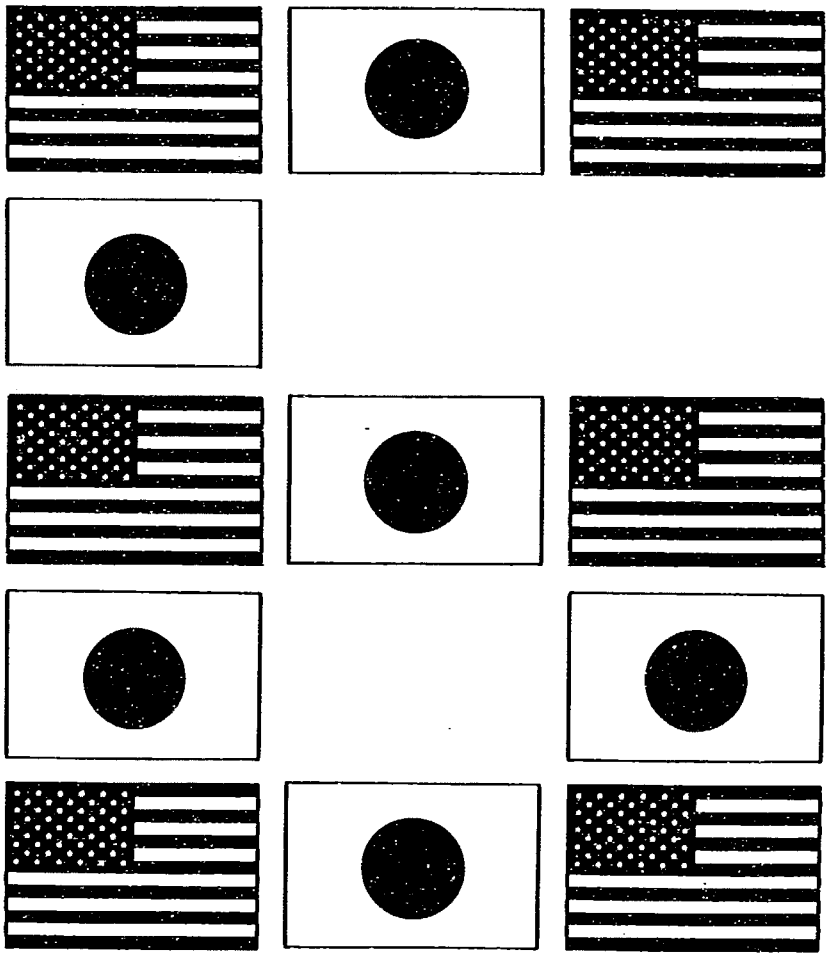
ISSN 0386-5878
Technical Memorandum
of PWRI No.3415

# PROCEEDINGS OF THE 6TH U.S.-JAPAN WORKSHOP ON EARTHQUAKE DISASTER PREVENTION FOR LIFELINE SYSTEMS



*JULY 18-19, 1995*
*OSAKA, JAPAN*

*PUBLIC WORKS RESEARCH INSTITUTE*
*MINISTRY OF CONSTRUCTION*

Copyright © (1994) by P. W. R. I.

All rights reserved. No part of this book may be reproduced by any means, nor transmitted, nor translated into a machine language without the written permission of the Director General of P. W. R. I.

この報告書は，土木研究所長の承認を得て刊行したものである。したがって，本報告書の全部又は一部の転載，複製は，土木研究所長の文書による承認を得ずしてこれを行ってはならない。

Technical Memorandum
of PWRI No. 3415

# PROCEEDINGS OF THE SIXTH U.S.-JAPAN WORKSHOP ON EARTHQUAKE DISASTER PREVENTION FOR LIFELINE SYSTEMS

JULY 18 AND 19, 1995
KKR HOTEL OSAKA,
OSAKA, JAPAN

**Synopsis:**

These proceedings document the results of the U.S.-Japan Workshop on Earthquake Disaster Prevention for Lifeline Systems which was held at KKR Hotel Osaka, Osaka, Japan, on July 18 and 19, 1995 under the auspices of the Panel on Wind and Seismic Effects, UJNR. The Workshop was organized by the Task Committee F "Disaster Prevention Methods for Lifeline Systems" (U.S. side chairman: R. M. Chung, NIST, Japan side chairman: Y. Koga, PWRI) of the Panel.

**Key word: Earthquake Disaster Prevention, Lifeline Systems, Pipeline, Gas, Telephone, Electricity, Water Supply, UJNR**

# FOREWORD

The following proceedings document the result of the sixth U.S.-Japan Workshop on Earthquake Disaster Prevention for Lifeline Systems, which was held at the KKR Hotel Osaka, Osaka, Japan, on July 18 and 19 1995. The workshop was co-sponsored by the Public Works Research Institute of Japan and the National Institute of Standards and Technology and the National Science Foundation of the United States under the auspices of task committee F "Disaster Prevention Methods for Lifeline Systems" (U.S. side chairman: Dr. R. M. Chung, Japan side chairman: Dr. Y. Koga) of the Panel on Wind and Seismic Effects, UJNR.

The purposes of this workshop were (1) to bring together experts from both countries to discuss current efforts in the area of lifeline seismic risk assessment and design, (2) to offer a forum for individuals to study specific measures being incorporated by agencies or companies to mitigate the effect of earthquakes on their systems, (3) to discuss the results of studies of the two recent large earthquakes which occurred in the United States and Japan, i.e., the January 17, 1994 Northridge Earthquake and the January 17, 1995 Hyogo-ken Nanbu Earthquake and (4) to identify future needs and opportunities between the two countries for cooperative research and exchange of data, information and research personnel. With these goals in mind, the Workshop program was developed so that it would help advance of the long-term objectives in lifeline earthquake engineering of both counties. It should be mentioned that three lifeline experts of New Zealand were also invited to the workshop to broaden our knowledge of the directions of research in the other parts of the world.

A broad range of special technical topics were presented at the Workshop. These included the following items.

1) Lifeline systems such as water, sewerage, gas, electric power, telecommunication, and transportation damaged by recent earthquakes
2) Effects of liquefaction and countermeasure for design and construction
3) Seismic monitoring
4) Risk assessment and socioeconomic impact
5) Post-earthquake fires
6) Post-earthquake lifeline function and restoration
7) Seismic design and retrofit of lifeline facilities

In total, 32 papers were presented in the two days of plenary sessions; 19 papers from Japan and 11 papers from U.S. and 2 papers from New Zealand.

In addition, the Workshop was highlighted by:

1) Active question and answer periods after each session;
2) Two-day field trip to the Central Load Dispatching Center of Kansai Electric Power Co., the Port Island Gas Plant of Osaka Gas Co., the Okuhirano Purification Plant of the Water

Supply Bureau, Kobe City, the Higashinada Sewage Treatment Plant of the Sewage Works Bureau, Kobe City, Akashi Kaikyo Bridge of Honshu Shikoku Bridge Authority, Nojima-Fault in Awaji Island and several bridges in Kobe area;

3) Resolutions fully supported by all the participants that identify future research priorities and cooperative activities between both countries.

The materials in this proceeding are presented as follows: (1) all technical papers that were presented during the workshop are provided in their order of presentation; (2) resolutions that were unanimously adopted by the participants during the closing session of the workshop; (3) appendices that include the workshop program, list of participants, study tour report, and photos to commemorate the workshop.

In concluding the foreword, We wish to express our profound gratitude and sincere appreciation to all participants in the workshop for supporting the workshop by active discussions. In particular, we would like to thank Dr. R. M. Chung, Leader of Earthquake Engineering Group, National Institute of Standards and Technology for his encouragement to hold the workshop. We also thank Mr. R. T. Eguchi of EQE International for organizing the U.S. and New Zealand members and Ms. L. A. Johnson of Spangle Associates for completing the beneficial study tour report. We were able to close a very successful workshop in which participants from U.S., New Zealand and Japan came to understand the problems and solutions used by each country for earthquake hazard mitigation through the exchange of important technical information on earthquake disaster prevention for lifeline systems.

Grateful thanks are extended to Kansai Electric Power Co., Osaka Gas Co., the Water Supply Bureau and the Sewage Works Bureau of Kobe City and Honshu Shikoku Bridge Authority for their generous cooperation during the study tour. We also would like to thank Public Works Research Center for their kind help to organize the workshop. Special appreciation also goes to the assisting staff members, Messrs Y. Ninomiya, T. Hamada J. Hoshikuma and K. Nagaya of PWRI for the smooth progress of the schedule.

October, 1995

Yasuyuki Koga
Hisanori Otsuka
Toru Terayama
Shuichi Tamoto
Earthquake Disaster Prevention Department
Public Works Research Institute

TABLE OF CONTENTS

Papers

Session–2 Effects of Liquefaction (1) ..... 1

Case History of Pipeline Response to Ground Deformation at Balboa Blvd., 1994 Northridge Earthquake

(T.D. O'Rourke) ..... 3

Liquefaction–Induced Ground Displacement and Its Caused Damage to Lifeline Facilities

(Masanori Hamada) ..... 21

Microfine Cement Grouting as a Countermeasure against Liquefaction

(Masaaki Sano) ..... 45

Analysis of Behavior and Effect of Geosynthetic Reinforced Embankments at the Occurrence Liquefaction

(Naozo Fukuda) ..... 57

Session–3 Effects of Liquefaction (2) ..... 69

Study on Flow of Liquefied Ground by means of Model Pipe Tests

(Ikuo Towhata) ..... 71

Countermeasures against the Floatation of Buried Pipes due to Liquefaction

(Susumu Yasuda) ..... 79

Dependence of Longitudinal Subgrade Reaction to the Buried Pipe on Displacement Velocities and Cycles of the Ground.

(Mio Kobayashi) ..... 91

Session–4 Water & Sewage ..... 107

Damages to Kobe Water System by the Hanshin Awaji Great Earthquake and Restoration Plan

(Makoto Matsushita) ..... 109

Performance of Sewerage System During the 1994 Hokkaido Toho–oki Earthquake

(Masaru Kitaura) ..... 129

Damage to Sewerage Facilities in Recent Earthquakes

(Shuji Tanaka) ..... 141

Water and Sewer Lifelines: Lessons Learned from Recent Earthquakes

(Le Val Lund) ..... 149

Performance of Lifeline Systems During the 1995 Great Hanshin Earthquake

(Shiro Takada) ..... 165

Session–5 Seismic Monitoring and Restoration ..... 185

A Study on the Development of An Immediate Detection System for Seismic Damage to Lifelines Using GPS and GIS.

(Fusanori Miura) ..... 187

Development of SIGNAL : Seismic Information Gathering Network Alert System

(Yoshihisa Shimizu) ..... 199

Conditional Non−Gaussian Fields
(Masaru Hoshiya) ..... 211
Real Time Conditional Simulation of Earthquake Ground Motion
(Tadanobu Sato) ..... 221
Optimization of Post−Earthquake Restoration of Lifeline Networks Using Genetic Algorithms
(Koji Ichii) ..... 235
Session−6 Gas, Electricity and Telecommunication ..... 251
Damages of Gas Facilities by Great Hanshin Earthquake and Restoration Process
(Shojiro Oka) ..... 253
Impact of the Earthquake of Southern Hyogo Prefecture on Electric Power Facilities
(Tohru Yoshikawa) ..... 271
Damage of Underground Telecommunication Facilities in the 1995 Great Hanshin Earthquake
(Kenichi Honda) ..... 289
Power Systems: Comparing the Kobe and Northridge Earthquake Experiences
(Anshel J. Schiff) ..... 301
Session−7 Risk Assessment and Impact of Seismic Effects (1) ..... 315
Pipeline Performance Parameters for Earthquake Vulnerability
(Donald Ballantyne) ..... 317
Economic Impact of Lifeline Disruption: Current Models and Preliminary Observations from the Hanshin Earthquake
(Stephanie E. Chang) ..... 333
Application of GIS Technology to Seismic Risk Assessment of Lifeline Systems in Shelby County, Tennessee
(Howard H.M. Hwang) ..... 349
Session−8 Risk Assessment and Impact of Seismic Effects (2) ..... 365
Functional Interactions of Lifeline Systems under Earthquake Conditions
(Masanobu Shinozuka) ..... 367
Regional Approach to Assessment of Impact on Lifelines and Response to Earthquakes in New Zealand
(John L. Lumsden) ..... 381
New Trends in the Use of Earthquake Scenario Exercises
: Opportunities for Mitigating Vulnerable Lifeline Systems
(Laurie A. Johnson) ..... 389
Rapid Post−Earthquake Damage Assessment for Lifeline Facilities
(Ronald T. Eguchi) ..... 399
Session−9 Transportation and Fire ..... 413
Resources Required to Rebuild Wellington
(David C. Hopkins) ..... 415
A Fundamental Study on Innovative Menshin System for Underground Structures
(Jun−ichi Hoshikuma) ..... 427

A Bridge Prioritization Method Based on Transportation System Performance Using GIS
(Anne S. Kiremidjian) ..... 437
Fire Following the Hanshin and Northridge Earthquakes : A Comparative Analysis
(C. Scawthorn) ..... 451

Resolutions ..... 469

Appendices ..... 473
Kobe at Six Months —A Phoenix on the Horizon— (A Study Tour Report)
(Laurie A. Johnson) ..... 475
Workshop Program ..... 515
Participants ..... 519


6th U.S.-Japan Workshop on Earthquake
Disaster Prevention for Lifeline Systems

# Session-2

## Effects of Liquefaction (1)

(U-1) Case History of Pipeline Response to Ground Deformation at Balboa Blvd.,1994 Northridge Earthquake
(T.D.O'Rourke and S.Toprak)

(J-1) Liquefaction-Induced Ground Displacement and Its Caused Damage to Lifeline Facilities
(Masanori Hamada, Ryoji Isoyama and Kazue Wakamatsu)

(J-2) Microfine Cement Grouting as a Countermeasure against Liquefaction
(Osamu Matsuo,Junichi Koseki, Masaaki Sano and Masao Shimoda)

(J-3) Analysis of Behavior and Effect of Geosynthetic Reinforced Embankments at the Occurrence Liquefaction
(Osamu Matsuo,Takao Shimazu, Junichi Koseki, Naozo Fukuda, Teruhisa Fujii and Nobuo Tajiri)

# CASE HISTORY OF PIPELINE RESPONSE TO GROUND DEFORMATION AT BALBOA BLVD., 1994 NORTHRIDGE EARTHQUAKE

by

T.D. O'Rourke[1] and S. Toprak[2]

## ABSTRACT

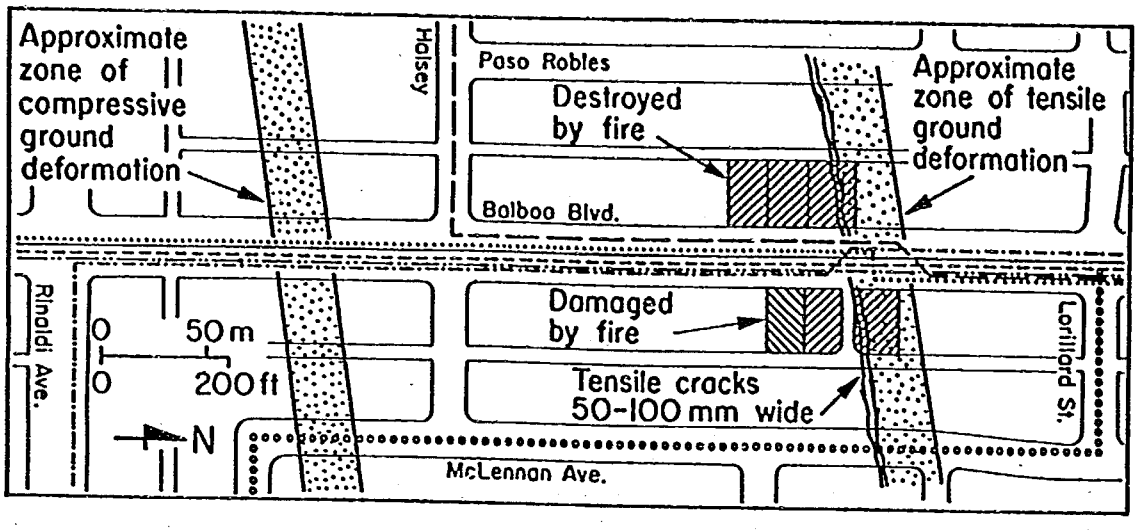
Permanent ground deformation on Balboa Blvd. and McLennon Ave. during the 1994 Northridge earthquake affected four gas transmission, one oil transmission, and two water trunk pipelines. Three of the pipelines failed with serious consequences, and four of the pipelines were not damaged. Accordingly, a case history evaluation of this incident is important for understanding factors contributing to the vulnerability of buried lifelines, calibrating analytical models, and taking corrective measures to improve performance. Deformation occurred as sliding of a relatively coherent soil mass parallel to the longitudinal axes of the pipelines. Relevant pipe, soil, and geometric conditions are reported in this paper. Analytical results from sliding block models of soil-pipeline interaction are compared with field observations, and shown to compare favorably with field performance.

## INTRODUCTION

During the 1994 Northridge earthquake, permanent ground deformation (PGD) occurred in Holocene alluvial sediments along Balboa Blvd. Hecker, et al. (1995) have mapped and described the ground deformation in this area. They report that deformation most likely involved shallow seated (< 10 m deep) displacements caused by one or more of the following phenomena: slope failure, lurching of surficial deposits, compaction of loose sediment, and liquefaction. O'Rourke and Palmer (1994) have described the response of buried pipelines in this area. Information from their study has been combined with additional observations and measurements at site to provide the case history database for this work.

Figure 1 is a map of the pipelines near Balboa Blvd. in the PGD zones. There were two 762-mm-diameter gas transmission lines and a 406-mm-diameter petroleum pipeline that were not damaged. Two water trunk lines operated by the Los Angeles Department of Water and Power (LADWP), the 1,245-mm-diameter Granada and the 1,727-mm-diameter Rinaldi Trunk Lines, failed in tension and compression in the tensile and compressive zones of ground deformation, respectively. Gas pipeline damage on Balboa Blvd. occurred in Old Line 120, a 559-mm-diameter

1 - Professor, School of Civil and Environmental Engineering, Cornell University, Hollister Hall, Ithaca, NY
2 - Graduate Research Assistant, School of Civil and Environmental Engineering, Cornell University, Hollister Hall, Ithaca, NY




Legend:

- 762 mm dia. gas Line 3003
- 762 mm dia. gas Line 3000
- 559 mm dia. gas Old Line 120
- 610 mm dia. gas New Line 120
- 406 mm dia. oil Mobil Oil
- 1245 mm dia. water Granada Trunk Line
- 1727 mm dia. water Rinaldi Trunk Line
- House destroyed
- House damaged

Figure 1. Map of Pipelines Affected by PGD

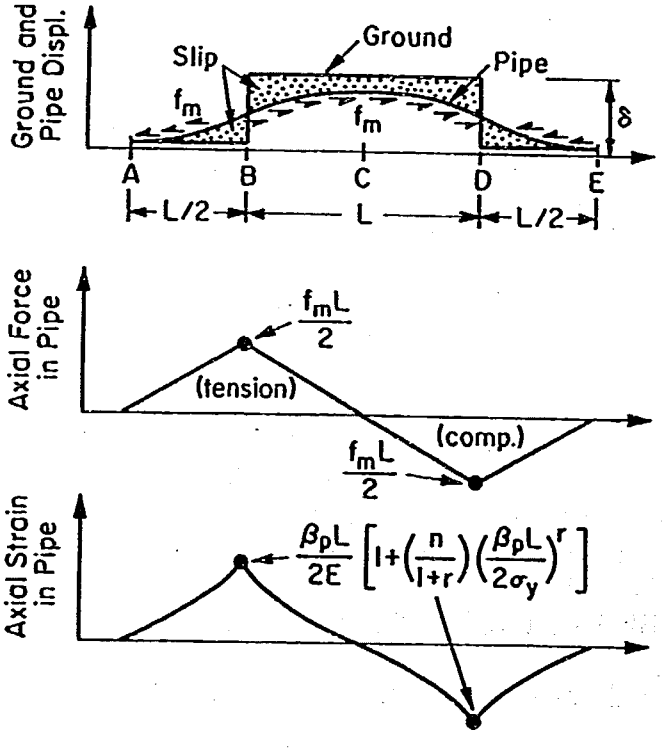



Figure 2. Case I Conditions

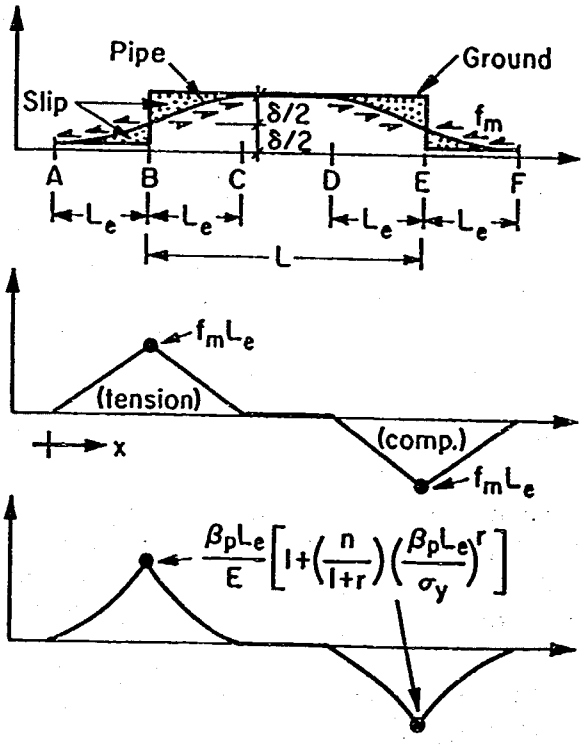



Figure 3. Case II Conditions

steel pipeline which was constructed in 1930. The line had been scheduled for replacement, and a new 610-mm-diameter pipeline (New Line 120) had been constructed parallel to the older one along McLennon Ave. It had not been opened for gas flow at the time of the earthquake. Even though it crossed similar zones of tensile and compressive ground deformation, it was not damaged.

A detailed examination of sections of Old Line 120 and the Granada Trunk Line, which were removed from the compressive ground deformation zone, each disclosed a compressive shortening of approximately 250 mm. In each case, the compressive shortening and line failure occurred at a welded joint. Observations of Old Line 120 in the tensile ground deformation zone showed a separation of approximately 250 mm at a ruptured welded joint.

In this paper, relevant pipe, soil, and geometric conditions are reported. Analytical results from sliding block models of soil-pipeline interaction (O'Rourke and Nordberg, 1992) are compared with observed pipeline performance. The analytical approach is similar to that described by O'Rourke and O'Rourke (1995); several of the analytical results and site descriptions in this paper are identical to those published by O'Rourke and O'Rourke (1995). Recommendations are made for future analysis, design, and pipeline testing.

## ANALYTICAL MODEL

The analytical model used in this work is based on the sliding block model for PGD effects on pipelines proposed by O'Rourke and Nordberg (1992). Two cases were considered in their work for a buried pipeline subject to a block pattern of longitudinal PGD. In Case I, the amount of ground movement $\delta$ is large and the pipe strain is controlled by the length, L, of the PGD zone. In Case II, L is large and the pipe strain is controlled by $\delta$.

The distribution of pipe axial displacement, force, and strain are shown in Fig. 2 for Case I and Fig. 3 for Case II, where $f_m$ is the frictional force per unit length at the pipe-soil interface and $L_e$ is the effective length over which $f_m$ acts. The frictional force can be expressed by:

$$f_m = (c + \mu\gamma H)\pi D \qquad (1)$$

where c is the soil cohesion or the undrained shear strength, $\mu$ is the coefficient of friction at the soil-pipe interface, $\Upsilon$ is the effective unit weight of soil, H is the depth to centerline of the pipeline, and D is the outside diameter of pipe.

Over the segment AB in both cases, the force in the pipe is linearly proportional to the distance from Point A. Using a Ramberg-Osgood model for the pipe material, the pipe strain, $\varepsilon_{max}$, for Case II can be expressed as follows:

$$\varepsilon_{max} = \frac{\beta_p L_e}{E}\left\{1+\frac{n}{1+r}\left(\frac{\beta_p L_e}{\sigma_y}\right)^r\right\} \qquad (2)$$

in which n and r are Ramberg-Osgood parameters, E is the modulus of elasticity of the pipe steel, $\sigma_y$ is the effective yield stress, $\beta_p$ is the pipe burial parameter, and $L_e$ is the distance from point A to point B in Fig. 3. A similar equation can be developed for Case I conditions, as shown in Fig. 2.

For granular soil typical of the backfill at Balboa Blvd. (c = 0), the pipe burial parameter $\beta_p$ can be computed by:

$$\beta_p = \frac{\mu\gamma H}{t} \qquad (3)$$

in which the frictional coefficient $\mu$ = ktan$\phi$, $\phi$ is the soil friction angle, and k is a coefficient related to the conditions at the soil-pipe interface.

As described by Tawfik and O'Rourke (1985) welded slip joints are used in many high-pressure water transmission pipelines and are vulnerable during earthquakes to axial compressive loads generated by ground movements. A welded slip joint is composed of a belled, or flared, pipe end into which a straight cylindrical, or spigot, section of the pipe fits. The bell and spigot are joined by means of a circumferential weld. Because the slip joint introduces a local eccentricity and change in curvature, its axial load-carrying capacity is decreased. Tawfik and O'Rourke (1985) analyzed the compressive failure mode associated with plastic flow in the curvilinear, belled ends of the joints. The governing equations for this mode are presented here because it was the observed compressive failure mode in the water trunk lines.

The dimensionless axial load-carrying capacity of a welded slip joint, $P_{II}$, is expressed by:

$$P_{II} = \frac{(2\rho + 1)p_r \pm \sqrt{(2\rho+1)^2 p_r^2 - 4(\rho^2+\rho+1)(p_r^2 - \sin^2\phi)}}{2(\rho^2+\rho+1)} \qquad (4)$$

where $\rho$ is dimensionless curvature, $\phi$ is an angle, and $p_r$ is dimensionless internal pressure. The values of $\rho$ and $\phi$ are determined by the shape of the slip joint. A cosine representation for the joint is adopted here. It was shown by Tawfik and O'Rourke (1985) that there is good agreement between the measured shapes of LADWP joints and the cosine representation. The dimensionless parameters, $\rho$ and $\phi$ are given by:

$$\rho = \frac{\frac{\zeta\pi^2}{2\lambda^2}\cos\frac{\pi\eta}{\lambda}}{1 + \frac{\zeta^2\pi^2}{4\lambda^2}\sin^2\frac{\pi\eta}{\lambda}} \tag{5}$$

and

$$\sin^2\phi = \left[1 + \frac{\zeta^2\pi^2}{4\lambda^2}\sin^2\frac{\pi\eta}{\lambda}\right]^{-1} \tag{6}$$

where $\zeta$, $\eta$, and $\lambda$ are dimensionless offset, coordinate, and length of the curved portion of the bell respectively. They are defined as follows:

$$\zeta = \frac{h}{R_o}, \eta = \frac{Z}{R_o}, \lambda = \frac{\ell}{R_o} \tag{7}$$

where h, z, l and $R_o$ are shown in Figure 4. The value of $p_r$ can be calculated by:

$$p_r = \frac{pR_o}{f_y t} \tag{8}$$

where p is internal pressure, $f_y$ is uniaxial yield stress, and t is thickness.

The axial compressive load capacity of a welded slip joint is given by:

$$P = P_{\Pi} 2\pi R_o f_y t \tag{9}$$

The Committee on Gas and Liquid Fuel Lifelines [CGLFL] (1984) suggests that compressional pipe wrinkling begins at a strain of 1/3 to 1/4 the theoretical value of 0.6 t/R, where t is pipe wall thickness and R is pipe radius. Assuming that wrinkling starts at the midpoint of this range:

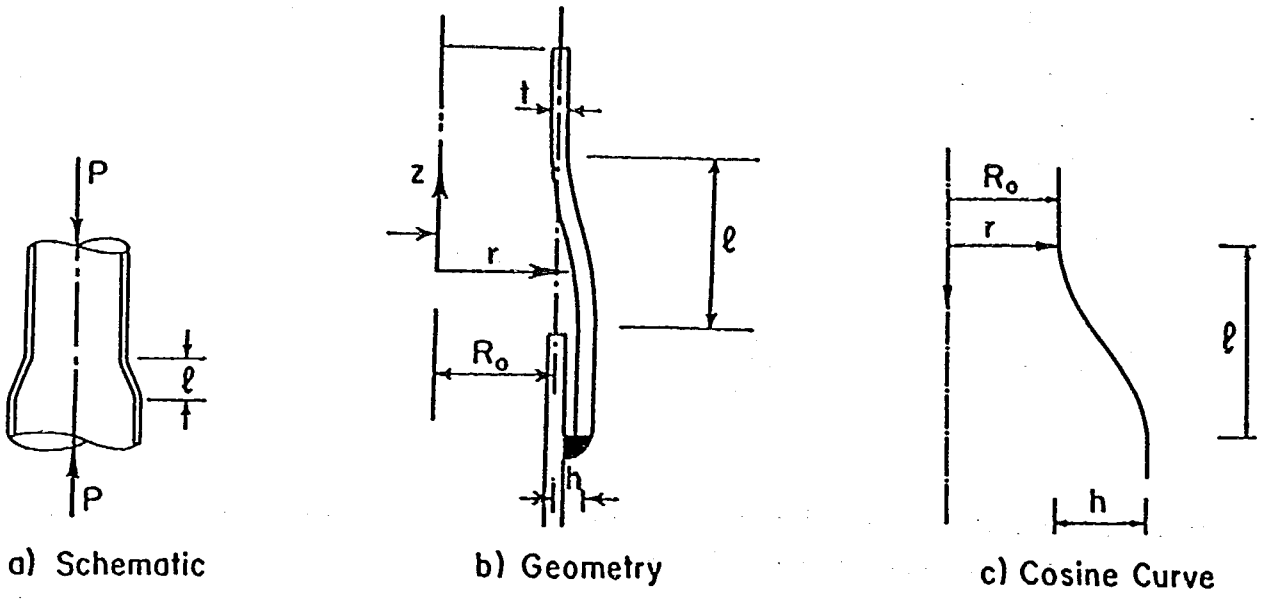



Figure 4. Schematic View, Geometry, and Cosine Curve For Welded Slip Joints (After Tawfik and O'Rourke, 1985)

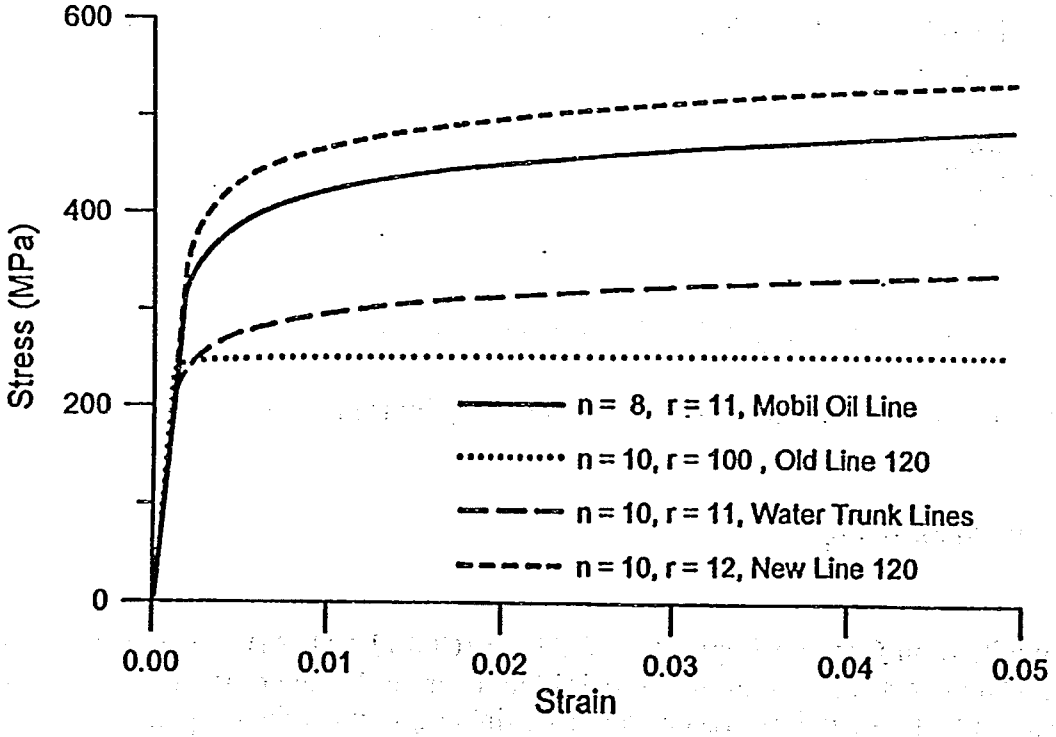



Figure 5. Stress-Strain Relationships for Pipe Steel

$$\varepsilon_{cr} = 0.175 \frac{t}{R} \qquad (10)$$

The strain associated with tensile rupture is on the order of 3% to 5% (CGLFL, 1984). In this study, an ultimate tensile value of 4% is assumed, above which the pipeline is considered to have failed in tension.

The critical length, $L_{cr}$, is established from Eqn. 2 by setting peak strain equal to the critical strain and solving for the corresponding effective length. The critical length, the length of the PGD zone at the onset of failure, is then twice this effective length.

## PIPE, SOIL, AND GEOMETRIC CHARACTERISTICS

Table 1 summarizes relevant pipe, soil, and geometric characteristics pertaining to the transmission and trunk lines on Balboa Blvd. and McLennon Ave. The unit weight of soil, $\gamma$, was assumed to be 19.65 kN/m$^3$. Of special importance are the frictional coefficient, stress-strain characteristics of pipe steel, and pipeline joints, which are discussed under the following headings.

### Frictional Coefficient

The frictional coefficient, $\mu$, was determined by assuming $\phi = 37°$, which is typical of medium dense sandy soil. The coefficient, k, was chosen on the basis of published test results related to the interface shear resistance between granular soil and various concrete and polymeric surfaces (e.g., O'Rourke, et al., 1990). Cement mortar coating is rough, and the appropriate k is 1.0. For smooth polyethylene and fusion bonded epoxy, k was chosen as 0.54. For coal tar epoxy, an appropriate k is 0.87.

### Pipe Steel

The stress-strain characteristics of the pipe steel were modeled by means of Ramberg-Osgood parameters, as shown in Figure 5. The Mobil Oil pipeline, Line 3000 and Line 3003, are composed of X52 steel, and the stress-strain characteristics were derived from tensile coupon tests of X52 pipe steel performed at Cornell University. New Line 120 is composed of X60 steel, and the stress-strain characteristics were derived similarly from tests at Cornell University. The stress-strain characteristics of steel in the Granada and Rinaldi Trunk Lines were derived from tensile coupon tests at Cornell for pipe steel of similar grade and age. No test results were available for steel typical of Old Line 120. It was assumed that older pipe steel will have a relatively flat post yield stress-strain relationship, which is more representative of the metallurgical characteristics of steel products manufactured during the 1930s.

Table 1. Pipeline Characteristics

| Pipeline | Joints | D[b] mm | t[c] mm | Coating | μ[e] | SMYS[d] MPa | Burial Depth, m |
|---|---|---|---|---|---|---|---|
| Old Line 120 | Unshielded Electric Arc | 559 | 7.1 | Coal Tar Epoxy | 0.65 | 242 | 1.5 |
| New Line 120 | Electric Arc[a] | 610 | 6.4 | Fusion Bonded Epoxy | 0.41 | 415 | 1.5 |
| Line 3000 | Electric Arc[a] | 762 | 9.5 | Coal Tar Epoxy | 0.65 | 360 | 5.2[f] 2.4[g] |
| Line 3003 | Electric Arc[a] | 762 | 9.5 | Coal Tar Epoxy | 0.65 | 360 | 2.4 |
| Granada Trunk Line | Welded Slip Joint and Mechanical Coupling | 1245 | 6.4 | Cement Mortar | 0.75 | 249 | 1.8 |
| Rinaldi Trunk Line | Welded Slip Joint | 1727 | 9.5 | Cement Mortar | 0.75 | 249 | 2.7 |
| Mobil Oil | Electric Arc[a] | 406 | 9.5 | Poly-ethylene | 0.41 | 360 | 1.5 |

a - refers to full penetration girth welds by shielded electric arc practices
b - nominal outside diameter d - Specified Minimum Yield Stress, equivalent to $\sigma_y$
c - wall thickness e - coefficient of friction
f,g - at tensile and compressive ground rupture zone, respectively

## Pipeline Joints

Modern oil and gas pipeline joints are full penetration girth welds administered with shielded electric arc procedures. The welded joints of pipelines, like the Mobil Oil Line, Line 3000 and Line 3003, and New Line 120 typically are stronger than adjacent pipe.

As previously mentioned, Tawfik and O'Rourke (1985) studied the load carrying capacity of welded slip joints on pipelines operated by the LADWP and their equations for calculating axial compressive capacity were used.

Unshielded electric arc joints involved the joining of two belled pipe ends around a steel liner, or chill ring. The interior ring provided a backing for welding the two belled ends. Unshielded arc practices, such as those used for Old Line 120, exposed the molten weld to the atmosphere, thereby increasing the likelihood of gas inclusions and uneven heating when compared with modern, shielded electric arc techniques. No published test results or studies of the load carrying capacity and stress-strain characteristics of these joints are available. It is likely, however, that the compressive and tensile strength of this type of joint are less than those determined from the yield strength of the pipe steel.

## ANALYTICAL RESULTS

As illustrated in Figure 1, there were six pipelines which crossed both the tensile and compressive ground rupture zones, including Mobil Oil Line, the Granada Trunk Line, and the Rinaldi Trunk Line, Old Line 120, Line 3000 and New Line 120. Line 3003 crossed only the tensile ground rupture zone. The analytical assumptions and results for each of the pipelines are discussed under a separate subheading as follows:

### Mobil Oil Line

The soil-pipeline interaction for the Mobil Oil Line is similar to that for Case I (see Figure 2). As shown in Figure 1, there is a bend in the line just north of the tensile ground rupture zone that was treated analytically as an anchor. The analytical procedure was modified to account for the asymmetric distribution of pipeline displacement and strain, as explained in Appendix A. The final form of the equation is:

$$a^2 + 2La - L^2 = 0 \qquad (11)$$

where L is the length of the permanent ground displacement zone and a is the distance between the compressive zone and the point where the pipe displacement is zero or a maximum. Application of this equation for the Mobil Oil Line, knowing that L is equal to 275 m, gave a value of a of 114 m. Calculated displacement and strain values are shown in Figure 6a.. The analytical strains are well below the compressive and tensile failure limits of the pipe.

### Granada Trunk Line

The Granada Trunk Line was pulled from a mechanical joint at the tensile rupture zone. Because the pullout resistance of a conventional mechanical joint is very low, free slip was assumed in the analysis. Compressive wrinkling of welded slip joints was considered in the analysis of the pipeline in the compressive rupture zone.

The axial capacity of the pipeline, $P_{II}$, was evaluated by using the Tawfik and O'Rourke (1985) procedure described previously. In this calculation, the internal pressure of the pipeline was assumed to be 0.7 MPa, which is conservative for these lines. Referring to Equations 5 and 6, the average value of $\lambda$ was 0.2 as determined by field measurements. The h value was evaluated by adding 0.8 mm to pipe wall thickness.

The failure stress for welded slip joints of the Granada Trunk Line is calculated as 92 MPa. Because of this low axial capacity, the onset of compressive wrinkling at the welded slip joint near the compressive rupture zone occurred at a relatively small level of soil and pipeline movement as shown in Figure 6b.

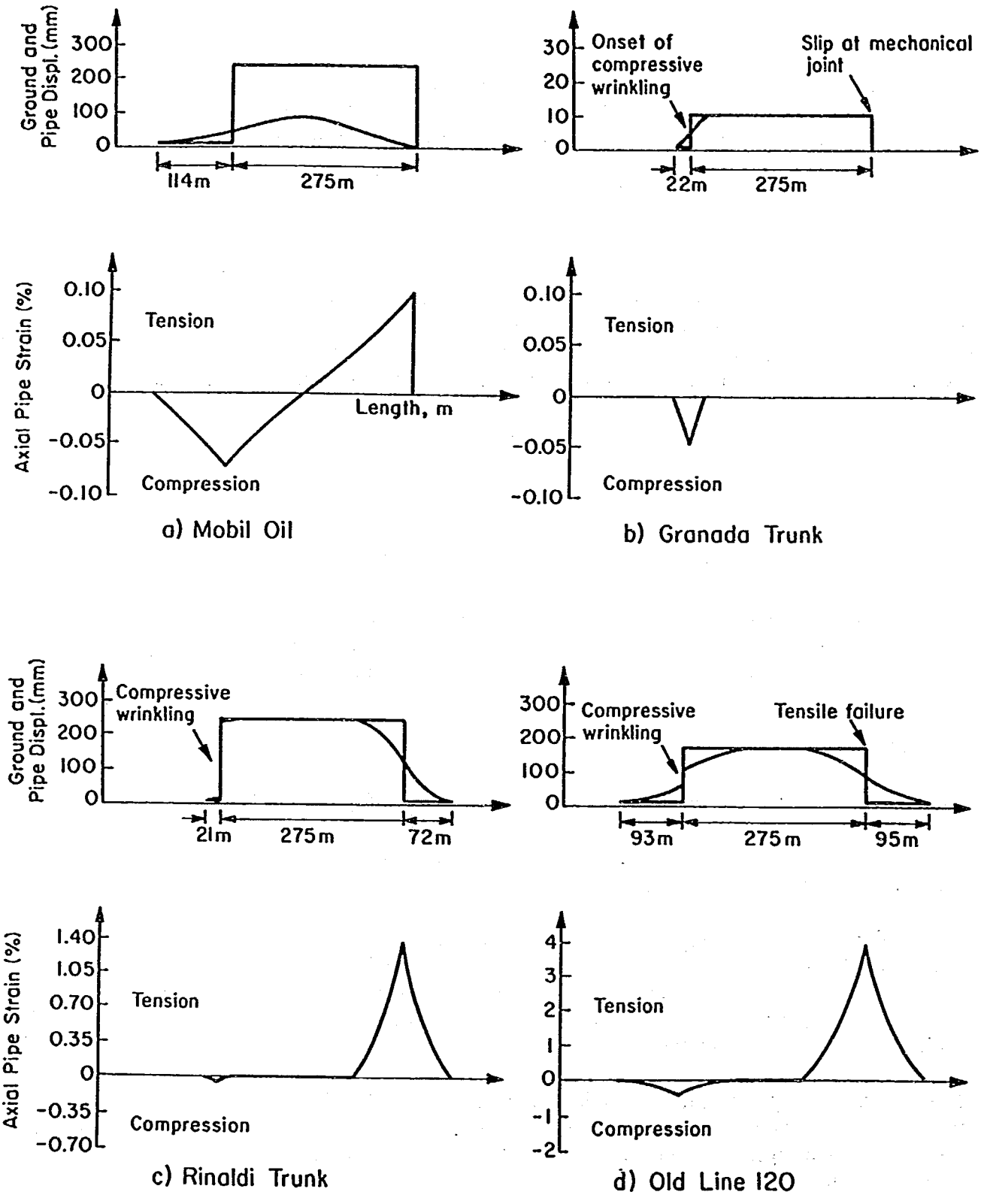



Figure 6. Analytical Results for Mobil Oil Line, Granada Trunk, Rinaldi Trunk, and Old Line 120

### Rinaldi Trunk Line

The analysis of the compressive wrinkling of welded slip joints in the Rinaldi Trunk Line in the compressive rupture zone was performed using the same parameters employed in the analysis of the Granada Trunk Line. The failure stress for the joints was computed as 87 MPa.

The results in Figure 6c show that the onset of plastic wrinkling in the compressive ground rupture zone occurs at relatively small displacement and strain levels. Tensile strains of approximately 1.4% was calculated in the pipe at the tensile ground rupture zone. This strain corresponds to an axial tensile stress of 300 MPa, which is likely to exceed the tensile capacity of a welded slip joint. Hence, the analytical results are consistent with the observed compressive and tensile failures at welded slip joints.

### Old Line 120

The results in Figure 6d show both compressive and tensile failure of the pipe are predicted for the relatively flat post yield stress-strain characteristics assumed (see Figure 5). Because failure was observed at unshielded electric are welded joints, it can be inferred that the strength of these joints is less than that determined from the yield strength of the pipe steel.

### Line 3000

Since Line 3000 has different burial depths at the tensile and compressive ground rupture zones, two separate analyses were made to determine the pipe response at the two zones by using the corresponding burial depths. Furthermore, there are some important geometric details which may need consideration in the analysis of Line 3000. There is a bend near the tensile ground deformation zone and a 90° bend approximately 120 m south of the compressive ground deformation zone at the junction of Balboa Blvd. and Rinaldi Street.

The bend near the tensile ground deformation zone was treated analytically as an anchor. An equation, which accounts for nonlinear stress-strain characteristics, was developed to perform the analysis. The derivation is provided in Appendix B. The final equations for displacement and strain are:

$$\delta = \frac{\beta_p L_e^{\,2}}{2E}\left[1 + \left[\frac{2}{r+2}\right]\left[\frac{n}{1+r}\right]\left[\frac{\beta_p L_e}{\sigma_y}\right]^r\right] \tag{12}$$

$$\varepsilon_{max} = \frac{\beta_p L_e}{E}\left[1 + \left[\frac{n}{1+r}\right]\left[\frac{\beta_p L_e}{\sigma_y}\right]^r\right] \tag{13}$$

No additional modeling was necessary to account for the 90° bend because the analysis showed that sufficient axial friction force is developed between the bend and the compressive ground rupture zone to accommodate the pipe displacement caused by soil block movement. Analytical calculations (see Figure 7a) indicates that strains developed both at tensile and compressive rupture zones are below the assumed critical strain levels, which is consistent with observations.

### Line 3003

Line 3003 has a bend north of the tensile ground rupture zone that was treated analytically as an anchor as in the case of Line 3000. Equations derived for Line 3000 were used in the analysis. Tensile strains of approximately 1.3% were calculated in the pipe at the tensile ground rupture zone (see Figure 7b) which is below the assumed critical strain limit.

The 90° bend in Line 3003 at the junction of Balboa Blvd. and Halsey Street, approximately 200 m south of the tensile ground deformation zone, did not affect the resistance of the pipeline because the pipe displacement approached the ground displacement north of the bend point, after which the pipe and ground displacements would be the same.

### New Line 120

The soil-pipeline interaction for New Line 120 is similar to that for Case I (see Figure 2), because of the low interface friction angle as well as the shallow burial depth. There is a 90° bend in New Line 120 approximately 40 m south of the compressive rupture zone that was treated analytically as an anchor. As a result, the pipe displacement was no longer symmetric. The analytical model was modified to account for this condition.

The derivation of the equation for this analysis is provided in Appendix C. In the derivation, linear stress-strain characteristics were assumed. Calculated strain values were checked to verify that they were in the linear range. The final form of the equation is:

$$L_1^2 - (4L + 2a)\,L_1 + (2L^2 + a^2) = 0 \qquad (14)$$

where L is the length of the permanent ground displacement zone, a is the distance between the anchor point and the compressive ground rupture zone, and $L_1$ is the distance between the compressive zone and the point where the pipe displacement is a maximum. The equation was solved for $L_1$ with known values of L and a, 275 m and 40 m, respectively. The calculated $L_1$ value was about 148 m. The results in Figure 7c show the evaluated displacement and strain values using this $L_1$ value. The strains are well below the critical strain levels.

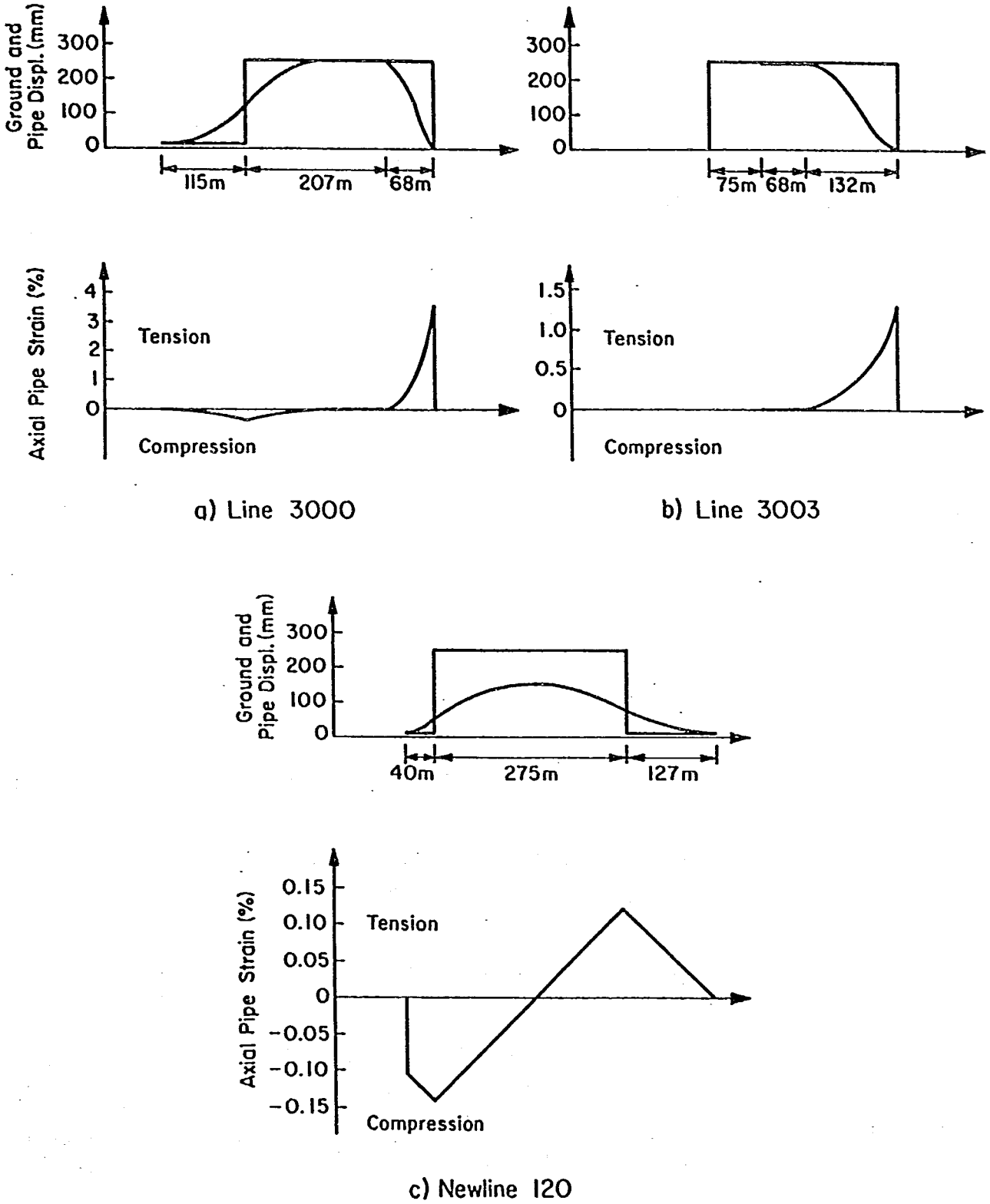



Figure 7. Analytical Results for Line 3000, Line 3003, and New Line 120

## CONCLUSIONS

The analytical results compare favorably with field performance, thus indicating that the sliding block model is an appropriate analytical tool for future design and planning purposes. The analytical results show that the successful performance of the Mobil Oil Line, Line 3000, Line 3003, and New Line 120 was related primarily to the relatively high strength of their electric arc welded joints and post-yield performance characteristics of the steel. The low strains calculated for the Mobil Oil Line and New Line 120 were influenced by the relatively low frictional coefficient of their coatings. Compressive and tensile pipeline failures occurred at welded joints, involving belled pipe with fillet welds for water trunk lines and unshielded electric arc welds for the oldest gas pipeline. It would be advantageous to perform full scale tensile and compressive tests on these types of joints and to determine more reliably the stress-strain characteristics of pipe steel representative of the older oil and gas pipelines in service.

## ACKNOWLEDGMENTS

Support for the research described in this report was provided by the National Center for Earthquake Engineering Research (NCEER). Some of the analytical approaches and results contained in this paper were developed with Professor Michael O'Rourke at Rensselaer Polytechnic Institute, and his contributions are gratefully acknowledged. Laurie McCall prepared the manuscript and Ali Avcisoy prepared the figures.

## REFERENCES

Committee on Gas and Liquid Fuel Lifelines, "Guidelines for the Seismic Design of Oil and Gas Pipeline Systems", ASCE, New York, NY, 1984.

Hecker, S., et al., "Ground Deformation in Granada Hills and Mission Hills Resulting from the January 17, 1994, Northridge, California Earthquake", Open File Report 95-62, USGS, Menlo Park, CA, 1995.

O'Rourke, M.J. and C. Nordberg, "Longitudinal Permanent Ground Deformation Effects on Buried Continuous Pipelines", NCEER-92-0014, NCEER, Buffalo, NY, June, 1992.

O'Rourke, T.D. and M.S. Tawfik, "Load-Carrying Capacity of Welded Slip Joints", Journal of Pressure Vessel Technology, ASME, Vol. 107, Feb. 1985, pp. 36-43.

O'Rourke, T.D., S.J. Druschel, and A.N. Netravali, "Shear Strength Characteristics of Sand-Polymer Interfaces", Journal of Geotechnical Engineering, ASCE, Vol. 116, Mar. 1990, pp. 451-469.

O'Rourke, T.D. and M.C. Palmer, "The Northridge, California Earthquake of January 17, 1994: Performance of Gas Transmission Pipelines", NCEER-94-0011, NCEER, Buffalo, NY, May, 1994.

O'Rourke, T.D. and M.J. O'Rourke, "Pipeline Response to Permanent Ground Deformation: A Benchmark Case", Proceedings, 4th U.S. Conference on Lifeline Earthquake Engineering, San Francisco, CA, Aug. 1995 (in press).

## APPENDIX A

There is a bend in the Mobil Oil Line just north of the tensile ground rupture zone that was treated analytically as an anchor. The analytical model was modified to account for asymmetric distribution of pipeline displacement and strain. The derivation of the necessary equation is as follows.

To satisfy the equilibrium and continuity requirements, the displacement of the pipe at the compression zone should be half of the maximum displacement of the pipe, as shown schematically in Figure A1a. A linear, rather than nonlinear, stress-strain relationship is assumed for simplicity. If the calculated strain values satisfy this assumption, then the derivation can be accepted. Otherwise, a nonlinear stress-strain relationship should be incorporated into the derivation.

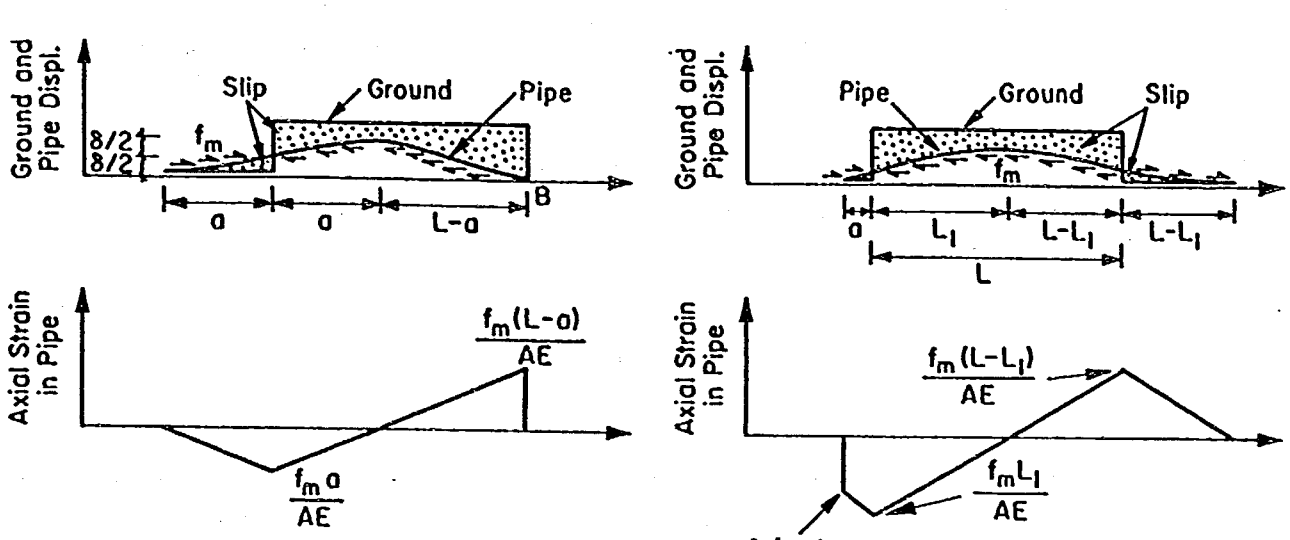
The displacement of the pipe in the compressive ground rupture zone is:

$$\frac{\delta}{2} = \int_{o}^{a} \frac{f_m x}{AE}\, dx \qquad (A.1)$$

where all values are defined previously. The displacement of the pipe in the tensile ground rupture zone is:

$$\delta = \int_{o}^{L-a} \frac{f_m x}{AE}\, dx \qquad (A.2)$$

After equating the two displacements with each other and arranging, the final equation becomes:




a) Mobil Oil

b) New Line 120

Figure A.1. Schematic Illustration of Pipe Displacements and Strains for Mobil Oil Line and New Line 120

$$a^2 + 2La - L^2 = 0 \qquad (A.3)$$

If this equation is solved for a with known value of L, 275 m, it yields the value of a = 114 m. This L value results in strain values of 0.07% and 0.1% in the compressive and tensile ground rupture zones, respectively. Since these strain values fall in the linear portion of the stress-strain curve of this pipeline, the initial assumption is valid and the derived equation can be used for the analysis.

## APPENDIX B

Line 3000 has a bend near the tensile ground rupture zone which was treated analytically as an anchor. Since initial analysis showed that nonlinear stress-strain characteristics should be incorporated into the analysis, the equation derived for the Mobil Oil Line cannot be used for this case. Therefore, a new and more general equation was derived as follows.

The strain can be expressed by:

$$\varepsilon(x) = \frac{\beta_p x}{E}\left[1+\left(\frac{n}{1+r}\right)\left(\frac{\beta_p x}{\sigma_y}\right)^r\right] \qquad \text{(B.1)}$$

For the section of the pipe anchored at the edge of the ground rupture zone, the displacement is:

$$\delta = \int_0^{L_e} \varepsilon(x)\, dx \qquad \text{(B.2)}$$

After substituting the strain equation into the displacement equation and integrating, the final equation is:

$$\delta = \frac{\beta_p L_e^2}{2E}\left[1+\left[\frac{2}{r+2}\right]\left[\frac{n}{1+r}\right]\left[\frac{\beta_p L_e}{\sigma_y}\right]^r\right] \qquad \text{(B.3)}$$

## APPENDIX C

There is a 90° bend in New Line 120 approximately 40 m south of the compressive rupture zone that was treated analytically as an anchor (See Fig. A1b). A new equation was developed for this situation as follows.

Maximum pipe displacement is expressed in different forms in the compressive and tensile zone. In the compression zone, the maximum pipe displacement is:

$$\delta = \int_0^a \left(\frac{f_m x}{AE} + \frac{f_m L_1 - f_m a}{AE}\right) dx + \int_0^{L_1} \frac{f_m x}{AE}\, dx \qquad \text{(C.1)}$$

In the tension zone, pipe displacement is:

$$\frac{\delta}{2} = \int_{o}^{L-L_1} \frac{f_m x}{AE} dx \qquad (C.2)$$

Combining and rearranging the above expressions results in:

$$L_1^2 - (4L + 2a) L_1 + (2L^2 + a^2) = 0 \qquad (C.3)$$

For the New Line 120, L and a values are known. They are 275 m and 40 m, respectively. The final equation yields a $L_1$ value of 148 m. The calculated strain values are 0.14% and 0.12% for the compressive and tensile ground rupture zones, respectively. Since these strains are on the linear part of the stress-strain curve for this pipe, the initial assumption was valid. Hence, the derived equation can be used in the analysis of New Line 120.

# LIQUEFACTION-INDUCED GROUND DISPLACEMENT AND ITS CAUSED DAMAGE TO LIFELINE FACILITIES

by

Masanori Hamada[1], Ryoji Isoyama[2]
and Kazue Wakamatsu[3]

## ABSTRACT

This paper introduces an outline of liquefaction-induced large ground displacement and its caused damage to lifeline facilities, and foundations of buildings and bridges piles during the 1995 Hyogoken-Nanbu (Kobe) earthquake. Some typical examples of large ground displacements which were measured by aerial survey are presented and the causal relationship of damage to buried pipes and foundation piles with ground displacement is introduced. Furthermore, the present paper outlines the soil and geomorphological conditions of the areas where the liquefaction and the large ground displacements occurred.

## INTRODUCTION

The 1995 Hyogoken-Nanbu (Kobe) earthquake caused severe soil liquefaction in extensive area of reclaimed lands in Kobe and its neighboring cities. The soil liquefaction also induced large ground displacements in the horizontal direction, which resulted in serious damage to buried lifeline facilities and foundations of structures. Since liquefaction-induced large ground displacements were firstly observed by using aerial photographs at the time of the 1983 Nihonkai-Chubu earthquake, a collaborative research has been conducted between U.S. and Japan in order to investigate the mechanism of the liquefaction-induced large ground displacements and to develop effective countermeasures. However, the 1995 Hyogoken-Nanbu earthquake again induced large ground displacements in a huge area of the reclaimed lands, and caused devastating damage to buried lifelines, and foundations of buildings and bridges.

---

1) Professor, The School of Science and Engineering, Waseda University.
2) Deputy Director, Earthquake Disaster Mitigation Division, Japan Engineering Consultants Co. Ltd.
3) Guest Researcher, Advanced Research Center for Science and Engineering, Waseda University.

The authors measured the liquefaction-induced ground displacements in reclaimed lands along the waterfront of Kobe area by an aerial survey using pre- and post-earthquake photographs. They also drew maps of the liquefaction-caused ground failures such as fissures and sand boils by interpreting post-earthquake aerial photos as well as by referring the results from field survey. Furthermore, they investigated the soil and geomorphological conditions of the areas where the liquefaction and large ground displacement occurred by collecting exiting borehole logs.

This paper introduces an outline of the measured ground displacement, ground failures and the related damage, and a summary of subsurface conditions. The whole result of the research is reported in Hamada et al.(1995).

## SUBSURFACE CONDITIONS

The survey area, which is located at the southern foot of the Rokko Mountains, is approximately 3 km wide in the north-south direction and 20 km long in the east-west direction. The Rokko Mountains, with elevations of more than 900 m in the eastern part and about 400 m in the western part, is comprised of granite formed by igneous activities in the Cretaceous period. The granite easily weathers and decomposes known as "Masado", which is characterized by low plasticity, low cohesion, high permeability and ease of erosion (JSSMFE ed., 1974).

Many fans have developed along the southern foot the Rokko Mountains. They are composed of coarse granite materials including sand, gravel and boulder. The materials were transported by rivers such as the Ikuta, Sumiyoshi, Ashiya and Shuku, which flow out from the Rokko Mountains.

The area between the fans and the south of National Highway (former shoreline) in Kobe and Ashiya is a relatively flat coastal plain, which simply consists of two geomorphological units, sand bar and back marsh. Sand bars developed along the coast, on which old city areas are located. The poorly drained area behind the bar is back marsh, composed of very soft clayey soils. The area south of Route 43 comprises filled areas.

Filling of Kobe Port began in the 1880's in earnest. Wharves such as Hyogo wharf and Piers Nos. 1 to 8 were built by 1940. From 1953, projects of cut and fill was performed in which mountains and hills including the Rokko Mountains and Awaji Island were systematically excavated and the material was dumped into the sea along the shoreline (Miyanaga and Takeyama, 1991). The filled areas include Mikage-hama, Uozaki-hama, Port Island and Rokko Island as shown in Table 1. Similar filling operations have been carried out in the cities of Ashiya and Nishinomiya (The third Port and Harbor Bureau, Ministry of Transport, 1967; Toyo Corporation, 1987; the Enterprise Agency of Hyogo Prefecture, 1995;

the Housing Public Corporation of Hyogo Prefecture, 1995), which are also shown in Table 1.

In the filled areas, soil improvements such as sand drain and pre-loading methods were applied for the areas where major structures were built to accelerate consolidation of the alluvial marine clay. Vibration compaction and sand compaction pile methods were applied in order to compact fill against liquefaction and differential settlement for the foundation ground where structures are supported by spread foundation. The areas where these soil improvements were performed include Port Island, Rokko Island and Minami-Ashiya-hama, second stage of Port Island, Ashiya-hama Seaside Town, Nishinomiya-hama and Koshien-hama (after the Enterprise Agency of Hyogo Prefecture, 1995).

On the basis of existing borehole data (e.g. Kobe City, 1980), 37 sections across filled areas were developed to determine subsurface conditions (Hamada et al. 1995). Typical soil profiles among them are shown in Fig. 1.

The geology of the reclaimed areas is essentially fill (F) overlying soft Holocene marine clay (Ac) which, in turn, rests on a series of Pleistocene deposits: alternate layers of dense sand and stiff clays (Dsc), stiff clay (Dc) and dense gravel (Dg).

Fill (F) is mainly composed of decomposed granite, excavated from the Rokko Mountains and Awaji Island near the epicenter and Pliocene deposits of mudstone, sandstone and conglomerate of Kobe Group from western Kobe, partially of Pleistocene marine clay and gravel of Osaka Group and dredged sands. The fill also contains rubble and refuse from construction sites.

Thickness of the fill in the survey area varies from 5 m to 25 m. Generally it increases toward the offing. Soil type of fill is sand and gravel with clay containing boulders of diameter 30-60 cm. The diameter of the gravel ranges from 2 to 60 mm and sand is mainly decomposed granite of medium to coarse grades. On the whole, the SPT N-value ranges between 5 to 20 but sometimes it exceeds 50. Unit weight of decomposed granite is about 2.0 tf/m$^3$ and that of the sandy soil of Kobe Group is 1.8 tf/m$^3$, respectively.

There is no doubt that fills liquefied during the current earthquake judging from the similarity in grain size distribution and color of fill and ejected sands. However, it was not clear as to whether all the fills below water level liquefied or not.

In addition, according to an electric pore pressure transducer installed at a depth of 39 m within the alluvial sand layer below the center of the second stage of Port Island, an excess pore pressure which built up to approximately 50 percent of the initial effective overburden pressure (17 m head of water) was recorded at 6 a.m., about 13 minutes after the earthquake

(Tanimoto, 1995).

In past earthquakes, estimation of the liquefied layer was made using the simplified procedures such as that outlined in the Japanese Highway Bridge Code and applying the peak observed acceleration during the earthquake. The results of the estimation compared well with the actual behavior of the ground and structures. However, the peak accelerations observed during the present earthquake were too large to apply the procedure described in the above code. The grain size characteristics were also beyond the limits of applicability of the code. Therefore an estimation of the liquefied layers was not made for the sections shown in Fig.1.

## SURFACE GROUND FAILURES

Identifications of the locations of the soil liquefaction had been carried out by field survey during past earthquakes. However, it was impossible to determine the liquefaction areas using such a method, because the region to be investigated was too large and there were many areas that were inaccessible. Also, in the case of such a field survey, there is the possibility of variations in individual judgment or variations due to the time when the survey is carried out.

The authors identified the locations of the liquefaction-caused ground failures based on photographic interpretations and drew maps of sand boils, sand volcano and fissures. The degree of resolution of the survey of ground failures depends on scales of the aerial photographs and is estimated to be around 15 cm. It should be noted that there are places where elevated roads or trees caused a visual obstruction for evaluation.

The survey based on these aerial photographs was carried out along the coastal region extending from Suma-ku, Kobe City, to the Mukogawa River that forms the border between Nishinomiya and Amagasaki cities.

It is fact that not all cases of surface ground failures have been confirmed by this evaluation of aerial photographs. Indeed, as mentioned previously, there are many places that were hidden by trees or elevated roads, and only instances of sand boil that were confirmed with certainty were plotted. As a result, there are possibly a large number of other locations or areas where liquefaction occurred. On the other hand, at Port Island and at Rokko Island, considerable sand boiled and flowed out, resulting in very wide sand boil deposits on these islands. Although these areas were identified as sand boil areas, it should be noted that this does not necessarily indicate that liquefaction occurred over the entirety of these areas.

Figure 2 shows the region covered by the survey of surface ground failures. The results of the survey were plotted on the 48 maps (Hamada, et al. 1995).

The aerial photographs used in the photographic interpretation were taken on the following dates. The earthquake occurred on January 17, 1995.

| | |
|---|---|
| ① January 18, 1995 | From Suma-ku to Hyogo-ku in Kobe |
| ② January 20, 1995 | From Kobe City Center to Rokko Island |
| ③ January 21, 1995 | East of Rokko Island |

The altitude was about 1,300 m in the case of photographs ① and ②, and about 1,800 m for photographs ③. In all cases the scale was 1/8,500. A total of around 120 photographs were used in this survey.

The accuracy of the photographic interpretation of ground failures cannot be expressed quantitatively as in the cases of aerial photogrammetry. However, in the case of ground fissures, it is believed that cracks of widths exceeding around 15 cm could be discerned from of the scale of the aerial photographs(1/8,500). The accuracy of the displacement of the sea walls fell to around 50 cm depending on the accuracy of the coordinates of standard control points used in the survey.

As previously stated, cases of sand boil that could not be identified with certainty were removed. Nevertheless, there still remains the possibility that there are cases where, due to existence of water on the ground surface or for some other reasons, what appeared to be sand boil in the photographs was mistakenly identified. However, the discernment ratio for cases of sand boil (number of sand boil identifications/the actual number of sand boil cases), including those not photographed due to obstruction by structures or trees as well as those overlooked, can be considered lower than for ground fissures. During the course of the field survey, there were many cases where sand boils had occurred depositing gray sand on gray road, most of these cases were impossible to discern.

The results of the photographic interpretation of surface ground failures from the aerial photographs was originally plotted on 1/2,500 scale maps, and was reduced to 1/4,000 scale in Hamada et al. (1995).

Figure 2 shows an outline of the surface ground failures in the whole region surveyed. In the figure, the old coastline based on the topographical maps (Geographical Survey Institute) made during 1,908~1,910s is also shown. It was found that, in general, ground failures occurred in the reclaimed area, and were considerable in the southern part (newly reclaimed area).

The surface ground failures in Port Island, Rokko Island, Uozaki-hama and Ashiya-hama are shown in Figs. 3 to 6 as typical examples. From a detailed examination of the reclaimed

land, for examples, Port Island and Rokko Island, difference can be seen in the ground failures occurring according to the area within the island. In the case of both islands, few ground failures occurred in the areas where city development has been carried out. In the case of Rokko Island, while extensive disruption occurred in the north of the island, disruption in the south (excepting the area near the sea wall) was considerably less. There is a necessity to make detailed geological and geomorphological studies of such characteristics including the materials used for the fill, methods of soil improvements, the thickness of the filled layer and elevation of ground surface.

Ground failures have also occurred at various points in the northern part of the old coastline as shown in Fig. 2. It should be noted that occurrence of soil liquefaction was confirmed at not all points by field survey. Future investigations are necessary, including on-site interviews, and studies of the old topography, to determine the causes of ground failures.

## LIQUEFACTION-INDUCED GROUND DISPLACEMENT

Liquefaction-induced ground displacements were measured in the two manmade islands (Port and Rokko Islands), and reclaimed lands in Kobe, and the neighboring cities.

Two sets of aerial photographs, which were taken in the same area before and after the earthquake, are necessary for measurement of ground displacements. The following sets of aerial photographs were used for measurement:

| | | |
|---|---|---|
| Pre-earthquake, Scale | : | 1/12,500 |
| Date | : | May 1990, May 1993 and May 1994 |
| Post-earthquake, Scale | : | 1/8,500 |
| Date | : | Jan. (18th~21st .) 1995 |

Three dimensional coordinates before as well as after the earthquake were measured on objects fixed on ground surface such as manholes and corners of drainage channels, and/or of corners of roofs of reportedly un-damaged structures. The liquefaction-induced ground displacements were obtained by subtracting coordinates before the earthquake from ones after the earthquake.

The accuracy of each aerial survey before and after the earthquake depends on reduction scales of the aerial photographs, human errors in reading the coordinates etc. The accuracy of aerial survey before the earthquake was estimated as $\pm 24$ cm in the horizontal and $\pm 27$ cm in the vertical, while it was estimated as $\pm 23$ cm in the horizontal and $\pm 46$ cm in the vertical after the earthquake. An attention should be paid to that these accuracies were estimated as a standard variation of the residual errors between the coordinates of the standard control points determined from on-ground surveys and the ones from the aerial survey. The

maximum error in this measurement is ±56 cm in the horizontal and ±54 cm in the vertical before the earthquake, while ±84 cm in the horizontal and ±98 cm in the vertical after the earthquake. Therefore, it should be noted that errors with such magnitude can be occurred at some observation points. However, the accuracy of the surveys after the earthquake can be improved, if the coordinates of the standard control points will be measured with higher accuracy in future.

The accuracy of liquefaction-induced ground displacements is given as a root-mean square of the accuracies of those before and after the earthquake, and is estimated as ±33 cm in the horizontal and ±53 cm in the vertical.

Relative displacements between two observation points, namely ground strains are much important to investigate failure process of buried pipelines. The accuracy of relative displacements does not depend on the accuracies of the coordinates of the standard control points, but on reduction scales of the aerial photographs. The accuracy of the relative displacement (in the horizontal direction) is $7.6\times10^{-6}$ m before the earthquake and $12.8\times10^{-6}$ m after the earthquake in the aerial photos' scale. The accuracies of the relative displacement before and after the earthquake are estimated as $7.6\times10^{-6}\times12{,}500 = 0.09$ m and $12.8\times10^{-6}\times8{,}500 = 0.11$ m, respectively. Finally, the accuracy of the relative displacement is estimated to be 14 cm as a root mean square of the above two standard variations.

The area where the ground displacements were measured is most of the reclaimed land shown in Fig.2. The whole result of the measurement is included in Hamada et al. (1995). In this report, the authors show in some typical examples of the ground displacements and their related damage to burried pipelines and foundations.

Figure 7 shows the ground displacements of the northern part of the Rokko Island where suffered severe liquefaction. The sea wall along the north end of the island moved toward the sea at maximum 3.5 m, and largely subsided about 2.0 m. At the Point ① in the figure a simply supported steel girder of the Port Liner bridge dropped from the pier as shown in Photo. 1, because the pier moved toward the sea due to the large displacement of the surrounding ground. According to the on-ground survey which was conducted by Kobe city after the earthquake, the top of the concrete caisson of the foundation displaced about 80 cm toward the sea.

It is noteworthy that the ground about 100 m far from the sea wall also moved toward the sea with a magnitude of about 1 m. It can be seen that a large movement of the sea wall affected a wide area behind it because of the liquid behavior of the liquefied soil.

The soil condition in this area is shown in Fig.1 as a part of the soil profile cross section G-G'.

The filled soil with a thickness of about 15 m is considered to be liquefied. The ground surface slightly inclined toward the Rokko Bridge (to the north), which coincided with the direction of the ground displacements.

Figure 8 shows the ground displacements in the north area of the Port Island. The quay wall line moved toward the north with a maximum magnitude of about 4m, and also largely subsided. At Point ② in the figure, the concrete pier of Kobe Bridge slightly inclined towards the sea due to the movement of the surrounding ground, as shown in Photo. 2. It is reported that the pier was supported on pile foundations the tips of which reached into a firm soil layer of Pleistocene age.

A welded steel pipe with a diameter of 60cm for the water trunk line was raptured at point ③ in the figure as shown Photo 3. It was reported that a heat affected zone by the welding was ruptured due to a large ground strain caused by the liquefaction. Furthermore, at Points ④ and ⑤, concrete piles were vertically broken at the top of the pile as shown in Photos. 4 and 5, due to a excessive bending moment caused by large ground displacements. It should be noted that the building at Point ⑤ located about 100 far the sea wall, but the foundation piles was also broken due to the ground displacement.

The soil condition in this area is shown in Fig. 1 as a part of the soil profile cross section E-E'. The filled soil with a thickness of about 10 m is also considered to be liquefied.

Figure 9 shows the ground displacement along the Pier No. 4 of the Kobe Wharf. The ground spread towards the sea at a maximum of about 3.0 m. At Point ⑥, a two-stories steel bridge girder dropped due to a large movement of the pier, as shown in Photo. 6. According to the aerial survey, the end of the non-collapsed girder moved about 90 cm toward the sea and this movement was considered as the direct cause of the fall of the girders. Along the Pier No.4, a concrete common conduit with a cross dimension of 4.0 m×3.0 m was buried, but it was reported that the concrete at the joints were slightly separated, and the inside of the conduit was flooded. Furthermore, it was also reported that a concrete caisson for the foundation of the Kobe Bridge moved toward the sea and inclined due to the ground movement.

Severe liquefaction was also occurred in the reclaimed land in the mainland side such as Uozaki, Fukae etc., and resulted in damage to buried pipelines and buildings. Figure 10 shows the measured ground displacements in Uozaki-hama, where a sewage plant was extensively damaged due to liquefaction and the ground displacements. Along the canal in the north of the plant, both banks moved toward the water 1~2 m. Photo. 7 shows the situation at Point ⑦ in Fig.10 where the foundation of a stair of a bridge over the canal displaced about 2.0 m due to the movement of the surrounding ground. In the sewage plant it was reported that the concrete piles of the buildings were broken and the concrete conduit was largely separated due to the ground movement. The soil condition in this area is shown

in Fig. 1 as a part of D-D' section. The filled soil as thick as more than 10 m is considered to be liquefied.

Figure 11 also shows an example of the large ground displacement in the reclaimed area in the mainland side. The both bank of the Miya River in Asiya-hama moved towards the river center about 1~2 m. Photo. 8 shows that a steel girder of a bridge over the river overlays the road on the river bank at Point ⑧ in Fig.11. This suggests that the river bank moved toward the water. Photo. 9 shows the river bank after the earthquake and it is noteworthy that the line of river bank keeps mostly straight even after the movement of about 2 m and the river bank did not collapsed. It can be guessed that the river bank moved on the underlying liquefied soil, which flowed toward the river.

## CONCLUDING REMARKS

The Hyogoken-Nanbu earthquake raised tasks about earthquake hazard prevention in urban areas. One of the most urgent tasks is how to assess liquefaction-induced large ground displacements and how to prevent their caused damage. Research into the mechanisms of such ground displacements and associated earthquake resistant design should be promoted strongly, never to repeat a disaster such as the Hyogoken-Nanbu earthquake. For this purpose, The authors conducted a survey of the liquefaction-induced ground displacements in the reclaimed land in Kobe and its neighboring cites and developed maps of the liquefaction-induced ground failures such as sand boils and fissures. Furthermore, the subsurface conditions of the liquefied area were investigated by collecting existing database for ground conditions.

After the Hyogoken-Nanbu earthquake, many committees were established by professional organizations to investigate the cause of damage to structures. The authors hope that this report can assist those investigations by providing fundamental database about ground displacements, ground failures, and subsurface conditions in the liquefied areas.

Earthquake engineering in Japan was initiated primarily through the tragic experience of the 1923 Great Kanto earthquake. Advancements in the earthquake engineering after the Kanto earthquake resulted in the construction of numerous infrastructures in Japan such high dams, large bridges and urban lifeline systems. However, the 1995 Hyogoken-Nanbu earthquake caused devastating damage in Kobe area, and exposed many deficiencies in the measures for earthquake disaster prevention and in the standards for the earthquake resistant design. Therefore, it is realized that earthquake engineering in Japan should be renewed by the experience of the earthquake.

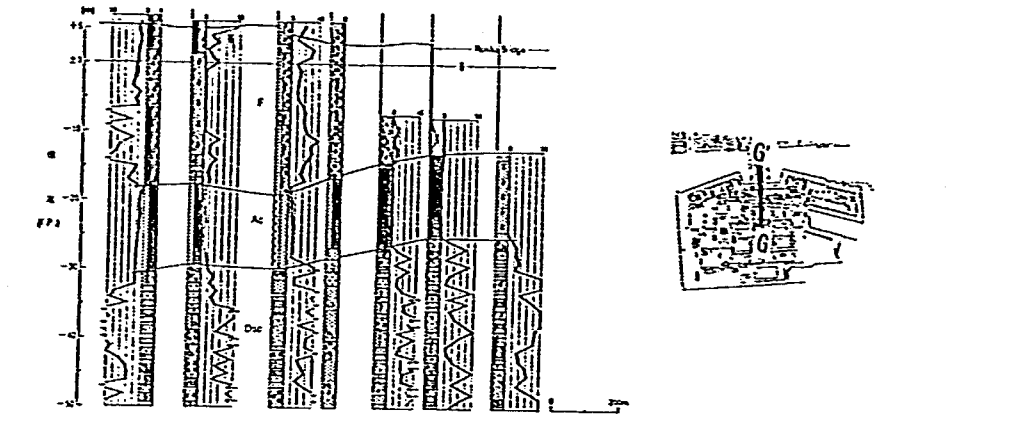
## REFERENCES


1. Hamada, H., Isoyama, R. and Wakamatsu, K. (1995): "The Hyogoken-Nanbu (Kobe) Earthquake, Liquefaction, Ground Displacement and Soil Condition in Hanshin Area", Association for Development of Earthquake Prediction, The School of Science and Engineering, Waseda University and Japan Engineering Consultants Co., Ltd.
2. Japanese Society of Soil Mechanics and Foundation Engineering (JSSMFE) ed. (1974): "Local Soils in Japan, "JSSMFE, pp.85-141 (in Japanese).
3. Kobe City (1980): "The Ground of Kobe", (in Japanese).
4. Miyanaga, S. and Takeyama, S. (1991): The History of the Reclamation in Kobe, Tsuchi-to-Kiso, JSSMFE, Vol.39, No.1, pp.42-45 (in Japanese).
5. Tanimoto, Y. (1995): Ground Failures Caused by the Hyogoken-nanbu Earthquake, "Special Lecture for the 30th Japan National Conference on Soil Mechanics and Foundation Engineering (in Japanese).
6. Private communication with The Enterprise Agency of Hyogo Prefecture (1995).
7. Private communication with The Housing Public Corporation (1995).
8. The Third Port and Harbor Bureau, Ministry of Transport (1967): "The Record on Construction of Maya Wharf", (in Japanese).
9. Toyo Corporation (1987): "The History of Naruo-Hama Project", (in Japanese).

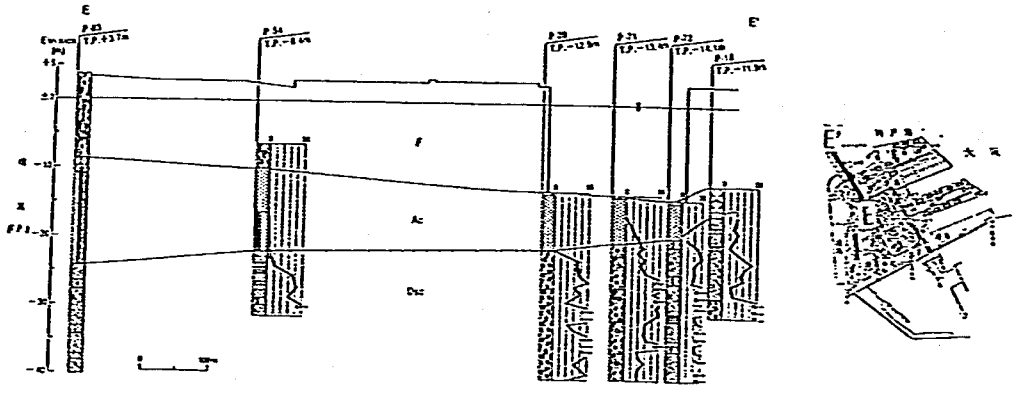
Table 1 Summary of Reclamation in Kobe, Ashiya and Nishinomiya

| | Area to be filled | Project organization | Work Period | Source of fill | Geology of fill |
|---|---|---|---|---|---|
| First Stage | Sotohama, Komagabayashi-minami | Kobe City | 1957-1967 | Suma Ward, Kobe | Rokko Granite*1 |
| | Karimojima | ditto | 1963-1968 | ditto | ditto |
| | Tohya-hama | ditto | 1960-1966 | Suma Ward, Kobe | ditto |
| | Nada-hama-higashi | ditto | 1953-1967 | Nada Ward, Kobe | ditto |
| | Mikage-hama, Sumiyoshi-hama | ditto | 1960-1968 | ditto | ditto |
| | Uozaki-hama | ditto | 1961-1968 | Higashi-Nada Ward, Kobe | ditto |
| | Fukae-hama | ditto | 1964-1970 | Suma Ward, Kobe | ditto |
| Second Stage | Port Island | ditto | 1966-1980 | ditto | ditto |
| | Rokko Island | ditto | 1972-1990 | Suma and Nishi Wards, Kobe | Rokko Granite, Kobe Group*2, Osaka Group*3 |
| | Port Island 2nd stage | ditto | 1986-1996 | Nishi Ward, Kobe | Kobe Group, Osaka Group |
| Maya Wharf | | Ministory of Transport | 1959-1967 | Nada Ward, Kobe Kobe Port | Rokko Granite Marine Sand |
| Ashiya-hama | | Hyogo Prefecture | 1969-1975 | Okayama Prefecture, Awaji Island | Marine sand Ryoke Granite*4 |
| Minami-Ashiya-hama | | Hyogo Prefecture | 1971-1996 | Awaji Island | Ryoke Granite |
| Nishinomiya-hama | | Hyogo Prefecture | 1971-1992 | ditto | ditto |
| Koshien-hama | | Hyogo Prefecture | 1971-1994 | ditto | ditto |
| Naruo-hama | | Private enterprise | 1967-1975 | ditto | ditto |

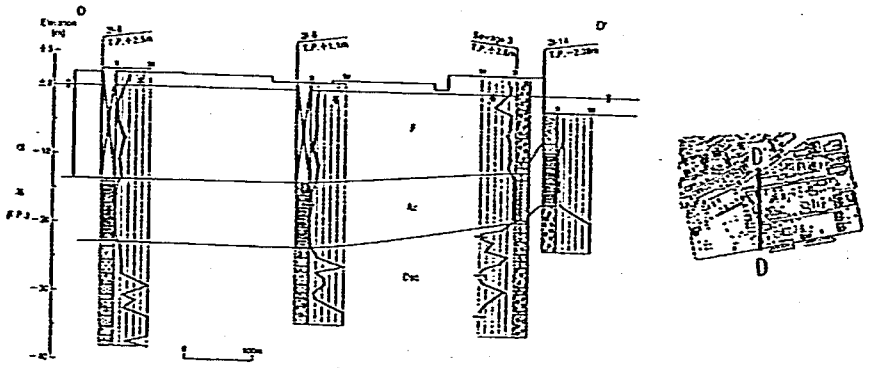
*1 : Granite including decomposed granite (Late Cretaceous)
*2 : Mainly consists of lacustrine mudstone, sandstone, and conglomerate embeded with intermediate layers of tuff (Miocene)
*3 : Mainly consists of marine clay embeded with intermediate layers of gravel and volcanic ash (Early Pleistocene)
*4 : Granite including decomposed granite (Early to Late Cretaceous)



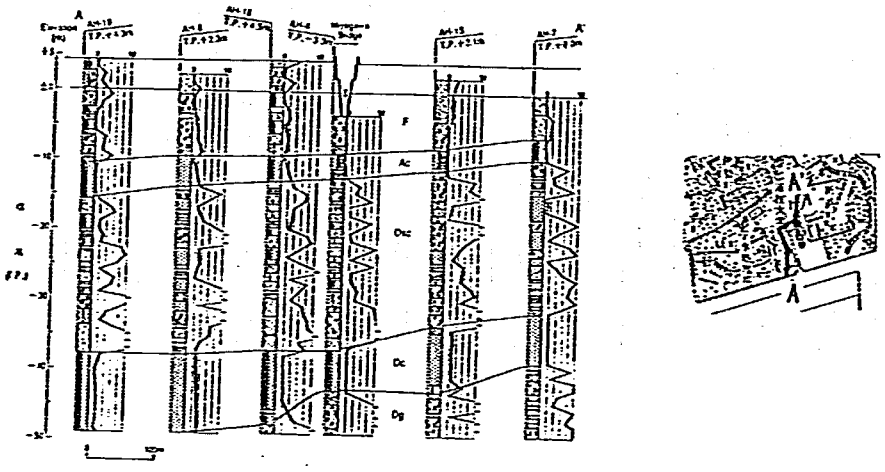

ROKKO ISLAND G-G'(South-North)




PORT ISLAND E-E'(South-North)




UOZAKI-HAMA D-D'(South-North)




ASHIYA-HAMA A-A'(South-North)

Fig.1 Typical Soil Profiles in Filled Area

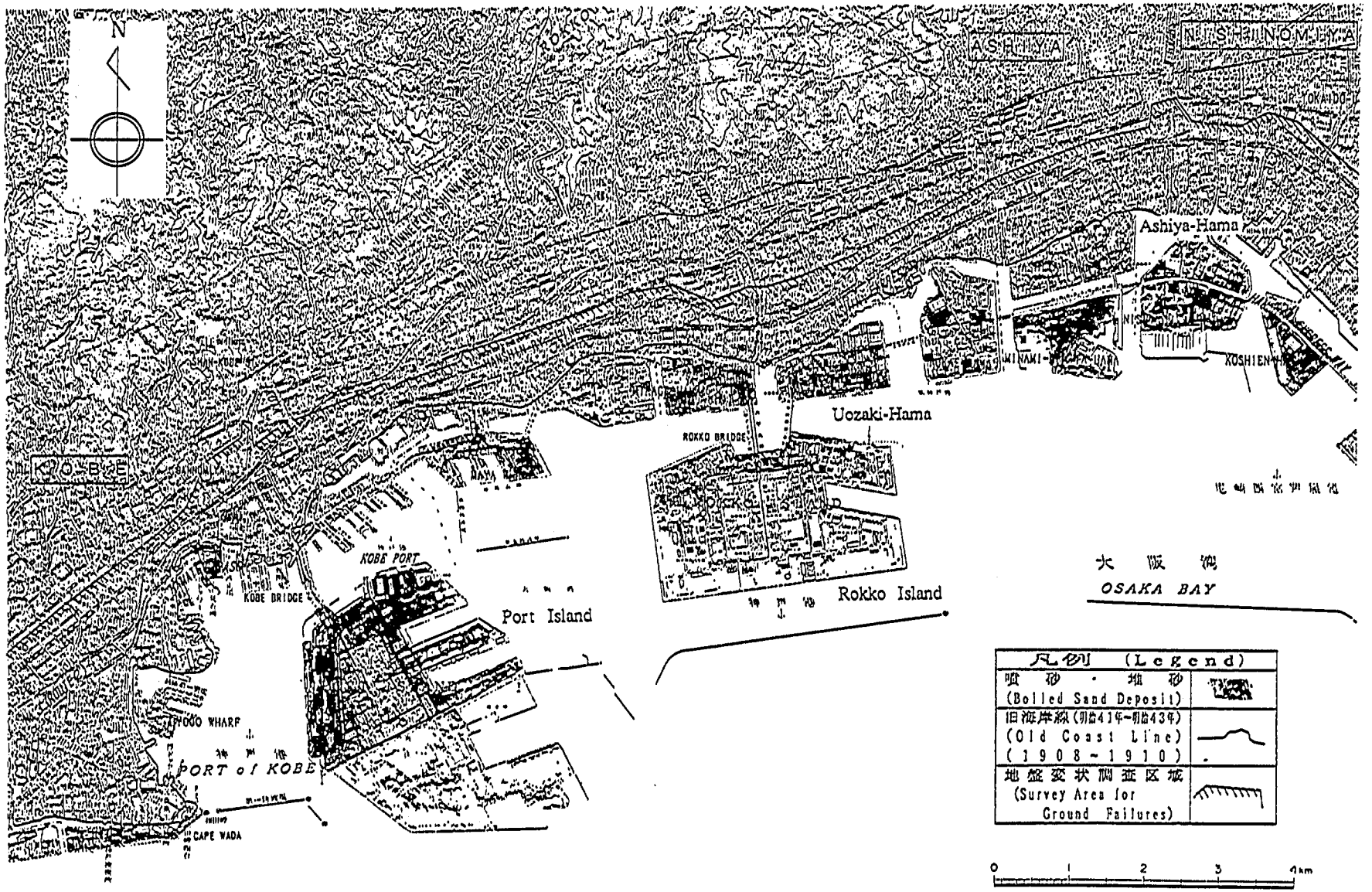



Fig.2 Survey Area for Surface Ground Failures and Outline of Surface Ground Failures

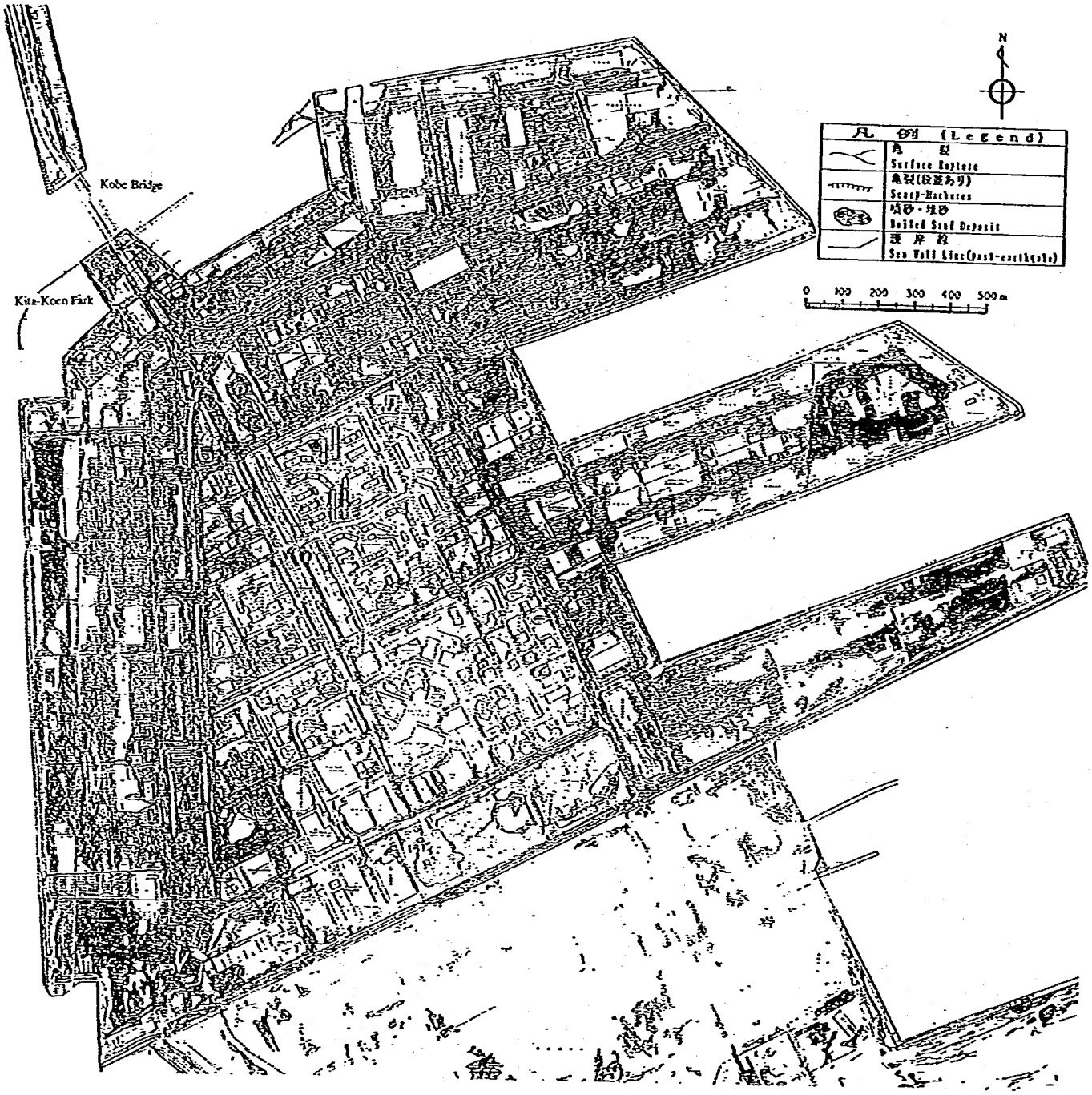



Fig.3 Surface Ground Failures in Port Island

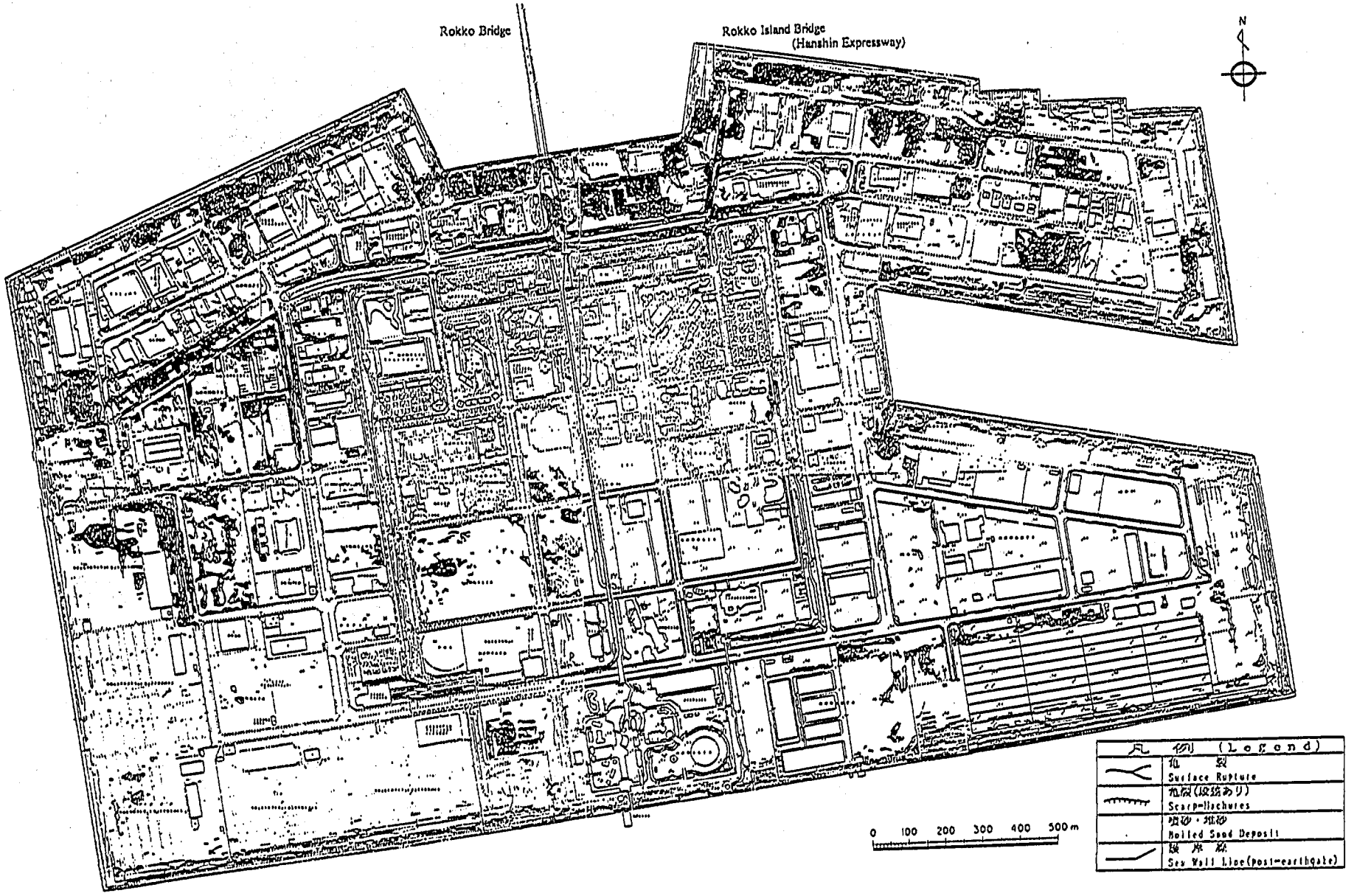



Fig.4 Surface Ground Failures in Rokko Island

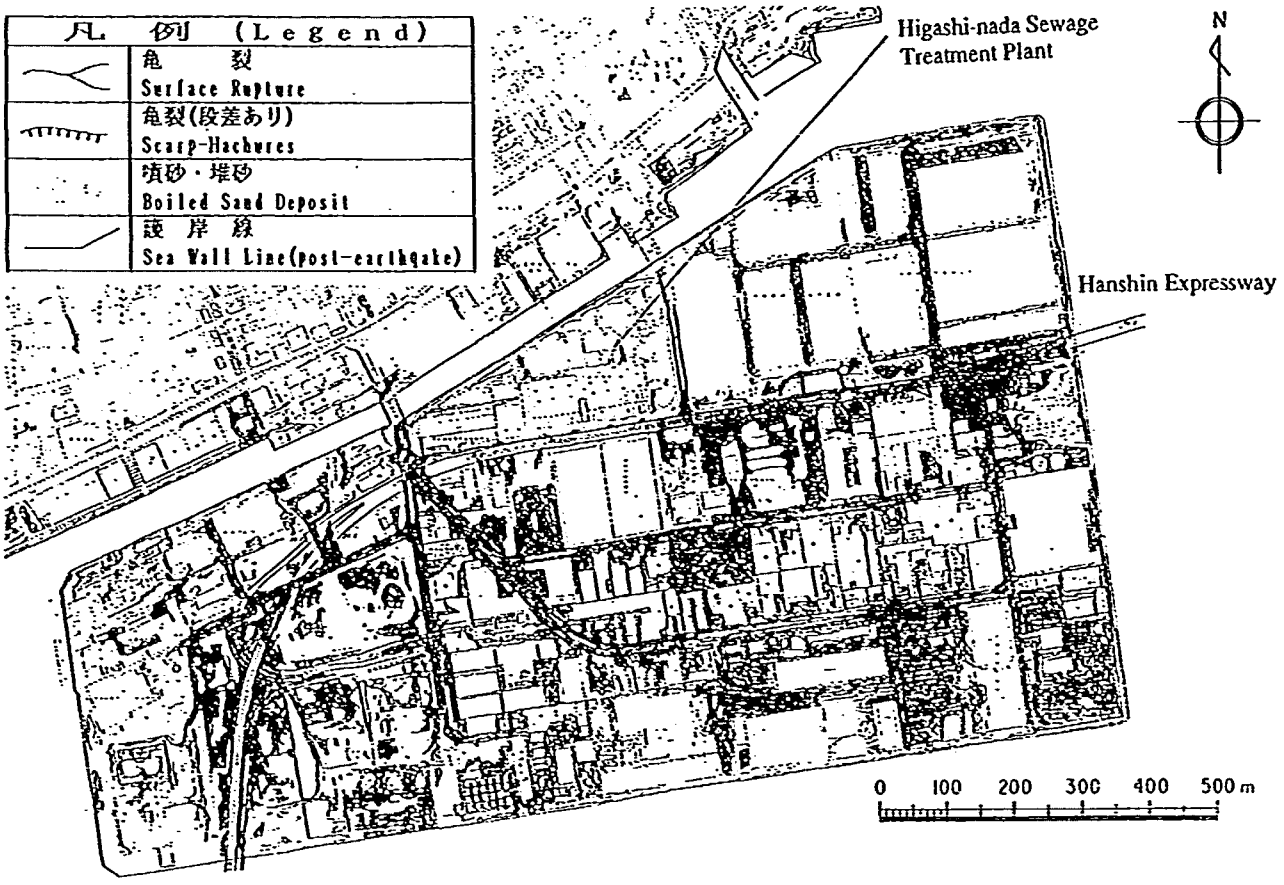



Fig.5 Surface Ground Failures in Uozaki-Hama

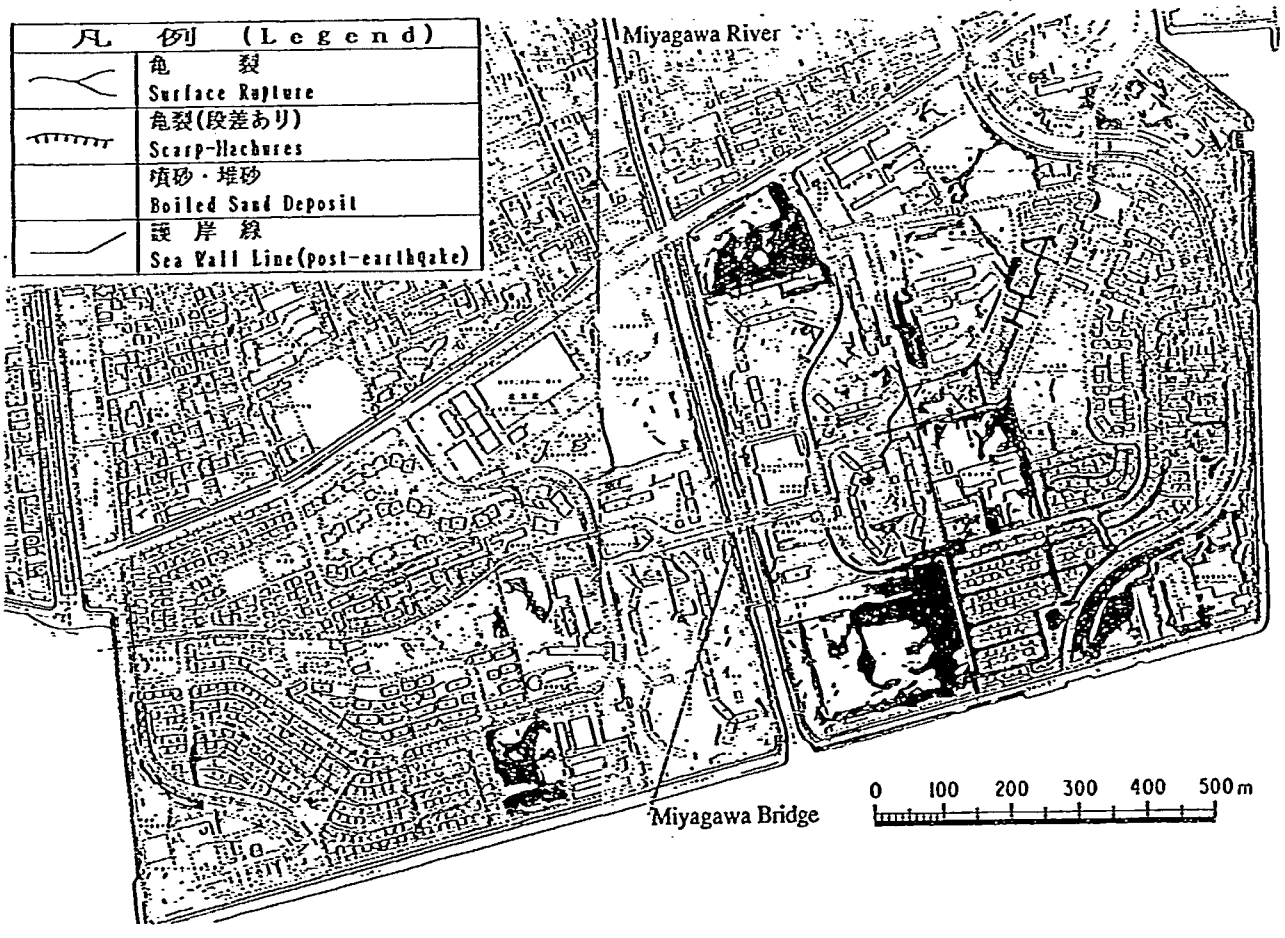



Fig.6 Surface Ground Failures in Ashiya-Hama

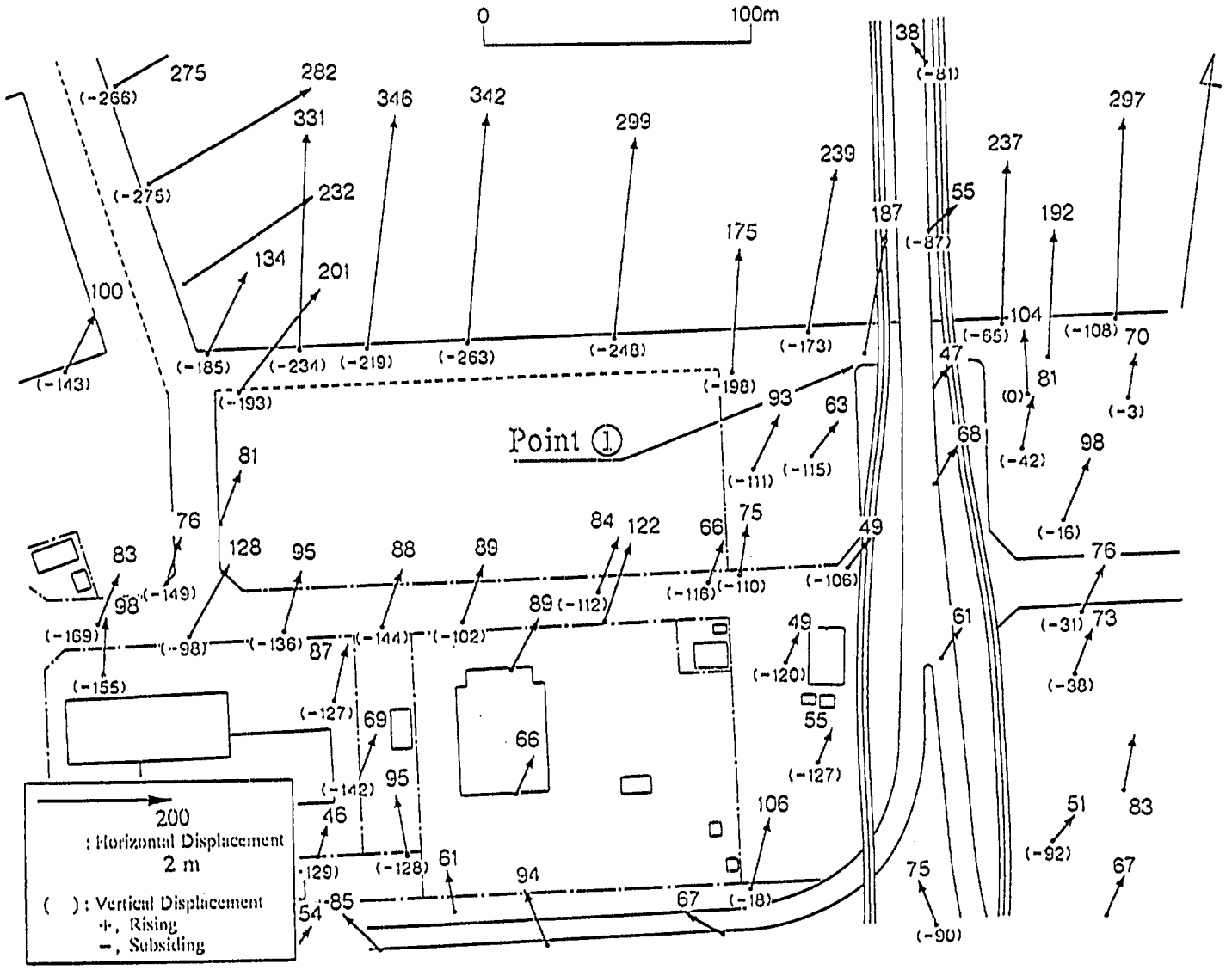



Fig.7 Liquefaction-Induced Ground Displacement in Northern Part of Rokko Island

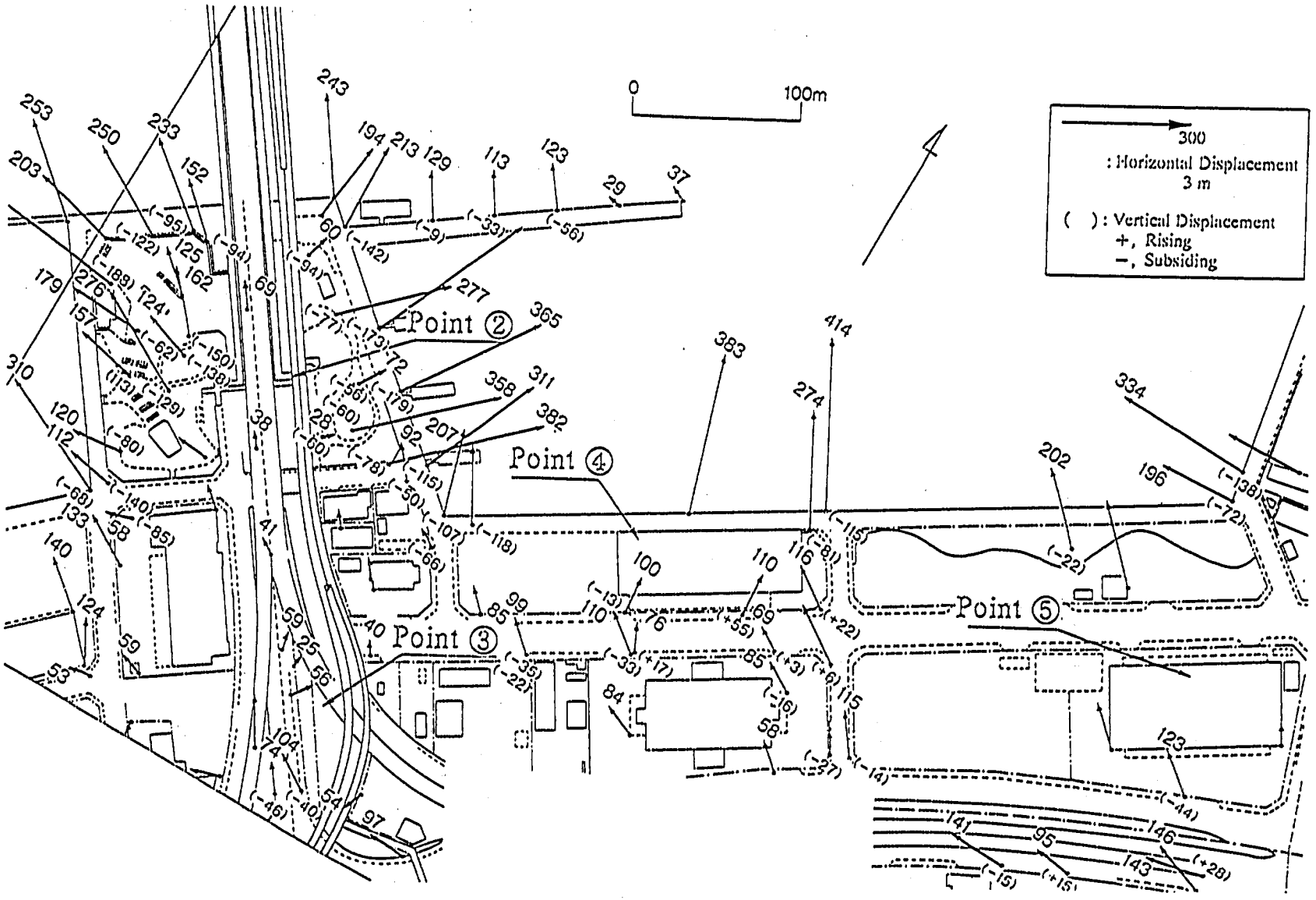



Fig.8 Liquefaction-Induced Ground Displacement at North Park of Port Island

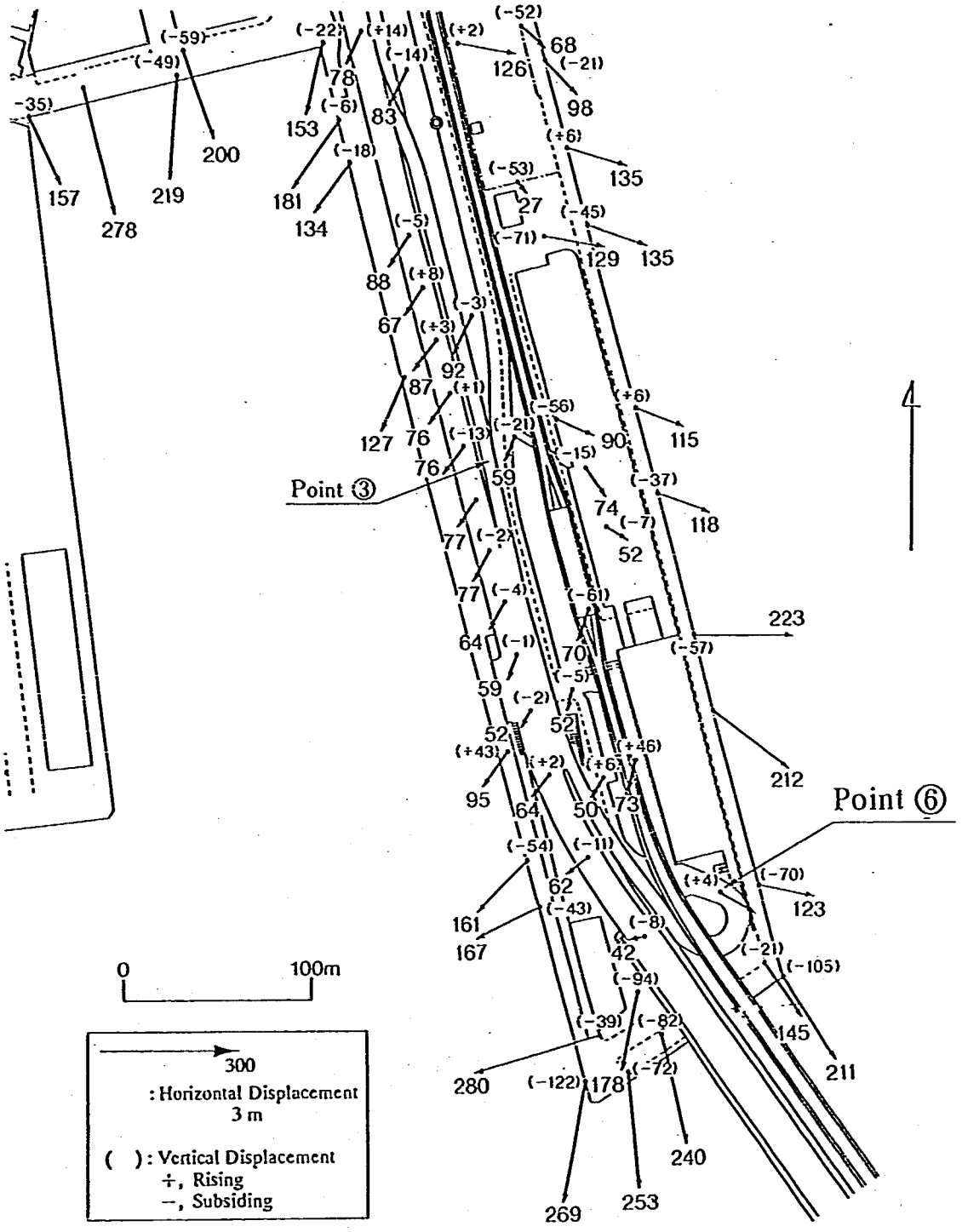



Fig.9 Liquefaction-Induced Ground Displacement at Pier No.4 of Kobe Wharf

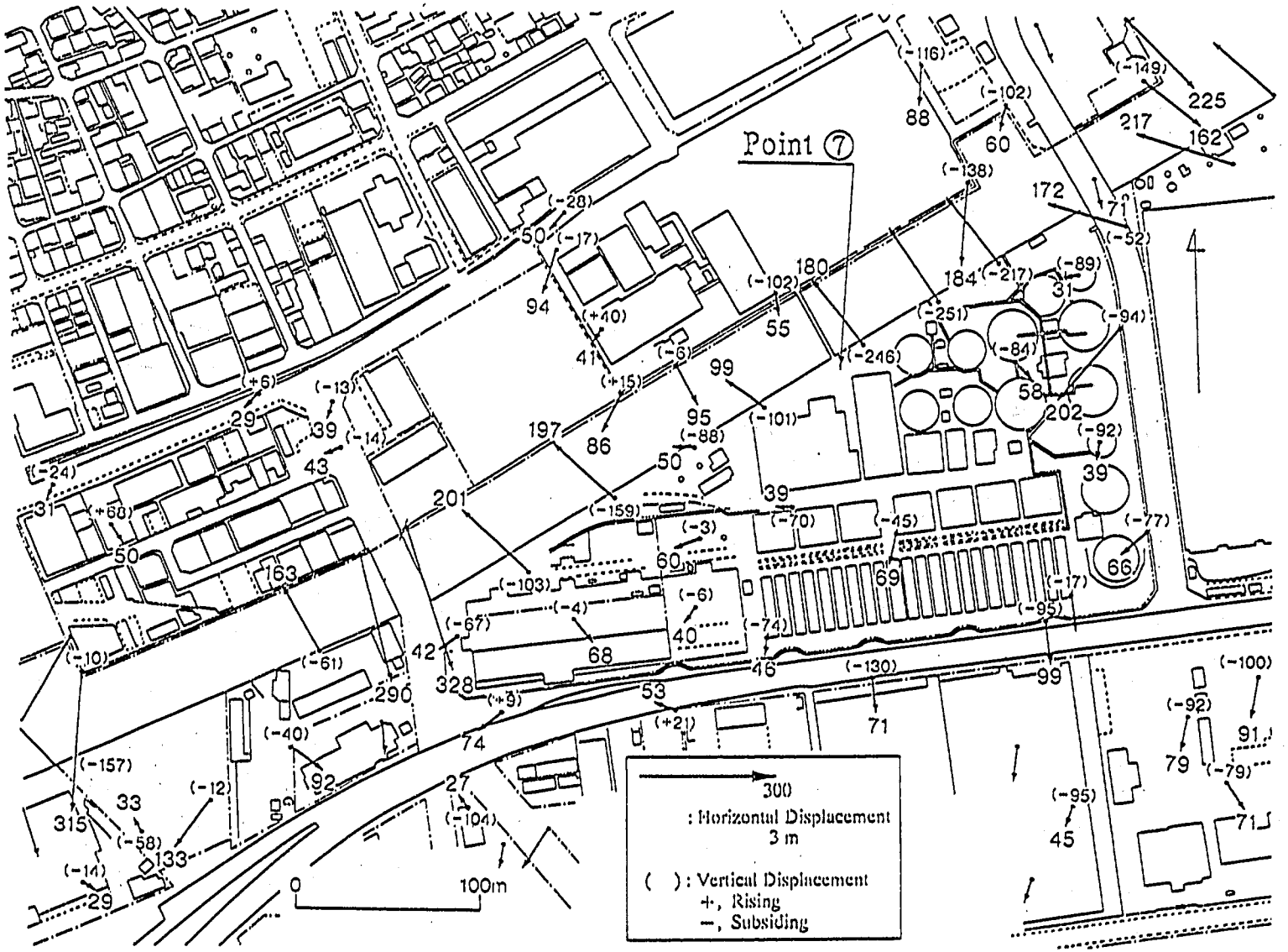



Fig.10 Liquefaction-Induced Ground Displacement at Higashi-Nada Sewage Plant in Uozaki-Hama

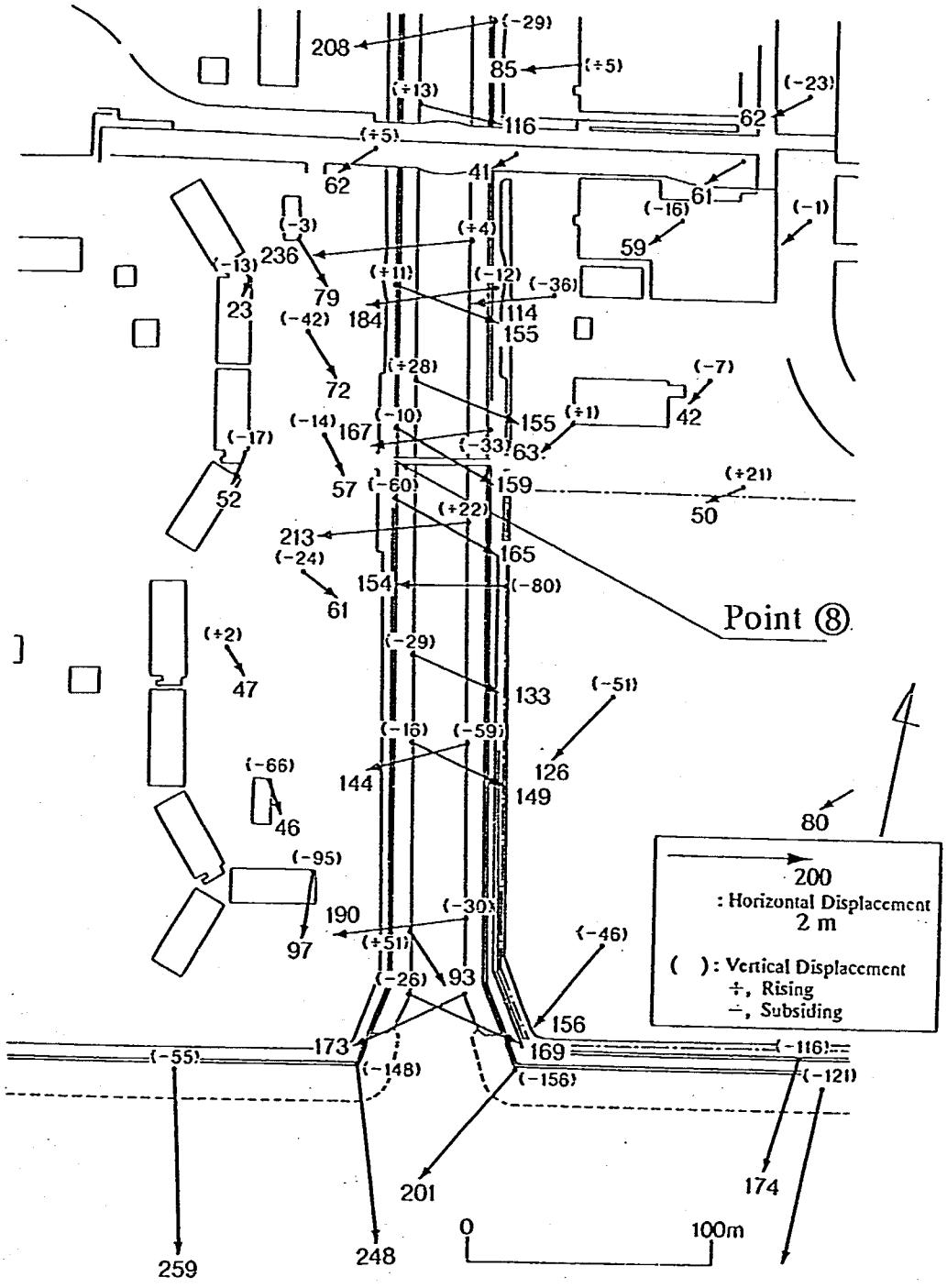



Fig. 11 Liquefaction-Induced Ground Displacement at Ashiya-Hama

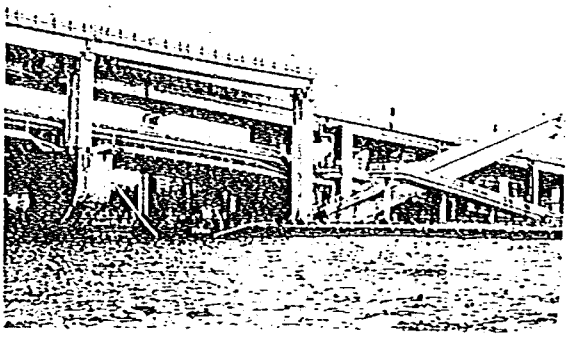


Photo. 1 Dropped Bridge Girder due to Ground Displacement (Point ① in Fig.7)



Photo. 2 Slightly Inclined Concrete Pier due to Ground Displacement (Point ② in Fig.8)

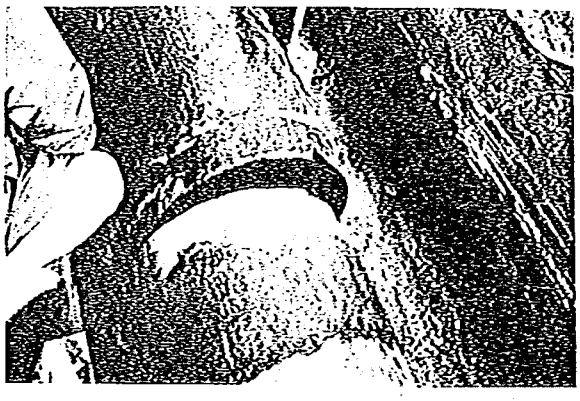


Photo. 3 Rupture of Welded Steel Pipe for Water Trunk Line (Point ③ in Fig.8)



Photo. 4 Breakage of Concrete Pile (Point ④ in Fig. 8)



Photo. 5 Breakage of Concrete Pile (Point ⑤ in Fig. 8)

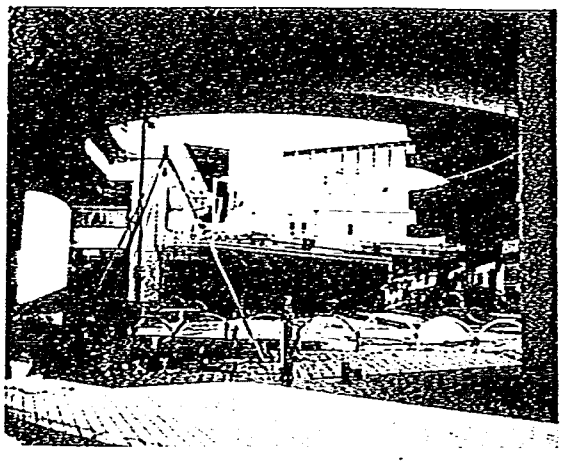


Photo. 6 Fall of Bridge Girder due to Ground Displacement (Point ⑥ in Fig.9)

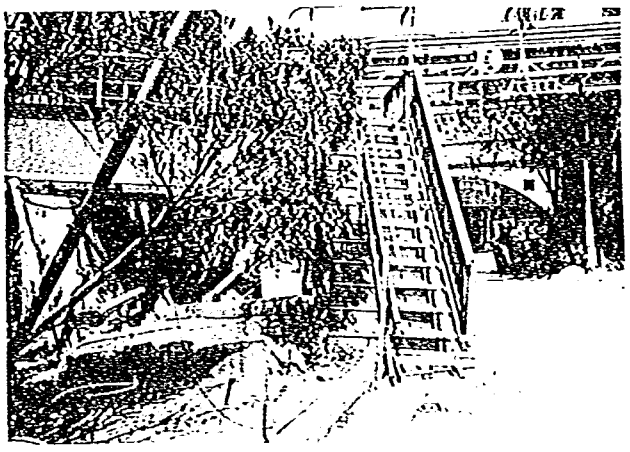


Photo. 7 Movement of Foundation for Stairs of Over-canal Bridge at Uozaki-hama (Point ② in Fig.10)

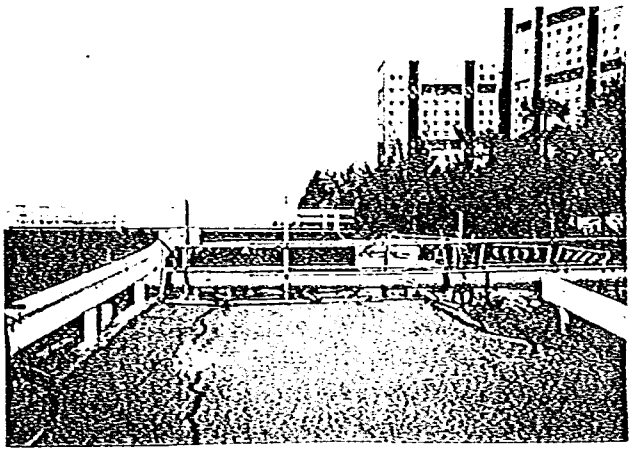


Photo. 8 Movement of River Bank at Ashiya-hama (Point ⑧ in Fig.11)

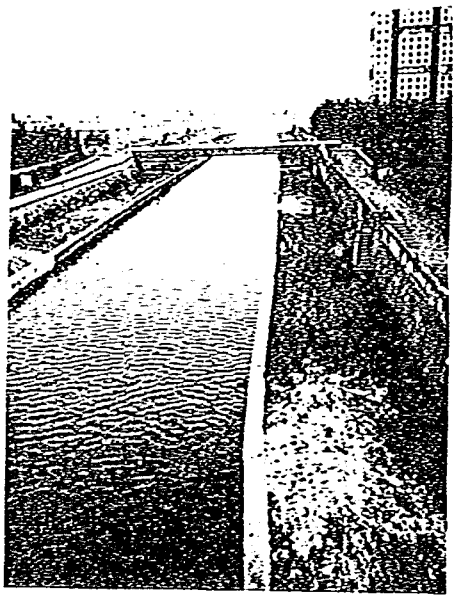


Photo. 9 River Bank after Ground Movement at Ashiya-hama

# Microfine Cement Grouting as a Countermeasure against Liquefaction

by

Masaaki Sano
Research Center, Onoda Chemico Corporation

Osamu Matsuo
Public Works Research Institute, Ministry of Construction

Junichi Koseki
Institute of Industrial Science, University of Tokyo

Masao Shimoda
Research Center, Onoda Chemico Corporation

## ABSTRACT

One-dimensional permeation test on microfine cement was carried out in the laboratory to investigate its permeative properties for use as an countermeasure against liquefaction of sandy ground. An unconfined compression test on its consolidated body was carried out in the laboratory to investigate the long-term durability and its strength retardation effect. And based on results of these labolatory test, three-dimensionsl permeation test was carried out in large scale experimental ground .

## INTRODUCTION

At the present time, a solution of liqid glass is used most commonly as a grouting material. However, it lack in durability. In order to establish a new grouting method as a countermeasure against liquefaction, the grouting material should have both a fine permeability into sandy ground and a long-term durability. This study confirms the permeative properties of microfine cement and the long-term durability properties of its consolidated body.

### 1. The permeative properties of the suspension of microfine cement

One-dimensional permeation grouting test was carried out to determine the kind of dispersing agent which produces the best permeability of the microfine cement suspension, the best water cement ratio of grout and the best mixture rate of the dispersing agent.

1. 1. Samples and test procedures

Microfine cement (specific gravity of 3.0,average grain size of 4μm, Blaine's specific surface area of 9000 $cm^2/g$ or over) was used as grout. Tohokuilica sand #7 (fine content of Fc= 2 to 5%, mean diameter $D_{50}$ = 0.1to 0.2mm) was used as sand sample.The grain size distsribution is shown in Figure 1[1].

The test specimen (length of 192cm, filter size of 4cm + 4cm) used in the one-dimensional permeation grouting test was made by putting air-dried sand sample intoan acrylic pipe with a length of 2m and an inside diameter of 50mm. Several layers were formed, each layer compacted by means of horizontal percussions so that a relative density Dr=50% was achieved. $CO_2$ was passed through the layers and the specimen was saturated by deaerated water. The test device is shown in Figure 2. Grout was filled from the bottom. The object of the test shown in Table 1 is to find the kind of dispersing agent with the best permeability. Some typical dispersing agents were mixed with grout, and grouting was done with a fixed pressure and water cement ratio, until the volume of grout flowing sufficiently diminished and no change in colortone could be seen (hereinafter referred to as critical grouting).

In Cases 1 to 10 of the test, refer to Table 2, grouting was done with a fixed pressure but with the water cement ratio W/C varied in the range from 250 to 3000% to find the best water cement ratio. Cases 11 to 14 were conducted with the mixture rate of dispersing agent varied in the range of B/C (the ratio of dispersing agent to grout) = 6 to 12%.

1. 2 Permeative properties of the grout

1) The best kind of dispersing agent

Figure 3 shows the test results obtained under the conditions depicted in Table 1. The best dispersing agents are found to be β-naphthalene and naphthalene in spite of their low mixture rates in comparison with others. They both passed through a 2m mold with a mixture .

2) The best water cement ratio

Figure 4 shows the results of Cases 1 to 10. As the water cement ratio gets larger,a longer consolidated body is formed but when the ratio exceeds W/C = 1000% and reaches W/C = 3000%, the length of the consolidated body decreases. A longer consolidated body can be formed if the dispersing agent mixture rate B/C is raised.

Figure 5 shows the relation between the grouting time and volume passing through a 2m mold for B/C 4% and 5%(herein after reffered to as grouting rout). These figures show that as water cement ratio gets larger, a larger volume of grout is filled, and the grouting rate does not drop even after a long period of grouting. Even when there is a variation in the mixture rate of the dispersing agent, grouting routes do not change as long as there is no change in the water cement ratio. From this, it is assumed that a grouting route is affected by the water cement ratio. Therefore, in fixed volume grouting, as the water cement ratio becomes larger, the grouting pressure remains low, which is desirable when considering the influences on adjacent structures.

When the ratio reaches over W/C = 1000%, the length of the consolidated body becomes smaller (Figure 4), but a monotonous increase in grouting volume is seen in Figure 5. It is presumed from this that cement particles may be restrained (probably somewhere around the grouting ports) by the filtration phenomenon of soil particles.

Figure 6 shows the measurement results of changes in the grout viscosity with the passage of time under the conditions shown in Table 3. From this figure, it can be seen that compared with the suspension composed of simple microfine cement, the viscosity of the suspension mixed with dispersing agent is 50% lower, and even 120 minutes later there is no rise in viscosity. The viscosity of the suspension with W/C= 1000% and with B/C= 5% is 3.5cp, which is very similar to the prime viscosity of 2.5cp of liquid glass grout. This is one of the factors proving the excellency of this suspension in permeability.

From the above mentioned length and permeative properties of a consolidated body and the change in viscosity over time, it can be said that the best water cement ratio should be around W/C = 1000%.

3) The best mixture rate of a dispersing agent

Figure 7 shows the test results obtained in Cases 4, 9 and 11 to 14 shown in Table 2, where W/C was fixed to 1000%. As the suspension passes through a 2m mold when the mixture rate rises over 3%, the data given in these figures are confined to the ones from the starting time to the time of passing through a 2m mold. When there is a change in the mixture rate of the dispersing agent, the grouting route does not change. However, as more amount of dispersing agent is mixed, the volume of the suspension needed to pass through is less, which indicates a better permeation effect.

The permeation effect can be discussed based on the filling ratio, which is foundby dividing the grouting volume by the void volume to be consolidated before grouting. The nearer this ratio is to 1 the better the permeation effect. Figure 8 shows the filling ratio obtained in Cases 4, 9, and 11 to 14. As more dispersing agent is mixed, the filling ratio is seen to reduce, and it reaches its lowermost limit at a mixture rate of 10%.

The best mixture rate of a dispersing agent is therefore about 10%.

## 2. The strength properties of a consolida-ted body using microfine cement suspension

As a pre-condition of any countermeasures against liquefaction is to secure enough strength and long-term durability so that the improved ground is not liquefied, strength tests with various mixing rates of adispersing agent were conducted.

### 2. 1. Test procedures

The test specimen (length of 23cm, filter size of 1cm + 1cm) used in the test was made by putting air-dried sand samples into an acrylic pipe with length of 25cm and inside diameter of 50mm. The samples were compacted by means of horizontal percussions so that the relative density Dr has a value equal to 50%, $CO_2$ was then passed through it,and deaerated water was used to saturat the test specimen. The testing device, sand sample, and

grout used in this test are the same as those used in the one-dimensional permeation test as shown in 2.1.

Table 4 shows the grouting conditions of the test specimen with various volumes of dispersing agents. The mold was removed after confirming the color (bluish green) which serves as an indicator of the degree of consolidation, and then it was cured in still water. The curing water was renewed once a month.

## 2. 2. strength properties of the consolidated body

Figure 9 shows the test results obtained under the grouting conditions shown in Table 4. Although the cases with mixture rates over 4% are sixty percent inferior in peak strength to the case in which the dispersing agent mixture rate is 1%, no deterioration in strength can beseen even after a curing of six months. There appeared to be no problem in long-term durability even when a dispersing agent was increased, and the target unconfined compression strength ($qu=1kgf/cm^2$) was sufficiently met.

Figure 10 shows the curing time necessary for the mold removal which was used for a long-term strength confirmation test. Manifestation of strength delayed with a rise in the mixture rate of a dispersing agent. The delay was especially large in the case of the grout with the dispersing agent mixture rates of over10%.

## 3. Injection experiment with large scale experimental ground container

Injection experiment with large scale experimental ground container was carried out to investigate three-dimensional permeation properties and the shape of consolidated bodies.

### 3.1. Preparation of experimental ground

TOHOKU silica sand #7 dried in air was fallen down from a certain height into a experimental ground of 4.00X3.55X4.20m to obtain uniform height of sand layer of 50 cm. This process was repeated 7 times and then this sand was saturated with water poured from the bottom of the ground. The weight in unit volume by measuring the height of sand after seven times' falling down of about 7 tons of sand was measured, and the ground thus obtained had relative density (Dr) of 48 %, coefficient permeability (k) of $7.1x10^{-3}$(cm/sec), porosity (n) of 48 %.

The experimental ground was surrounded with gravel layer for drainage and the wire netting having 75μm opening was placed between the gravel layer and experimental ground. Concrete having a thickness of 10 cm was placed on the ground. Pore water pressure meter, earth pressure meter and displacement meter were provided to measure the change of each value in the inner portion or at the surface portion of the ground during grouting. Figure 11 shows the position of each meter and the outline of the experimental ground.

### 3.2. Combination of grout material and the method for its injection

From the experimental result of one-dimensional permeation test, the material combination for permeating grout into experimental ground was determined as follows. W/C of 1,000 % and β-naphthalene type dispersing agent of 10% to the grout weight were used.

The grouting was performed from the center of experimental ground container at 10ℓ/min using double packer system until rapid change of injection pressure or blowoff of the suspension occurs.

### 3.3. The state and the result of grouting

The injection was stopped after 8 hr 55 min from the start as we could recognize the blowoff of the suspension from the side of upper portion. Total amount of grout injected was 5292 ℓ. During the injection, clear change was not be observed with respect to the earth pressure meters and displacement meters.

The changes of injection pressure and pore water pressure by pore water pressure meters placed at 50 cm horizontal interval during grouting are shown in Figures 12 and 13, respectively.

Figure 12 shows that at the start of grouting, the pressure rose to 2.0 kgf/cm$^2$, and was stabilized at 2.0 kgf/cm$^2$ until 200 min, then gradually increased until 300 min to about 3.0 kgf/cm$^2$, and maintained between 3.5 to 3.9 kfg/cm$^2$ until pressure dropped by blowing off.

Fig. 13 shows the clear change in pore water pressure measured at the position horizontally separated 50 cm from the grout inlet as described below. The pressure was stabilized at 0.02 kgf/cm$^2$ until 50 min, then increased to the peak of 0.11 kgf/cm$^2$ at 180 min and then gradually decreased. Such clear change was not recognized in other pore water pressure meters.

The pore water pressure was much lower than the injection pressure, and the displacement of the ground did not occur, which is desirable when considerating the influences on adjacent structures.

### 3.4. The shape of consolidated bodies

In order to confirm the shape of consolidated bodies, unsolidified sand was gradually taken off from the upper portion. The shape of the horizontal sections of the consolidated body at the depth interval of 25 cm from the upper portion of the body, the shape of its vertical sections from west to east and from north to south are respectively shown in Figures 14, 15 and 16.

Its maximum horizontal diameter was 2.3m and its maximum vertical diameter was 1.4m.

## 4. Summary

From our tests using Tohoku-Silica Sand #7, we were able to determine the best kind of dispersing agent ($\beta$-naphthalene, naphthal-ene), the best water cement ratio (around W/C=1000%) and the best mixture rate of a dispersing agent (around B/C=10%). We, also, found that there was no negative influence on the long-term durability even when there is a rise in the mixture rate of a dispersing agent.

When we performed the experimental injection using this combination grout in the experimental ground container, we could obtain consolidated body having horizontally elongated shape with maximum horizontal diameter of 2.3 m and maximum vertical diameter of 1.4m.

In the future we would like to confirm the permeation limit according to the changes in coefficient of permeability and fine grain content of ground which is to be improved, and the relation between the changes in coefficient of permeability and the shape of consolidated bodies.

This report summarizes the study carried out by the first author as a visitingresearcher in Soil Dynamics Division of the Public Works Research Institute in the Ministry of Construction during the period from April 1994 through March 1995.

## Referrences

1) The Japanese Society of Soil Mechanics and Foundation Engineering: Study on chemical grouting, from design to execution, p.3 1985.

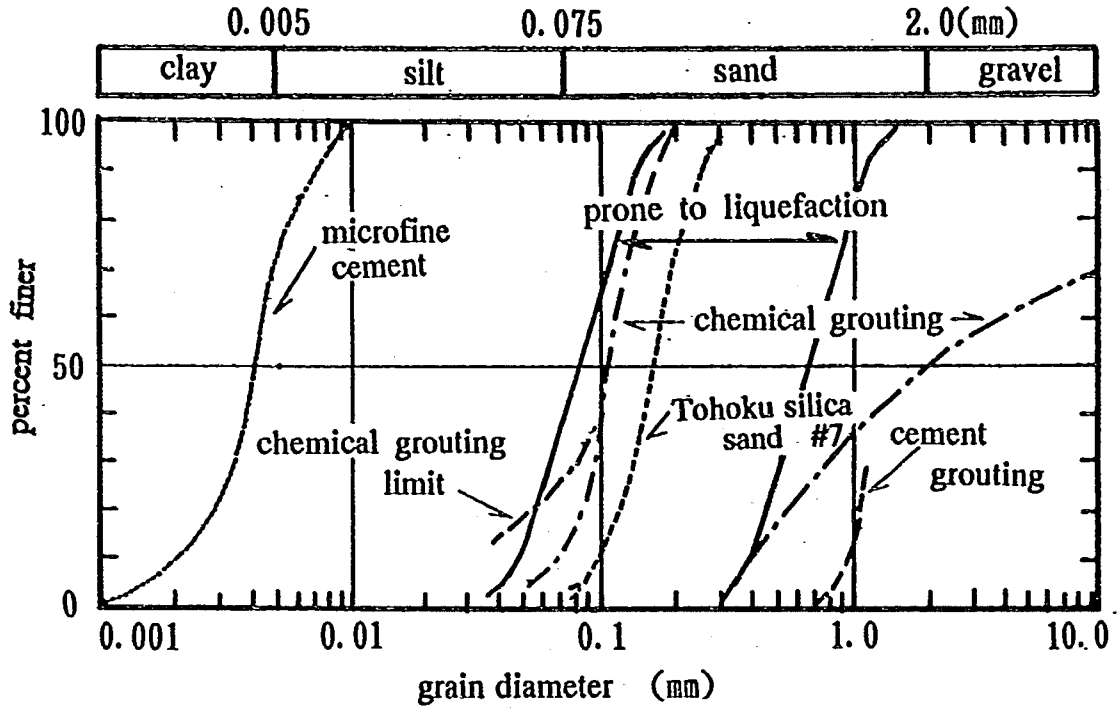



Figure 1 Grain size distribution

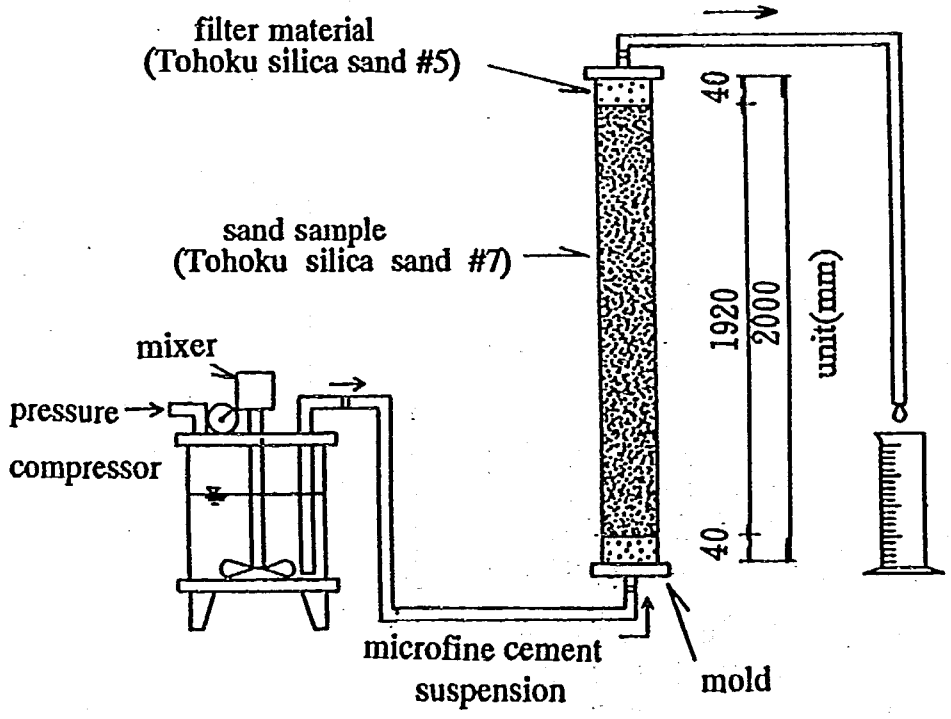



Figure 2 experimental device

Table 1 Condition 1 in one-dimensional permeation grouting

| dispersing agent | mixure rate of dispersing agent(%) | grouting pressure (kgf/cm²) | W/C (%) |
|---|---|---|---|
| polycarboxylic acids | 4 | 1.0 | 1000 |
| lignins | 4 | | |
| aromatics | 4 | | |
| β-naphthalene | 1, 2, 3 | | |
| naphthalene | 1, 2, 3 | | |

Table 2 Condition 2 in one-dimensional permeation grouting

| case | dispersing agent | mixure rate of dispersing agent(%) | grouting pressure (kgf/cm²) | W/C (%) |
|---|---|---|---|---|
| 1~5 | β-naphthalene | 4 | 1.0 | 250, 500, 750 1000, 3000 |
| 6~10 | | 5 | | 250, 500, 750 1000, 3000 |
| 11~14 | | 6, 8, 10, 12 | | 1000 |

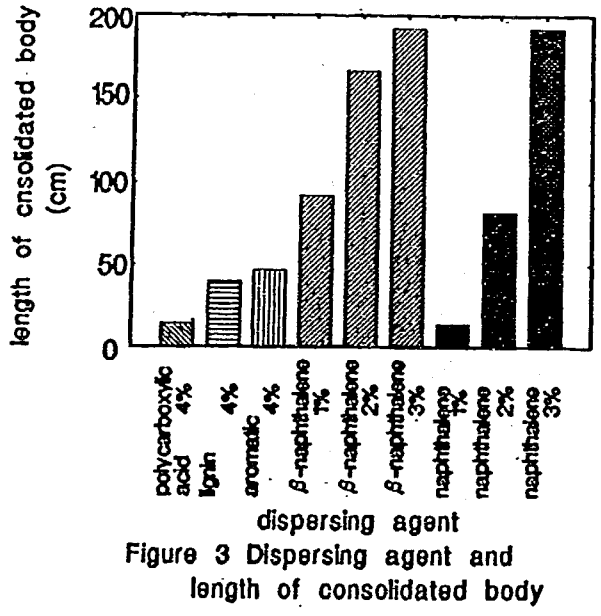



Figure 3 Dispersing agent and length of consolidated body

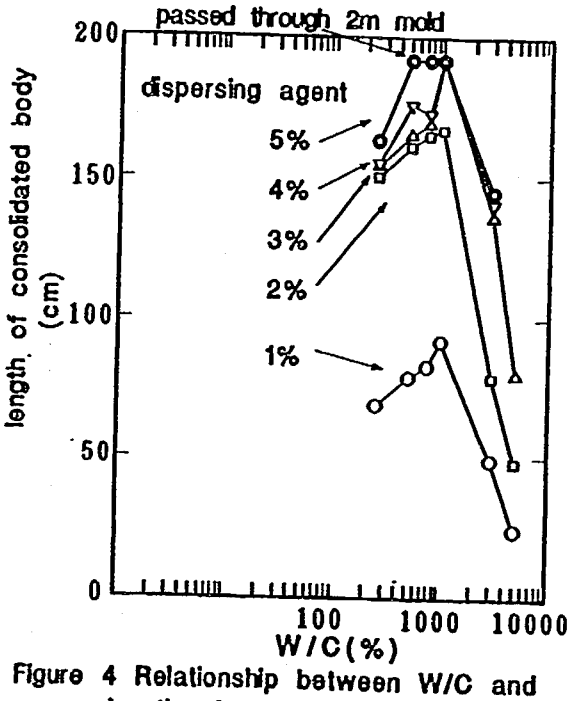



Figure 4 Relationship between W/C and length of cnsolidated body

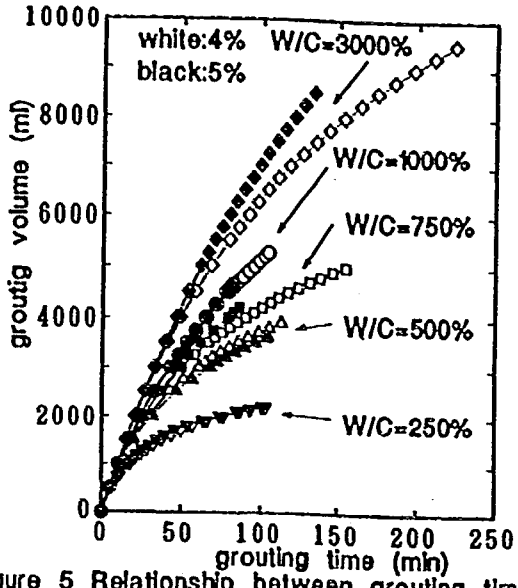



Figure 5 Relationship between grouting time and volume at the time of passing though a 2m mold (mixture rate of dispersing agent:4 and 5%)

Table 3 Mixing proporation of micro fine cement for viscosity measurement

| dispersing agent | mixure rate of dispersing agent(%) | W/C (%) |
|---|---|---|
| β-naphthalene | 0, 5 | 1000 |
| | 0, 3, 5 | 750 |
| | 0, 5 | 500 |

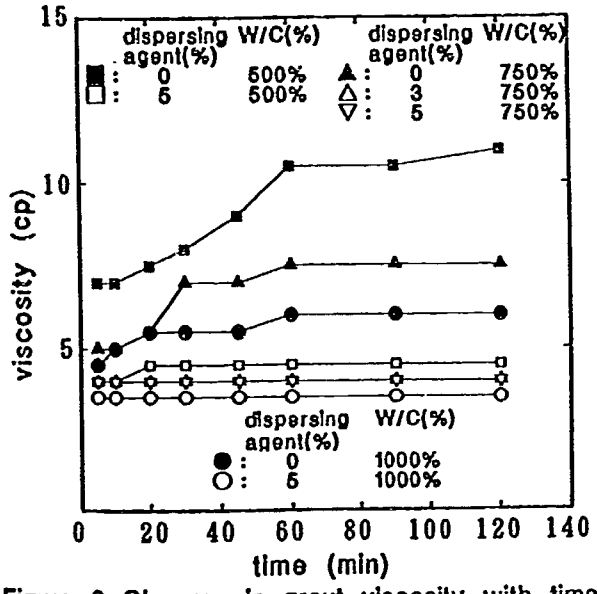



Figure 6 Changes in grout viscosity with time dispersing agent: β-naphthalene

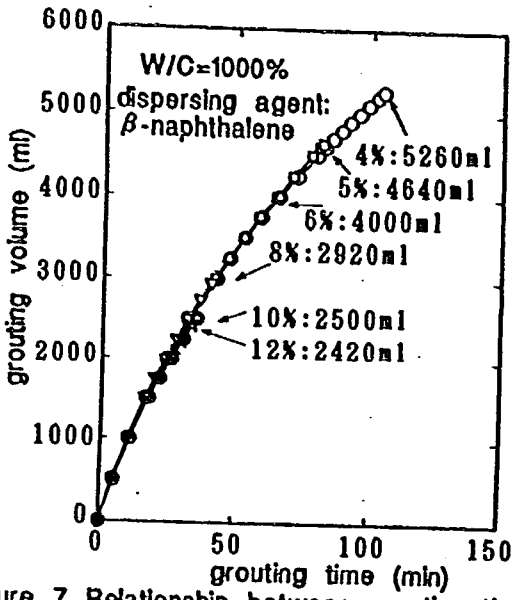



Figure 7 Relationship between grouting time and volume at the time of passing through a 2m mold (W/C=1000%)

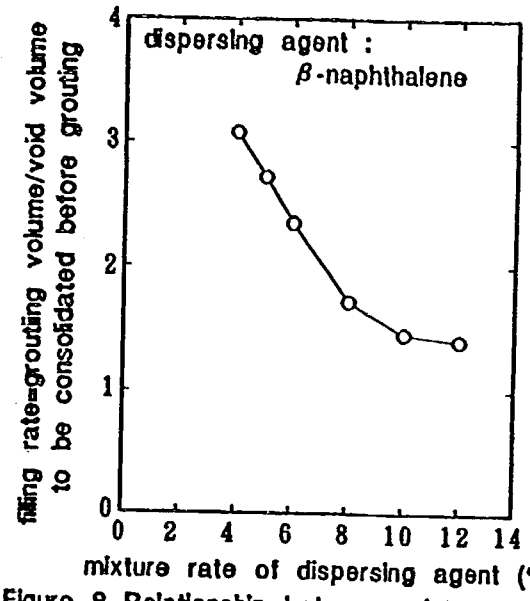



Figure 8 Relationship between mixture rate of disperesing agent and filling rate (W/C=1000%)

Table 4 Grouting condition for a long-term strength confirmination test

| grouting volume | mixure rate of dispersing agent(%) | grouting pressure (kgf/cm²) | W/C (%) |
|---|---|---|---|
| void volume ×1.2 | 1, 4, 5, 6, 8, 10, 12 | 3.0 | 1000 |

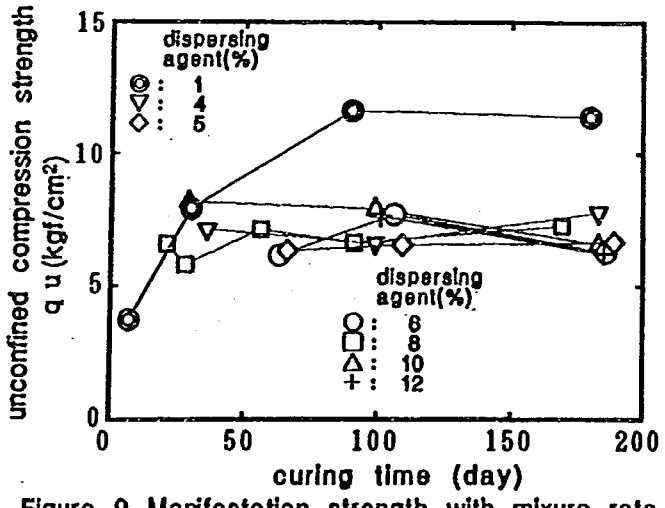



Figure 9 Manifestation strength with mixure rate of dipersing agent : β-naphthalene

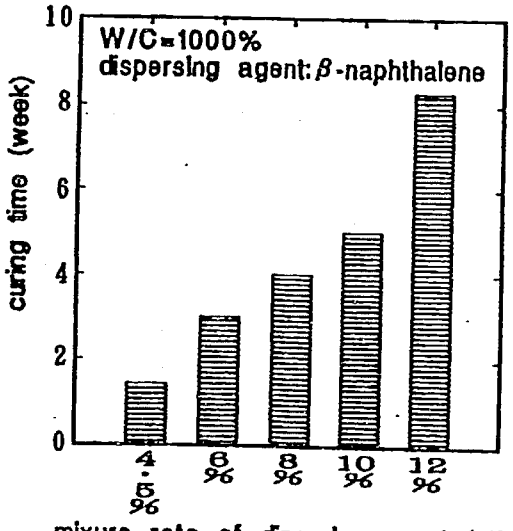



Figure 10 Curing time necessary for the form removal of a mold with mixture rate of dispersing agent :β-naphthalene

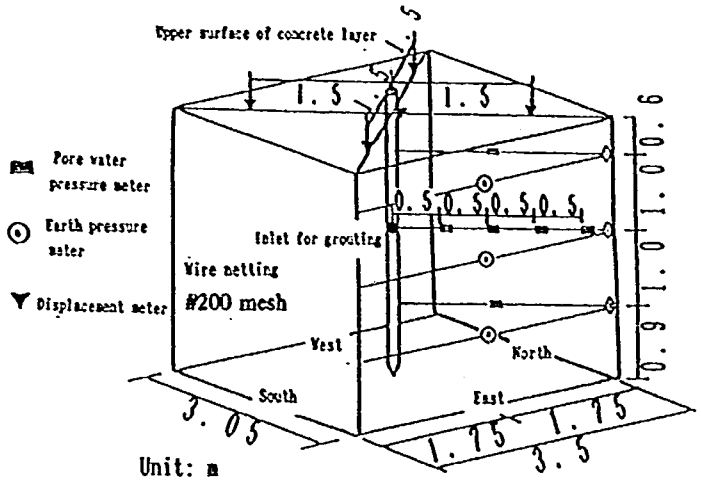



Figure 11 Outline of experimental ground

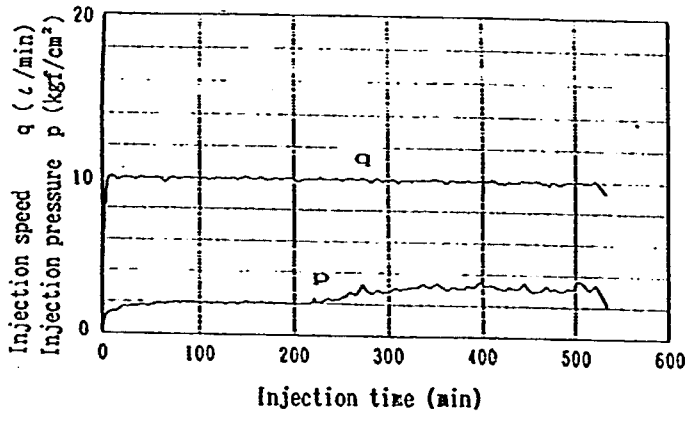



Figure 12 Change of injection pressure and rate of grouting

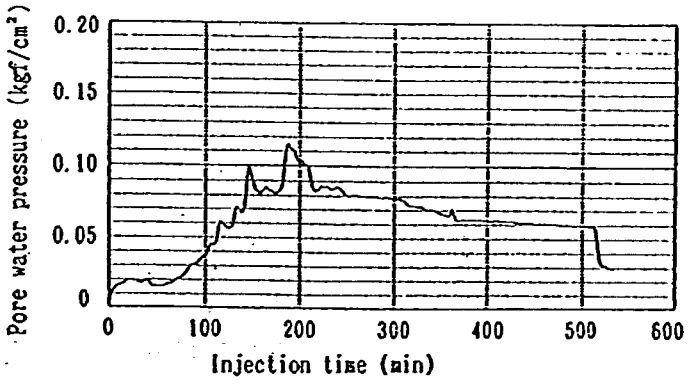



Figure 13 Change of pore water pressure during grouting (at the position horizontally separated 50 cm from the grout inlet)

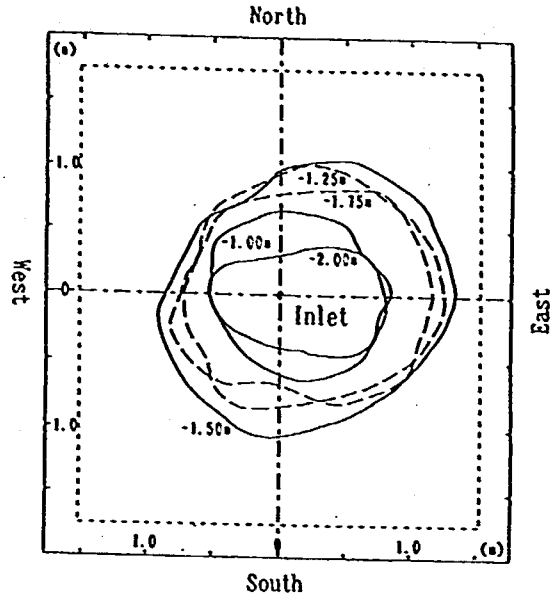



Figure 14 Horizontal section of consolidated body

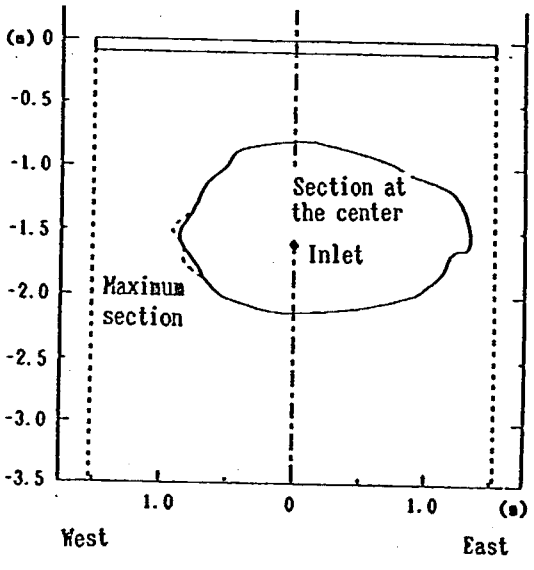



Figure 15 Vertical section of cnsolidated body from west to east

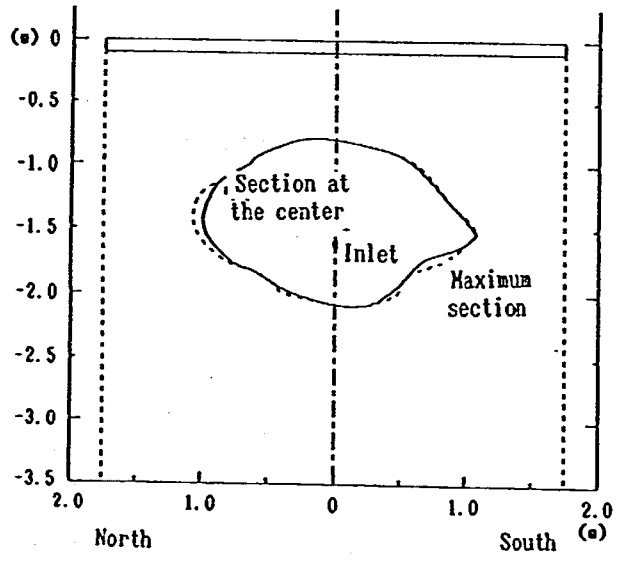



Figure 16 Vertical section of cnsolidated body from north to south

# Analysis of Behavior and Effect of Geosynthetic Reinforced Embankments at the Occurrence of Liquefaction

Osamu MATSUO[1], Takao SHIMAZU[1], Junichi KOSEKI[2],
Naozo FUKUDA[3], Teruhisa FUJII[3] & Nobuo TAJIRI[3]

## ABSTRACT

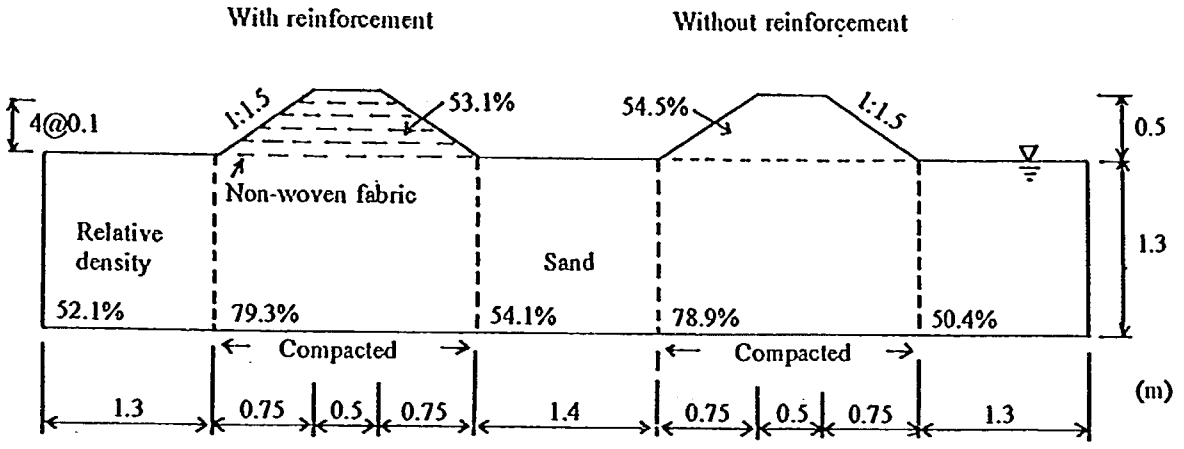
This paper reports of two-dimensional seismic response analyses of unreinforced and geosynthetic reinforced embankments both on a liquefactive ground during medium- and large-scale earthquakes. As a result of these analyses, it was ascertained that the geosynthetic, enhancing their stability at the same time, is more effective in unifying, or consolidating, individual embankments against earthquakes which cause smaller differential subsidence of the base grounds through liquefaction.

## 1. INTRODUCTION

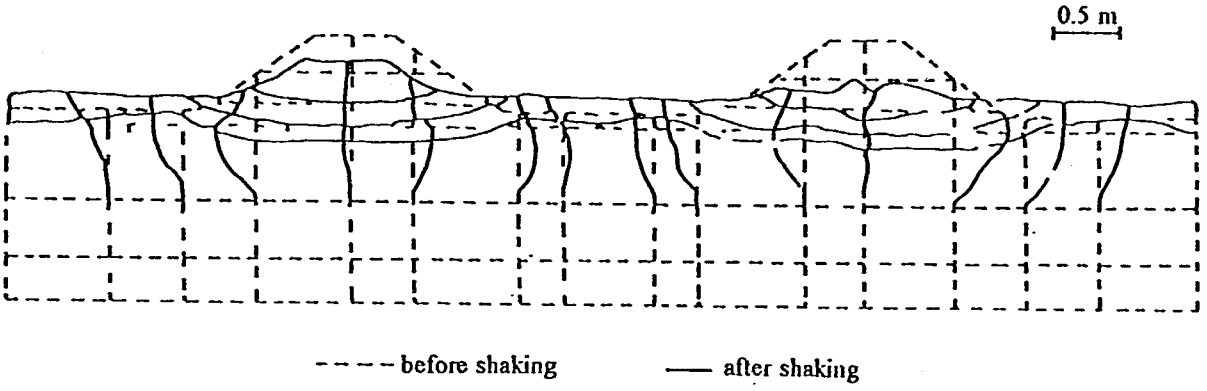
Soil structures on soft grounds have often sustained damage from liquefaction in their grounds during earthquakes. To address this subject, Mochizuki, Fukushima, et al.[1), 2), 3)] analyzed the improving effect of geosynthetic reinforced soils on liquefaction strength of grounds through dynamic tests and shaking table tests. Moreover, Futaki, et al.[4)] ascertained the subsidence-resistant effect of the geosynthetic reinforced embankments through large-scale liquefaction tests, seeking the reinforcement of foundations of houses. On the other hand, the Public Works Research Institute has been performing shaking table tests of embankment models reinforced with geosynthetics, etc[5)]. As a result of these tests, it was ascertained that although reinforced embankments subside when liquefaction occurs in their grounds, their subsidences tend to be somewhat smaller than those of unreinforced embankments as shown in Fig. 1. Measures like this can not be a positive one, but the effect to maintain the shapes of embankments, to sustain their functions as roads or banks, and thus to make easier the restoration of damaged areas can be expected[6)].

In this paper, models of unreinforced and geosynthetic reinforced embankments are set up, results of two-dimensional seismic response analyses of permanent deformations during medium- and large-scale earthquakes are presented, and evaluation of the subsidence-resistant effect of the reinforcement and subjects for the future are discussed.

[1] Public Works Research Institute, Ministry of Construction, Tsukuba, Japan
[2] Institute of Industorial Science, University of Tokyo, Tokyo, Japan
[3] Fukken Co., Ltd., Consulting Engineers, Hiroshima, Japan




(a) Initial condition before tests




(b) Final condition after tests at 240 gal

Fig. 1 Results of past shaking table tests[9].

## 2. CONDITIONS FOR ANALYSIS

### 2.1 Analysis method

The permanent deformation analysis method developed by the Public Works Research Institute of the Ministry of Construction was used[7,8]. This analysis method is based on the conception that plastic strain accumulates in the soil elements of an embankment and its ground due to shearing stress during an earthquake and the accumulated plastic strain causes permanent deformation in the embankment. Analysis programs used are SADAP and GSTR2. Analysis models were of an unreinforced embankment and of a geosynthetic reinforced one both on a liquefactive sand ground. Seismic motions of medium- and large-scale earthquakes were assumed. The flow chart of the analysis is shown in Fig. 2.

### 2.2 Setup of ground and embankment conditions

As shown in Fig. 3, the base ground of the analysis model was assumed to consist of an upper sand stratum, a lower sand stratum and a clay stratum beneath them, and an embankment to be constructed on the base ground. Soil parameters of the embankment and the base ground were assumed as shown in Table 1.

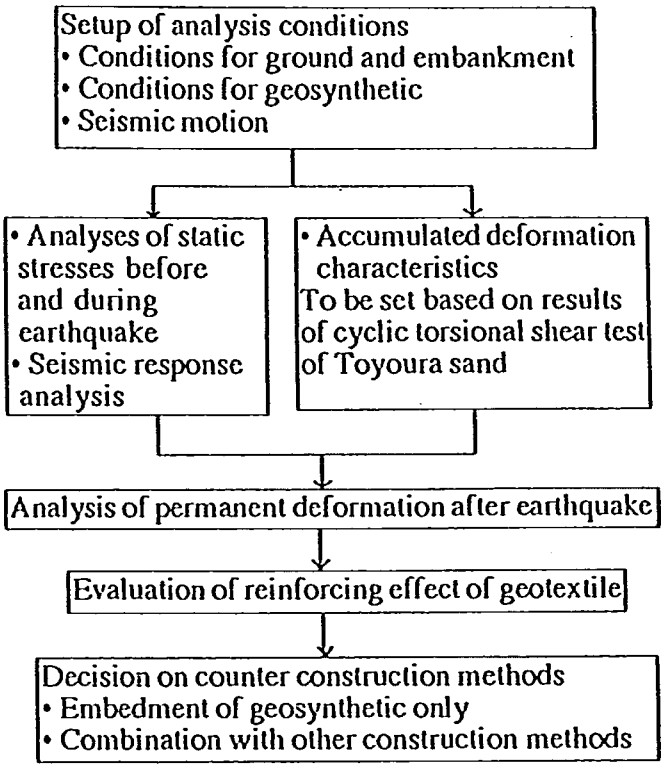



Fig. 2 Flow chart of Analysis.

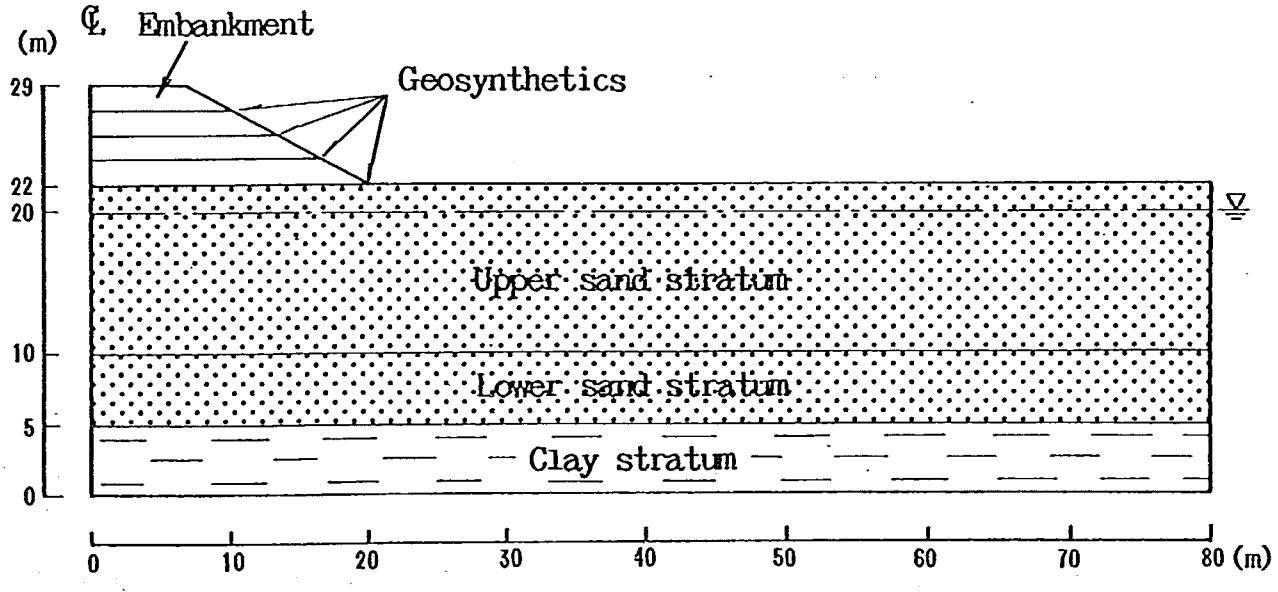



Fig. 3 Section of analysis model.

Table 1 Soil property parameters of embankment and base ground of analysis model.

| Soil Property Parameters | | Embankment | Upper Sand Stratum | | Lower Sand Stratum | Clay Stratum |
|---|---|---|---|---|---|---|
| | | | Above groundwater level | Below groundwater level | | |
| Wet unit weight $\gamma_t$(tf/m$^3$) | | 1.900 | 1.798 | 1.930 | 1.971 | 1.800 |
| Cohesion $c'$(tf/m$^2$) | | 1.0 | 0.0 | 0.0 | 0.0 | 10.0 |
| Internal friction angle $\phi'$(° ) | | 25.0 | 39.0 | 39.0 | 43.0 | 0.0 |
| Poisson's ratio | Static | 0.3333 | 0.3333 | 0.3333 | 0.3333 | 0.3333 |
| | Dynamic | 0.4999 | 0.4999 | 0.4999 | 0.4999 | 0.4999 |
| Coefficients to determine shear modulus $Go=\alpha \cdot \sigma_m^n$ | $\alpha$[(tf/m$^2$)$^{1-n}$] | 2,386 | 4,055 | 4,055 | 4,698 | 2,070 |
| | $n$ | 0.4 | 0.4 | 0.4 | 0.4 | 0.4 |
| Liquefaction strength | | – | – | 0.197 | 0.413 | – |

2.3 Setup of geosynthetic

2.3.1 Geosynthetic embedment plan

Geosynthetic was embedded only in the embankment. Each of the vertical spaces was 1.75 m, dividing 7 m height of the embankment into 4 layers of the same thickness as shown in Fig. 4.

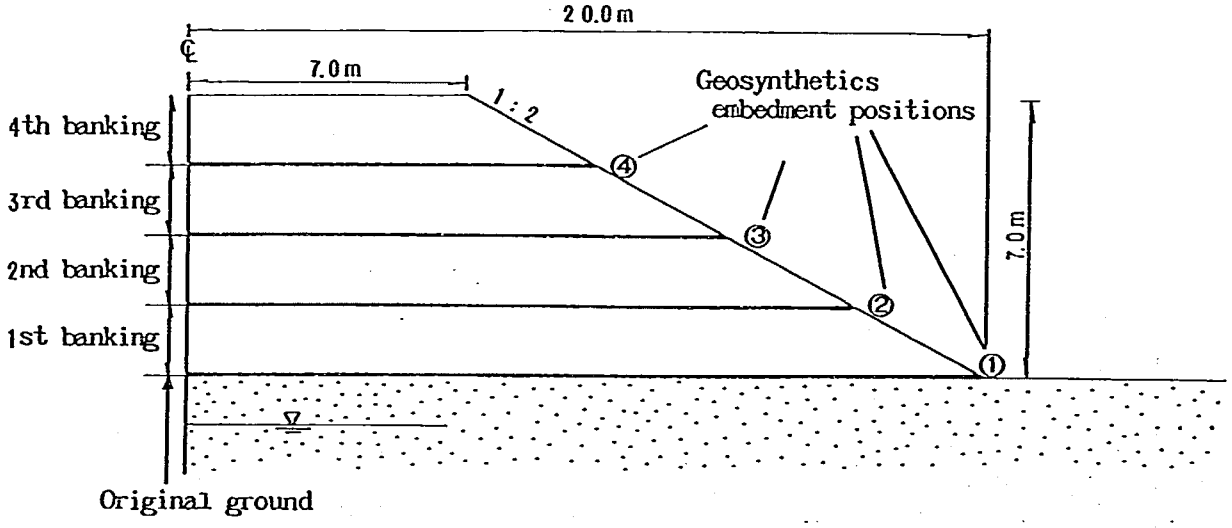



Fig. 4 Positions and spaces of geosynthetic embedment.

2.3.2 Physical properties of geosynthetic

Such a geogrid as commonly adopted in reinforced-soil construction methods was assumed to be used.

In this analysis, the geosynthetic was treated as a girder element, and because the rigidity of the geosynthetic is far different from that of the embankment's soil, they were modeled by providing a joint element between them. The physical properties of the geosynthetic were assumed as indicated

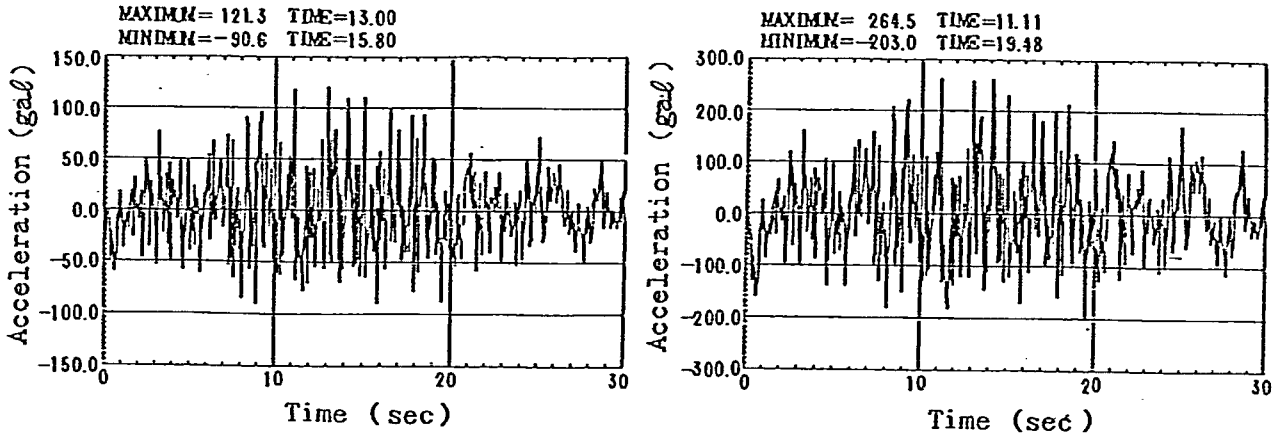
in Table 2.

Table 2 Geosynthetic's physical property values used in analyses.

| Item | Set Value | Remark |
|---|---|---|
| $E \cdot A$<br>$E$:Modulus of elasticity<br>$A$:Sectional area | $E \cdot A$=100 tf<br>$E$=100.0 tf/m$^2$<br>$A$=1.0 m$^2$ | $E \cdot A$:Tension test result<br>$E$ and $A$:Provisionally set for the convenience of input |
| $I_t$:Moment of inertia of area | $I_t$=0.01 m$^4$ | Evaluated as tension member |
| $\gamma_t$:Unit weight | $\gamma_t$=10$^{-6}$ tf/m$^3$ | Value small enough<br>Geosynthetic's dead weight not considered |

2.4 Seismic motion

Two kinds of input seismic motions, one for a medium-scale earthquake (hereinafter referred to as "Level-1") and the other for a large-scale earthquake ("Level-2"), were derived from the amplitudes and frequency characteristics of the existing strong-motion earthquake records and used in this analysis. Fig. 5 shows the input seismic motion-time graphs. The maximum accelerations of Level-1 and Level-2 are 121.3 gal and 264.5 gal,respectively.




(a)Level-1($\alpha_{max}$=121.3 gal)　　(b)Level-2($\alpha_{max}$=264.5 gal)

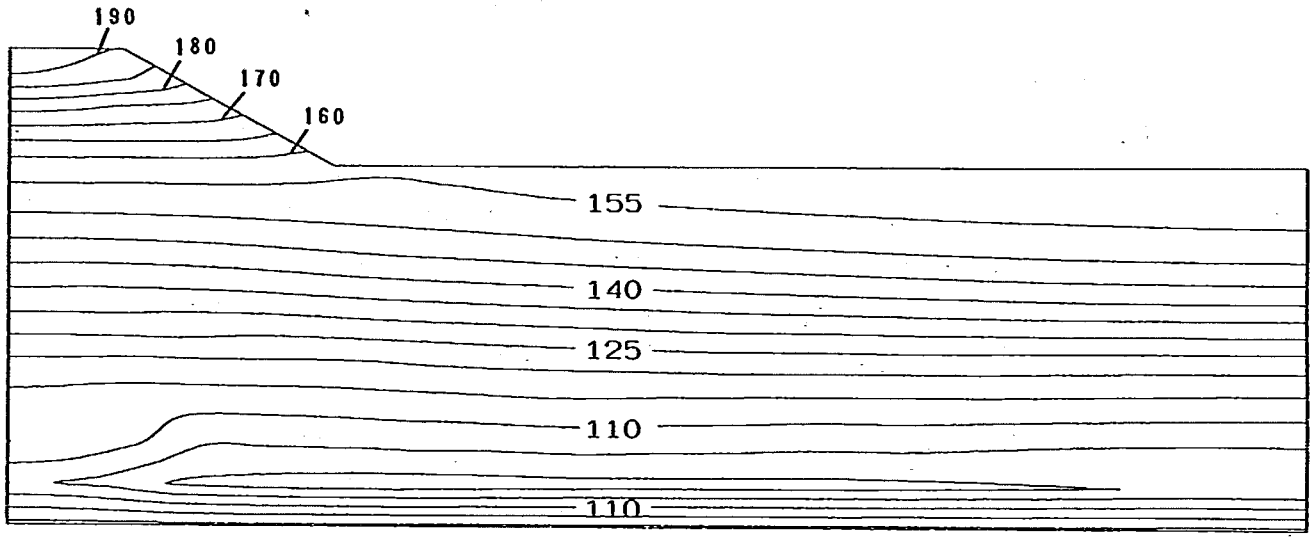
Fig. 5 Input seismic motion-time graphs used in analyses.

## 3. ANALYSIS RESULTS

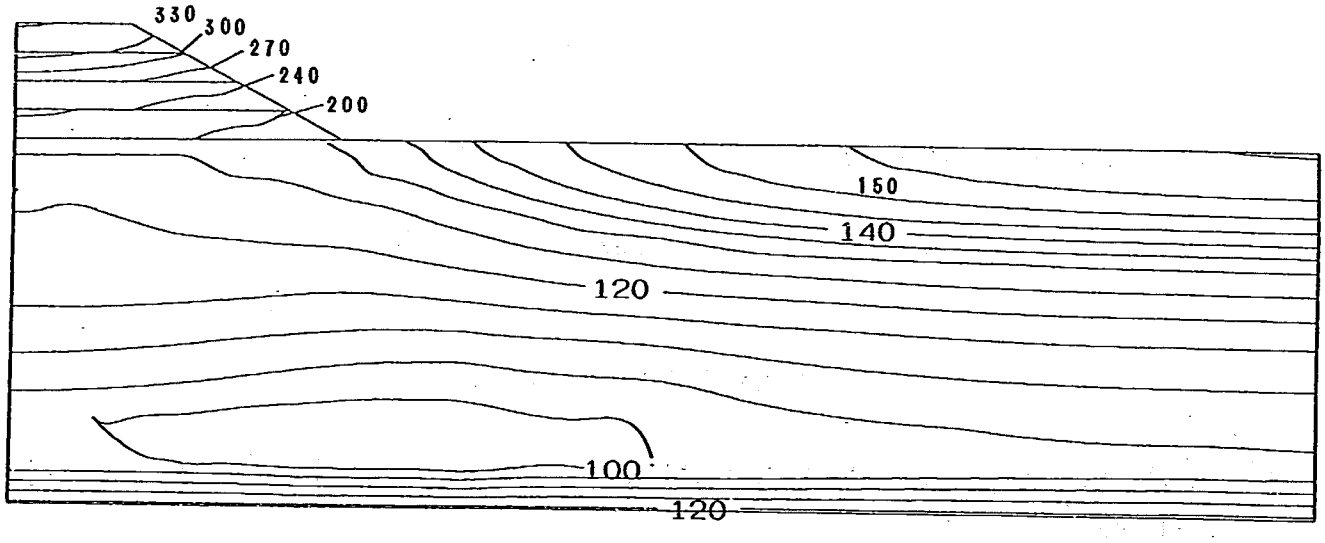
3.1 Acceleration response scale factors (Maximum horizontal acceleration/maximum input acceleration)

Fig. 6 shows the distribution of maximum horizontal accelerations in the unreinforced and

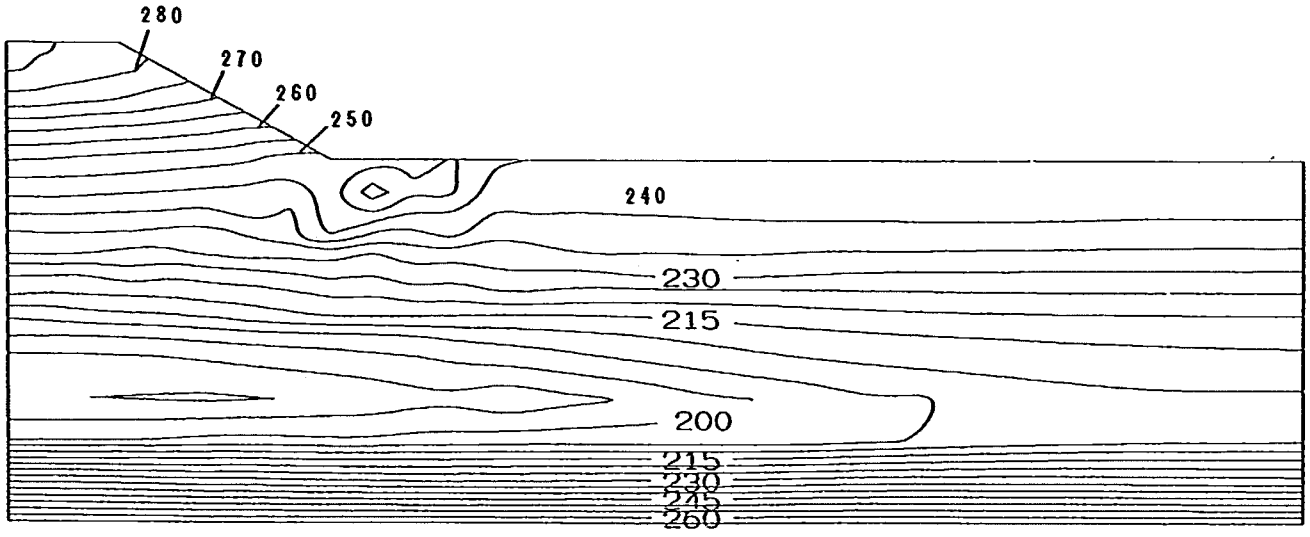
reinforced embankments under each of the Level-1 and Level-2 seismic motions. In the base ground, while the acceleration response scale factor with the unreinforced embankment is larger than that with the reinforced one under the Level-1 seismic motion, no significant difference can be observed between the scale factor with the unreinforced embankment and that with the reinforced one under the Level-2 seismic motion. In the embankments, on the other hand, the acceleration response scale factor of the reinforced embankment is larger than that of the unreinforced one under both the Level-1 and -2 seismic motions. This can be considered due to the embankment's rigidity increased by embedding the geosynthetic.



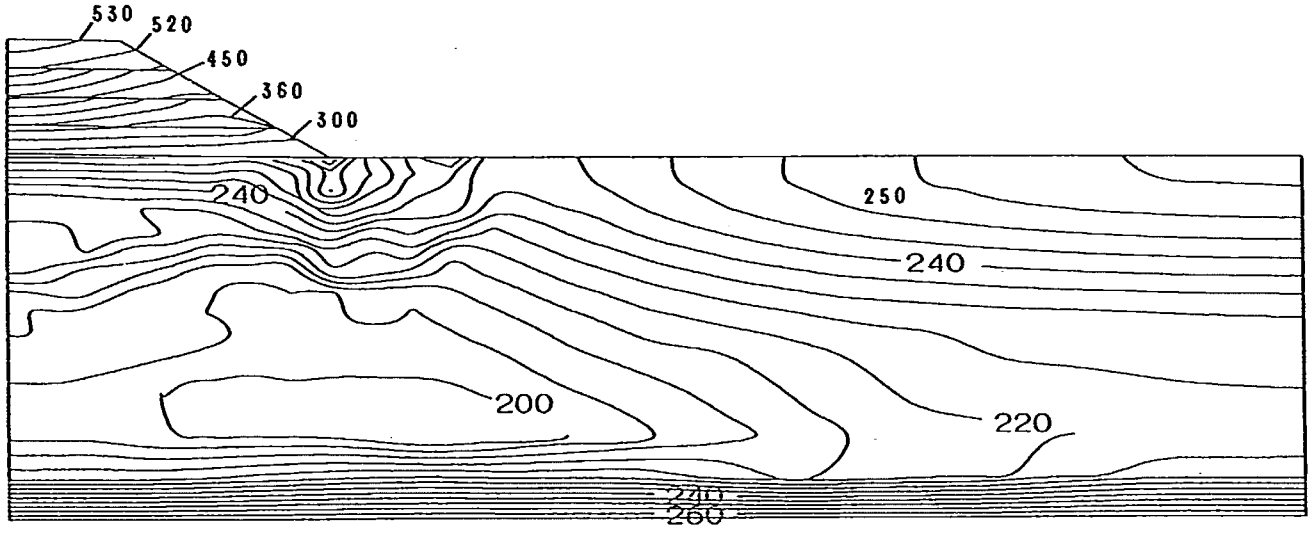

(a)Level-1, unreinforced




(b)Level-1, geosynthetic reinforced




(c)Level-2, unreinforced



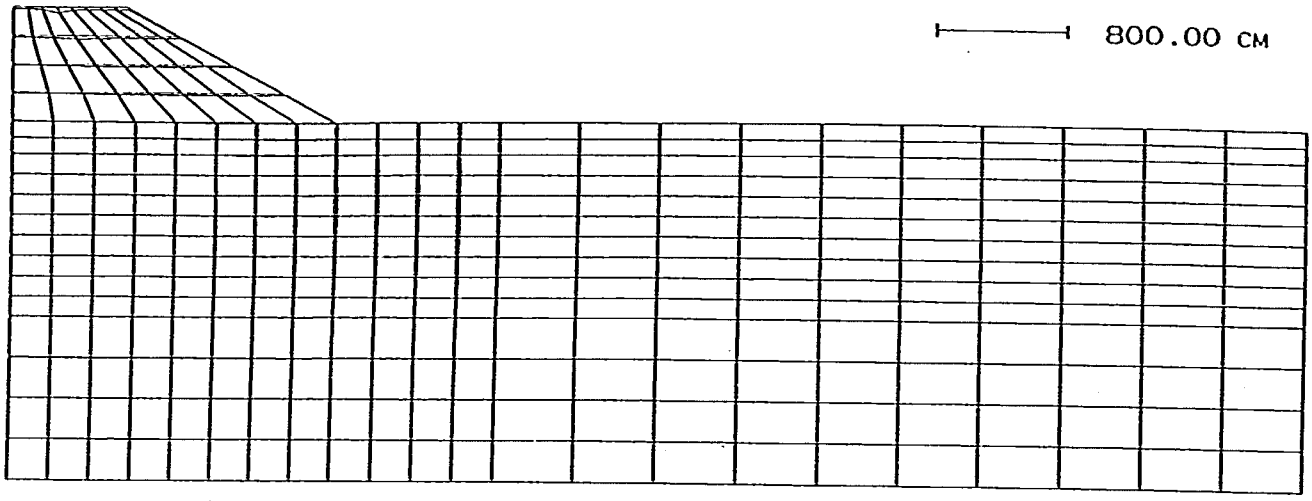

(d)Level-2, geosynthetic reinforced

Fig. 6 Maximum horizontal acceleration distribution charts.

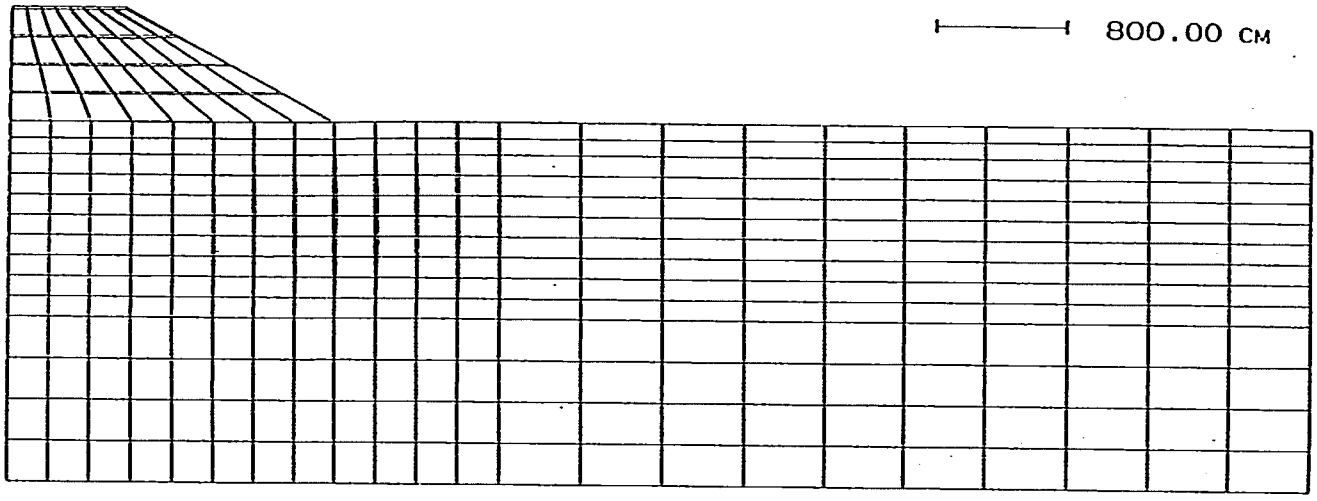
3.2 Permanent deformation

Fig. 7 shows the results of permanent deformation analyses of the unreinforced and reinforced embankments. Fig. 8 shows the relation between the maximum input acceleration and the subsidence at the top center of the embankment. It can be observed from Fig. 7 that the subsidence of the reinforced embankment is smaller than that of the unreinforced one under both the Level-1 and -2 seismic motions, which demonstrates the reinforcing effect of the embedded geosynthetic. It can also be observed from Fig. 7 that the deformation in the base ground near the toe of the slope was reduced by embedding the geosynthetic. On the other hand, Fig. 8 indicates that the subsidence at the top center of the embankment was reduced by 12 - 15% by embedding the geosynthetic under

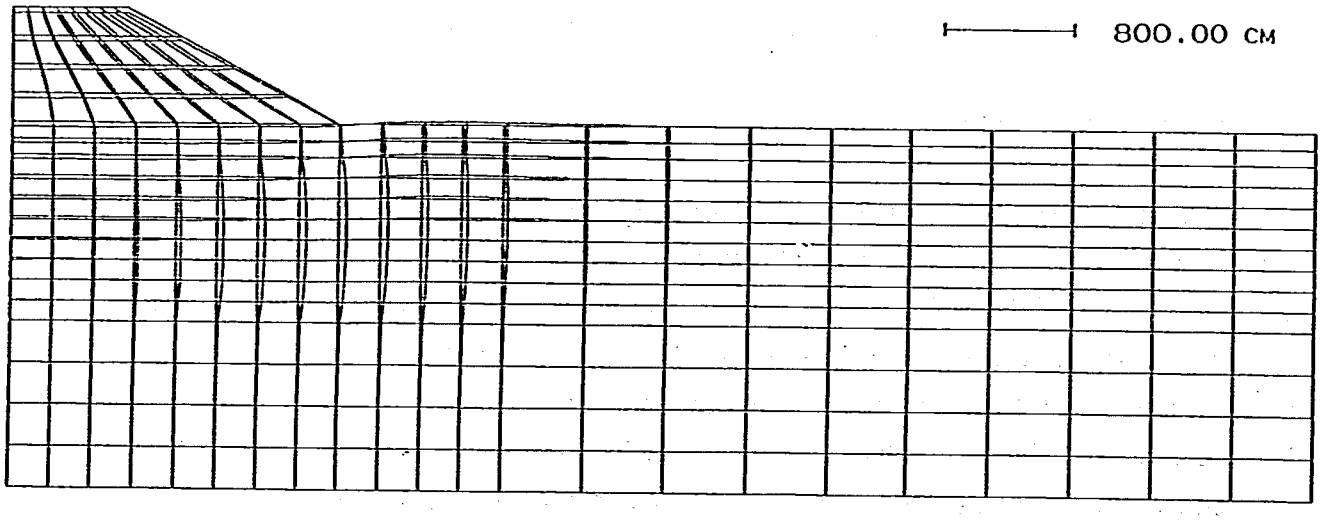
both the Level -1 and -2 seismic motions.



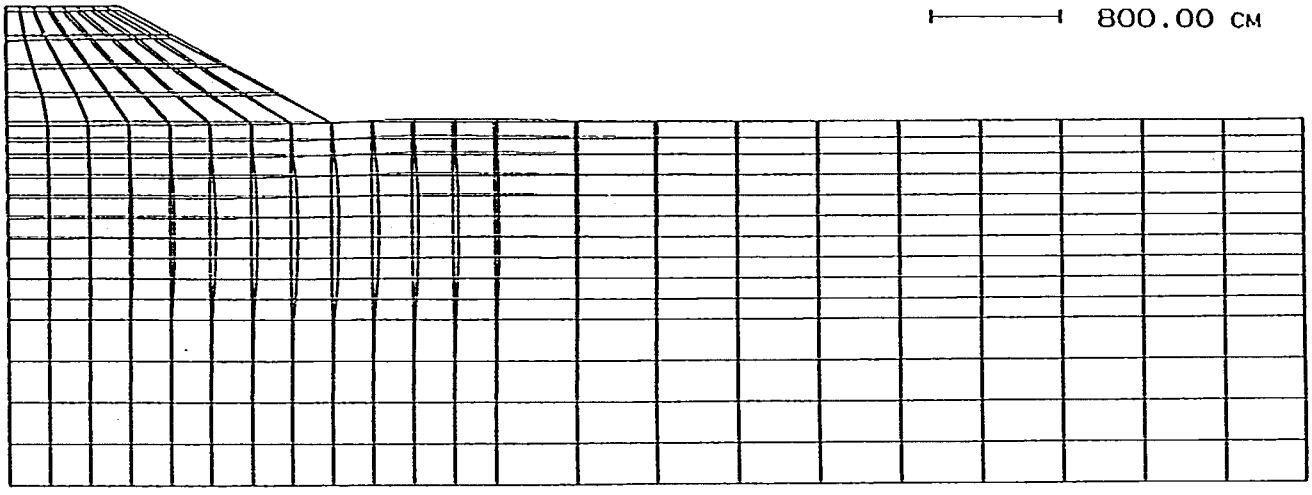

(a)After Level-1 seismic motion, unreinforced




(b)After Level-1 seismic motion, geosynthetic reinforced




(c)After Level-2 seismic motion, unreinforced




(d)After Level-2 seismic motion, geosynthetic reinforced

Fig. 7 Comparison between deformations of unreinforced and reinforced embankments.

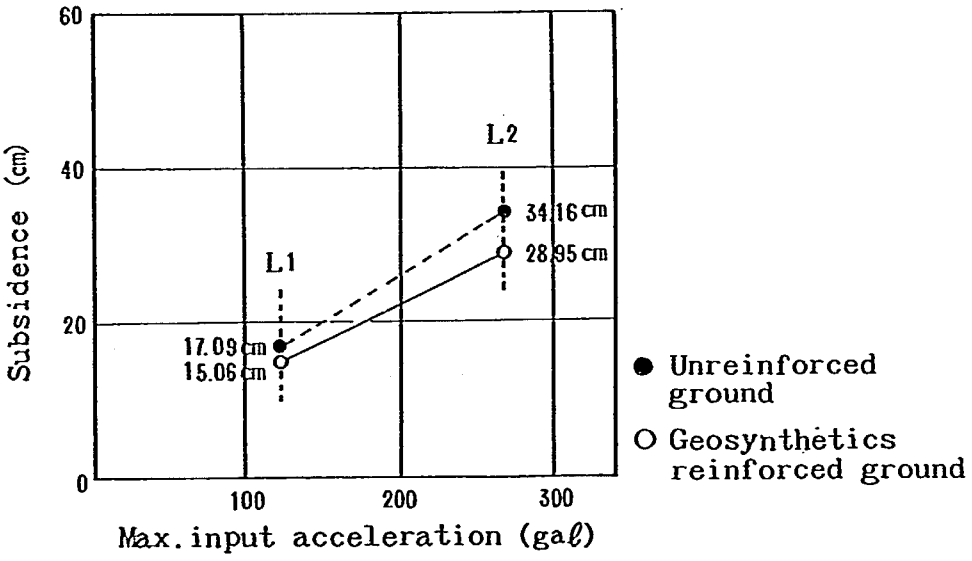
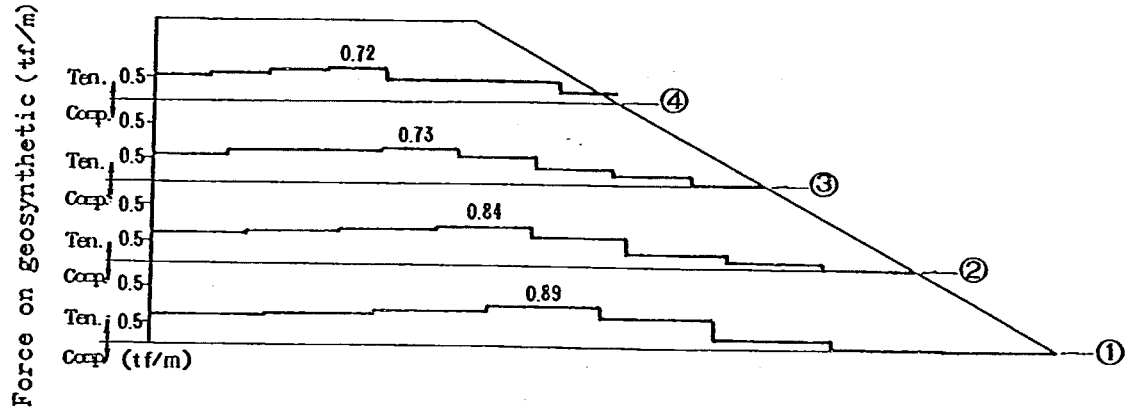



Fig. 8 Relation between maximum input acceleration and subsidence at the top center of embankment.

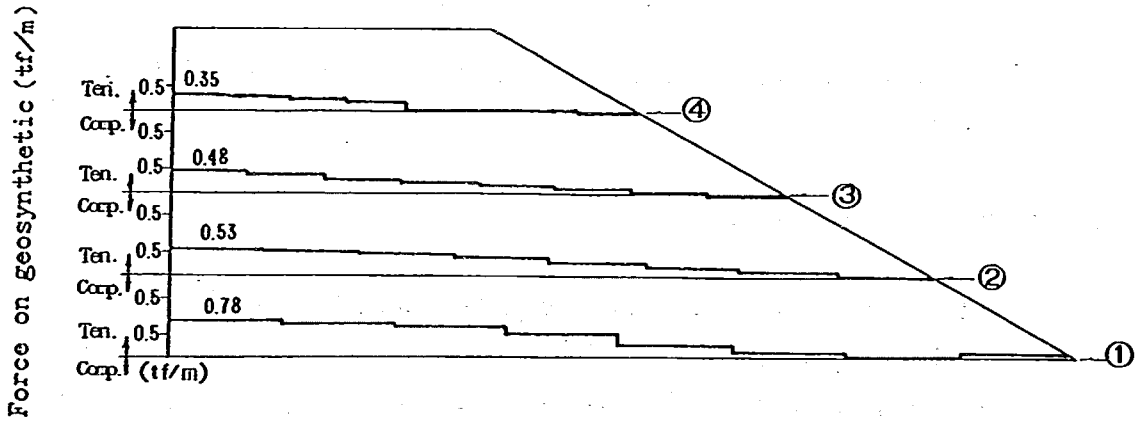
3.3 Force on reinforcing geosynthetic

Fig. 9 shows the force distribution on the geosynthetic after the seismic motions. In both the cases of the Level-1 and -2 seismic motions, the maximum tensions caused are in the range of 0.4 - 0.9 tf/m, and a tendency can be observed that the lower the geosynthetic position in the embankment, the larger the tension. However, because the tensile yield stress of the geosynthetic is approximately 6.3 tf/m, it is far from yielding. In case of Level-1, tension is produced evenly from the center to a certain distance and decreases rapidly near the slope face. In case of Level-2,

on the other hand, the tension is largest at the center of the embankment, it decreases gradually when the position moves toward the slope, and compressive force occurs in the upper area of the slope face. It seems that large subsidence occurred at the center of the embankment under the Level-2 seismic motion, which in turn caused the pull-out of the geosynthetic in the vicinities of the slope faces, which again in turn caused the compressive areas with bending in the vicinities of the slope faces. (See Fig. 10.) This suggests that making smaller the base ground's subsidence (including lateral flow) due to liquefaction improves the effect of unifying, or consolidating, the embankment and thus higher stability of the embankment can be secured.




(a)After Level-1 seismic motion




(b)After Level-2 seismic motion

Fig. 9 Distribution charts of force on geosynthetic.

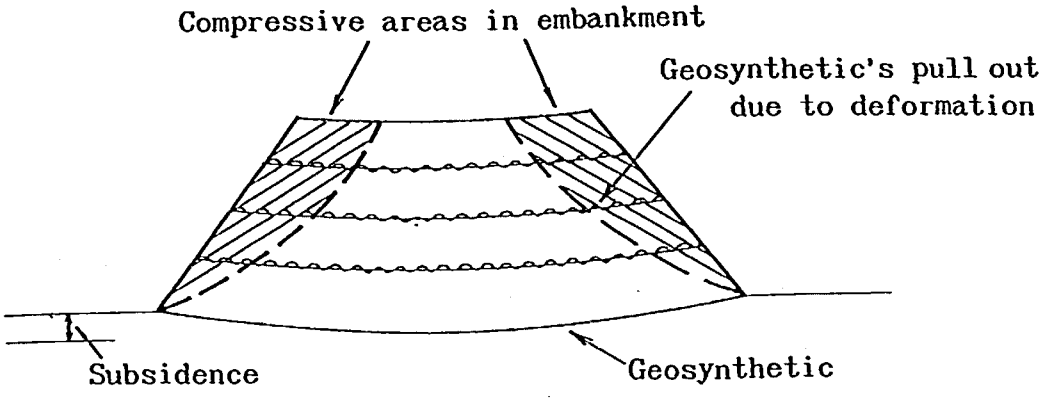



Fig. 10 Mechanism of occurrence of compressive areas under Level–2 seismic motion.

## 4. CONCLUSION

Regarding the effect of reinforcing embankments with geosynthetics on liquefactive sand grounds, a ground model was set up and seismic response analysis was performed. The results can be summarized as follows:

(a) In the base ground, while the response acceleration was reduced by reinforcing the embankment under the Level–1 seismic motion, no significant difference could be observed between the response acceleration with the unreinforced embankment and that with the reinforced one under the Level–2 seismic motion. In the embankment, on the other hand, the response acceleration was increased by reinforcing the embankment.

(b) Under both the Level–1 and –2 seismic motions, the subsidence at the top center of embankment was reduced 12 – 15% by embedding the geosynthetic in the embankment.

(c) While the distribution chart of force on the geosynthetic after the Level–1 seismic motion shows tensile force in almost all the areas, the chart after the Level–2 seismic motion shows compressive force on the upper, slope area, which means the reduction of the embankment unification, or consolidation, effect.

Further study has yet to be made about conditions of base grounds, configurations of embankments, kinds of reinforcing materials, reinforcement embedding patterns, and combination with other construction methods.

This paper is a summary of a part of the 1994 results[9] of the "Joint Research for Earthquake–Resistant Construction Method for Soft Grounds," among the Public Works Research Institute of the Ministry of Construction and 17 private companies for 5 years from 1992.

## REFERENCE

1) Mochizuki, M., Fukushima, S. and Kagawa, K.: Applicability of reinforced–soil construction

methods as countermeasures for the prevention of liquefaction, 1st Geotextile Symposium, pp. 15–18, 1986.

2) Mochizuki, M., Fukushima, S. and Kagawa, K.: Shaking–table model tests of reinforced sand, 2nd Geotextile Symposium, pp. 10–13, 1987.

3) Mochizuki, M., Fukushima, S., Kagawa, K. and Kuno, G.: Applicability of reinforced–soil construction methods to countermeasures for the prevention of liquefaction, Soils and Foundations,Vol. 35, No. 4, pp. 5–10, 1987.

4) Futaki, M. and Minamizaka, T.: Large–scale liquefaction tests of a polymer–grid reinforced sand ground, 23rd Japan National Conf. on Soil Mechanics and Foundation Eng., pp. 2223–2226, 1988.

5) Koga, Y. and Fukuda, N.: A course, A reinforced–soil construction method using geotextile 11, View on seismic design (No. 1), Soils and Foundations, Vol. 42, No. 2, PP. 71–76, 1994.

6) The Public Works Research Institute, the Ministry of Construction: Research of seismic subsidence of embankments and countermeasures, Public Works Research Institute Report, No. 2769, pp. 55–106, 1989.

7) Sasaki, Y., Matsuo, O and Karasawa, Y.: A analysis method of permanent deformation of embankments by earthquakes and its application example, Civil Engineering Report, 27–3, pp. 46–51, 1985

8) Koseki, J. and Matsuo, O.: Permanent deformation analysis of dynamic centrifugal model tests of embankments on liquefactive grounds, 29th Japan National Conf. on Soil Mechanics and Foundation Eng.,pp. 1053–1056, 1994.

9) The Public Works Research Institute, the Ministry of Construction, et al.: Joint research report (No. 2) for earthquake–resistant construction method for soft grounds, Joint Research Report, No. 104, 1994.

# Session-3

## Effects of Liquefaction (2)

(J-4) Study on Flow of Liquefied Ground by means of Model Pipe Tests
(Ikuo Towhata and William Vargas-Monge)

(J-5) Countermeasures against the Floatation of Buried Pipes due to Liquefaction
(Susumu Yasuda, Hideo Nagase, Shigeru Itafuji and Keiichiro Mine)

(J-6) Dependence of Longitudinal Subgrade Reaction to the Buried Pipe on Displacement Velocities and Cycles of the Ground.
(Mio Kobayashi, Hirokazu Ando and Noritake Oguchi)

# STUDY ON FLOW OF LIQUEFIED GROUND BY MEANS OF MODEL PIPE TESTS

William Vargas-Monge[1]
Ikuo Towhata[2]
Department of Civil Engineering
University of Tokyo
7-3-1 Hongo, Bunkyo-ku
Tokyo 113, Japan

## 1. INTRODUCTION

Lateral flow of liquefied soil in gentle slopes has been the subject of recent research carried out in Japan. This type of ground failure has increasing economic significance due to the number of lifelines, buried pipelines, foundations and other underground structures located in liquefiable areas. Although important, the phenomenon is not fully understood yet because until recently, research had emphasis on understanding why, where, when and how liquefaction happened and not on what happened after liquefaction.

Estimation of potential damage that buried structures may suffer after liquefaction requires appropriate assessment of stresses induced by lateral flow and of behavior of liquefied soil at large deformations. The role of properties of liquefied soil, such as dilatancy, residual strength and viscosity (strain-rate dependency of stress) and the influence of loading conditions in ground must be clarified for that purpose.

Flowing liquefied ground in the field, as in lateral flow of gentle slopes (Doi and Hamada, 1992), and in shaking table experiments with models is similar to liquid (Sasaki et al., 1992). However, behavior of flowing liquefied soil in small specimens at large deformations (under 30% of shear strain) is commonly described only in terms of residual or steady-state shear strength (Verdugo, 1992; Ishihara, 1993). Strain-rate dependency (or viscosity) is not generally included in models of soil behavior but it becomes important when trying to explain the behavior observed in shaking table experiments.

The purpose of this study was to examine the behavior of flowing liquefied sand in experiments conducted with a small-scale pipe in a model ground. The focus was the drag exerted by flowing liquefied soil on a buried pipe under different loading conditions. From the observations, some properties of liquefied soil, such as viscosity could be examined.

## 2. EXPERIMENTAL CONDITIONS

### 2.1 *Material*

Standard Japanese Toyoura sand was used in all tests. It has a density $\rho_s$=2.65 g/cm$^3$, a mean diameter $D_{50}$=0.17 mm, and a uniformity coefficient $C_u$=1.4. The maximum and minimum void ratios are $e_{max}$=0.974 and $e_{min}$=0.605, respectively.

---

[1]Graduate Student

[2]Professor

## 2.2 *Equipment*

Figure 1 shows the layout of the container used in tests. It was a welded steel tank with acrylic windows in the lateral walls. Its interior dimensions were 400 mm in width, 700 mm in length and 600 mm in height. On one side of the tank, an attached steel arm held an electric motor. On the opposite side and near the base of the tank there was a water inlet with a porous stone.

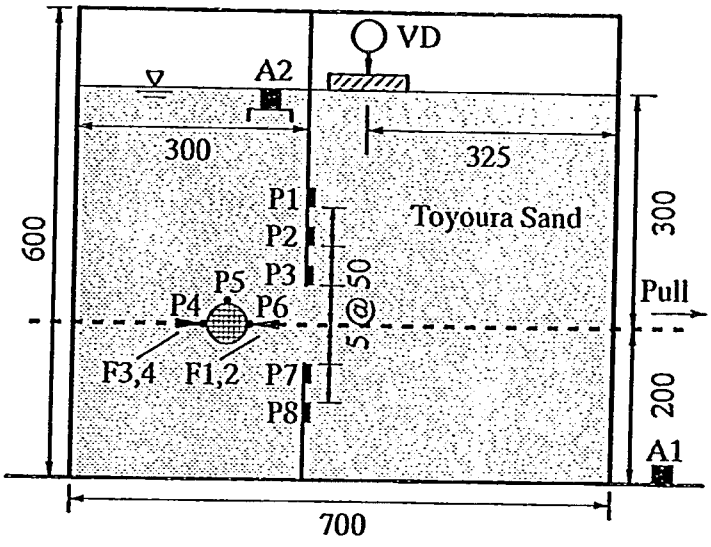



**Figure 1** Layout of container used in the experiments with location of transducers. A: accelerometer, F: load cell, P: pressure meter, VD: vertical displacement meter. Units: mm

The model pipe was a hollow steel cylinder 30 mm in diameter and 300 mm in length, with an apparent density of 2.0 g/cm$^3$. It was fixed in its ends to two parallel guide bars 6 mm in diameter, placed inside the container. Those bars extended beyond the back and front walls of the container through grease-locked cells and were attached to a motor in the front and connected by a transverse bar in the rear to form a frame. This frame kept the pipe at a constant height of 200 mm from the bottom of the container. The motor pulled the structure with adjustable constant velocity. When the pipe was in motion, the volume of structure inside the container was constant.

To measure the horizontal force acting on the pipe, four load cells were installed between the pipe and the guide bars. This setting allowed the calculation of the net force, canceling the effect of friction between the guide bars and the container's walls. Excess of pore water pressure was measured by transducers installed on the front, top and rear of the pipe, and at four other locations in the sand mass, above and below the pipe, as shown in Figure 1. Accelerometers measured the input at the base of the container and the model ground acceleration at the surface. Surface settlement was also recorded at the center. All data were recorded by a digital system.

Tests were carried out on three unidirectional shaking tables. One shaking table had a hydraulic motor that generated a sinusoidal motion with adjustable amplitude and frequency. The other two were manually operated and generated a constant-frequency sinusoidal motion with variable amplitude.

## 2.3 *Model preparation*

In the field, sand with potential to flow is typically loose ($D_r$<40%) and exhibits contractive behavior (negative dilatancy) when sheared (Ishihara, 1993). Very loose sand models have to be constructed to achieve contractive behavior at the low levels of confining stress in shaking table tests at normal gravity. A separate study has proved that this type of very loose ground flows (Toyota and Towhata, 1994) in such conditions. With densities similar to that of a prototype, behavior of a model would always be dilative and flow would stop when shaking is switched off (Toyota and Towhata, 1994). A previous study with the same equipment and material (Orense, 1992) was done in the latter conditions, with sand at a relative density of $D_r$=30%.

Wet tamping (Ishihara, 1993) was used to prepare very loose sand models. Each model was

built in ten layers of approximately 5 cm in thickness from sand previously moistened with 5% of water. The amount of sand for one layer was placed by hand inside the container with care taken to shatter clusters. Then the surface was softly pressed to remove large voids and leveled off. Except in the loosest models ($e$=1.10), compaction was applied with a tamper using the same energy in every blow until the preset thickness had been attained. After tamping, the surface was scratched to reduce excessive local compaction, to improve continuity between layers and general uniformity.

Once completed, water was supplied through the bottom inlet to inundate the models, until the water level coincided with the ground surface. Depending on the aimed void ratio, some collapse occurred as saturation progressed. The initial void ratio was computed with measurements taken at the end of saturation. Resulting relative densities ranged from $D_r$=-30% to $D_r$=-10%.

### 2.4 *Testing procedure*

The equipment used in the experiments did not allow the actual flow of the model ground and instead, lateral flow was simulated by moving the model pipe inside liquefied ground. In fluids, when the Reynolds number has the same, small value (laminar flow), both cases are perfectly analogous. Those conditions were verified in every test.

Tests were conducted in three different conditions that allowed the study of different aspects of behavior: monotonic displacement after the end of the shaking, monotonic displacement during shaking and cyclic displacement during and after shaking. The first two types of loading represent possible conditions in reality: lateral flow after the end of the seismic load and flow during the earthquake. The third type does not represent a prototype loading condition and was employed to study behavior.

#### 2.4.1 Monotonic displacement after shaking

A strong shaking of short duration was applied to trigger liquefaction. After the end of shaking and while the ground was still liquefied, the pipe was moved with constant velocity through a maximum stroke of 250 mm or till the force in the transducers was nearing their allowable load.

Different ranges of void ratios, velocities (rates of deformation), and amplitudes of cyclic acceleration were studied. Frequency of input motion was kept constant, between 3.5 and 5 Hz. Velocity of movement was limited by the motor to 19 mm/s. The range of velocities used in the experiments was between 4 mm/s and 19 mm/s (strain rates of approximately 10 $s^{-1}$ and 60 $s^{-1}$, if the velocity is normalized by the pipe's diameter).

#### 2.4.2 Monotonic displacement during shaking

Flow during shaking was simulated by applying continuous, constant-amplitude shaking and moving the pipe with constant velocity after liquefaction had started. Amplitude of acceleration was kept at around 400 Gals and the void ratio at approximately 1.05. Two manual shaking tables allowed the study of soil response when vibration was applied in two main directions, parallel and perpendicular to the pipe's displacement, respectively.

#### 2.4.3 Cyclic displacement

Finally, the response of liquefied sand to cyclic loading was studied. This type of load was created by cyclic movement of the pipe. It started after liquefaction and continued for a short time after the end of shaking. The input acceleration was kept at 400 gals and the void ratio at approximately 1.05.

## 3. RESULTS

Figure 2 shows the graphs of a typical test result in which pipe's movement started after shaking. Models showed a considerable settlement of the surface when liquefaction was triggered. Volume decreased mainly during shaking but continued to decrease throughout the duration of the pipe's movement. The void ratio changed in that process but measurements showed that the final average void ratio was still in the range for which contractive behavior has been observed in triaxial tests (Verdugo, 1992). Results are reported with respect to the initial void ratio.

The amplitude of acceleration recorded on the model ground was as much as four times smaller than the amplitude of the input motion, and the difference increased after liquefaction occurred.

### 3.1 *Behavior in monotonic loading after shaking:*

An important difference between models and prototypes of flowing liquefied slopes was the absence of the static shear stress caused by gravity (the component of weight parallel to slope) in models. In level models, gravity induced reconsolidation but not shearing. Besides that, in small-size tanks the duration

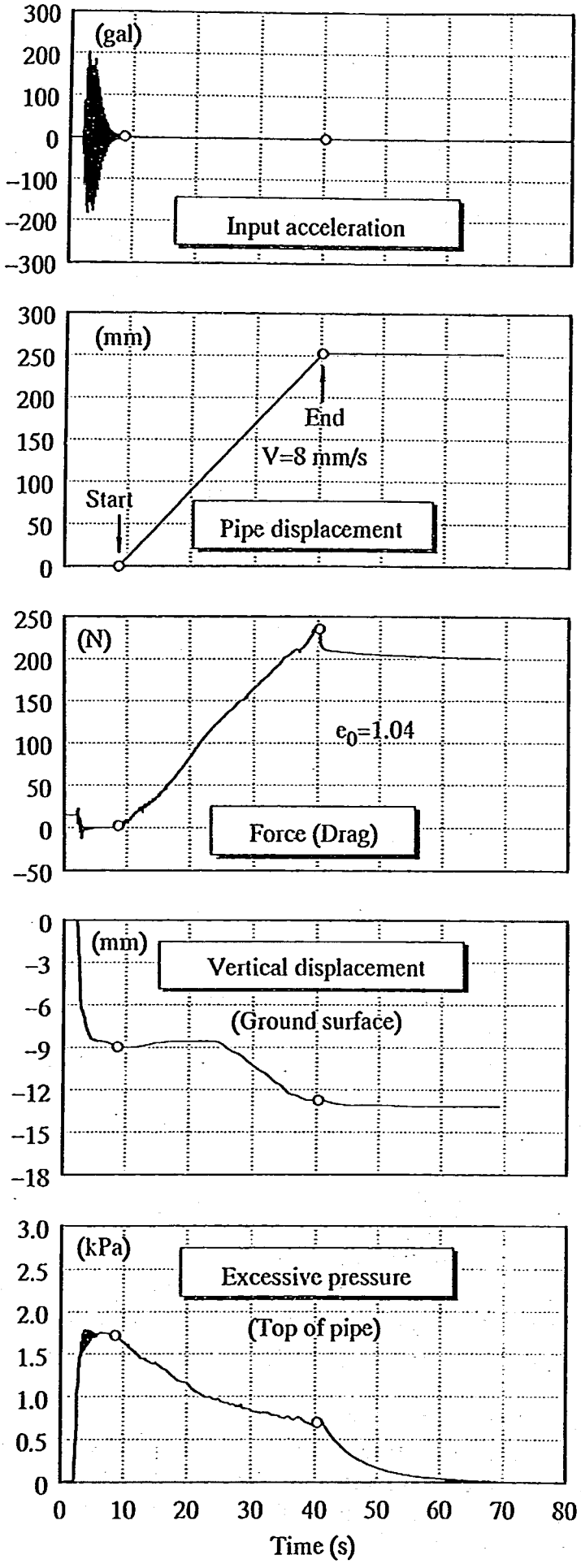



**Figure 2** (at right) Time histories of acceleration, displacement, drag, surface settlement and excessive pressure for a typical test

of complete liquefaction is very short and lateral flow of even very loose model slopes is limited (Toyota & Towhata, 1994). The combination of these two factors made the measurement of drag at 100% liquefaction difficult in this type of loading.

Moreover, the pipe's movement induced dilatancy and accelerated dissipation of excessive pore water pressure. Dissipation of the excessive pressure ended the condition of complete liquefaction and caused the soil to recover strength. As a result, the measured drag increased steadily from an initial small value, as seen in Figure 2. Thereafter, the observed model behavior could be more related to the postliquefaction phase in a prototype.

Only the initial drag that occurred while the ground was still completely liquefied was used in the analysis, since pore pressure dissipation affected the subsequent increase in force. Its value was assessed from detailed time histories of force, as shown in Figure 3. The sudden increase in the force at the start of movement was measured directly from the records or from detailed plots and the resulting value was taken as the initial drag.

Figure 4 shows the computed values of drag plotted with the results of a previous study (Orense, 1992) done under similar conditions on denser models ($D_r$=30%). The observed tendency was the same in both studies: the drag exerted by liquefied sand increased with velocity. The effect was more pronounced at higher densities. This suggests that viscosity of completely liquefied sand also depended on density. In the same figure, dashed lines represent the theoretical drag

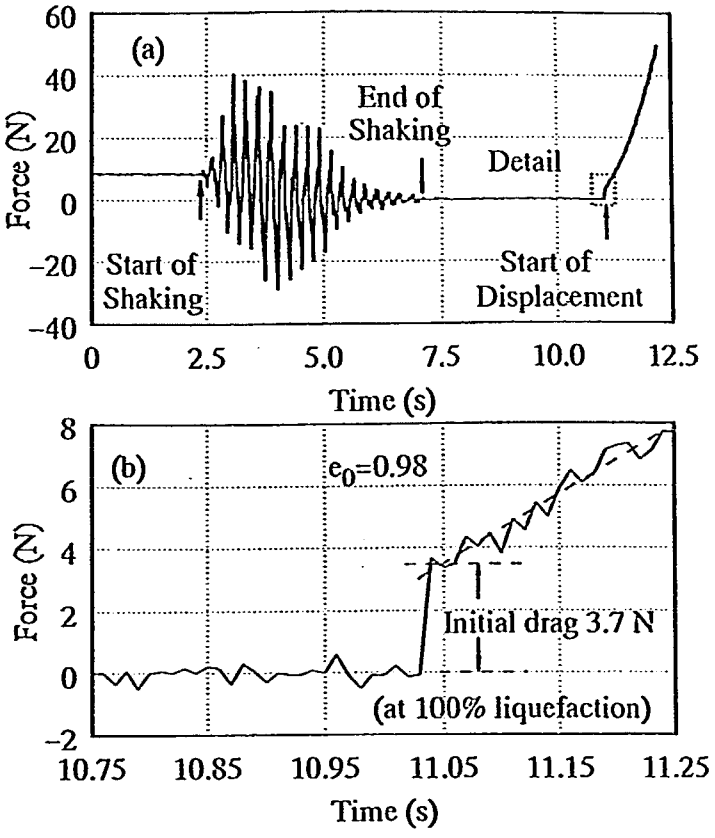



Figure 3 Details of time history of force (a) and measurement of initial drag (b).

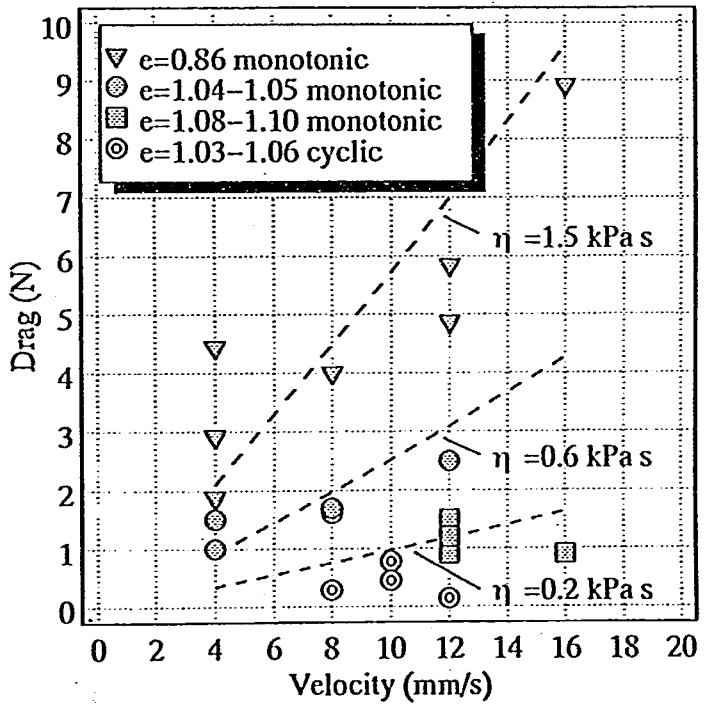



Figure 4 Measured drag of liqued sand and theoretical curves for the indicated viscosities

on an infinite cylinder of a fluid with the same densities and indicated coefficients of viscosity, computed with Lamb's formula (Lamb, 1932).

### 3.2 *Monotonic displacement during shaking*

Under continuous shaking, the excess of pore water pressure was maintained at its maximum, allowing the study of behavior of completely liquefied sand. It was observed that behavior was affected by the direction of shaking. When shaking was applied in the direction of flow (or pipe's displacement), liquefied sand exhibited some residual stiffness. This is shown by the increase in drag in Figure 5(a).

Drag was constant when the direction of shaking was perpendicular to flow, as in Figure 5(b). These observations suggest that inertia (acceleration) of sand particles may induce anisotropy and influence the behavior of liquefied ground.

The drag could be properly assessed only in the second case, when it was constant as in Figure 5(b). For the same conditions (density and velocity), the magnitudes were similar to those of the initial drag obtained from monotonic displacement after shaking.

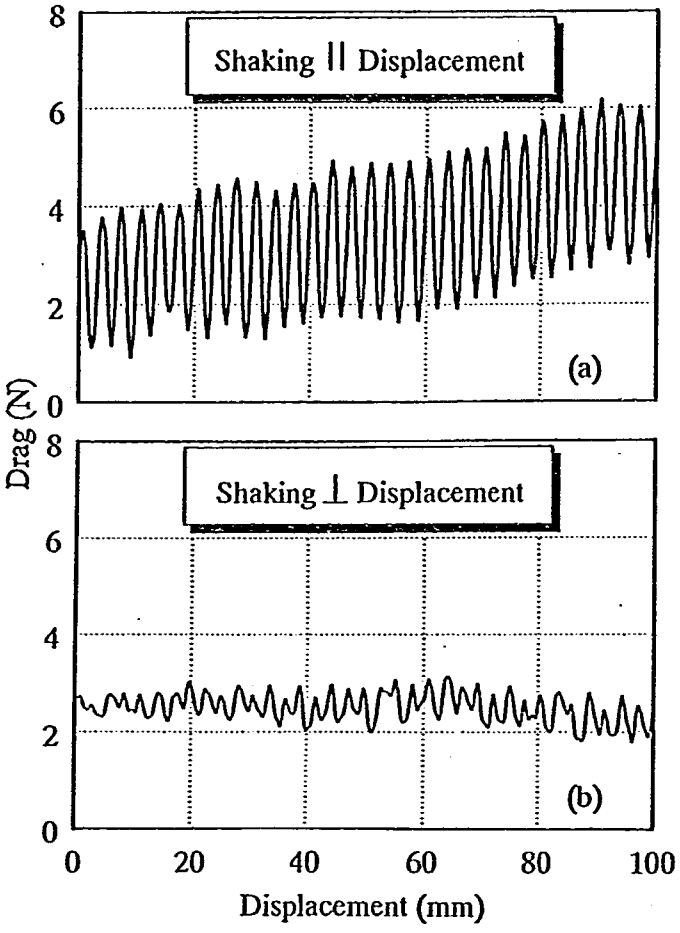



**Figure 5** Drag of liquefied sand under continuous shaking. $e_0$=1.05, V=12 mm/s.

### 3.3 *Behavior in cyclic loading*

Figure 6 shows an example of the measured drag when the pipe was moved cyclically inside liquefied sand undergoing continuous shaking.

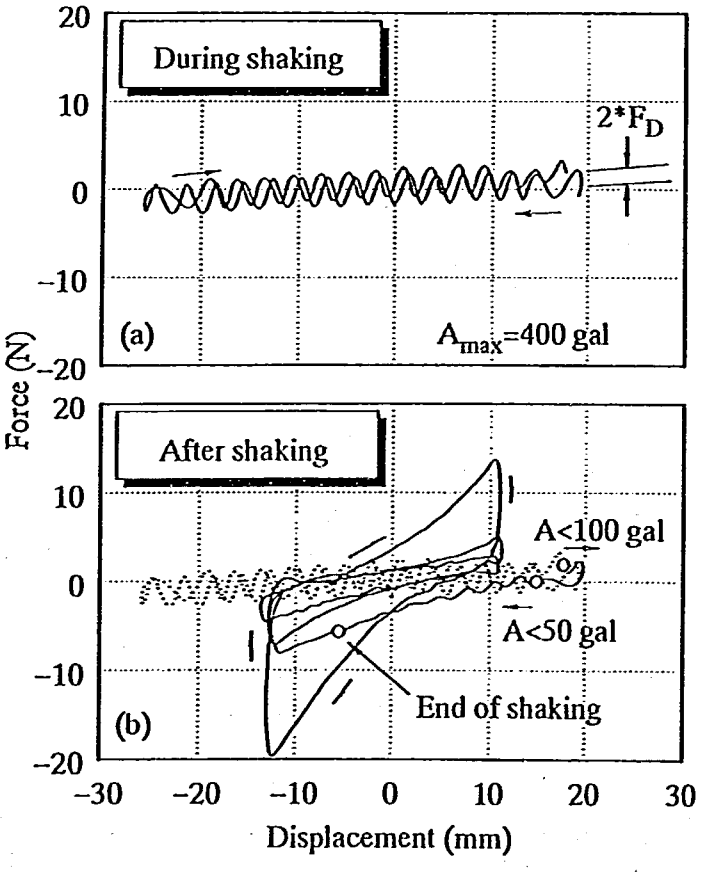



Figure 6 (at right) Behavior of liquefied sand under cyclic loading: during shaking (a) and after shaking (b). $e_0$=1.05, V=10 mm/s.

Like in the previous case, behavior of liquefied sand was influenced by the direction of shaking.

The drag during cyclic motion was taken as half the difference between the average values obtained in two consecutive half-cycles. This is shown schematically in Figure 6(a). The magnitudes of drag computed in this way were compatible with those found when the pipe underwent monotonic displacement, as shown in Figure 4.

Figure 6(b) shows that the behavior of the mass changed and a hardening process started when the amplitude of the input acceleration was reduced below approximately 100 Gals. After that, liquefied soil entered cyclic mobility, with higher values of force and higher rate of pore-pressure dissipation reached on every cycle, at the same displacement.

## 4. CONCLUSIONS

Behavior of flowing liquefied sand in lateral flow could be studied with the use of model pipe tests. The results of the experiments suggested that properties of liquefied soil depended on density, phase and degree of liquefaction and characteristics of loading.

Results of various tests showed that the drag of completely liquefied sand was proportional to the velocity of flow and increased with density. The strain-rate dependent behavior of liquefied sand was interpreted as viscosity and the coefficient viscosity was computed from the measured drag. Its values were in the same range as other reported in literature. The average coefficient of viscosity of liquefied Toyoura sand at 30% of relative density was 1.5 kPa·s.

Movement of the pipe (flow) accelerated the dissipation of excessive pore pressure after shaking stopped and caused the drag to increase steadily in models. This observation suggests that the total stress caused by flowing liquefied ground on buried structures may be the result of a combination of viscous drag and dilatancy. It also suggests that structures inside flowing liquefied ground act as dissipating mechanisms by inducing dilatancy. Therefore, properly set walls or groups of piles could be used as countermeasures against excessive deformations due to lateral flow of liquefied ground.

Test results also show that besides the initial state of the ground (defined by the void ratio and the effective confining stress) the type of dynamic loading and the degree of liquefaction determined the type of predominant behavior. The direction of shaking relative to the direction of flow influenced the behavior of liquefied sand undergoing continuous shaking. Liquefied ground behaved more stiffly when shaking was applied in the same direction as flow (pipe's movement). It was concluded that the inertia of particles induced anisotropy in the behavior of liquefied sand. Lower values of the coefficient of viscosity obtained under continuous shaking also show that dynamic loads affect the behavior of liquefied sand.

## ACKNOWLEDGEMENTS

The Ministry of Education, Science and Culture of Japan (Monbusho) provided financial support for this study. Part of the experimental work was done with the valuable assistance of Mitsuhiro Yao.

REFERENCES

Doi, M. & Hamada, M. (1992); A summary of case studies on liquefaction-induced ground displacements. *Proceedings from the Forth Japan-U.S. Workshop on Earthquake Resistant Design of Lifeline Facilities and Countermeasures for Soil Liquefaction.* Edited by M. Hamada and T.D. O'Rourke. NCEER, Buffalo, N.Y., U.S.A. Vol 1, 115-129.

Ishihara, K. (1993); Liquefaction and flow failure during earthquakes. *Géotechnique.* Vol 43, 2:351-415.

Lamb, H. (1932); *Hydrodynamics.* Cambridge Universtiy Press. Sixth edition.

Orense, R. P. (1992); *Modeling of permanent displacement of liquefied ground and its effects on structures.* Doctoral Thesis. Department of Civil Engineering, University of Tokyo, Japan.

Sasaki, Y., Towhata, I., Tokida, K., Yamada, K., Matsumoto, H., Tamari, Y. & Saya S. (1992); Mechanism of permanent displacement of ground caused by seismic liquefaction. *Soils and Foundations*, Vol. 32, 3:79-96.

Toyota, H. & Towhata, I. (1994); Post-liquefaction ground flow in shaking table tests. *Proceedings from the Fifth Japan-U.S. Workshop on Earthquake Resistant Design of Lifeline Facilities and Countermeasures for Soil Liquefaction.* Preprint.

Verdugo, R. (1992); *Characterization of sandy soil behavior under large deformation.* Doctoral Thesis. Department of Civil Engineering, University of Tokyo, Japan.

# COUNTERMEASURES AGAINST THE FLOATATION OF BURIED PIPES DUE TO LIQUEFACTION

by

Hideo NAGASE, Associate Professor, Kyushu Institute of Technology, JAPAN
Susumu YASUDA, Professor, Tokyo Denki University, JAPAN
Shigeru ITAFUJI, Engineer, Fukken Co.,Ltd, Consulting Engineers, JAPAN
Keiichiro MINE, Graduate Student, Kyushu Institute of Technology, JAPAN

## ABSTRACT

Several shaking table tests were conducted to demonstrate the effectiveness of two types of simple countermeasures to prevent floatation of buried pipes due to soil liquefaction. The countermeasures tested were ①insert a pair of plates or nettings, and ②attach a pair of blades in horizontal direction or vertical direction. Test results showed that the speed of floatation of pipes with the measures were slower than the speed of the pipes without measures, though the excess pore pressure ratio at the bottom of the pipes increased up to 1.0.

## INTRODUCTION

Many manholes and sewage pipes were floated due to liquefaction during the 1993 Kushiro-oki earthquake in Japan. The authors have carried out several shaking table tests under several conditions of soil densities, specific gravitates of pipes, water levels and diameters of pipes, to study the mechanism of the floatation. Tests were also conducted on the model grounds in which a trench was excavated and then backfilled with loose sands. Test results show that the speed and height of floatation are affected by soil densities, specific gravity of the pipes or manhole, water level, and width and depth of the trench. Moreover, it was observed that the soil grains surrounding a pipe moved toward the bottom of the pipe during the floatation.

Then, two types of simple countermeasures against the floatation, which prevent the movement of the soil grains, were developed. And several shaking tests were carried out to demonstrate the effectiveness of the measures.

## TEST METHODS TO STUDY THE MECHANISM AND THE EFFECT OF COUNTERMEASURES

The soil container used was 100cm in length, 70cm in depth and 60cm in width, as shown in Fig.1. A foam rubber of 5cm in thickness was attached to the inside of both walls to induce uniform cyclic shear strain in a soil model during shaking. Very clean Toyoura sand with a mean diameter of 0.175mm was used. A model pipe or box was buried in the model ground as shown in Fig.1. Three piezometer and two accelerographs were installed in the model ground. One piezometer was attached at the bottom of the pipe. The floatation of the pipe was measured by the displacement of a string which was connected to the pipe. Shaking motion was applied in one direction parallel to horizontal axis in Fig.1, at a frequency of 3Hz and with an acceleration of 250gals or 400gals, until the floatation of pipes is terminated.

First of all, several tests were carried out under the following conditions to study the mechanism:

1. Relative density: 0%, 30%, 50% and 70%
2. Type of buried structure: pipe and box(10cm in width)
3. Diameter of pipes: 6.0cm, 11.4cm and 16.5cm
4. Specific gravity of pipes: 0.5, 1.5, 1.7, 1.8 and 1.9
5. Specific gravity of the box: 1.0
6. Water table: GL-0cm and GL-15cm
7. Acceleration of shaking: 250gals and 400gals

Then, several tests were carried out to study the effect of liquefaction of backfill soil under following test conditions, by using the model shown in Fig.2:

1. Relative density of backfill soil: 30%
2. Relative density of the surrounding ground: 90%
3. Type of buried structure: pipe(11.4cm in diameter) and box(10cm in width)
4. Specific gravity of the pipe: 0.75
5. Specific gravity of the box: 1.0
6. Width of a trench: 20cm, 25cm, 30cm and 90cm
7. Depth of a trench: 35cm, 40cm, 45cm and 50cm
8. Permeability of the boundary between a trench and surrounding ground: impermeable and permeable
9. Water table: GL-0cm
10. Acceleration of shaking: 250gals

The following test conditions were selected to study the effect of countermeasures:

1. Relative density: 30%
2. Types of countermeasures: plates, wire nettings and blades(shown later)
3. Type of buried structure: pipe(0.5 or 1.5 of specific gravities)

4. Diameter of a pipe: 6.0cm and 11.4cm
5. Water level: GL-0m
6. Acceleration of shaking: 250gals

## BRIEF REVIEW OF THE TESTS TO STUDY THE MECHANISM AND EFFECT OF LIQUEFACTION OF BACKFILLED SOIL

Based on the first tests to study the mechanism of floatation, the following main conclusions were derived (Yasuda et.al., 1995):

1. The speed of floatation decreased with soil density, diameter of the pipe, the specific gravity of the pipe and water level.
2. The speed of floatation increased with the acceleration of shaking, namely severity of liquefaction.
3. The speed of floatation was not constant during the floatation in low-density soil and with pipes of low specific gravity as shown at the upper position in Fig.3 and 4. Arrows in these figures show the movement of soil grains, measured by the displacement of chips of noodles installed between soil and front glass, during the floatation. As shown in these figures, the soil grains upper and below the pipe moved to up, and the soil grains right and left sides of the pipe moved toward the bottom of the pipe. It is noted that the soil grains 30cm far from the pipe moved also toward the bottom of the pipe.

According to the test results for the study on the effect of liquefaction of backfill soil, following conclusions were derived (Yasuda et.al., 1995) :

1. The speed and the maximum height of floatation increased with the width of a trench. as shown in Fig.5.
2. The speed and the maximum height of floatation also increased with the depth of a trench as shown in Fig.6.
3. If the boundary between a trench and surrounding ground is permeable, excess pore pressure increased in the backfill soil dissipated to the surrounding ground and the pipe was not floated.

## RESULTS OF TESTS TO STUDY THE EFFECT OF COUNTERMEASURES

Several measures have been developed to prevent the occurrence of liquefaction or liquefaction associated floatation. Those are densification method, gravel drain method, and pile supporting method. As these methods are expensive and hard to apply the existing buried pipes, simple methods which are economic and applicable for existing pipes were derived.

The simple methods studied were :①insert a pair of plates or screens, and ②attach a pair of blades in horizontal direction or vertical direction. In the first methods, a pair of wooden plates or wire nettings were inserted as shown in Fig.7. The width of the plates or nettings changed from 12cm to 30cm. The diameter of the pipe was 11.4cm. Figures 8 and 9 show the test results for the wooden plates and wire nettings, respectively. The speed and the maximum height of floatation decreased with the decrease of the width of plates or nettings, though excess pore water pressure ratio at the bottom of the pipe increased up to 1.0. Figures 10 and 11 show the movement of soil grains in both tests. The soil grains outer the plate could not move to the bottom of the pipe in the case of wooden plates. As shown in Fig.11, the soil grains outer the netting slightly tended to move toward the bottom of the pipe due to the flow of water, however, the movements were prevented by the nettings. These results imply that the movements of soil grains toward the bottom of the pipe are necessary for the floatation of the pipe, though the excess pore water pressure ratio increased up to 1.0. Anyway, the driving of sheet piles or something geotextile may be effective for the floatation of buried pipes.

In the second methods, a pair of blades were attached in horizontal direction or vertical direction as shown Fig.12. The length of the blades changed from 2.5cm to 20cm. Figures 13 and 14 show the test results for the horizontal blades and the vertical blades, respectively. The speed and the maximum height of the floatation decreased with the length of blades. And the horizontal blades were more effective than the vertical blades. Figures 15 and 16 show the movements of soil grains. The movements of soil grains surrounding the pipe were slightly prevented by attaching the blades.

## CONCLUSIONS

Shaking table tests were carried out to study the effect of two types of simple countermeasures to prevent the floatation of a buried pipe due to liquefaction. The following conclusions were derived based on the tests:

1. Driving of sheet piles or geotextiles beside an existing buried pipe may reduce the floatation of the pipe even liquefaction is induced in the ground.
2. A pair of blades attached to a pipe may reduce the floatation of the pipe even liquefaction occurs in the ground.

As the conclusion was derived from only the model tests, more study must be necessary for the application of these methods.

## REFERENCE

Yasuda, S., Nagase,H., Itafuji,S, Sawada,H. and Mine,K. : A Study on the Mechanism of the

Floatation of Buried Pipes due to Liquefaction, Soil Dynamics and Earthquake Engineering, pp.125-132, 1995.

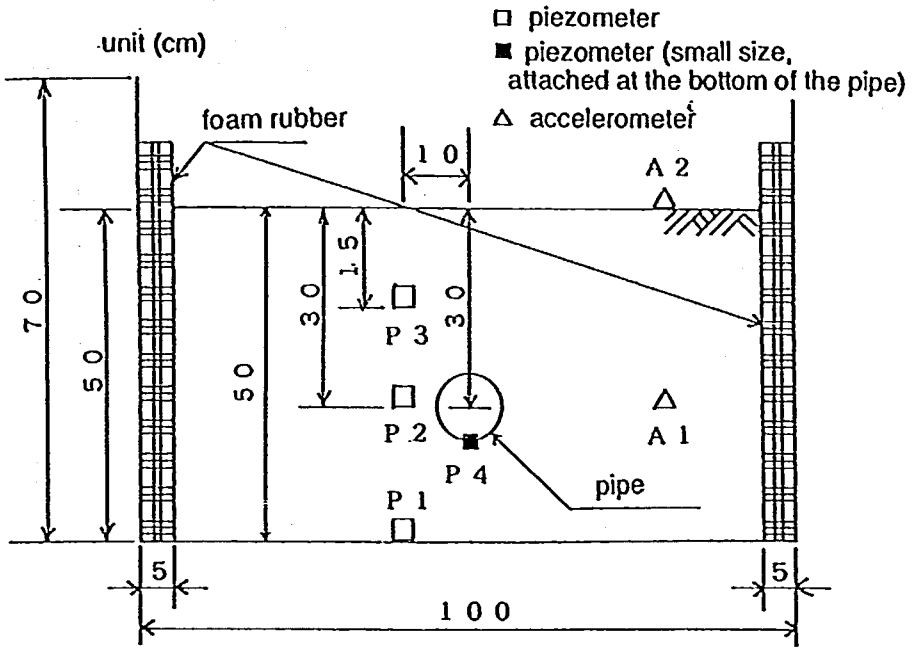



Fig.1 Diagram of apparatus for shaking table test

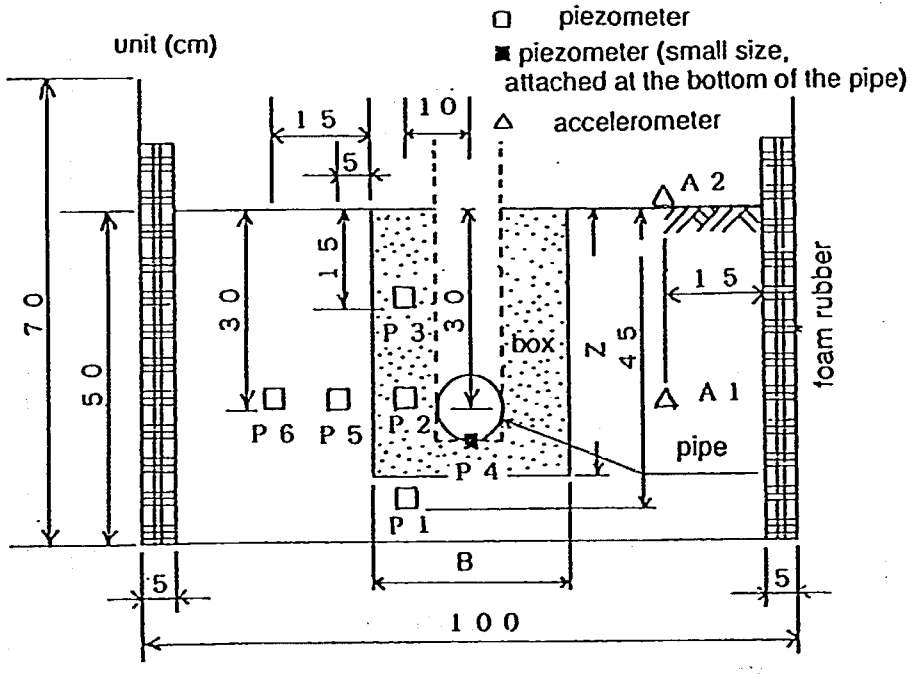



Fig.2 Diagram of apparatus for tests on the effect of backfill soil

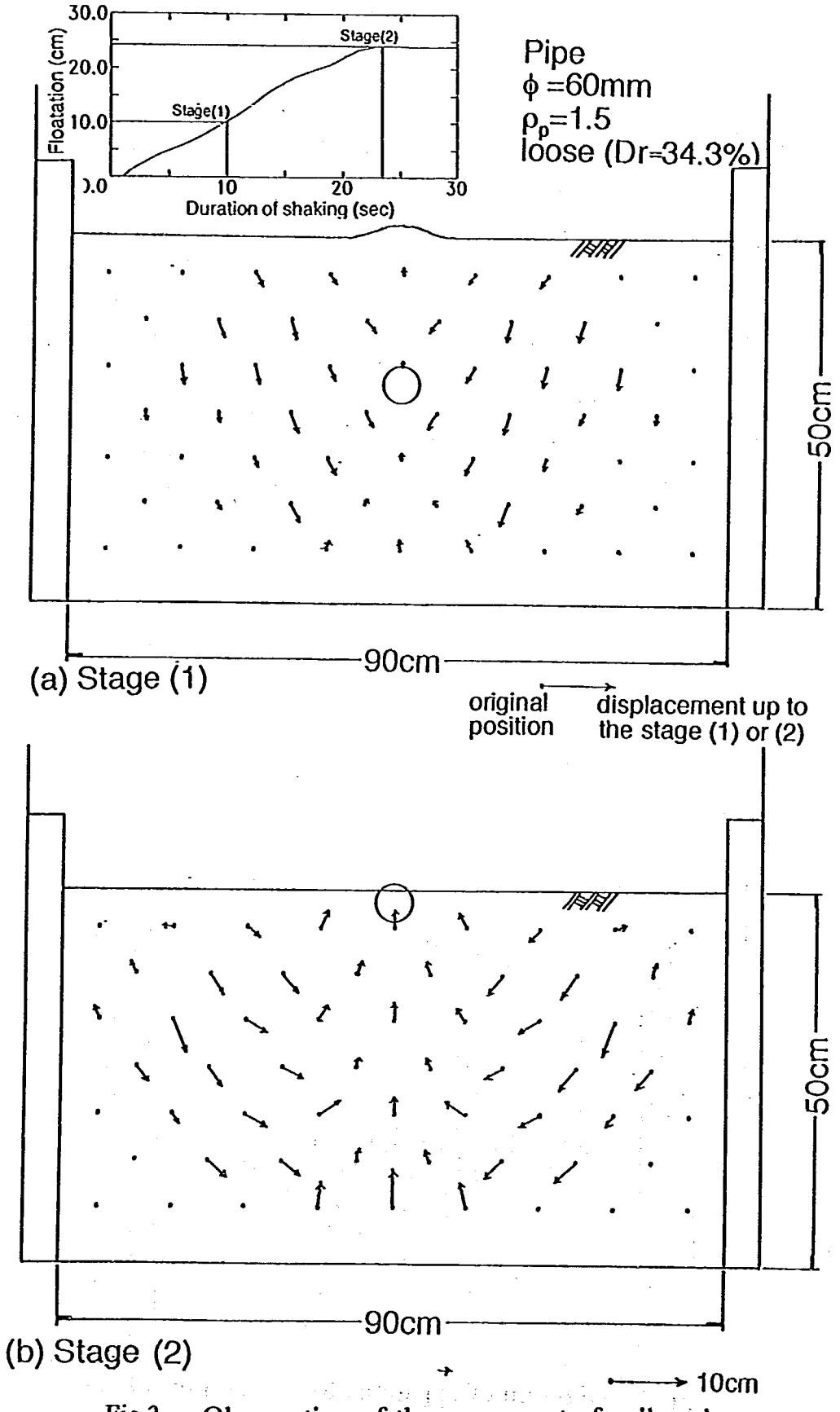



Fig.3 Observation of the movement of soil grains during the floatation of a buried pipe ($\phi$=60mm, $\rho_p$=1.5)

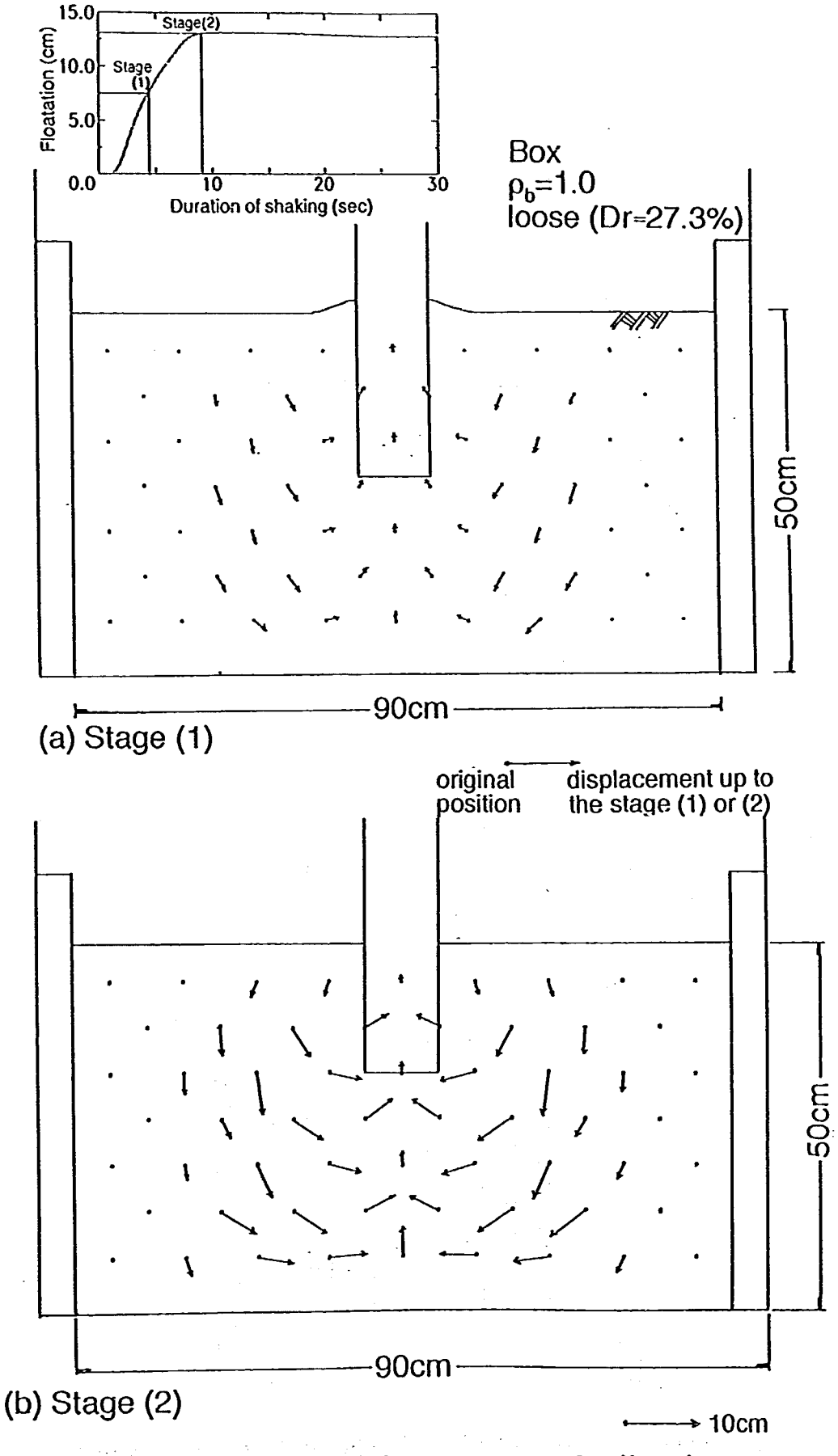



Fig.4 Observation of the movement of soil grains during the floatation of a buried box (width of the box is 35cm, $\rho_b$=1.0)

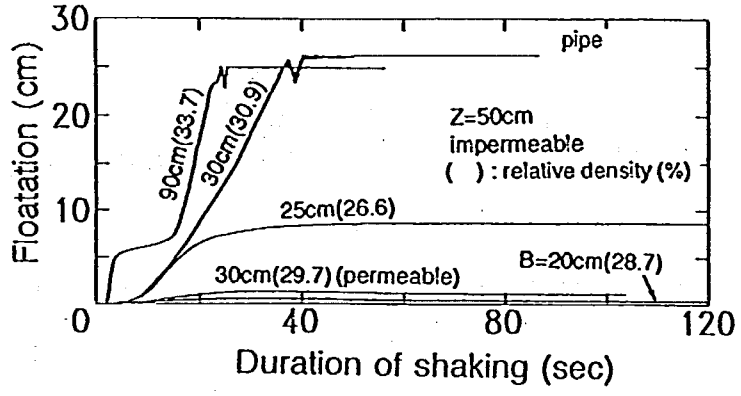



Fig.5 Effect of the width of a trench on the floatation of a pipe

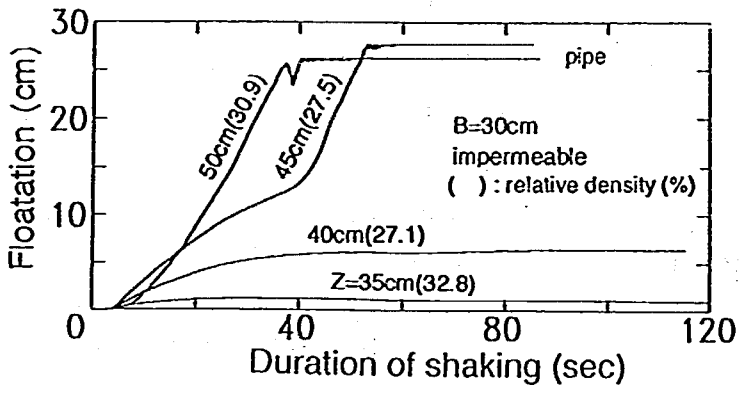



Fig.6 Effect of the depth of a trench on the floatation of a pipe

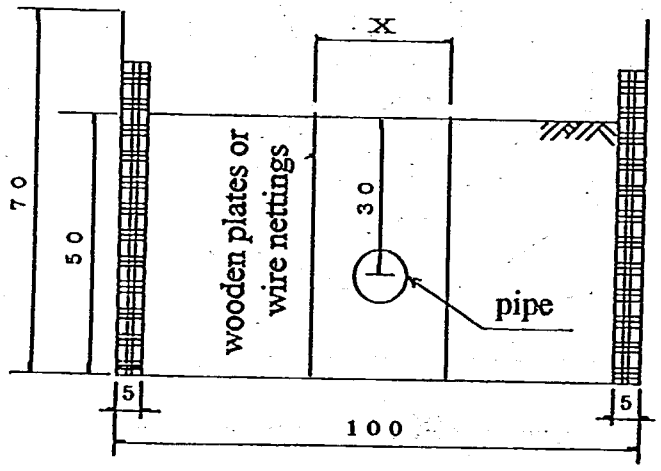



Fig.7 Countermeasures by a pair of wooden plates and wire nettings

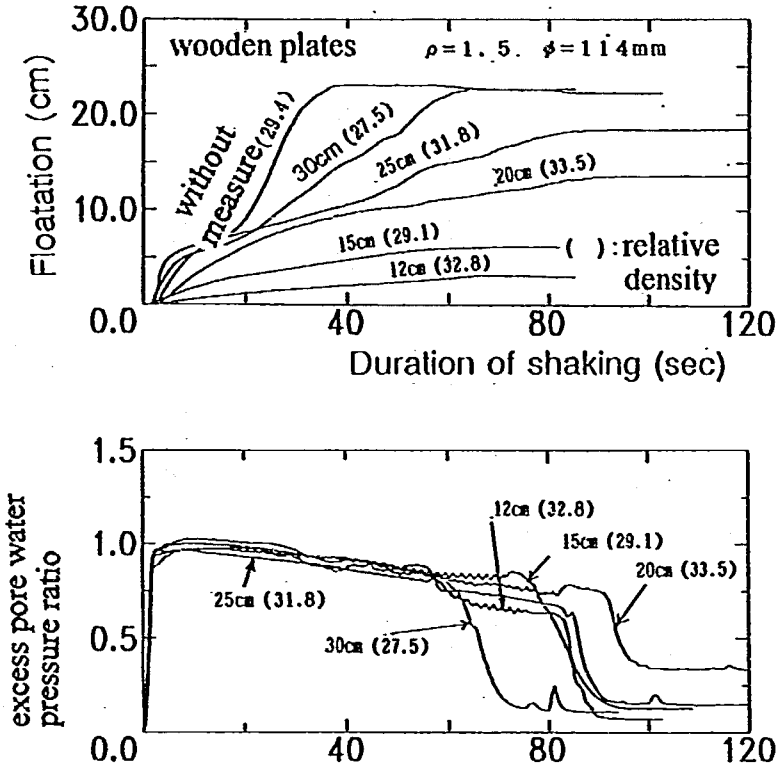



Fig.8 Test results for wooden plates

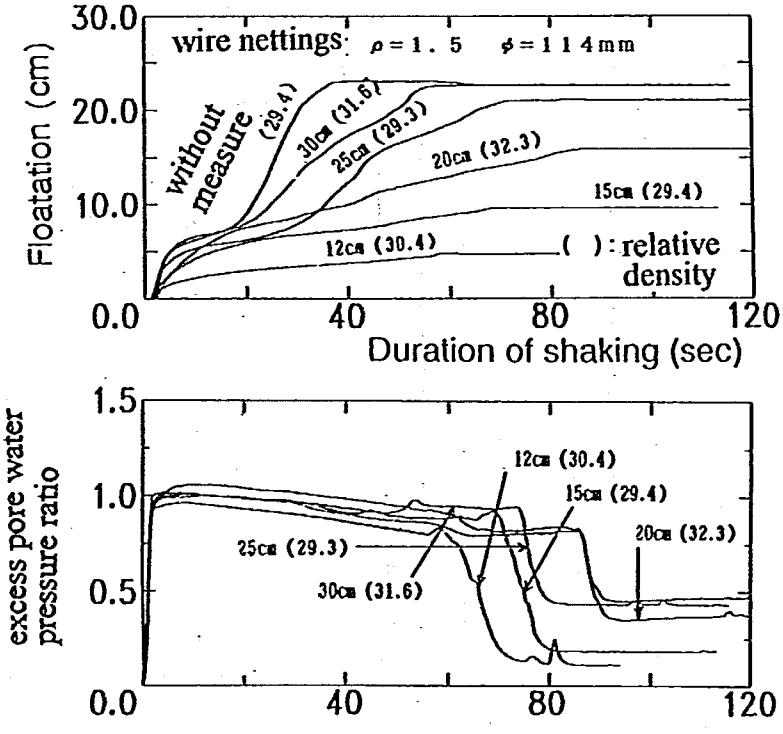



Fig.9 Test results for wire nettings

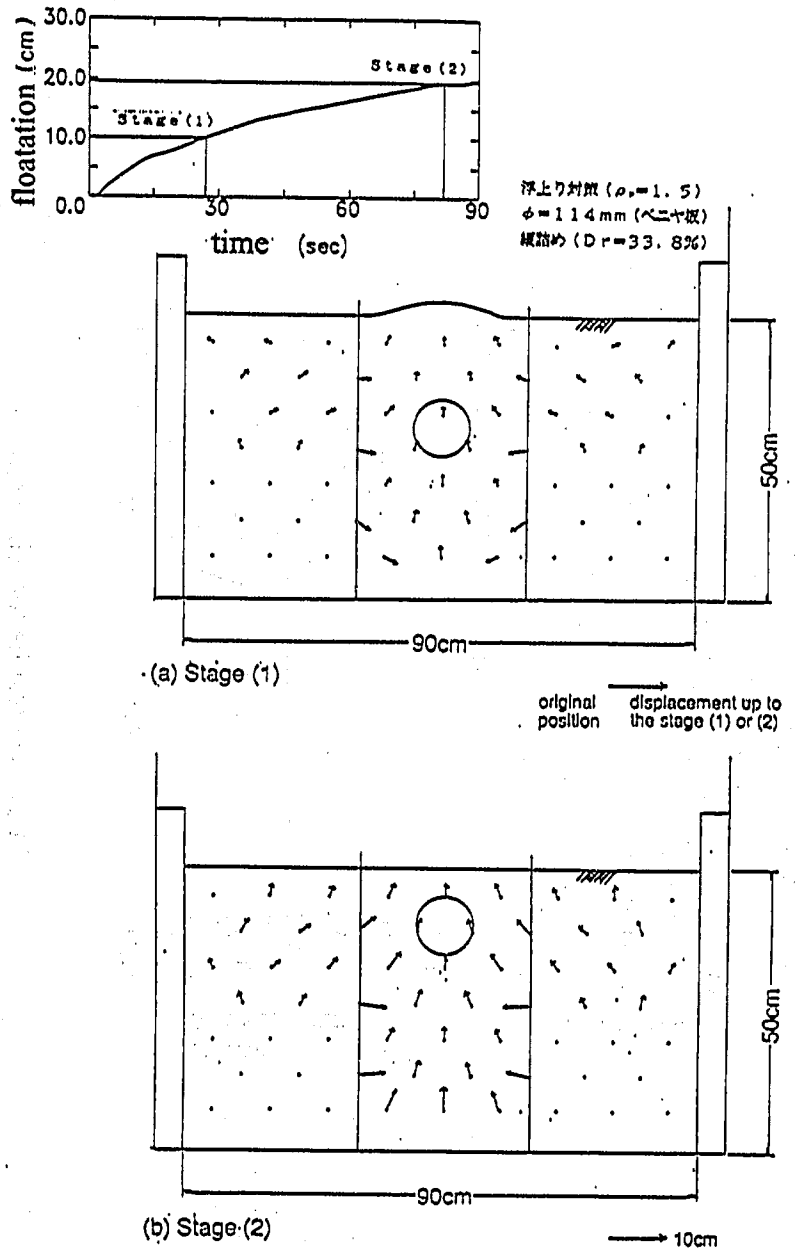



Fig.10 Movements of soil grains (wooden plates)

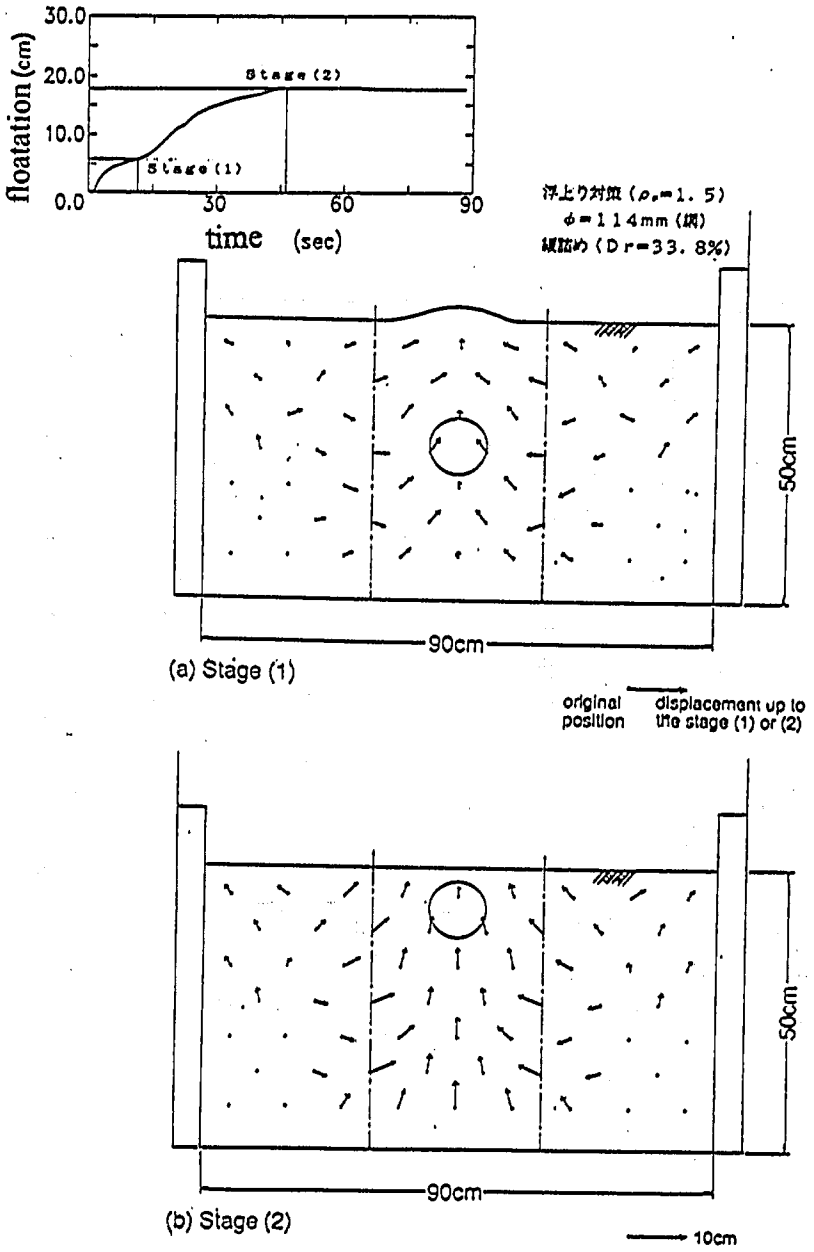



Fig.11 Movements of soil grains (wire nettings)

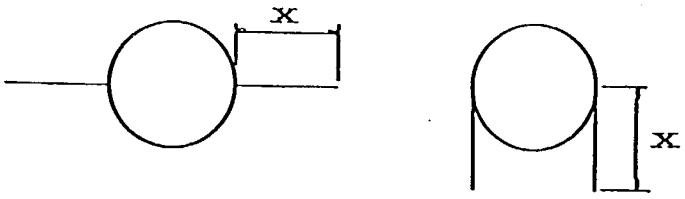



Fig.12 Models of attaching blades

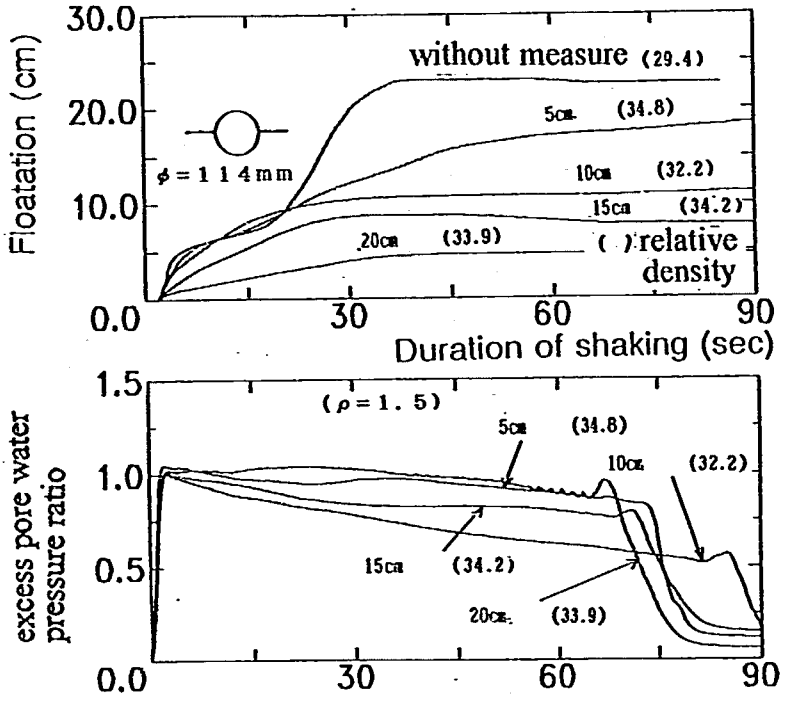



Fig.13 Test results for horizontal blades

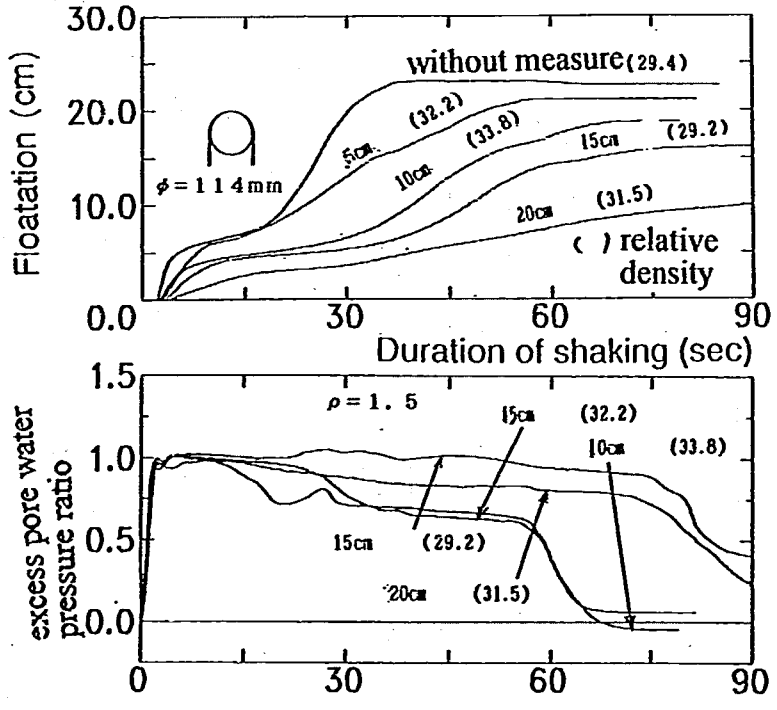



Fig.14 Test results for vertical blades

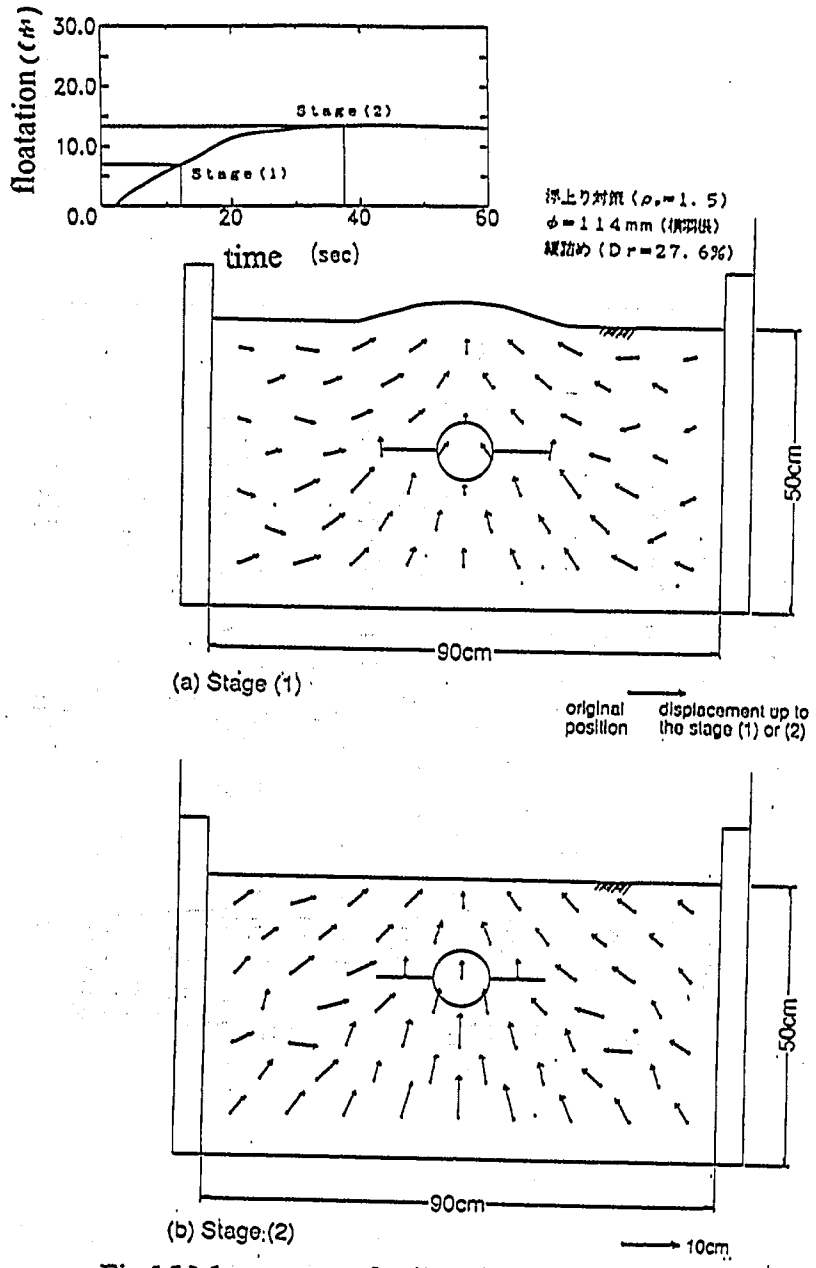



Fig.15 Movements of soil grains (horizontal blades)

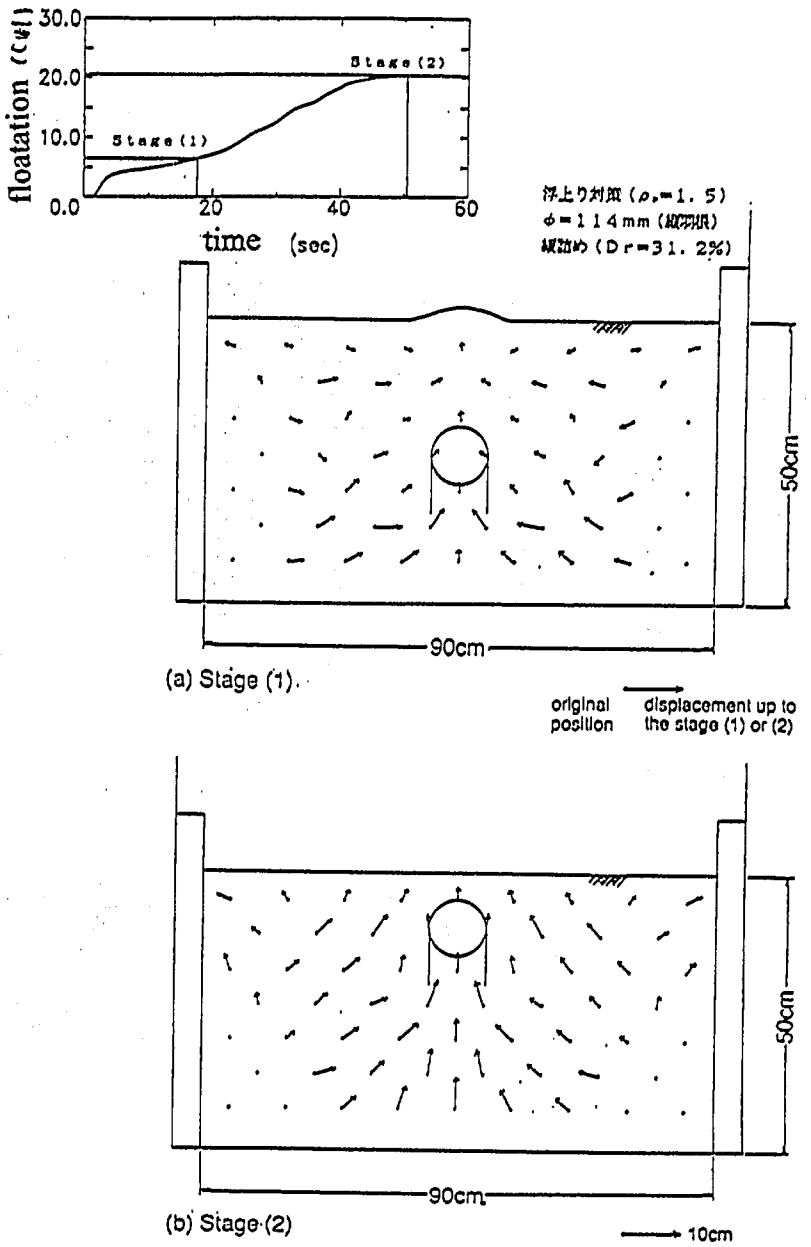



Fig.16 Movements of soil grains (vertical blades)

# DEPENDENCE OF LONGITUDINAL SUBGRADE REACTION TO THE BURIED PIPE ON DISPLACEMENT VELOCITIES AND CYCLES OF THE GROUND

Mio KOBAYASHI
Hirokazu ANDO
Noritake OGUCHI

Fundamental Technology Research Laboratory, Tokyo Gas Co., Ltd.,
Minato-ku, Tokyo, 105, Japan

## ABSTRACT

Subgrade reaction is an important factor to analyze behavior of buried pipelines. It has generally been considered that the subgrade reaction is in proportion to the amount of one directional movement. However, strong earthquake occurs with large cyclic deformations. It should, therefore, be considered that effect of displacement velocity and cycles to subgrade reaction are taken into account. Shaking table test was carried out to examine the effect. The main conclusions are as follows.

In case of the plastic coated steel pipes of 150 and 300 mm diameters, there was no considerable dependence of longitudinal subgrade reaction on displacement velocity and cycles. No differences were observed in the result of the subgrade reaction regardless of different shaking conditions or the pipe diameters. The subgrade reaction reached its upper limit in the extent of the minimal displacement even in any shaking condition.

## INTRODUCTION

To understand how buried pipes move during an earthquake, it is necessary to estimate the precise displacement of the buried pipes caused by heterogeneous movements at the ground. In estimation, we can calculate the interaction between the ground and pipes by using the subgrade reaction, that represents the spring-constant between the ground and pipes. When the relative displacement is minimal even in the reciprocal actions of the pipes and the ground, the subgrade reaction and the deformation of the ground in the vicinity of the pipes give a linear relationship. If the reciprocal actions are larger, slippage may occur between the ground and the pipes. In such the case we must consider the non-linearity in the deformation of the ground around the pipes.

We have therefore hypothesized what would happen during a large earthquake and have conducted an experiment using a shaking table to establish an evaluation method of the subgrade reaction. The method is based on the non-linearity of the subgrade reaction in the axial direction caused by relative displacement, relative velocity in cyclic mode. This report discusses results of the experiment.

## THE EXPERIMENT

Concept The subgrade reaction that acts on the pipes in the axial direction is produced by the different displacements of the ground and the pipes. Figure 1 illustrates this behavior.

Traditional idea was to assume a linear model, where the subgrade reaction increases with the relative displacement, rather than to consider the non-linear behavior. Lot of experiments have, however, assured that subgrade reaction reaches an upper limit and the critical displacement appears at that limit. There have also been experiments where this relationship is approximated by a bi-linear model for practical design.

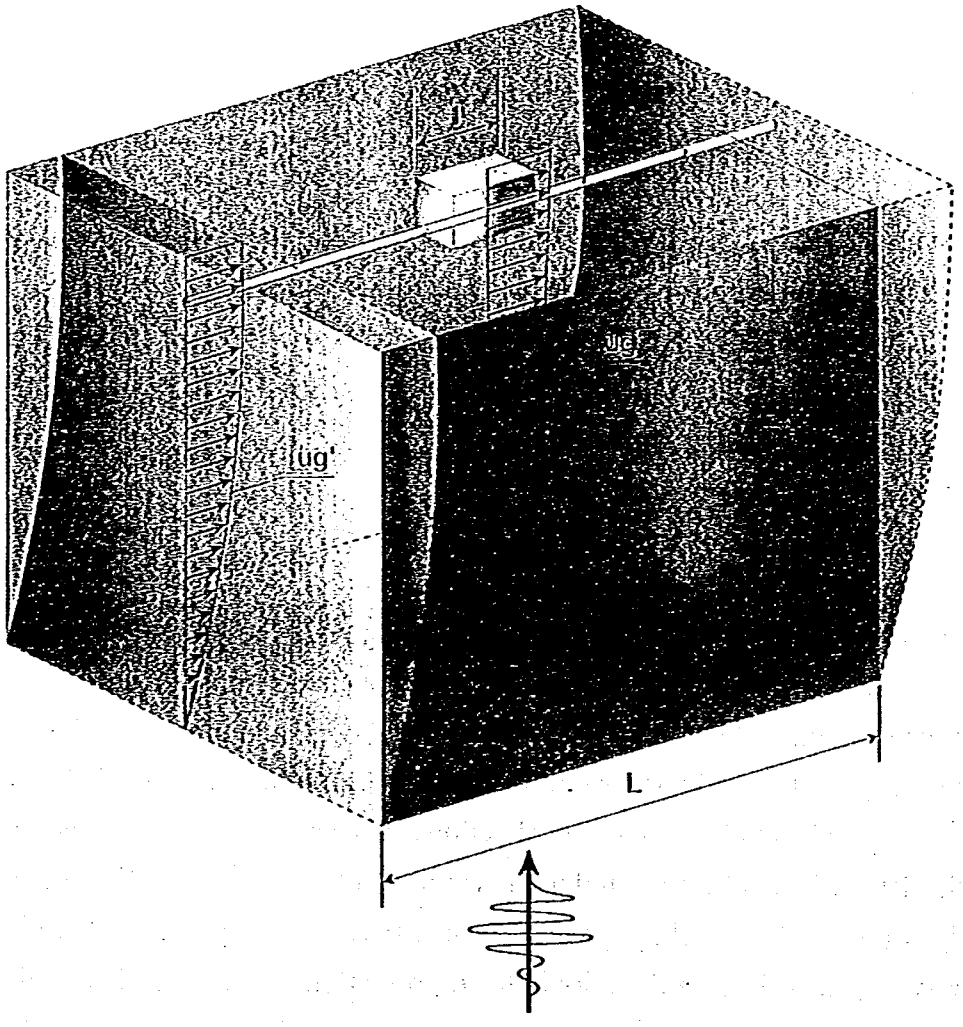



Figure 1 Concept of this experiment.

To evaluate the subgrade reaction more realistically, the relative velocity, the confined pressures and the cyclic effects of subgrade reactions must be taken account into the calculations in addition to the relationship of the subgrade reaction and the relative displacement. Generally, we can define the subgrade reaction ( $\tau_p$) as the function given in equation (1).

$$\tau_p = f(\delta, V, N, \sigma_g) \quad (1)$$

In this equation, $\delta = u_g - u_p$, where $u_g$ and $u_p$ denote displacements of the ground and the pipe respectively. V is the relative velocity, N is the number of cycles of the subgrade movement, and $\sigma_g$ is the confined pressure of the ground, The $\sigma_g$ acts in the normal to the pipe and varies depending on the type of subgrade together with the direction of the ground displacement, the depth of the buried pipe, and the conditions of the pipe surface. All the factors, of course, are time dependent.

In our experiment, we paid close attention to how $\delta$, V and N affect the subgrade reaction of the ground. We set conditions so that the subgrade reaction would remain constant.

There have been several experimental reports concerned about the relative velocity and the factor of the cyclic ground movement. These experiments have, however, been insufficient because most of them have been examined in the range of 10 ke. There were some unreliabilities —— in their experiment such as inaccurate measurement of $\delta$ associated with use of the pipe of long length and influence of the inertial force on the pipe.

To evaluate the subgrade reaction accurately, we realize the conditions like Figure 1 as precisely as possible. We conducted an experiment of a sand container using a shaking table. There is a pipe of small diameter in the container so that the factor of pipe elongation could be ignored.

Apparatus We made the apparatus shown in Figure 2, and equipped measurement system. We conducted the experiment using a steel sand box of 1.2m depth, 1.8m length, and 1.9m width. We then buried steel pipes coated of polyethylene at a depth of 1.2m. Sand was compacted at the rate of higher than 95%. The characteristics of the sand are given in Table 1. Sort of the sand was usually used for backfilling, and we buried the pipe at the standard depth. The compatibility of the sand was slightly excessive; nevertheless, we accepted this compatibility to be on the conservative side. Thus, the subgrade reaction was indeed dependent on the ground confined pressure because the subgrade reaction can be formulated by the following equation (2).

We used steel pipes of two different diameters: The first was 300mm (outer diameter Do = 318.5mm, wall thickness t = 6.9mm); the second was 150mm (outer diameter Do = 165.2mm, wall thickness t = 5.0mm).

To keep the confined pressure $\sigma_z$ constant, we increased the rigidity of the sand box to prevent relative displacement of the sand. And we didn't set any apparatus such as place rubber on the inside of the box.

To evaluate precisely the subgrade reaction in the axial direction, the pipes were laid horizontally. For preparatory measurement, we got horizontal displacements many times and set up the experiment so that the pipe was horizontal at an accuracy of 1mm or less. We measured the acceleration in the direction of Z, and also checked the horizontality of the pipes.

In the experiment, we first attached a load cell to either end of each pipe which was fixed to the reaction wall, and then produced relative displacement between the ground and the pipe by shaking the box. We set up the pipe fixing rig and other equipment paying close attention so that there would be no shifting of the rig in its fastened location or no locking of the shaking box in a direction of Y & Z.

As be shown in Figure 2, we placed a velocimeter, displacement meters and accelerometers in the sand box. We glued 24 strain gauges on the internal surface of each pipe at every 45 degrees circumferencially, and then coated them with a polyethylene material. We then measured the subgrade reaction by the load cell. All dynamic measurements were recorded at 0.01-second intervals.

Table 1 Properties of sand

| Gs | Gravel(%) | Sand(%) | Silt,Clay(%) |
|---|---|---|---|
| 2.72 | 0 | 96 | 4 |
| Uc | Wopt(%) | C(kgf/cm2) | $\phi$(deg) |
| 2.1 | 20.9 | 0.22 | 36.66 |

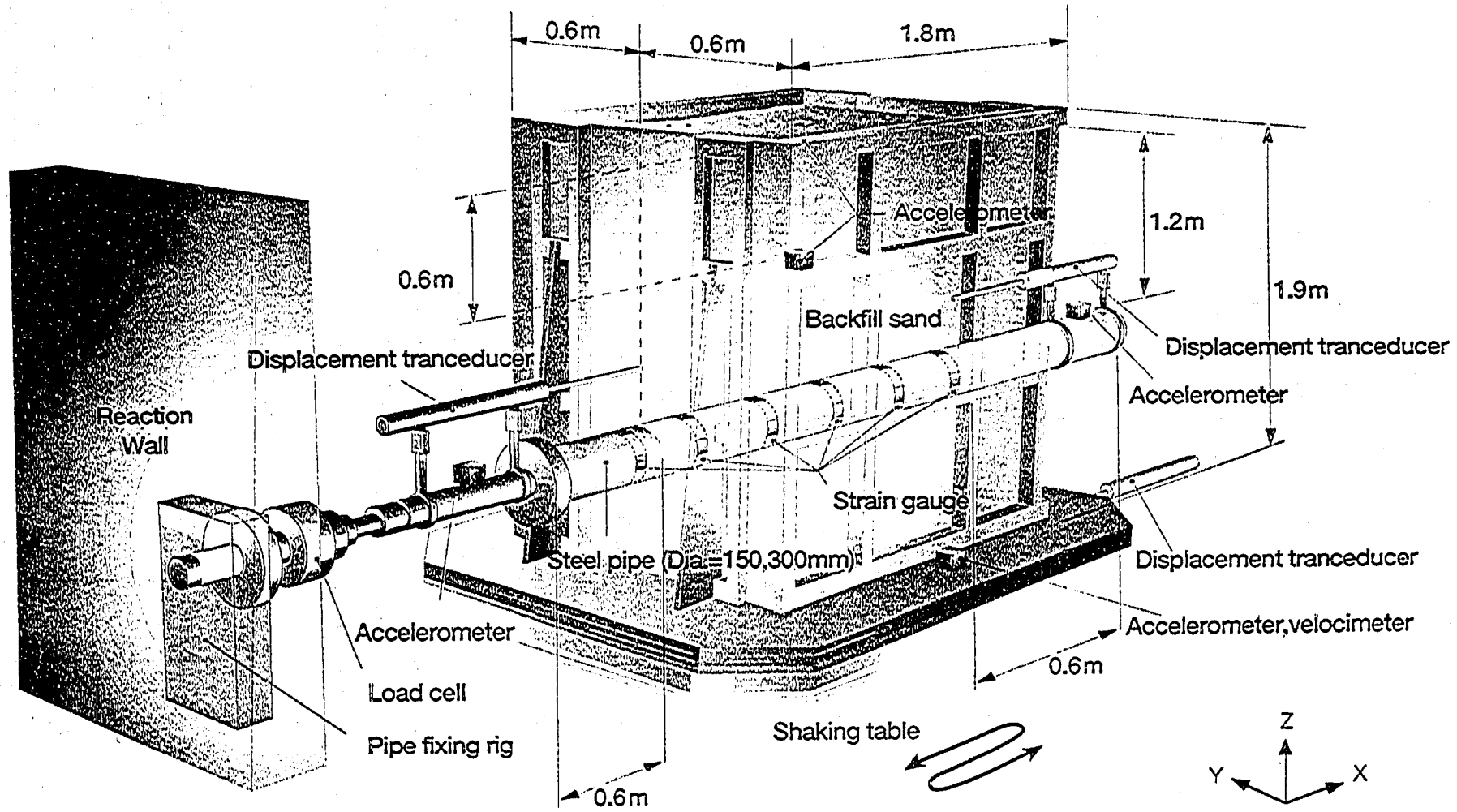



Figure 2 Experiment Devices

Shaking Conditions Table 2 shows the shaking conditions. During this investigation, we focused on the effects of the relative velocity (V), and the effects of cyclic ground movement on the subgrade reaction. We determined the influence of the relative velocity by changing the maximum velocity into 3 steps;- 50 ke, 5 ke, and quasi-static 0.5 ke. This change was made by sine waves with a constant displacement amplitude. We examined the effects of slow change of the amplitude together with that of a random amplitude during actual earthquakes. According to three different experiments of the limited velocity, a constant amplitude and a variable amplitude, we understood that the characteristics of subgrade reaction appeared cyclically under various conditions.

We set the maximum amplitude of the tapering waves at 10mm and 100mm. As the waves of an actual earthquake, we selected the wave of NS directional components (maximum acceleration Amax = 258gal.) that was observed on the first floor of a building at Tohoku University during the Miyagiken-Oki Earthquake in 1978, and the wave of NS directional component (maximum acceleration Amax = 818gal.) that was observed at the Kobe Kaiyo Meteorological Observatory during the Southern Hyogo Earthquake in 1995.

Both of these earthquakes caused immense damage to buried pipes, including gas pipelines. To reproduce the motions of both earthquakes as precisely as possible, we utilized a reproduction control system in the shaking table. As a result, we achieved wave forms with a maximum velocity of about 36 ke and a maximum displacement of 110mm for the Miyagiken-Oki earthquake, and 76 ke and 120mm for the Hyogo earthquake. Both the velocity and the displacement of the waves of the actual earthquakes are different from those produced in the experiment. We however, judged, that this was acceptable for determining the subgrade reaction under the critical conditions, and used these conditions unchanged.

We set the confined pressure( $\sigma_s$ ) as a constant. In order to confirm this condition, we set up accelerometers in both the horizontal and vertical directions at the top and bottom of the ground. The conditions seemed to be satisfied because the observed values through this experiment varied little, like the behavior of rigid body was exhibited.

Table 2 Testing condition

| Testing condition | Number of cases | | Remarks |
|---|---|---|---|
| | 300A | 150A | |
| 50kine | 2 | 4 | 1Hz of sine wave ,Maximum100mm. Including the cases which conducted from compression side and after 25days. |
| 5kine | 1 | 2 | 0.1Hz of sine wave ,Maximum100mm. |
| 0.5kine | 1 | 2 | 0.01Hz of sine wave ,Maximum100mm. |
| Tapering wave | 2 | 2 | |
| Miyagiken-Oki Eq. | 1 | 2 | |
| Southern Hyougo Eq. | 1 | - | |

## EXPERIMENTAL RESULTS

Dependency of Velocity and Comparison of Shaking Conditions It is necessary to compare the subgrade reaction under various shaking conditions while paying attention to its dependency on ground velocity. The subgrade reaction is given as F/ $\pi$ DL, where F is measured by the loadcell.

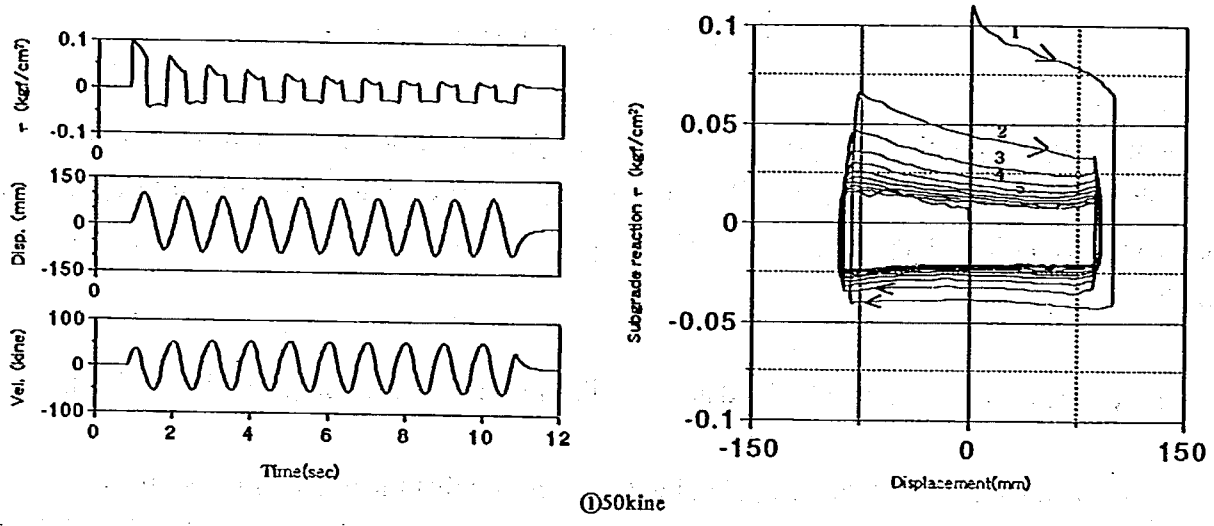
Figure 3 shows the results obtained at three different the maximum ground velocities.

Even when we changed the ground velocity, we found that the value of the subgrade reaction remained nearly the same. This force was not dependent on the diameter of the pipe. We also found that the subgrade reaction reached its upper limit with minimal relative displacement ( $\delta$ ).

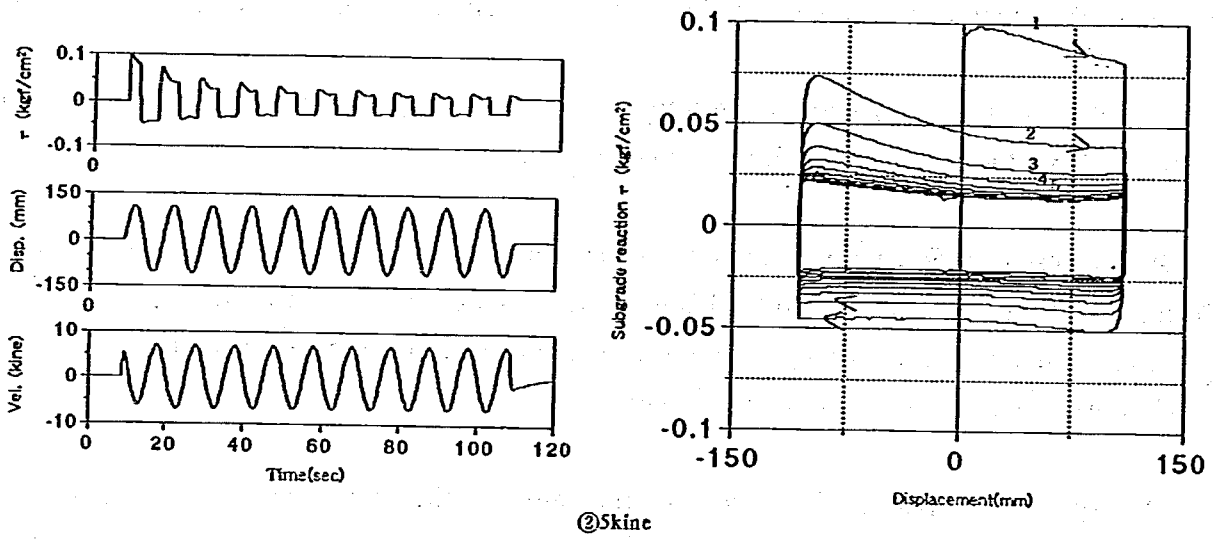
The results of the experiment at the slow change of the displacement amplitude are given in Figure 4. Only the results of the 300mm-diameter pipe is shown.

Due to these results, we assured that the subgrade reaction reached its upper limit at minimal displacement. This was understood to be no relation to the degree of the critical displacement $\delta_a$ because there were no differences found in behavior even during experiments which set the maximum displacement as 10mm and 100mm.

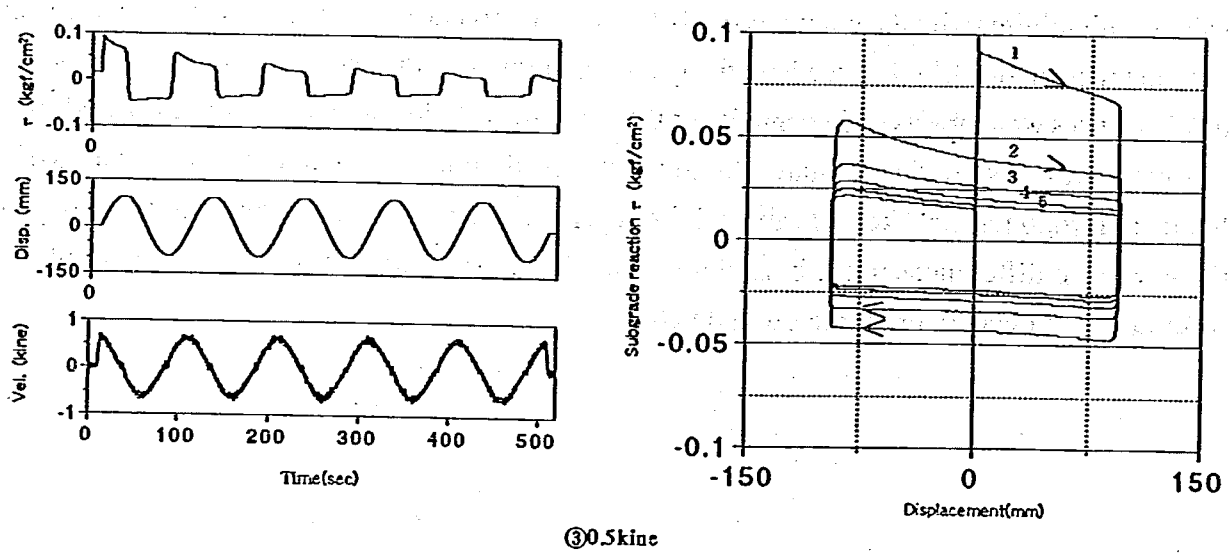
The experimental results obtained using the values of the actual seismic waves are given in Figure 5. When tapering waves were applied, the subgrade reaction was found to reach critical values with minimal displacement as well. There were no particular differences in this tendency even in the main displaced area where the greater amplitude of displacement appeared. Moreover, no differences were observed in behavior of the subgrade reaction associated with the two different seismic waves. As previously stated, although the maximum velocity of the seismic waves of the Southern Hyogo Earthquake were about 2 times greater than that of the Miyagiken-Oki earthquake, there were no differences in the behavior of the subgrade reaction. It is convinced that subgrade reaction is not dependent on the ground velocity.




①50kine



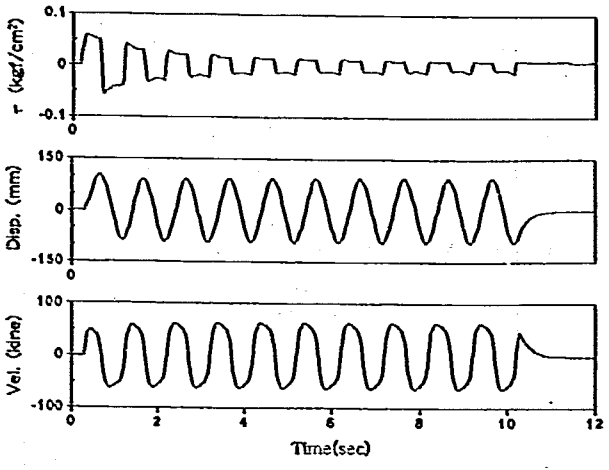

②5kine

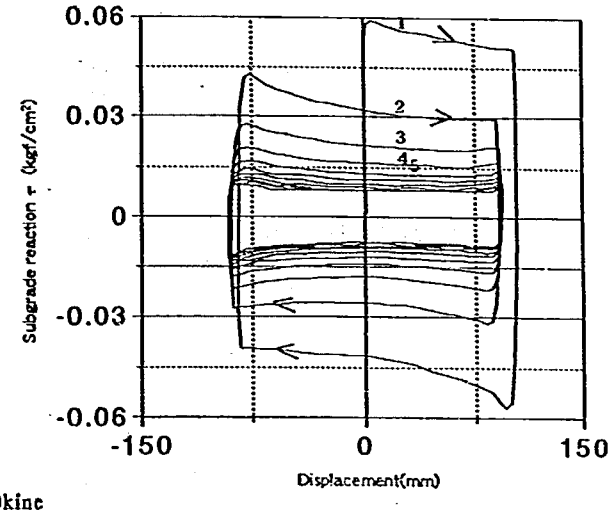



③0.5kine

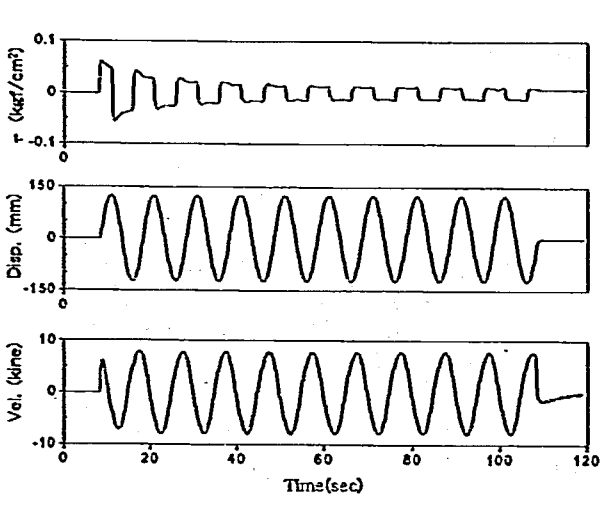
a) 300A

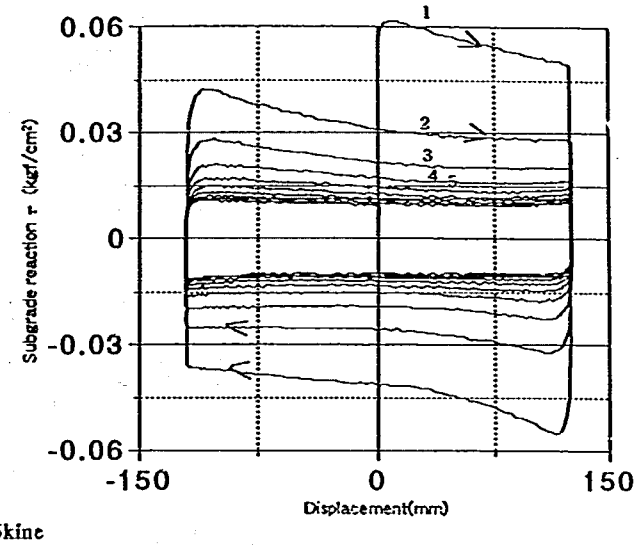
Figure 3-1 Influence of relative velocity



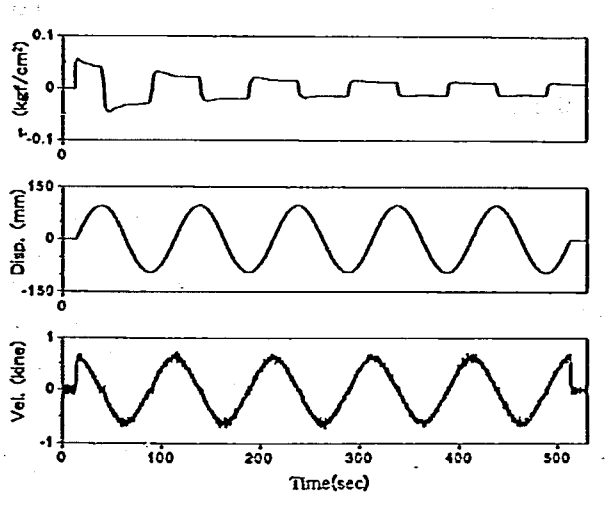



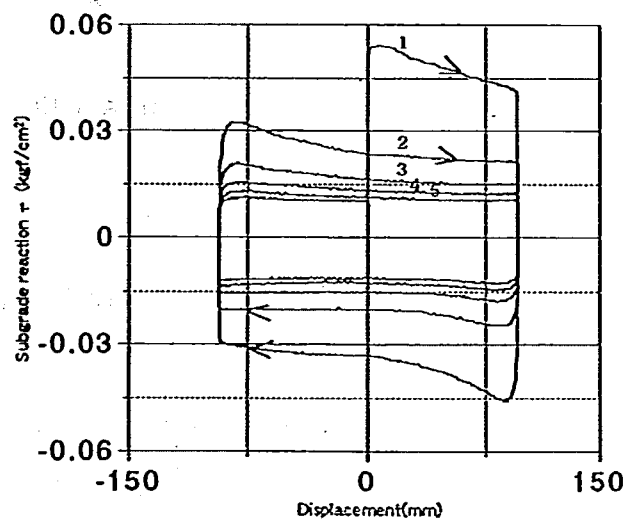

①50kine




②5kine

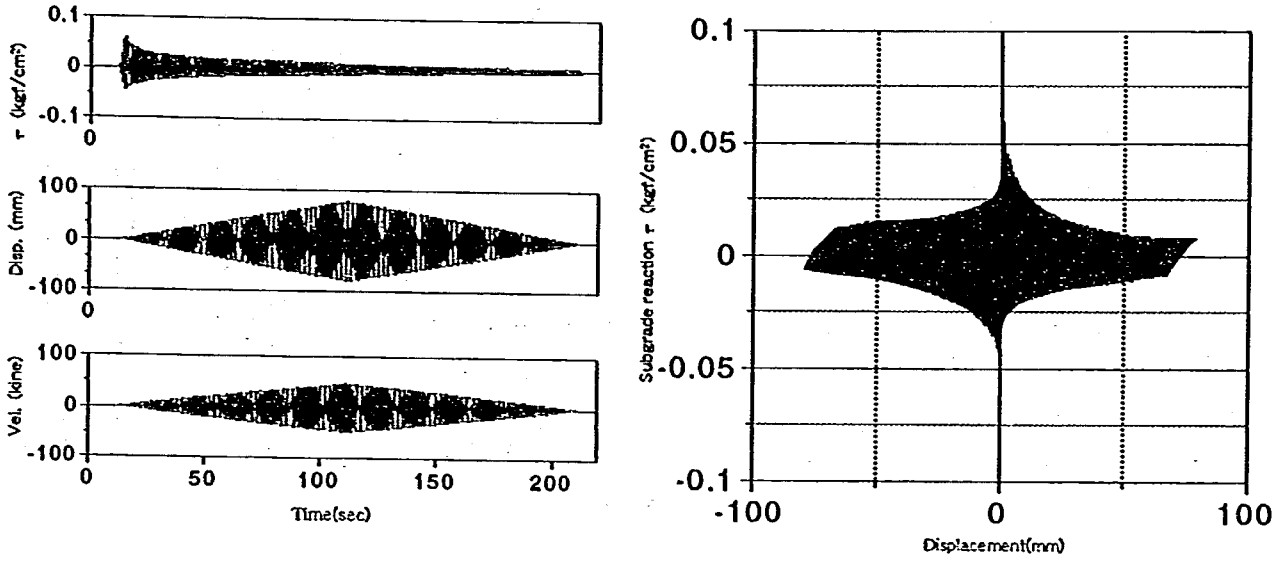


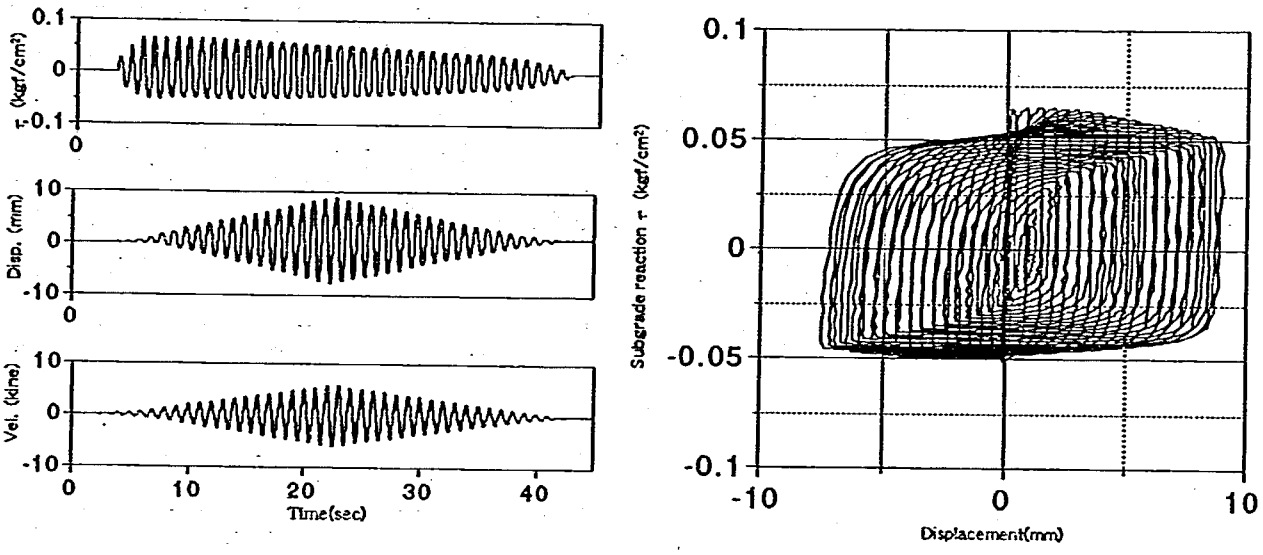

③0.5kine

b) 150A

Figure 3-2 Influence of relative velocity

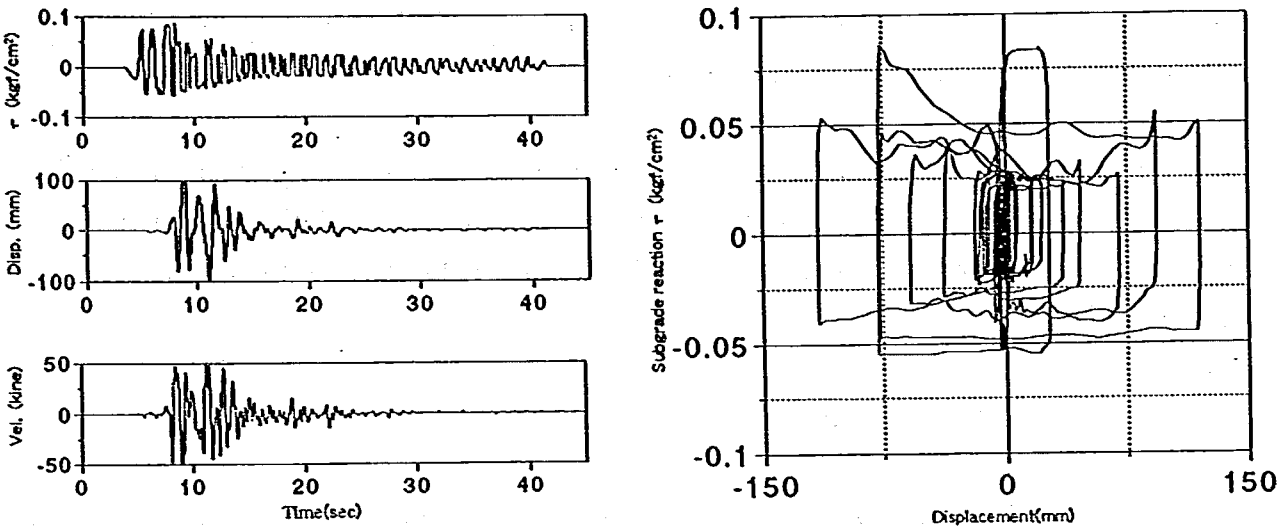



a)Amplitude = 100mm

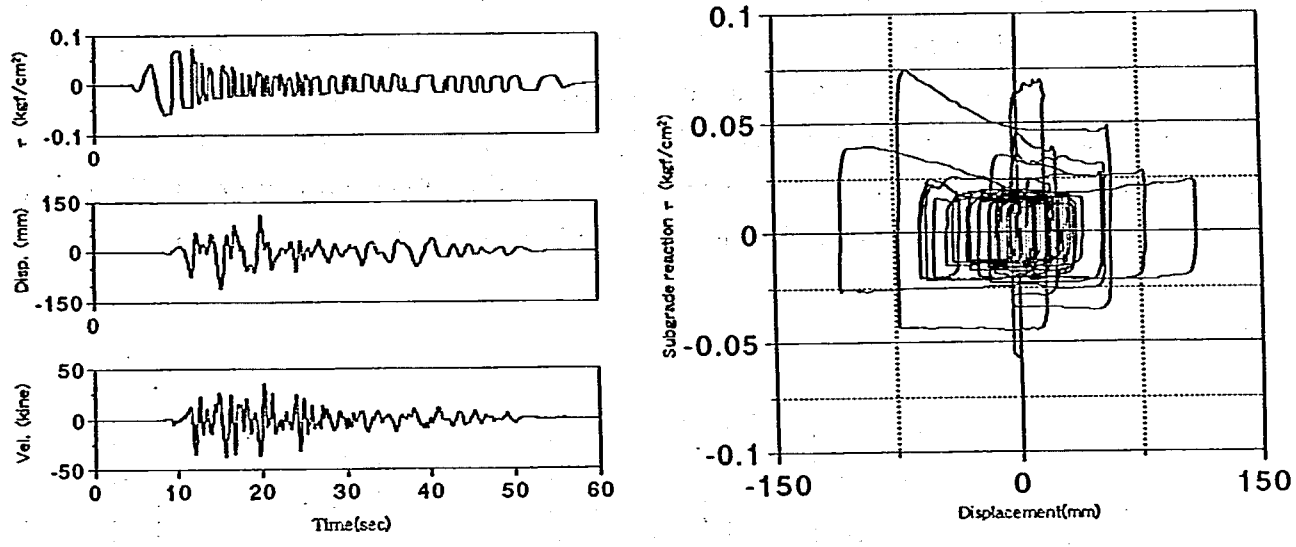



b)Amplitude = 10mm

Figure 4 Tapering wave




a)Southern hyougo Eq.




b)Miyagiken-oki Eq.

Figure 5 Earthquake wave

We then compared the maximum subgrade reactions under various shaking conditions. The results of this comparison are given in Figure 6.

These results clarified that the maximum subgrade reaction is not dependent on shaking conditions, and the value $\tau_{pa}$ is almost constant at the range of 0.06 to 0.11 kgf/cm². The critical shearing force of the sand is calculated by Eq.(2) of Mohr Coulomb's criterion in the vicinity of the top of the buried pipe.

$$\tau_{sa}=C+\gamma_t H \tan\phi \qquad (2)$$

where C is the adhesion of the sand, $\gamma_t$ is the unit volume weight of the sand, and $\phi$ is the friction angle. These are already given in Table 2. Because the depth of the buried pipe was H=1.2m, $\tau_{sa}$ was approximately 0.4kgf/cm². These results show that the critical subgrade reaction $\tau_{pa}$ was less than 25% of $\tau_{sa}$. We observed a tendency for the critical subgrade reaction acting on the 300mm-diameter pipe to be somewhat larger than that acting on the 150mm-diameter pipe. Although this was same at a depth to the top of the pipe for both pipes, that such difference in the critical subgrade reaction is estimated to be slightly greater on the 300mm-diameter pipe because the confined pressure increases with the depth. Nevertheless, we found no significant differences in our results. We two assured that subgrade reaction is not dependent on diameter size.

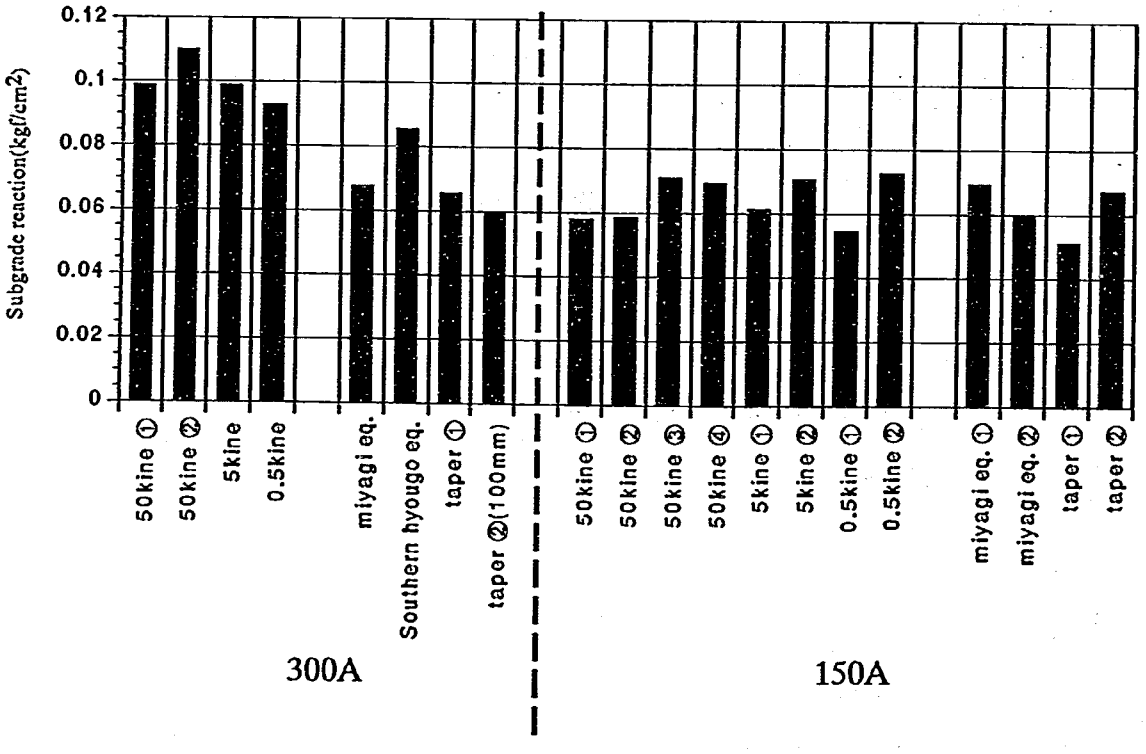



Figure 6 Maximum subgrade reaction

We used strain distribution developed along the pipe to confirm that uniform subgrade reaction acted on the surface of the pipe. These results are shown in Figure 7. The results were observed when the critical subgrade reaction was acting on the pipe of 150mm-diameter while we changed the ground velocity.

These results show that the strains linearly decrease as the distance from the reaction wall. It is supposed that there was a uniform subgrade reaction along the pipe.

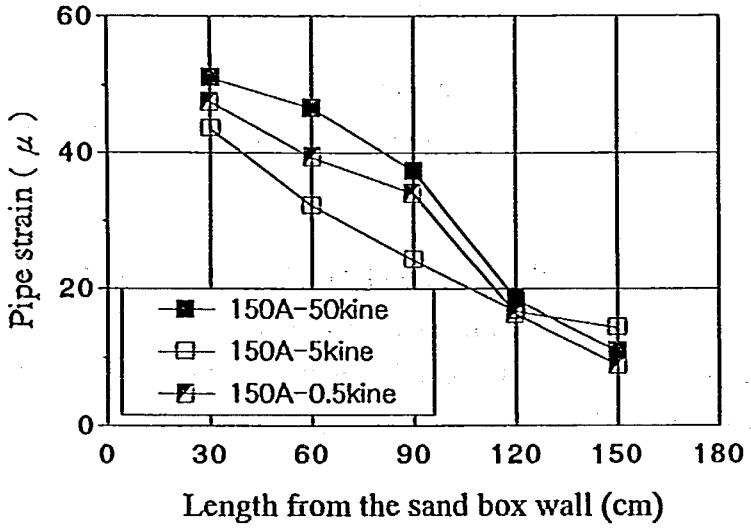



Figure 7 Strain Distribution

Cyclic Characteristics Figure 8 shows the relationship between the critical subgrade reaction and the number of cycle under shaking conditions. Because there were little difference between the pipes of the two diameter, we can discuss only the results of the 300mm-diameter pipe. The critical subgrade reaction have been normalized to the same maximum value found in the experiments of the various cycles.

It was found that the subgrade reaction had the maximum during the initial cycling in the experiment where a large amplitude was applied. It decreased to about 30% at the fifth cycle.

In the experiment where the tapering and earthquake waves were applied, subgrade reaction reached its maximum value after a number of cycles of minimal subgrade reaction. In this case, it as well fell to about 30% after about 10th cycle. Further investigation is required to understand why reduction of the subgrade reaction at tapering and earthquake waves slackened off relative to its behavior at constant amplitudes.

After completing the experiments in each case discussed so far, we again shook the pipes in the boxes, this time for a maximum of half a day, to confirm the recover of the subgrade reaction. The results from these experiments confirmed that the original subgrade reaction was not recovered and that the values again fell down to 25% as discussed previously.

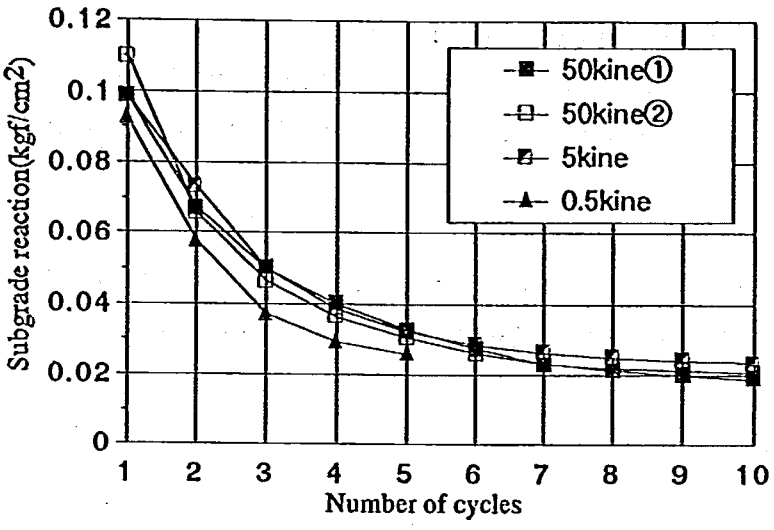



Figure 8 Effect of velocity on subgrade reaction (300A)

Critical Relative Displacement We make it clear the behavior of the relative displacement between the ground and the pipe before its critical value. The results are shown in Figure 9. These are in particular, in case of the initial cycling, which occurs before the critical values drop. We considered only the results of the 300mm-diameter pipe with velocity controlled waves of 50 ke.

The results show that, the subgrade reaction $\tau_p$ clearly increased until displacement $\delta = 0.3$ to 0.5mm under all shaking conditions, but that it remained almost constant or decreased gradually afterward. We can therefore determine critical relative displacement $\delta_\alpha$ independent of the shaking conditions. Because this critical relative displacement value is extremely small, the subgrade reaction behaves almost as plastic material.

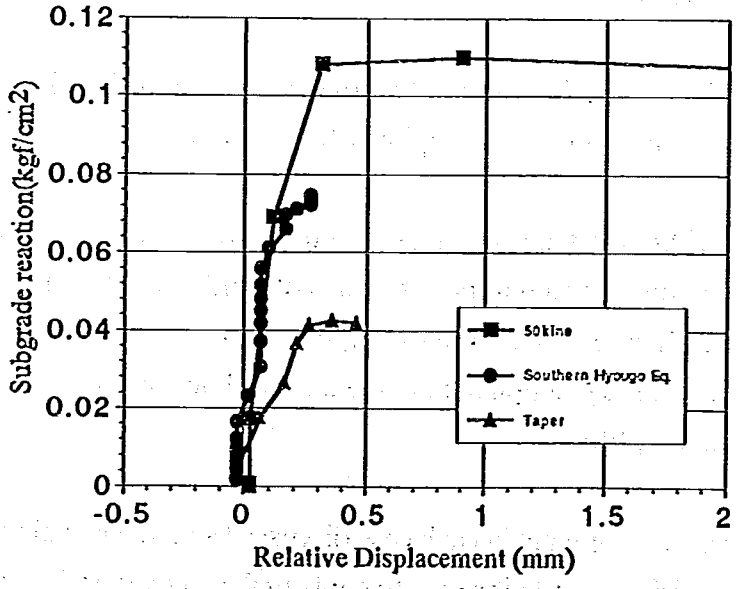



Figure 9 Critical relative displacement

## CONCLUSIONS

Regarding the subgrade reaction that acts in the axial direction on buried pipes during an earthquake, we evaluated the characteristics of cycling and dependency on the ground velocity, using a shaking table test on two polyethylene-coated steel pipes of 300mm and 150mm diameters. The following results were clarified by our experiment:

We conducted two types of experiments: one in which we changed the maximum velocity and displacement amplitude with the sine waves, and another in which we applied random relative amplitude by using actual earthquake waves, including those recorded in the Southern Hyogo Earthquake of 1995. In both of these experiments, no differences were observed in the behavior of subgrade reaction due to the shaking conditions or the pipe diameter.

Subgrade reaction was not dependent on the relative velocity of the ground and the pipe, and no differences were observed between the experimental results obtained at the tests of the maximum velocity of 50 ke and in the quasi-static state. This was also confirmed in the experiments using the seismic waves of the two actual earthquakes where the maximum velocities are different.

Subgrade reaction was not dependent on the shaking conditions and reached its upper limit at an extremely small relative displacement less than 1mm between the ground and the pipe. At greater displacements, there was a tendency for the subgrade reaction to remain constant or to decrease gradually, and the subgrade reaction behaved almost as plastic, even when displacement occurred cyclically. Critical subgrade reaction was small, at approximately 0.1 kgf/cm$^2$. Using this figure, we calculated the dynamic subgrade reaction between the sand and the polyethylene surface to be approximately 25% of the critical shear force of the sand.

The subgrade reaction reached its upper limit in the region of the minimal relative displacement between the ground and pipe. As a result, there were no differences in the behavior of either experiment where we gradually raised or lowered the amplitude of the displacement or in the experiment where we used random amplitudes in the real earthquakes.

Under all the shaking conditions, the subgrade reaction decreases as the cycle of the relative displacement between the ground and the pipe increases. It reduced at about 30% at the 10th cycle from the initial. It was confirmed through the experiment where shaking continued for approximately half a day that the subgrade reaction fell at every cycle and did not recover.

## REFERENCES

1) O'Rourke,T. et al, Soil springs for buried pipeline axial motion, *Journal of Geotechnical Engineering*, ASCE Vol.114 No,11 pp.1335-1339,1988

2) Recommended Practice for Earthquake Resistant Design of High Pressure Gas Pipeline, Japan Gas Association, 1982 (in Japanese)

3) Investigation on the seismic design of buried pipes, Technical Memorandum of PWRI No,1073, 1975 (in Japanese)

4)Behavior investigation of buried steel pipe, Tokyo Electric Power Co., Ltd. 1968 (in Japanese)

# Session-4

## Water & Sewage

(J-7) Damages to Kobe Water System by the Hanshin Awaji Great Earthquake and Restoration Plan
(Makoto Matsushita)

(J-8) Performance of Sewerage System During the 1994 Hokkaido Toho-oki Earthquake
(Masaru Kitaura and Masakatsu Miyajima)

(J-9) Damage to Sewerage Facilities in Recent Earthquakes
(Shuji Tanaka)

(U-2) Water and Sewer Lifelines: Lessons Learned from Recent Earthquakes
(Le Val Lund)

(J-10) Performance of Lifeline Systems During the 1995 Great Hanshin Earthquake
(Shiro Takada and Junichi Ueno)

# DAMAGES TO KOBE WATER SYSTEM BY THE HANSHIN AWAJI GREAT EARTHQUAKE AND RESTORATION PLAN

by

Makoto MATSUSHITA

Assistant Manager, Planning Division, Kobe Municipal Waterworks Bureau,
Sionogi Kobe bldg. 4-1-6, Isogami-dori, Chuo-ku, Kobe, 651, Japan

## ABSTRACT

Southern Hyogo Area (Hanshin area) was hit by a large earthquake. The epicenter was on the Island of Awaji, 20km south-west of Kobe City Center.

Water service was disrupted throughout Kobe City, especially in the south of Rokko mountain area (Shigaichi-chiku) owing to thousands of water pipeline failures, and it took up to ten weeks to fully restore water service.

## 1. INTRODUCTION

The Hanshin Awaji Great Earthquake hit upon the southern area of Hyogo Prefecture at 5:46 AM on Tuesday, 17 January 1995. (Ms 7.2) In Kobe City over 3800 residents died and over 86,000 houses were destroyed. Due to this earthquake, the water supply system in Kobe City suffered the complete disruption and lost its principle functions. However, owing to the great efforts of repair persons gathered from all over Japan, our water system was almost repaired by the end of February except some part of the water front district and was completely repaired by 17 April.

Before starting this report, I would like to express our deepest thanks to all who were concerned in repair works of Kobe Water System.

## 2. CHARACTERISTIC FEATURES OF KOBE WATER SYSTEM

Kobe City Waterworks Bureau was established in 1900 as the seventh modern water supply system in Japan. The characteristic features of the sytem are as follows:

(1)Water Resource (Figure-1)

As there are few large rivers within the city, three resvoirs were constructed to ensure a stable supply for citizens. However, these sources provide only 200,000

$m^3$/day and is mostly supplied by the Hanshin Water Supply Authority.

(2)Two Transmission Tunnels

The water from the Hanshin Water Authority comes through two tunnels in Rokko Mountains along the famous Shinkansen line. These tunnels are situated approximately 90m above sea level and supply water to the lower part of the city by gravity flow.

(3)Layer and Block Distribution System (Figure-2)

Urban Kobe is situated on a long and narrow strip of land. Moreover, the residential areas occupy land ranging between 0 meter and 300 meters above sea level. To overcome difficulties in supplying water to such areas, the water distribution system has been divided into layers at 30m each and a large number of water distribution facilities have been constructed. There are currently 119 water reservoirs and 44 pump stations.

(4)Telemeter/Telecontrol System

As mentioned above, it is neccesary to operate many facilities to allocate water successfully. There is the Central Control Center in the Okuhirano Purification Plant which controls all the reservoirs and pump stations by Telemeter/Telecontrol System.

## 3. EARTHQUAKE POLICY IN KOBE CITY

Before this earthquake, Kobe City had structured the Earthquake Policy figured in Table-1. As to the waterworks facilities, the construction of Emergency Shut-off Valve System and the replacement of aged pipes have been consistently carried out. Emergency Water Supply had been prepared according to the Kobe City's District Disaster Program.

(1)Emergency Shut-off Valve System

This system consists of three seismometers, electric butterfly valve which is equipped in either of paired service reservoirs, and control system thereof. This system is intended to secure water 3 $\ell \times 7$ days in a reservoir in case of an earthquake and to supply water for fire-fighting in another reservoir. The decision making is based on the data from both seismometer and abnormal flow rate. The emergency water supply facilities are provided in each reservoir site, so as to be able to start emergency water supply operation in the early stage of disaster. The construction of this system was startd in 1985 and 21 valves had been completed before the Hanshin Awaji Great Earthquake.

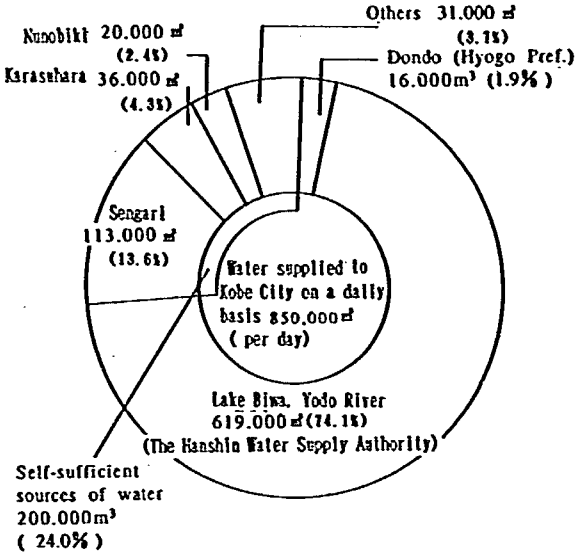



Figure-1. Daily Water Supply Capacity in Kobe

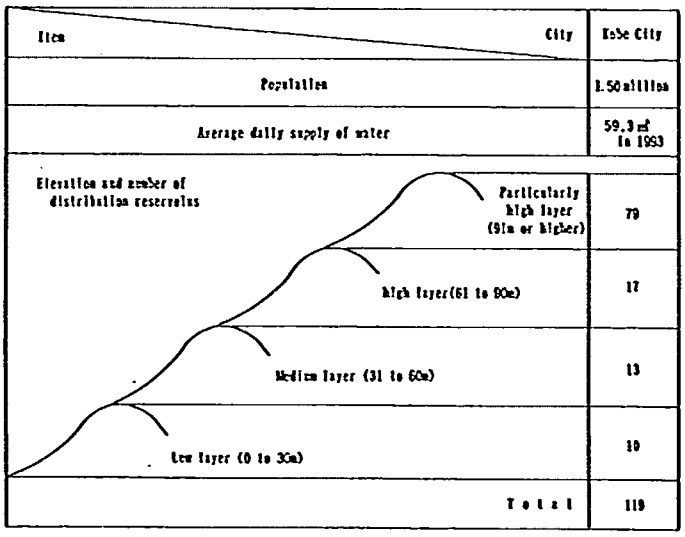
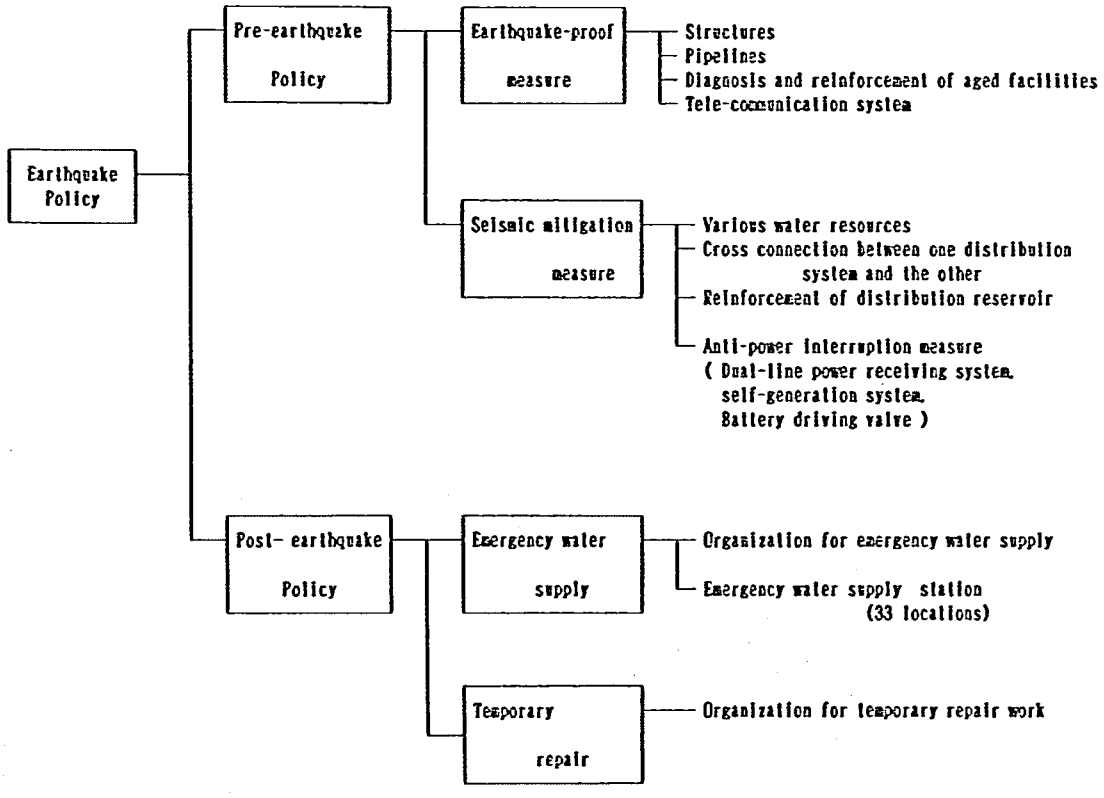



Figure-2. Water Distribution System by Elevation

## Table-1 Earthquake Policy in Kobe City



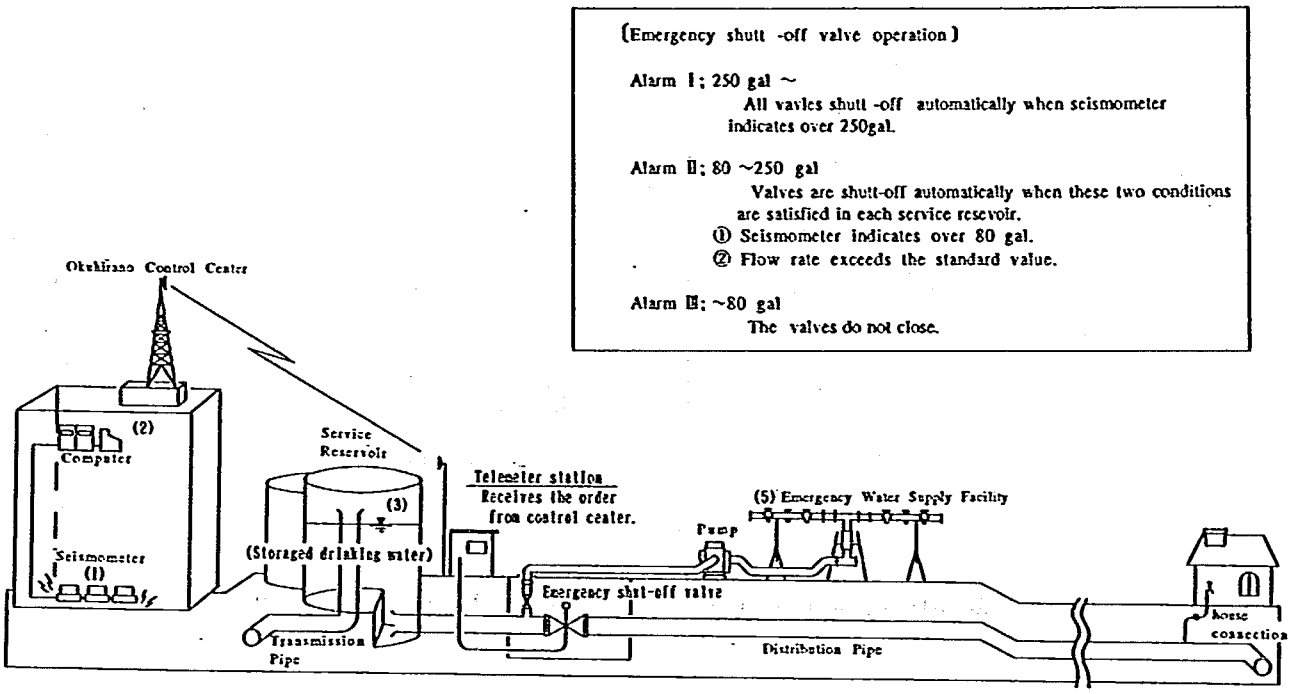



Figure-3. Emergency Shut-off Valve System

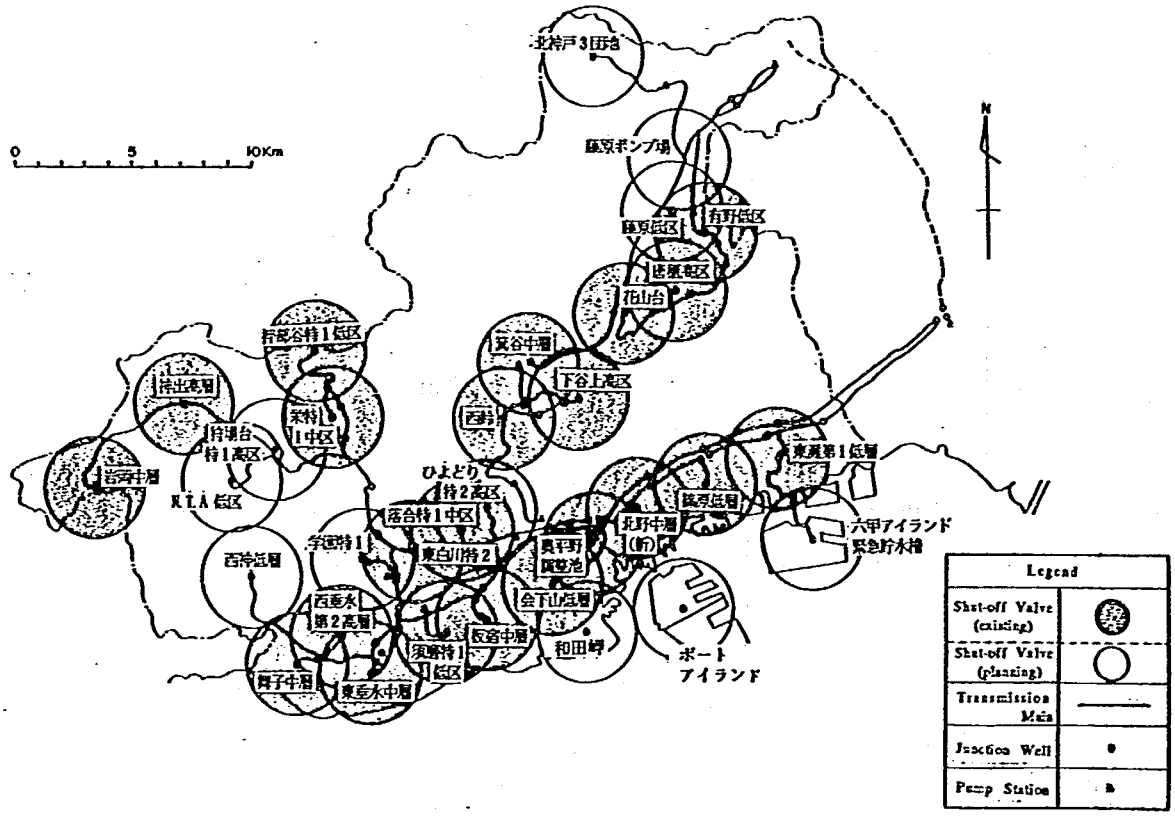



Figure-4. Layout Plan of Emergency Shut-off Valve System

(2)Replacement of Aged Pipes

It is very important to enhance the earthquake durability by updating pipe materials. In Kobe City the replacement by ductile iron pipe has been intensively performed for these 30 years. In order to replace effectively, we classify the earthquake level into three categories(Level 1~3) according to pipe materials and joint types, as shown in Table 2 and 3. In the same table also is shown the pipe length corresponding to each category and in each ward. After studying this table, it can be seen that pipe replaced rate is low in old towns, on the other hand, new materials are widely used in a newly developed housing areas. (Suma, Tarumi, Nishi and Kita) Before the earthquake the total pipe length belonging to Level 1 and 2 exceeded 90%. This is the main reason why the joint separation occurred rather than the pipe-break itself.

Therefore the usage of restraint joint would be essential in consideration of Kobe City's full restoration plan.

## 4. DAMAGES TO WATERWORKS FACILITIES

(1)Characteristic Features of Damages

The dameges to water purification plants and distribution reservoirs are few because these facilities are constructed on hard soil which is in good ground condition. The repair works were done in a short time, and we were able to regain the ability to produce water again.

On the other hand, distribution pipes and service pipes suffered too heavy dameges to repair in a short time. When earthquake occurred, too many pipe breaks and joint separations were brought in many places at the same time. The water inside the pipes were lost simultanously, which led to the low water pressure and made it difficult to identify leakage locations.

(2)Basic Facilities

①Dams

There are small cracks in dam bodies of Nunobiki and Karasuhara Reservoirs. Also seen are landslides and bridge failures to the road along Nunobiki Reservoir.

②Aquaduct (Photo-1)

Some collapses and cracks were seen in Sengari Aquaduct Tunnel.

Table-2 Pipe Length in Each Ward

| Ward | DCIP&SP km (%) | CIP&VP km (%) | Total Length (km) |
|---|---|---|---|
| Higashi Nada | 373.1 (85.7) | 62.4 (14.3) | 435.5 |
| Nada | 168.5 (70.2) | 71.5 (29.8) | 240.0 |
| Chuo | 254.3 (83.7) | 49.5 (16.3) | 303.8 |
| Hyogo | 177.5 (77.9) | 50.4 (22.1) | 227.9 |
| Nagata | 219.6 (82.1) | 47.8 (17.9) | 267.4 |
| Suma | 343.3 (90.3) | 36.9 (9.7) | 380.2 |
| Tarumi | 522.8 (94.1) | 32.7 (5.9) | 555.5 |
| Nishi | 716.9 (94.3) | 43.3 (5.7) | 760.2 |
| Kita | 744.8 (94.0) | 47.8 (6.0) | 792.6 |
| Total | 3,520.8 (88.8) | 442.3 (11.2) | 3,963.1 |

Table-3. Pipe length according to material and joint type

| Earthquake-proof Level | Materials | Joint Type | Pipe Length km (%) |
|---|---|---|---|
| Level 1 | DCIP | S, S II | 237.3 (6.0) |
| | SP | welded | 103.3 (2.6) |
| Level 2 | DCIP | T, K, A | 3,180.2(80.2) |
| Level 3 | CIP | leaded | 7.0 (0.2) |
| | | A | 308.9 (7.8) |
| | VP | —— | 126.4 (3.2) |
| Total | | | 3,963.1(100.0) |

DCIP : Ductile Cast Iron Pipe
SP : Steel Pipe
CIP : Cast Iron Pipe
VP : Vinyl Pipe

Table-4

Diameter and type of failure (distribution main)

| dia-meter (mm) | length (m) | cases | cases /length (—/km) | type of failure A | B | C |
|---|---|---|---|---|---|---|
| 50 | 63.143 | 15 | 0.24 | 7 | 8 | 0 |
| 75 | 165.051 | 49 | 0.30 | 9 | 33 | 7 |
| 100 | 790.329 | 313 | 0.40 | 73 | 193 | 47 |
| 150 | 1,455.137 | 565 | 0.39 | 117 | 378 | 68 |
| 200 | 744.689 | 263 | 0.35 | 62 | 181 | 20 |
| 250 | 39.706 | 21 | 0.53 | 8 | 13 | 0 |
| 300 | 388.606 | 222 | 0.57 | 36 | 157 | 29 |
| 350 | 18.195 | 5 | 0.27 | 0 | 4 | 1 |
| 400 | 79.700 | 48 | 0.60 | 9 | 25 | 14 |
| 450 | 3.082 | 0 | 0.00 | 0 | 0 | 0 |
| 500 | 88.450 | 28 | 0.32 | 3 | 8 | 17 |
| 600 | 45.224 | 16 | 0.35 | 1 | 3 | 12 |
| 700 | 45.857 | 29 | 0.62 | 1 | 6 | 22 |
| 800 | 10.264 | 9 | 0.88 | 1 | 7 | 1 |
| 900 | 26.131 | 26 | 0.99 | 3 | 11 | 12 |
| 1000 | 498 | 1 | 2.01 | 0 | 0 | 1 |
| total | 3,963.062 | 1,610 | mean 0.41 | 332 | 1027 | 251 |

type of failure A: Pipes (breakdown, etc.) (April, 1995)
B: Joints (pulled out, etc.)
C: Fittings(fire-hydrants, etc.)

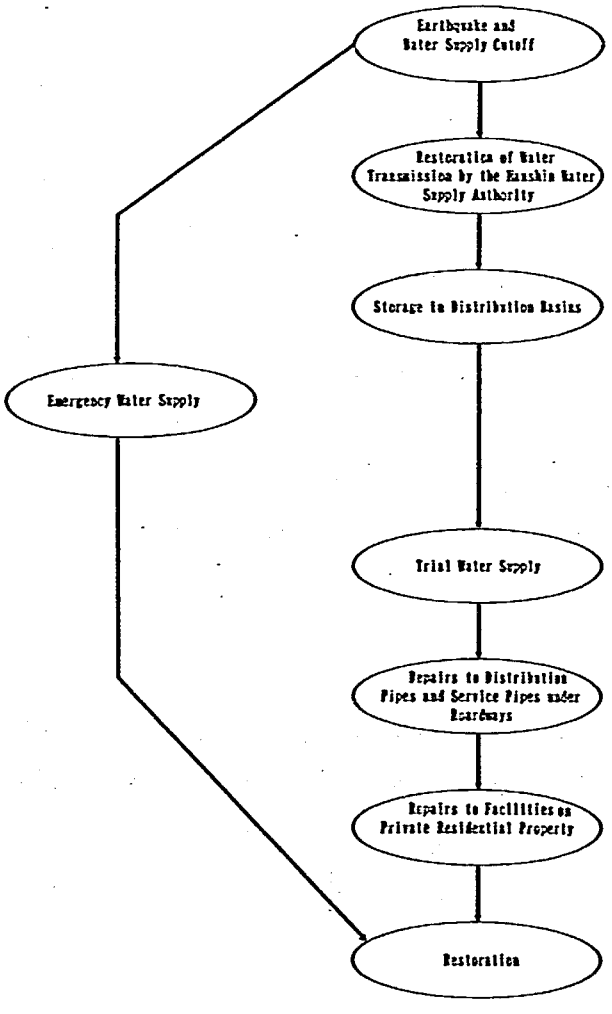



Figure-5. Restoration Process

③Purification Plant (Photo-2)

The damages to Uegahara Purification Plant is the severest in seven purification plants of Kobe City. These damages are done to slow sand filter, rapid sedimentation basin, washing water tank and wastewater treatment facilitiy. In Motoyama Purification Plant there were some cracks in washing water tank and some leakages in plant pipings.

④Water Transmission Tunnels and Pipes

No failures were seen in two water tunnels which send water to Kobe City. However, there were some leakages in the pipelines to Jumonji and Konan service reservoirs. And some collapses of concrete structure were seen in Motoyama and Kumochi water pipeline tunnels.

⑤Service Resrvoir (Photo-3)

In Egeyama Service Reservoir there occurred the fatal cracks between old structure and new structure, from which all the stored water was lost. At present no failures are found in rest of 118 service reservoirs.

⑥Others

The buckling of steel tower in Okuhirano Control Center which is used for telemeter and telecontrol.

(3)Pipelines (Photo-4, 5, 6)

Pipelines suffered the most severe damages from this earthquake. The number of pipeline failures reached over 1400 in the end of March. As the table-4 shows, the largest cause of failure is joint separation(60 %). The rests are pipe break (20 %) and pipe fittings failure (20 %). Besides these pipe failures, there are still too many leakages which cannot be found by leakage survey team yet.

There are some artificial islands within Kobe City, the famous ones are Port Island and Rokko Island. The water pipe bridges, which connect these islands with main land, suffered fatal damages and it became a large barrier against the quick recovery of water service.

(4)Service Connection

Till the end of April, the number of service connection repairs reached to 12,827 on the road and 58,408 in private property. Therefore the total of service connection repairs is 71,235. Most of them are caused by pipe breaks and joint separation following fall down of houses and road deformation. These tremendous number of failures would be the main reason of rapid water loss from distribution pipeline.

# Basic Facilities

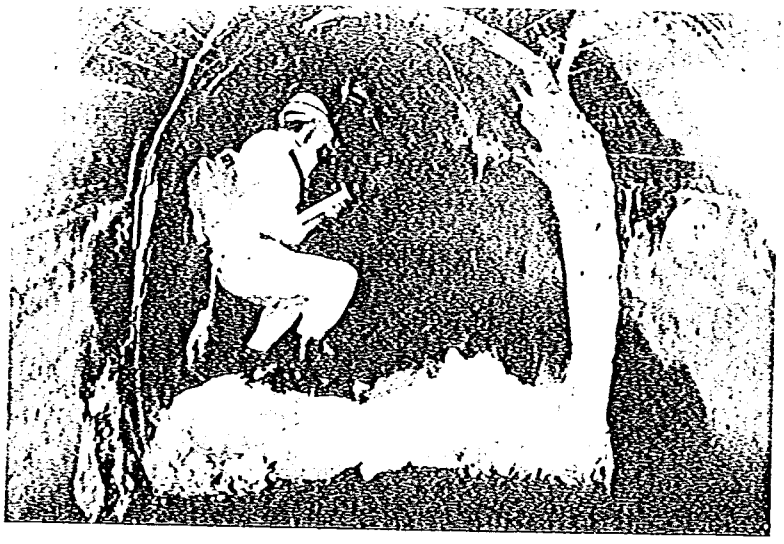


Photo-1
Collapse of Concrete tunnel
of Sengari Aquaduct

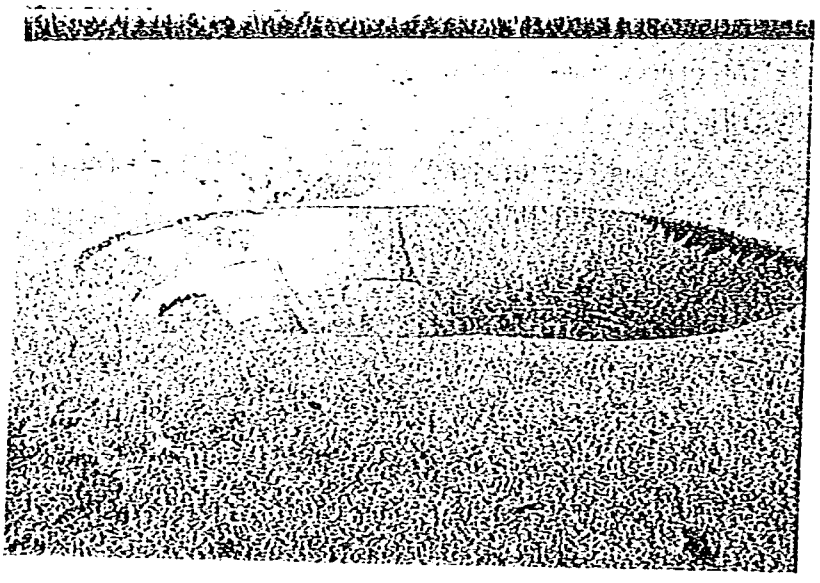


Photo-2
The crater of slow sand
filter bed in Uegahara
Purification Plant

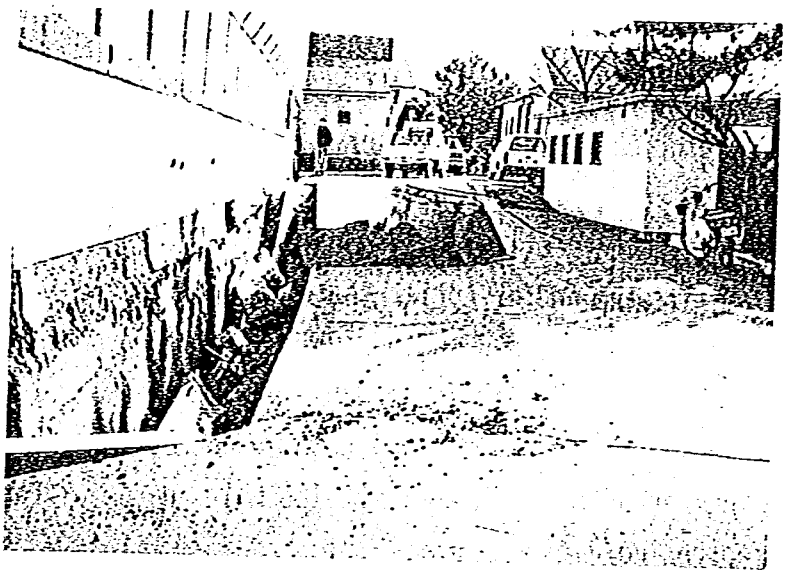


Photo-3
Subsidence in Egeyama
Reservoir

## Pipelines

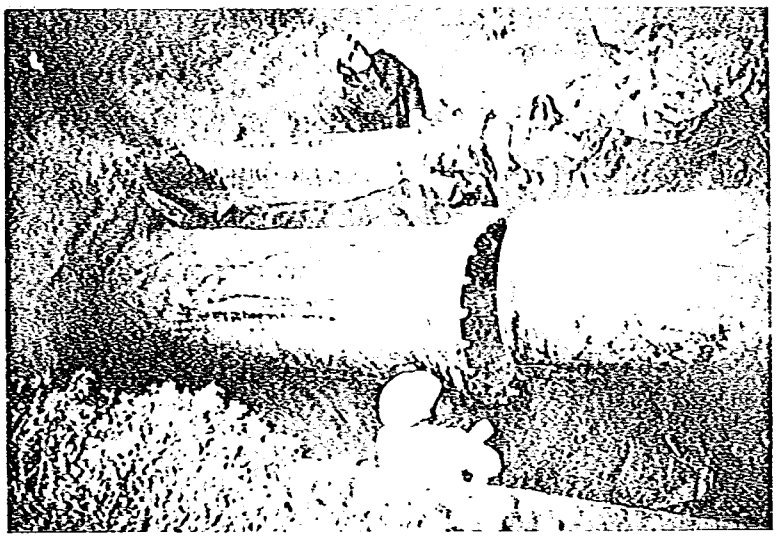


Photo-4
Joint Separation of
Ductile Iron Pipe ($\phi$800mm)



Photo-5
The break of Cast Iron Pipe
($\phi$800mm)

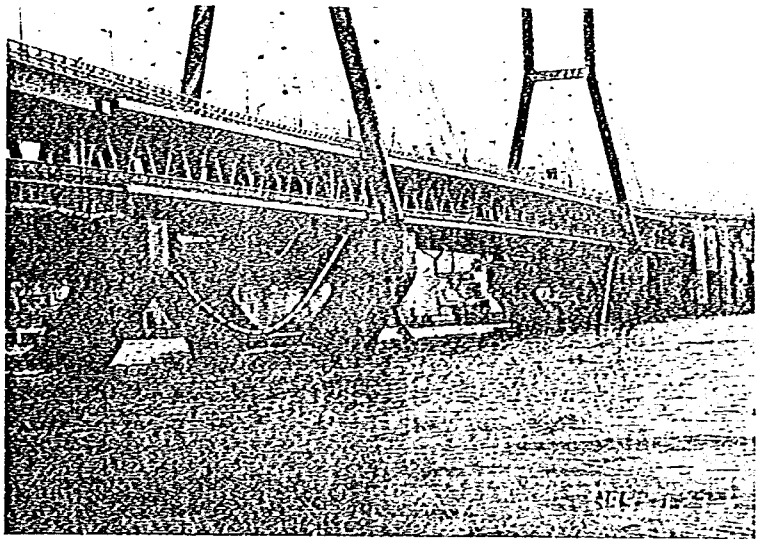


Photo-6
Failure of water pipe
attached to Rokko Bridge
(to Rokko Island)

## 5. PROCESS OF RESTORATION

Restoration of waterworks is enforced by supplying emergency water to citizens and by identification of leakage points and repair works.

Specially in the case of Kobe City, we rely most part of supply on Hanshin Water Supply Authority. Therefore it is necessary at first to secure the volume supplied from it and to store water in each distribution reservoir.
The restoration process is shown in Figure-5.

(1)Status of Water Resource and Storage in Service Reservoir

On the occurrence of the Earthquake, emergency shut-off valve system operated in 18 out of 21 service reservoirs, which secured 42,000 $m^3$ volume of water in total. 37,000$m^3$ of which was stored in urban districts. Assuming 3 $\ell$ is necessary per person a day, this amount is equivalent to the amount needed in Kobe City for 9.3 days or for 9.6 days in urban districts.

Troubles in electric system and leakage from the reservoirs are reasons why emergency shut-off valve system did not operate in three service reservoirs.

Water supply from Hanshin Water Supply Authority temporarily stopped due to a decline in capacity caused by the damage and to power failure. However, owing to emergency restoration works, transmission was resumed by the evening of the same day. Meanwhile, reserved volume of 86 distribution reservoirs in urban districts became zero. The numbers of service reservoirs are shown in Figure-6(right).

The effective volume in the urban districts was 401,870 $m^3$ and 338,455$m^3$ was stored at 5:00 AM on 17th January, directly before the earthquake. Stored volume decreased to the minimum of 94,908$m^3$ at 1:00 AM on 18 January. The volume secured by the emergency shut-off valve system is included in this figure.

The daily change of stored volume in distribution reservoir at 7:00 AM is shown in Figure-6. The stored volume is 109,560$m^3$ at 7:00 AM on 18 January gaining approximately 15,000$m^3$ since 1:00 AM. It returned to the level before the earthquake at the end of January. However, places of leakage increased as water supply area was expanded, and the stored volume decreased again at one time to 21,000 $m^3$ level.

(2)Emergency Water Supply (Photo-7,8)

After water was cut off in the entire city, Waterworks Bureau dispached water tank trucks. Since we had to cover so wide a range, it was very difficult. However, as the greatness of earthquake was reported through mass-media, water supply aid from neighbouring cities arrived first, and afterwards supports from Self-Defence Force and other cities arrived, which strengthened emergency water supply system.

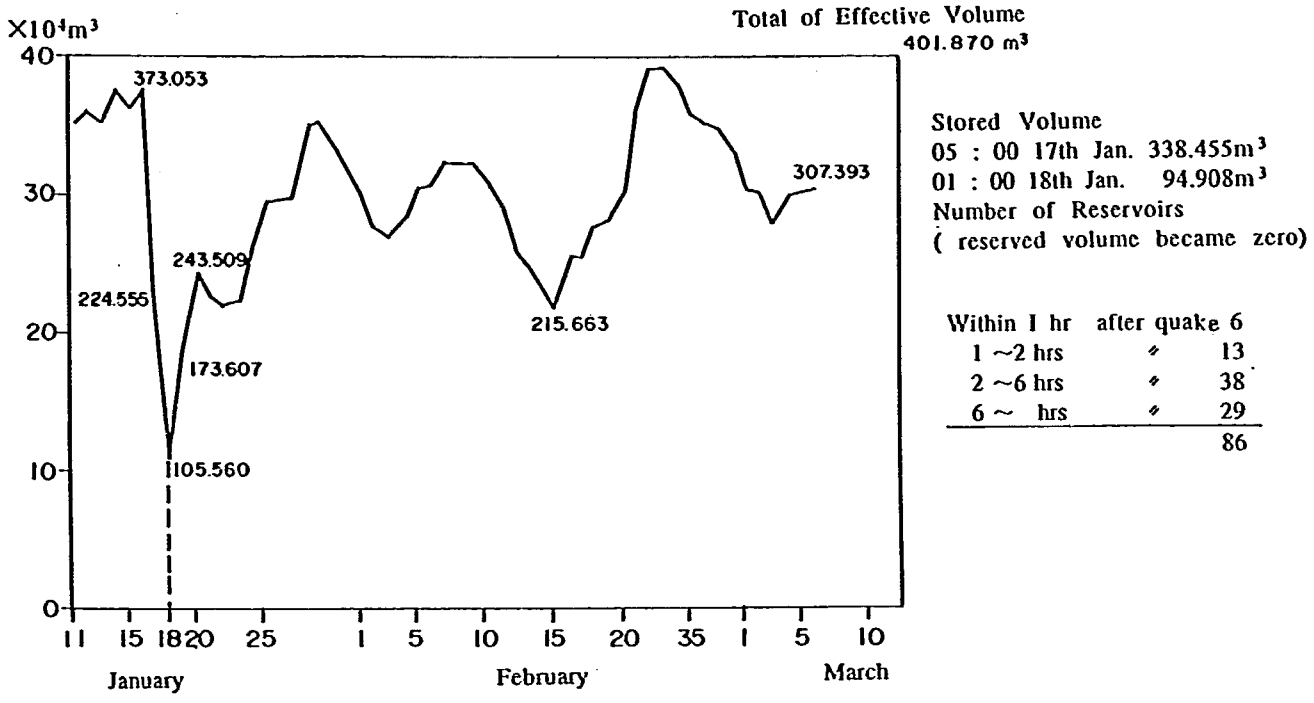



Figure-6. Change of Stored Volume in Shigaichi Service Reservoirs (Urban District)

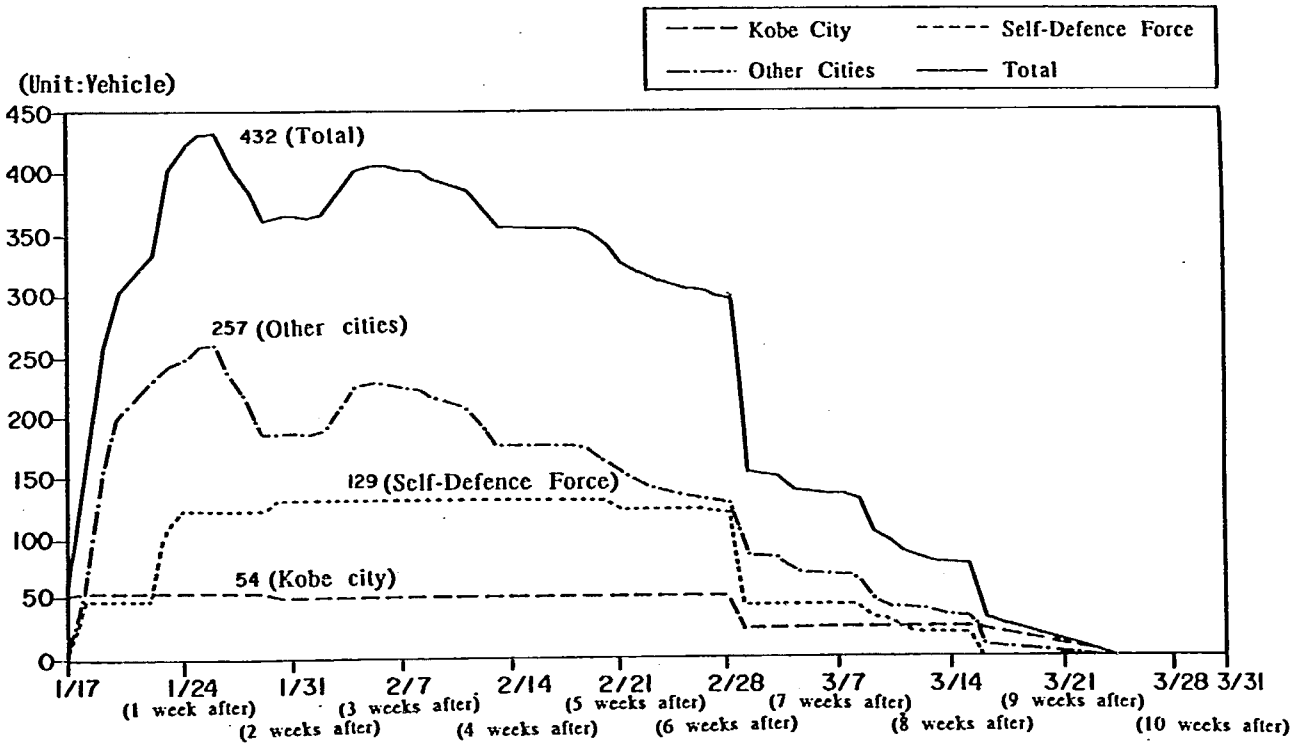



Figure-7. Number of Water Tank Trucks

## Emergency Water Supply

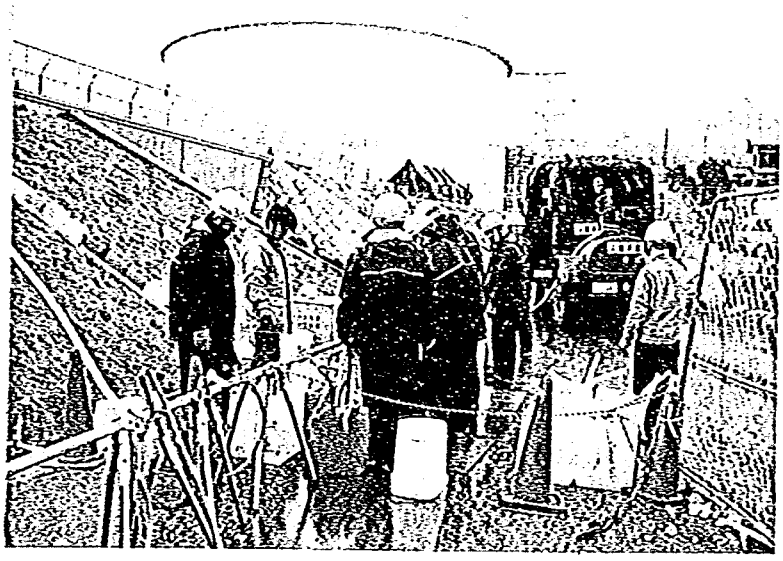


Photo-7
Emergency water supply
in Higasi-Nada Reservoir

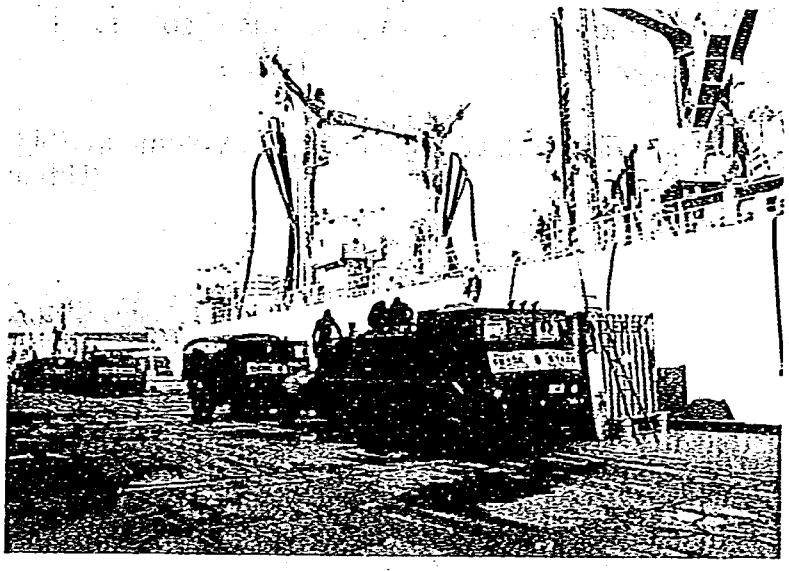


Photo-8
Self-Deffence Force ship
supplying water to
Water Tank Truck

In addition to this, it must be noted that many private volunteers cooperated in emergency water supply. The change of numbers of water trucks is shown in Figure-7.

Making use of the characteristic of Kobe as a port town, water was transported by ships from Marine Self-Defence Force, Maritime Safety and private shipping companies.

Ten quays became water supply points at a peak period.

(3)Temporary Restoration Work

As mentioned above, damage was mainly done to distribution pipes and service pipes. By extraordinarily great vibration of the earthquake, distribution pipes were broken, joints were pulled out and fittings such as air valves failed, and service pipes were pulled out or broken. The number of such cases mounted up to 1,600 as to distribution pipes and 60,000 as to service pipes at the end of April.

Although Waterworks Bureau tried hard to identify leakage points by trial water supply, as water-pressure was low at first, it was extremely difficult to identify the places of leakage. Further, as we were too short of hands, we called on The Japan Water Works Association(JWWA) for help in restoration works and received personnel support from many cities. Change of number of personnel from other cities is shown in Figure-8. It mounted up to 734 from 38 cities and became zero at the end of March.

(4)Recovery of Water Supply

The aforesaid temporary restoration was carried out enlarging restoration area by resumption and increase in volume of water transmission from Hanshin Water Supply Authority and by resumption of operation in each distribution reservoir. This process of trial water supply, identification of leakage, and repair was repeated and restoration rate increased gradually. Figure-9 shows the change of numbers of repair cases on the road (distribution pipe and service pipe) and within private properties. Figure-10 shows the restoration rate of each center.

As seen from the Figure-10, although in Kita Center(North Ward) and Tarumi Center(Tarumi and Nishi ward) where damege was not so severe, restoration was completed relatively early at the end of January or in the middle of February, in Tobu Center(Higashinada and Nada ward), Chubu Center(Chuo and Hyogo ward) and Seibu Center(Nagata and Suma Wards) restoration work was delayed due to the destruction of houses and road subsidence in waterfront areas.

The work was completed as a whole at the end of March when restoration rate reached 99.98 %.

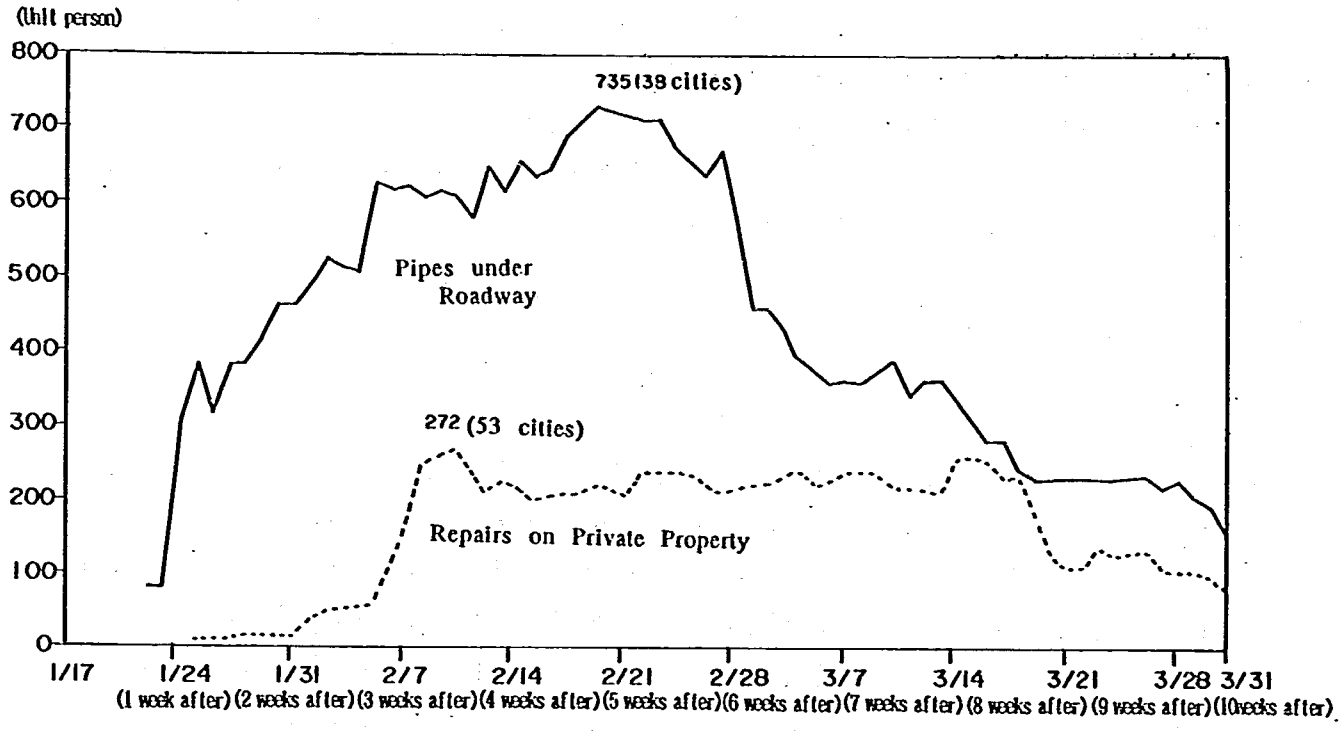



Figure-8. Repair Workers on Loan from Other Cities

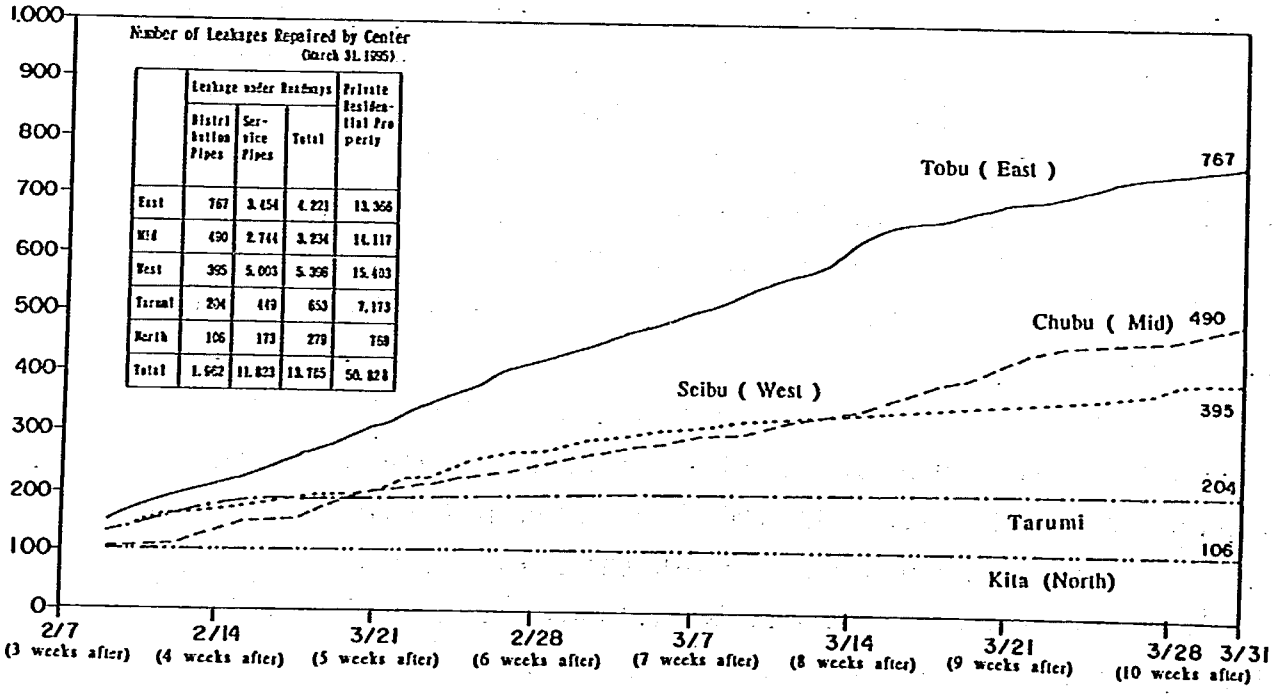



Figure-9. Number of Leaks Repaired

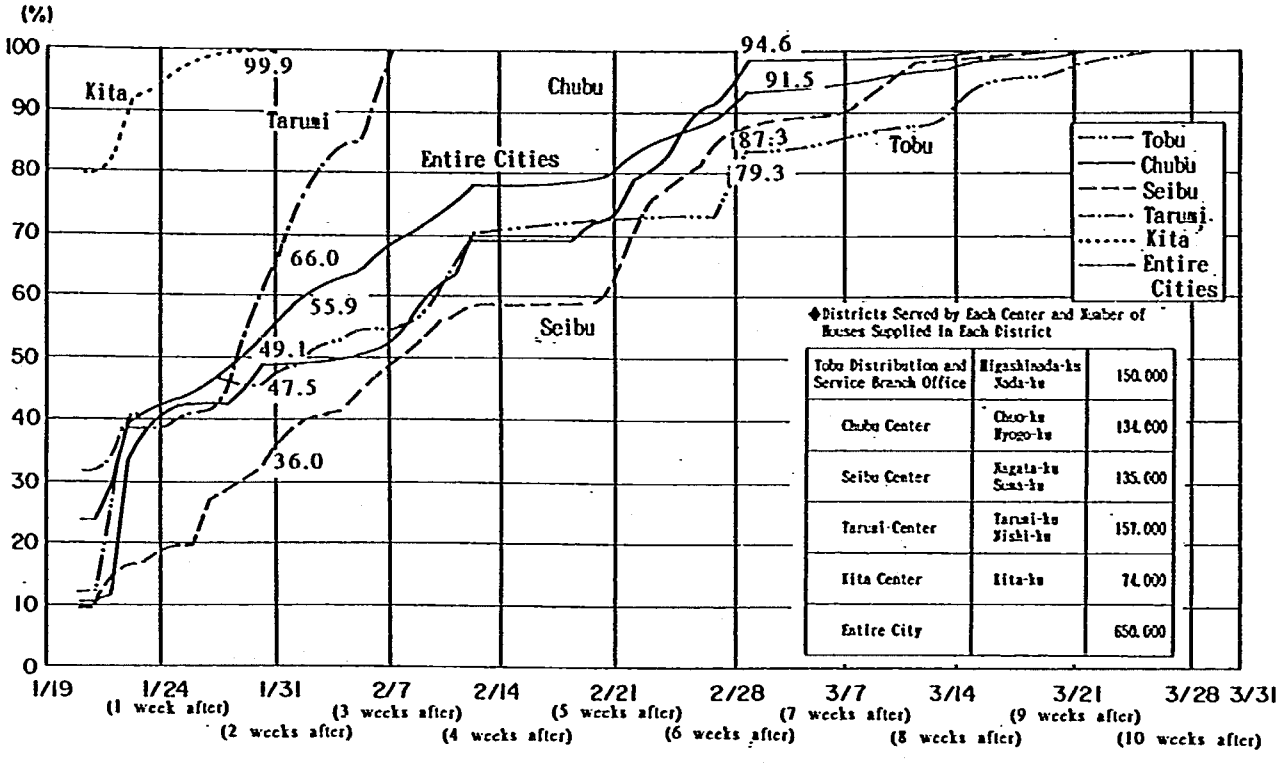



Figure-10. Restoration Curve of Water Supply

| | 1st stage | 2nd stage | 3rd stage | 4th stage |
|---|---|---|---|---|
| restoration period | ~ 3 days | 4~10 days | 11~21 days | 22~28 days |
| ℓ/person/day | | | | |
| 250 | | | | |
| 100 | | | | |
| 20 | | | | |
| 3 | | | | |

Figure-11. Planned Water Volume by Emergency Water Supply

## 6. WATERWORKS RESTORATION PLAN

(1)Basic concept

In enforcing the restoration of waterworks, due to new legislative action by the Government, restoration improving earthquake-resistance is now approved as the object of the government subsidy.

In March, "Basic concept for the restoration of waterworks facilities damaged in the Hanshin Awaji Great Earthquake" was indicated by the Ministry of Health and Welfare. It is now indispensable for the future maintenance of facilities to improve earthquake-resistance.

Planning of guideline and study for various restoration plans were done in Hyogo Prefecture and in Kobe City and are now on their way to realization. Kobe City Waterworks Bureau established Kobe City Waterworks Restoration Planning Committee in March and prepared "Guidline for Earthquake-resistible Waterworks in Kobe City. Further, we will make "Master Plan for Earthquake-resistible Waterworks in Kobe City" and also its "Working Plan".

(2)Guideline for Earthquake-resistible Waterworks in Kobe City

This Guideline is made to lay down the direction for the future costruction of Kobe City Waterworks in order to build "Diaster-resistible facilities" and "Quickly and Easily restorable facilities" .

The basic concepts for making the guideline are: anticipate occurrence of earthquake as large as Hanshin Awaji Great Earthquake, take the citizen's point of view concerning the use of waterworks and reflect characteristics of the terrain of Kobe.

Especially as to emergency water supply, taking into consideration the increase of necessary amount of water with the passage of time from the occurrence of disaster, our target is to secure 3 ℓ per person a day for first three days by using water stored against emergencies at each points and by supplying from reservoir with emergency shut-off valve or from large scale water tank, to fill the water to main pipe from the fourth day and to secure 20 ℓ by the tenth day, secure 100 ℓ by enlarging water filling work to branch pipes by the 21st day, and finally secure 250 ℓ by the 28th day. (Figure-11)

It is also one of our aims to complete temporary restoration in four weeks which took ten weeks this time.

Following concrete measures are now under consideration;

①improve earthquake-resistance of basic waterworks facilities

②emergency water storage system

③formation of earthquake-resistible pipe-network

④improve earthquake-resistance of water pipe bridges and pipe fittings

⑤improve earthquake-resistance of service connections

⑥installation of "Large Water Transmission Main" and large area backup system

It is also necessary to improve "the operation and maintenance system" to operate these facilities more effectively. (Figure-12, 13, 14)

(3)Master Plan for Earthquake-resistable Waterworks Facilities

The Master Plan is prepared based on the Guideline for Earthquake-Resistible Waterworks in Kobe City. It includes the installation of emergency shut-off valve system which was effective in the Hanshin Awaji Great Earthquake and achievement of the object (2) by adopting earthquake-resistible pipe network of 500m grid for main pipe and 200m grid for branch line.

As to receiving water supply from Hanshin Water Supply Authority, although it was planned to build the third mountain tunnel in addition to the existing two water transmission tunnels, a new plan is now under consideration, for diversification of risks, to build "Large Water Transmission Main" which go through urban districts in order to be able to supply water to populous districts in case of disaster. These service pipes are expected to function as large area back-up system facilities linking the right bank of Yodo River with Hanshin area and Awaji Island etc. in the future.

## 7. CONCLUSION

### ～ Towards Earthquake-resistible Waterworks for Citizens～

The Hanshin Awaji Great Earthquake Disaster claimed the lives of more than 5,500 people and had a great influence on the society. It is our mission to make use of the lessons we learned from the experience in our future waterworks projects.

It is our policy in the Kobe City Waterworks Bureau to do our best to enforce project for earthquake-resistible waterworks in conformity with "The Whole Kobe City Restoration Plan".

The newly-born earthquake-resistible Kobe City waterworks will be suitable for "the international disaster-proof model city---Kobe---" and also will be the waterworks which citizens can rely on and be proud of.

We would like to thank every one of those who cooperated in restoration of Kobe City Waterworks and it will be our pleasure if this report be of some help in considering future earthquake-resistible water supply system.

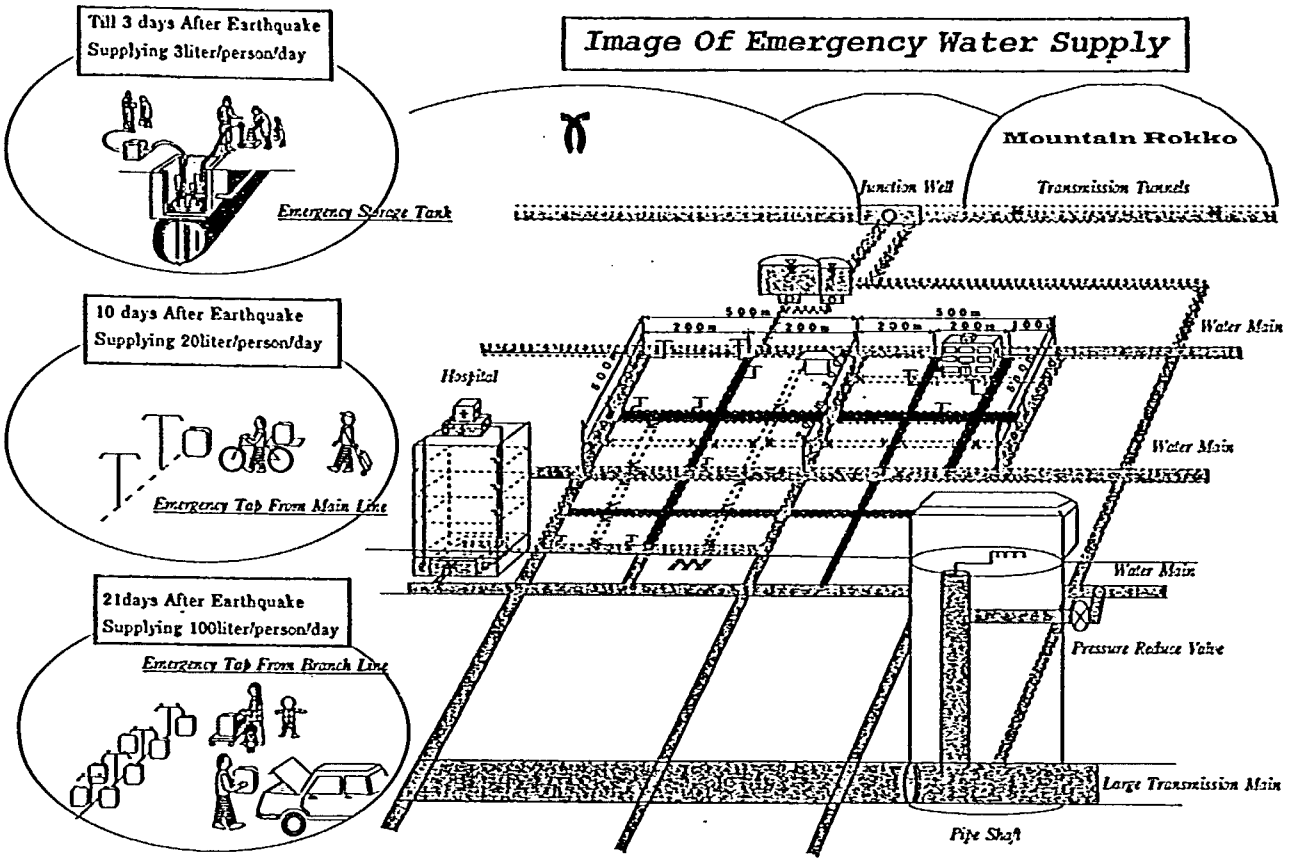



Figure-12. Image of Emergency Water Supply using earthquake-resistible pipe-network

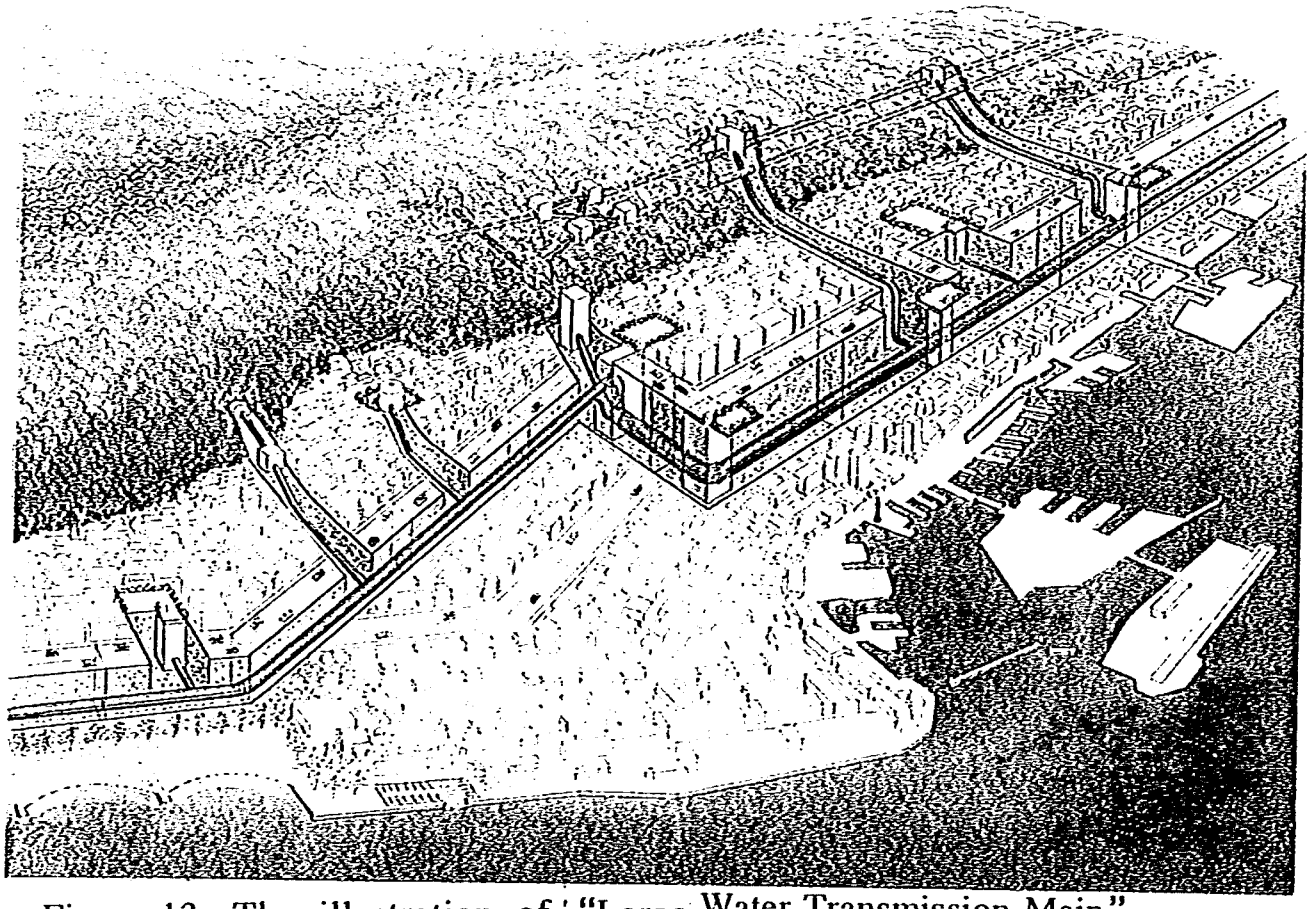


Figure-13. The illustration of "Large Water Transmission Main"

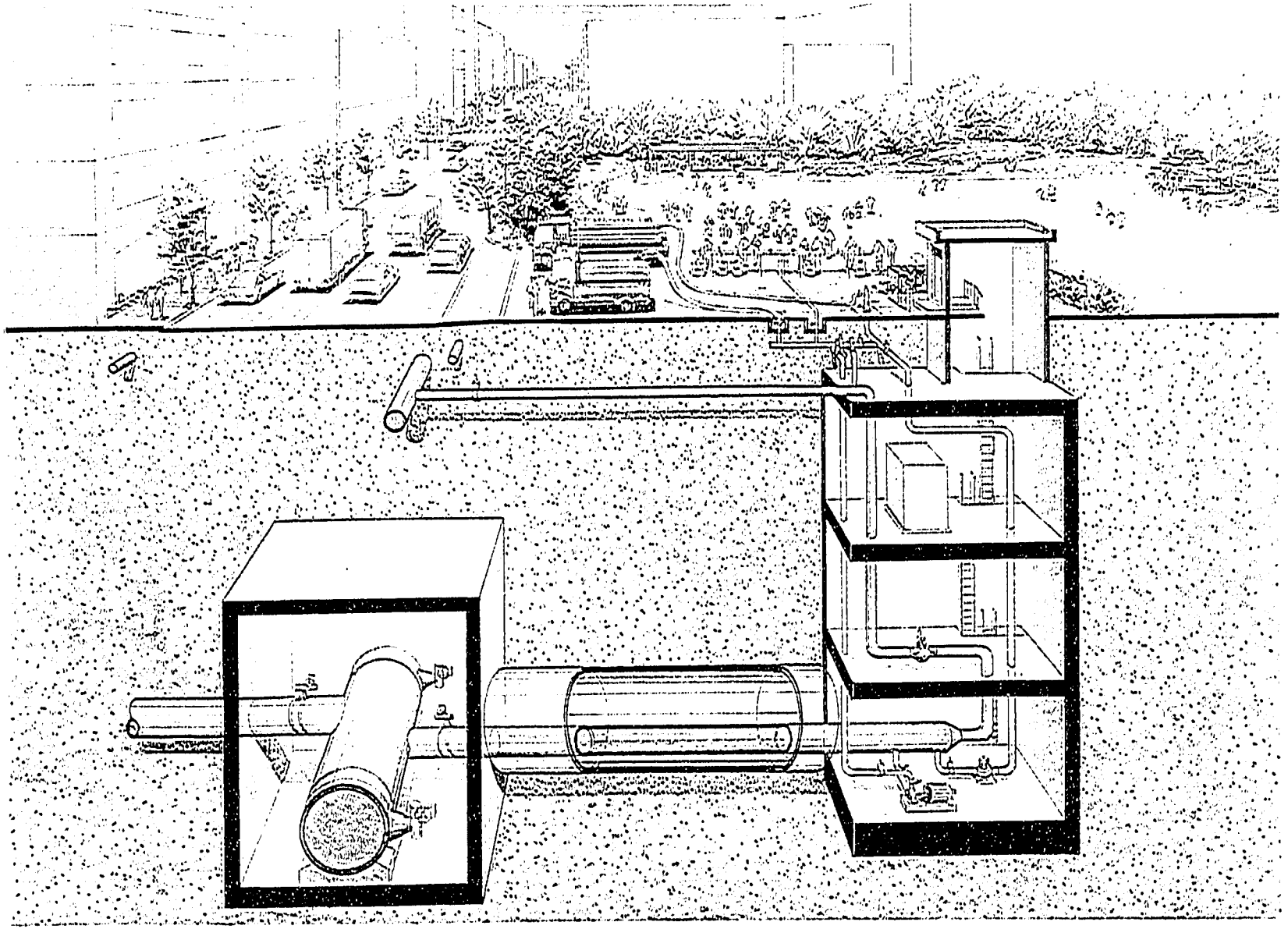


Figure-14. "Large Water Transmission Main" and Emergency Water Supply

# PERFORMANCE OF SEWERAGE SYSTEM DURING THE 1994 HOKKAIDO TOHO-OKI EARTHQUAKE

by

Masaru KITAURA[1] and Masakatsu MIYAJIMA[2]

1) Professor, Dept. of Civil Engineering, Kanazawa Univ., 2-40-20, Kodatsuno, Kanazawa, 920 Japan.
2) Associate Professor, ditto.

## ABSTRACT

An earthquake with magnitude of 8.1 rocked the eastern Hokkaido on October 4, 1994. The damage resulting from this earthquake included structural failure of houses and civil engineering structures, and widespread disruption of lifeline facilities in the east part of Hokkaido. Earthquake damage done to sewerage facilities was investigated, and an overviews of the damage to pipelines in Hokkaido is given. The floating of sewerage manhole is discussed in relation to the ground conditions.

## INTRODUCTION

Many manholes and sewerage pipes in Hokkaido were floated during the 1993 Kushiro-oki earthquake with magnitude of 7.8 in Japan. The mechanism of the floatation was investigated through shaking table tests by Yasuda et al. [1] Since this earthquake occurred in the middle of January, the surface soil layer was frozen. Although subsidence of surface ground was small because of frozen soil, the floating of manhole seemed to be caused by liquefaction.

The 1994 Hokkaido Toho-oki earthquake with magnitude of 8.1 also caused severe damage to sewerage system in Hokkaido. Many manholes were floated and subsidence of backfill soil was also occurred simultaneously at many places. Floatation of manholes and subsidence of the backfill soil obstructed the road after the earthquake. This could be a big problem for evacuation of residents and traffic of emergency vehicles if this kind of damage occurs at a high population density area.

The present paper deals with the damage to sewerage system during the 1994 Hokkaido Toho-oki earthquake. Firstly, an overview of the damage done to the sewerage system in Hokkaido is given. The paper focuses on the damage at Shibetsu town and the relation between the damage and ground conditions are investigated. The cause of damage to sewerage system is discussed.

## OVERVIEW OF THE EARTHQUAKE AND DAMAGE

The Hokkaido Toho-oki earthquake occurred at 22:23 on October 4, 1994. The seismic origin was 30 km below the sea bed about 150 km off Nemuro peninsula in the eastern Hokkaido. The earthquake triggered an enormous destructive tsunami and heavy damage due to tsunami was caused at the Russian-held disputed northern islands. Fig. 1 shows the JMA(the Japan Meteorological Agency) seismic intensity in Hokkaido. The greatest intensity in this earthquake was 6 in Kushiro and 5 was in Nemuro, Urakawa and Hiroo. The peak horizontal ground acceleration was 473 gal in EW component at the Kushiro meteorological observatory and 369 gal in NS component at the Nemuro meteorological station. The peak vertical ground acceleration was 193 gal at Kushiro and 183 gal at Nemuro [2]. Although the epicentral distance of Nemuro is smaller than that of Kushiro, the peak ground acceleration at Nemuro was smaller

than that at Kushiro. The topography and local soil conditions seems to affect the amplification of ground shaking.

Thirty two persons were seriously injured and 404 persons were slightly injured. Sixty one houses were completely destroyed, 348 houses were partially destroyed and 7,095 houses were damaged. The civil engineering structures, such as roads, railroads, bridges, ports , river dikes, etc. were also damaged extensively. The cost of reconstruction was estimated as 57.34 billion yen in Hokkaido.

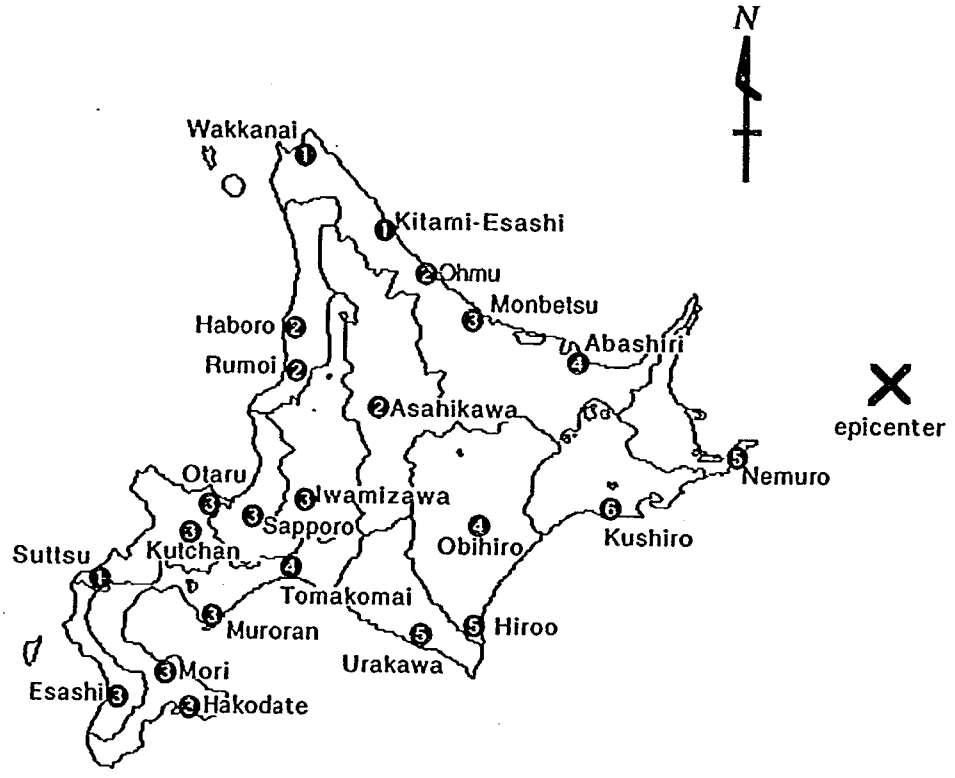



Fig. 1 JMA seismic intensity in the 1994 Hokkaido Toho-oki earthquake.

## OVERVIEW OF DAMAGE TO SEWERAGE SYSTEM IN HOKKAIDO

Fig. 2 shows the amount of cost for reconstruction in each district in Hokkaido. This figure also indicates the cost of reconstruction of damaged sewerage system. The total cost of reconstruction of sewerage system in Hokkaido was estimated as 5 billion yen. It is about 9 % of the amount of the reconstruction cost. Since the cost in Nemuro district was greatest, the reconstruction costs at each city and town in Nemuro district were shown in Fig. 3. The reconstruction cost of sewerage system was more than half of the amount of the reconstruction cost in Shibetsu town. The present paper focuses on the damage to sewerage system in Shibetsu town because the damage to sewerage system was severe as shown in Fig. 3.

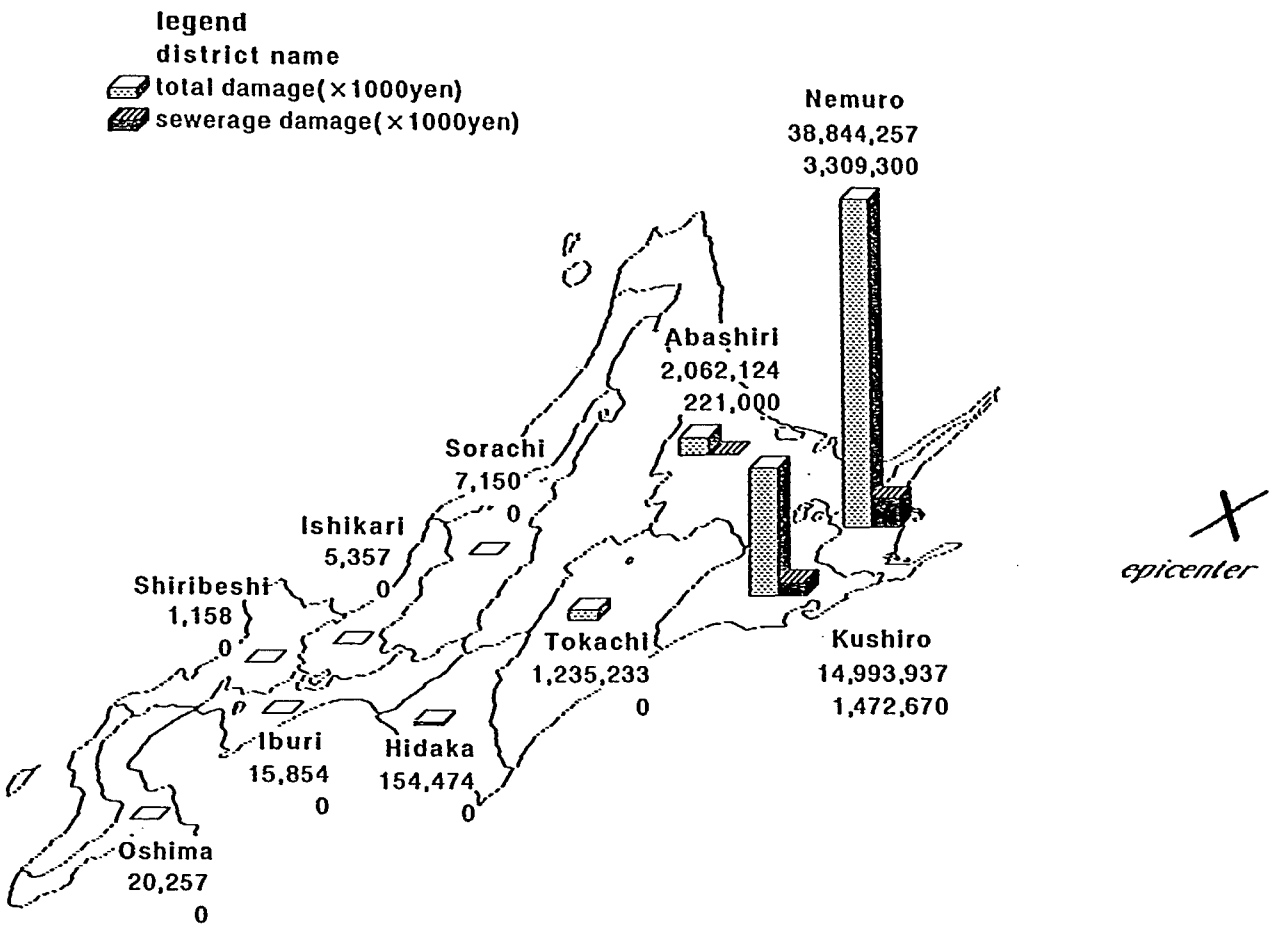



Fig. 2 Amount of cost for reconstruction in Hokkaido.

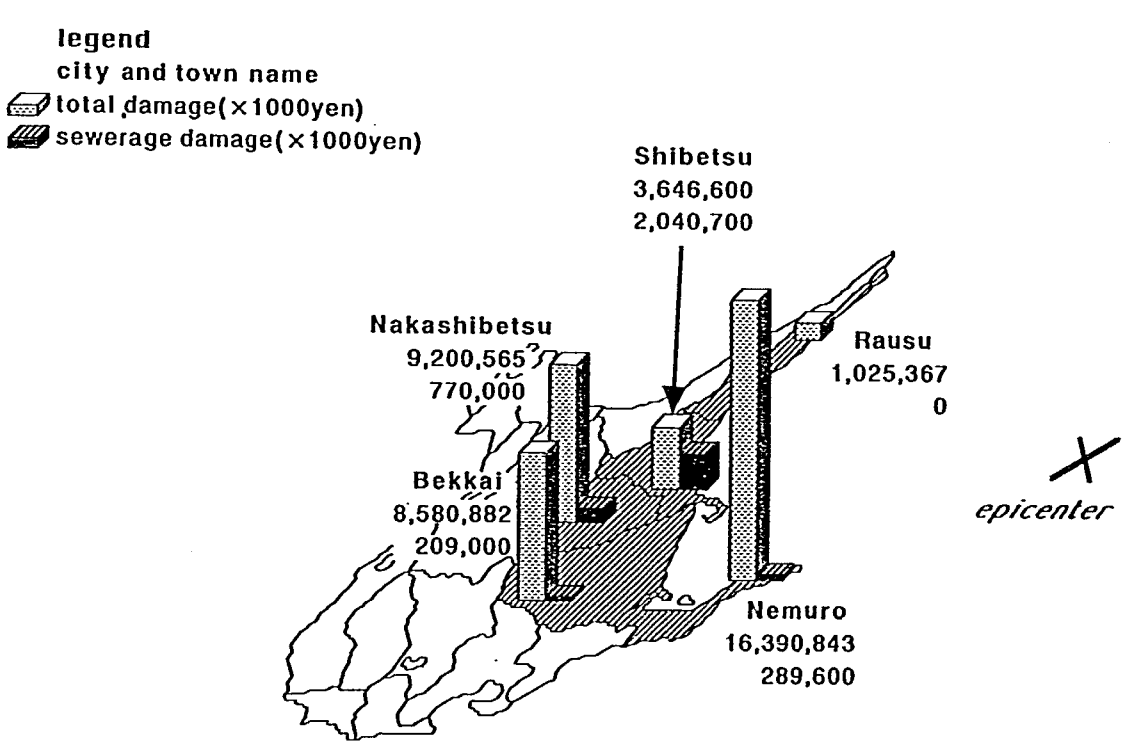



Fig. 3 Amount of cost for reconstruction in Nemuro district.

## DAMAGE TO SEWERAGE SYSTEM IN SHIBETSU TOWN

### Overview of damage

Shibetsu town with about 7,000 inhabitants has the sewerage system of 18.7 km pipelines. The pipelines is made up of vinyl pipe. Fig. 4 illustrates the piping length and damaged pipe length in relation to the pipe diameter. The total length of damaged pipeline was 10.5 km. The damage rate, defined as the damaged pipe length divided by the total piping length, was 0.56. Fig. 5 shows the damage rate in relation to the pipe diameter. This figure suggests that the damage rate was great at the pipeline with small diameter. Photos 1 and 2 show the damaged pipelines. The pipelines wound vertically and horizontally.

The floating of manhole and settlements of backfill soil were occurred simultaneously at many places in Shibetsu town as shown in Photo 3. According to this Photo, although the relative displacement of manhole was great, it is not clear that the manhole floated from the ground or the surrounding soil subsided. Therefore, the top of the manhole and level of the surrounding soil were measured. Fig. 6 illustrates the floating of manhole and settlements of the surrounding ground at Shinkawakami-chou, the northern part of Shibetsu town. This figure indicates that the settlements of the ground was 10 cm to 50 cm and the floating of the manhole was 0 to 20 cm, that is, the settlements of the ground was greater than the floating of the manhole.

### Ground conditions

The ground conditions of Shibetsu town is discussed here using 33 boring data obtained close to the pipelines. Fig. 7 shows the plot plan view of the damaged pipelines and boring sites. Fig. 8 illustrates the estimated soil profiles along A-A' line shown in Fig. 7 [3]. Since the depth of sewerage pipeline was about 5m, the pipeline was buried at peat layer. The peat layer is very soft and its SPT *N*-value is 1 to 3.

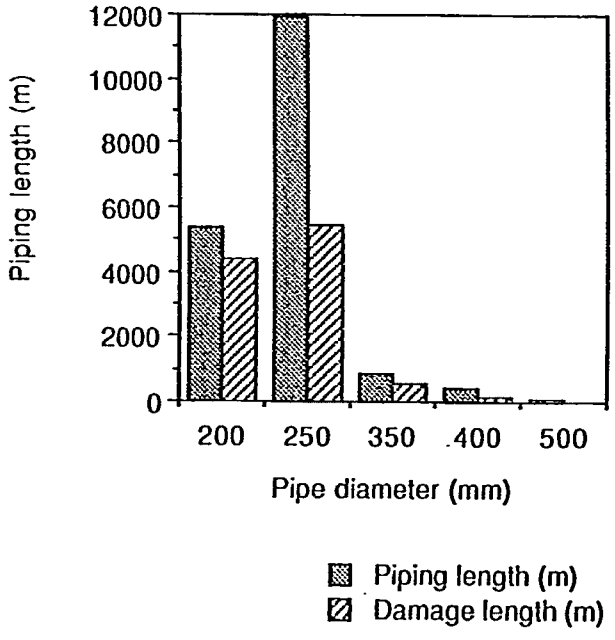



Fig. 4 Piping length and damaged pipe length.

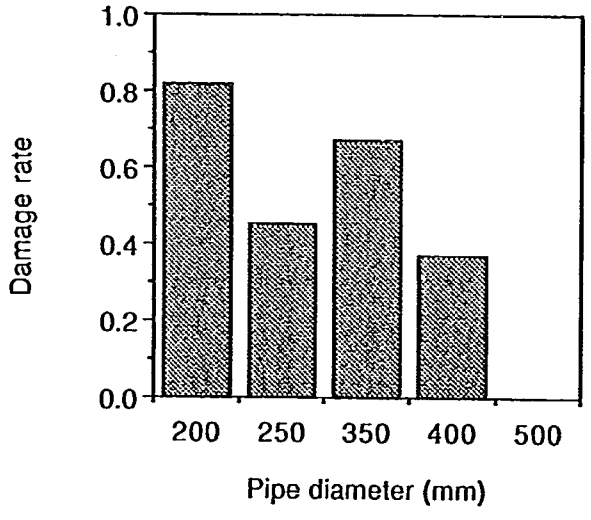



Fig. 5 Damage rate in relation to pipe diameter.

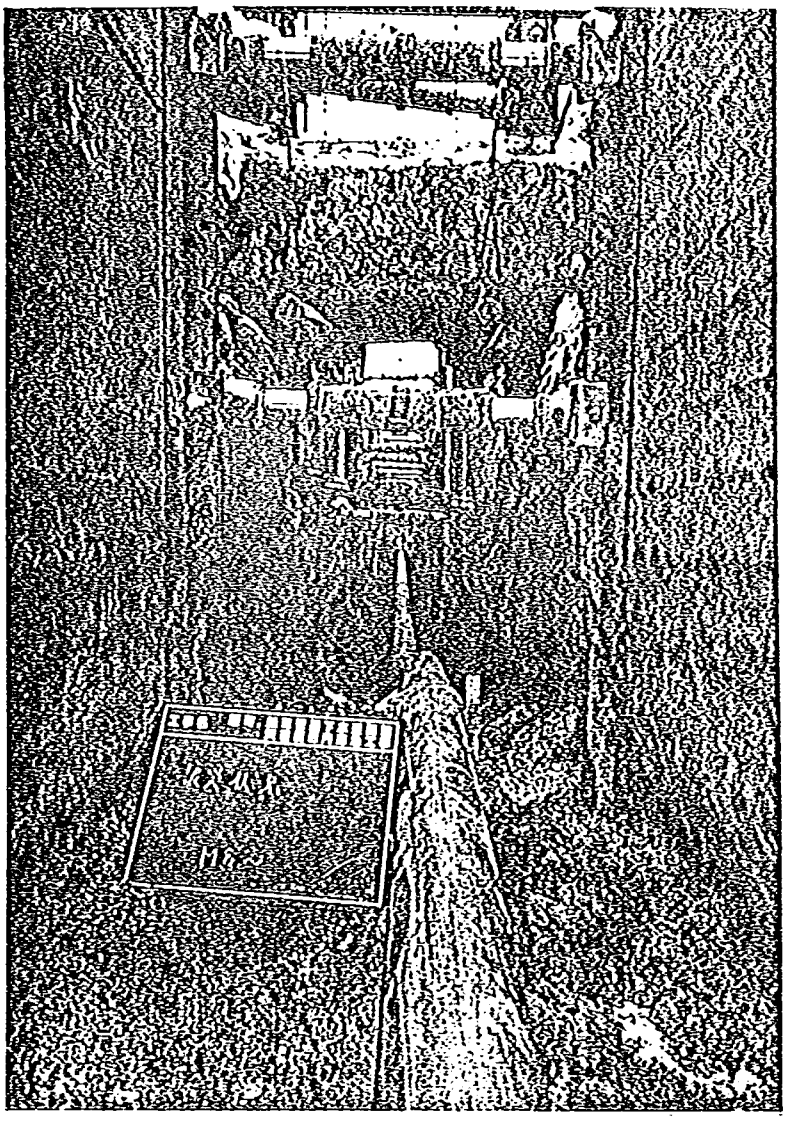


Photo 1 Damaged pipeline which wound vertically.



Photo 2 Damaged pipeline which wound horizontally.

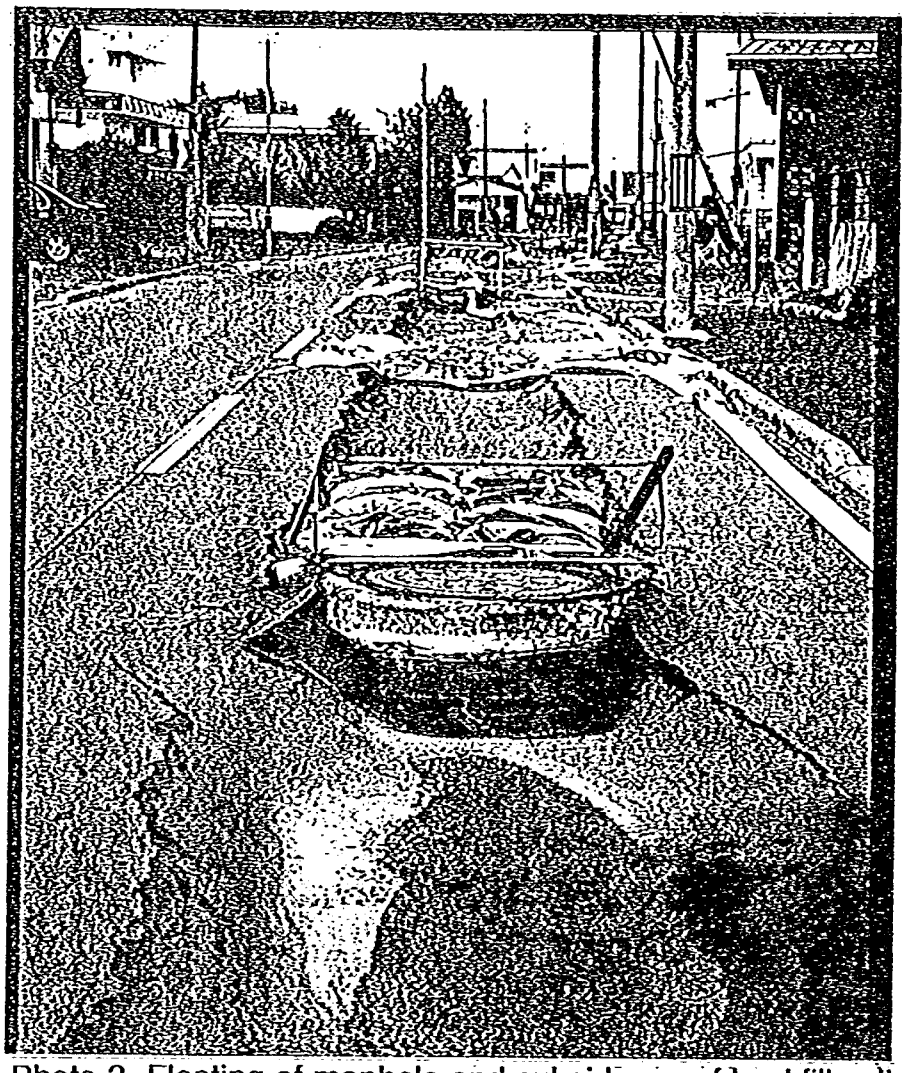


Photo 3 Floating of manhole and subsidence of backfill soil.

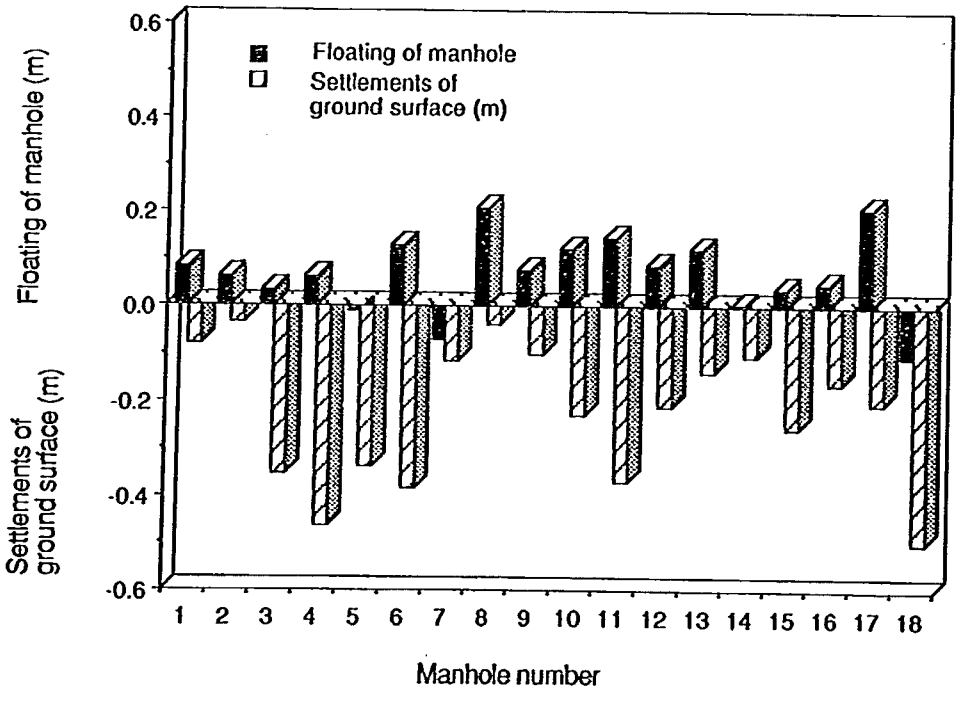



Fig. 6 Floating of manhole and subsidence of backfill soil at Shinkawakami-chou.

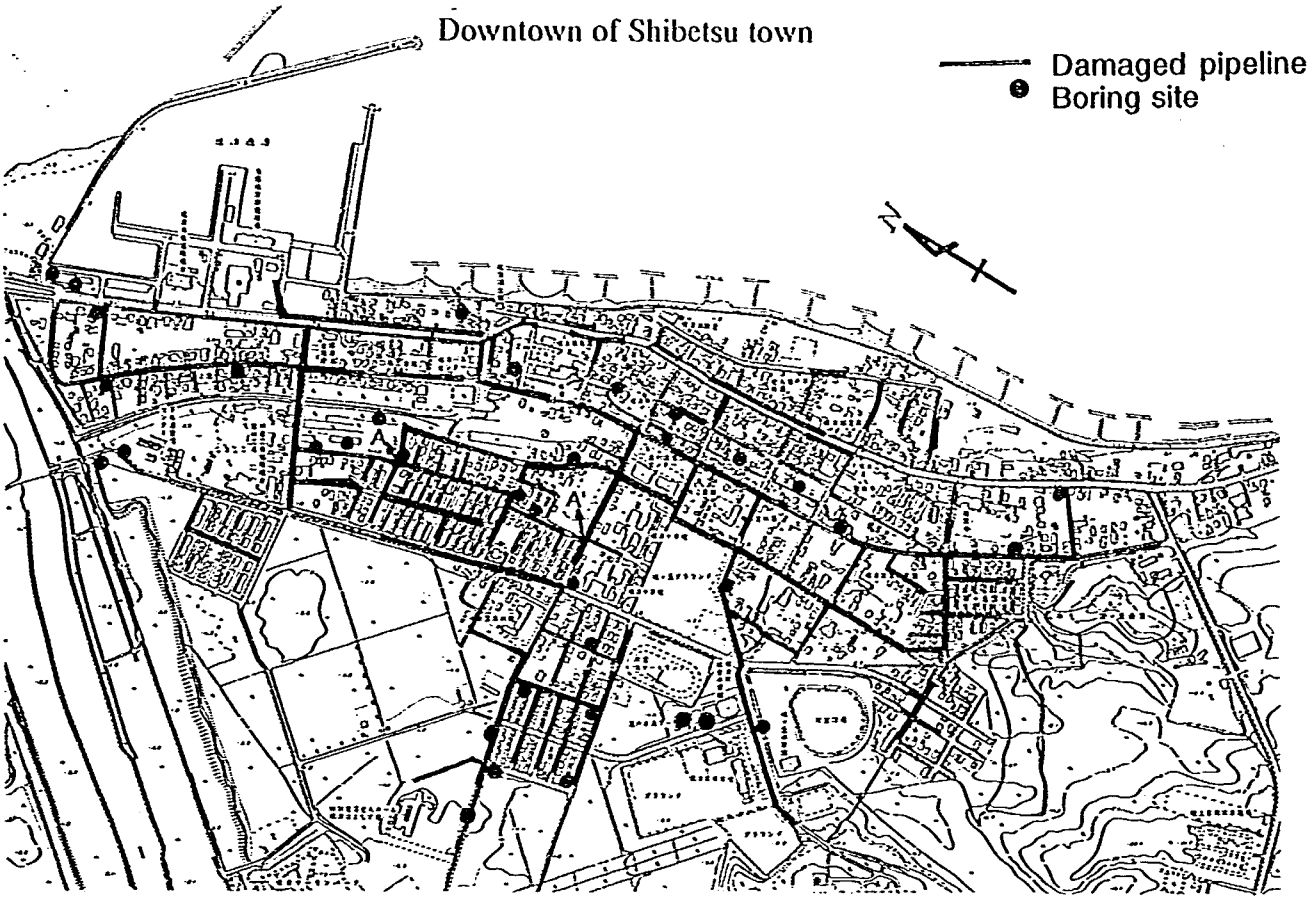



Fig. 7 Damaged pipelines and boring sites.

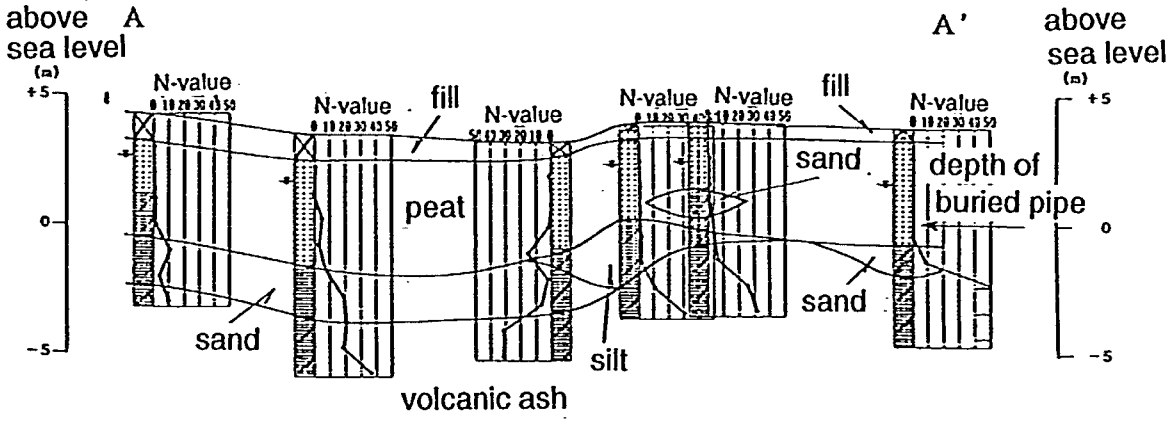



Fig. 8 Estimated soil profiles along A-A' line (after Kiso Jiban Consultant [3]).

Since the sand boils due to liquefaction appeared close to the damaged pipelines, the liquefaction resistance factor $F_L$ [4] was calculated using the boring data and the liquefied layers were estimated. The peak surface ground acceleration was assumed as 350 gal [5]. Fig. 9 illustrates the thickness of estimated liquefied layer at the sites of damaged pipeline and non-damaged pipeline. The thickness of estimated liquefied layer at the sites of damaged pipeline is 2 m to 6 m and that of the non-damaged pipeline is 0 to 3m. It suggests that liquefaction is one of the most influential factors to pipeline failure.

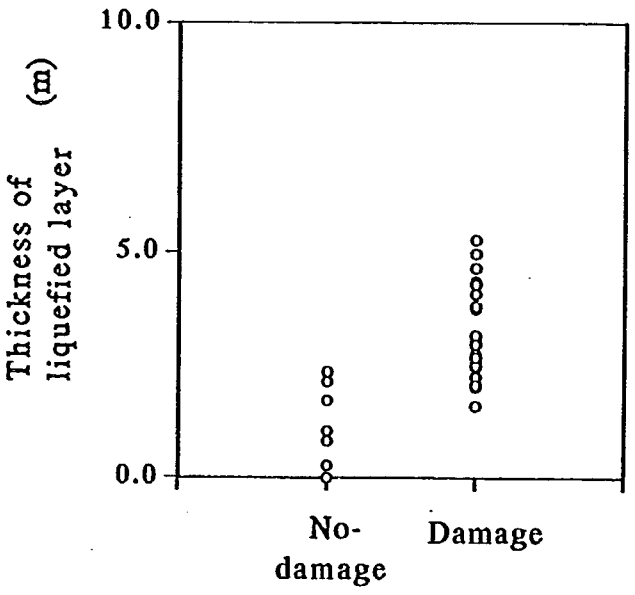



Fig. 9 Thickness of estimated liquefied layer at sites of damaged and non-damaged pipelines.

## Response simulation of layered soil deposit

The layered soil deposit shown in Fig. 10 was analyzed employing the 2-dimensional FEM proposed by authors [6]. The accumulation and dissipation of excess pore water pressure can be evaluated by this method. The accumulation of excess pore water pressure is evaluated by Martin, Finn and Seed model [7] and the dissipation is calculated by the equation of seepage in saturated-unsaturated porous media [8]. The model of layered soil deposits was established by using the boring data at Shinkawakami-chou. Fig. 11 shows model 2, that is, the trench with backfill soil exists in layered soil deposits. The backfill soil is neglected in model 1. The base rock motion was estimated by using the E-W component of the 1993 Kushiro-oki earthquake.

Fig. 11 shows time histories of excess pore water pressure ratios at each element in model 1. The excess pore water pressure ratios at the elements 15,21 and 33 reached 1.0, therefore, the liquefaction could occur at a depth of 1.5 m to 3.0 m and from 4.0 m to 5.0 m. Fig. 12 illustrates the time histories of excess pore water pressure ratios at each element in model 2. Fig. 12 (a) shows the ratios in the backfill soil. The backfill soil at a depth of 0.5 m to 5.0 m could liquefy, that is, most of backfill soil could liquefy. Since the vertical strain of liquefied sand is 5 to 10 %, the subsidence of backfill soil is estimated as about 20 to 50 cm. This value agrees with the subsidence occurred during the earthquake as shown in Fig. 6. Fig. 12 (b) illustrates the ratios at the surrounding soil of the trench with backfill soil. The comparison of both figures suggests that the liquefaction resistance of the backfill soil was smaller than that of the surrounding soil of the trench with backfill soil. Therefore, the liquefaction of the backfill soil was seemed to induce the subsidence of the ground and floating of manhole.

The reasons of liquefaction of backfill soil are considered as follows. SPT $N$-value of backfill soil was small and ground water level was shallow. The upper part of backfill soil was not permeable because the sewerage pipeline was buried below pave road. Since the trench for pipeline was installed at peat layer, the permeability of both side of backfill soil was also low. The backfill soil was, therefore, under the undrained condition during earthquake. Moreover, the shear strain of backfill soil could be great because of the soft peat layer at the both side. The backfill soil seems to be easy to liquefy. The above discussion seems to show that the peat layer strongly affected the liquefaction of backfill soil.

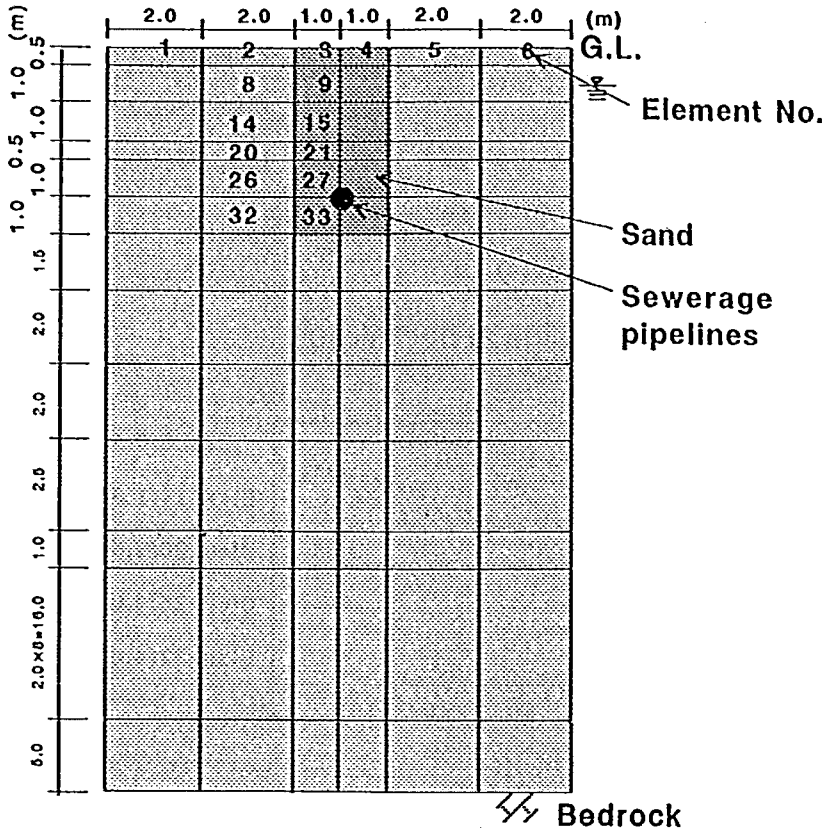



Fig. 10 Finite element model of the ground.

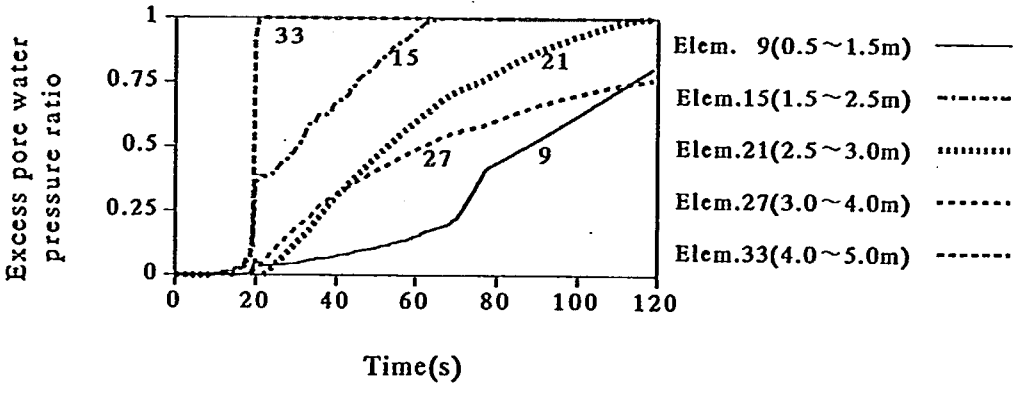
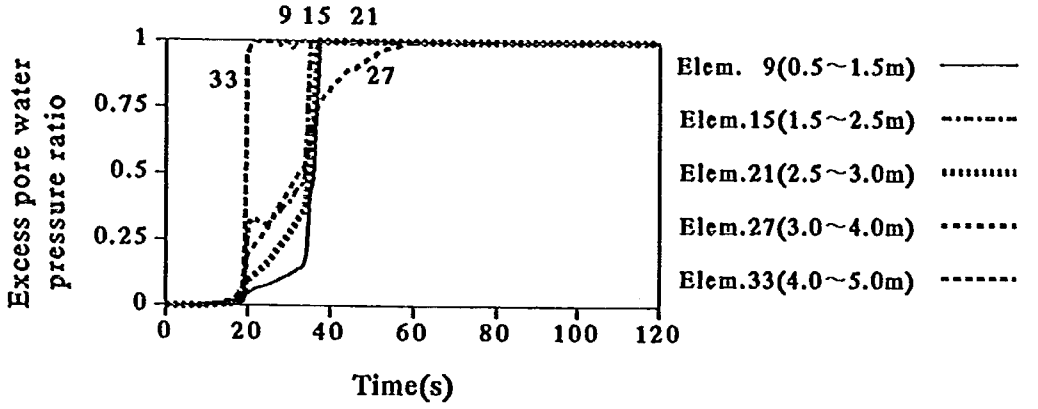
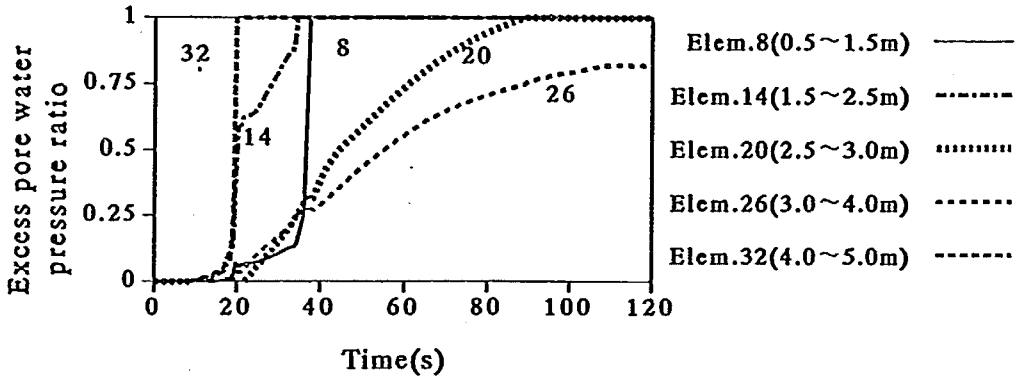



Fig. 11 Time histories of excess pore water pressure ratio (Model 1).




(a) The ratios at backfill soil.




(b) The ratios at surrounding soil.

Fig. 12 Time histories of excess pore water pressure ratio (Model 2).

## Analysis on floating of manhole

Floating of manhole was estimated by using safety index for uplift of manhole as shown in the following equation [9].

$$F_S = \frac{W_B + Q_B}{U_S + U_D}$$

Here, $W_B$ = weight of manhole, $Q_B$= frictional resistance at the side of manhole, $U_S$ = force of uplift acting on bottom of manhole due to static water pressure, $U_D$ = force of uplift acting on bottom of manhole due to excess pore water pressure.

If $F_S$ is below 1.0, manhole begins to float, and when $F_S$ is over 1.0, floating of manhole stops. Using the results of FEM analysis, the floating of manhole in Shibetsu town was calculated. Fig. 13

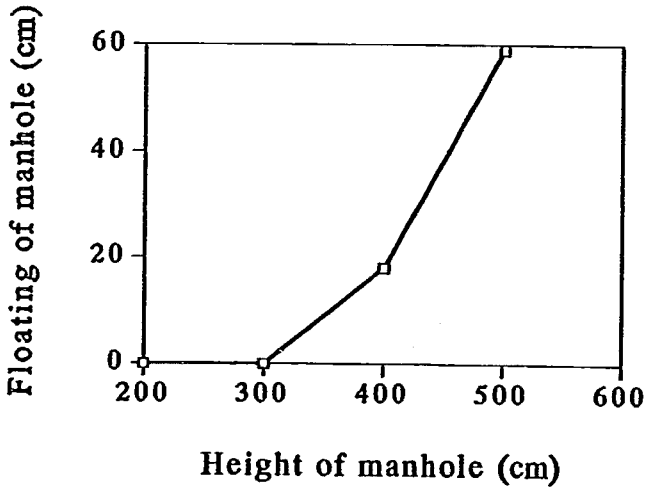



Fig. 13 Calculated floating of manhole at Shinkawakami-chou

illustrates the floating of manhole in relation to the height of manhole. The height of manhole coincides with depth of the bottom of manhole. This figure suggests that the floating of manhole buried at 4 to 5m below surface is 20 to 60 cm.

## CONCLUSIONS

An outline of the damage done to sewerage system by the 1994 Hokkaido Toho-oki earthquake was given and the relation of that damage to ground conditions discussed. The present paper focused on the damage at Shibetsu town in the eastern Hokkaido. The investigation leads to the following conclusions.

(1) Settlement of backfill soil estimated from the response simulation agreed with the actual settlements after the earthquake.
(2) Floating of manhole evaluated by using safety index for uplift of manhole coincided with the actual floating after the earthquake.
(3) Floating of manhole and subsidence of backfill soil seemed to be caused by liquefaction of backfill soil.
(4) Peat layer greatly affected the liquefaction of backfill soil.

## ACKNOWLEDGMENTS

The present paper is based on the data collected through the reconnaissance work. Many individuals and organizations generously helped with our reconnaissance activity. In particular, we are deeply indebted to Mr. T. Jouchi of Shibetsu town for his help. The authors wish to thank Mr. A. Murata and T. Fujino, graduate students of Kanazawa University for their special assistance. This study is supported in part by the Grant-in-Aid for Scientific Research from the Ministry of Education, Science and Culture of Japan (No.07650539).

## REFERENCES

1) Yasuda, S., Nagase, H. Itafuji, S, Sawada, H. and Mine, K.: Shaking Table Tests on Floatation of Buried Pipes due to Liquefaction of Backfill Sands, Proc. of 5th US-Japan Workshop on Earthquake Resistant Design of Lifeline Facilities and Countermeasures Against Soil Liquefaction, pp. 665-677, 1995 (in Japanese).
2) The National Research Institute for Earth Science and Disaster Prevention: Prompt Report on Strong-Motion Accelerations, Science and Technology Agency, No. 44, 1994.
3) Kiso-Jiban Consultants: Investigation Report on the 1994 Hokkaido Toho-oki Earthquake, 1994 (in Japanese).
4) Japan Road Association: Design Code for Road Bridge, V, pp. 16-20, 1990 (in Japanese).
5) Tobishima Construction Company: Investigation Report on the 1994 Hokkaido Toho-oki Earthquake, 1994 (in Japanese).
6) Kitaura, M., Miyajima, M. and Suzuki, H.: Response Analysis of Buried Pipelines Considering Rise of Ground Water Table in Liquefaction Processes, Proc. of JSCE, No. 380, pp. 173-180, 1987.
7) Martin, G.R., Finn, W.D.L. and Seed, H.B.: Fundamentals of Liquefaction under Cyclic Loading, Proc. of ASCE, Vol. 101, No. GT5, pp. 423-438, 1975.
8) Yoshikuni, H., Uno, H. and Yanagisawa, E.: Soil Mechanics (II), Gihodo-Shuppan, pp. 215-224, 1984 (in Japanese).
9) Japan Road Association: Design Code for Common Conduit, pp. 64-68, 1986 (in Japanese).

# DAMAGE TO SEWERAGE FACILITIES IN RECENT EARTHQUAKES

by

Shuji TANAKA

Head of Wastewater System Division, Water Quality Control Department,
Public Works Research Institute, Ministry of Construction,
Tsukuba Science City, Ibaraki-ken 305 Japan

## ABSTRACT

Many large earthquakes have occurred recently, and sewerage facilities have been damaged by these earthquakes. The following typical types of damages are outlined in this paper:

-Big surfacing of manholes by liquefaction of back fill sand in soft ground
-Uplifting of pipes by liquefaction of back fill sand in soft ground
-Continuous sinking of road in area where back fill sand has liquefied
-Gap of block of manhole

In liquefaction, the damage rate of pipes increases as the apparent specific gravity of pipes becomes smaller.

## INTRODUCTION

The length of sewerage pipes in Japan is about 220,000 km. The Japanese Government has set a target of providing sewerage facilities to 90% of the population by the early 21st century, when the length of pipes will reach 900,000 km or more. So far, when sewerage pipes are designed, earthquake countermeasures have rarely been considered, because there has been little experience of serious problems with sewerage facilities due to an earthquake. However, sewerage facilities have been severely damaged due to successive earthquakes recently, and engineers now recognize the necessity of earthquake countermeasures for sewerage pipes.

Sewerage pipes transport sewage by gravity flow. Therefore, the range of displacement tolerance of pipes is narrow. Moreover, the diameter of pipes ranges from 200 to 2000 mm or more, and the depth of pipe-laying underground ranges from 1 to 30 m or more. Therefore, analysis of damage to sewerage pipes is very useful when considering the earthquake-proofness of life line.

This paper explains typical damage to sewerage pipes in recent earthquakes.

## LIQUEFACTION DAMAGE IN SOFT GROUND

In the Kushiro-Oki, Hokkaido-Nansei-Oki, and Hokkaido-Touhou-Oki earthquakes, sewerage pipes received much liquefaction damage. The Kushiro-Oki and the Hokkaido-Touhou-Oki earthquake damages are occurred in large peat ground regions, and peat ground covers mainly on Hokkaido. In other prefectures, the peat layer covers an extremely small area. Peat ground is typically soft, and sewer damages of the Kushiro-Oki and Hokkaido-Touhou-Oki earthquakes occurred in soft ground. In the Kushiro-Oki earthquake, many manholes surfaced in Kushiro town (Figure 1). In the Hokkaido-Touhou-Oki earthquake, roads under which the

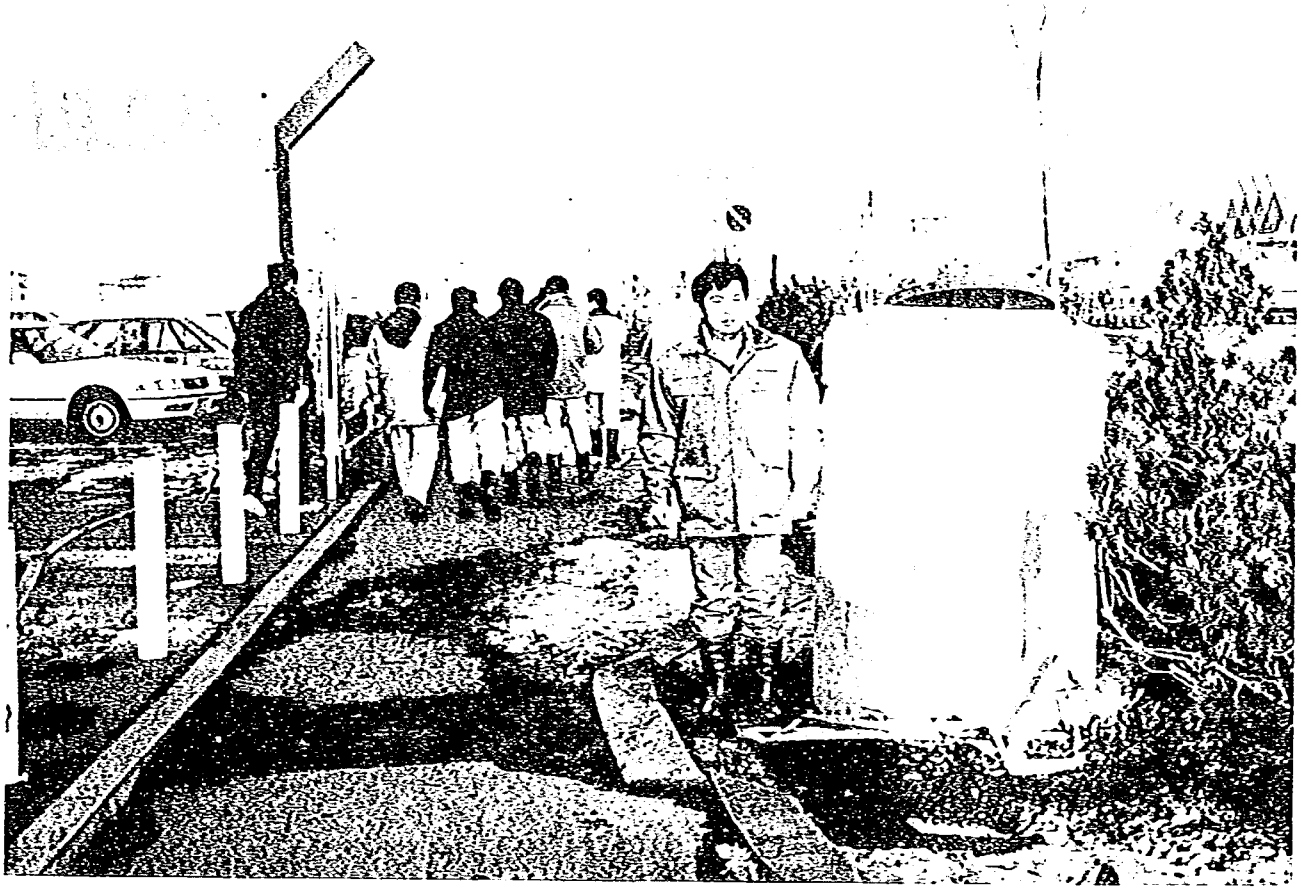


Figure 1. Surfaced manhole, Kusiro town

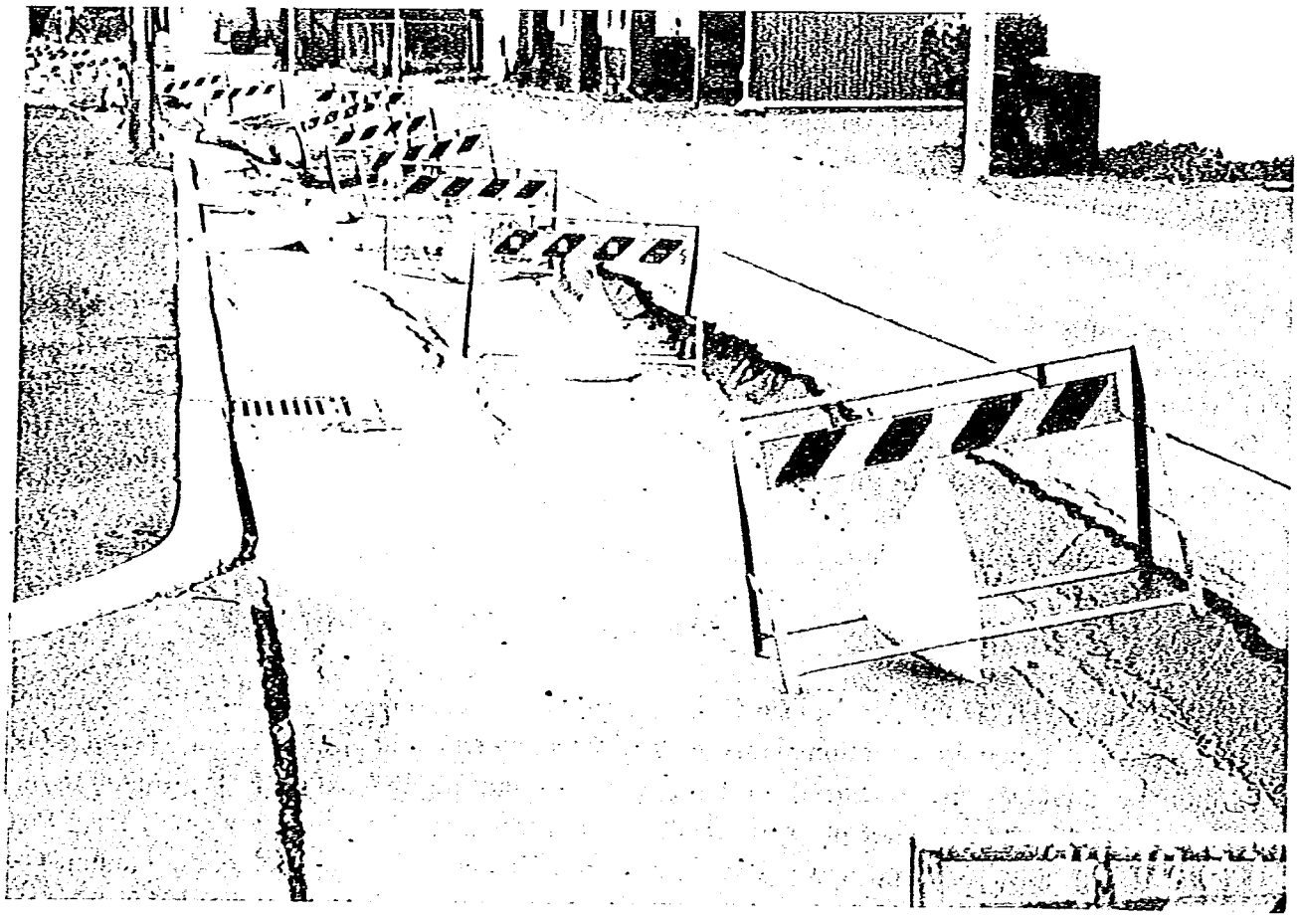


figure 2. Subsided road, Shibetsu town

sewer pipes were laid subsided severely in Shibetsu town and some other areas (Figure 2). Such damage which had not been experienced before attracted great attention.

Ground shaking becomes great in soft ground during an earthquake, therefore damage tends to increase in soft ground. However, though liquefaction usually dose not occur in soft ground, remarkable damage was caused by liquefaction both in the Kushiro-Oki and Hokkaido-Touhou-Oki earthquakes. This damage was generated as follows. When a sewer pipe is constructed by the open-cut method, sand is used widely instead of using excavated soft soil for the back filling material in soft ground region (Figure 3). Because the ground water level is very high in peat area, the back filled sand fills up with ground water, and so is liquefied by earthquake movement.

The displacement of pipes was measured during the restoration construction. This data was arranged in Figure 4 (Ninomiya et al., 1995). In this figure, the perpendicular displacement is more frequent than the horizontal displacement. In addition, uplifting is more common than subsidence in the perpendicular displacement. Consequently, liquefaction uplifted the sewer pipes from there normal position.

Surfacing of manholes was also typical damage caused by liquefaction in Kushiro town, rising 1.5m above ground level as a maximum. Such damage was caused by the same circumstances.

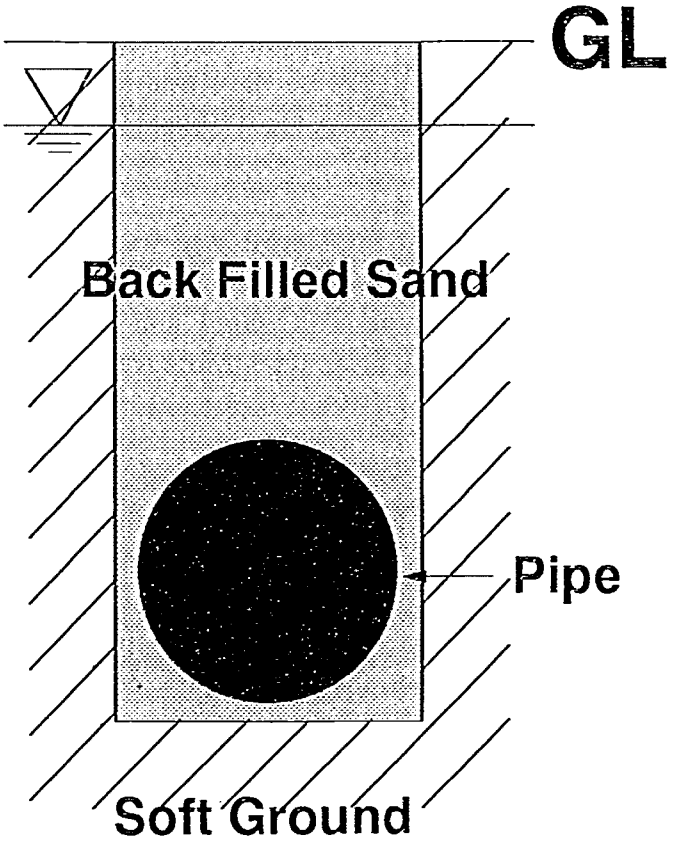



Figure 3.
Cross-sectional view
at Kushiro city

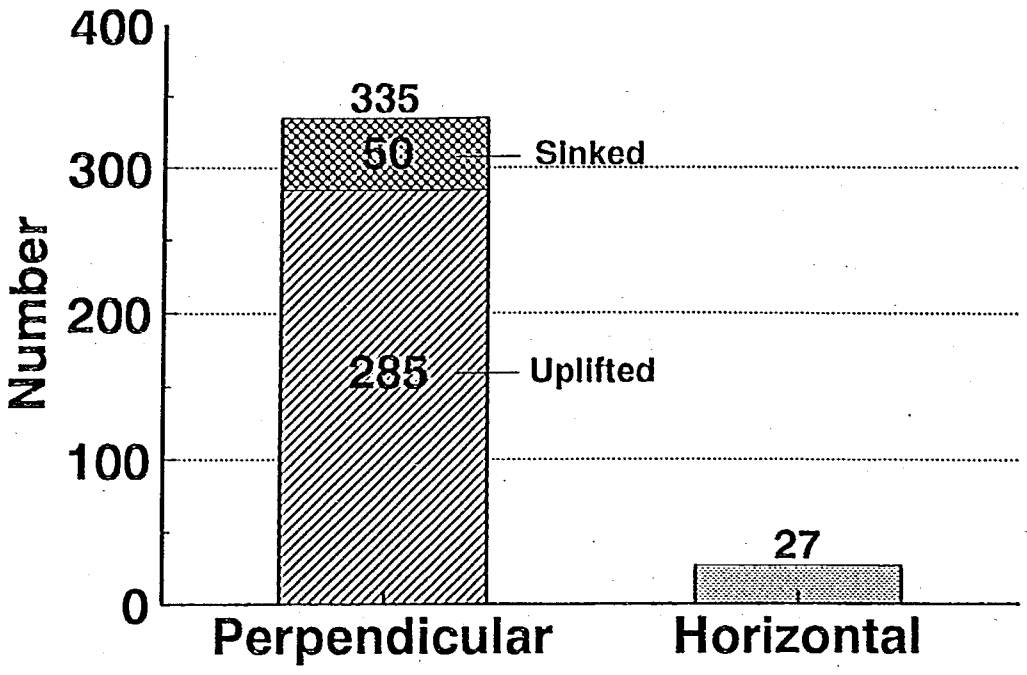



Figure 4. Pipe displacement at Kushiro city due to Kushiro–Oki earthquake

## DAMAGE RATE IN CASE OF LIQUEFACTION

The Kushiro-Oki and the Hokkaido-Touhou-Oki earthquakes struck almost the same region in a short term. The sewerage facilities in Kushiro city were badly damaged twice by these earthquakes. The length of pipes damaged by the Kushiro-Oki earthquake was 7,107 m, and totaling damage of 1,061 million yen. With the Hokkaido-touhou-oki earthquake, the figures were 6,234km, and 775 million yen.

The considerable earthquake damage in Kusiro city was caused by uplifting of pipes by liquefaction. The pipe damage length is divided into centrifugal reinforced concrete pipe (CRC pipe) and polyvinyl chloride pipe (PVC pipe), and classified by pipe diameter in table 1. PVC pipe was damaged more than CRC pipe. Moreover, the damage rate rose as the pipe diameter increased in the CRC pipe.

In sewerage pipes, sewage is transported by gravity flow. Sewage flows from branch lines to trunk lines and flows into a treatment plant. The length of small diameter of pipes accounts for most of the entire system. For instance, in Kushiro city's sewerage system, the pipe length of up to 300 mm accounts for 84%. And in flat places, the underground depth of sewerage pipes increases downstream. Therefore, the deeper the depth of pipe, the larger the pipe diameter,which means the larger the CRC pipe's depth became, the more the pipe is damaged.

The phenomenon of more damage as the pipe diameter became larger is the opposite to damage trends in previous earthquakes such as the Nihon-Kai-Chubu earthquake in 1983. Furthermore, the CRC pipe shows a higher damage rate than the PVC pipe in the Nihon-Kai-Chubu earthquake. However, in Kushiro city the PVC pipe shows a higher damage rate than the CRC pipe. The weight of PVC pipe is light, for example, PVC pipe weights about one-fourth of the same size CRC pipe for a diameter of 200 mm. Therefore,

Table 1. Damage rate and apparent specific gravity at Kushiro city and Shibetu town

| | Pipe Type | Diameter mm | Total-length m | Damaged-length m | | Damage rate % | | Apparent Specific Gravity |
|---|---|---|---|---|---|---|---|---|
| | | | | Kushiro-Oki -Earthquake | Touhou-Oki -Earthquake | Kushiro-Oki -Earthquake | Touhou-Oki -Earthquake | |
| Kushiro city (Furukawa treatment area) | CRC | 200 | 27114 | 211 | 41 | 0.78 | 0.15 | 1.016 |
| | | 250 | 247819 | 3001 | 3027 | 1.21 | 1.22 | 0.891 |
| | | 300 | 16173 | 503 | 325 | 3.11 | 2.01 | 0.811 |
| | | 350 | 4644 | 42 | 39 | 0.90 | 0.84 | 0.758 |
| | | 400 | 2270 | 179 | 0 | 7.89 | 0.00 | 0.726 |
| | | 450 | 4657 | 176 | 12 | 3.78 | 0.26 | 0.706 |
| | | 500 | 1244 | 0 | 0 | 0.00 | 0.00 | 0.705 |
| | | 600 | 3407 | 0 | 146 | 0.00 | 4.29 | 0.706 |
| | | 700 | 1460 | 0 | 0 | 0.00 | 0.00 | 0.707 |
| | PVC | 200 | 42195 | 166 | 457 | 0.39 | 1.08 | 0.185 |
| | | 250 | 5882 | 1658 | 1799 | 28.19 | 30.58 | 0.177 |
| | | 300 | 69 | 0 | 56 | 0.00 | 81.16 | 0.173 |
| Shibetu town | PVC | 200 | 5352 | - | 4378 | - | 81.80 | 0.185 |
| | | 250 | 11963 | - | 5425 | - | 45.35 | 0.177 |
| | | 350 | 866 | - | 580 | - | 66.97 | 0.168 |
| | | 400 | 415 | - | 153 | - | 36.87 | 0.165 |

because of it's light weight PVC pipe cannot resist a large uplift force when the ground became liquefied, which explains the high damage rate of PVC pipes. Moreover, in the CRC pipe the apparent specific gravity becomes small as the diameter increases, hence the pipe tends to be uplifted more easily with liquefaction. To clarify the relation between the damage rate and pipe size and type, the damage rates are shown by apparent specific gravity of pipes in Figure 5.

The damage rate increases as the apparent specific gravity decreases. However, in some cases even if the apparent specific gravity is small, the damage rate is small. The maximum damage rate in the figure may therefore reach an upper limit corresponding to the apparent specific gravity.

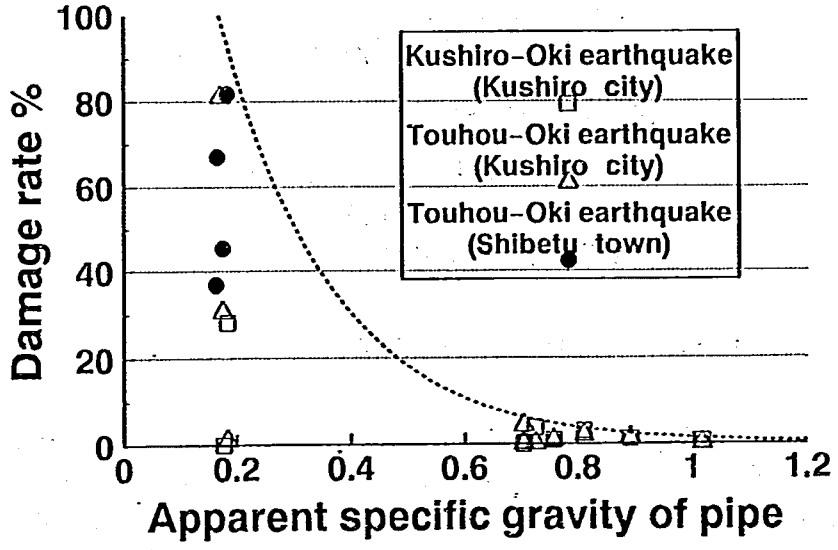



Figure 5. Damage rate in Liquefaction

## LIQUEFACTION CAUSED BY SMALL AMOUNT OF CUSHION SAND

Towada city suffered uplift of its sewers due to the Sanriku-Haruka-Oki earthquake. The type of damage is the same as that observed in Kushiro city, but the back fill soil condition was different from the case of the Kushiro city. Sandy gravel, which contains 60% or more gravel with grain diameter larger than 2 mm was used for the back fill soil. Sand was filled around the pipe as shown in Figure 6 as a cushion material to prevent the pipe being damaged by the gravel. Only the cushion sand is considered to have liquefied and to have displaced the pipe largely. It is unlikely that the back filled gravel liquefied, because undrained cyclic triaxial tests of disturbed samples showed a considerably large cyclic stress ratio of 0.35 which caused liquefaction in 20 cycles. A thorough examination is thus necessary for the cushion material even if its amount is relatively small.

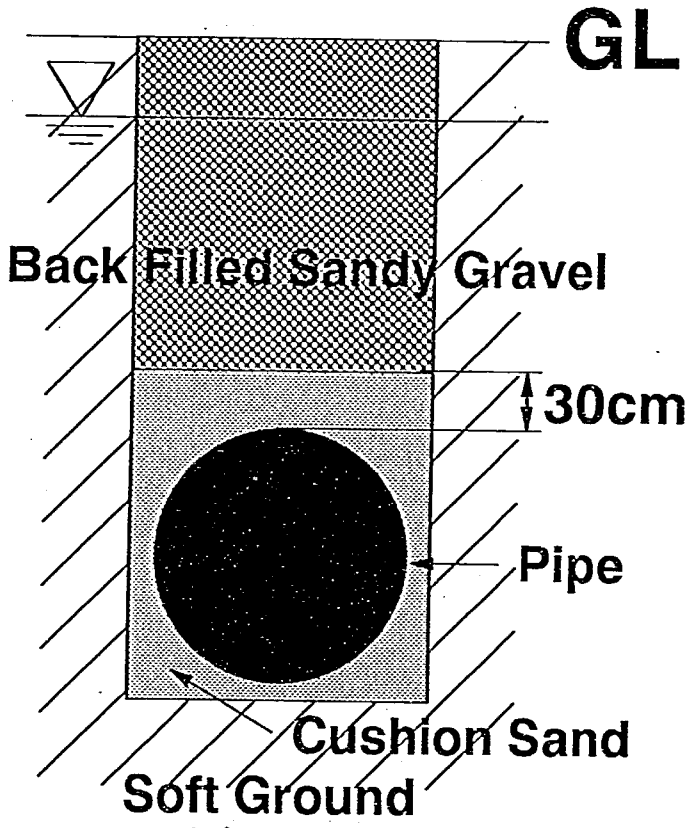



Figure 6.
Cross-sectional view
at Towada city

## DAMAGE DUE TO THE HYOGO-KEN-NANBU EARTHQUAKE

In the Hyogo-Ken-Nanbu earthquake, the earthquake gave damaged pipes in two prefectures and nine cities, in which the percent of sewered population exceeds 90%. A complete picture of the damage has not emerged yet because the pipe damage extends over a wide area and is very severe, and more time is required to assess the characteristics of the entire damage. Damaged facilities are now being restored in the city.

In the Hyogo-Ken-Nanbu earthquake, part of the ground in the area was liquefied. However, most pipe damage occurred in the non-liquefied region.

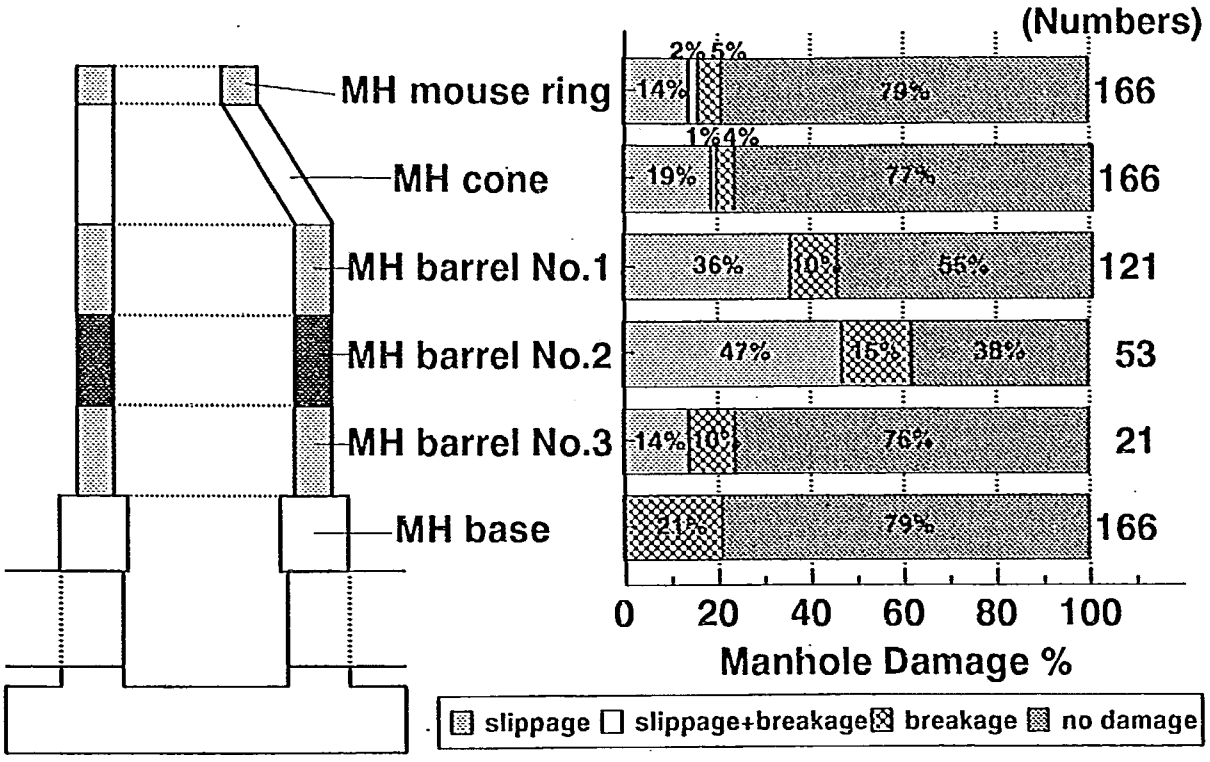



Figure 7. Manhole Damage

Figure 7 shows manhole damage. In the lower part, damage is great, which suggests the shear strain of ground reflecting the damage characteristic.

Pipes connected manholes were damaged more than other ones. In case of breakage, manhole connecting pipes were damaged about ten times to other ones. In case of joint displacement, they were 1.7 times.

## CONCLUSION

-In the case of liquefaction, (1) PVC pipe is damaged more than CRC pipe, (2) in the CRC pipe the damage increases with pipe diameter. These tendencies are both functions of the apparent specific gravity.
-Sand that was filled around the pipes caused liquefaction damage, even if the volume of sand was relatively small.
-In manholes, the lower part was easily damaged severely.
-Manhole connecting pipes were damaged severely.

## REFERENCES

Ninomiya Y. et al.(1995) Predictions and countermeasures for liquefaction damages to sewerage facilities.,PWRI annual report FY1994

# WATER AND SEWER LIFELINES
# LESSONS LEARNED FROM RECENT EARTHQUAKES

Le Val Lund, P. E., M. ASCE
Civil Engineer, Los Angeles, CA

## ABSTRACT

The interest in the seismic performance of water and sewer lifelines grew after the 1971 San Fernando, CA, USA earthquake. One of the American Society of Civil Engineers-Technical Council on Lifeline Earthquake Engineering goals is to study the lessons learned from the seismic performance of lifelines. Since the 1971 event there has been a number of earthquakes in California and Japan testing the performance of tanks, reservoirs, wells, pumping plants, water and wastewater treatment plants, pipes and lifeline agency emergency response. Some conclusions and lessons learned and relearned from these earthquakes are discussed.

## INTRODUCTION

The interest in the seismic performance of water and sewer lifelines developed after the 1971 San Fernando, CA, USA earthquake. C. Martin Duke, Professor of Civil Engineering, UCLA, initiated the lifeline study, which ultimately created the American Society of Civil Engineers-Technical Council on Lifeline Earthquake Engineering. One of ASCE-TCLEE goals is to study the lessons learned from the seismic performance of lifelines. Since the 1971 event there has been a number of earthquakes in California and Japan testing the performance of tanks, reservoirs, wells, pumping plants, water and wastewater treatment plants, pipes and lifeline agency emergency response and recovery.

Lifelines are those services vital to the health, safety, human and social activities of the community and particularity to the functioning of an urban and industrialized society. Lifelines are critical for the emergency response and recovery of a community after a disaster such as an earthquake.. Lifelines include electric power, communication, transportation (highways, airports, railroads and harbors), water, sewage, natural gas, and liquid fuel systems. Only water and sewer lifelines will be discussed in this report.

## EARTHQUAKES

San Fernando, USA, 6:01 a.m., (PST), February 9, 1971, M 6.6

Whittier Narrows, USA, 7:42 a.m., October 1, 1987, M 5.9

Loma Prieta, USA, 5:04 p.m., (PDT), October 17, 1989, M 7.1

Landers and Big Bear, 4:58 and 8:04 a.m., June 28, 1992, M 7.5 and M 6.6

Northridge, USA, 4:31 a.m., (PST), January 17, 1994, M 6.7

Kyogo-Ken Nanbu (Kobe), Japan, 5:46 a. m. (JT), January 17, 1995, M 6.9

## GENERAL

Some of the lessons learned and recommendations from these earthquakes are discussed. Typically lessons are learned from previous earthquakes, but due to limitations on funds and resources seismic mitigation is not performed and the lesson is relearned. The following are some

conclusions, lessons learned and recommendations to improve water and sewer lifeline performance in future earthquakes.

## Lifelines Importance

Since the 1971 San Fernando earthquake, lifelines have played an important role in emergency response and restoring the community after an earthquake. Telecommunications, radio and electronic media play a role in directing emergency response for essential services and the repairing of damaged lifelines. Water supply is necessary for public fire protection. Wastewater systems are necessary to prevent pollution and the potential for illness and the spread of diseases. Highways and roads are used to move rescue, repair, fire and medical teams and their supplies and equipment to the damaged areas for rescue and restoration.

## Seismic Performance

The 1994 Northridge event showed significant improvement in the seismic performance of lifelines from the 1971 San Fernando earthquake. Among the facilities and equipment installed, using modern seismic design, since 1971, with good seismic performance, but not totally inclusive is dams, steel and concrete tanks, wells, and pumping stations. Dams in California since 1971 have been constructed or retrofitted using dynamic finite element seismic design analysis. Steel and concrete tanks have been designed using the seismic criteria in AWWA Standards. Wells have been constructed using California well construction standards. Pumping and chlorination plants have been designed using the seismic criteria of the local building codes. In the Loma Prieta and Northridge earthquakes there has been damage to mechanical equipment in the basins of water and wastewater treatment plants due to shaking and sloshing within the basins. In all California and the Kobe, Japan earthquakes there has been significant damage to pipe systems. There is a continuing need to develop seismic guidelines and standards for all water and sewage lifelines.

## Emergency Response Plans

The 1971 San Fernando and 1987 Whittier Narrows earthquakes experience have encouraged lifeline agencies to prepare emergency response plans and emergency operations centers. These plans have been tested and implemented by lifeline agencies. Emergency operations plans are working. The regular earthquake exercises generally held in California, in April, of each year in various communities proved to be invaluable in

the lifeline response to earthquakes. The month of April is selected because it is the anniversary of the 1906 San Francisco, USA, earthquake. Lifeline emergency response plans need to be updated and practiced on a regular basis.

## Old Steel Tanks

Older steel tanks not seismically designed and constructed suffered buckling at the bottom (elephants foot bulge), damage to the tank shell and roof in the San Fernando, Landers/Big Bear and Northridge earthquakes. These tanks are not designed to take the horizontal and vertical shaking. There is a need to develop seismic guidelines and retrofit these older facilities.

## Steel and Concrete Tanks

Prestressed-concrete water tanks designed and constructed in excess of AWWA Standards for Wire-Wound Circular Prestressed-Concrete Water Tanks (AWWA D 110) performed very well in the Northridge event. There were welded steel tanks that performed well in the Northridge event; however, it is not known whether they were seismically designed and constructed under American Water Works Association (AWWA) Standards for Welded Steel Tanks for Water Storage (AWWA D-100). An AWWA designed tank in the Watsonville area performed well in the Loma Prieta earthquake. In Kobe most of the tanks are prestressed and they performed well. New steel and concrete tanks need to be designed and constructed with the seismic criteria provided in the AWWA standards.

## Tank Inlet and Outlet Piping

Above ground tanks usually have either one or two pipes, with valves, rigidly connected to the tank to provide for the filling the tank and draining the tank to meet the peak water demands in the water service area. In the San Fernando, Landers/Big Bear and Northridge earthquakes, there were cases were the piping or valves broke because the differential movement between the tank and the piping. Several methods have been developed for providing a more flexible connection between the tank and the piping to withstand the differential movement. There needs to be further study on economical and other methods of preventing storage tank inlet/outlet piping damage due to differential movement.

## Bell and Spigot Joint

Water supply lifelines use the bell and spigot pipe almost exclusively for welded steel pipe. Bells are fabricated by using a mandrel to expand the cold pipe to create the bell. There were a number of instances in the Northridge earthquake were the large diameter bell was cracked at the curvature point where the bell changes diameter. There is a need to study the seismic strength of welded steel bell and spigot joints and how to improve the seismic performance of the joint. The joint performance should be compared with the current (AWWA) Standard for Welded Steel Pipe.

## Cast Iron and Old Steel Pipe

Most damage to the water distribution system piping occurred in cast iron pipe with rigid joints (lead or cement caulked) and old steel pipe subject to corrosion in the San Fernando, Loma Prieta, Landers/Big Bear, and Northridge earthquakes. Programs are needed, including funding, to replace this older pipe in seismically active areas.

## Air Inlet and Air Release Valves

Air inlet and air release (air and vacuum) valves are located at high points on pipelines. This valve prevents a vacuum from collapsing the pipe when the water is rapidly released upon a pipe break or damage due a sudden pressure increase (water hammer). This valve is installed as an inverted pendulum above the ground surface. In the Northridge event many valves toppled, had cracked bodies or damaged floats (balls). Also the damage was caused by transient pressures in the pipeline. Replacement valves were available in two days. A study is required to improve the performance of these valves in an earthquake.

## Emergency Power Supply Operation

In past earthquakes most of the emergency power supplies, where installed and tested, worked for pumping stations and treatment plants when available. A water reclamation plant emergency generator automatically started in the Northridge event, but was shut down when strange noises occurred. In the Loma Prieta earthquake an auxiliary fire pumping plant used its supply of fuel in the day tank; however, since there was a commercial power outage, the electric pump could not transfer fuel from the reserve tank to the day tank. There is a need for transferring

fuel from the storage tank to the day tank, when the electric pumps are out of service. There is a continuing need to regularly test these emergency generators under load; to have adequate fuel for a longer term commercial power outage.

### Emergency Power Supply

There are number of wells, pumping stations and water treatment and water reclamation plants without emergency power or do not have capacity to provide for all their essential operations. In the Loma Prieta event a water agency operation and maintenance yard lost commercial power. Emergency generator provided power for the communication facilities which worked fine. The yard electric fuel pumps where not connected to the emergency power, which delayed the refueling of trucks and equipment necessary for the restoration effort. A portable generator was moved to the fuel pumps to solve the problem which required an electrician to make the electrical connections. Water and sewage facilities need emergency power and capacity to provide for all their essential operations. Also in cases where portable generators are used 'quick electrical connectors' expedite there operation.

### Shaking and Sloshing in Treatment Plant Basins

Shaking and sloshing in large basins in water filtration and water reclamation plants has cause damage in the 1994 Northridge and 1989 Loma Preita events. As an example, shaking and sloshing damaged the wood baffles in 2,082 ML/d (550 mg/d) water treatment plant and jammed the chain drive sludge scrapers in seven out of 44 final clarifiers of a 303 ML/d (80 mg/d) water reclamation plant in the Northridge event. Also, three of the four up-flow clarifiers in 303 ML/d (80 mg/d) water treatment plant in the Loma Prieta event was damaged. A laboratory worker reported that the wave almost reach the top of a 0.76 m (30-in) railing around the basin. Inside each clarifier is a floculator-center feed clarifier equipment supported on a one meter (39-in) steel column. The column, anchored at the base (a pendulum) rotated and cracked the rotating floculator gear-drive housing casting. Some of the launderers fell on and jammed the rotating sludge scraper. Although not critical, the damaged equipment can cause malfunction of other equipment. There is a continuing need to consider sloshing and shaking in the design of mechanical equipment and baffles in large basins of water and wastewater treatment plants.

## Redundancy

Customer water supply and wastewater service has been disrupting to a the population impacted by past earthquakes. Most of this disruption was due to distribution system damage and structural damage to residences and buildings. The water disruption has been reduced because redundancy has been provided by distribution system grid networks and alternate water supplies have been provided from reservoir storage, groundwater basins and alternate aqueduct systems. In the Northridge earthquake when the major supply lines were damage redundant alternate supplies were provided to the Santa Clarita, Simi and San Fernando Valleys from the groundwater basin, reservoir storage and imported supplies from the Colorado River Aqueduct, respectively. Redundancy needs to be expanded as it continues to play an important role in the providing and restoring of water and wastewater services.

## Essential Facilities Lifelines

The 1994 Northridge event demonstrated the vulnerability of lifelines within essential facilities, such as, hospitals, fire stations and emergency operating centers. Small breaks in water lines and automatic sprinklers caused flooding in lower floors, Roof top HVAC equipment was damaged which caused malfunction of other systems within the building. Most roof top equipment has been constructed as an add-on to the building without consideration of earthquake forces. Lifelines in essential facilities require seismic design. In some of the hospitals the lost of electric power and water supply impacted the operation of the facility. There is a need for emergency electric and water supplies for essential facilities.

## Alternate Work Locations

The Northridge earthquake because of the closure of major transportation highways (Interstate 10 and State Highway 14) identified several areas were there is a need for enhancing the ability of lifeline employees in their emergency response and recovery activities. This event cause transportation problems, because of the closed freeways, for lifeline employees to get from their homes to their regular work location. Alternate work locations or telecommuting where feasible should be considered.

## Emergency Food, Water and Housing

The Northridge earthquake showed the need for emergency food, water and housing; and adequate cash to purchase these items, for lifeline workers in the epicentral areas. Because of the loss of potable water, gas and electricity; restaurants, motels and banks (Automatic Teller Machines) were not in operation. This affected mutual aid agencies who came from a outside the Ventura and Los Angeles Counties area and Los Angeles Aqueduct employees, who came from a maintenance yard 161-km (100-miles) to the north to make their repairs. This required a 322-km (200-mile) round trip each day, because the Santa Clarita Valley motels and restaurants were not operating, since they were under a boil water notice.

## Family Communication Plan

There is need for a communications plan, which has been tested for lifeline employees and families to notify each other of their well being. This would allow employees to report directly to a restoration effort without worrying about their families. The telephone system would probably be jammed, because of tremendous increase in the number of call attempts. An amateur radio system has been used to limited degree in the Loma Prieta and Northridge earthquakes. This was not necessary in the in recent earthquakes, since they occurred early in the morning or at the beginning of the 1989 World Series baseball game and most of the employees were at home.

## Non-emergency Employee Training

Non-emergency response lifeline employees, in advance of an emergency, should be assigned and trained in emergency response activities. After the Loma Prieta earthquake non-emergency employees, in the Santa Cruz area, operated the radio system and issued warehouse supplies. In the Northridge earthquake, non-emergency response personnel documented the repairs for Federal Emergency Management Agency (FEMA) reimbursement. Only government water and waste water agencies are eligible for reimbursement. Investor owned utilities also must document their costs in order to apply for Small Business Administration loans.

## Emergency Response Employees Assistance

Lifeline emergency response personnel are concerned for the safety of their family and stability of their house after an earthquake. In the

Northridge event one water agency provided family counseling while another agency with their own engineering staff, not involved in the recovery operation, offered their services to help employees with their home earthquake inspections. These activities assisted those employees who were involved in the restoration activities in this emergency. Consideration should be given to help emergency response employees with their families and housing in an emergency.

## Mobile Water Quality Laboratory

In the Northridge event, because of the number broken water mains "boil water" notices were issued by the water agencies and California Department of Health Services (CDHS) in both Ventura and Los Angeles Counties. The boil water notice was issued on TV, radio and newspapers as a precautionary measure in case the water was polluted from the broken water mains. Customers were ask to boil their water for a specific period of time or add a specified amount of disinfectant. Notices were in effect until January 24th in the Simi Valley, January 29th in the San Feranado Valley and February 4th in the Santa Clarita Valley. Samples were collected in the field and transported to a CDHS certified laboratory before clearance was given to lift the notice. This was a time consuming operation. There is no indication that a boil water notice was given in the Kobe earthquake. Consideration should be given to developing a mobile water quality laboratory to expedite, in the field, after repairs have been made, the determination if the water is safe for drinking.

## Expedited Bacteriological Testing

After a water main is repaired the main must be pressure tested and disinfected to eliminate any possibility of pollution. Samples are collected and tested at a CDHS certified laboratory. Currently the bacteriological testing using the membrane filter method takes 48 hours to quantify the fecal coliform. However, during the Northridge event the Colilert test was used which require 24 hours to determine the absence or presence of fecal coliform. In Los Angeles, samples checked in this manner were rechecked using the membrane filter method. Bacteriological testing is time consuming to determine if the water is not contaminated and safe for drinking. Research should be done to expedite this process in order to determine if the water is safe for drinking and the boil notice may be lifted sooner.

## Confined Spaces Entry

Large diameter pipes, conduits and tunnels were repaired from the inside in the Northridge earthquake. In the United States, the Occupational Health and Safety Act (OSHA) requires specific air testing to determine the presence of poisonous gases. It also specifies specific emergency breathing equipment required before entering a confined space. The entering of large diameter pipes, conduits and tunnels requires compliance with OSHA requirements for entering confined spaces.

## Mitigation Financing

The Northridge event there was good performance of structures and equipment which had been seismically upgraded from the 1971 San Fernando event. Pipelines usually need replacement, while structures and equipment can be seismically retrofitted. Seismic upgrade of water and sewage equipment, buildings and facilities is very costly requires prioritizing, budgeting and some form of innovative financing. Innovative financing research is required to further improve the seismic performance of these lifelines.

## Seismic Vulnerability Assessments

After the 1971 San Fernando earthquake, Los Angeles made a seismic vulnerability assessment of its water facilities. Facilities were identified as low, medium and high cost for retrofit or replacement. A number of dams, pumping stations, chlorination stations and maintenance yards were seismically retrofitted or completely rebuilt at cost of nearly $200 million. Metropolitan Water District of Southern California and other water and sewer agencies have had similar programs. There was no reported damage to these facilities in the Northridge earthquake. All lifeline agencies should make seismic vulnerability assessments of their facilities to determine vulnerability to damage of their system. The assessment should prioritize, budget and schedule any required seismic mitigation.

## Collocation

Studies have been made of collocated lifelines in the Cajun Pass, California and Salt Lake City, Utah to determine their response to a scenario seismic event. On Balboa Boulevard in Granada Hills in the Northridge earthquake an actual collocation event occurred. There were nine lifelines including

the street at this location (gas, water, sewer, petroleum, telephone, cable TV, power and street lighting). A zone of tension and compression occurred approximately 275-meters (900-ft) apart causing damage to one sewer, two gas and two water lines. A fire erupted eventually causing the burning of five homes and severing the overhead telephone, cable TV, power and street lighting. Studies are required to develop mitigation scenarios for essential collocated lifelines.

## Direct and Indirect Losses

In past earthquakes the direct loss of the lifeline is small compared to the loss of the function of the lifeline. Highways and streets are necessary for use to gain access for restoration effort. The non availability of water could inhibit fire suppression and the loss of commercial power could prevent water pumping and treatment if back-up power is unavailable. Indirect losses could be considerably greater than the direct losses. Studies have been made; however, further studies should be made so that management decisions related to cost-benefit can be made for seismic retrofit or replacement.

## Emergency Water Supplies

In all of the California earthquakes cited above and the Kobe event there has been significant damage to water pipeline networks causing lack supply to the people for drinking, cooking and sanitary purposes and water for fire suppression. Construction and beverage water trucks, water tank trailers, portable tanks, fire hydrant hose bibb adaptations, portable treatment units, swimming pools, and portable hoses and pipeline systems have been used. These systems have been coordinated between water agencies, fire departments, military and the emergency services organizations. Emergency response plans should include emergency water supply and designate a specific organization to manage the emergency water supply.

## Geographical Information Systems

Pipeline repairs have been documented in the Loma Prieta and Landers/Big Bear earthquakes using the geographical information systems (GIS). ASCE-TCLEE created the TCLEE Pipeline Failure Database for these events. Northridge earthquake pipeline repairs is also being documented using GIS. GIS identifies the repairs by latitude and longitude and provides characteristics of the repair, i.e. pipe diameter, material, age, type of

damage and repair, etc. In California, a system is under development to determine an early assessment of damage using damage reports from past earthquakes, GIS and almost real time information as to the location and magnitude of earthquakes. This information could be of value to assist the lifeline agencies in directing their response for repair and recovery.

## SUMMARY

1. Lifelines performance in past earthquakes have continued to show their value in the emergency response and recovery of a community after a disaster such as an earthquake.

2. There is a continuing need to develop seismic guidelines and standards for lifelines where there are no current guidelines or standards.

3. All lifeline agencies should have an emergency response and recovery plan. The plan should be practiced and updated on a regular basis.

4. There is a need to seismically retrofit or replace older steel tanks.

5. New steel and concrete tanks need to be designed in accordance with the seismic provisions of the AWWA standards.

6. Research is required to develop flexibility in the inlet-outlet piping to prevent damage because of differential movement between the tank and the inlet/outlet piping.

7. A study is needed to improve the seismic performance of the bell and spigot joint for welded steel pipe.

8. A study is required to improve the seismic performance of air inlet and air release valves in an earthquake.

9. There is a continuing need to regularly test emergency generators under load, with adequate fuel for a longer term commercial power outage;

10. Emergency generators need a method for transferring fuel from the storage tank to the day tank, when the electric pumps are out of service because of the loss of commercial power.

11. Emergency generation capacity should be increased to cover all essential operations.

12. Portable generators with "quick electrical connectors" are of value for water and sewer electrical equipment.

13. Shaking and sloshing should be considered in the design of mechanical equipment in large basins of water and wastewater treatment plants.

14. Redundancy needs to be expanded as it continues to play an important role in the providing and restoring of water and wastewater services.

15. Lifelines in essential facilities (hospitals, fire and police stations, and emergency operation centers) require seismic design.

16. There is a need for emergency back-up electric and water supplies for essential facilities.

17. Where transportation problems exist preventing lifeline employees to get to their regular work location, alternate work locations or telecommuting where feasible should be considered.

18. There is need to provide emergency food, water and housing; and adequate cash to purchase these items, for lifeline workers in the seismically affected areas.

19. A communications plan is needed, which has been tested for lifeline employees and families to notify each other of their well being during the emergency restoration period.

20. Consideration should be given by lifeline agencies to help emergency response employees with their families and housing in an emergency, in order that they may be available to perform their restoration activities.

21. Consideration should be given to developing a mobile water quality laboratory to expedite, in the field, after repairs have been made, the determination if the water is safe for drinking.

22. Bacteriological testing is time consuming to determine if the water safe for drinking, after water mains are repaired. Research should be done to expedite this process, so that, the boil notice may be lifted sooner.

23. In the United States the entering of large diameter pipes, conduits and tunnels requires compliance with Occupational, Safety and Health Act

requirements (air testing and breathing equipment) for entering confined spaces.

24. A study of innovative financing is required to fund the design and construction to improve the seismic performance of water and sewage lifelines.

25. All lifeline agencies should make seismic vulnerability assessments of their facilities to determine vulnerability to damage of their system. The assessment should prioritize, budget and schedule any required seismic mitigation.

26. Studies are required to develop seismic mitigation scenarios for essential collocated lifelines.

27. Studies should be made of the relationship between direct and indirect losses of the loss of a lifeline function, so that management decisions can be made for seismic retrofit or replacement.

28. Regional emergency response plans should include a plan and designate a specific organization to manage emergency water supply after an earthquake.

29. Geographical information system information, along with almost real time earthquake information could be of value to assist the lifeline agencies in directing their response for repair and recovery.

## REFERENCES

Aqueduct, Metropolitan Water District of Southern California, Los Angeles, CA, March/April 1994.

Biagi, D. A. to R. F. Packard, Memo, '94 Earthquake After Action Report, Bureau of Sanitation, Los Angeles, CA, February 1994.

Disaster Report 1008, 1994 Northridge Earthquake, County Sanitation Districts of Los Angeles County, El Monte, CA, March 18, 1994.

Intake, Department of Water and Power, Los Angeles, CA, January/February 1994.

Lifelines Performance in the Landers and Big Bear Earthquakes of June 28, 1992, Bulletin of the Seismological Society of America, Volume 84, Number 3, University Park, PA, June 1994.

Loma Prieta Earthquake Reconnaissance Report, Supplement to Volume 6, Earthquake Spectra, Earthquake Engineering Research Institute, El Cerrito, CA, May 1990.

Lund, L., 1994, "How the Earthquake Affected Water Quality", Association of California Water Agencies, Water Quality Monitor, Volume 6, Number 1, January/February 1994, , Sacramento, CA.

Lund, L., 1994, Personal Communications and field investigations with cities and water and wastewater agencies in California and Kobe, Japan.

Northridge Earthquake of January 17, 1994 Reconnaissance Report, Supplement C to Volume 11, Volume 1, Earthquake Spectra, Earthquake Engineering Research Institute, Oakland, CA, April 1995.

Persson, V. H., 1994, "Assessment of Damage to State Jurisdictional Dams Caused by the Northridge Earthquake ($M_W$ 6.7) on January 17, 1994", Presented at the California Seismic Safety Commission meeting, March 3, 1994, Burbank, CA.

Whittier Narrows Earthquake of October 1, 1987, Volume 4, Number 2, Earthquake Spectra, Earthquake Engineering Research Institute, El Cerrito, CA, May 1988.

Water Environment & Technology, Water Environment Federation, March 1994.

## FIGURES

Figure 1 General vicinity map showing communities, highways and epicenter of the Northridge earthquake, January 17, 1994 (Caltrans).

6th US/Japan Workshop on Earthquake Disaster Prevention for Lifeline Systems, July 18-21, 1995, Osaka, Japan

Le Val Lund 6-29-95

# Performance of Lifeline Systems during the 1995 Great Hanshin Earthquake

by

Shiro TAKADA

Professor, Kobe University, Department of Civil Engineering, 1,Rokko-dai, Nada, Kobe, Japan

Junichi UENO

Senior Engineer, Department of Civil Engineering, Konoike Construction Co.,Ltd., 3-6-1, Kitakyuhoji-machi, Chuo-ku, Osaka, Japan

## ABSTRACT

This paper first represents on structural damage of lifelines such as electricity, gas, water, waste water and telecommunication systems during the 1995 Great Hanshin Earthquake. Then, emergency response and restoration process of their service are referred and compared. The future plan in the guideline prepared by the local government is also referred.

## Summary of Structural Damages for facility

(1) Electric facilities: Table 1 shows the summary of damage on power facilities. There were no damage for hydroelectric power plant and nuclear power plant located a little far from the epicenter. Ten thermal power plants, located along Osaka Bay in Amagasaki City and Osaka City, were damaged and 20 of failures were occurred in machineries. However, there were no damage for main facilities such as boiler, generating turbine and oil tank. Regarding with transformer facilities, damaged substations were located in Kobe City and its vicinity. The reason of power outage in Kobe area was due to damage occurred in three 275Kv transformer in Nishi-Kobe, Kobe and Shin-Kobe substations(Ref.

Photo 1). Within the area of seismic intensity VII(JMA), there are 29 transformer substations and 14 of them, 48%, were damaged. These damaged substations were all constructed before 1965, while seven substations constructed after 1975 were not damaged. As shown in Table 1, failures for transmission line occurred in 112 routes. Failures of underground lines were more than that of aerial lines. (There are 6 routes used both for underground and aerial.)

There were 5 damaged steel towers in Awaji Island, 13 in Kobe & Itami City and 2 in Osaka Prefecture. For distributing facilities, 660 of 12,109 routes were damaged. Damage ratios for underground and aerial are almost equal. The area of Sannomiya branch, which seismic intensity was VII(JMA), has a cable of 25km length. 4km (15%) among them was damaged, so 75 routes became unable to transmit. Within these 75 damages, 3 damages occurred in main lines and 72 damages occurred in service lines. Main mode of failures in the service lines were the dislocation of joint due to ground deformation caused by a relative displacement between building and pavement. An unnecessary temporal power restoration work was not performed in 64 routes because of severe damage of residential houses and office buildings.

(2) Gas facilities: Table 2 shows the summary of damage for gas facilities in the supplied area by Osaka Gas Co.Ltd..

There were no damage for LNG terminals located in Senboku (Sakai & Takaishi City) and Himeji(Himeji City) and for storage facilities like glove-shaped holders located in all over the area. There were no damage for high pressure trunk lines. But 95 locations had damaged for medium-A pressure and medium-B pressure lines. These were slight structural damages, but it was one of factors for the delay of restorations. It is very rare to record the damage for main gas lines due to past severe earthquakes in Japan. Main modes were failures on dresser joint of a valve and a leakage through flange due to looseness. Several welded steel pipes and cast iron pipes with aseismatic joints located in liquefied areas or near active faults were damaged(Ref. Photo 2). The restoration work was finished on January 31st for medium-A line and February 8th for medium-B line. Medium pressure lines which went through severely suffered

locations such as a cave-in over the Daikai subway station, a collapse of land-fill of Dai-2 Shinmei Road and a falling down of a girder of new tram lines on Rokko-Ohashi bridge to Rokko island, were damaged but there were no gas leakages. Regarding with low pressure lines, the final figure of total damages is about twenty six thousands. Most of them are the failures on a screw joint and a spigot joint. Osaka Gas Co. had already began to replace these old-type joints but 30% of them were still remained when the earthquake. No damage has found in polyethylene pipe so far. As for facilities of supply pipes located in user's house areas, pipe failure, which are all screw joint pipes, had occurred at the connection to basement of buildings or to heavy equipments. Gas facilities in a high rise apartment building in the Rokko island had not damaged. It can be said that the flexible joint, countermeasure for non-uniform settlements, were effective. For equipments inside buildings, they had never damaged as long as they are installed in sound buildings. In the rare case of damage, they were the leakage from the connection pipes with a water heater (especially in the case when a heater wasn't fixed to a wall firmly.) In the area of Sumoto Gas Co., four persons were killed due to CO gas poisoning during the gas leakage from the screw joint of a distribution pipe.

(3) Water facilities: Table 3 shows the summary of damage for a water system of Kobe city. Regarding with the water filtration plant and distribution reservoir, following damages were observed. Parapet on a top of the embankment was cracked and a pier of a management bridge was damaged in the Nunobiki reservoir. One vertical crack was found at the end of embankment and a stonewall for a maintenance road was damaged in the Karasuhara storage reservoir. Especially in the Uegahara water purification plant, a slow sand filtration plant was found to have cracks on the body and crater of the sand filter. For a rapid sedimentation basin, a damage of expansion joint and a leakage at a pipe from a water tank were found. For treatment facilities for drainage, there were many damages for a body, pipes and machineries(Ref. Table 3). Pulling out was occurred in a joint of a drainage pipe($\phi$1200mm) for the rapid treatment. There were also many damages for small pipes, retaining walls

and supplementary machineries. At the Motoyama purification plant, damages for a inflow pipe to a treatment water tank and an inflow pipe of a raw water and cracks for the tank were found. Number of damages for the transmission and distribution pipes at the Motoyama filtration plant were 5 and 13. At the Egeyama low layer distribution reservoir, there was a leakage from a connection between tank and well. (The distribution system is divided into 4 layers at 30m elevation each.) A vertical crack in the expansion joint inside the reservoir was found. A pump in the Karasuhara reservoir became out of operation because of flooding.

Next, for water transmission pipes, more than 10 damages were found including a pipe in the Uegahara water filtration plant ($\phi$1200mm) (Ref. Photo 3) and a pipe in the Egeyama reservoir($\phi$500mm). At the Motoyama tunnel for transmission pipes, a leakage from a joint of PC pipe($\phi$500mm) and a crack for a hume pipe($\phi$300mm) due to a collapse of the top of tunnel were found. For distribution pipes, 64,090 of damages were reported by the end of March, 1995. It consists of 1,439 for distribution pipes, 11,823 for service pipes and 50,828 in pipes inside buildings. Failure modes among 1,439 distribution pipe are 293 cracks for pipe bodies, 908 for joints and 238 for incidental equipments. Steel pipe($\phi$700mm) attached to the Rokko-Ohashi bridge had hung down. For a steel pipe($\phi$600mm) attached to the Kobe-Ohashi bridge, there were buckling and shear failures at a joint. At the joint of a ductile cast iron pipe($\phi$900mm), the socket crashed into the screw. A damage ratio of pipes of $\phi$75 to $\phi$400mm is within 0.3 to 0.5 (number of damage/km). There are following general features for pipe damages. The separation at joints exceeded in number than that of crack or snap at pipe body. There were also many damages for air valves or shut-off valves. Regarding with water main pipes, damages had concentrated on aged pipes. As there were few damages for pipes with an expansion and a flexible joint, their effectiveness were proved. The collapse of the sixth floor of the Kobe City-Office , where the bureau of waterworks was located, buried drawings of pipeline networks and facilities. The building where the east branch of the bureau of waterworks in Kobe City was located, was severely damaged. The west center was partly fired and the

Tarumi center was partly damaged. Several branch offices needed retrofitting for their buildings.

(4) Waste water facilities: A public waste water system covers 97.4% of Kobe City area. Within the 7 treatment plants, the failures occurred in 3 plants which are Higasinada, Chubu and Seibu. Among them, the damage of Higashinada treatment plant was most heavy. Contents of the damage were the failure of intake open channel, the breakage of an aeration tank and a final sedimentation tank, the inclination of a management building and a dryer machinery building, the collapse of canal quaywall, the destruction of a pavement, the inclination of a filter basin, the submergence of treatment facilities and the deformation of a sludge scraper, a sand filtration plant and a sludge drying machine. The treatment ability of these three plants decreased to 0%, 50% and 20%. Higashinada treatment plant had diverted the adjoining canal to the purpose of primary treatment by coffering with sheet piles. Regarding with the sewage pumping station, 20 of stations were damaged. At Uozaki pumping station, falling down of a sewage aqueduct bridge on the canal, the breakage of a joint in an outfall, the failure of a sedimentation clearing house, the sliding of pumps for sanitary and storm sewages and the deformation of a conveyor for screenings were occurred. At the Port island, pumping stations, No.1 to No.3, had lost function because of flooding. As Higashinada treatment plant and Uozaki pumping station were located in a soft reclaimed land, the settlement and lateral spreading due to liquefaction, which caused damages, were occurred. By the primary survey, the damage for manhole (rising, subsidence and slipping between components), a deformation of road surface, crack and clogging of pipes and invasion of sand in pipes were found. Secondary survey was done for pipes in the area where were judged as severely damaged by the primary survey. The check for the inside of pipe was done with the remote controlled television camera when the secondary survey. Then the failures (4.273km in length) in 23 routes were identified in sewer mains of 32 routes (83.9km of total length).

(5)Telecommunication facilities : Table 4 shows an outline of damages for NTT. NTT's offices from Chuo Ward to Nagata Ward are connected via a box culvert and a shield tunnel. The box culvert

was made with open-cut method and its average overburden depth is 3m. There was no damage for the shield tunnel. But for the box culvert, there were slight damages for side wall, expansion joint and connection to buildings. The box culvert on Kamisawa dori ,near severely damaged Daikai station, had slip 4cm laterally and 13cm vertically at an expansion joint. Then, liquefied sand and water had invaded(Ref. Photo 4). In suffered area, pipes which total length are about 370km is buried. 5.9% of them was damaged. Failure modes of them were the push in of pipes into manholes and the breakage of the manhole. Such a damage of underground pipelines hadn't led to the fatal damage like a cut off of main cables. The cut off was seen mostly at the connection from a buried pipe to buildings via a pole and aerial cable or poles. These cut off were due to collapse of poles and adjacent buildings and burn out of aerial cables by fires nearby. At a river crossing, a cable is attached to a bridge. Telecommunication cables attached to a bridge at a river crossing hadn't led to functional damages even in the case of twisted bridges. Regarding with the material of damaged pipes, pipe with jute cover and cast iron pipe had high ratio of damage. Regarding with a joint type, damage of a spigot joint and a screw joint which were installed from 1960 to 1970 were exceeded in number. The damage ratio on liquefied area was two to three times higher than on normal ground. A damage of poles and aerial cables due to building collapse and fires became one of main reason for severe functional damage. Following three buildings of NTT were damaged. Miyuki Bldg. became unable to use. The foundation of a parabola antenna on the top of the Minato Bldg. was damaged and removed later. As it inclined, residents of environ were once compelled to evacuate. The antenna on the top of Daikai Bldg. was retrofitted.

## Emergency response and restoration

(1) Electric system: Just after the earthquake, power outage occurred on the south of Hyogo prefecture and a part of adjacent Osaka prefecture. About 2,600,000 of households were affected (Ref. Figure 1). At restoring process, first priority was placed on emergency transmission with utilizing survived aerial

cables, high-voltage generator and tentative lines. On January 23rd, 6 days after earthquake, restoration was finished except for the area where is impossible to be restored with building damages. This quick recover of electricity expedited the recover of other lifelines by supplying power for their repair works through aerial cables. While it took long time to restore for underground facilities, because it was difficult to locate the damage and an excavation work was necessary. Reasons for the quick recovery are presumed as follows. ① Switching of transmission from damaged 154Kv to 77Kv ②Utilization of aerial cables ③Supplier's communication system ④Support from other electric companies ⑤ Pre-earthquake countermeasure for equipments

(2) Gas system: Osaka Gas Co. had 34 seismometers with telemeters installed in the supply area. So it was possible to distinguish the distribution of acceleration immediately after earthquake. Getting more information from administration office, mass media, customer via telephone and branch office via wireless phone, it was more cleared that there were many gas leakages, fires and possibility of second disaster. Being judged that it is impossible to respond case by case, the first decision of gas supply stop was done at 11:30. By the evening of that day, supply for five middle blocks, which contains 860,000 households, was stopped(Ref. Figure 2). Restoration work had began on 21st, January. The work basically started from the slight damaged areas. The priority of the work for an area was judged based on number of leakage, an extend of damage for roads and buildings, traffic loads and availability of materials and equipments. Exceptional priority was given to public facilities like hospitals. Besides the quickness, aseismatic material and device such as polyethylene pipes or aseismatic joints were introduced positively. The restoration work can not be judged it took too much time in considering of greatness of the damage and comparing with the speed of restoration work during the past earthquakes. The reasons for the delay were as follows. ①Gas line takes much time to repair due to its feature of a supply system, once a shutdown had occurred. ②It took much time to remove invaded water or liquefied sand from low pressure gas pipes when the water pipe was damaged nearby. ③Restoration

works was interrupted because of collapsed buildings and a traffic jam.

(3) Water system: It took two and a half months to finish restoration. Main reasons for this delay were too many numbers of a pipeline damage and a shortage of water pressure enough for locating water leakages. Survey and works were also delayed by the traffic jam and failure of roads. There were also the area where the width is too narrow for vehicle to access or a road was occupied by collapsed buildings or debris. There were the rare case that pipes were damaged by other lifeline's restoration work. Prior to this earthquake, the bureau of waterworks in Kobe City had prepared unique countermeasures which are a wide area telemeter control system and emergency shut off valve system for distributing reservoirs. The former one worked well and it became possible to know the situation of facilities of the whole water supply system. With the latter system, each distributing reservoir consists of two reservoirs and an emergency shut off valve which is attached to one of the two reservoirs. When the intensity level of earthquake and a flow volume of water exceed a certain level, one with a valve keeps water and the other one continues to supply. This time 18 valves of all 21 worked correctly. Then 40,000 tons of water was hold for emergency drinking water.

(4) Waste water facilities : Many failures were occurred at most of the components such as sewer pipe, pumping station, treatment plant and so on. Treatment plants and pumping stations were restored smoothly by emergency countermeasures except for Higashinada treatment plant. It can be judged that the influence of the above failures towards the daily life of citizen was minimum as possible. It is also confirmed that the sewage can flow through most of the conduit. Although another issue about lavatory had emerged. That was the shortage and delay of locating of portable rest room for refugee shelter. The way to treat the raw sewage from portable rest room was also the problem. For the people whose house was not collapsed, to obtain the water for flushing was the problem. If it was impossible to flush because of the failure on conduits, the problem would have become more serious. If so, the raw sewage would have overflown from manhole and the sanitary countermeasure would have become

necessary. For the area where the structural damage was heavy, the delay of restoration of water supply might have hidden above problem on sewage system.

(5)Telecommunication system: NTT set up the head quarter for the disaster at 8:30 and began to check and restore. Switching unit without back up power had revived by the end of 18th because vehicles with the generator were located. Then 285,000 lines of interruption was decreased to 85,000 lines by Jan.19th.. Checks for the tunnel containing communication cables in Kobe city was finished by 18th. Restoration works had done by 1,000 workers of Kobe branch and 3,000 workers from other branches. 11 vehicles with the generator and 6 vehicles with satellite communications were put in it. On January 31st the restoration was finally over except for 38,000 lines which was impossible to restore with building collapse and so on.

## Aseismatic countermeasures for lifelines

(1)Restoration curves : Figure 3 shows restoration curves for the electricity, gas, water and telecommunication systems. The axis of ordinates shows the ratio of restoration. But its physical meaning depends on the kind of the lifeline. For the electricity and telecommunication, it means the ratio of reduction for power outage and suspension of phone by the complete restoration. For the gas and water, it means the ratio of re-supplied households by the permanent restoration. The restoration of the electricity and telecommunication turns out to be far quicker than that of the gas and water, because it is easy to switch the route for the electricity and telecommunication by manipulating a managing software and is not so easy for the gas and water. It also took much time to restore vast amount of underground facilities in downstream of the water and gas systems. How to expedite the recovery is an important subject for the lifeline system. The way to shorten the restoration process, in other words way to minimizing the slash lined area in Figure 3, is so important.

(2) Structural countermeasure : The welded steel pipe and the aseismatic joint in pipelines buried in the area where is liquefied or close to active fault was damaged. But the newly

constructed line using above material or device was not damaged except for above area. Figure 4 shows the time history of velocity calculated from the record of acceleration on Kobe oceanic weather station. It is assumed that the area which seismic intensity was over VII(JMA) experienced the velocity around 100 kine. If the propagation velocity of the seismic wave is assumed to be 100m/sec, the strain of ground is 1%. If the strain transmit to buried pipe perfectly, the ground displacement for the pipe of 5m length is absorbed by the joint which ability for tension or compression is 50mm. So it is considered that the component considered as aseismatic ones such as welded steel pipe, GM-II type joint or S-II type joint could withstand for this earthquake. But the situation of the damage caused by the large ground displacement such as active fault or liquefaction should be examined closely. Table 5 shows current seismic countermeasures for hardware, which are planned by each supplier of the lifelines. They are based on the consideration that most of failures occurred on the facilities which are not followed by the latest seismic design codes. They are all giving priority to the way to improve aseismatic performance of buried pipes too. The polyethylene pipe which is excellent in elongation ability will be used more in the future. It is also necessary to develop a large diameter polyethylene pipe which has the required rigidity.

(3) Systematic(software) countermeasure : Lifeline systems have been expanded with the increase of population and their own function and they still have left outmoded components in their system. It takes quite long time to strengthen all the components of a lifeline system which consists of huge amount of facilities. At the same time, they are required to provide service consistently. Then, the post-earthquake countermeasure for quick recovery of function toward structural damages should be presumed. Table 6 shows the software countermeasures of the lifelines. Besides the contents considered in Table 6, there are problems of the interaction of damages or the collaboration of restoration works between lifelines. As stated before, sand and water leaked from water pipes became the obstacle for restoration of the gas system and an electric pole recovered quickly aided restoration of the telecommunication. To manage

the schedule of the restoration work for different kinds of lifeline, an information of buried lifelines should be gathered and governed unitary by a common administrator. It is also necessary to provide the source or database to get the real-time information on the failure location, accessibility and/or updated schedule of restoration works. The system to publicize the recovery schedule and to collect complaints are also necessary for citizen.

## Aseismatic city and recovery of lifeline

(1)Acceptable risk of lifeline : Now, government offices of cities or prefectures suffered from this earthquake are preparing the guideline for restoration. Their presupposition is to rebuild or develop the area to be sustainable for the earthquake such as the present earthquake. In the process to make these guide lines, there were some opinions that the scale of scenario earthquake can be decreased as the big earthquake , which return period was over a thousand years, had already occurred. But the both near field earthquake such as this earthquake and oceanic distant earthquake were employed as the scenario earthquake in the guidelines for the restoration. Although it may be impossible to rebuild all the infrastructures to proof against these supposed earthquakes. As mentioned in previous chapter, it is impossible to make lifeline structures aseismatic economically in a short term. It can be judged that lifeline facilities following current seismic codes could bear the this earthquake and consequently it was proved that the update of outmoded structures is in a great hurry. The effort for update has to be continued to minimize structural damages. Notwithstanding this effort, it is impossible to minimize the damage perfectly. So the effort to make the system restorable quickly after earthquake is also necessary. The restoration planning considering seismic intensity VII(JMA) is to make critical facilities tolerable to VII(JMA) and to provide the post-earthquake countermeasure for quick restoration for the facilities which have possibility of the damage. Regarding with this possibility of damage, acceptable or not should be judged depending on the purpose of a facility. In other words the

acceptable risk of lifeline should be different from that of other structures, such as building, railroad, bridge and so on. The bureau of waterworks in Kobe City, which is now preparing a restoration plan of facilities had analyzes the demand and complaint of citizen during restoration period. As a result of it, the bureau set the minimum volume of supplying water during emergency restoration period in their plan. They are 3 litter/day/person (3days from earthquake), 20 litter/day/person (4-7days), 50 litter/day/person (8-14days), 150 litter/day/person (15-21days) and 250 litter/day/person (22-28days). Presupposition in this plan is to keep the life of the citizen safe.

(2)Aseismatic utility conduit and lifeline box : The pipeline included in a box culvert or a shield tunnel had never damaged during this earthquake. Crack on the wall of a culvert and displacement at the joint were found but it was more aseismatic than the buried pipelines. The plan for the large scale aseismatic utility conduit crossing the Kobe city from east to west has started considering the existing culvert plan. Regarding with the water system, the plan to enclose large capacity trunk line in the above conduit as the part of the wide area trunk line network. And conduit from north to south for trunk line is also considered now. If the grid of these conduits is made, water can be conveyed to the points nearby for all the citizen just after this kind of large earthquake. For the distribution level, the plan to insert distribution pipes close to consumers into the "lifeline box" under the pavement is considered. This may not be aseismatic structurally, but quick restoration will be possible without excavation. The culvert of this type for gas and water pipeline is named "lifeline box" and the similar culvert is named "cc box" for electricity and telecommunication. The connecting device from the above box to consumer has to be developed more but the construction as a test case in redeveloping area is planning now.

## Reference

Kobe University, Department of Civil Engineering;Hyogo-ken Nanbu Earthquake damage survey report (Vol.1, Feb.1995), (Vol.2, March 1995)

Asahi Newspaper Publishing Co., Monthly Journal of Science, Kagaku Asahi, extra number March 1995.

Table 1 Damage for electric facilities

| Facilities | | Unit | Number of damage | |
|---|---|---|---|---|
| | | | Main facilities | Others[1] |
| Power plant | | Location | 5 | 5 |
| Transformer Substation | | Location | 17 | 33 |
| Transmission | Aerial | Line | 11 | 12 |
| | Buried | Line | 3 | 92 |
| Distribution line | | Line | 649 (11[2]) | 0 |
| Communication | | Line | 0 | 76 |

1)Damage to other facilities including slight damage to main facilities
2)Special high voltage distribution line

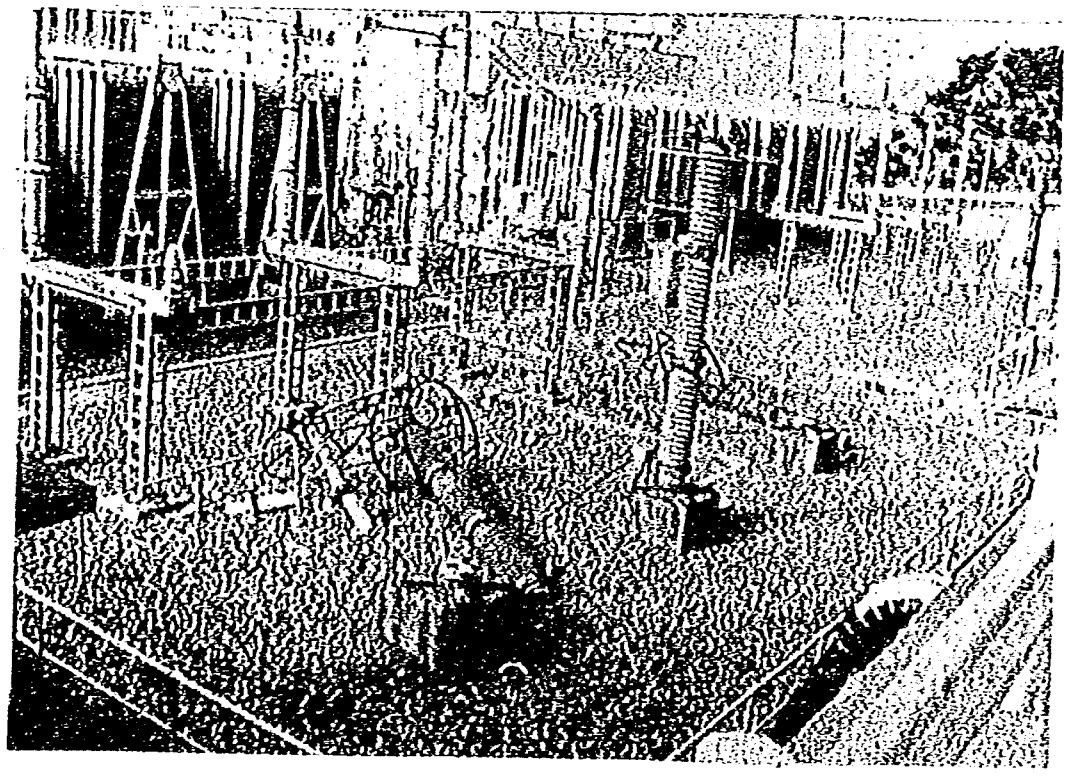


Photo 1 Damage on transformer substation

Table 2 Damage for gas facilities

| Facilities | Damages | remarks |
|---|---|---|
| LNG terminal | None | |
| Storage | None | |
| High pressure trunkline | None | |
| Medium pressure line | Leakage of 95 locations | Failure on dresser joint<br>Crack on welding of low-grade steel pipe,e.t.c. |
| Low pressure line | Leakage of over a few thousands | Concentrated on screw joint and spigot joint |



Photo 2 Failure of welded steel pipe

Table 3 Damage for water facilities

| Facilities | | Damage (number of location) | remarks |
|---|---|---|---|
| Reservoir | | 3 | Crack on embankment<br>Failure on service road |
| Purification plant | | 2 | at Uegahara & Motoyama |
| Transmission pipe | Tunnel | None | |
| | Pump | 1 | Stop by flooding at Karasuhara |
| | Pipe | 10 | |
| Distribution pipe | Reservoir | 1 | Leakage from joint at Egeyama |
| | Pipe | 1439* | Pull out in joint<br>Break of pipe |
| Service pipe | Beneath road | 11823* | |
| | Within customer site | 50828* | |
| Office building | | over 4 | Main,West,East and Tarumi office |

*Figure at the end of March

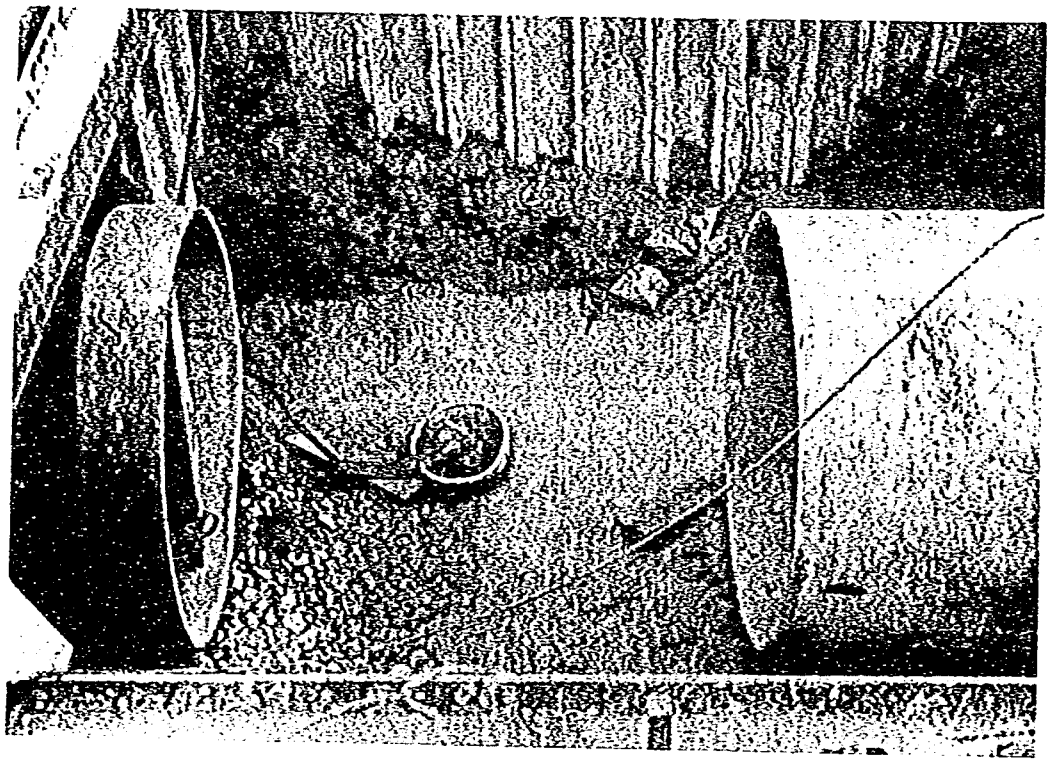


Photo 3 Failure of pipe in treatment plant

Table 4 Damage for telecommunication facilities

| Facilities | Damage | Remarks |
|---|---|---|
| Tunnel | 7 locations | Crack on wall<br>Displacement at joint |
| Road | 5.9 % | Cast iron pipe, spigot joint |
| Manhole | 10.0 % | |
| Buried cable | 0.23 % | % of replaced cable |
| Pole | 1.5 % | |
| Aerial cable | 1.7 % | % of replaced cable |

| | Power outage restored date | Number of power outage households |
|---|---|---|
| | 1/17, 7:30 | 1,000,000 |
| | 1/18, 8:00 | 400,000 |
| | 1/20, 6:00 | 110,000 |
| | 1/23, 15:00 | — |

• Power distribution center

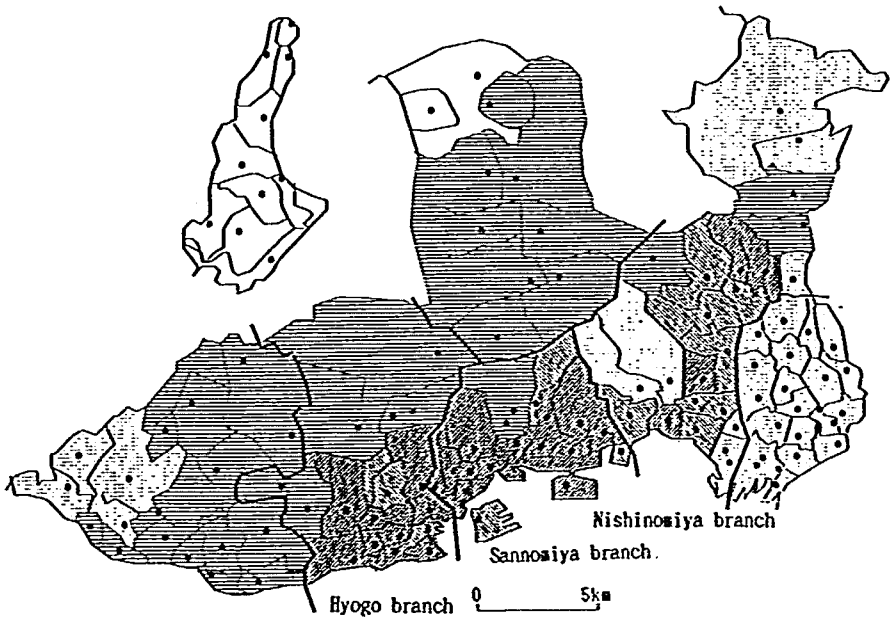



Figure 1 Power outage area and resumed date

| | Gas supply-stop date | Name of block | Number of gas supply-stop households (×1000) |
|---|---|---|---|
| | 1/17, 11:30 | Kobe②, ③ | 336 |
| | 1/17, 16:15 | North Osaka ⑦ | 103 |
| | 1/17, 19:10 | Kobe① | 220 |
| | 1/17, 21:00 | Kobe④ | 124 |
| • | 1/18, 5:00~ | Supply-stop in small block | 23 |

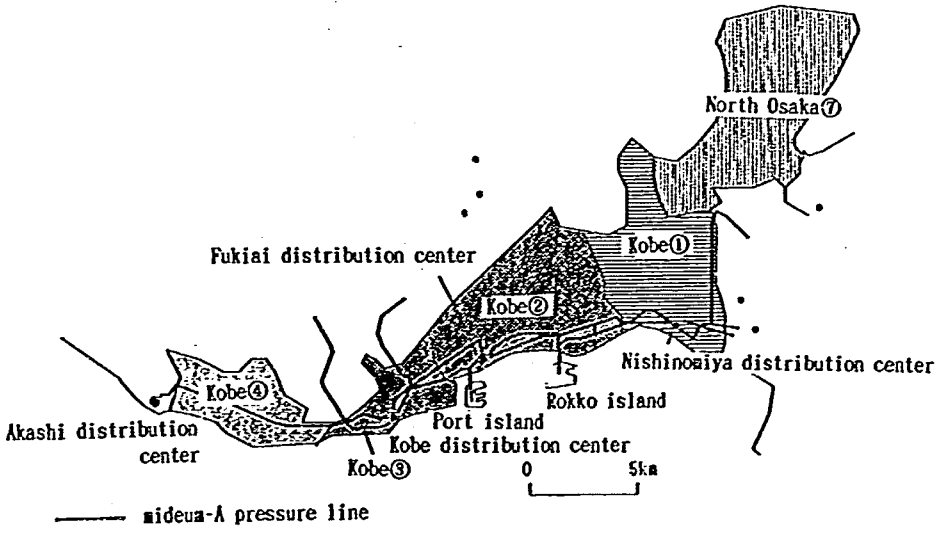



Figure 2 Gas supply stopped area and time of shut down

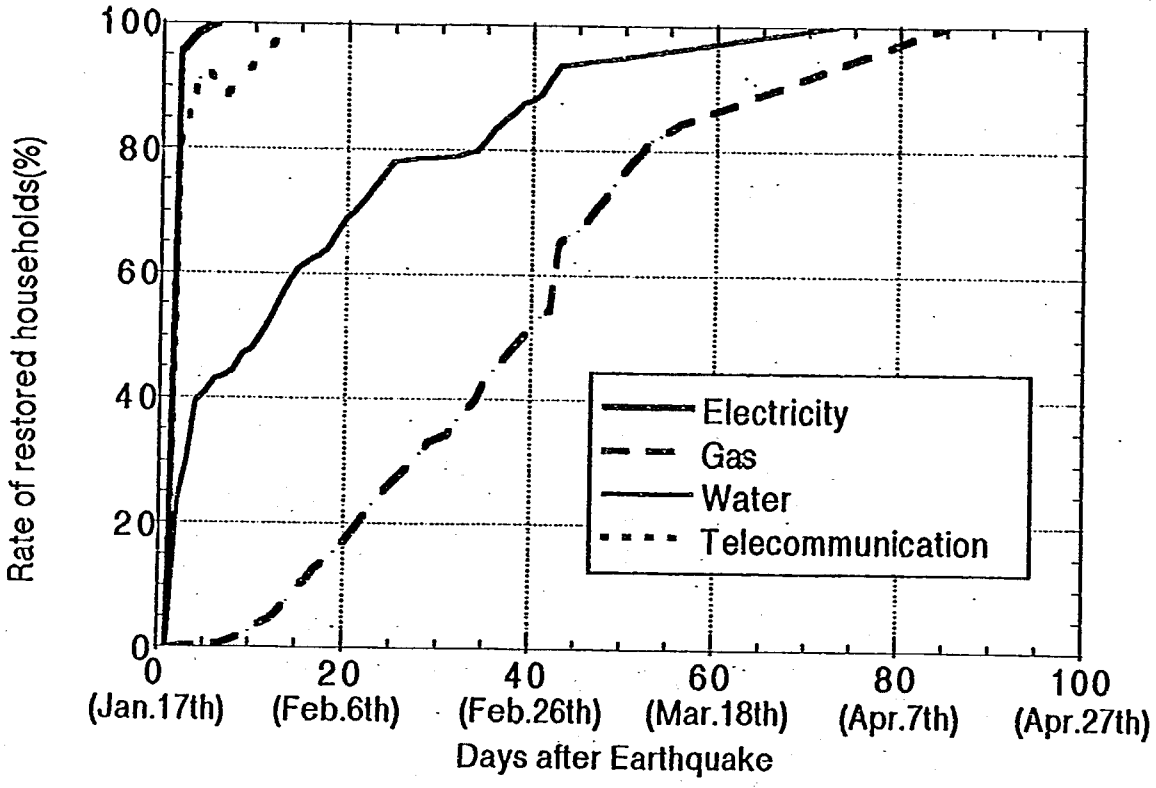



Figure 3 Restoration curves for lifelines

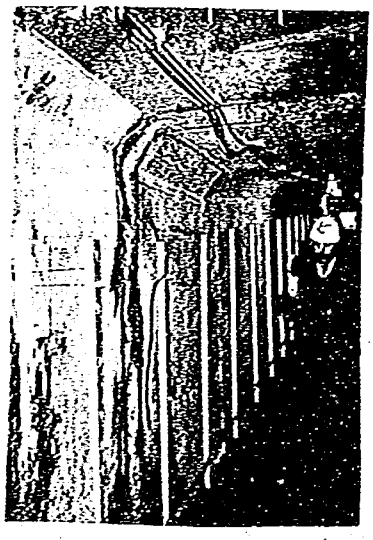


Photo 4 Displacement at joint of box culvert

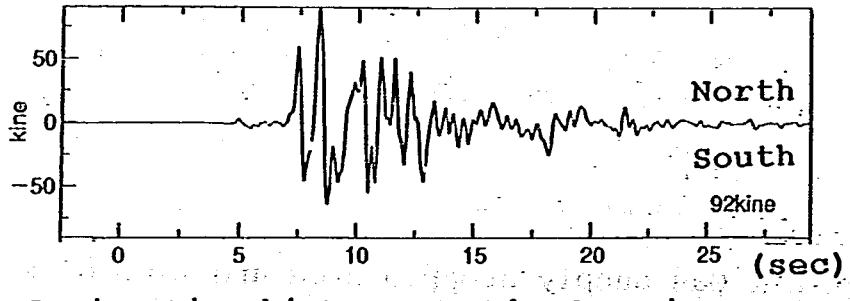



Figure 4 Velocity-time history at Kobe Oceanic Weather Station

Table 5 Structural countermeasures for lifelines

| type | Structural countermeasure |
|---|---|
| Electricity | 1. Aseismatic reinforcement for steel tower and aerial line<br>2. Aseismatic reinforcement for pre-1975 transformer plant<br>3. Aseismatic reinforcement for buried pipe<br>4. Aseismatic reinforcement for electric pole |
| Gas | 1. Replacement of old-type pipes in medium and low pressure lines<br>2. Introduction of PE pipe<br>3. Replacement with automatic shut-off gas meter |
| Water | 1. Arrangement for pipeline network with appropriate durability<br>2. Introduction of aseismatic joint and flexible pipe<br>3. Introduction of emergency shut off valve with telemeter for distribution reservoir<br>4. Aseismatic reinforcement for old type equipment for water transmission and distribution<br>5. Aseismic reinforcement for service equipment |
| Telecommunication | 1. Aseismatic reinforcement for steel tower on building roof<br>2. Aseismatic reinforcement for equipment within office<br>3. Aseismatic reinforcement for existing buried cable and adoption of medium diameter underground pipe<br>4. Aseismatic reinforcement for joint of box culvert |
| Waste water | 1. Liquefaction countermeasure for treatment plants<br>2. Aseismatic reinforcement for conduits and manholes |

Table 6 Software countermeasure for lifelines

| type | Systematic and operational countermeasure |
|---|---|
| Electricity | 1. Multiple back up for main line<br>2. Back up by aerial line for distribution line |
| Gas | 1. Subdividing of middle block<br>2. Introduction of shut off valve with telemeter for middle block<br>3. Stipulation of decision making process for supply stop |
| Water | 1. Blocking of distribution lines<br>2. Decentralization of managing system |
| Telecommunication | 1. Decentralize arrangment of communication centers<br>2. Development of overload-proof system<br>3. Development redundant main line network<br>4. Diversification of communicating methods<br>5. Development of method to locate damages |
| Waste water | 1. Decentralize arrangment of treatment plants<br>2. Development of method to treat sewer |

# Session-5

## Seismic Monitoring and Restoration

(J-11) A Study on the Development of An Immediate Detection System for Seismic Damage to Lifelines Using GPS and GIS.
(Fusanori Miura and Junji Kiyono)

(J-12) Development of SIGNAL: Seismic Information Gathering Network Alert System
(Yoshihisa Shimizu, Fumio Yamazaki, Shigeru Noda, Ryuji Isoyama and Youichi Yoshikawa)

(J-13) Conditional Non-Gaussian Fields
(Masaru Hoshiya)

(J-14) Real Time Conditional Simulation of Earthquake Ground Motion
(Tadanobu Sato and Hiroshi Imabayashi)

(J-15) Optimization of Post-Earthquake Restoration of Lifeline Networks Using Genetic Algorithms
(Tadanobu Sato and Koji Ichii)

# A STUDY ON THE DEVELOPMENT OF AN IMMEDIATE DETECTION SYSTEM FOR SEISMIC DAMAGE TO LIFELINES USING GPS AND GIS

by

Junji KIYONO* and Fusanori MIURA**

* Assoc. Prof., Faculty of Eng., Yamaguchi Univ., Tokiwadai, Ube, Yamaguchi 755, JAPAN
** Prof., Faculty of Eng., Yamaguchi Univ., Tokiwadai, Ube, Yamaguchi 755, JAPAN

## ABSTRACT

The 1995 Hyogo-ken Nanbu earthquake is one of the worst disasters in recent Japan history, not only because of the total number of casualty but also the fact that the earthquake struck a highly urbanized area where the population, buildings, transportation systems and other urban facilities were concentrated. The property damage caused by this earthquake roughly amounts to more than 10 trillion yen and about 6% is for lifelines (gas, water, electricity and telecommunication systems). The lifelines are important infrastructure and their contribution to our social life is very significant. They must at least maintain the facilities even if a large earthquake occurs. The lifeline systems, however, revealed very vulnerable features to this Hyogo-ken Nanbu earthquake. Three countermeasures to the disaster are available; 1) predict the disaster and take measures in advance, 2) reduce the vulnerability of the system, and 3) make an immediate response to minimize the damage. We here report a study for the third one. The objective of this study is to construct a theory to develop an immediate detection system for seismic damage of lifelines. Moreover, this damage mostly relates to the deformation of the ground. Hence, a theory to assess the lifeline damage based on the ground deformation using GPS and GIS is proposed. Furthermore, as the disaster changes from time to time, the proposed system incorporates new information and updates the assessed damage.

## INTRODUCTION

It is very important to know an outline of the great disaster and review the lifelines' damage in order to design the system proposed in this study. The 1995 Hyogo-ken Nanbu earthquake (the 1995 South Hyogo Prefecture earthquake) struck Hanshin (Kobe and Osaka) area at 5:46 am on January 17, 1995. The magnitude was 7.2 on the Japan Meteorological Agency (JMA) Scale. Kobe city extends in a east-west direction like a corridor between Rokko Mountain and Osaka Bay and the earthquake occurred in such geographically worst area. The event claimed about 5,500 lives and more than 35,000 persons were injured. More than 80,000 houses were collapsed and more than 60,000 houses were severely damaged. The property damage amounted to more than 10 trillion yen. Bridges of transportation systems such as railways and express motor ways fell down and lifelines were cut off everywhere. As of May 15, the estimated property damage for buildings was 5.8 trillion yen, 34 billion yen for railways, 55 billion yen for highways, 1 trillion yen for port and harbors, 5 billion yen for water supply system, 19 billion yen for gas supply system, 23 billion yen for electric power supply system and 12 billion yen for telecommunication system [1].

In the following chapter, damage to lifeline systems is summarized. Then the basic idea of the proposed system will be given. After that, we will mention the algorithm to update the information about the damage after obtaining new information.

## SUMMARY OF THE DAMAGE TO LIFELINE SYSTEMS[2]

Water cut-off area spread over nine cities and five towns (Kobe, Amagasaki, Nishinomiya, Ashiya, Itami, Takarazuka, Kawanishi, Akashi, Miki; Tsuna, Awaji, Hokutan, Ichinomiya, Higashiura) in Hyogo prefecture. Water was supplied for about 3,426,000 populations and the total amount of supplied water was 1,363,000$m^3$/day. The number of water-supplied households was 1,356,000 and about 85% households suffered water cut-off. Fig. 1 shows the comparison of water cut-off households for the past large earthquakes. Water supply was cut off to 50,000 households for the Northridge earthquake, which occurred just a year past of the Hyogo-ken Nanbu earthquake. The total number of water cut-off households becomes 20 times larger than that of the Northridge earthquake. Fig.2 shows the restoration process of water supply system. It has completed after 91 days. Because of so many cracks and separations of pipes, leakages were difficult to find.

Electricity in Hyogo, Osaka and Kyoto prefectures is supplied by Kansai Electric Power Co. Inc.. Electricity of 2.6 million households was cut off just after the earthquake. In the 1994 Northridge earthquake, electricity cut off was upto 1.1 million households (Fig.3). It takes six days to restore urgently. Fig. 4 shows the comparison of restoration days for the past large earthquakes. A preliminary restoration had finished very quickly despite its heavy damage. The speedy restoration had a good influence on the other lifeline systems.

Gas in the earthquake-affected area is supplied by Osaka Gas Co. Ltd. The area including 5.7 million households is divided into eight super-blocks and each super-block is composed of several middle-blocks. Fig. 5 shows the middle-blocks in which gas supply was cut off. The total number of gas cut-off households was 860,000 (Fig.6). Fig. 7 shows the comparison of restoration days for the past large earthquakes. It took 85 days, the longest, for preliminary restoration. The shutdown decision for gas supply was done six hours after the event for lack of information.

About 285,000 telecommunication lines were cut, of which about 193,000 lines were due to cables and facilities damage. The remaining interrupted lines were due to electricity cut-off. The number of phone calls on that day was 50 times more than the usual and the next day, 20 times more. Fig. 8 shows the restoration process of the interrupted lines. The preliminary restoration had completed in two weeks after the earthquakes except the lines for burned or collapsed houses.

Disaster occurred in an urban region is usually characterized by damage to lifelines. The counter-measures for the disaster are classified into three phases; prior protection, immediate protection and posterior protection. In Japan, strategies of the prior and the posterior protection have been explored relatively well. But the immediate or emergency planning is not sufficient. Several systems for the emergency protection such as UrEDAS for JR, CUBE for Caltech/USGS and SIGNAL for Tokyo Gas Co. Ltd. have already been developed. With the Hyogoken-nanbu earthquake as a turning point, these kinds of systems will increase more and more. In this study, we develop a theory to detect the damage to lifelines for the immediate protection strategy. The tools used in the theory are GIS and GPS.

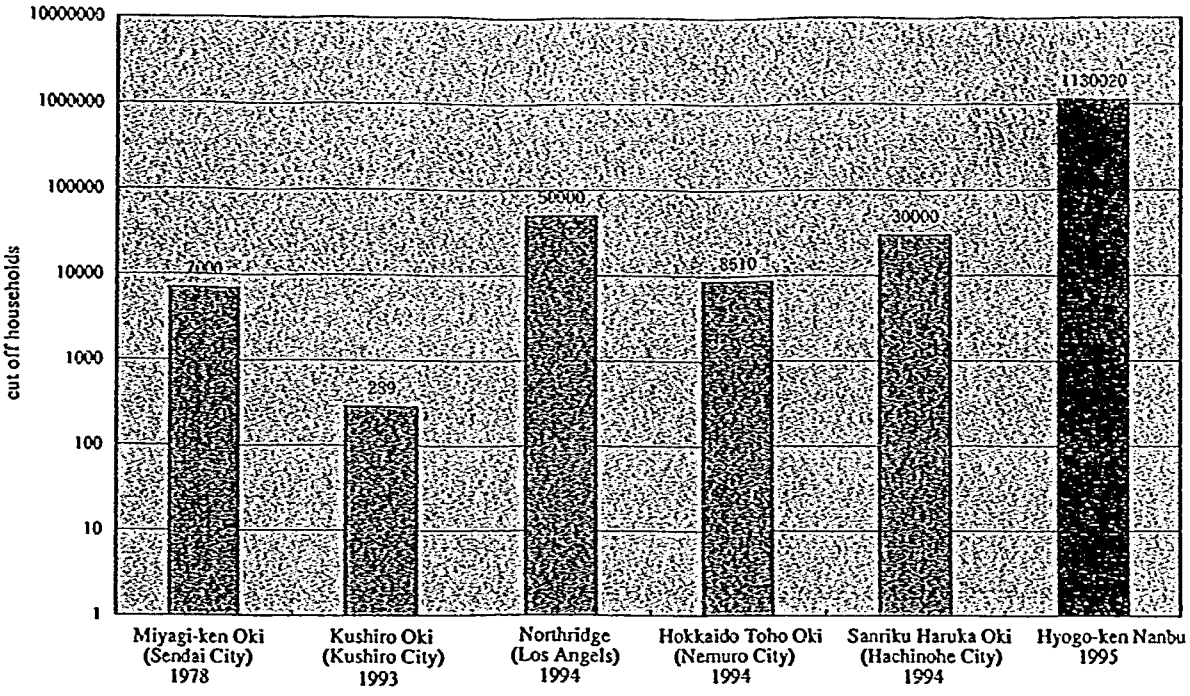



Fig. 1 Comparison of water cut-off households for the past large earthquakes

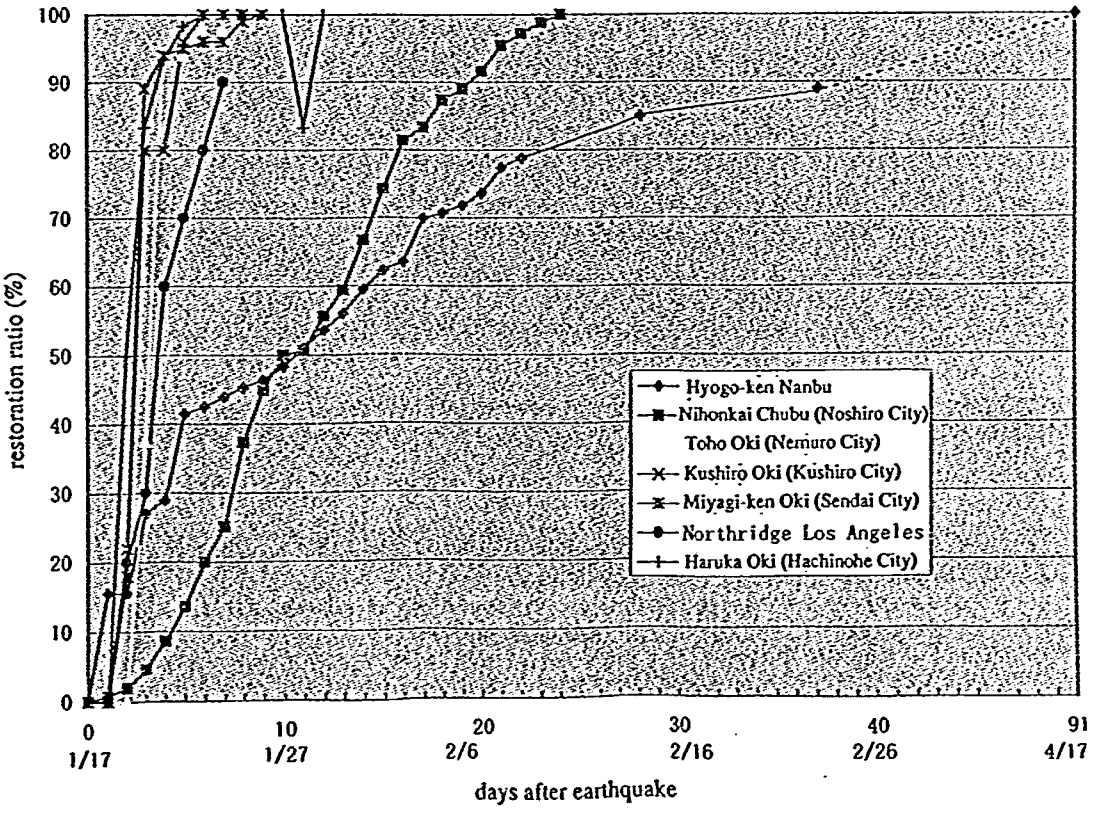



Fig. 2 Restoration process for water supply system

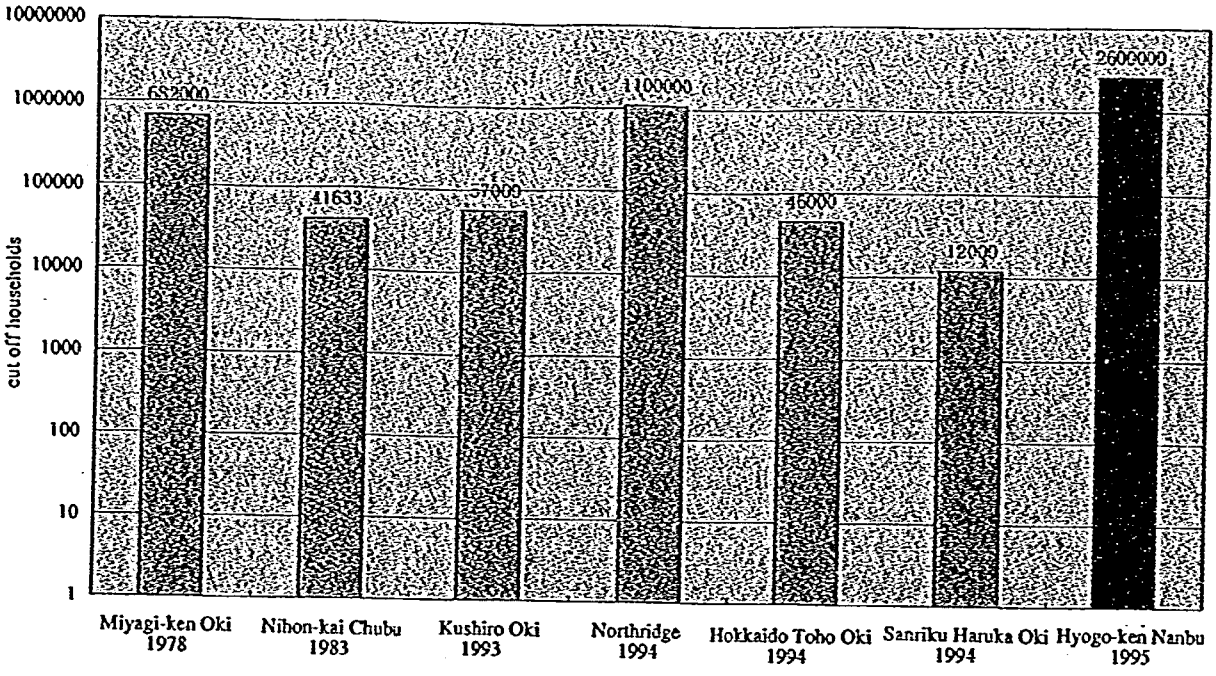



Fig. 3 Comparison of electricity cut-off households for the past large earthquakes

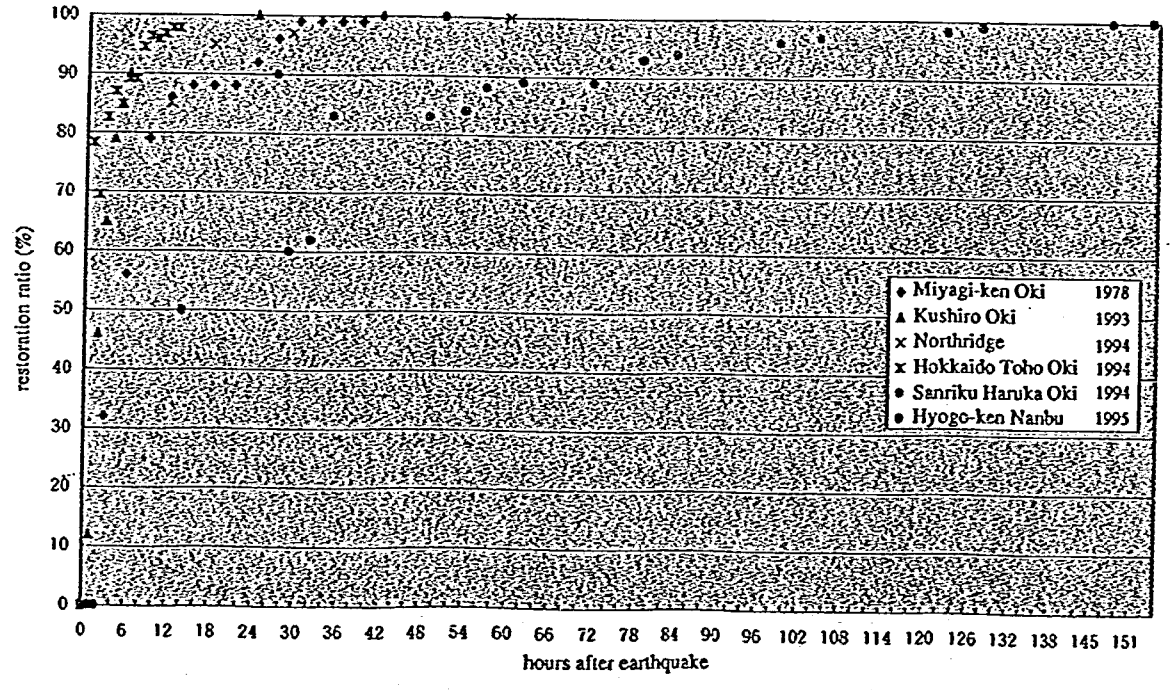
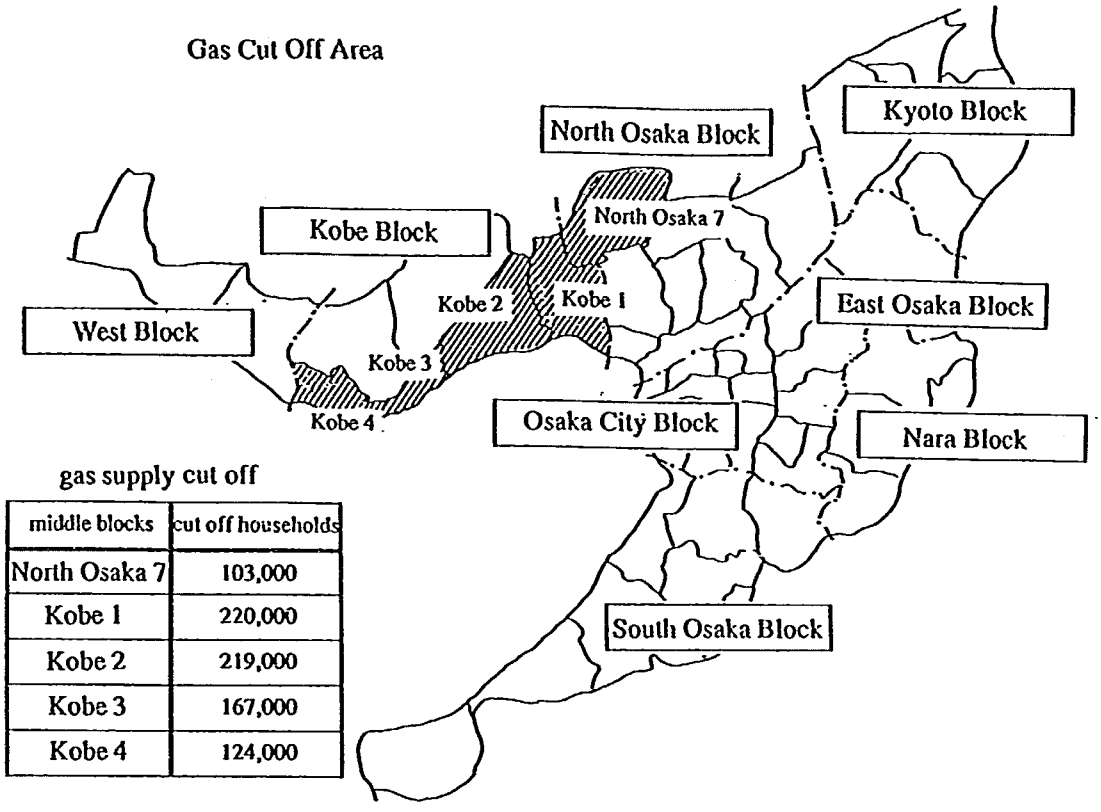



Fig. 4 Comparison of restoration days for the past large earthquakes (electricity)




gas supply cut off

| middle blocks | cut off households |
|---|---|
| North Osaka 7 | 103,000 |
| Kobe 1 | 220,000 |
| Kobe 2 | 219,000 |
| Kobe 3 | 167,000 |
| Kobe 4 | 124,000 |

Fig. 5 Gas cut-off area

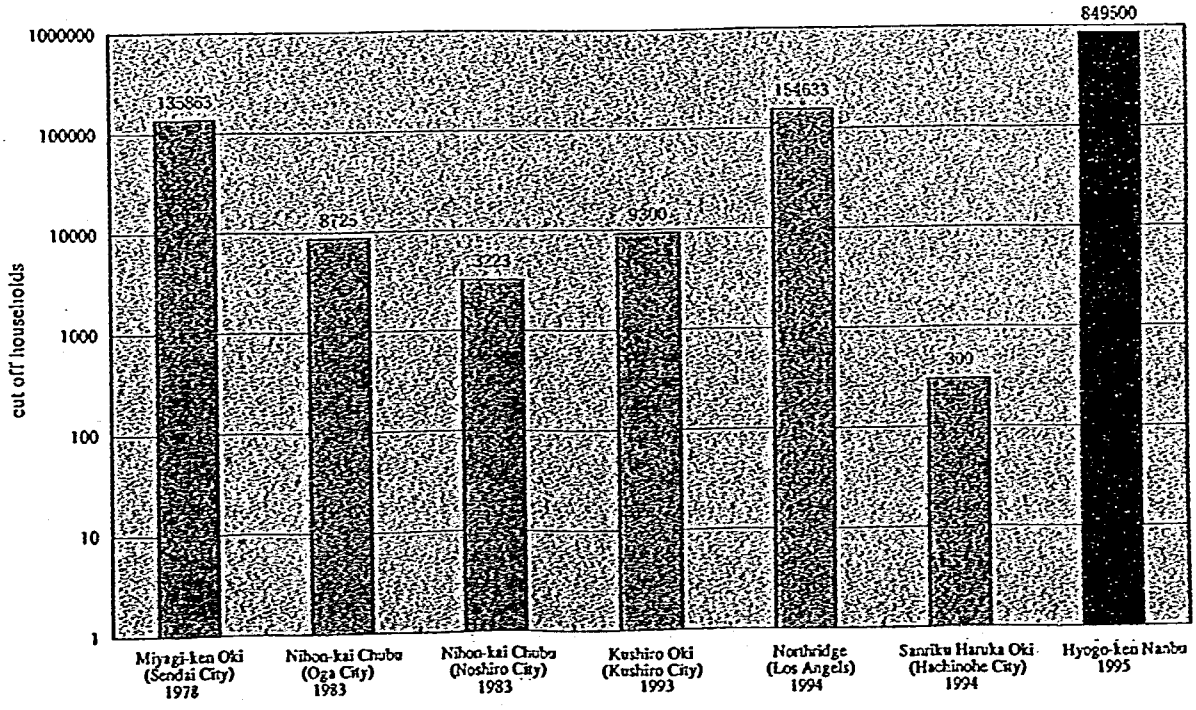



Fig. 6 Comparison of gas cut-off households for the past large earthquakes

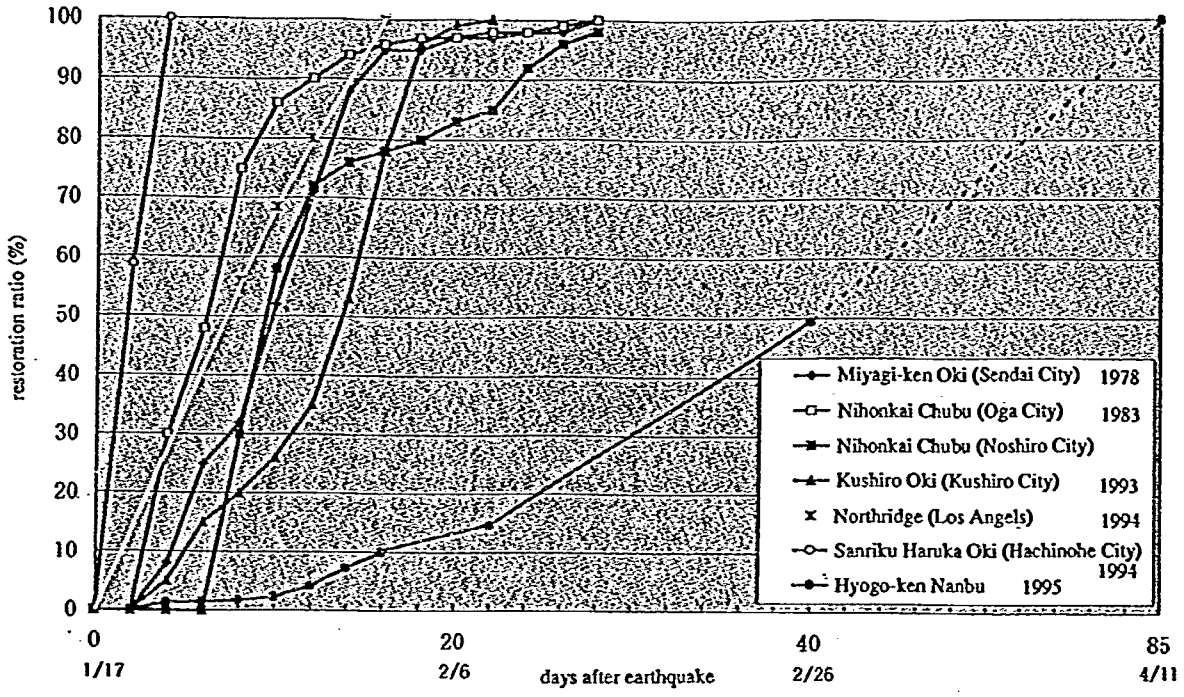



Fig. 7 Comparison of restoration days for the past large earthquakes (gas)

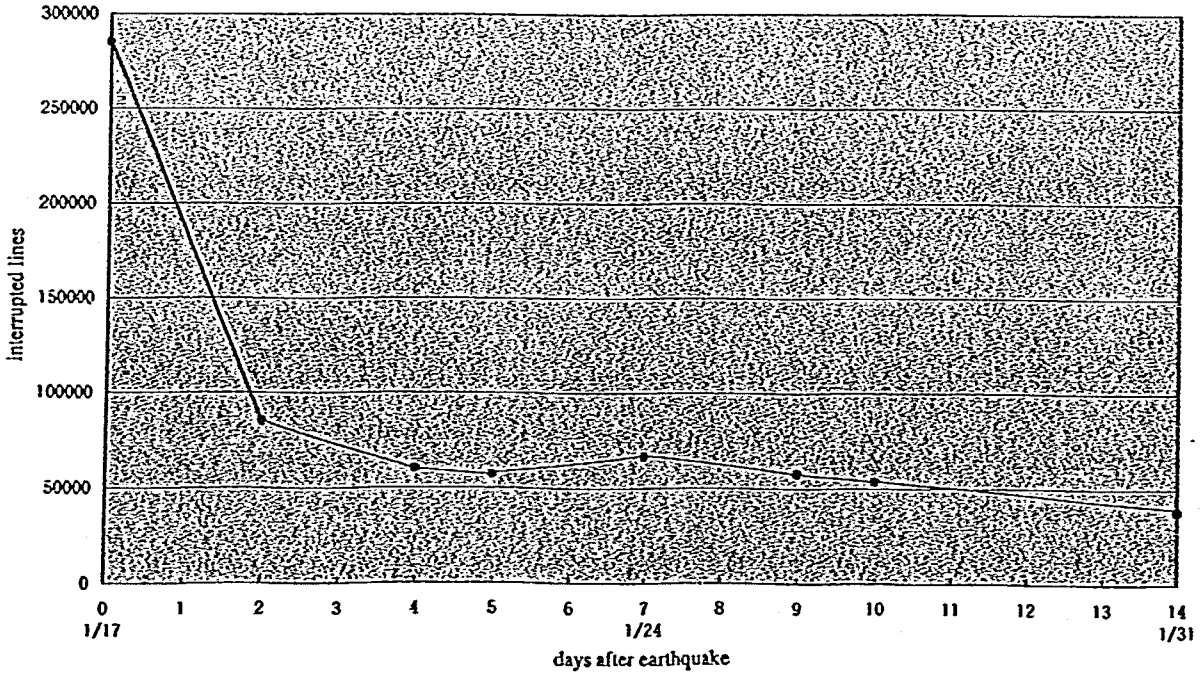



Fig. 8 Restoration process for telecommunication system

## DEVELOPMENT OF IMMEDIATE DETECTION SYSTEM

### GPS and GIS

Observations by satellites are the powerful means for weather information or environmental investigation. Movement of cloud observed by weather satellites and practical use of Landsat data are good examples. Electromagnetic waves that are reflected from the objects are used as remote sensing data. The remote sensing technique is indispensable to the analysis of environmental problems. The Global Positioning System (GPS) positioning provides the geocentric position for individual receivers or the relative positions between co-observing receivers by using signals with codes and messages transmitted by the satellites. GPS is developed and operated by the U.S. Department of Defense. Now, the 24 satellites are successfully operating and provide 24-hour, all weather navigation and surveying capability worldwide[3]. There are many civilian uses of GPS (Fig. 9). In this study, we construct the theory to make a precise survey for monitoring ground deformation. Fig. 10 shows the outline of the satellites' surveying system. In the field of seismology, the change of the distance between two points is precisely surveyed by using GPS. The order of the distance is from a few km to a few hundreds km. Our plan is to make a dense network of receivers and to monitor ground deformation or strain in a distance of a few tens meters or a few hundred meters before and after the earthquake.

The Geographical Information System (GIS) is designed to deal with the spatial or geographical information. It is frequently applied to many geographically oriented system [5]. A variety of information system indicates that the field of GIS has expanded rapidly in recent years. On the basis of the tasks performed, three facilities can be identified: database, information analysis and presentation. Collected data for various themes are placed in specific data layers for convenience in analysis and decision making support. This capability of GIS is very useful for the immediate detection of lifeline damage. After collecting and analyzing the satellites' data by GPS, the different data layers are combined, visualized and used for decision making through GIS, with this as the first information for the outline of lifeline damage, the next stage is the update of damage estimated.

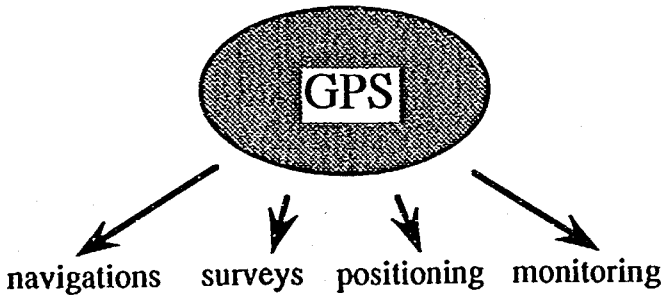



Fig. 9 Examples for civilian uses of GPS

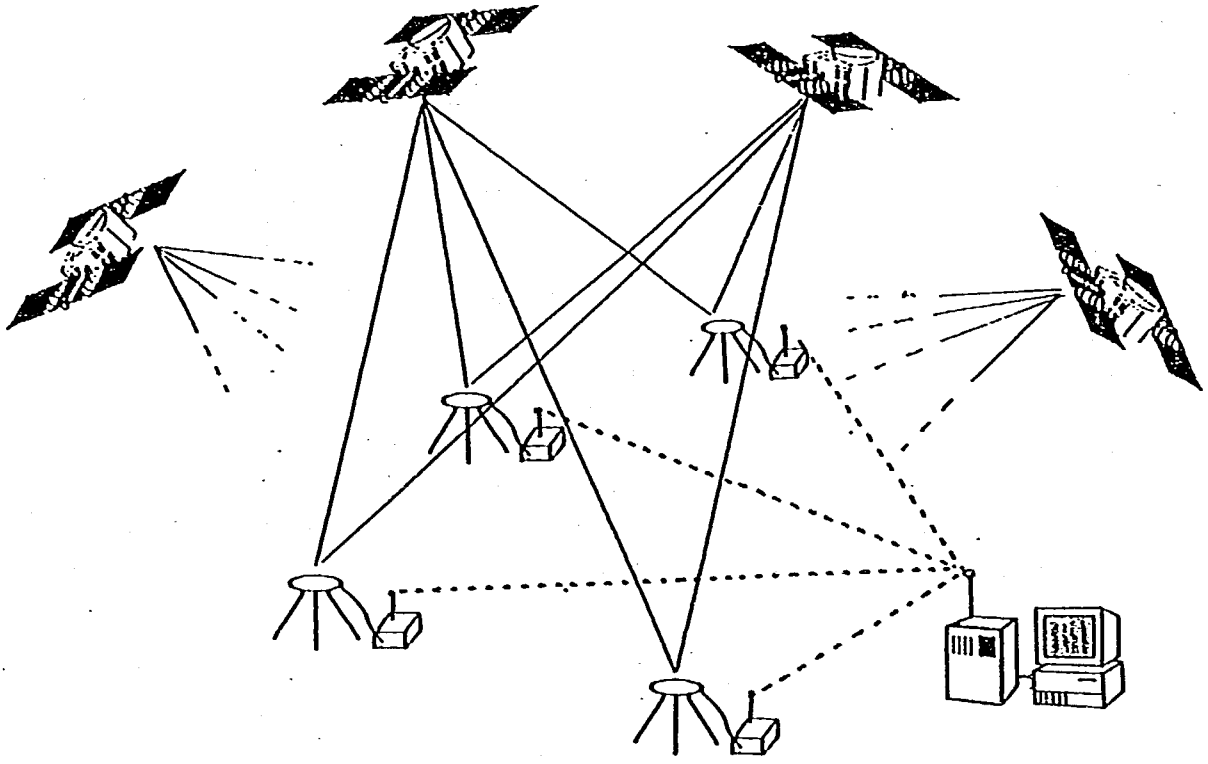


Fig. 10 Outline of satellites surveying system

Damage Function

Ohta [4] describes a relationship between earthquake input and earthquake disaster in human society as follows.

$$D = PVE \tag{1}$$

in which D is a scale of earthquake disaster, P the number of dangerous elements, V damage function and E an intensity of the earthquake. Even if the ground deformation in a quake-struck area is surveyed by GPS, it does not directly connect with damage to lifeline systems. The relationship between the ground deformation and the damage must be established. Strain of the ground is easily calculated from observed deformations. By using the ground strain, $\varepsilon$, the damage function, which expresses vulnerability of the system, is given by

$$V = f(\varepsilon) \tag{2}$$

in which V is the vulnerability of lifeline system of which parameter is ground strain.

Real Time Monitoring

In order to build a robust city for disasters, not only strengthening hardware such as aseismic reinforcement of structures but also constructing real time collection and response systems are indispensable. Various information about damage, evacuation, secondary disaster, rescue, etc. has to be collected in real time. Several systems for the emergency protection such as UrEDAS for JR, CUBE for Caltech/USGS and SIGNAL for Tokyo Gas Co. Ltd. have been already developed. The objective of this study is to obtain damage information from GPS observation for ground strain or deformation in real time and to take various countermeasures. Now high-resolution GPS receivers are very expensive. But as new receivers are continuously being developed, we will be able to obtain them at moderate price in the near future.

Ground strain at an arbitrary point can be easily calculated by using the displacements obtained by GPS surveying. Consider a triangle area surrounded by the point i, j and k (Fig. 11). Assuming that displacement vector at three nodes is $\delta$, displacement, u, in an arbitrary point in the triangle is given according to the same procedure as FEM.

$$u = N\delta \tag{3}$$

In which N is the shape function matrix. As the displacement is expressed as Eq. (3), element strains, $\varepsilon$, are written as

$$\varepsilon = B\delta \tag{4}$$

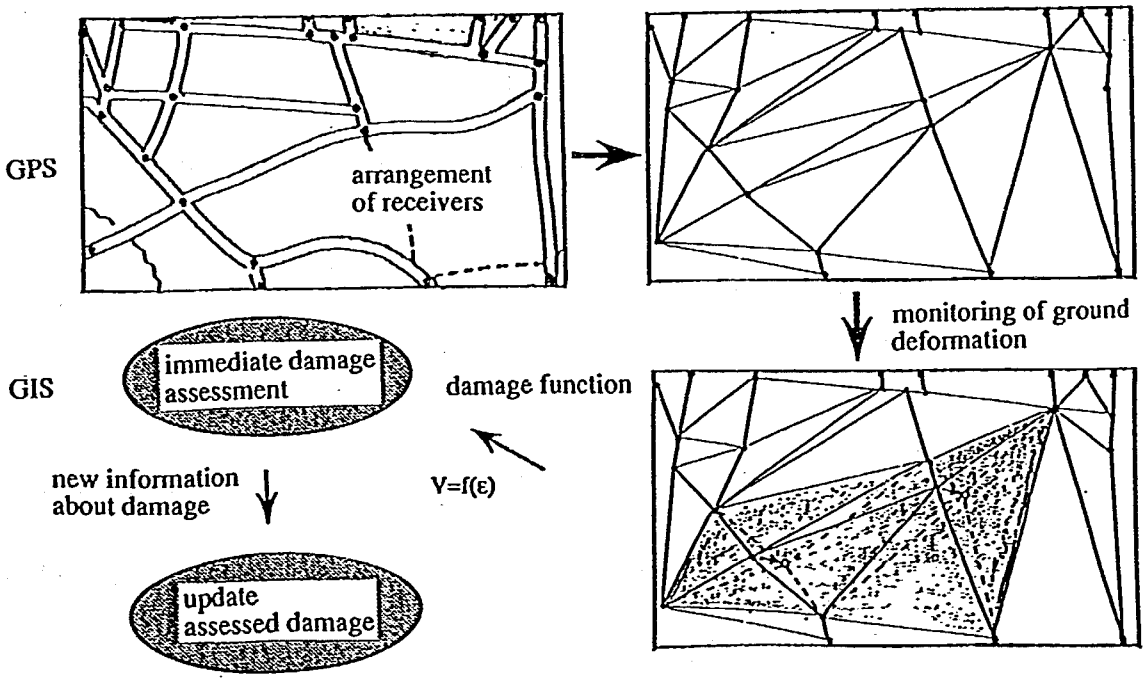



Fig. 11 Immediate detection and update system by GPS and GIS

in which B is the strain-displacement matrix. Once the displacements in specified points are obtained, ground strain can be computed immediately. when extreme ground deformations such as cracks and local lateral spreadings exist, they can be directly measured. Consequently damage to lifeline systems can be estimated according to Eq. (2). Then, next step is the update operation of disaster estimation by incorporating observed data. This algorithm is mentioned below.

Update Algorithm

The observed values which express damage to lifelines, $y_m(x)$, and their state variables, $z_n(x)$, are

$$y_m(x) = \{y(x_1)\, y(x_2) \cdots y(x_m)\}^T \tag{5}$$

$$z_n(x) = \{z(x_1)\, z(x_2) \cdots z(x_n)\}^T \tag{6}$$

Generally $y_m$ and $z_n$ are the m- and n-dimensional vectors while x is the position vector. For simplicity, we assumed n=m. The observation equation is given by

$$y_n(x) = M_n z_n(x) + R_n w_n(x) \tag{7}$$

in which $y_n$, $z_n$ and $w_n$ are the n-dimensional vectors, $M_n$ and $R_n$ are matrices with the dimensions n x n. $y_n$ is rewritten by using estimated value, $z(x_0)$, for the state variable at an additional arbitrary point, $x_0$, except observation points $x_i$ (i=1,...., n)

$$\begin{aligned} y_n(x) &= [0 \mid M_n]\{z(x_0)\, z_n^T(x)\}^T + R_n w_n(x) \\ &= M_{0_n} z_{0_n}(x) + R_n w_n(x) \end{aligned} \tag{8}$$

in which $z_{0n}(x)$ is the (n+1)-dimensional vector and $M_{0n}$ is n x (n+1) matrix.

An optimum estimation equation for $z_{0n}(x)$ is summed to be linear combination of n observations;

$$\hat{z}_{0_n}(x) = \Lambda_n y_n(x) \tag{9}$$

$$\hat{z}_{0_n}(x) = \{\hat{z}(x_0)\, \hat{z}(x_1) \cdots \hat{z}(x_n)\}^T \tag{10}$$

in which $\Lambda_n$ is (n+1) x n weight matrix. The trace of estimation error covariance matrix is

$$C = \mathrm{tr}\, E[\{z_{0_n}(x) - \hat{z}_{0_n}(x)\}\{z_{0_n}(x) - \hat{z}_{0_n}(x)\}^T] \tag{11}$$

$\Lambda_n$ which minimizes above equation becomes

$$\Lambda_n = Q_n M_{0_n}^T (M_{0_n} Q_n M_{0_n}^T + R_n W_n R_n^T)^{-1} \tag{12}$$

in which $Q_n$ and $W_n$ are correlation and error covariance matrix respectively;

$$E\{z_{0_n}(x)z_{0_n}^T(x)\} \tag{13}$$

$$E\{w_n(x)w_n^T(x)\} \tag{14}$$

The estimation error covariance matrix, $P_n$, is represented by

$$P_n = Q_n - Q_n M_{0_n}^T (M_{0_n} Q_n M_{0_n}^T + R_n W_n R_n^T)^{-1} M_{0_n}^T Q_n^T \tag{15}$$

When the (n+1)th observation is obtained, $y_{n+1}(x)$ is

$$y_{n+1}(x) = \{y(x_1) \cdots y(x_n)\ y(x_{n+1})\}^T \tag{16}$$

The optimum estimation is

$$\hat{z}_{0_{n+1}}(x) = \{\hat{z}_{0_n}^T(x) \mid \hat{z}(x_{n+1})\}^T \tag{17}$$

By using (n+2) x (n+1) weight matrix, $\Lambda_{n+1}$, the optimum estimation is given in the same manner as Eq.(9);

$$\hat{z}_{0_{n+1}}(x) = \Lambda_{n+1} y_{n+1}(x) \tag{18}$$

According to the same procedure for Eq.(11), it is rewritten

$$\hat{z}_{0_{n+1}}(x) = A\hat{z}_{0_n}(x) + K y_{n+1}(x) \tag{19}$$

Given (n+1)th observation, the optimum estimation can be calculated by the sum of the optimum estimation when n data are given and weighted. The estimation is updated by incorporating new observations [6]. According to this algorithm, damage information estimated by input information and damage function just after the earthquake is updated by the succeeding new information.

## CONCLUSIONS

The 1995 Hyogo-ken Nanbu earthquake has given enormous damage to lifeline systems. The possible countermeasures for the disaster are three phases. But disaster protections done so far are mainly for prior and posterior ones. All three phases including immediate protection do not work continuously. In this paper, we dealt with an issue of emergency protection. A system proposed is an immediate detection system for lifeline damage. The information about ground deformation is collected immediately by using GPS. The damage to lifeline systems is assessed by damage function and monitored by using GIS. The outcome can be used for the decision support. The updating algorithm, which is indispensable to incorporate new damage information in the measures, was developed.

REFERENCES

[1] Reconnaissance Team on Great Hanshin Earthquake in Kobe Univ.: 2nd Report on Great Hanshin Earthquake, 1995.3.
[2] Takada, S., T. Sato, F. Miura and J. Kiyono: Damage to lifeline systems, Reconnaissance report on the 1995 Hyogo-ken Nanbu earthquake, Ministry of Education, Science and Culture (Grant No.06306022), Edited by T. Fujiwara, pp.286-325, 1995.3 (in Japanese).
[3] Alfred Leick: GPS Satellite Surveying, John Willey & Sons, Inc., 1995.
[4] Ohta, Y.: Seismic Strong Motions as Key Information for Earthquake Disaster Prevention, Zishin 2, 47, pp.113-136, 1994 (in Japanese with English abstract).
[5] Edger Falkner: Aerial Mapping, Lewis Publishers, 1995.
[6] Kiyono, J. and F. Miura: Development of assessment system for seismic damage to lifelines, Proc. of 50th National Conf. on Civil Engineering, 1995.

# DEVELOPMENT OF SIGNAL

(Seismic Information Gathering Network Alert System)

by

Yoshihisa SHIMIZU Manager, Center for Supply Control and Disaster Management ,Tokyo Gas Co.,Ltd ,1-5-20 Kaigan ,Minato-Ku ,Tokyo ,105 Japan

Youichi YOSHIKAWA Senior Manager ,ditto

Fumio YAMAZAKI Associate Professor, Institute of Industrial Science , The University of Tokyo, 7-22-1 Roppongi ,Minato-Ku , Tokyo 106, Japan

Shigeru NODA Associate Professor, Dept. of Social Systems Engineering, Tottori University, Minami 4-101, Koyama-cho ,Tottori 680 Japan

Ryoji ISOYAMA Deputy Director, Civil Engineering Dept, Japan Consultants Co.,Ltd. 33-11 Honcho 5 Chome, Nakano-ku ,Tokyo 164 Japan

## ABSTRACT

Tokyo Gas supplies city gas to 8 million customers around Tokyo metropolitan area and has social responsibility to secure safety even after big earthquake. To prevent gas-caused secondary disaster after earthquake ,it is necessary to make prompt and reasonable decision. For this purpose, SIGNAL (Seismic Information Gathering Network Alert System)has been developed to support to make decision and has been in operation since June, 1994. SIGNAL can make on-line damage estimation using 356 seismic sensors located on site and existing mapping system database, then the result can be used to make decision quickly.

# INTRODUCTION

Tokyo Gas Co., Ltd. supplies city gas to 800,000,000 customers in most congested area, Tokyo metropolitan area, through 44,000 km length pipeline network and needs to bear social responsibility to secure safety at anytime, even during a big earthquake. Therefore Tokyo Gas has made a lot of effort to conduct countermeasures against earthquake. Basic concept of Tokyo Gas's countermeasures against earthquake is as follows,

1) Earthquake resistant design for important facilities to prevent any major damage on them during earthquake

2) Emergency measures(including gas shut-off) to prevent secondary disaster just after earthquake or to continue gas supply in little/no damaged area.

3) Quick service restoration

SIGNAL(Seismic Information Gathering Network Alert System) has been developed for emergency measures and this paper describes it,

In the event of a large-scale earthquake it is necessary to prevent secondary disasters, such as fire caused by explosion, while maintaining a gas supply to those service areas that are not badly damaged. For this reason ,we have already developed a pipeline segmentation system capable of limiting service shutoff only to affected areas by segmenting the entire service network into regional blocks.

However it is necessary to promptly and reasonably assess gas pipe damage block by block immediately following an earthquake and then to determine whether a block should continue to receive gas or be shut off. Then, we have developed SIGNAL capable of automatically processing computerized ground and gas pipe information and radio-transmitted real-time seismic data, and which estimates pipe damage promptly and accurately through the use of 356 seismic sensors installed over the entire service region. This system supports us to determine whether to shut off or continue to supply gas in the event a major earthquake.

## SIGNAL SYSTEM CHARACTERISTICS

1) Estimates pipeline damage from ground motion data collected in real time from 331 SI sensors through exclusive radio network
2) Provides detailed database for each mesh (175 x 250 m)
3) Promptly and exactly estimates hypocenter information on the earthquake occurring near the service area

## CONFIGURATION OF SIGNAL

SIGNAL consists of two parts, "Seismic Information Monitoring Part" and " Damage and Hypocenter Assessment Part" as shown in Fig.1. There are two sub-parts in " Damage and Hypocenter Assessment Part" , one is " Damage Estimation System Part" and the other is "Hypocenter Estimation System Part" .

(1) Seismic Information Monitoring System (Fig.2)

The 331 SI(Spectrum Intensity) sensors[1] has been put on site within the service area, which measure the spectrum intensity and the peak ground acceleration(PGA) at each point. These two values (SI and PGA) will be transmitted to SIGNAL HOST SYSTEM in control center by radio network when earthquake occurs ,then they will be used in damage estimation system.

Liquefaction sensors[2] are installed at 20 locations of the service area prone to soil liquefaction to detect the occurrence of liquefaction. Measured pore water rises will be also sent to control center.

In addition, five accelerometers (bed-rock seismometer) Installed deep underground along the outer periphery of the service area, continuously transmit acceleration waveform data used mainly for hypocenter estimation.

All sensor information is transmitted to the Center for Supply Control and Disaster Management through reliable private radio network(Fig.3) which enables prompt and exact assessment of the distribution of ground motion intensity in the service area within approximately only three minutes after the occurrence of an earthquake.

(2) Hypocenter Estimation System

This system estimates the specific magnitude (Richter scale) of an earthquake and its hypocenter using waveform data from accelerometers installed at five locations in a couple of minutes. The hypocenter estimation system[3] is designed for the prompt detection of earthquakes, and is especially accurate for those occurring directly below the supply area, due to 5 monitoring points installed in the

service area.

(3) Damage Estimation System

Detailed database is prepared in the computer system based on each mesh (250 m, east-westward x 175 m, south-northward about 80,000 in total) (Fig.4 and 5). The soil is classified into four categories based on topography and natural period, with the database storing information relating to liquefied layer thickness, pipeline density by pipe type and pipe diameter used, the number of customers, etc. Some meshes, which are considered to have the same soil characteristics, are combined together into groups, and each group has one seismometer in it. Its seismic information is considered to represent ground motion of each group. Then, damage to gas pipes and buildings are assessed for each mesh based on 331 real-time monitored SI values and database information.[4] Damage can be totaled by block.

The system automatically processes these transactions and displays results on-screen. Collection of information and damage estimations can be made within approximately ten minutes after an earthquake has occurred. In addition, the system can support to determine the need for service shutoff for each block by combining invariably monitored gas flow rates and pressure fluctuations with field damage information.

## CASE STUDY

After installation of SIGNAL, case study can be conducted for the damage estimation and the hypocenter estimation system. Fig.6 shows the estimated pipeline damage which is the result of simulation under the assumption of ANSEI-EDO earthquake (in 1855, 7.0 in Richter Scale).

This result shows significant damages on several low-pressure pipeline blocks, especially in Tokyo lowland areas where liquefaction occurrence is expected. This simulation enables us to conduct valuable emergency drills.

## CONCLUSION

SIGNAL has been developed to gather real-time seismic information and to conduct damage estimation in a short period just after earthquake occurs.

This system has been in operation successfully since June, 1994 and used for support of decision making on emergency measures in order to prevent second disasters.

However after the 1995 Great Hanshin Earthquake, the further investigation is considered to be necessary especially for the damage estimation part, and some modification and improvement measures will be conducted. from now on.

## REFERENCES

(1) Katayama,T.,Sato,N.,and Saito, K. "SI sensor for identification of destructive earthquake ground motion." Proc. of the 9th World Conf. on Earthquake Engineering Ⅶ (1988):667-672

(2) Yasuda,S.,Morimoto,I.,and Shimizu,Y. " Development of Liquefaction Sensor" UJNR Remedial Treatment of Liquefiable Soils (1991):125-136

(3)Noda,S., and Kono,H. "Hypocenter estimation system for earthquake countermeasures."Journal of Natural Disaster science,VOL.15, 1(1993):53-90

(4) Yamazaki,F.,Katayama,T., and Yoshikawa,Y. " On-line damage assessment of city gas networks based on dense earthquake monitoring. "Proc. of the 5th U.S. National conference on Earthquake Engineering,VOL.4,(1994 a):829-837

# SIGNAL

(Seismic Information Gathering and Network Alert System)

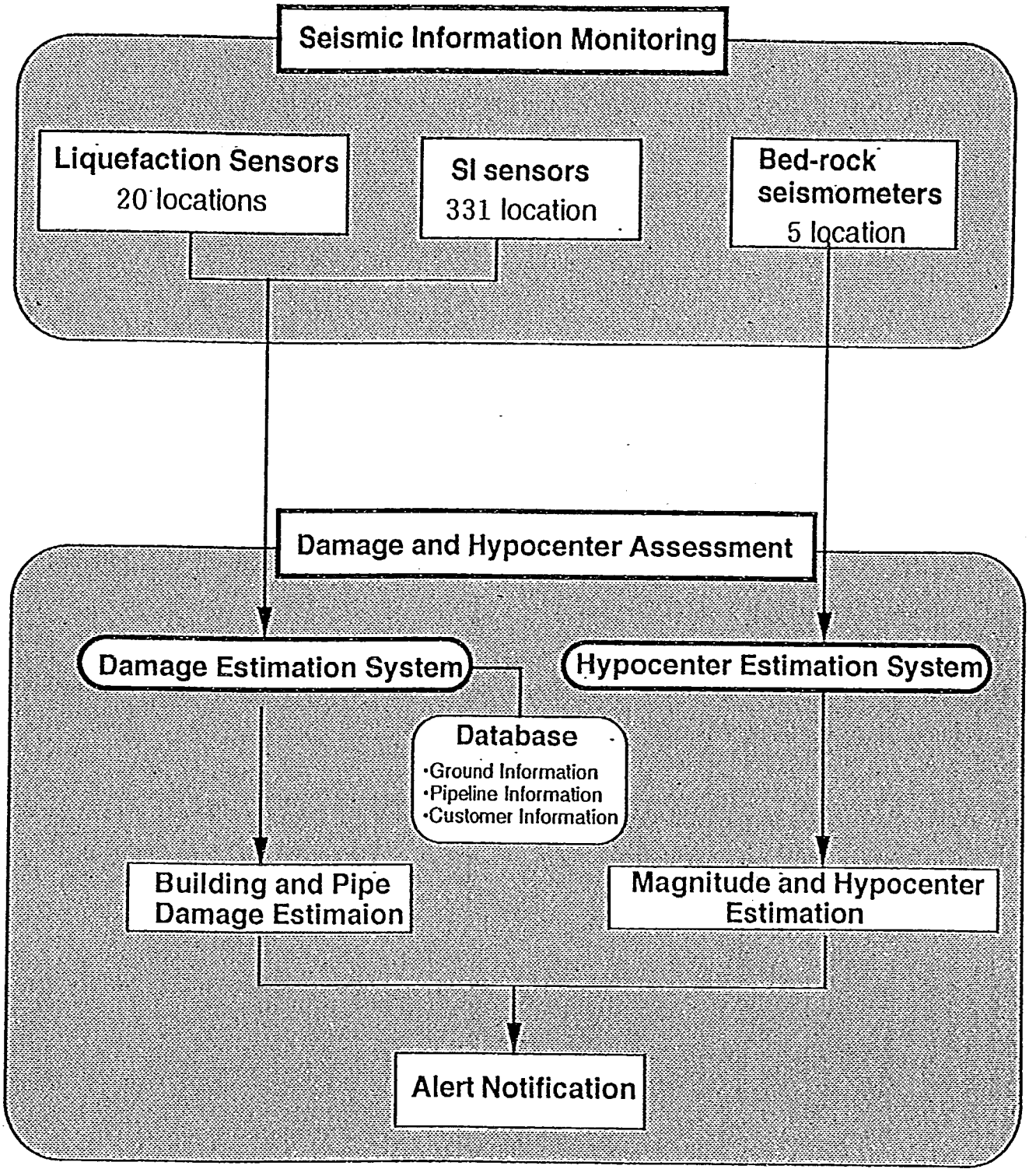



Fig. 1 Configuration of SIGNAL

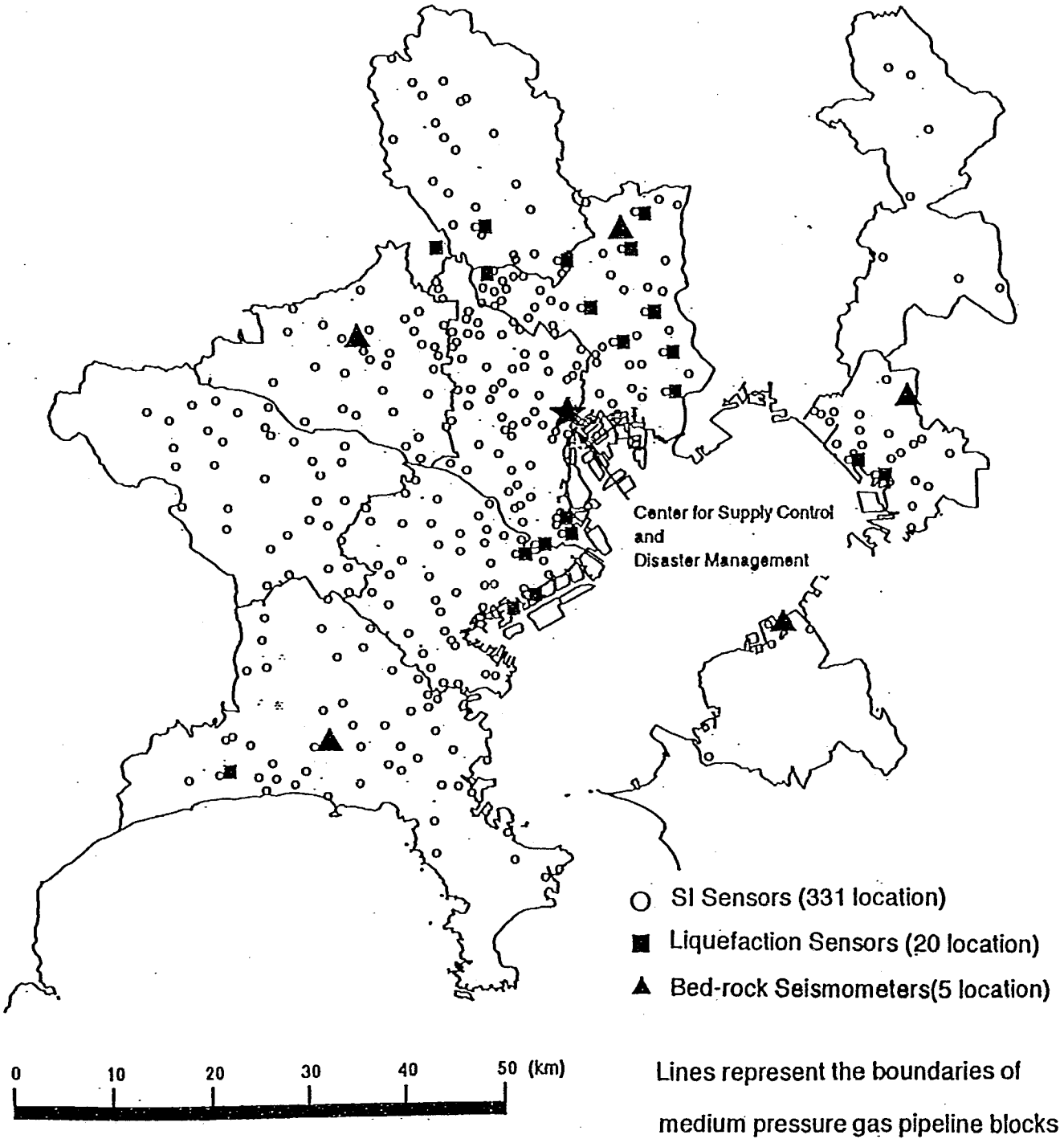



Fig. 2 Distribution of Seismic Sensors

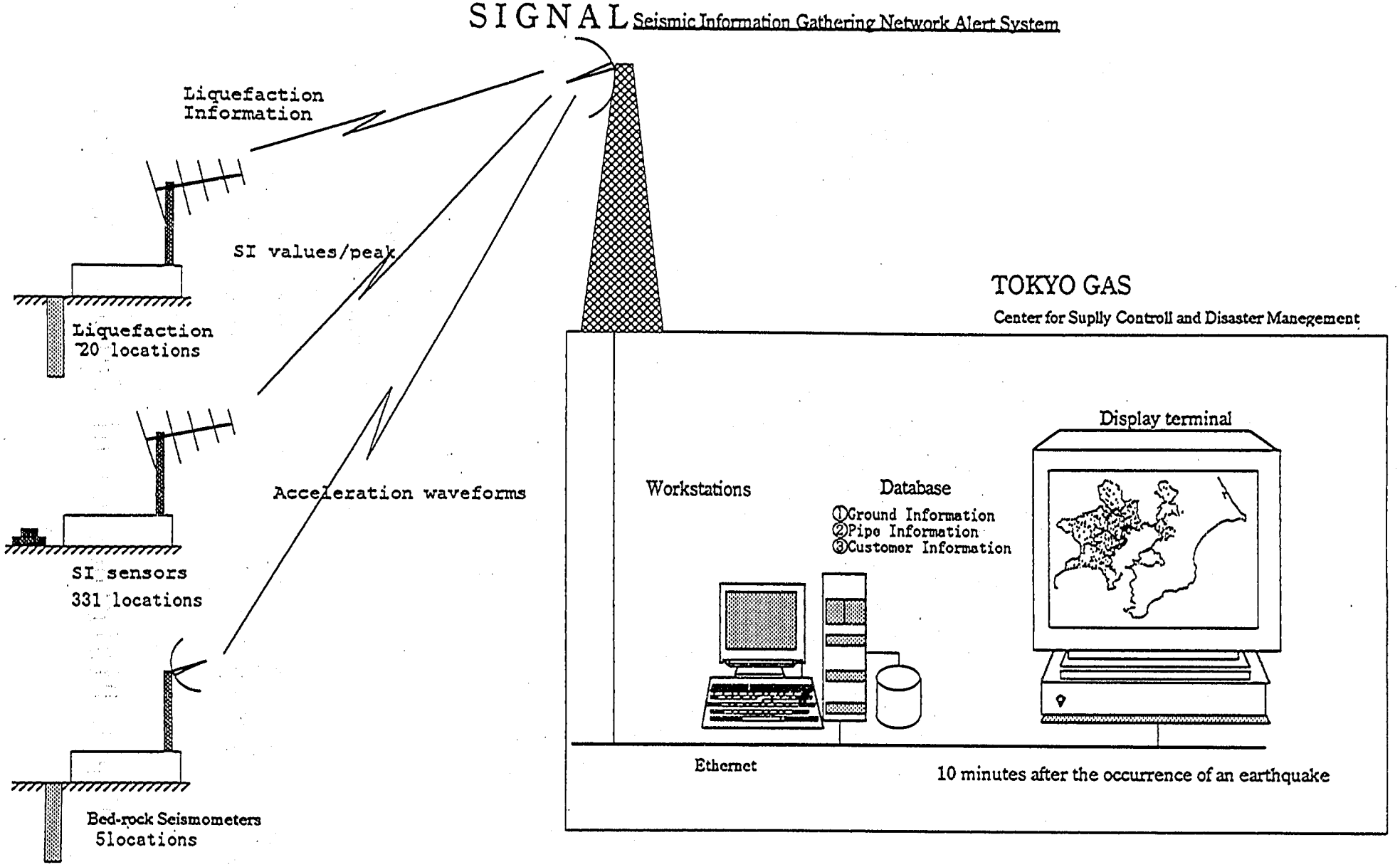



Fig. 3 Seismic Information Monitoring

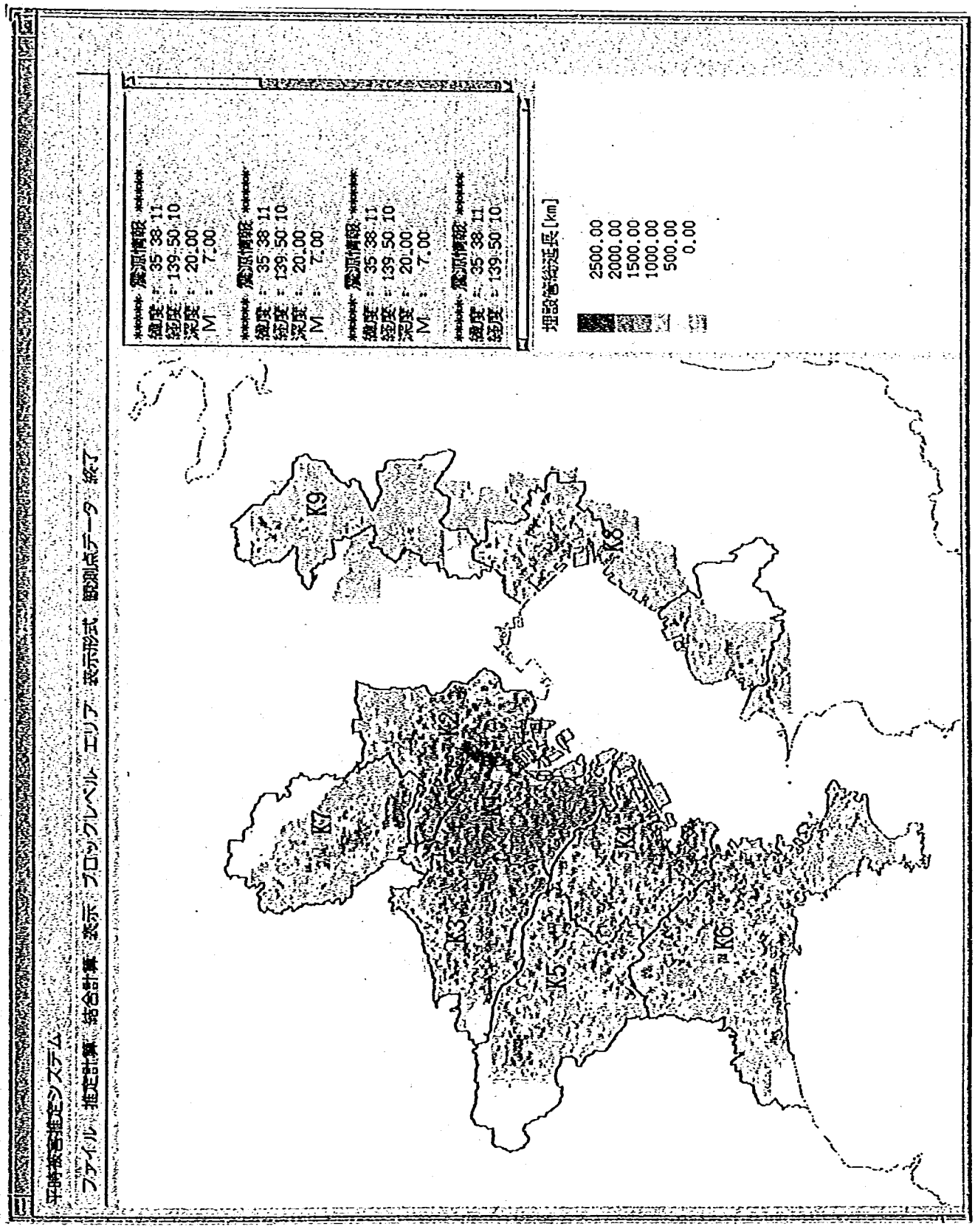



Fig. 4 Density of Pipe per Mesh

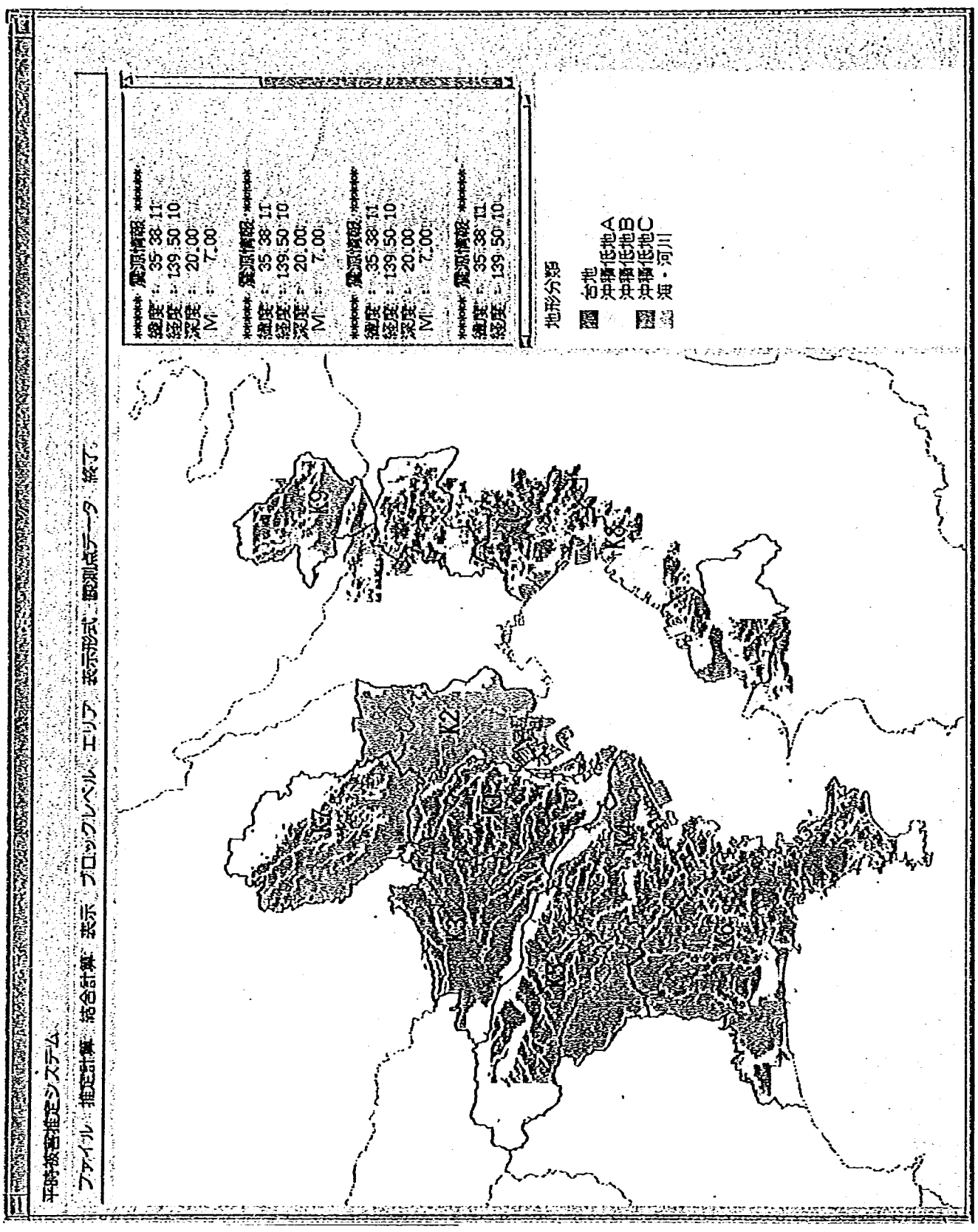



Fig.5 Topographical Classification

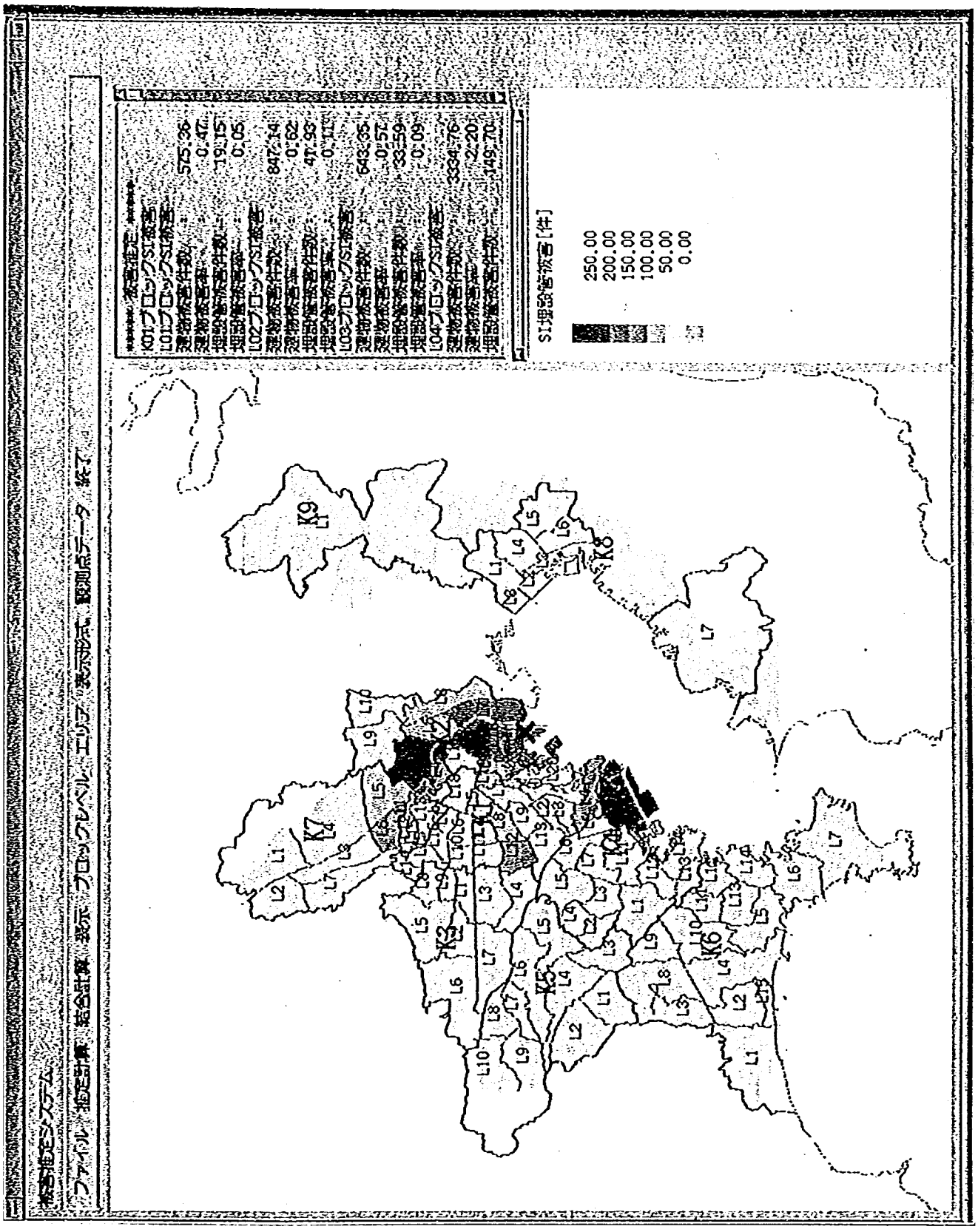



Fig. 6 Pipe Damage Estimation
(ANSEI Earthquake)

# CONDITIONAL NON-GAUSSIAN FIELDS

by
Masaru HOSHIYA

Professor of Civil Engineering, Musashi Institute of Technology, Setagaya-ku, Tokyo 158 Japan

## ABSTRACT

A theoretical formulation of non-Gaussian fields is presented to simulate sample fields conditioned by observed data at discrete points. The formulation is based on a conditional probability density function, which includes Gaussian fields as a special case and the formulation can be also applied to non-Gaussian random processes when spatial points are replaced by temporal points. Interpolation and extrapolation of environmental and geotechnical problems, and simulation of conditional real time random processes of earthquake type phenomena are typical examples in the application.

## INTRODUCTION

Consider a non-Gaussian and non-homogeneous stochastic field $x_i$ at a discrete spatial point $i$, where the marginal probability density function $f_{Xi}(x_i)$ and the correlation coefficient $\rho_{ij}$ are prescribed. Since $\rho_{ij} = E\left[(x_i-\mu_i)(x_j-\mu_j)\right]/\sigma_i\sigma_j$ in which the means $\mu_i$ and $\mu_j$, and the standard deviations $\sigma_i$ and $\sigma_j$ are spatially dependent, $x_i$ is generally non-homogeneous.

Now consider that a set of sample realization $\underline{\mathbf{X}}_{n-1} = (\underline{x}_1, \underline{x}_2, \cdots, \underline{x}_{n-1})^T$ of $\underline{\mathbf{X}}_{n-1}$ at discrete points $i = 1, \cdots, n-1$ is observed, and a sample realization $\underline{x}_n$ at an unobservation point $n$ is to be estimated. If $\underline{x}_n$ can be estimated, then as many data as we need can be estimated at other unobservation points by treating estimated ones $\underline{x}_n, \underline{x}_{n+1}, \cdots$ as if they were observed. Hereinafter, therefore a theoretical formulation is derived to simulate $\underline{x}_n$ conditioned on $\underline{\mathbf{X}}_{n-1} = (\underline{x}_1, \underline{x}_2, \cdots, \underline{x}_{n-1})^T$.

If we assume the discrete spatial point $i$ as a discrete time subscript with $t = i\Delta$ where $\Delta$ is a sampling interval, the formulation may be also directly applied to a random process $(x_1, x_2, \cdots, x_{n-1}, x_n)$ in which $\underline{x}_n$ is to be conditionally estimated with given $\underline{x}_1, \underline{x}_2, \cdots, \underline{x}_{n-1}$ in a sequential time order.

Conditional simulation of a Gaussian stochastic field has been already investigated by the Kriging least error variance method (1),(2),(3) and its solutions may easily stem from the present formulation as a special case.

A well known interpretation on the coefficients of a Gaussian autoregressive model and the model error is also made clear based on the formulation.

## THEORETICAL FORMULATION

The formulation is derived by forming a conditional density function $f_{X_n}(x_n|x_i, i=1,\cdots,n-1)$ via the mapping of non-Gaussian random variable into Gaussian variable. Once $f_{X_n}(x_n|x_i, i=1,\cdots,n-1)$ is obtained, $x_n$ can be easily simulated by the ordinary Monte Carlo method. The expansion to a multiple point simulation is easy if the step by step expansion method available is applied (1),(2),(3).

The law of mapping gives

$$F_{X_i}(x_i) = \Phi(z_i) \tag{1}$$

where $F_{X_i}(x_i)$ = the marginal probability distribution function of $x_i$,

$\Phi(z_i)$ = standard Gaussian probability distribution function,

and $z_i$ is a standard Gaussian random variable.

The joint probability distribution function of $\mathbf{X}_n = (x_1, x_2, \cdots, x_n)^T$ is then expressed by

$$\begin{aligned} F_{\mathbf{X}_n}(\mathbf{X}_n, \mathbf{R}_n) &= \text{Prob}\left[(X_1 \le x_1) \cap (X_2 \le x_2) \cap \cdots \cap (X_n \le x_n)\right] \\ &= \text{Prob}\left[(Z_1 \le z_1) \cap (Z_2 \le z_2) \cap \cdots \cap (Z_n \le z_n)\right] \\ &= \Phi_n\left[\Phi^{-1}\{F_{X_1}(x_1)\}, \Phi^{-1}\{F_{X_2}(x_2)\}, \cdots, \Phi^{-1}\{F_{X_n}(x_n)\}, \mathbf{R}'_n\right] \end{aligned} \tag{2}$$

where $\Phi_n$ = standard Gaussian joint probability distribution function,

$\mathbf{R}_n$ = the correlation coefficient matrix of $\mathbf{X}_n$ whose components are $\rho_{ij}$

and $\mathbf{R}'_n$ = the correlation coefficient matrix of $\mathbf{Z}_n = (z_1, z_2, \cdots, z_n)^T$, whose components are $\rho'_{ij}$.

It is noted that while $\mathbf{R}_n$ is prescribed, $\mathbf{R}'_n$ is not known at this stage and is to be estimated. Actually, $\mathbf{R}'_n$ may be numerically evaluated by utilizing the mapping law of correlation coefficients of $\rho_{ij}$ and $\rho'_{ij}$ except for a few special distributions such as a lognormal distribution.

The joint Gaussian probability density function of $\mathbf{X}_n$ may be obtained from eq(2) as follows.

$$f_{Xn}(\mathbf{X}_n,\mathbf{R}_n)=\frac{\partial^n F_{\mathbf{X}_n}(\mathbf{X}_n,\mathbf{R}_n)}{\partial x_1\partial x_2\cdots\partial x_n}$$

$$=\varphi_n(z_1,z_2,\cdots,z_n,\mathbf{R}_n')\frac{f_{X_1}(x_1)f_{X_2}(x_2)\cdots f_{X_n}(x_n)}{\varphi(z_1)\varphi(z_2)\cdots\varphi(z_n)} \tag{3}$$

where $\varphi_n$= standard Gaussian joint probability density function,

$f_{X_i}(x_i)$= the marginal probability density function of $x_i$,

and $\varphi(z_i)$= standard Gaussian probability density function.

This equation(3) is called the Nataf model and is shown in the reference(4).

If the non-Gaussian variable $x_i$ is expressed as a function of the standard Gaussian variable $z_i$ as

$$x_i=g(z_i) \tag{4}$$

where $g(z)$ is an increasing function, then equation(3) may be converted to the following expression.

Since $\text{Prob}(Z_i\le z_i)=\text{Prob}(X_i\le g(z_i))$, we have

$$\Phi(z_i)=F_{X_i}(g(z_i))$$

and therefore we have

$$\varphi(z_i)=f_{X_i}(x_i)g'(z_i) \tag{5}$$

Substitution of eq(5) in eq(3) leads to

$$f_{\mathbf{X}_n}(\mathbf{X}_n,\mathbf{R}_n)=\frac{\varphi_n(z_1,z_2,\cdots,z_n,\mathbf{R}_n')}{g'(z_1)g'(z_2)\cdots g'(z_n)} \tag{6}$$

This equation(6) is shown in the reference(5). Regarding eq(4), we have for a lognormal distribution of $x_i$

$$g(z_i)=\exp(\varsigma_i z_i+\lambda_i) \tag{7}$$

where $\lambda_i=E[\ln x_i]$ and $\varsigma_i=\sigma_{\ln x_i}>0$.

As mentioned before, the most important is the conditional probability density function of $x_n$ which may be easily obtained by using eqs(3) or (6) as below.

From the definition of conditional probability, we have with eq(3)

$$f_{X_n}(x_n|x_i,i=1,\cdots,n-1)=\varphi(z_n|z_i,i=1,\cdots,n-1)\frac{f_{X_n}(x_n)}{\varphi(z_n)} \tag{8}$$

If we use eq(6), instead of eq(3), we have

$$f_{X_n}(x_n|x_i,i=1,\cdots,n-1)=\varphi(z_n|z_i,i=1,\cdots,n-1)/g'(z_n) \tag{9}$$

Observe that the right hand sides of both eqs(8) and (9) are specified except for the conditional standard Gaussian density function $\varphi(z_n|z_i,i=1,\cdots,n-1)$ which needs the correlation coefficients $\rho_{ij}'$. These correlation coefficients may be numerically obtained from the following relationships respectively (4).

In the case of eq(8),

$$\rho_{ij} = \int_{-\infty}^{\infty}\int_{-\infty}^{\infty}\left(\frac{x_i-\mu_i}{\sigma_i}\right)\left(\frac{x_j-\mu_j}{\sigma_j}\right)\varphi_2\left(z_i,z_j,\rho'_{ij}\right)dz_i dz_j \tag{10}$$

In the case of eq(9),

$$\rho_{ij} = \int_{-\infty}^{\infty}\int_{-\infty}^{\infty}\left(\frac{g(z_i)-\mu_i}{\sigma_i}\right)\left(\frac{g(z_j)-\mu_j}{\sigma_j}\right)\varphi_2\left(z_i,z_j,\rho'_{ij}\right)dz_i dz_j \tag{11}$$

If $\mathbf{X}_n = (x_1, x_2, \cdots, x_n)^T$ is jointly lognormal, then we have

$$\rho'_{ij} = \frac{\ln\left(1+\rho_{ij}\delta_i\delta_j\right)}{\sqrt{\ln\left(1+\delta_i^2\right)\ln\left(1+\delta_j^2\right)}} \tag{12}$$

where $\delta_i, \delta_j$ = coefficients of variation.

Once the correlation coefficients are determined, the conditional probability density function $\varphi\left(z_n|z_i, i=1,\cdots,n-1\right)$ may be expressed as a Gaussian probability density function with the conditional mean

$$\mu_{n|cond} = \mathbf{Z}_{n-1}^T \mathbf{R}'^{-1}_{n-1}\mathbf{S}'_{n-1} \tag{13}$$

and the conditional variance

$$\sigma^2_{n|cond} = 1 - \mathbf{S}'^T_{n-1}\mathbf{R}'^{-1}_{n-1}\mathbf{S}'_{n-1} \tag{14}$$

where $\mathbf{R}'_{n-1}$ and $\mathbf{S}'_{n-1}$ are submatrices of $\mathbf{R}'_n$ and are given by

$$\mathbf{R}'_n = \begin{bmatrix} \mathbf{R}'_{n-1} & \mathbf{S}'_{n-1} \\ \mathbf{S}'^T_{n-1} & 1 \end{bmatrix} \tag{15}$$

The evaluation of the inverse matrix $\mathbf{R}'^{-1}_{n-1}$ may be carried out by the following recursive equation so that simulation at multiple points may be efficiently performed.

$$\mathbf{R}'^{-1}_{n-1} = \begin{bmatrix} \mathbf{R}'^{-1}_{n-2} + \mathbf{R}'^{-1}_{n-2}\mathbf{S}'_{n-2}\mathbf{S}'^T_{n-2}\mathbf{R}'^{-1}_{n-2}/\sigma^2_{n-1|cond} & -\mathbf{R}'^{-1}_{n-2}\mathbf{S}'_{n-2}/\sigma^2_{n-1|cond} \\ -\mathbf{S}'^T_{n-2}\mathbf{R}'^{-1}_{n-2}/\sigma^2_{n-1|cond} & 1/\sigma^2_{n-1|cond} \end{bmatrix} \tag{16}$$

The conditional simulation of non-Gaussian fields based on eqs(8) or (9) are now to be performed since we have an efficient method of constructing the conditional Gaussian probability density function $\varphi\left(z_n|z_i, i=1,\cdots,n-1\right)$. It is noted that for the expansion to multiple point simulation, $\varphi\left(z_{n+1}|z_i, i=1,\cdots,n\right)$ can be easily obtained with eq(16).

Based on eq(9), the simulation procedure is very much ordinarily done by the Monte Carlo method.

(1) First, generate an uniform random variable $\underline{a}$ from the uniform distribution between zero to one.

(2) Solve the following equation for $\underline{x}_n$

$$\int_{-\infty}^{\underline{x}_n} f_{X_n}\left(x_n|x_i, i=1,\cdots,n-1\right)dx_n = \underline{a} \tag{17}$$

If we substitute eq(9) in the integrand with $x_n = g(z_n)$, the eq(17) is transferred to an integration with respect to $z_n$ instead of $x_n$ as follows.

$$\int_{-\infty}^{\underline{z}_n} \varphi(z_n|z_i, i=1,\cdots,n-1)dz_n = \underline{a} \tag{18}$$

and $$\underline{z}_n = \Phi^{-1}(\underline{a}|z_i, i=1,\cdots,n-1) \tag{19}$$

(3) The sample value at the spatial point $n$ is obtained by

$$\underline{x}_n = g(\underline{z}_n) \tag{20}$$

If we use eq(8), equation(20) may be replaced by

$$\underline{x}_n = F_{X_n}^{-1}\{\Phi(\underline{z}_n)\} \tag{21}$$

since eq(1) is valid.

## LEAST MEAN SQUARE ESTIMATION

Instead of a sample realization $\underline{x}_n$, we want to estimate $\hat{x}_n$ at an unobservation point so that the mean square error is minimum. So, we have

$$\begin{aligned} E\left[(x_n - \hat{x}_n)^2\right] &= \int_{-\infty}^{\infty}\cdots\int_{-\infty}^{\infty}(x_n - \hat{x}_n)^2 f_{X_n}(\mathbf{X}_n, \mathbf{R}_n)d\mathbf{X}_n \\ &= \int_{-\infty}^{\infty}\cdots\int_{-\infty}^{\infty} f_{X_{n-1}}(\mathbf{X}_{n-1}, \mathbf{R}_{n-1})\int_{-\infty}^{\infty}(x_n - \hat{x}_n)^2 f_{X_n}(x_n|x_i, i=1,\cdots,n-1)dx_n d\mathbf{X}_{n-1} \end{aligned} \tag{22}$$

Since the integrand above is nonnegative, it suffices to minimize

$$\int_{-\infty}^{\infty}(x_n - \hat{x}_n)^2 f_{X_n}(x_n|x_i, i=1,\cdots,n-1)dx_n$$

This integral is the second moment of the conditional probability density function $f_{X_n}(x_n|x_i, i=1,\cdots,n-1)$ with respect to $\hat{x}_n$, and therefore this moment is minimum if

$$\hat{x}_n = \int_{-\infty}^{\infty} x_n f_{X_n}(x_n|x_i, i=1,\cdots,n-1)dx_n = E\left[x_n|x_i, i=1,\cdots,n-1\right] \tag{23}$$

This is an unbiased estimator, since $E[\hat{x}_n] = E\left[E\left[x_n|x_i, i=1,\cdots,n-1\right]\right] = E[x_n]$.

If we use eq(9), this becomes

$$\hat{x}_n = \int_{-\infty}^{\infty} g(z_n)\varphi(z_n|z_i, i=1,\cdots,n-1)dz_n = E\left[g(z_n)|z_i, i=1,\cdots,n-1\right] \tag{24}$$

The least mean square error is then

$$E\left[(x_n - \hat{x}_n)^2\right] = E\left[x_n^2\right] - 2E[x_n\hat{x}_n] + E\left[\hat{x}_n^2\right] \tag{25}$$

where

$$E\left[x_n^2\right] = \int_{-\infty}^{\infty} x_n^2 f_{X_n}(x_n)dx_n \tag{26}$$

$$E[x_n\hat{x}_n] = \int_{-\infty}^{\infty}\cdots\int_{-\infty}^{\infty}(x_n\hat{x}_n)f_{X_n}(\mathbf{X}_n, \mathbf{R}_n)d\mathbf{X}_n \tag{27}$$

$$E\left[\hat{x}_n^{\,2}\right] = \int_{-\infty}^{\infty}\cdots\int_{-\infty}^{\infty}\hat{x}_n^2 f_{X_{n-1}}(\mathbf{X}_{n-1},\mathbf{R}_{n-1})d\mathbf{X}_{n-1} \tag{28}$$

The error variance is

$$\sigma^2_{(x_n-\hat{x}_n)} = \sigma_n^2 + \sigma^2_{\hat{x}_n} - 2Cov(x_n,\hat{x}_n) \tag{29}$$

By the way, the conditional variance of $x_n$ is given by

$$\begin{aligned}\sigma^2_{x_n|cond} &= E\left[x_n^2|x_i, i=1,\cdots,n-1\right] - \hat{x}_n^2 \\ &= E\left[g^2(z_n)|z_i, i=1,\cdots,n-1\right] - E\left[g(z_n)|z_i, i=1,\cdots,n-1\right]^2 \\ &= \sigma^2_{g(z_n)|z_i,i=1,\cdots,n-1}\end{aligned} \tag{30}$$

Equations (23) to (30) are valid for any non-Gaussian field as far as $x_n = g(z_n)$. We summarize that (1) the best estimator is equal to the conditional mean of $x_n$ (eq(23)) , and is equivalent to the conditional expectation of $g(z_n)$ (eq(24)) . $\hat{x}_n$ is of course dependent upon sample realization $\underline{x}_i, i=1,\cdots,n-1$.

(2) The least mean square error (eq(25)) is dependent upon the locations of sample observation, but independent of the values of $\underline{x}_i, i=1,\cdots,n-1$.

(3) The conditional variance (eq(30)) is not equal to the least error variance of eq(29) (or the least mean square error (eq(25)) ).

These observations are already commented for a lognormal field by the Kriging approach in the references (6),(7).

## GAUSSIAN FIELD

If $\mathbf{X}_n = (x_1, x_2, \cdots, x_n)^T$ is Gaussian, eqs(10) or (11) will give the following result.

$$\rho_{ij} = \rho'_{ij} \quad (\mathbf{R}_n = \mathbf{R}'_n) \tag{31}$$

and since $(x_n - \mu_n)/\sigma_n = z_n$ , we have

$$g(z_n) = \sigma_n z_n + \mu_n \tag{32}$$

In this case, equation(9) becomes

$$f_{X_n}\left(x_n|x_i, i=1,\cdots,n-1\right) = \varphi\left(\frac{x_n-\mu_n}{\sigma_n}|z_i, i=1,\cdots,n-1\right)\Big/\sigma_n \tag{33}$$

With eqs(13) and (14), equation(33) is a conditional Gaussian probability density function with the mean of

$$\mu_{n|cond} = \mu_n + \sigma_n \underline{\mathbf{Z}}^T_{n-1}\mathbf{R}^{-1}_{n-1}\mathbf{S}_{n-1} \tag{34}$$

and the variance of

$$\sigma^2_{n|cond} = \sigma_n^2 - \sigma_n^2\mathbf{S}^T_{n-1}\mathbf{R}^{-1}_{n-1}\mathbf{S}_{n-1} \tag{35}$$

It is noted that the results of eqs(34) and (35) coincides naturally with the solutions for the Kriging estimator of a Gaussian field in the references (1),(2),(3).

If we use the following matrices and vectors

$$\mathbf{C} = \begin{bmatrix} \mathbf{C}_{n-1} & \mathbf{D} \\ \mathbf{D}^T & c_{nn} \end{bmatrix} ; \text{covariance matrix} \tag{36}$$

$$c_{nn} = \sigma_n^2 \tag{37}$$

$$\mathbf{C}_{n-1} = \sigma_{n-1}\mathbf{R}_{n-1}\sigma_{n-1} \tag{38}$$

$$\mathbf{D} = \sigma_n \sigma_{n-1}\mathbf{S}_{n-1} \tag{39}$$

$$\mu_{n-1} = (\mu_1, \mu_2, \cdots, \mu_{n-1})^T \tag{40}$$

$$\text{and} \quad \sigma_{n-1} = \begin{bmatrix} \sigma_1 & & & \\ & \sigma_2 & & \\ & & \ddots & \\ & & & \sigma_{n-1} \end{bmatrix} \tag{41}$$

then we have another expressions for eqs(34) and (35) respectively.

$$\mu_{n|cond} = \mu_n + \mathbf{D}^T\mathbf{C}_{n-1}^{-1}(\underline{\mathbf{X}}_{n-1} - \mu_{n-1}) \tag{42}$$

$$\sigma_{n|cond}^2 = \sigma_n^2 - \mathbf{D}^T\mathbf{C}_{n-1}\mathbf{D} \tag{43}$$

## GAUSSIAN AUTOREGRESSIVE MODEL

A Gaussian AR model may be expressed as

$$x_n = \mathbf{a}_{n-1}^T\mathbf{X}_{n-1} + \varepsilon_n \tag{44}$$

where the subscripts of $x_n, \mathbf{X}_{n-1}$ and $\varepsilon_n$ represent time $t = n\Delta$ in which $\Delta$ is the sampling interval.

The coefficient vector $\mathbf{a}_{n-1} = (a_1, a_2, \cdots, a_{n-1})^T$ may be obtained by minimizing the mean square error, and we have

$$\mathbf{a}_{n-1} = \mathbf{C}_{n-1}^{-1}\mathbf{D} \tag{45}$$

and the error variance becomes

$$\sigma_{\varepsilon_n}^2 = \sigma_n^2 - \mathbf{D}^T\mathbf{C}_{n-1}^{-1}\mathbf{D} \tag{46}$$

We also have the mean of the error as

$$\mu_{\varepsilon_n} = \mu_n - \mathbf{D}^T\mathbf{C}_{n-1}^{-1}\mu_{n-1} \tag{47}$$

Consider the conditional mean of $x_n$ when the past data $\underline{\mathbf{X}}_{n-1}$ are given, and we have from eq(44)

$$\begin{aligned} \mu_{n|cond} &= \mathbf{a}_{n-1}^T\underline{\mathbf{X}}_{n-1} + \mu_{\varepsilon_n} \\ &= \mu_n - \mathbf{D}^T\mathbf{C}_{n-1}^{-1}(\mathbf{X}_{n-1} - \mu_{n-1}) \end{aligned} \tag{48}$$

Similarly the conditional variance is

$$\sigma_{n|cond}^2 = \sigma_{\varepsilon_n}^2 = \sigma_n^2 - \mathbf{D}^T\mathbf{C}_{n-1}^{-1}\mathbf{D} \tag{49}$$

The interpretation of $\mathbf{a}_{n-1}$ and $\varepsilon_n$ in eq(44) is self-explanatory since eqs(48) and (49) coincide with eqs(42) and (43) respectively.

## CONCLUDING REMARKS

Theory of conditional non-Gaussian fields is discussed by the theory of conditional probability incorporated with mapping of non-Gaussian variable to Gaussian variable. The following results are obtained.

(1) Simulation of a sample field $\underline{x}_n$ at an unobservation point conditioned by observation data $\underline{\mathbf{X}}_{n-1}=(\underline{x}_1,\underline{x}_2,\cdots,\underline{x}_{n-1})^T$ can be performed based on the conditional probability $f_{X_n}(x_n|x_i,i=1,\cdots,n-1)$ of eq(8) or eq(9).

(2) Expansion of the simulation to multiple points can be efficiently performed with the recursive evaluation of the inverse matrix of the equivalent Gaussian field correlation coefficients by eq(16) which is necessary for the step by step expansion procedure.

(3) The properties of the best estimator $\hat{x}_n$ at an unobservation point based on the least mean square estimation are clarified by eqs(23) to (30). The error variance of eq(29) does not coincide with the conditional variance of eq(30) in general, which is clearly different from the results of Gaussian fields.

In addition, the following well known facts are discussed.

(4) A special solution from the theory developed herein leads to the properties of Gaussian fields obtained by the Kriging approach, when $\mathbf{X}_n$ is Gaussian.

(5) The conditional mean and the conditional variance of an autoregressive model are identical to the Kriging estimator and the error variance, if the coefficient vector of the model is determined by minimizing the mean square error.

## REFERENCES


(1) Hoshiya, M.,Simulation of a Conditional Stochastic Field,Jour. of JSCE, No. 459/I-22, pp113-118,1993.1. (in Japanese)

(2) Hoshiya, M.,Conditional Simulation of a Stochastic Field, 6th Inter. Conf. on Structural Safety and Reliability, Innsbruck, Austria, pp349-353,1993.8.

(3) Hoshiya, M.,Kriging and Conditional Simulation of Gaussian Field, Jour. of Eng. Mech. ,ASCE, Vol.121, No.2, pp181-186,Feb.,1995.

(4) Pei-Ling Liu and A. Der Kiureghian, Multivariate distribution models with prescribed marginals and covariance, Jour.of Prob. Eng. Mech., Vol.1, NO.2, pp105-112,1986.

(5) Grigoriu ,M.,Crossings of Non-Gaussian Translation Processes,Jour. of Eng. Mech., ASCE ,Vol.110(4), pp610-620,April,1984.

(6) Noda, S.,Hoshiya, M. and Tsukamoto, H.,Universal Kriging in Lognormal Stochastic Field,9th Symp. on Japan Earthquake Engineering ,pp253-258,1994.12. (In Japanese)
(7) Noda, S and Hoshiya, M., Identification of Conditional Stochastic Lognormal Field, 9th Symp. on Japan Earthquake Engineering , pp247-252,1994.12. (In Japanese)

# REAL TIME CONDITIONAL SIMULATION OF EARTHQUAKE GROUND MOTION

by

Tadanobu Sato[1] and Hiroshi Imabayashi[2]
[1]Professor, Disaster Prevention Research Institute, Kyoto University
[2]Engineer, Toda Cooperation

## ABSTRACT

A method is presented for simulating earthquake ground motions at local-field points under the condition that the recorded motions are specified at several locations and the stochastic characteristics of the field also are designated. The simulated motions at observation points coincide with observed records. The state equation expressing the spatial and temporal field of earthquake ground motion compatible with the modeled stochastic field is derived by using the autoregressive process. The Kalman filtering technique is used to identify the best adaptive estimator of a stochastic field from observations made at discrete spatial and temporal points. To take into account the nonstationarity and nonhomogeneity of earthquake ground motions, the algorithm to identify the stochastic characteristics of the field from observed earthquake motions is also developed and introduced to the conditional simulation algorithm. This analytical method is very promising for conditional simulation of earthquake motion at unobserved locations.

## 1. INTRODUCTION

Earthquake ground motions vary in time and space. Various methods for simulating space-time correlated ground motion have been proposed. The one most widely used is a probabilistic approach based on the cross-correlation function or cross-spectrum. The theory of random fields and its application to digital simulation of earthquake ground motions are well established [1]. As substantial databases of earthquake ground motions based on the dense strong motion arrays have been formed, the stochastic characteristics of the space-time correlation of earthquake motions are modeled by the function of the separation distance between two points, the traveling time of the wave, the frequency, and the wave number. Waves simulated by the random field theory, however, are only sample waves.

Conditional simulation methods must be devised that allows realization of a sample field at an unobserved location which satisfies the properties of a stochastic field and is compatible with measured values at observed locations. To obtain this kind of simulation a method that used closed form solutions of conditional probability functions for Fourier coefficients [2], nonstochastic conditional simulation [3], and application of the Kriging method [4,5] has been developed. In these analyses, as all time histories of propagating waves at observation points must be known apriori, are not applicable to the real-time conditional simulation of earthquake motions. The

use of observed real-time earthquake motions obtained from existing array observation systems to simulate earthquake motions at several unobserved locations on real-time is main concern of this paper.

## 2. SPACE-TIME EQUATION OF EARTHQUAKE MOTION

The temporal and spatial fields of earthquake motion are assumed to be expressed by a spatially correlated autoregressive process

$$z_t = -A_1 z_{t-1} - A_2 z_{t-2} - \cdots - A_q z_{t-q} + \Gamma w_t \tag{1}$$

in which $z_t$ is a vector composed of $n$-dimensional earthquake motion at time $t$

$$z_t = \{g_1(t), g_2(t), \cdots, g_n(t)\}^T \tag{2}$$

When we define the following vector

$$Z_{t-1} = \{z_{t-1}^T, z_{t-2}^T, \cdots, z_{t-q}^T\}^T \tag{3}$$

Eq.(1) can be rewritten

$$z_t = -\Phi Z_{t-1} + \Gamma w_t, \quad \Phi = [A_1, A_2, \cdots, A_q] \tag{4}$$

in which $w_t$ is the system noise with covariance matrix $Q_t = E[(w_t - \bar{w}_t)(w_t - \bar{w}_t)^T]$ and $\bar{w}_t$ the mean value of noise at time $t$. When the posterior best estimator of $Z_{t-1}$ is given by $\hat{Z}_{t-1}$, the apriori best estimator of $z_t$ is calculated as

$$\bar{z}_t = -\Phi \hat{Z}_{t-1} + \Gamma \bar{w}_t \tag{5}$$

Defining the difference between $z_{t-k}$ and $\bar{z}_{t-k}$ for arbitrary $k$

$$\tilde{z}_{t-k} = z_{t-k} - \bar{z}_{t-k} \tag{6}$$

The covariance matrix of $z_t$ is given by

$$M_t = E[\tilde{z}_t \tilde{z}_t^T] = \Phi P_{t-1} \Phi^T + \Gamma Q_t \Gamma \tag{7}$$

in which $P_{t-1}$ is the system covariance matrix at time $t-1$. If the earthquake motion is assumed to be a stochastic field that is homogeneous in time and stationary in space, this matrix is defined as

$$P_{t-1} = E[\tilde{Z}_{t-1} \tilde{Z}_{t-1}^T] = \begin{bmatrix} R(0) & R(-1) & \cdots & R(1-q) \\ R(1) & R(0) & \cdots & R(2-q) \\ \vdots & \vdots & \ddots & \vdots \\ R(q-1) & R(q-2) & \cdots & R(0) \end{bmatrix} \tag{8}$$

in which $\tilde{Z}_{t-1} = Z_{t-1} - \hat{Z}_{t-1}$, $\hat{Z}_{t-1}$ is the posterior best estimator of $Z_{t-1}$, and $R(p)$ the cross correlation matrix with dimension $(n \times n)$ defined by

$$R(p) = E[\tilde{z}_{t-k} \tilde{z}_{t-l}^T], \quad (p = l - k) \tag{9}$$

The coefficient matrices $A_i$ of the autoregressive process can be calculated by use of the cross correlation function of $z_t$. Subtracting Eq.(5) from Eq.(1) and taking its transverse then multiplying by $\tilde{z}_{t-k}$ $(k = 1, 2, \cdots, q)$ from the left;

$$E[\tilde{z}_{t-k}\tilde{z}_t^T] = -E[\tilde{z}_{t-k}\tilde{z}_{t-1}^T]A_1^T - E[\tilde{z}_{t-k}\tilde{z}_{t-2}^T]A_2^T - \cdots - E[\tilde{z}_{t-k}\tilde{z}_{t-q}^T]A_q^T \tag{10}$$

Taking into account Eq.(9), Eq.(10) is transferred to the following simultaneous equation to define the coefficient matrices of the autoregressive process in Eq.(1)

$$-\begin{bmatrix} R(0) & R(-1) & \cdots & R(1-q) \\ R(1) & R(0) & \cdots & R(2-q) \\ \vdots & \vdots & \ddots & \vdots \\ R(q-1) & R(q-2) & \cdots & R(0) \end{bmatrix} \begin{bmatrix} A_1^T \\ A_2^T \\ \vdots \\ A_q^T \end{bmatrix} = \begin{bmatrix} R(1) \\ R(2) \\ \vdots \\ R(q) \end{bmatrix} \tag{11}$$

Once the cross correlation matrix defined by Eq.(9) and the observed time series of earthquake motion from time $t-q$ to $t-1$ are given, earthquake motion at time $t$ can be simulated by Eq.(1).

## 3. CONDITIONAL SIMULATION OF EARTHQUAKE MOTION

Consider the case in which the total number of points for which the earthquake ground motion needed is $n$, but records of earthquake motion are obtained only at $m$ $(m < n)$ observation points as defined by

$$y_t = \{g_1(t), g_2(t), \cdots, g_m(t)\} \tag{12}$$

The observation equation then is

$$y_t = [H]\, z_t, \quad H = [I \;\; 0] \tag{13}$$

in which $H$ is the observation matrix with the dimension $(m \times n)$ and $I$ the unit matrix with the dimension $(m \times m)$. This is a special case in that the observation vector $y_t$ and the vector $z_t$ to be estimated have the same physical values [6]. The covariance matrix of the observation noise, $S_t$, is therefore assumed to be the zero matrix

$$S_t = 0 \tag{14}$$

The Kalman filtering technique [7] is used to obtain the posterior best estimator of earthquake motion at time $t$ conditioned by the observation equation. Because the apriori best estimator and its covariance matrix are given by Eqs.(5) and (7), the posterior best estimator of $z_t$ and its covariance matrix $P_t$ are

$$\hat{z}_t = \bar{z}_t + K_t(y_t - H\bar{z}_t) \tag{15}$$

$$P_t = M_t - K_t H M_t \tag{16}$$

in which $K_t$ is a Kalman gain at time $t$ and is defined as

$$K_t = M_t H^T (H M_t H^T + S_t)^{-1} \tag{17}$$

Partitioning the matrix $M_t$ into the observed and unobserved parts

$$M_t = \begin{bmatrix} M_{t;m,m} & M_{t;m,n-m} \\ M_{t;n-m,m} & M_{t;n-m,n-m} \end{bmatrix} \tag{18}$$

and substituting the $H$ matrix given in Eq.(13) and Eq.(18) into Eqs.(16) and (17), the Kalman gain and covariance matrix $P_t$ yield

$$K_t = \begin{bmatrix} I \\ M_{t;m,n-m}^T M_{t;m,m}^{-1} \end{bmatrix} \tag{19}$$

$$P_t = \begin{bmatrix} 0 & 0 \\ 0 & M_{t;n-m,n-m} - M_{t;m,n-m}^T M_{t;m,m}^{-1} M_{t;m,n-m} \end{bmatrix} \tag{20}$$

Substituting Eqs.(19) and (20) into Eq.(15) the best posterior estimator of earthquake motion is

$$\hat{z}_t = \begin{Bmatrix} \hat{z}_{t;m} \\ \hat{z}_{t;n-m} \end{Bmatrix} = \begin{Bmatrix} y_t \\ \bar{z}_{t;n-m} + M_{t;m,n-m}^T M_{t;m,m}^{-1} (y_t - \bar{z}_{t;m}) \end{Bmatrix} \tag{21}$$

These results show that the posterior best estimators of earthquake motion at observation points are identical to the observed values and that the components of covariance matrix become zero.

To obtain sample earthquake motion at an unobserved point we must add a sample fluctuation to the posterior best estimator of earthquake motion. The sample field is simulated by

$$z_{t;n-m} = \hat{z}_{t;n-m} + e \tag{22}$$

in which $e$ is the sample error function vector simulated by multiply-correlated process with a zero mean vector, and covariance $P_{t;n-m,n-m}$ being defined by

$$\begin{aligned} P_{t;n-m,n-m} &= E[(z_{t;n-m} - \hat{z}_{t;n-m})(z_{t;n-m} - \hat{z}_{t;n-m})^T] \\ &= M_{t;n-m,n-m} - M_{t;m,n-m}^T M_{t;m,m}^{-1} M_{t;m,n-m} \end{aligned} \tag{23}$$

By factoring matrix $P_{t;n-m,n-m}$ the error sample function is

$$e = L_t N, \quad P_{t;n-m,n-m} = L_t L_t^T \tag{24}$$

in which $N$ is an $n-m$ dimensional sample noise vector generated by the standard normal distribution density function.

## 4. STOCHASTIC MODEL OF EARTHQUAKE MOTION

We assume that earthquake motion at point $i$ and time $t$ is expressed by the cross correlated $m$ stochastic processes $u_i(t)$ $(i = 1, 2, \cdots, m)$ [1] as

$$u_i(t) = \sum_{p=1}^{i} \sum_{n=1}^{N} | H_{ip}(\omega_n \sqrt{\Delta\omega}) | \sqrt{2} \cos(\omega_n t + \theta_{ip} + \phi_{pn}) \tag{25}$$

in which $\phi_{pn}$ are mutually independent uniformly distributed variables over $-\pi$ to $\pi$ and

$$\omega_n = n \cdot \Delta\omega = \frac{2n\pi}{T} \tag{26}$$

in which $T$ is the duration of earthquake motion. $H_{ip}(\omega_n)\sqrt{\Delta\omega}$ is obtained by factoring the cross spectrum $S_{ij}(d_{ij}, \omega_n)$ defined in the field as

$$\begin{bmatrix} S_{11}(d_{11},\omega_n)\Delta\omega & \cdots & S_{1m}(d_{ij},\omega_n)\Delta\omega \\ \vdots & \ddots & \vdots \\ S_{m1}(d_{11},\omega_n)\Delta\omega & \cdots & S_{mm}(d_{ij},\omega_n)\Delta\omega \end{bmatrix} =$$

$$\begin{bmatrix} H^*_{11}(\omega_n)\sqrt{\Delta\omega} & \cdots & 0 \\ \vdots & \ddots & \vdots \\ H^*_{m1}(\omega_n)\sqrt{\Delta\omega} & \cdots & H^*_{mm}(\omega_n)\sqrt{\Delta\omega} \end{bmatrix} \begin{bmatrix} H_{11}(\omega_n)\sqrt{\Delta\omega} & \cdots & H_{m1}(\omega_n)\sqrt{\Delta\omega} \\ \vdots & \ddots & \vdots \\ 0 & \cdots & H_{mm}(\omega_n)\sqrt{\Delta\omega} \end{bmatrix} \tag{27}$$

and $\theta_{ip}$ is calculated by

$$\theta_{ip} = \tan^{-1}\left\{\frac{I_m[H_{ip}(\omega_n)\sqrt{\Delta\omega}]}{R_e[H_{ip}(\omega_n)\sqrt{\Delta\omega}]}\right\} \tag{28}$$

The cross spectrum is assumed to be given by the equation

$$S_{ij}(d_{ij},\omega_n)\Delta\omega = S_T(\omega_n)\Delta\omega \cdot \exp(\frac{-i\omega_n d_{ij}}{c}) \cdot \exp(\frac{-\alpha\omega_n \mid d_{ij} \mid}{2\pi c}) \tag{29}$$

in which $d_{ij}$ is the relative distance between points $i$ and $j$, $c$ the propagating wave speed, and $S_T(\omega_n)$ the discretized homogeneous and stationary power spectrum density function at the circular frequency of $\omega_n$ and is defined by the following equation, provided the discrete Fourier *cos* and *sin* series amplitudes of $a_n$ and $b_n$ are given at a certain point in the concerned field,

$$S_T(\omega_n)\Delta\omega = \frac{a_n^2 + b_n^2}{2} \tag{30}$$

To make the conditional simulation of earthquake ground motions, the cross correlation function must be defined in the field obtained by inverse Fourier transform of the cross spectrum;

$$\begin{aligned} R_{ij}(d_{ij},\tau) &= \frac{1}{2}\int_{\infty}^{\infty} S_{ij}(d_{ij},\omega)\exp(i\omega\tau)d\omega \\ &= \frac{1}{2}\sum_{n=1}^{N}(a_n^2 + b_n^2)\exp(\frac{-\alpha\omega_n \mid d_{ij} \mid}{2\pi c}) \cdot \cos\left\{\omega_n(\tau - \frac{d_{ij}}{c})\right\} \end{aligned} \tag{31}$$

in which $\tau$ is the relative time delay of earthquake motion between points $i$ and $j$.

Eq.(31) is intended only to illustrate the procedure, but it does show some characteristics of the empirical correlation functions obtained from dense accelerograph

array data. Fig.2 shows the simulated sample fields of a one-dimensional wave propagation with velocity of c=1000m/s and $\alpha = 0.02$ from Eq.(25). Each point is separated by 100m. In the simulation earthquake ground motion at the left edge point is assumed to be given and its discrete Fourier spectrum amplitude calculated (Fig.1), after which the wave forms of the remaining points can be simulated.

## 5. IDENTIFICATION OF AUTOREGRESSIVE PROCESS

### 5.1 Identification of Observed Parts

So far we have assumed that the temporal and spatial stochastic characteristics are defined in the concerned field apriori. Because of nonstationarity and nonhomogeneity of earthquake ground motions these stochastic characteristics must be identified from observed motions.

When the time history of earthquake ground motions at all observed stations are assumed to be given, Eq.(4) is rewritten in the form of observation equation

$$\{g_1(t), g_2(t), \cdots, g_m(t)\} = H_t \begin{bmatrix} A_1^T \\ A_2^T \\ \vdots \\ A_q^T \end{bmatrix}_t + v_t \tag{32}$$

in which $v_t$ is the observation noise and the observation matrix is defined by

$$H_t = Z_{t-1} = -\left\{z_{t-1}^T, z_{t-2}^T, \cdots, z_{t-q}^T\right\} \tag{33}$$

in which $z_t$ is a vector composed of $m$-dimensional observed earthquake motion at time $t$; $z_t = \{g_1(t), \cdots, g_m(t)\}$. The state space description of the coefficient matrices of the autoregressive process is given by

$$\begin{bmatrix} A_1^T \\ A_2^T \\ \vdots \\ A_q^T \end{bmatrix}_t = [I] \begin{bmatrix} A_1^T \\ A_2^T \\ \vdots \\ A_q^T \end{bmatrix}_{t-1} \tag{34}$$

To apply the Kalman filtering algorithms for identifying autoregressive process the coefficient matrix appeared in Eqs.(32) and (34) is rearranged as a matrix composed of column vectors $a_{k,t}$ ($k$=1, $\cdots$, $m$)

$$\begin{bmatrix} A_1^T \\ A_2^T \\ \vdots \\ A_q^T \end{bmatrix}_t = [a_{1,t} a_{2,t} \cdots a_{m,t}] \tag{35}$$

The state space and observation equations can be rewritten

$$a_{k,t} = [I]\, a_{k,t-1} \quad g_k(t) = H_t a_{k,t} + v_{k,t} \tag{36}$$

in which

$$H_t = -\left\{z_{t-1}^T, z_{t-2}^T, \cdots, z_{t-q}^T\right\}$$

The algorithm of the Kalman filtering for Eq.(36) are formulated as developed in[8]

(1)Initial conditions: $\hat{a}_{k,0} = a_0$, $P_{k,0} = P_0$, $R = R_0$, $t = 0$
(2)Time step increase: $t = t + 1$
(3)Predicted state estimation: $\bar{a}_{k,t} = \hat{a}_{k,t-1}$, $M_{k,t} = P_{k,t-1}$
(4)Kalman gain: $K_{k,t} = M_{k,t}H_t^T(H_tM_{k,t}H_t^T + R)^{-1}$
(5)Corrected state estimation: $\hat{a}_{k,t} = \bar{a}_{k,t} + K_{k,t}(g_k(t) - H_t\bar{a}_{k,t})$
(6)Estimation of error covariance matrix: $P_{k,t} = M_{k,t} - K_{k,t}H_tM_{k,t}$

Through the steps from (1) to (6) the posterior best estimator of coefficient matrices of autoregressive process is calculated.

### 5.2 Identification of Unobserved Parts

To identify the coefficient matrices of autoregressive process related to unobserved parts the cross-correlation function of the concerned field must be given. Because we assume the form expressed by Eq.(31) for cross-correlation function, identification of the parameters $\alpha$ and $c$ from observed earthquake ground motions are enough to define the cross-correlation function. Once this function identified Eq.(11) is rewritten as

$$\mathrm{RA} = \mathrm{r} \tag{37}$$

in which R, A and r are the matrices rearranged their components and partitioned into the observed and unobserved parts as

$$\mathrm{R} = \begin{bmatrix} \mathrm{R}^{oo} & \mathrm{R}^{ou} \\ \mathrm{R}^{uo} & \mathrm{R}^{uu} \end{bmatrix} \quad \mathrm{A} = \begin{bmatrix} \mathrm{A}^{oo} & \mathrm{A}^{ou} \\ \mathrm{A}^{uo} & \mathrm{A}^{uu} \end{bmatrix} \quad \mathrm{r} = \begin{bmatrix} \mathrm{r}^{o} \\ \mathrm{r}^{u} \end{bmatrix} \tag{38}$$

The partitioned matrix $\mathrm{A}^{oo}$ can be identified by using observed earthquake ground motions as mentioned in the section 5.1. The components of autoregressive matrices related to unobserved points can be determined by solving following equations

$$\left.\begin{aligned} \textstyle\sum_{j=1}^{m\times q} \mathrm{R}_{ij}^{oo}\mathrm{A}_{jl}^{oo} + \sum_{j=1}^{(n-m)\times q} \mathrm{R}_{ij}^{ou}\mathrm{A}_{jl}^{uo} &= \mathrm{r}_{il}^{o} \\ \textstyle\sum_{j=1}^{m\times q} \mathrm{R}_{kj}^{uo}\mathrm{A}_{jl}^{oo} + \sum_{j=1}^{(n-m)\times q} \mathrm{R}_{kj}^{uu}\mathrm{A}_{jl}^{uo} &= \mathrm{r}_{kl}^{u} \end{aligned}\right\} \tag{39}$$

$$\left.\begin{aligned} \textstyle\sum_{j=1}^{m\times q} \mathrm{R}_{ij}^{oo}\mathrm{A}_{js}^{ou} + \sum_{j=1}^{(n-m)\times q} \mathrm{R}_{ij}^{ou}\mathrm{A}_{js}^{uu} &= \mathrm{r}_{is}^{o} \\ \textstyle\sum_{j=1}^{m\times q} \mathrm{R}_{kj}^{uo}\mathrm{A}_{js}^{ou} + \sum_{j=1}^{(n-m)\times q} \mathrm{R}_{kj}^{uu}\mathrm{A}_{js}^{uu} &= \mathrm{r}_{ks}^{u} \end{aligned}\right\} \tag{40}$$

in which $(l = 1, 2, \cdots, m)$, $(s = m+1, m+2, \cdots, n)$, $(i = 1, 2, \cdots, m \times q)$ and $(k = 1, 2, \cdots, (n-m) \times q)$. Solving Eq.(40) the unknown values of $\mathrm{A}_{jl}^{ou}$ and $\mathrm{A}_{jl}^{uu}$ can be determined. As can be seen from Eq.(39) the number of unknown values is $(n-m) \times q$ but the number of equation is $n \times q$. We can apply the least square estimation algorithm to define the most appropriate values of $\mathrm{A}_{jl}^{uo}$.

## 6. NUMERICAL EXAMPLES

To verify the applicability of the autoregressive process for simulating multi-correlated earthquake motions, we assume that the sample earthquake motions shown in Fig.2 are observed at all points up to time $t-1$ and that earthquake motions at time $t$ are simulated by Eq.(4) with no system noise. The coefficient matrices of the autoregressive process are determined by solving Eq.(11) and assigning $\alpha = 0.02$ an $c = 1000$m/sec for Eq.(31). The results shown in Fig.3 are in good agreement with the sample motions shown in Fig.2.

When the stochastic characteristics, i.e. the cross-correlation function of the field, and earthquake motions at several points in Fig.2 are given up to time $t-1$ as observed motions, the motions at the intermediate points at time $t$ are interpolated from Eq.(21). The results shown in Fig.4(a) agree well with the sample motions shown in Fig.2. Fig.4(b) is the interpolated earthquake ground motions for the case of $\alpha = 0.1$ and $c = 1500$m/s. As the value of $\alpha$ increases the distortion of propagating wave becomes large. Even such a case the developed interpolation algorithm works well.

Increasing the number of observation points improves the accuracy of the posterior estimation of earthquake motion at an unobserved point. Consider a realistic two-dimensional field, in which an unobserved point is located at the center of the field and one observation point (No.4) is added to the already distributed three observation points (No.1,2,3) as shown in Fig.5. The side length of each grid is 100m. Earthquake motion propagating in the 45° direction to horizontal axis with a wave velocity of 1000m/sec and $\alpha = 0.02$ is assumed, and sample motions are simulated at five points including unobserved point (Fig.5). The resulting time history for the unobserved point becomes the exact time history when the posterior estimation of earthquake motion is introduced. The interpolated motion at the unobserved point obtained from records providing three observation points is shown in Fig.6(a) and the time history that takes into account the record for a newly added observation point is in Fig.6(b). As the number of observation points increases, the estimated earthquake motion comes close to the exact time history as can be seen in Fig.6(c).

When the stochastic characteristics of the field are not given apriori we must identify the cross-correlation function and the coefficient matrices of the autoregressive process from the observed earthquake motions. To demonstrate the application of the algorithm developed in the section 5, sample earthquake motions are simulated and we select three of them as observed earthquake motions (Fig.7). Examples of identified cross-correlation functions and components of coefficient matrices of autoregressive process are shown in Figs.8 and 9, respectively. In Fig.8 the thick line is the identified correlation function and thin line is the function used to simulate sample earthquake motions. Fig.9 is time histories of the identified autoregressive coefficient matrix components related to observed points. For conditional interpolation of earthquake ground motions the components of the coefficient matrices of autoregressive process related to unobserved points must be calculated by Eqs.(39) and (40). The accuracy of calculated results is shown in Fig.10 in which the abscissa is the exact values and the ordinate the calculated values. Because all calculated

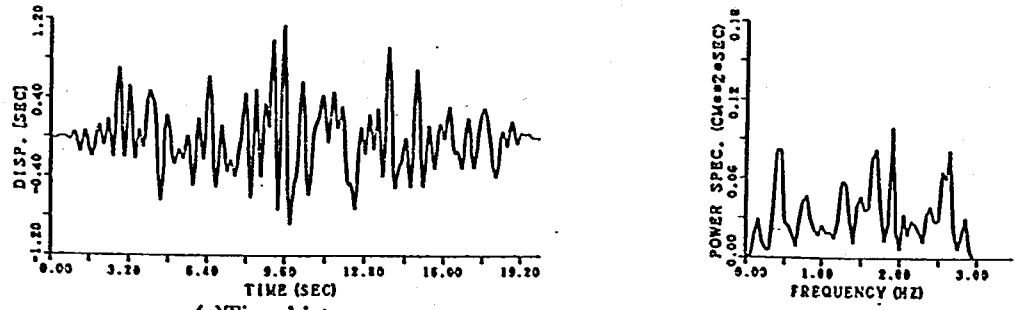
components lie on the line with 45° to abscissa, we can confirm the algorithm to identify the autoregressive process only from observed data. Once the coefficient matrices of autoregressive process are identified we can interpolate earthquake motions at unobserved points from observed motions. Fig.11 shows the ability of the proposed method.

## 7. CONCLUSION

We have proposed a stochastic interpolation method for the conditional simulation of earthquake motion. It combines the methodology of the multi-autoregressive process for simulating earthquake motions and the Kalman filtering technique in which the state vector, including unknown parameter, is updated based on observations. This method provides the best estimator of earthquake motions at unobserved points that coincide with sample motions at observed points. Its application to earthquake ground motion simulation is illustrated by several examples.

## REFERENCES


1. Vanmarcke E.H., Random fields, MIT Press, Massachusetts, 1983.
2. Kawakami H., Simulation of space-time variation of earthquake ground motion using a recorded time history, Proceedings of Japan Society of Civil Engineers, No.441/I-18, pp.167-175, 1992 (in Japanese).
3. Kameda H. and Morikawa H., An interpolating stochastic process for simulation of conditional random fields, Probabilistic Engineering Mechanics, 7(4), pp.243-254, 1992.
4. Vanmarck E.H. and Fenton G.A., Conditional simulation of local fields of earthquake ground motion, Journal of Structural Safety, 10, pp.247-264, 1991.
5. Hoshiya M. and Murayama O., Stochastic interpolation of earthquake wave propagation, Proceedings of 6th International Conference on Structural Safety and Reliability, Innsbruck, August 1993.
6. Hoshiya M. and Yoshida I., Identification of conditional stochastic Gaussian field, Submitted to ASCE, Journal of Engineering Mechanics Division, dated September 1993.
7. Kalman R.E., A new approach to linear filtering and prediction problems, Journal of Basic Engineering, 82(1), pp.35-45, 1960.
8. Sato T. and Toki K., Active control of seismic response of structures, Journal of Intelligent Material Systems and Structures, 1(4), pp.447-475, 1990.




(a)Time history. (b)Fourier spectra.

Fig.1 Input earthquake motion into the time space field.

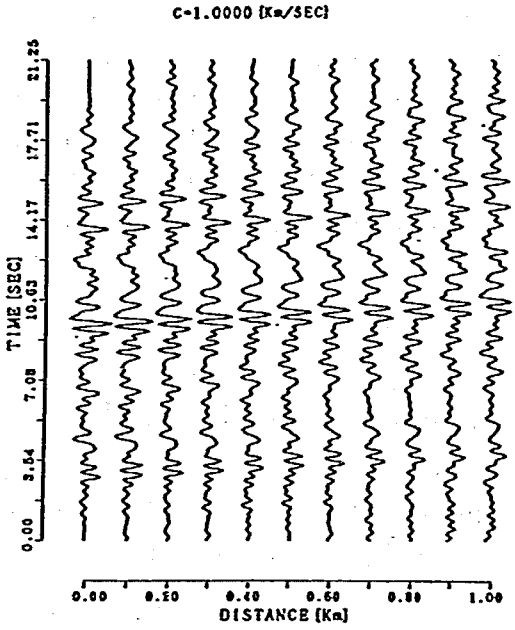



Fig.2 Sample earthquake ground motions simulated by Eq.(25).

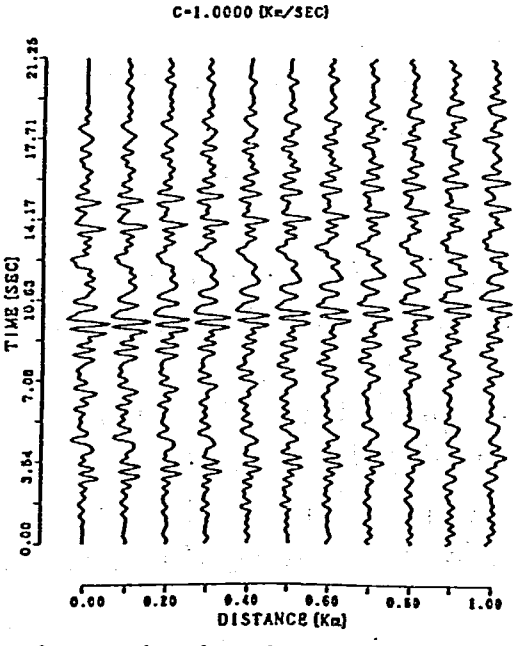
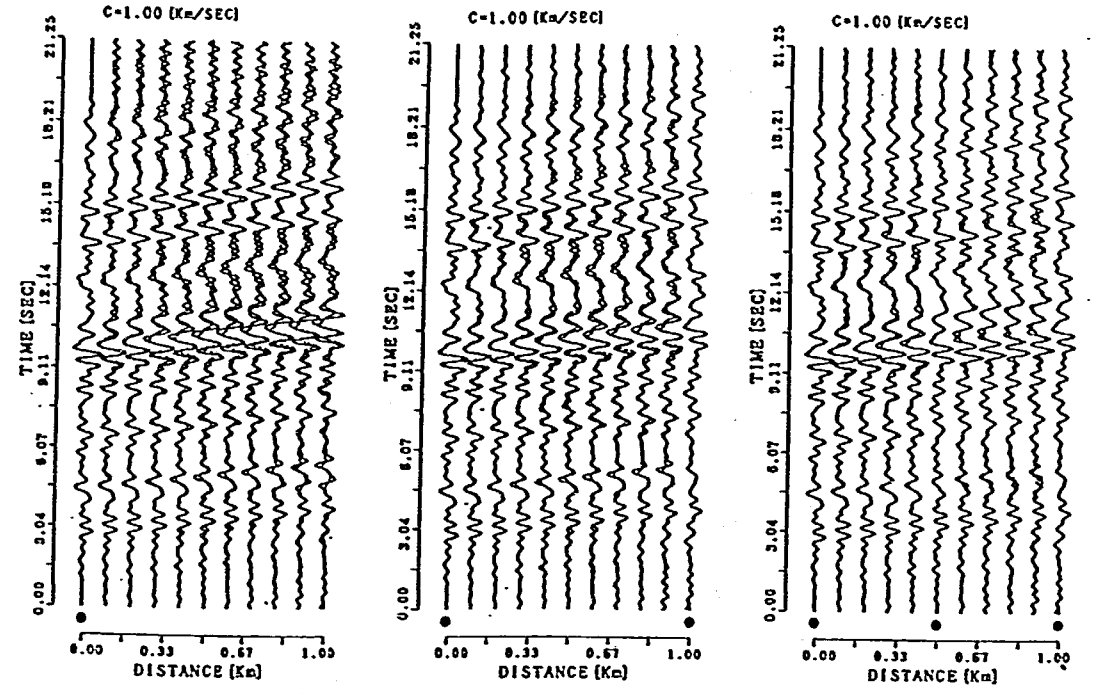
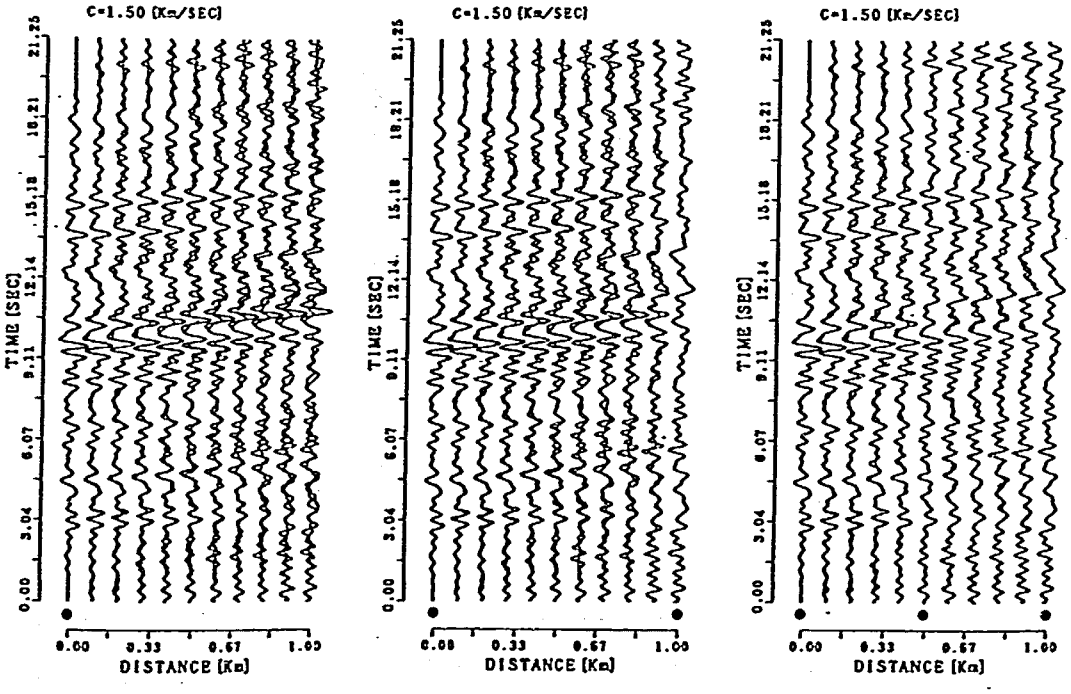



Fig.3 Earthquake ground motions simulated by the autoregressive process defined by Eq.(4) with no system noise. The coefficient matrix of AR process are obtained by solving Eq.(11) provided the cross-correlation function of the concerned field is given by Eq.(31).




(a) For the case of c=1000m/s and $\alpha$ =0.02




(b) For the case of c=1500m/s and $\alpha$ =0.1

Fig.4 Interpolated earthquake ground motions(thin lines) when earthquake motions(thick lines) at points expressed by ● are given. For the comparison the sample earthquake motions simulated by Eq.(25) are shown by broken lines.

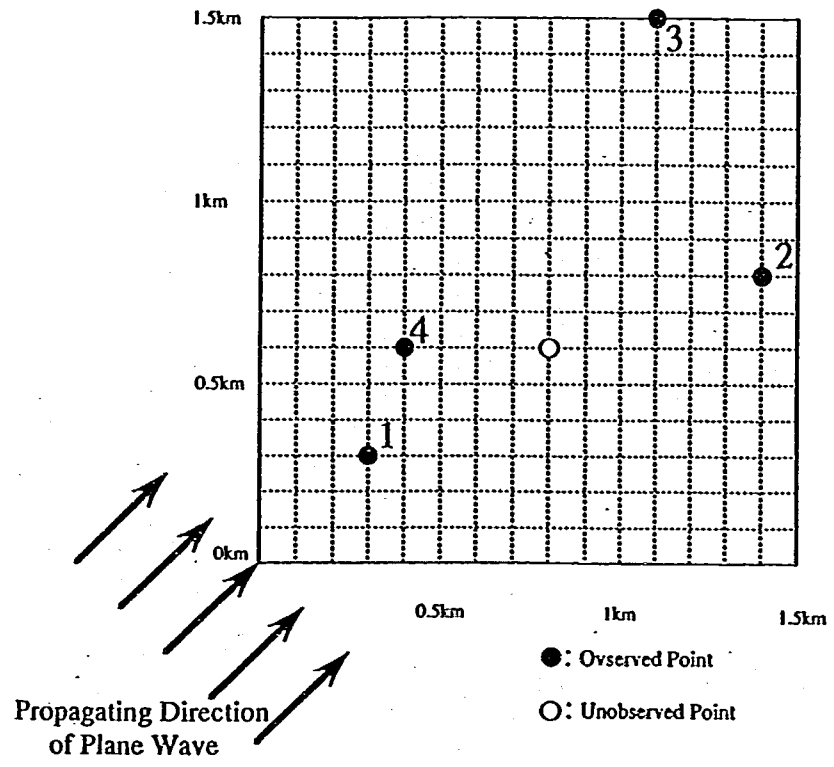
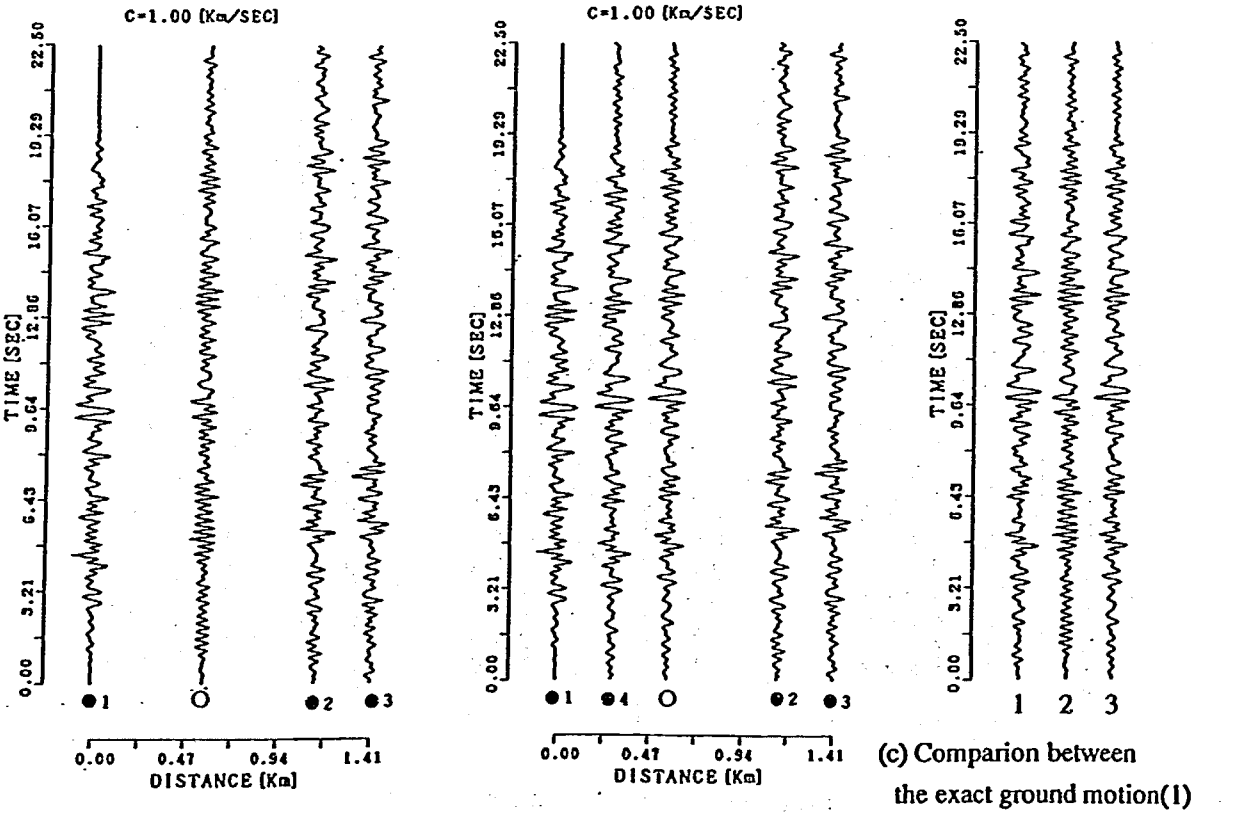



Fig.5 Location of observation points and an unobserved point.




(a) The case of three points observations(●).

(b) The case of four points observations(●).

(c) Comparion between the exact ground motion(1) and interpolated ones {2:from case(a),3:from case(b)}.

Fig.6 Increase in interpolating accuracy for earthquake ground motion at an unobserved point as the number of observation points increases.

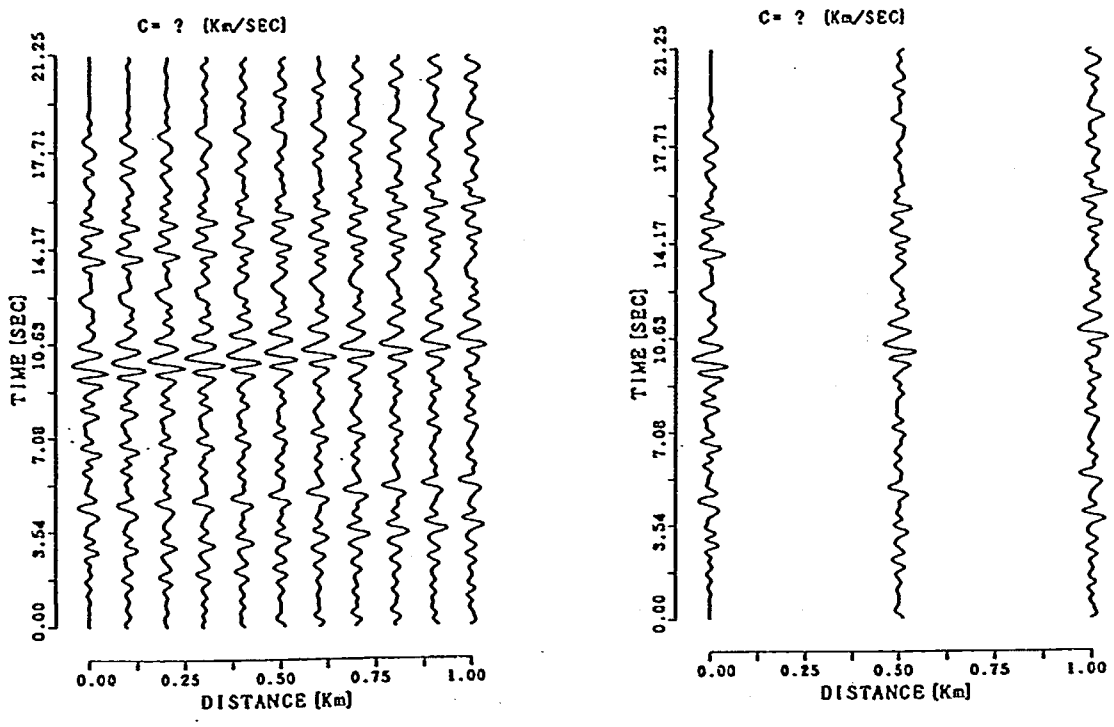



Fig.7 Sample earthquake motions(left) and earthquake motions assumed to be observed(right).

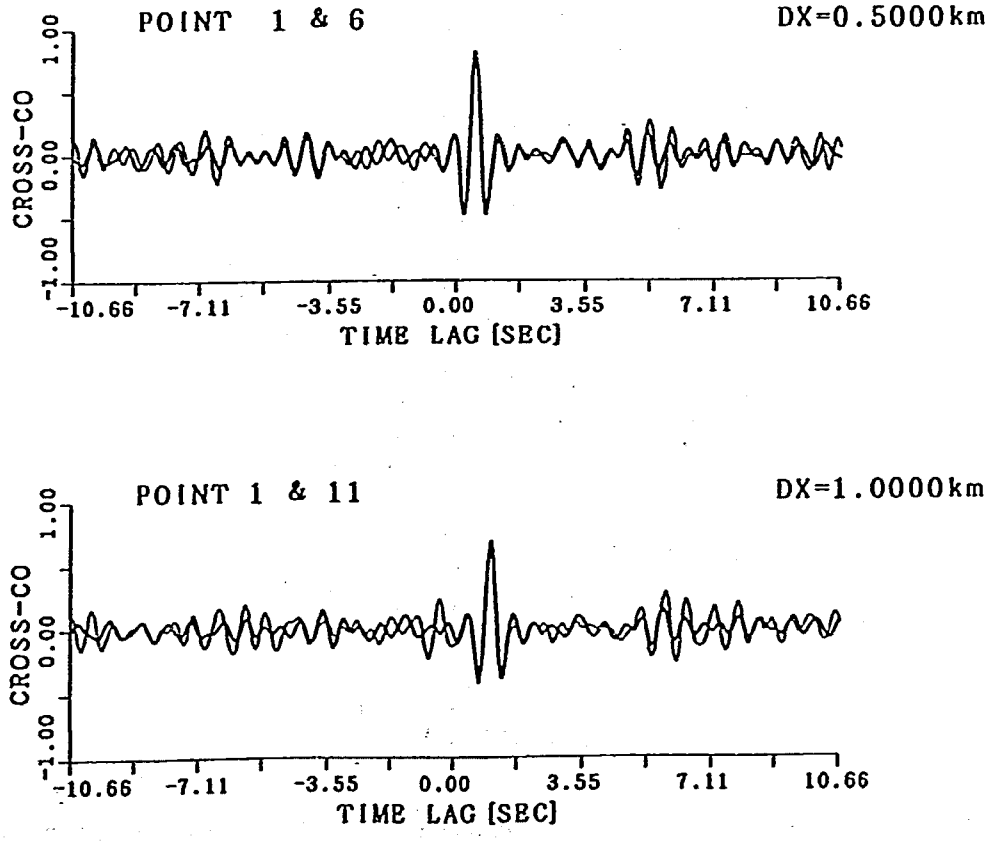



Fig.8 Examples of identified cross-correlation fuction(thick line) from ground motions and one defined in the time-space field cross-correlation(thin line).

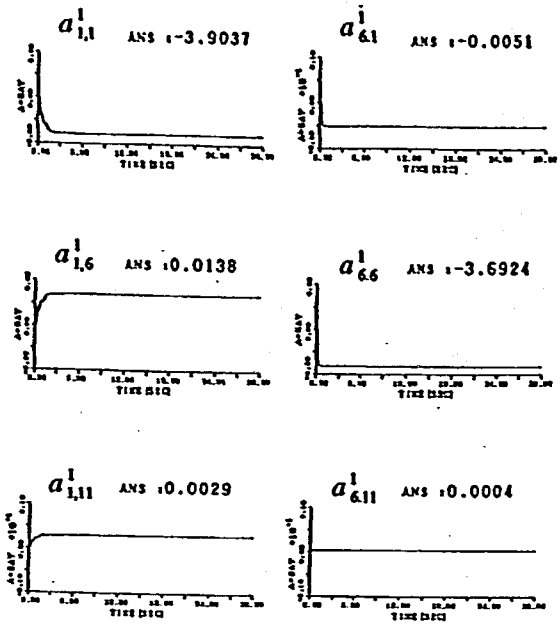



Fig.9 Examples of identifing process of AR coefficient matrix components

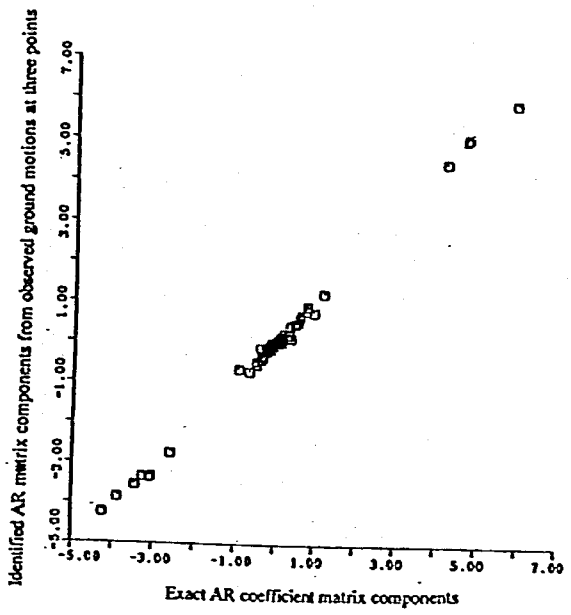



Fig.10 Comparison between the identified AR coefficient matrix components and the exact ones.

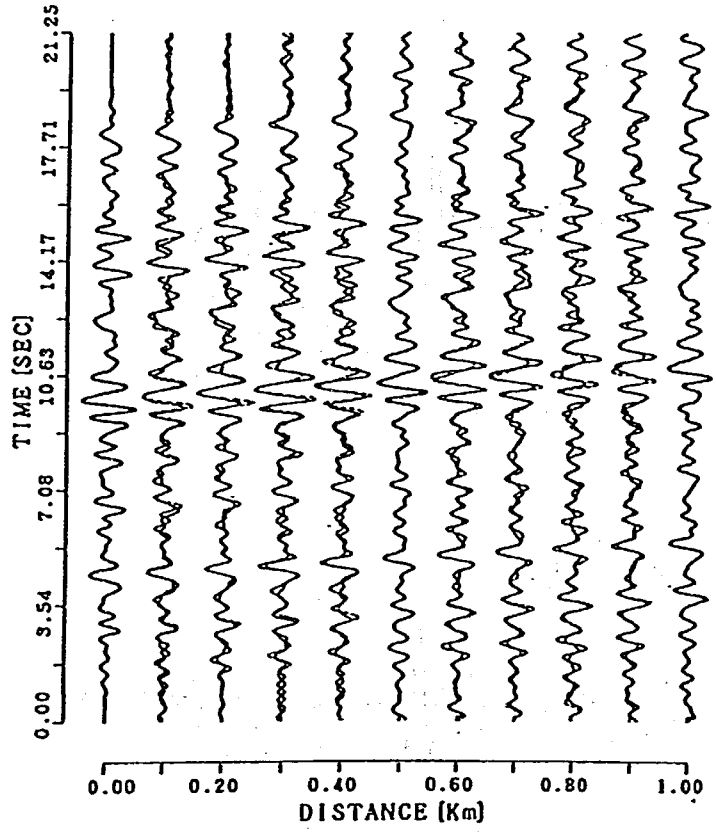



Fig.11 Interpolated earthquake ground motions(thin line) by using identified AR matrix components when earthquake motions are assumed to be given at three points expressed by ●.

# OPTIMIZATION OF POST-EARTHQUAKE RESTORATION OF LIFELINE NETWORKS USING GENETIC ALGORITHMS

by

Tadanobu SATO[1] and Koji ICHII[2]

[1]Professor , Disaster Prevention Research Institute , Kyoto University

[2]Research Engineer , Port and Harbour Research Institute , Ministry of Transport

## ABSTRACT

This study is concerned with methods to optimize restoration process of damaged lifelines by earthquakes. We develop algorithms by using Simple Genetic Algorithms (Simple GA) and Hybrid Genetic Algorithms (Hybrid GA) to decide the priority of component to restore. Simulation results show that Hybrid Genetic Algorithms is useful tool.

We also apply Single Populated Genetic Algorithms (SPGA) to distribute restoration teams at damaged sites for optimizing the restoration process of lifeline networks.

## 1. INTRODUCTION

Countermeasures to mitigate earthquake disaster to lifeline systems can be classified as follows[1]; 1) prevention of direct damage by reinforcing components, 2) increase of system redundancy to maintain the post earthquake serviceability, 3) prevention of damage propagation by implementing an efficient emergency shutdown system, and 4) rapid recovery of the system from earthquake damage.

This paper concerns with the 4th item. There were many researches to fined out the optimal restoration process of lifeline systems damaged by earthquakes. Shiraishi and Toki developed a system to support decision making to restore an earthquake damage to gas network by using the dynamic programing technique[2]. Nojima and Kameda applied the Horn's algorithm to optimize the restoration process of hierarchically separated lifeline networks[3]. Noda applied a neural-network algorithm to optimize post-earthquake restoration of a telephone system[4]. Hoshiya et al. developed the method to predict the restoration process of lifelines[5]. They pointed out difficulties to optimize the restoration process of lifeline networks damaged by earthquakes. Because lifeline systems consist of many components the enumeration of restoration order of components becomes very large. For the network with N components we must evaluate and compare total restoration times for N! combinations of restoration order of

components. If we add the case to distribute the different number of restoration teams for several damaged components, the enumeration becomes too large and long computation time is necessary accordingly to find the best solution. The dynamic programing technique can not be applied to calculate optimal distribution of restoration teams because it assumes non-correlation between the total restoration time of a network and the restoration order of components. The index to evaluate restoration efficiency may change at each restoration stage and the restoration policy of the concerned network may be altered accordingly. After defining the efficient index to measure the restoration efficiency, algorithms to manage the restoration process base on the such index must be developed.

In this paper, we study the feasibility of applying Genetic Algorithms (GA) to optimize the restoration process of lifeline networks. GA is a random search method which uses an analogy with biological evolution.

## 2. INDEX TO MEASURE THE EFFICIENCY OF RESTORATION PROCESS

Restoration process of a earthquake damaged lifeline network is expressed by the time history of restoration ratio[3]as shown in Fig.1. The area of upper-side of the restoration curve (an area of oblique lines in Fig.1) is defined as the total un-restored ratio and is used as the index to evaluate the efficiency of restoration. Because the degree of inconvenience due to the functional loss of the earthquake damaged lifeline could be changes as time proceeds. We multiply a weighting time function, w(t), to the time function of restoration ratio, R(t) and integrate it up to time, T, to define the weighted total un-restored ratio, TR as follows:

$$TR = \int_0^T w(t) \cdot [1 - R(t)] dt \qquad (1)$$

The algorithm to be developed in this paper can determine the restoration order of components in an earthquake damaged lifeline network by which we can minimize the value of TR providing the restoration time of each damaged component in the network.

## 3. OPTIMIZATION OF RESTORATION ORDER OF DAMAGED COMPONENTS USING GENETIC ALGORITHMS

### (1) Outline of Genetic Algorithms

Genetic Algorithms are stochastic search algorithms introduced by Holland[6] in the 70's. These algorithms are based on ideas and techniques from genetic and evolutionary theory. Genetic algorithms simulate an evolutionary process with N individuals which represent points in a search space. Every individual is encoded as a string called a genotype. The cost function is defined for such a string. In each step of the genetic algorithm, called a generation, every individual is evaluated with regard to the entire population. This value is called the relative

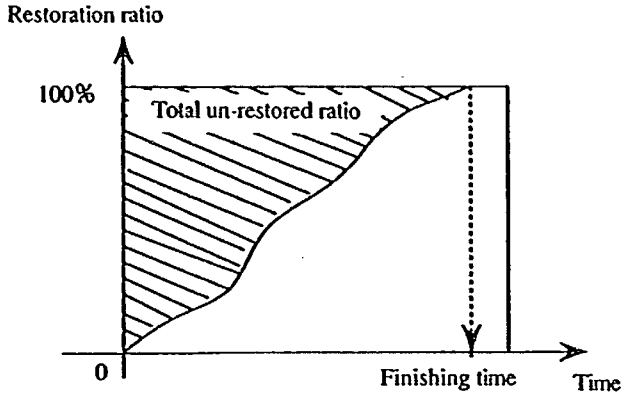



Fig1 Evaluation function of restoration process

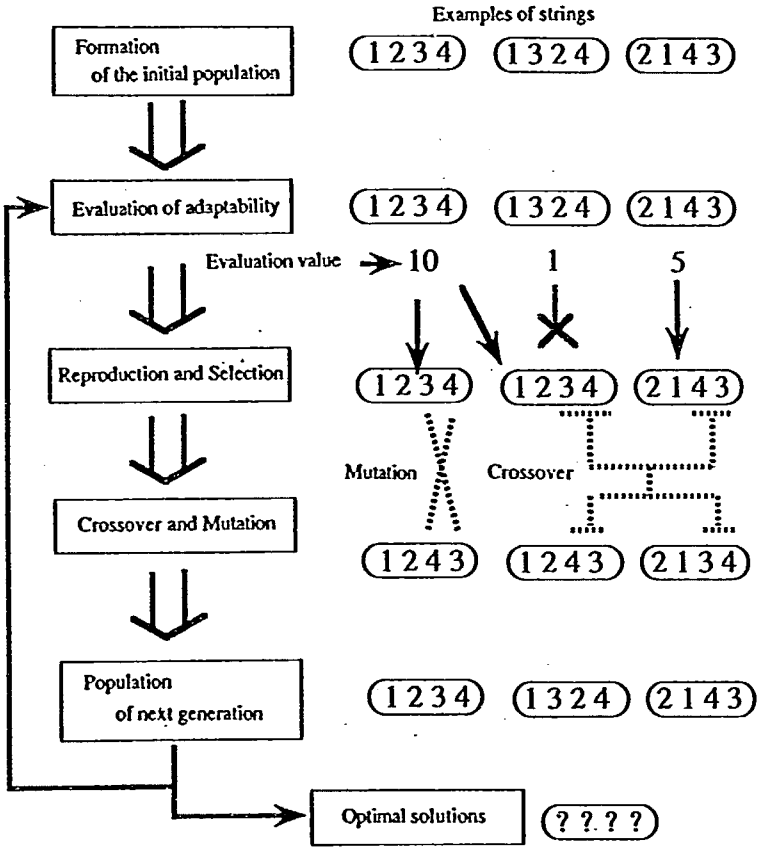



Fig2 A simple explanation of Genetic Algorithm(GA)

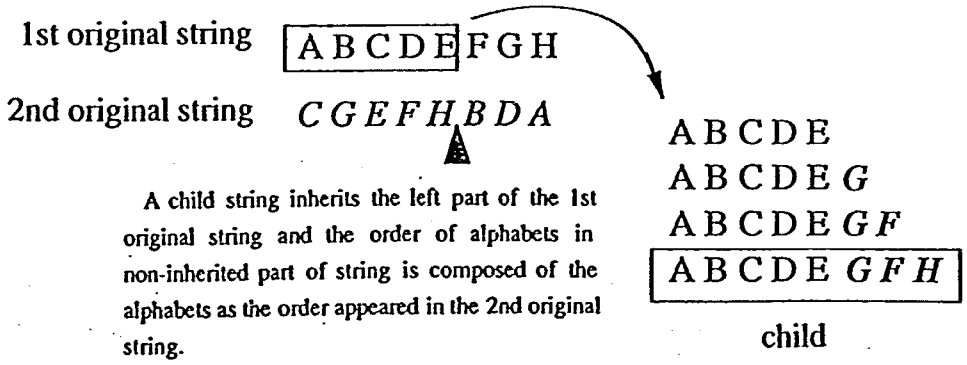



Fig3 Schema of order crossover

fitness of an individual. According to natural evolution offsprings are produced using genetic operators. The selection operator chooses individuals with a probability that corresponds to the relative fitness. Two chosen individuals produce a descendant using the crossover operator which exchanges substrings of the codes of the two chosen individuals. The descendant replaces an individual in the population after the generation step is complete. Another genetic operator, call mutation, changes the genotype of the descendant, with a small probability (mutation rate). Mutation and crossover cause variation in the search process. The mutation operator allows a search close to a point in the search space, because only a small number of changes occur. Crossover causes longer jumps in the search space. Only selection, however, leads the search in a specific direction. Substrings of individuals that are more fit than others are kept for the next generation.

Although. Genetic Algorithms are still developing methods and many variety of Genetic Algorithms are proposed. The outline of a simple genetic algorithms shown in Fig.2. The first step in this algorithm is coding of design parameters in a genotype which is expressed by a line of digits. An example of genetic operations being shown in Fig.2 has a space with three populations. The fitness of each genotype is evaluated by a cost function. In Fig.2, genotype of strings 1234, 1324 and 2134 get respective fitness values of 10, 1 and 5. In selection process the parents to generate descendants are chosen by using those fitness value. An individual with genotype possessing the high fitness value must have high probability to be selected more and an individual with low fitness value must be died out. In Fig.2, an individual with genotype 1234 with the fitness value 10 increases its populations from one to two and a genotype 1324 is died out. In the crossover process, the exchange of substrings is done at a certain probability (crossover rate) between randomly selected two individuals. Two genotypes 1243 and 2143 are generated from parent genotypes 1234 and 2143. As an example of the mutation process a genotype 1234 is altered to 1243. We repeat those process until the entire populations satisfy a given convergent condition or reach to a decided generation. We can find the best solution from all genotypes being generated during all generations. There are many variations to code the genotype and to define selection, crossover and mutation operators. We have to design the best Genetic Algorithm fitting to the problem.

(2) Design of Genetic Algorithm to decide restoration order of damaged components.

In this analyses only links in the networks are assumed to be damaged and those are numbered. A genotype to express a restoration process is a string composed of a line of those numbers. For example, when we restore damaged links in the order of 1 -> 2 -> 3 -> 4, a genotype for that process is expressed by a string 1234 and the length of genotype is equal to the number of damaged links. Genotypes of initial individuals are generated by a random process. Fitness value of each genotype is calculated using linear normalization technique[7]. We calculate the

total un-restored ratios for all produced genotypes and arrange them by the order starting with the smallest un-restored ratio. The fitness value of the ith genotype is defined by

$$f(i) = \max(a - bi, 1) \quad (2)$$

in which i is the order of the genotype, a is maximum fitness value and b is reducing ratio. For example of 20 populations, and a=100 and b=10. The best genotype (i=1) gets 90 score as the fitness value because 100-10x1=90. The second best genotype gets 80 score. Fitness values of genotypes become equal to 1 beyond the 10th genotype because the value of a-bi for i larger than 10 becomes less than 0. If the reducing ratio, b, has a large value, only the small number of genotypes have high fitness values, these superior genotypes increase accordingly in the next generation and production of too many resemble genotypes reduces the search space of solution. The roulette wheel selection technique is used to select parents. The total sum of fitness values of all individuals is calculated. Choosing an arbitrary number, p, between 0 to the total sum of fitness values and summing the fitness values in the order from the highest fitness value, we select an individual as a parent when the summing fitness values exceeds p. We repeat this process until we get enough parents for the next generation. For example, the total of all fitness is 461 in the case of 20 populations, and a=100 and b=10. We select 20 random number within 1 to 461. Assuming the first number of p is 132, it is bigger than 90 which is the best fitness value but smaller than 170 which is the sum of fitness values of the first and second best genotypes. We select the genotype with the second best fitness value as the first parent of next generation. If the second number of p is smaller than 90, we select the best genotype as the second parent. We repeat this process until 20 parents are generated.

A cutting point in the two pair of genotypes (parents genotypes) is selected randomly in the order crossover technique as shown in Fig.3. The first descendant inherits a longer substring from the first parent and replace the genes of shorter substring in the order of genes appeared in the second parent. The second descendant inherits a main substrings from the second parent and the order of genes of remaining substrings is decided by the first parent. In the example shown in Fig.3, the first descendant inherits the substring of ABCDE from the first parent and the remaining substring of FGH is replaced by GFH which is the order of genes (alphabets) appeared in the second parent. In mutation process, we replace the two genes of the string of a descendant at a small probability.

(3) Numerical example using sample network

We compare the efficiency of genetic algorithm with that of random search algorithm using the sample network shown in Fig.4. The number attached to each link is a restoration time assigned randomly. Because this network have tree structure, we can calculate the exact solution for the restoration process of the damaged components using Horn's algorithms without searching all possible solutions[3].

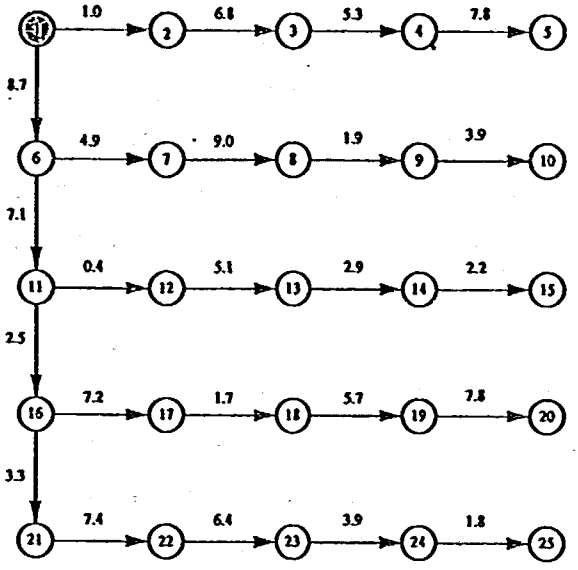



Fig4 Network model

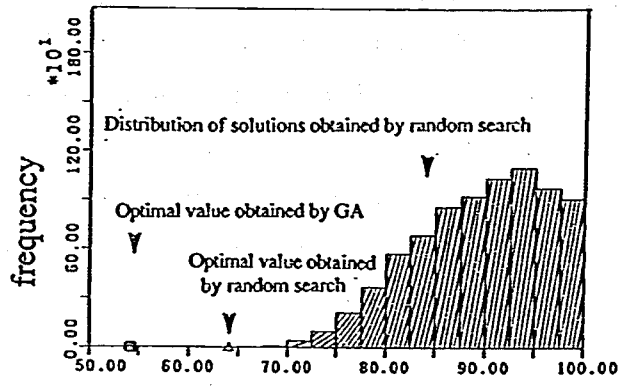



Fig5 Comparison between the optimal values obtained by GA and by random search

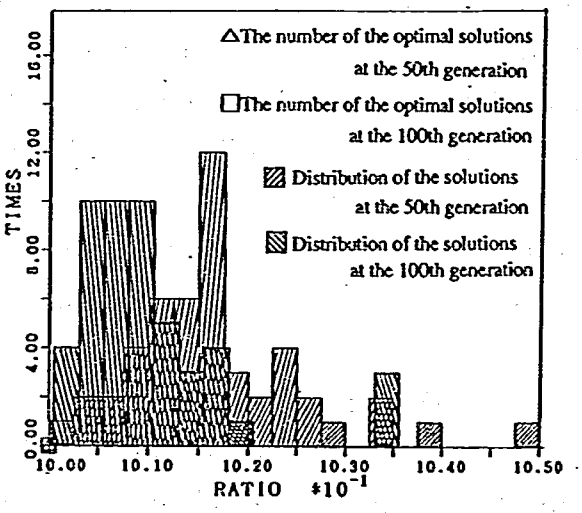



Fig6 Distribution of the solutions obtained by GA

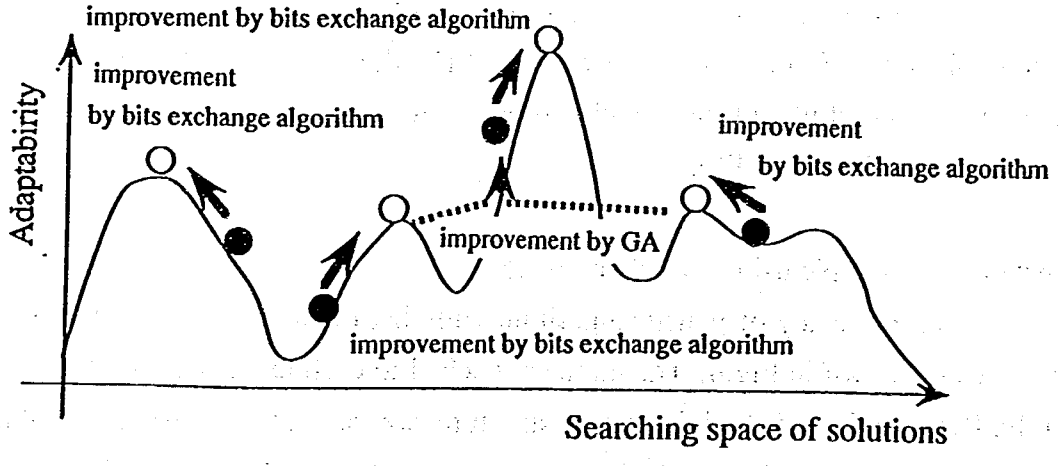



Fig7 Schema of Hybrid GA

For the calculation using the genetic algorithm we assign a crossover rate of 0.5, a=100, b=20 and a mutation rate of 1.0 after several numerical trials to find the best solution. For the case of random search we selected randomly 10000 cases of restoration order of all links. In this genetic algorithm, we use populations of 50 and maximum generations of 100. The histogram of calculated all total un-restored ratios is shown in Fig.5. The restoration order of links with the lowest total un-restored ratio is the best solution of the restoration process in the random search algorithm. In Fig.5, △ is the best solution obtained by the random search and □ is the average value of solutions obtained by the five trials of the genetic algorithm using different initial distribution of individuals. Though the required calculation time used for the genetic algorithm is equal to that for 5000 times random search, the solution obtained by the genetic algorithm is far better than that obtained by the random search (△).

Next, we compare the solutions obtained by the genetic algorithm with the exact solution in order to check the distribution of solutions obtained by the genetic algorithm. We generated 10 cases of damaged networks with same network configuration as shown in Fig.4 but different restoration times assigned for links. For each case the best un-restored ratio is calculated using the genetic algorithm for five different initial distributions of the individuals. Fig.6 shows the histogram of 50 solutions obtained by the genetic algorithm. The horizontal coordinate is the ratio of GA's solutions to the exact solution. The bars with left down slant lines show the distribution of solutions after 50 generations and the bars with right down lines show the distribution of solutions after 100 generations, The symbols △ and □ plotted at origin shows the number of solutions reached to the exact solution after 50 and 100 generations. Since the number of links is 24, there are $24! \approx 6.2 \times 10^{23}$ combination of restoration order. Though the genetic algorithm dose not give the exact solution , 68% (34 out of 50) of solutions after 100 generations is distributed within a tolerance of 1% from the exact solution.

## 4. OPTIMIZATION OF RESTORATION ORDER USING HYBRID GENETIC ALGORITHMS

### (1) The idea of Hybrid GA

Using the genetic algorithm to search wide solution space is easy but fairly difficult to get the exact solution. One of effective methods to improve this week point in the genetic algorithm is the hybrid method[7] combining the genetic algorithm and the improved iteration method[8] (Hybrid GA). The idea of Hybrid GA is shown in Fig.7. The symbols ● and ○ show individuals (representatives of possible solutions). The solutions ● improve to the solutions ○ by using the improved iteration method and exchanging the genes between two solutions of ○ by using the genetic algorithm we can move a searching space to a different location. In the process of genetic algorithm a crossover operation between two solutions reaching to local

maximum solutions jumps the solution space to the places near another mountains. But the convergence to the local maximum by GA becomes very slow as the solution reaches to the local maximum solution. We can increase the convergence speed using the improved iteration method.

(2) Design of Hybrid GA using improved iteration methods

The original solution is improved to a better solution by changing the genes of own genotype slightly from the original configuration of genes[8]. The original solution is replaced by a new solution when it is improved and this replacement is continued until we cannot improve the solution. We here investigate the efficiency of two different types of improved iteration methods. The first method is to exchange an arbitrary pair of genes in a genotype and if its fitness value is larger than the fitness value of the original genotype we replace it by the new genotype. Exchange of two genes in a genotype is continued until we get the best solution. For example, if we express a component with restoration priority of ith order by $a_i$, the genotype expressing the restoration order of components is

$$a_1 a_2 a_3 \cdots a_i \cdots a_n \qquad (3)$$

We evaluate the efficiency of all restoration processes obtained by exchanging all pairs of $a_i$ and $a_j$. The most efficient solution is assigned as a solution improved locally. For a network with n damaged components the computation time to find the improved solution is proportional to n(n-1). The second method is to exchange only a series pair of genes in a genotype for finding a local best solution. For the genotype expressed by Eq.(3) the efficiency of restoration processes is evaluated for all genotypes obtained by exchanging a pair of $a_i$ and $a_{i+1}$ (i=1,2,...,n-1). For a network with n damaged components the computation time proportional to n-1 in this method. In the second method even after we exchange the restoration order of $a_i$ and $a_{i+1}$, the restoration order of components before $a_{i-1}$ and after $a_{i+2}$ is not changed. The difference of restoration efficiency of genotypes before and after pair of genes exchanged can, therefore, be evaluated by comparing two restoration processes with two components of $a_i$ $a_{i+1}$ and $a_{i+1}$ $a_i$. We can, therefore, save computation time than that of first method.

There are two ways to design Hybrid GA ; 1) The genetic algorithm is applied to obtain the solutions converged to a certain level and improved iteration method is used to find the best solution. 2) In each generation of the genetic algorithm the improved iteration method is applied to all individuals at the beginning of generating descendants. The second algorithm is formulated as

1. Generation of initial individuals using random process
2. Application of the improved iteration method for all individuals to get local solutions
3. Application of the genetic operations i.e. selection, crossover and mutation for the local solutions.
4. Return to the step 2

(3) Application to the sample network

We generated 10 cases of damage to the network with same network configuration as shown in Fig.4 and for each case the best un-restored ratio is calculated for 5 different initial distribution of individuals. The populations and the maximum generation used for the calculation are 10 and 50 respectively. Fig.8 shows the histogram of solutions obtained by Hybrid GA for the sample network. The horizontal coordinate is the ratio of GA's solution to the exact solution obtained by Horn's algorithm. The bars with left down slant lines and right slant lines are the respective distribution of solutions after 10th and 50th generations. Figures (a) and (b) are the results obtained by using the first and second types of hybrid genetic algorithm respectively. Symbols △ and □ show the number of solutions reached to the exact solution after 10th generation and 50th generation. Even though the populations is small, at 50th generations the solutions of 37 and 44 out of 50 reached to the exact solution by using the respective first and second types of hybrid genetic algorithm. Furthermore, the number of solutions within a tolerance of 1% from the exact solution (from 1.00 to 1.01 in horizontal axis) is 46 for the type1 and 50 for the type2 algorithm. By comparing the convergence characteristics of type1 and type2 algorithms at 10th generation (bars with left down slant lines), we can see that solutions of type1 distribute near the exact solution and 36 out of 50 solutions reach to the exact solution. This means that the convergence is very fast in type 1 algorithm but tend to converge to local solution. This characteristic of type1 algorithm confirmed by the fact that we can get better result from type 2 algorithm at 50th generations.

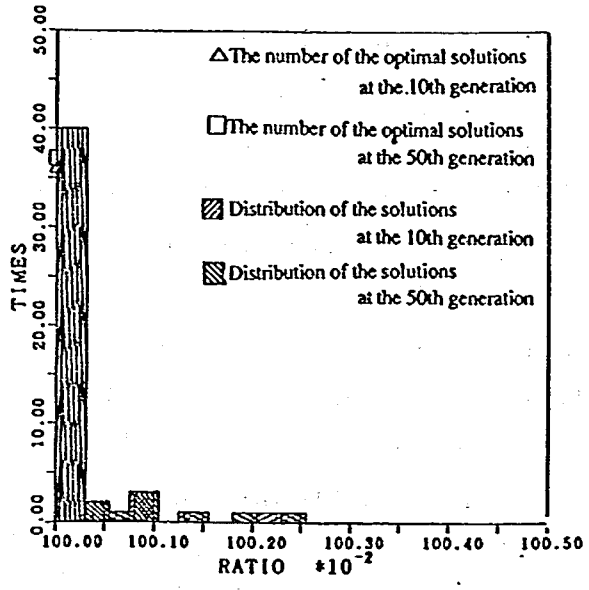
(4) Application to a road network

In this section, we optimize the restoration process of the road network in Izu peninsula damaged by the 1978 Off Izu-oshima earthquake. The initial condition for the restoration process is assumed to be the stage that an emergency restoration is finished and traffic in each link is secured at the minimum level. The concerned optimization is, therefore, of the restoration process to reduce the inconvenience of the damaged road network. Fig.9 shows the damaged road network and the number attached to each link is the steps needed to restore. The parameter of each link used to this calculation is given in the reference [9].

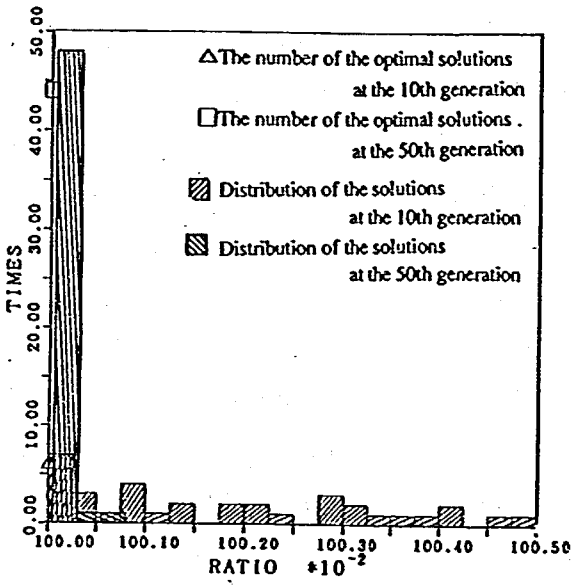
We define the restoration ratio using total travel times of vehicles. The travel time $T_{Si}$ in each damaged link is defined by

$$T_{Si} = T_i \cdot \frac{(1+\alpha S)}{(1+S)} \tag{4}$$

in which S is the steps remained to restore the ith link, $T_i$ the traffic time at normal condition, and $\alpha$ the weight. The traffic time $T_{Si}$ becomes $\alpha$ times of $T_i$ when many restoration steps are remained. We assume the traffic time $T_i$ at normal condition as the linear function of traffic volume. The traffic time of ith link at normal condition is given by




(a) Type 1 (exchanging arbitrary pair of digits and evaluating the restoration time)




(b) Type 2 (exchanging neighboring digits and evaluating the restoration time)

Fig8 Distribution of solutions obtained by Hybrid GA

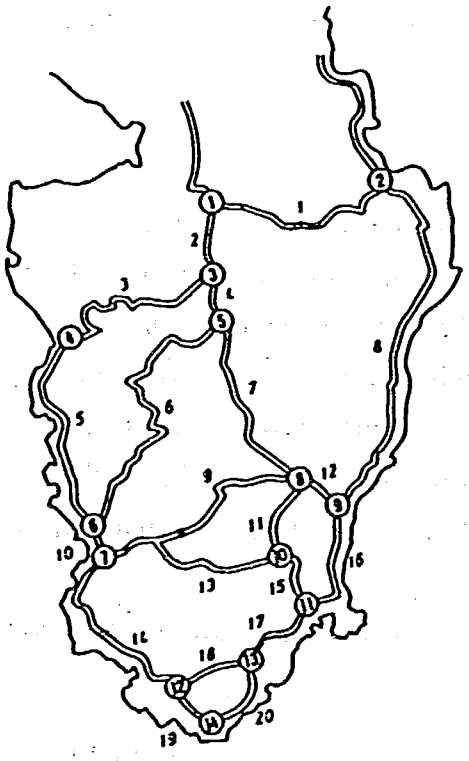


Fig9 A road network model in the Izu Peninsula

$$T_i = L_i\left(\frac{\beta Q_i}{Q_{oi}} + \frac{1}{V_{oi}}\right) \tag{5}$$

in which $L_i$ is the length of the link, $Q_i$ the traffic volume of the link, $Q_{oi}$ the traffic capacity of the link , $V_{oi}$ the fastest traffic velocity in the link and $\beta$ the inclination of traffic time function. The restoration ratio is assumed to be defined by the total traffic time $\tau(t)$. The total traffic time at time t is defined as follows.

$$\tau(t) = \sum_{i=1}^{N} Q_i(t) \cdot T_i(t) \tag{6}$$

in which $Q_i(t)$ and $T_i(t)$ the traffic volume and time at time t ,respectively, and N the number of links in network. As the restoration of links proceeds the total traffic times decrease, the restoration ratio of the concerned road at time t is defined by

$$RR(t) = \frac{\tau(t_0) - \tau(t)}{\tau(t_0) - \tau(t_E)} \tag{7}$$

in which $t_0$ is the starting time of restoration and $t_E$ the completion time of the restoration. The traffic volume of each link is obtained by the dividing method of OD traffic (the number in division is 10). The OD table for traffic to use for simulation is given in the reference [10]. We apply the second type hybrid genetic algorithm to get the best solution. We search the solutions over the 10 generations using individuals with the population of 10 because a long calculation time is needed.

The weighted total un-restored ratio is used as a criteria to evaluate the restoration process. We simulated the cases for two different weighting time function. One is the case of linearly increasing weight with time by which we can express an increase of inconvenience due to the delay of restoration. The other is the case of linearly decreasing weight with time which express the importance of emergency restoration. Furthermore, we calculated a time history of restoration ratio using the maximum gradient method in order compare the results obtained by these methods. The maximum gradient method decides a restoration order of links as to maximize the gradient of the restoration curve.

Fig.10 shows the restoration curve for the case using the linearly increase weight. The solid line is the restoration curve by Hybrid GA and the dotted line is the restoration curve by maximum gradient method. From time step 10 to 30, the solid line is under the dotted line and restoration by Hybrid GA accordingly proceeds in slow pace. But during the time step from 35 to 40, the solid line is above the dotted line and the delay of restoration is recovered. The weighted total un-restored ratio is 6.82 for the restoration curve obtained by Hybrid GA and 6.86 by maximum gradient method. It means that Hybrid GA gives the better restoration process than maximum gradient method. Fig.11 shows the restoration curve for the case using

the weight decrease linearly. During the time step from 10 to 40, solid line is above the dotted line and the restoration by Hybrid GA proceeds faster than that by the maximum gradient method. The weighted total un-restored ratio obtained by Hybrid GA is 35.97 and smaller than 36.09 by the maximum gradient method. From these simulation, we can conclude that the solution obtained by Hybrid GA is sensitive to the definition of the problem and we can search the solution which fit the problem.

## 5. OPTIMIZATION OF THE DISTRIBUTION OF RESTORATION TEAMS USING SIMPLE POPULATED GENETIC ALGORITHMS

(1) The outline of Simple Populated Genetic Algorithms

Although Genetic Algorithms are efficient methods to find the optimal solution for a problem with large universe, to define the proper genotype is not so easy task and to execute the algorithm need sometime long calculation time when the parameters to be considered become too many. An example of such a case is to optimize the distribution of restoration teams to large number of damaged components. We apply the single populated genetic algorithm (SPGA) to solve this problem. This is a genetic algorithm using only one genotype[11] in which the mutation operation is only used to search the optimal solution. This idea comes from asexual reproduction which is common in bacteria or sea anemones.

The algorithm of the SPGA is formulated as

1) Production of a initial parent.
2) Application of the mutation operation to the parent to produce a descendant and evaluation of a fitness value of the descendant.
3) Replacement of the parent by the descendant when the fitness value of the descendant is larger than that of the parent.
4) Return to 2) or finish SPGA when the convergent condition satisfy.

(2) Design of the SPGA to optimize the distribution of restoration teams

A genotype to be used for optimizing the plan to distribute restoration teams during restoration process of a damaged lifeline network is defined by a matrix

$$p=\begin{bmatrix} a_{11} & a_{12} & \cdots & a_{1n} \\ a_{21} & a_{22} & \cdots & a_{2n} \\ \vdots & \vdots & \ddots & \vdots \\ a_{m1} & a_{m2} & \cdots & a_{mn} \end{bmatrix} \qquad (8)$$

in which the element $a_{ij}$ expresses the component number to be repaired at jth order by the ith restoration team. For example, $a_{23}=4$ means that the second restoration team restores the

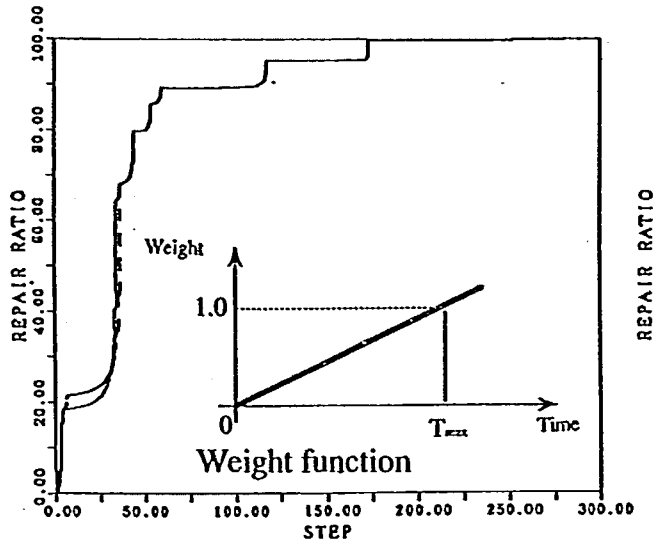



Fig10 Restration ratio cueve with the weight increasing linearly with time

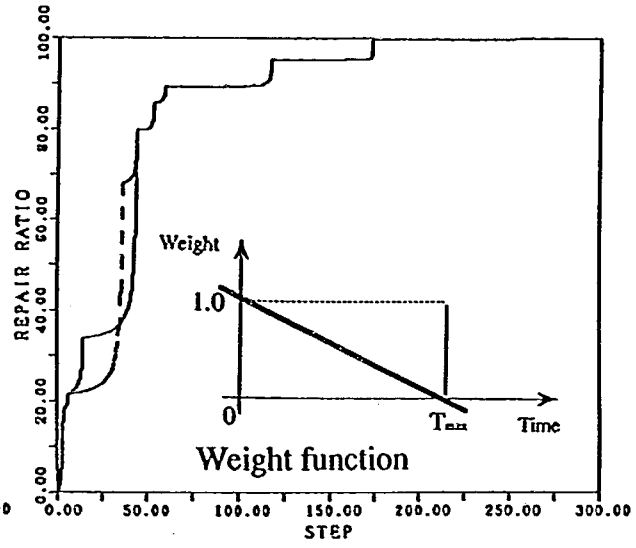



Fig11 Restoration ratio cueve with the weight decreasing linearly with time

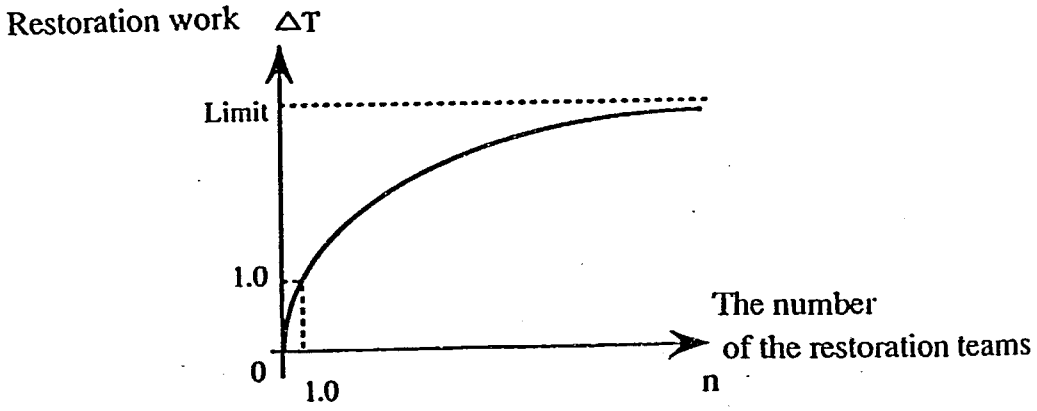



Fig12 Saturation of restoration efficiency

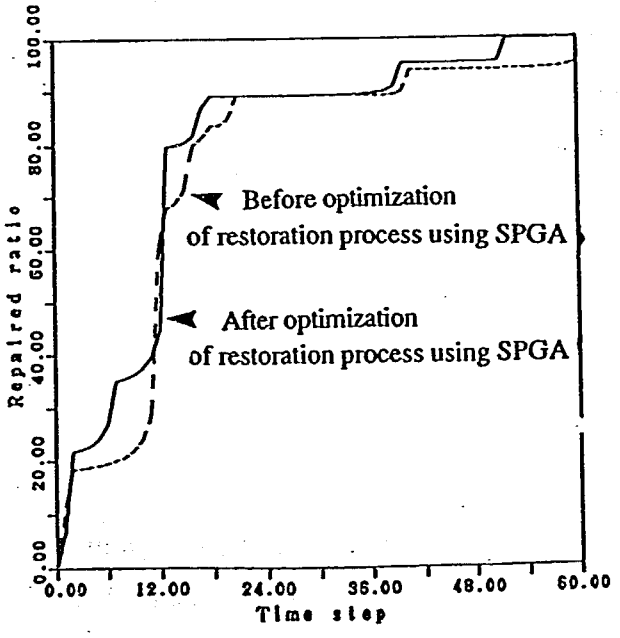



Fig13 Restoration ratio curve of the damaged road network with 5 teams ,taking account of the saturation of restoration efficiency

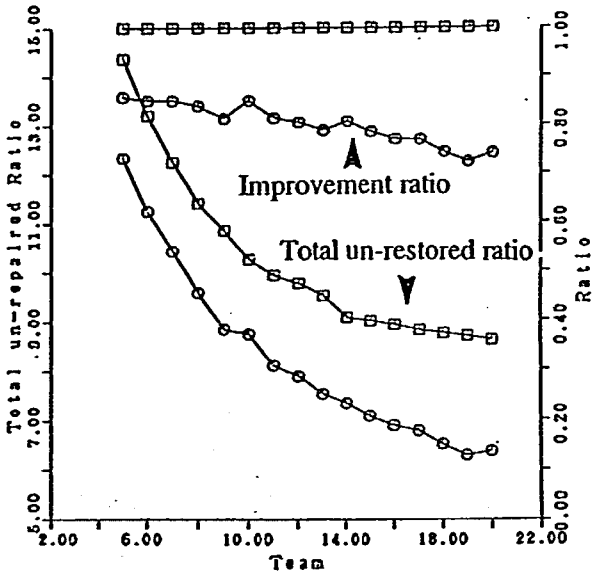



Fig14 Improvement of restoration efficiency by using SPGA

fourth component at third order. In this matrix, row and column express the order of restoration and the restoration team number respectively.

As the initial genotype, we assume that all restoration teams restore the components in same order. For example, considering the case to distribute three restoration teams and four damaged components, if the restoration order of components 1 -> 2 -> 3 -> 4 is assigned to all restoration teams, the initial genotype p is given as

$$p=\begin{bmatrix}1 & 2 & 3 & 4\\ 1 & 2 & 3 & 4\\ 1 & 2 & 3 & 4\end{bmatrix} \qquad (9)$$

For mutation operation we select a gene $a_{ij}$ randomly and replace the selected gene $a_{ij}$ with a neighboring gene $a_{ij+1}$. We replace only a pair of genes in one generation, but we increase the number of replacements for the case when the solution falls in the local minimum or there is no improvement of the solution in successive 5 generations.

(3) Distribution of restoration teams taking into account non-linear restoration efficiency We usually assume a linear relation between the number of restoration teams and restoration efficiency. In other wards, the restoration time is proportion to the number of restoration teams. When we concentrate restoration teams to a component the efficiency of restoration process, however, may not be increased as we expect because a saturation phenomenon of restoration efficiency usually can be seen. This means that we have to take into account a non-linear relation between the number of restoration teams and the restoration efficiency . To define this non-linear relation we have to simulate the actual restoration process using system dynamics or other method. In this paper, we assume the following relation. The amount of restoration work $\Delta T$ during one restoration step is assumed to be expressed as a function of the number of restoration teams n.

$$\Delta T = f(n) \qquad (10)$$

if this relation is linear

$$\Delta T = n \qquad (11)$$

in this section, we assume the relation given by

$$\Delta T = -\frac{p(p-1)}{n+p-1}+p \qquad (12)$$

in which p is the maximum restoration work during one restoration step. This is shown as a function n in Fig.12. The saturation effect on the restoration work can be seen when n is increased.

A numerical simulation of the restoration process for the road network (Fig.9) is shown in Fig.13 of the case of p=5.0. This figure shows the restoration curves for the case that 5

restoration teams are distributed to restore the network. The solid line is the restoration curve obtained by the SPGA at 100 generations which takes into account the saturation effect to distribute restoration teams and the dotted line is that obtained by the maximum gradient method without considering saturation effect. From this figure we conclude that the optimization of the restoration process is well performed by the SPGA. Fig.14 shows how well we can optimize the restoration process by the SPGA when we increase the number of restoration teams from 5 to 20. The two thin lines show the total un-restored ratio and the two bold lines the ratio of improvement. In each line, □ shows the restoration process without considering the saturation effect and ○ shows the restoration process taking into account the saturation effect obtained by the SPGA. Horizontal coordinate shows the number of restoration teams. It shows that we can reduce the total un-restored ratio from 15% to 30 % when we take into account the saturation effect.

## 6.CONCLUSIONS

In this research, we developed simple optimization methods in order to support a decision for restoring earthquake damaged lifeline networks. The simple genetic algorithms and the hybrid genetic algorithms are applied to determine the most effective restoration order of damaged components in lifeline networks. From results obtained by numerical simulations for a damaged road network, we can conclude that the hybrid genetic algorithm is useful tool to decide the restoration order of components to restore the damaged network.

We developed an algorithm which can take into account the saturation effect to distribute restoration team to restore the damaged lifeline network. The single populated genetic algorithm was applied. Numerical example demonstrated well the efficiency of the developed algorithm.

## 7.REFERENCES


1) Hiroyuki Kameda and Nobuoto Nojima : Development of Lifeline Earthquake Engineering , Proceedings of Workshop on CHINA-JAPAN Joint Research for Earthquake Disaster Prediction and Mitigation , 1992.
2) Koji Shiraishi and Kenzo Toki : Research for System to Support Decision Making at Post-Earthquake Restoration of Damaged Gas Networks , Proceedings of the 43th annual conference of JSCE , pp.792-793 , 1988
3) Nobuoto Nojima and Hiroyuki Kameda : On Algorithm for Optimum Post-Earthquake Restoration of Hierarchically Separated Lifeline Networks , Proceedings of JSCE , No.450 / I-20 , pp171-180 , 1992.
4) Shigeru Noda : Optimum post-earthquake restoration of a telephone system using neural

networks , J. of Natural Disaster Science , Vol.15 , pp.91-111 , 1993.
5) Masaru Hoshiya , Seiichi Koike and Masatoshi Miyazaki : Prediction of Seismic Damage Restoration of Underground Water Pipeline Systems , Proceedings of JSCE , No.322 , pp.25-35 , 1982.
6) Holland,J. : Adaptation in Natural and Artificial Systems, The University of Michigan , 1975. and MIT Press , 1992.
7) Davis, L. : Handbook of Genetic Algorithms, Van Nostrand Reinhold , 1991.
8) Iichi Nishikawa et al. : Optimization , Iwanami (in Japanese) , 1982.
9) Yoshikazu Yamada , Hirokazu Iemura , Shigeru Noda and Kazuyuki Izuno : Evaluation of the Optimum Restoration Process for Transportation Systems After Seismic Disaster , Proceedings of JSCE , No.368 / I-5 , pp.355-362 , 1986.
10) Hideji Kawakami : Evaluation of Earthquake Performance of Transportation Systems , Proceedings of JSCE , No.327 , pp.1-12 , 1982.
11) Koji Morikawa , Takeshi Furuhashi and Yoshiki Uchikawa : Application of Single Populated Genetic Algorithms , Proceedings of 2nd Neural Network Symposium (in Japanese) , pp.131-138 , 1991.

# Session-6

## Gas, Electricity and Telecommunication

(J-16) Damages of Gas Facilities by Great Hanshin Earthquake and Restoration Process
(Shojiro Oka)

(J-17) Impact of the Earthquake of Southern Hyogo Prefecture on Electric Power Facilities
(Tohru Yoshikawa and Yoshiaki Mino)

(J-18) Damage of Underground Telecommunication Facilities in the 1995 Great Hanshin Earthquake
(Kenichi Honda,Yuzo Yamaguchi and Shinji Mataki)

(U-3) Power Systems: Comparing the Kobe and Northridge Earthquake Experiences
(Anshel J. Schiff)

# Damages of Gas Facilities by Great Hanshin Earthquake and Restoration Process

Shojiro Oka
Central Control Office, Distribution Department
Osaka Gas Co., Ltd.

## ABSTRACT

This paper reports the damages caused on gas facilities by Great Hanshin Earthquake and the process of restoration works.

## INTRODUCTION

The Hanshin Earthquake shook the western Japan with strong jolts on January 17, 1995. In the service area of Osaka Gas Co., Ltd., seismometers installed in Kobe and Nishinomiya recorded maximum accelerations of 833 gal and 792 gal, respectively, that are equivalent to seismic intensities of 7 by Meteorological Agnecy of Japan (MAJ). The Hanshin Earthquake having an intensity of 7 by MAJ, highest recorded in Japan since Fukui Earthquake of 1948, caused over 5,500 deaths and nearly 200,000 houses to collapse or damaged. Transportation facilities severely damaged. Three railways, JR, Hankyu and Hanshin, connecting Osaka and Kobe, and Kobe line and Wangan line of Hanshin Expressway were disrupted, completely crippling the transportation in the earthquake-stricken region. Damages on the lifeline were also devastating. 2.6 million households suffered from power outage, 1.2 million households were cut off from water supply, 380,000 telephone lines were disrupted and 860,000 households were cut off from town gas supply. Furthermore, over 300,000 people who lost their homes or could not return to their unsafe homes were forced to take shelters in schools or tents amid the continuing aftershocks in the mid-winter cold.

## GAS SUPPLY SYSTEM

Osaka Gas Co., Ltd. supplies gas to about 5.7 million customers in six prefectures in Kinki Region. It sold about 5.5 billion square meters of gas in fiscal 1994. While households account for 95% of the total number of customers, industrial and business use accounted for 63% of the total sales volume.

Gas from a gas manufacturing terminal is sent through high-pressure, medium-pressure and low-pressure pipeline network and distributed to the customers. High-pressure pipeline networks are operated normally at pressures from 1 to 4 MPa, and are used in long-distance transportation and to send fuel gas to electric power stations. Gas which has been transported

through a high-pressure pipeline network enters a governor where the pressure is decreased, then fed into a medium-pressure pipeline network. Medium-pressure pipeline networks are divided into two stages of medium-A pressure and medium-B pressure. Medium-A pressure pipeline networks are operated at pressures from 0.3 to 1 MPa, and medium-B pressure pipeline networks are operated at pressures from 0.1 to 0.3 MPa. Medium-pressure pipeline networks, both A and B, are used in inter-city transportation and in gas supply to large hospitals, hotels, factories and other institutions. Gas holders which provide buffers for the daily fluctuation of gas demand are part of medium-pressure gas distribution facilities. Commercial and industrial institutions of medium to small scales and households are supplied from low-pressure pipeline networks via governors which decrease the pressure of the gas received from the medium-pressure pipeline networks. The pipelines are made of welded steel pipes, ductile cast iron pipes, polyethylene pipes, etc., as shown in table 1, all having earthquake-resistant property.

Table 1 Gas distribution systems of Osaka Gas

| Pressure class | Working pressure | Material | Major applications |
|---|---|---|---|
| High-pressure | 1.0～4.0MPa | Steel pipe (Welded) | Long-distance gas transportation, Gas supply to power stations |
| Medium-A pressure | 0.3～1.0MPa | Steel pipe (Welded) | Medium-distance gas transportation, Gas supply to hospitals, factories and other large-volume customers |
| Medium-B pressure | 0.1～0.3MPa | Steel pipe (Welded)<br>Ductile cast iron pipe | |
| Low-pressure | 1.0～2.5kPa | Steel pipe (Welded,mechanically joined)<br>Cast iron pipe<br>Polyethylene pipe<br>Steel pipe (Screw joint) | Gas supply to households, medium & small-scale businesses and industrial customers |

## ANTI-EARTHQUAKE MEASURES

Anti-earthquake measures implemented by Osaka Gas. are summarized in Table 2. The measures in the category of hardware includes the construction of earthquake-resistant facilities and the introduction of microcomputer-controlled intelligent gas meters. Production facilities and gas holders are designed in conformity with the requirements of relevant legal regulations and constructed after confirming the earthquake-resistant performance by means of dynamic structural analysis and other advanced techniques. We have also been strengthening the pipeline networks to make them earthquake-resistant by using earthquake-resistant joints for joining the pipes and employing polyethylene pipes which have enough flexibility to accommodate large deformation. Gas meters of households have been replaced with the intelligent meters that shut off gas flow when a strong tremor of an earthquake is detected.

Table 2 Anti-earthquake measures of Osaka Gas

| Hardware measures | Software measures |
|---|---|
| (1)Construction of earthquake-resistant facilities<br>* Dynamic analysis of production facilities and gas holders<br>* Reinforcement of pipeline networks to make them earthquake-resistant (Earthquake-resistant joint, polyethylene pipe, etc.)<br>(2) Introduction of intelligent meter | (1) Division of the service area into earthquake isolation blocks<br>(2) Preparation of disaster program and other manuals<br>(3) Practice of earthquake drills<br>(4) Operation of security communications network |

As measures in the category of software, division of the service area into earthquake isolation blocks and other measures have been implemented. As our gas distribution services cover an extended region, different portions of the service area expect to suffer damages of significantly different degrees of severity from an earthquake, depending on the location of the epicenter. For this reason, we have divided the service area into several blocks so that severely affected blocks can be isolated from other blocks. Our whole service area is divided into 8 "Super Blocks" and they are sub-divided into 55 "Middle Blocks".

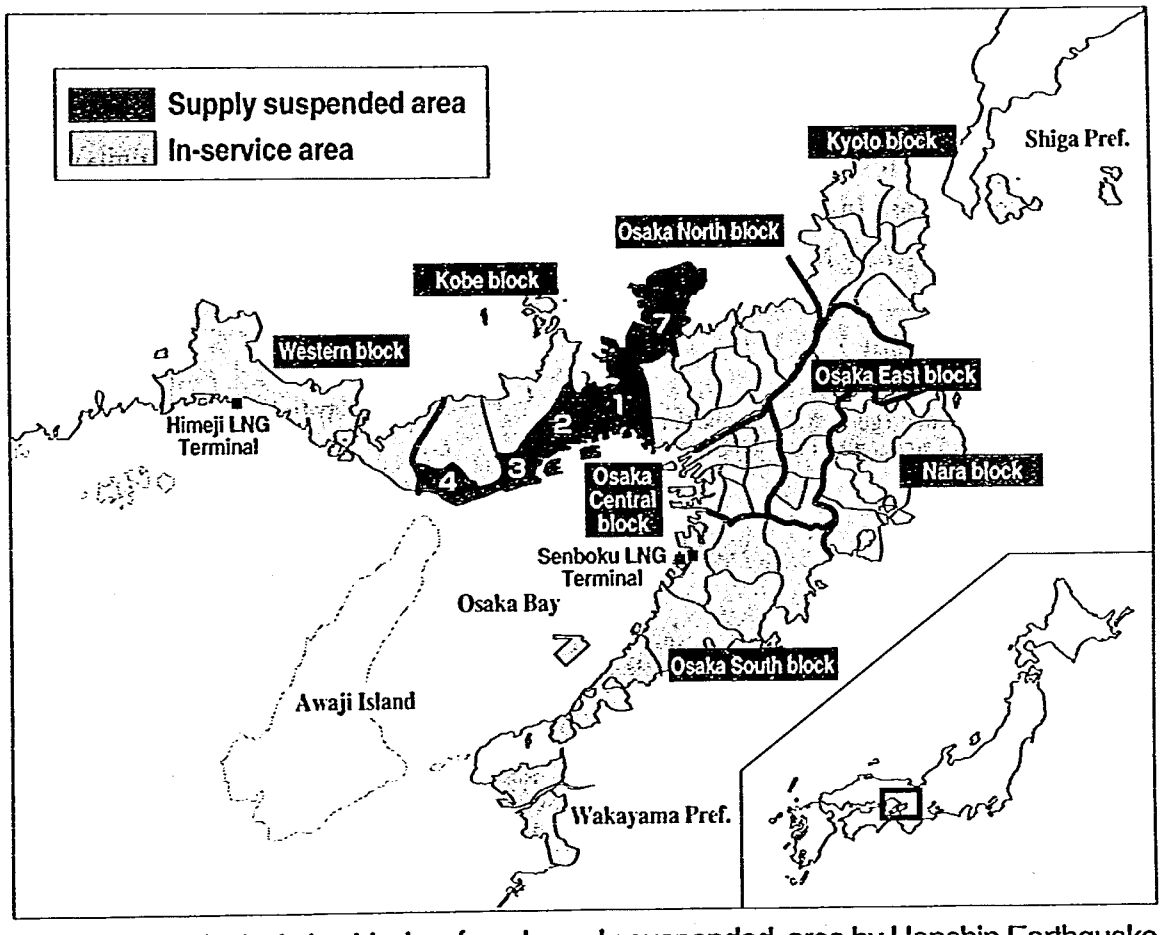



Fig.1 Earthquake isolation blocks of and supply-suspended area by Hanshin Earthquake

In blocks which suffer severe earthquake damages, gas supply is suspended in order to prevent secondary disasters while continuing the gas supply in unaffected blocks. By the Hanshin

Earthquake, we suspended our gas to five middle blocks as shown in Fig.1.We worked out a disaster program and accordingly have been conducting company-wide earthquake drills once a year. We also have an emergency action manual that states the criteria on which our employees determine whether they should report immediately to their office in the event of a disaster and specifies which corporate organization should deal with a specific situation. A radio communications network operated by Osaka Gas for security communications also serves for information transmission, remote monitoring and control of facilities in emergency.

## DAMAGES ON FACILITIES

### Production facilities

Major production facilities were not affected by the earthquake on Jan. 17, and continued their operations. Some minor impairments were caused, however, on material handling facilities, roads and vacant lands that surround the facilities, as shown below, due to liquefaction .

* Instrumentation boxes were tilted.
* Air leaked through a flanged portion of instrumentation air piping.
* Water leaked through flanged portions of industrial water piping and sea water piping.

As for the gas holders, maximum ground surface acceleration of 833 gal was recorded in Fukiai supply station, although no damage was sustained by the two gas holders. Also no damage was caused in our gas holders located near the epicenter; Nishinomiya (4 units), Kobe (1 unit), Akashi (1 unit), Kita-kobe (1 unit), Kanzakigawa (2 units) and Senri (3 units).
None of 3212 governors installed in our service area were damaged, including those installed in the area where level 7 by MAJ was recorded.

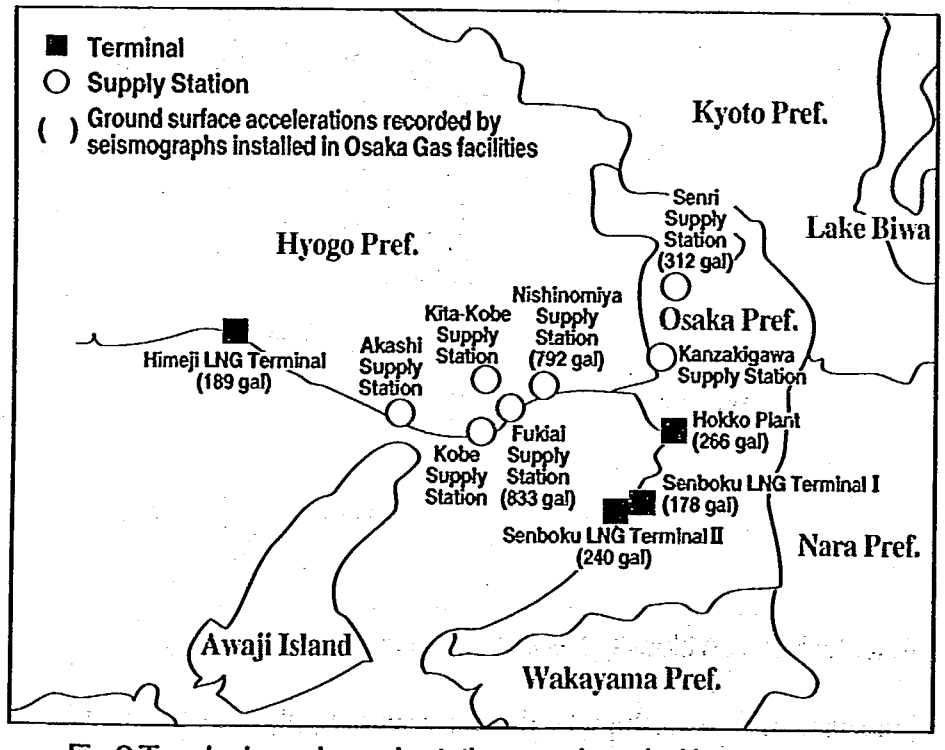



Fig.2 Terminals and supply stations equipped with gas holders

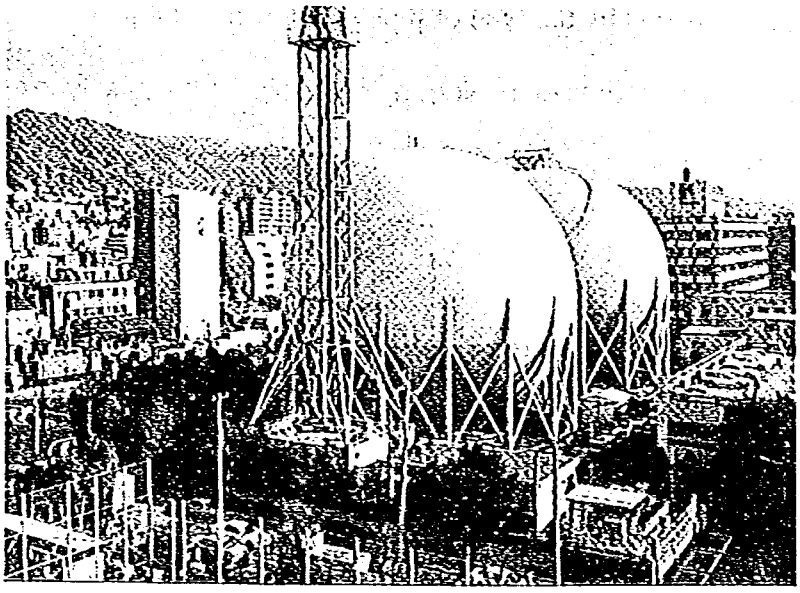


Photo 1 Overview of gas holder

**High-pressure pipeline**

The high-pressure pipelines (total length 490 km) sustained no damage. In Akashi district of Hyogo prefecture where accelerations over 400 gal were observed, in particular, the high-pressure pipelines remained intact.

In Tenpozan district along Osaka Bay, although sand boil, fissure and ground subsidence occurred due to the liquefaction, no damage was sustained by the high-pressure pipelines.

**Medium-pressure pipeline**

The medium-pressure pipelines sustained failures at 106 points. Table 3 shows the numbers of failures by the block where the gas supply was suspended and by the pressure classification. Table 4 shows the numbers of failures in the medium-pressure pipelines in the blocks where the gas supply was not suspended.

Table 3 Failures of medium-pressure pipelines in service suspended blocks

| Block / Pressure | Kobe 1 | Kobe 2 | Kobe 3 | Kobe 4 | Osaka North 7 | Other | Total |
|---|---|---|---|---|---|---|---|
| Medium-A pressure | 12 | 16 | 3 | 1 | 1 | 0 | 33 |
| Medium-B pressure | 19 | 27 | 10 | 1 | 5 | 0 | 62 |
| Total | 31 | 43 | 13 | 2 | 6 | 0 | 95 |

Table 4 Failures of medium-pressure pipelines in blocks where gas supply continued

| Administrative district / Pressure | Hyogo pref. | Osaka city (Osaka District Pipeline Office) | Osaka pref. (Hokubu District Pipeline Office) | Other | Total |
|---|---|---|---|---|---|
| Medium-A pressure | 1 | 1 | 0 | 0 | 2 |
| Medium-B pressure | 3 | 5 | 1 | 0 | 9 |
| Total | 4 | 6 | 1 | 0 | 11 |

Numbers of failures classified by the type of pipe are shown in Table 5.

Table 5 No. of failures of medium-pressure pipelines by the type of pipe

(No. of failure)

| | Steel pipe | | | | | Cast iron pipe | | | | Total for joints | Total for pipe bodies | Grand total |
|---|---|---|---|---|---|---|---|---|---|---|---|---|
| | Weld joint | Flange joint | Mechanical joint (dresser) | Sub-total | Pipe body | Mechanical joint | | Sub-total | Pipe body | | | |
| | | | | | | GM II | Bell-and-spigot | | | | | |
| Medium-A pressure | 8 | 5 | 22 | 35 | 0 | — | — | — | — | 35 | 0 | 35 |
| Medium-B pressure | 6 | 17 | 38 | 61 | 0 | 3 | 7 | 10 | 0 | 71 | 0 | 71 |
| Total | 14 | 22 | 60 | 96 | 0 | 3 | 7 | 10 | 0 | 106 | 0 | 106 |

"—" in the table indicates that it is not installed.

Situations of the failures can be summarized as follows.

* Most of the failures were leaks caused by loosened dresser joint. (Fig.3, photo 2)
* Welded portions of steel pipes were cracked at 14 points, all due to low grade welding process. (Photo 3)
* Leakage from the pipelines did not occur at the sites of seismic ground failures including cave-in of ground surface to largest depth of about 2.5m extending about 27m due to the collapse of Kobe subway Daikai station, collapse of road filling soil in about 100m section of Daini Shinmei highway, and collapse of revetments due to liquefaction below Karumo bridge. (Photos 4 through 6, Figs. 4 through 6)
* No leakage occurred from bridge-mounted pipes. (Investigated at 370 places.)
* No leakage occurred in pipelines made of cast iron pipes reinforced by rehabilitation technique (reverse lining process). (Table 6)

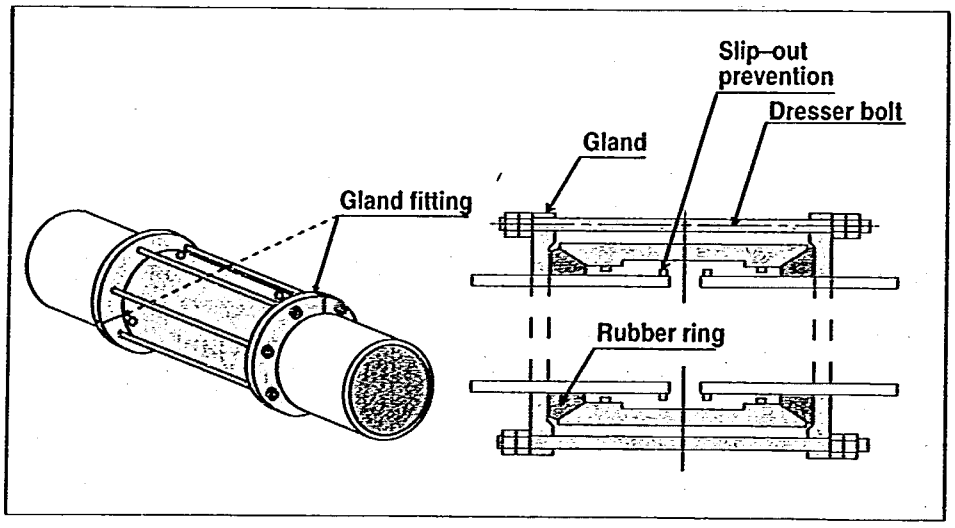



Fig.3 Dresser

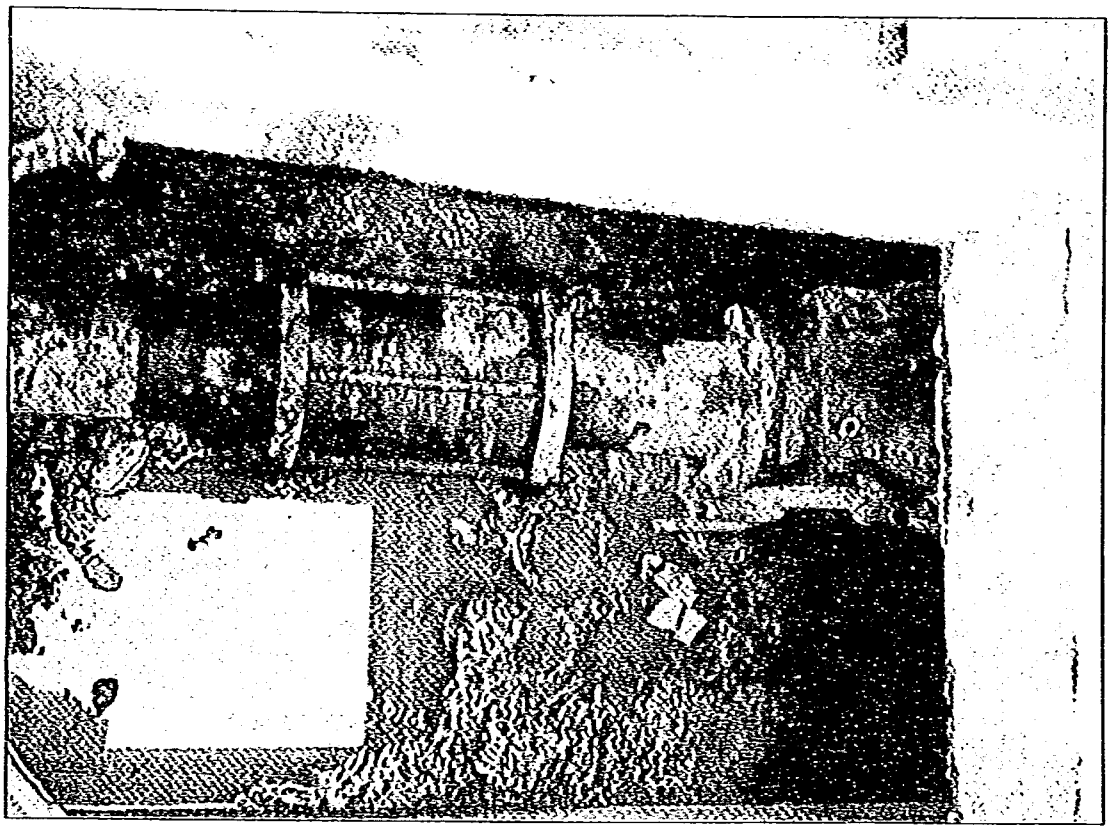


Photo 2 Failure in dresser

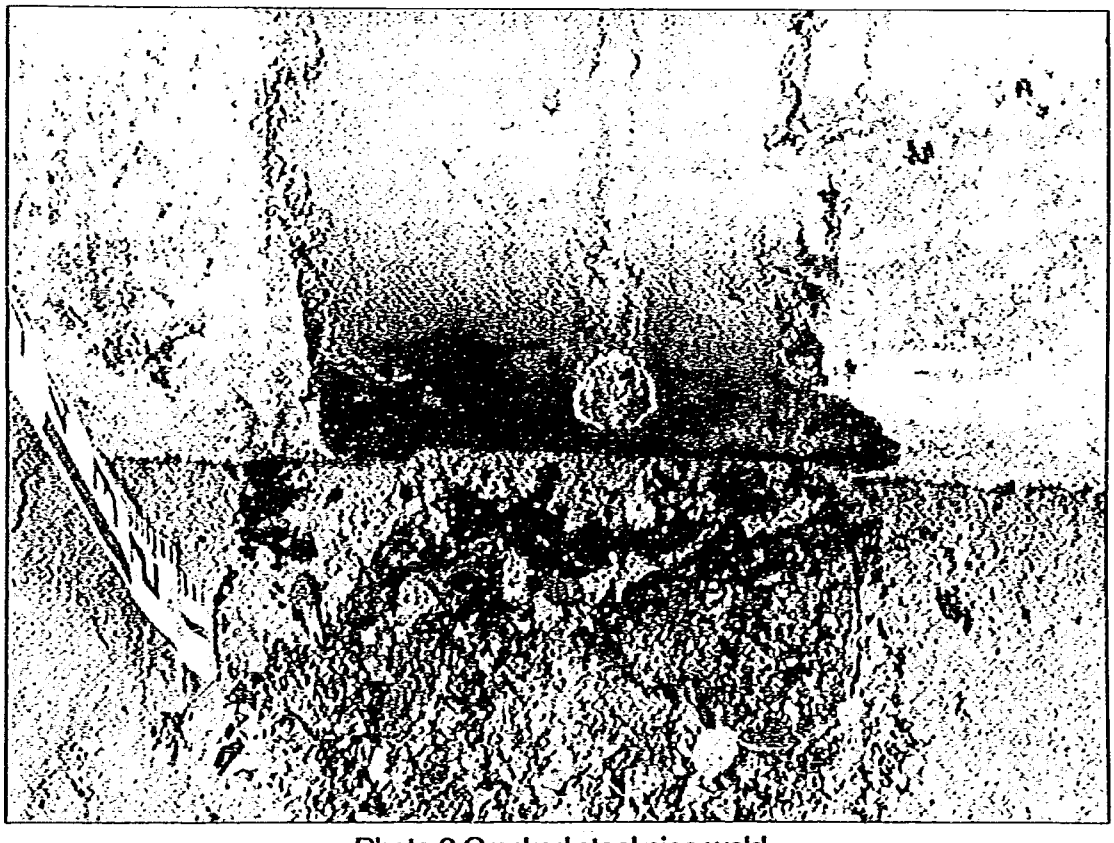


Photo 3 Cracked steel pipe weld

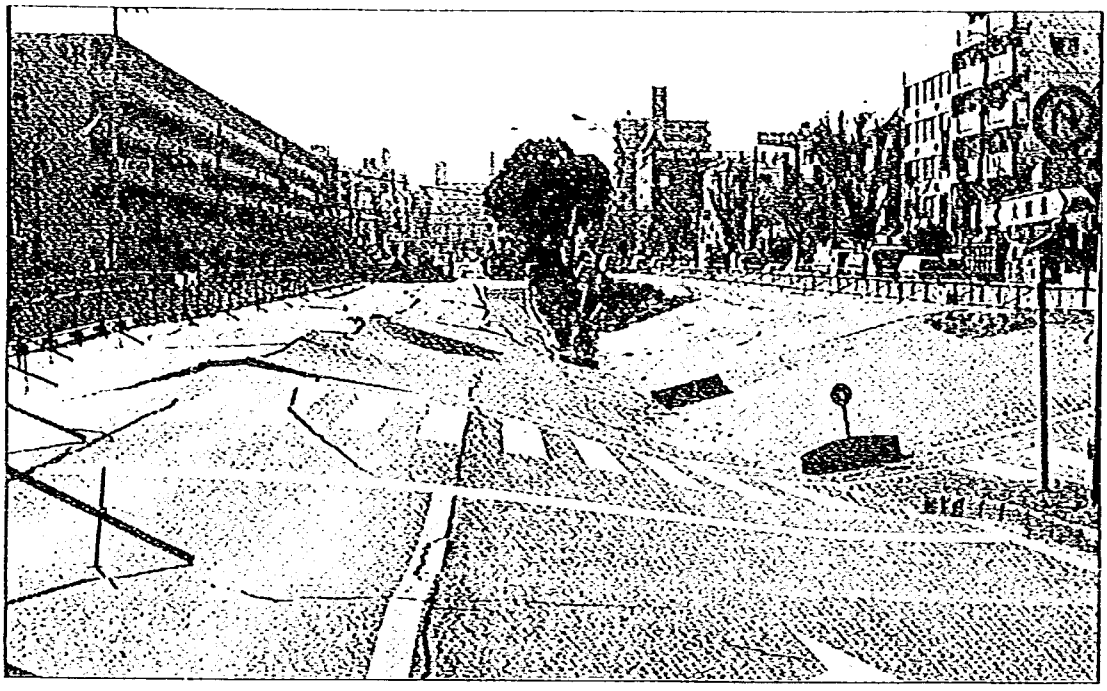


Photo 4 Road surface caved in near Daikai station

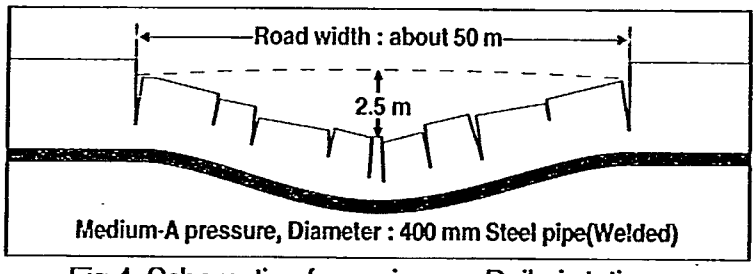



Fig.4 Schematic of cave-in near Daikai station

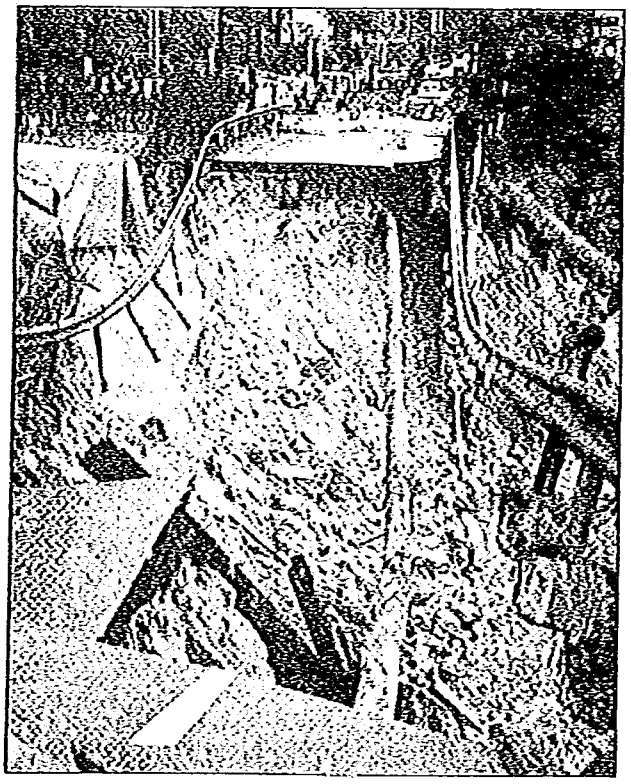


Photo 5 Landslide in Daini Shinmei highway at Okuradani

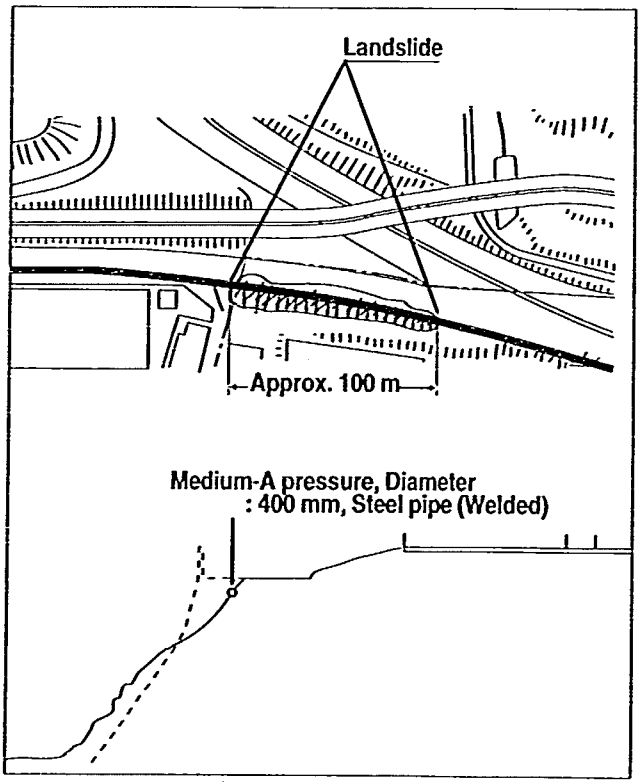



Fig. 5 Geographical sketch of landslide in Daini Shinmei highway at Okuradani

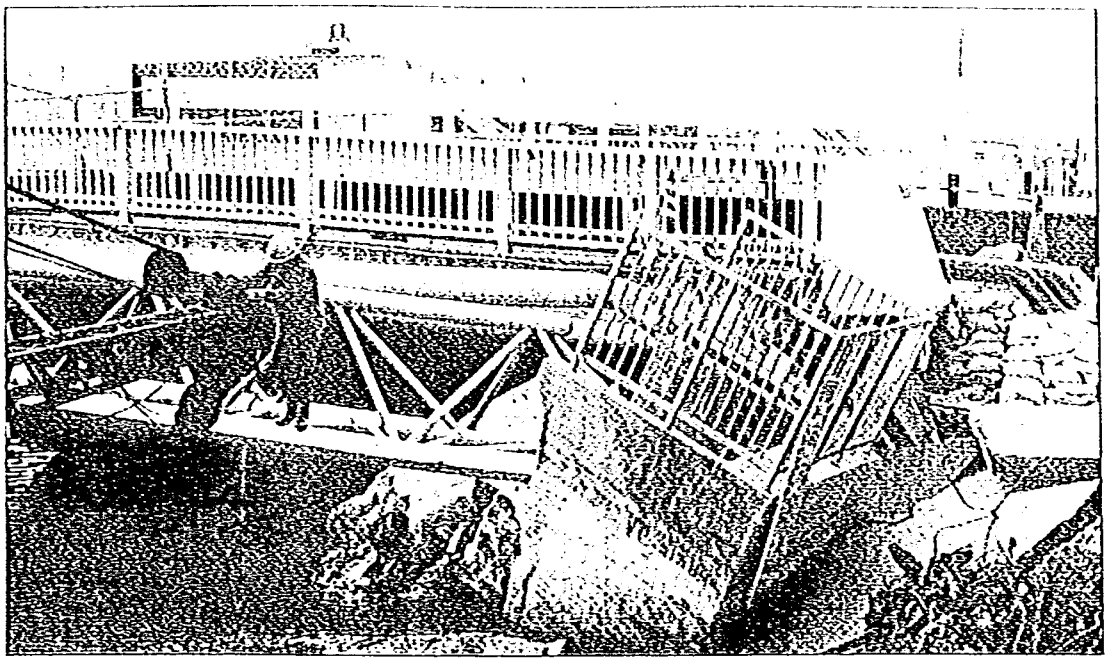


Photo 6 Damage on Karumo bridge

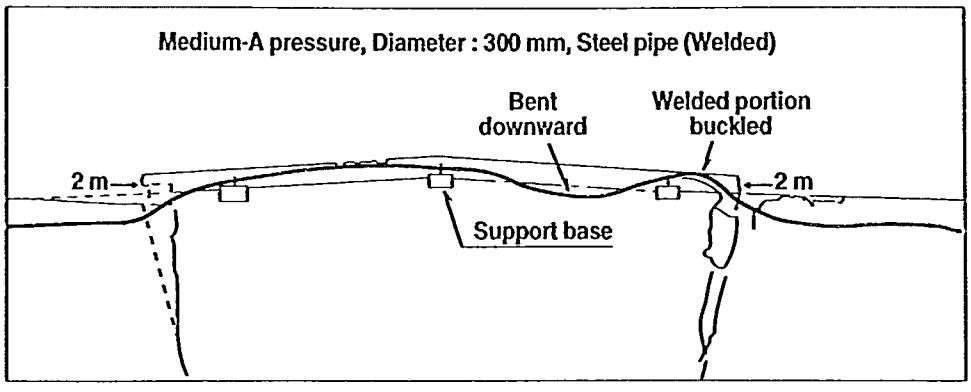



Fig.6 Schematic of damage on Karumo bridge

Table 6 Examples of medium-pressure pipelines where rehabilitation technique (reverse lining process) was applied

| Administrative district | Pipe material | Diameter | Total length | Leakage |
|---|---|---|---|---|
| Nishinomiya City | Cast Iron | 300mm | 455m | No leakage |
| Kobe City | Cast Iron | 300mm | 593m | No leakage |
| Kobe City | Cast Iron | 300mm | 247m | No leakage |
| Kobe City | Cast Iron | 500mm | 778m | No leakage |

**Failures of low-pressure pipelines**

Low-pressure pipelines in the area where the gas supply was suspended failed at 21,647 places. Number of failures by the block in the service suspended area is shown in Table 7. Number of failures in the service sustained area is shown in Table 8.

Table 7 Number of failures of low-pressure pipelines by the block in the service suspended

(No. of failure)

| | Kobe 1 | Kobe 2 | Kobe 3 | Kobe 4 | Northern Osaka 7 | Other | Total |
|---|---|---|---|---|---|---|---|
| Main | 185 | 116 | 88 | 83 | 23 | 8 | 503 |
| Branch | 993 | 889 | 803 | 567 | 583 | 102 | 3,937 |
| Service pipe | 1,339 | 1,859 | 1,445 | 271 | 355 | 40 | 5,309 |
| Service pipe on customer 's property | 996 | 1,025 | 688 | 280 | 138 | 51 | 3,178 |
| House pipe | 2,796 | 2,254 | 2,048 | 956 | 590 | 76 | 8,720 |
| Total | 6,309 | 6,143 | 5,072 | 2,157 | 1,689 | 277 | 21,647 |

Table 8 Number of failures of low-pressure pipelines in on-service areas

(No. of failure)

| | Hyogo pref. | Osaka city (Osaka District Pipeline Office) | Osaka pref. (Hokubu District Pipeline Office) | Other | Total |
|---|---|---|---|---|---|
| Main | 53 | 22 | 5 | 0 | 80 |
| Branch | 358 | 200 | 110 | 2 | 670 |
| Service pipe | 512 | 260 | 89 | 14 | 875 |
| Service pipe on customer 's property | 398 | 144 | 236 | 21 | 799 |
| House pipe | 1,382 | 450 | 491 | 65 | 2,388 |
| Total | 2,703 | 1,076 | 931 | 102 | 4,812 |

Number of failures by the type of pipe is shown in Table 9.

Table 9 Number of failures of low-pressure pipelines by the type of pipe

(No. of failure)

| | Steel pipe | | | | | | Cast iron pipe | | | | | PE | Flexible steel pipe | | Total for joints | Total for pipe bodies | Grand total |
|---|---|---|---|---|---|---|---|---|---|---|---|---|---|---|---|---|---|
| | Welded | Flanged | SGM | Screw | Sub-total | Pipe body | GM II | Bell-and-spigot type | Socket type | Sub-total | Pipe body | | Joint | Pipe body | | | |
| Main | 0 | - | - | - | 0 | 0 | 76 | 439 | 34 | 549 | 34 | 0 | - | - | 549 | 34 | 583 |
| Branch | - | - | 156 | 4451 | 4607 | 0 | - | - | - | - | - | 0 | - | - | 4607 | 0 | 4607 |
| Service pipe | - | - | 106 | 6045 | 6151 | 0 | 5 | 28 | - | 33 | 0 | 0 | - | - | 6184 | 0 | 6184 |
| Service pipe on customer's property | 0 | 0 | 59 | 3906 | 3965 | 0 | 3 | 7 | 0 | 10 | 2 | 0 | - | - | 3975 | 2 | 3977 |
| House pipe between meter and cock | 0 | 0 | 13 | 11085 | 11098 | 0 | 1 | 1 | 0 | 2 | 0 | 0 | 8 | 0 | 11108 | 0 | 11108 |
| Total | 0 | 0 | 334 | 25487 | 25821 | 0 | 85 | 475 | 34 | 594 | 36 | 0 | 8 | 0 | 26423 | 36 | 26459 |

Failures can be summarized as follows.

* Much failures are concentrated in screw joints. (Photo 7)

* Polyethylene pipes and welded steel pipes sustained no failures. (Photo 8)

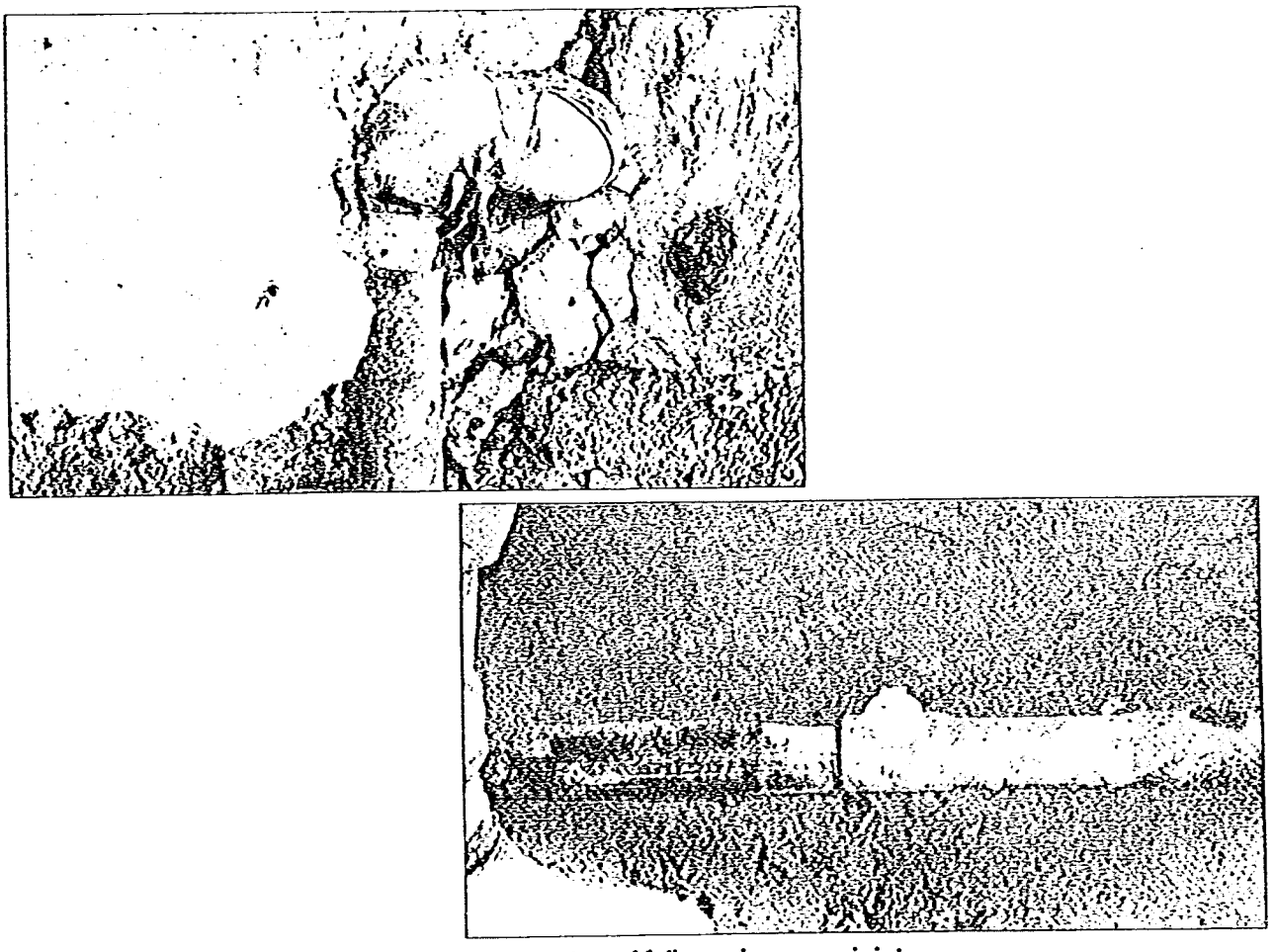
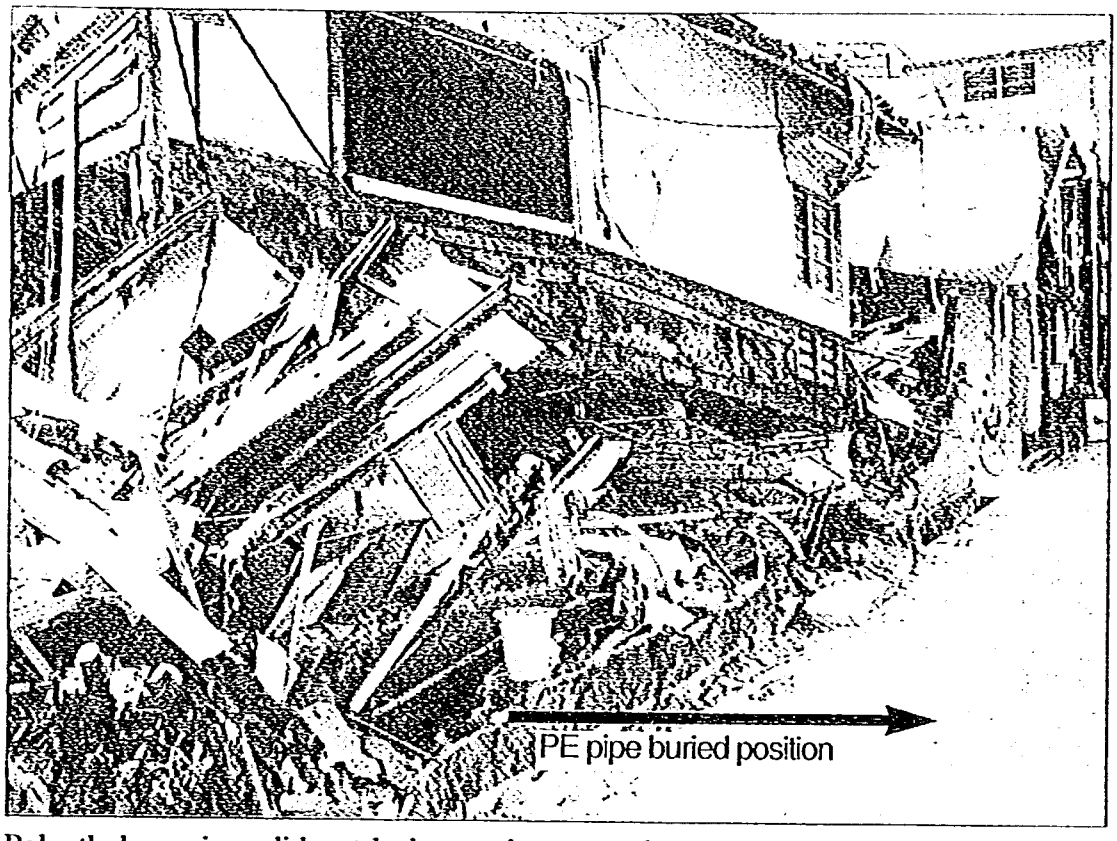
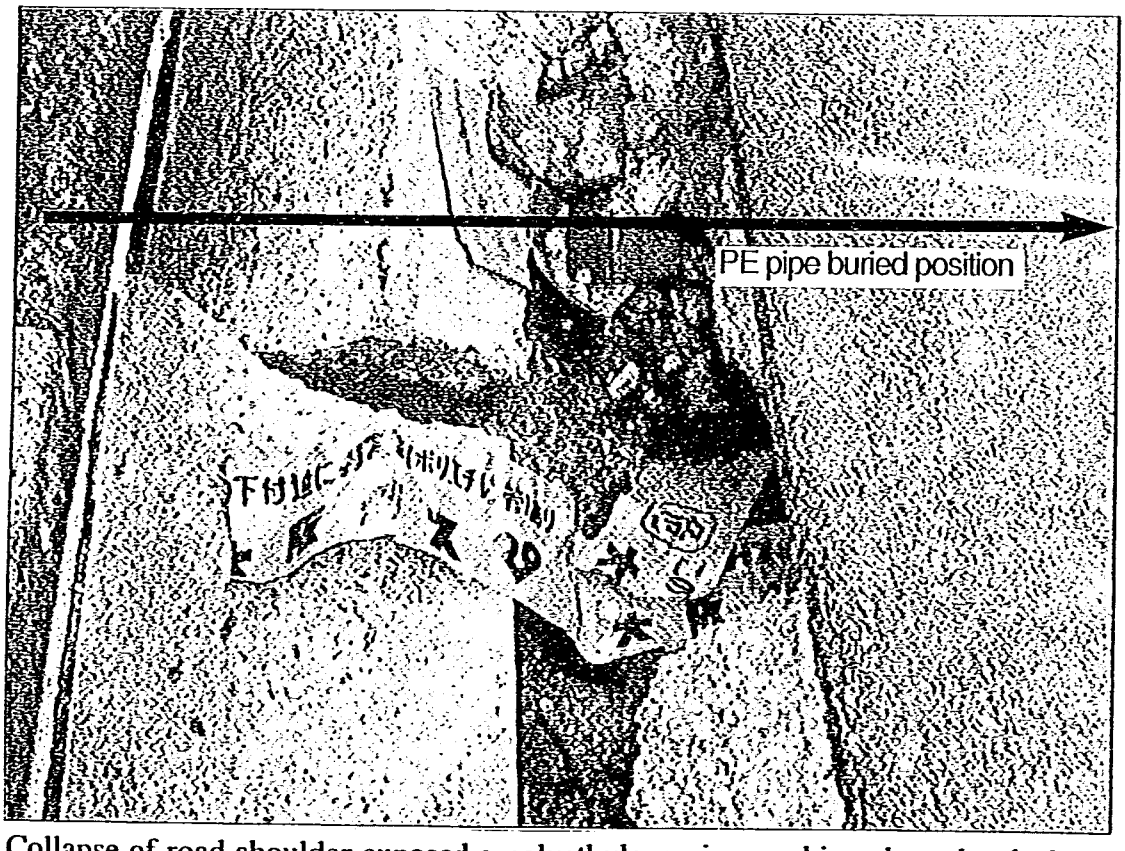


Photo 7 Examples of failures in screw joints




Polyethylene pipes did not leak even in areas where many houses were destroyed. (Kitaguchi-cho, Nishinomiya)




Collapse of road shoulder exposed a polyethylene pipe marking sheet, but leakage did not occur. (Horakucho, Nishinomiya)

Photo 8 Examples of polyethylene pipe surviving the earthquake

## SERVICE SUSPENSION

On January 17, Osaka Gas stopped the gas supply to about 860,000 customers in order to prevent secondary disaster due to gas leakage. Areas where the gas supply was suspended are five blocks located between Osaka and Kobe as shown in Fig.1, where the earthquake damages were severest among the service area. The largest number of customers ever affected by service suspension due to earthquake in Japan had been about 160,000 in the case of Miyagi Off-shore Earthquake that occurred in June 1978. Suspension of service to 860,000 customers was unprecedented incidence not only for Osaka Gas but for the Japanese gas industry as a whole.

## RESTORATION WORKS

### Restoration program

Fig.7 shows the restoration program for the areas where the gas supply is suspended. In the restoration work of town gas system, top priority is placed on securing the safety. For this reason, gas supply service can be resumed only after completing the inspection and repair of the gas facilities of all customers, not to say the main pipes buried under roads. Restoration works proceed as follows. First, our personnel visit every customer and close the customer's gas meter cock. Then cut off the connection of the mains to form a block (called the restoration sector) of a size from three to four thousand customers. Upon establishing the restoration sectors, the mains and branches of each sector are inspected and, in case there is a leakage, repaired. If water and/or sand are found to have entered the pipe, they are discharged. After repairing the mains, our personnel inspect the gas facility of every customer. If the inspection of gas pipe in the customer's premise showed no leakage and the inspection of the air-intake and flue ventilation system showed no abnormality, supply of gas is resumed. This process is repeated for every restoration sector.

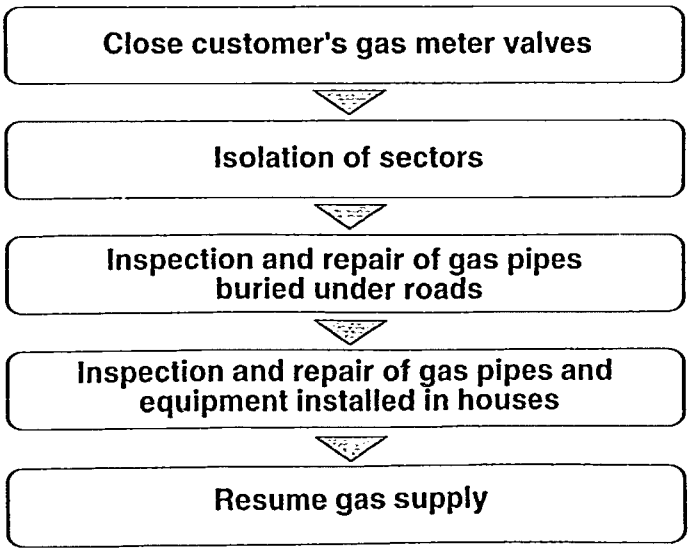



Fig.7 Procedure of restoration works

### Organization and restoration

As the restoration works for the gas supply system need tremendous manpower as described above, we mobilized six thousand employees from other areas such as Osaka, Kyoto, Nara, Wakayama and Shiga prefectures. Japan Gas Association asked its member companies, throughout the country from Hokkaido to Okinawa, to send reinforcement workers to help our restoration efforts. Thus the restoration works involved 9700 workers and 4800 vehicles at a time in the peak period.

Immediately after the earthquake struck, Osaka Gas organized the emergency operation headquarters in the company headquarters and, at the same time, established the front operation headquarters in Imazu, Nishinomiya which is located at the edge of the earthquake-stricken area on the east. Restoration workers, repair materials and food supplies were transported not only by land, but by extensive use of ships for marine transportation. Advance operation bases were established near the sites of restoration works by using sports grounds of universities and private companies through their courtesy.

### Progress of restoration works

We carried out the restoration works by dividing the five middle blocks where the gas supply was suspended into over 220 restoration sectors. Restoration works were started in fringe areas, where the damages were not serious, adjacent to areas not affected by the earthquake. This schedule was chosen for the purpose of resuming the gas supply service to as many customers and as early as possible.

Restoration works for one sector can normally be completed in four days. But in the earthquake-stricken areas, it required unexpectedly long time and much labor to remove large quantities of water and sand/mud which had entered the gas pipes. Thus it often took us over one week to restore one sector. Our restoration efforts were also impeded by wrecked houses which blocked roads.

Despite such worst conditions, we continued our best possible efforts and managed to complete the restoration works on April 11, except for a small number of customers where the circumstances prohibited to set to the restoration work.

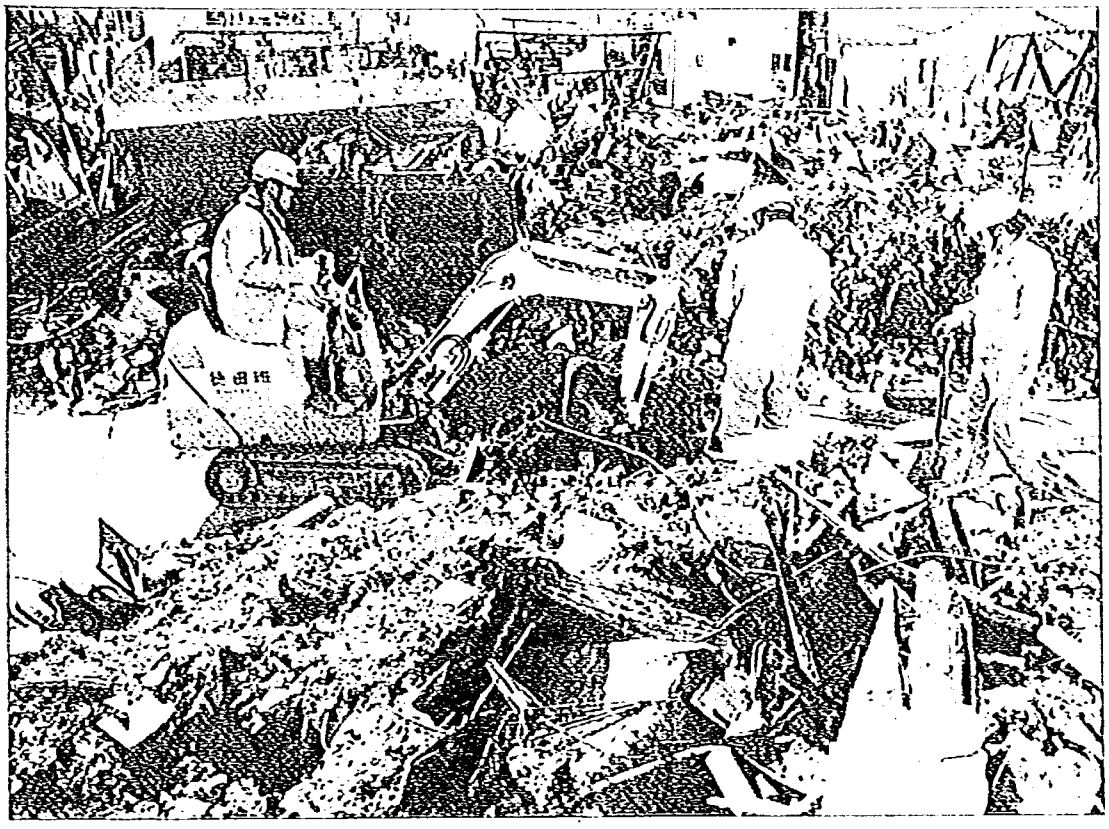


Photo 9 Gas restoration work amid rubble

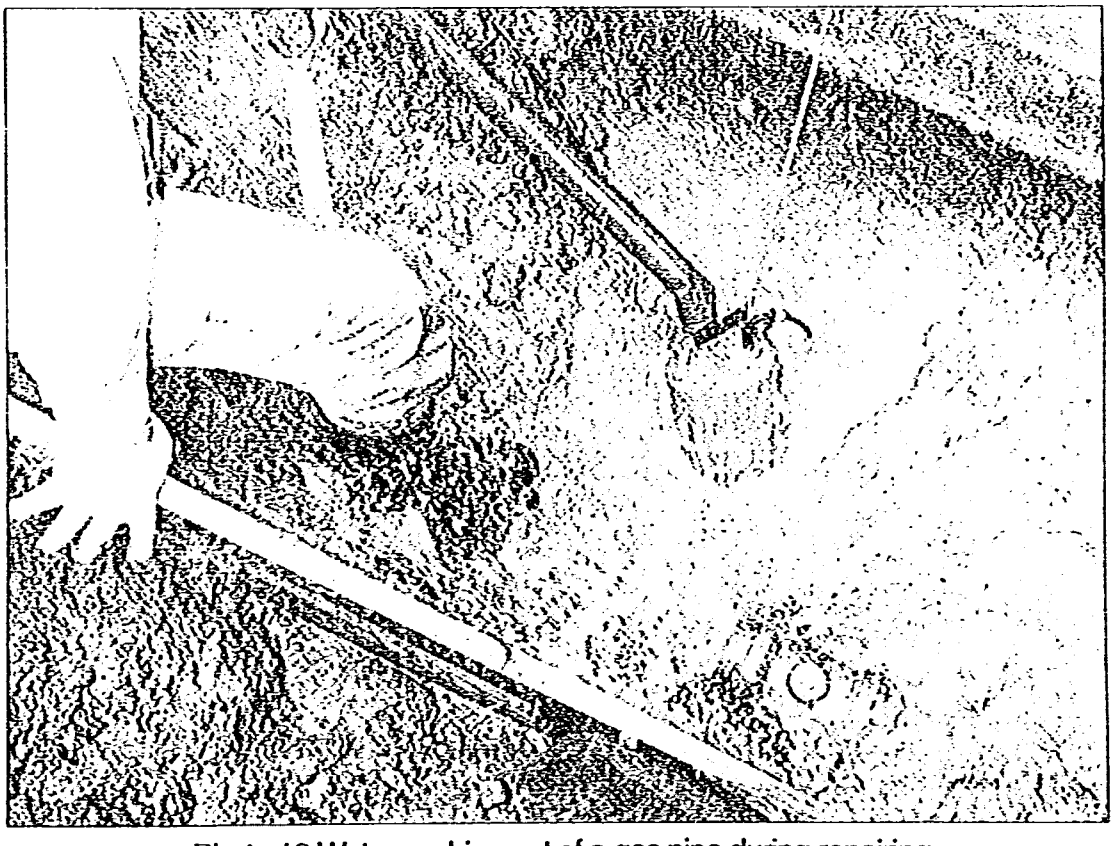


Photo 10 Water gushing out of a gas pipe during repairing

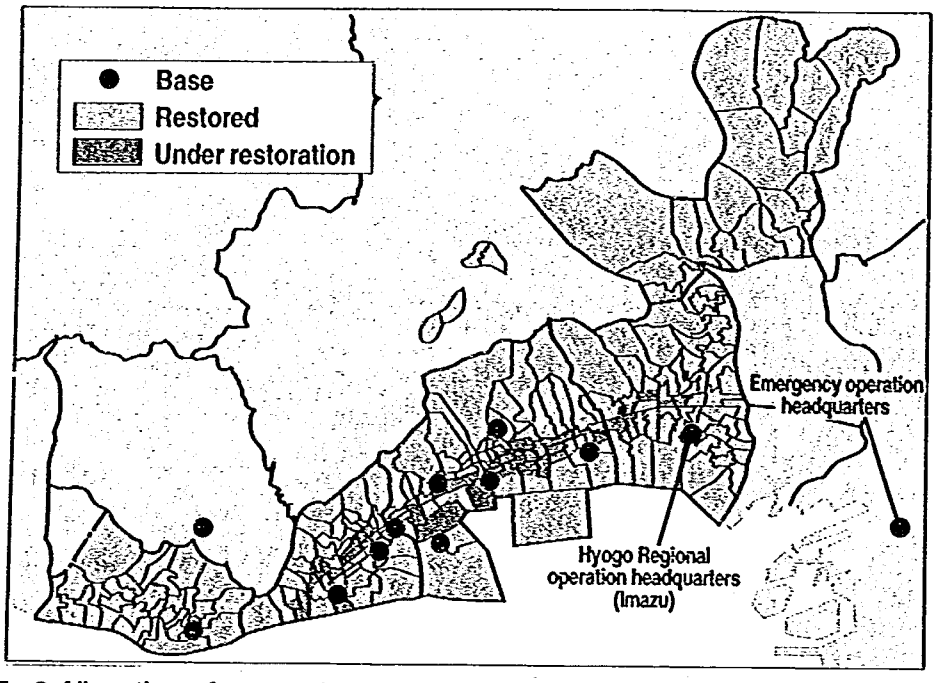



Fig.8 Allocation of restoration sectors and operation bases (End of March)

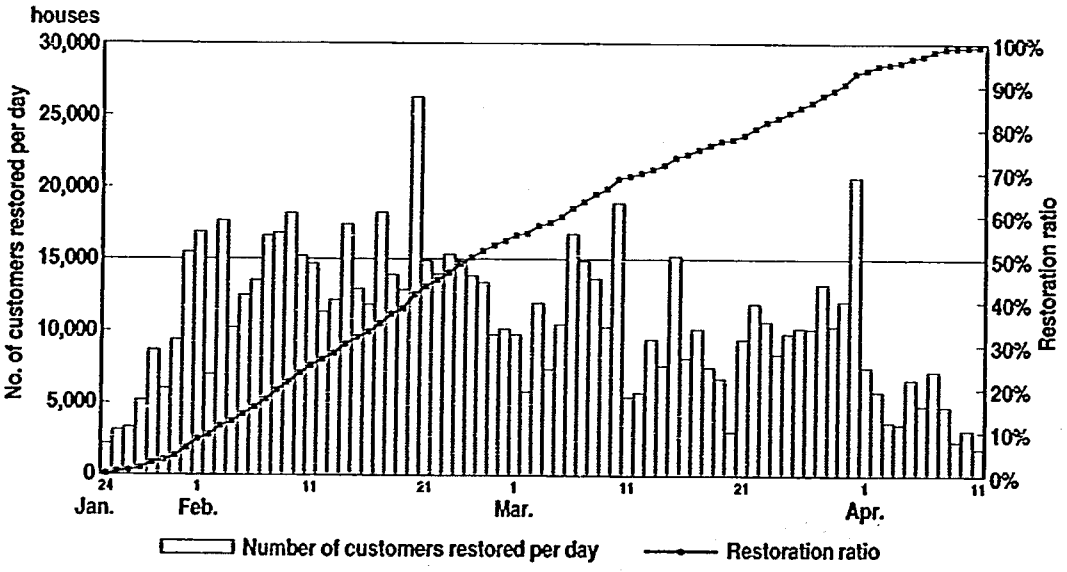



Fig.9 Progress of restoration

## TEMPORARY SERVICES TO MEET CUSTOMER NEEDS

As we suspended the gas supply over an extended region, we immediately started to supply alternative fuels to hospitals and other institutions which had important social functions. The alternative fuels included portable cooking stoves, LPG (liquid propane gas) bombs, LNG (liquefied natural gas), CNG (compressed natural gas) and LPG air.

We also installed temporary showering facilities at places used as shelters, and temporary baths at our premises and those borrowed from other private corporations, for the convenience of local residents. Total man-times of the use of our showering facilities and baths reached about 90,000.

For customers whose gas supplies cannot be restored because the restoration works were blocked by heaps of rubble made in the final stage of wreckage removal, we offered them LPG burning baths and heat sources for cooking with the cooperation of other companies.

## PROGRAMS TO MAKE THE GAS SUPPLY SYSTEMS EARTHQUAKE-RESISTANT

To be earthquake-prepared, it is most important to make facilities earthquake-resistant and, if ever earthquake disaster occurs, to prevent secondary disasters from taking place and make provisions to complete restoration works as early as possible. We are studying to add the following measures to our existing anti-earthquake measures:

* More extensive use of polyethylene and other pipe materials which have higher strength against earthquake
* Earlier installation of intelligent gas meters to all households
* Installation of additional seismometers
* Subdivision of isolation blocks

In addition to these measures, we plan to implement disaster programs paying due consideration to a report expected from Anti-earthquake Gas Supply System Study Committee which is currently studying the requirements for anti-earthquake measures as a private advisory body of Director General of the Agency of Natural Resources and Energy.

## ACKNOWLEDGEMENT

We could resume the gas supply service to 860,000 customers in a short time, less than three months. We owe this achievement very much to the cooperative understanding and efforts of the government organizations, local administrative bodies, many companies and customers. We would like to express hearty thanks to these organizations and numerous people.

## REFERENCE

Eguchi, H. (1995)Effect of Hanshin-Awaji Earthquake on town gas system. Proceeding of the ENERGY SYMPOSIUM-95 (to be printed), Tokyo:Waseda University

# IMPACT OF THE EARTHQUAKE OF SOUTHERN HYOGO PREFECTURE ON ELECTRIC POWER FACILITIES

by
Tohru YOSHIKAWA
Yoshiaki MINO

The Kansai Electric Power Co., Inc.
3-22, 3-Chome Nakanoshima, Kitaku, Osaka 530, Japan

## ABSTRACT

On January 17th 1995, a strong earthquake occurred directly beneath southern Hyogo Prefecture. The Kansai Electric Power Company suffered heavy damage of the facilities and power service was disrupted for approximately 2.6 million customers. The company completed emergent restoration 6 days after the earthquake.

## 1. PREFACE

The Kansai Electric Power Co., Inc. (Kansai Electric) is one of the nine major investor-owned electric utility companies in Japan. The service area of the Company is located in the central part of the main island in the Japanese archipelago. The area has a population of about 20 million people, and the Company supplies electricity to 11.7 million customers in the area. The region, generally known as "Kansai", constitutes an economic area of prime importance for the nation, ranking second to the Tokyo metropolitan area.

The total installed generating capacity is 35,035 MW that is composed of 9,768 MW of nuclear power, 18,581 MW of fossil fuel power and 6,686 MW of hydroelectric power. The backbone of the main power system is a 500 kV radial configuration. (Figure-1)

The Southern Hyogo Prefecture Earthquake occurred at 5:46 a.m., on January 17th this year with a magnitude of 7.2 on the Richiter scale. The epicenter was located in the northern tip of Awaji Island, and the earthquake focus was at a depth of about 20km. It was only about 20km away from the center of Kobe City where about 1.5 million people live. The earthquake took the lives of more than 5,500 people, destroyed about 180,000 buildings and private houses, collapsed railways, expressways and seaports.

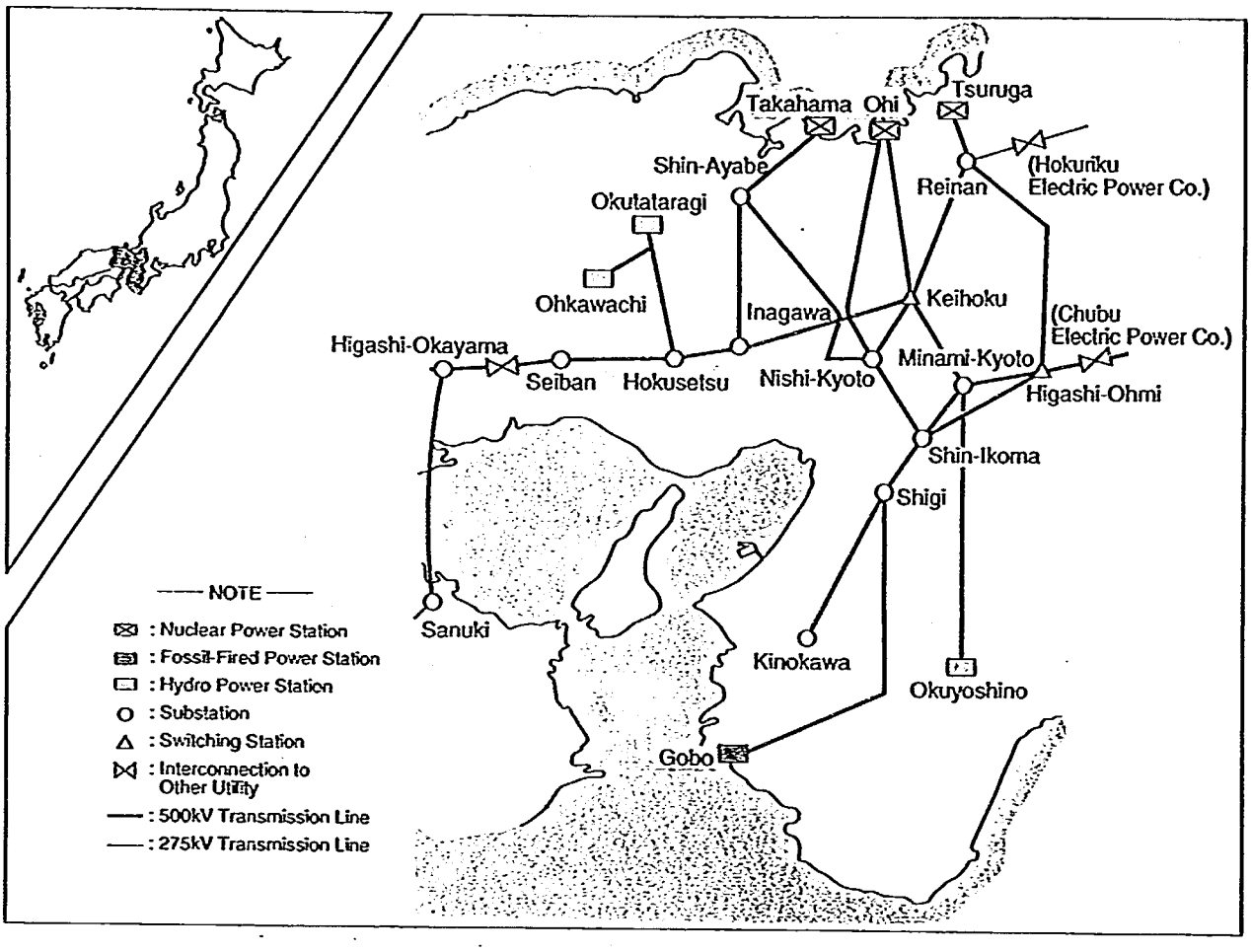



Figure-1 Power System in 1994 (Present)

The facilities operated by Kansai Electric also suffered major damages from the tragic earthquake. The number of customers without power amounted to approximately 2.6 million. Restoration activities were carried out with four steps, that is, emergent power supply, temporary restoration, permanent restoration and full scale reconstruction. Considering the importance of electricity as life line, Kansai Electric made utmost effort for restoration and it completed emergent restoration on January 23rd.

## 2. SUPPLY AND DEMAND OF ELECTRICITY

### 2-1 Generation and Load Balance Immediately after the Earthquake

Kansai Electric lost 1,760 MW of power generation immediately after the earthquake. Loss of load due to damage to the power system, however, was greater than the loss of generation. As a result, the frequency increased by 0.45 Hz, and the voltage at the 500 kV Hokusetu and Inagawa substations, which supply electricity to the greater Kobe region, went up by 20 kV. The central load

dispatching center decided to operate pumped storage power stations and managed to stabilize the frequency in few minutes. (Figure-2)

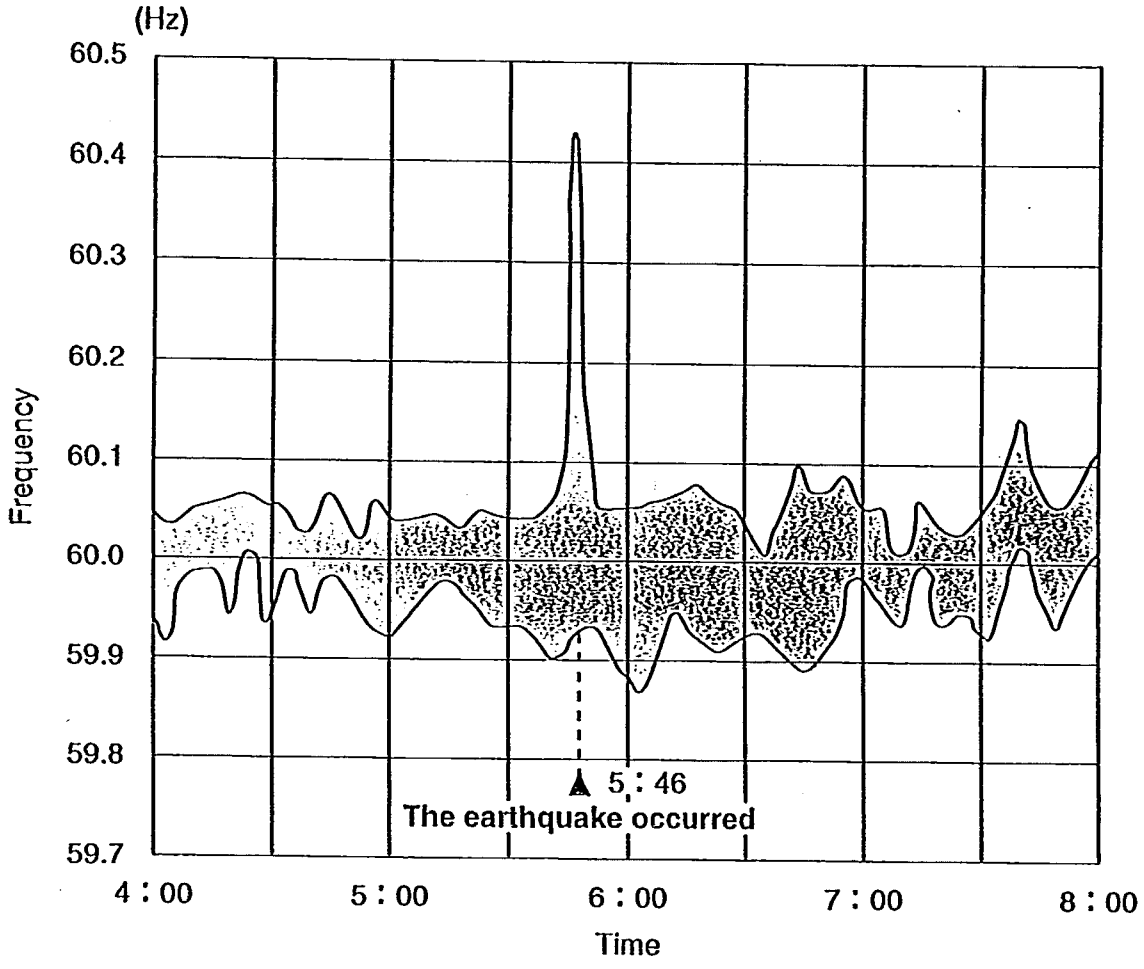
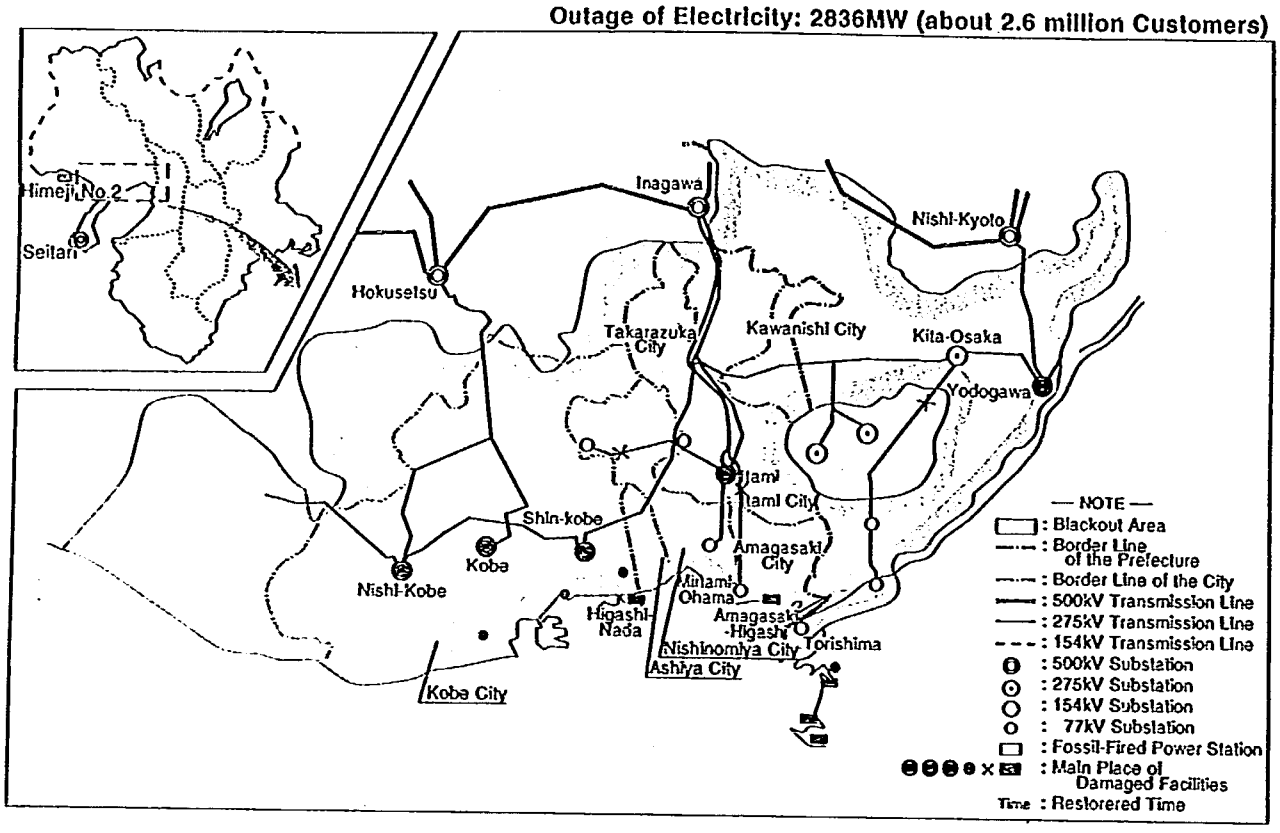



Figure-2 Frequency at January 17, 1995

2-2 Interruption of Electricity Supply

Immediately prior to the earthquake, The Kansai Electric Power Company's total electric power demand was on the order of 13,000 MW. The earthquake took roughly 20 % of the total power system out of operation. Six 275 kV substations, the Yodogawa, Kita-Osaka, Itami, Sin-Kobe, Kobe, and Nishi-Kobe substations, and two 154 kV substations, the Torishima and Minami-Ohama substations, were damaged by the earthquake vibrations and completely out of service. As a result, power supply was cut off throughout a wide area stretching from Akashi City in Hyogo Prefecture to the southwestern region of Kyoto Prefecture. The areas affected by the outage of electric power represented a total demand of 2,836 MW from approximately 2.6 million customers. (Figure-3)




Figure–3 Blackout Area just after the Earthquake

2–3 Restoration of Electricity Supply

Immediately after the earthquake, operators on nightduty began to inspect and restore the power system by switching properly functioning equipment at disabled substations over to systems that were still running. At about 7:30 a.m., two hours after the earthquake hit, the number of customers left without electricity had been reduced to approximately 1.0 million, mostly in Kobe and Nishinomiya cities.

At the same time Kansai Electric organized the Emergency Countermeasure Headquarters in its Head Office for obtaining information of damages and establishing restoration organization, and began to carry out repairs to damaged facilities.

The other electric power companies of Japan provided assistance to Kansai Electric by sending mobile generator vehicles, personnel for restoration activities.

By 8:00 a.m. on January 18th, one day after the earthquake occurred, all of the substations were restored to a temporary operating condition, and the number of customers left without electricity was further reduced to about 0.4 million.

The restoration work on the distribution lines was carried out under extremely difficult circumstances. Many of the roads were in poor condition, and it was necessary to confirm which buildings had collapsed or were unoccupied.

The emergent restoration works were completed by 3:00 p.m. on January 23rd, just over six days after the earthquake hit. After emergent restoration activities, providing against the rainy season, peak demand of summer and typhoon, Kansai Electric has been continuously making efforts to enhance facilities safety and increase distribution capacity. As for the permanent restoration it is expected to take six to twelve more months except Higashi-Nada Gas Turbine Power Station that was damaged heavily. (Figure-4)

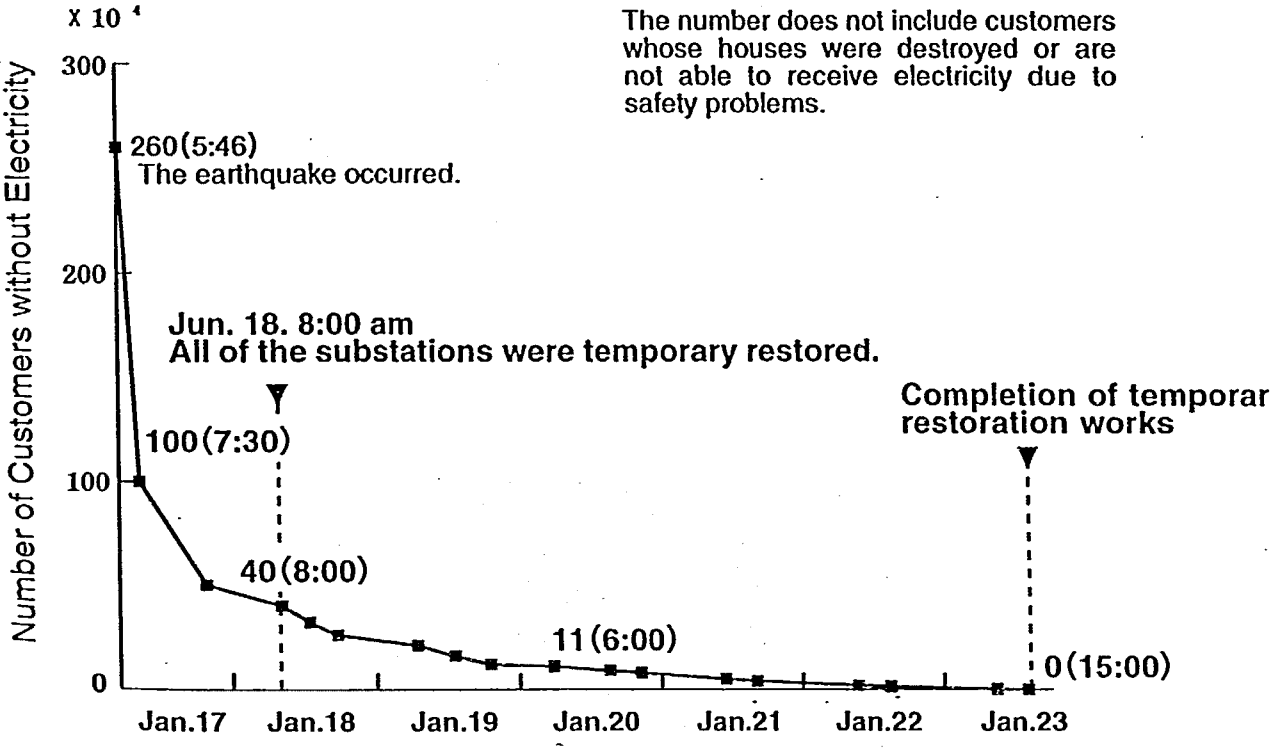



Figure-4 Number of Customers without Electricity

## 3. EARTHQUAKE DAMAGES TO ELECTRIC POWER FACILITIES

### 3-1 Generation Plants

The earthquake did not damaged any nuclear power generation plants or hydroelectric power generation plants.

The Kansai Electric operates 21 fossil-fired thermal generation plants, comprising 64 units. Among these, 20 units located at 10 different power stations suffered damage, typically to the boiler tubes. (Figure-5)

All the units necessary to meet immediate demand were up and running by January 27th. With a just few exceptions, the damages of the other units had been repaired by the beginning of February.

However, it will probably take until June of 1996 to resume full operations at the Higashi-Nada Gas Turbine Power Station having two 60 MW generators. This particular power station is located near the epicenter, and suffered serious damage from the earthquake. Land subsidence occurred through the power station, and caused the uneven settlement of the soil beneath the foundations supporting major equipment.

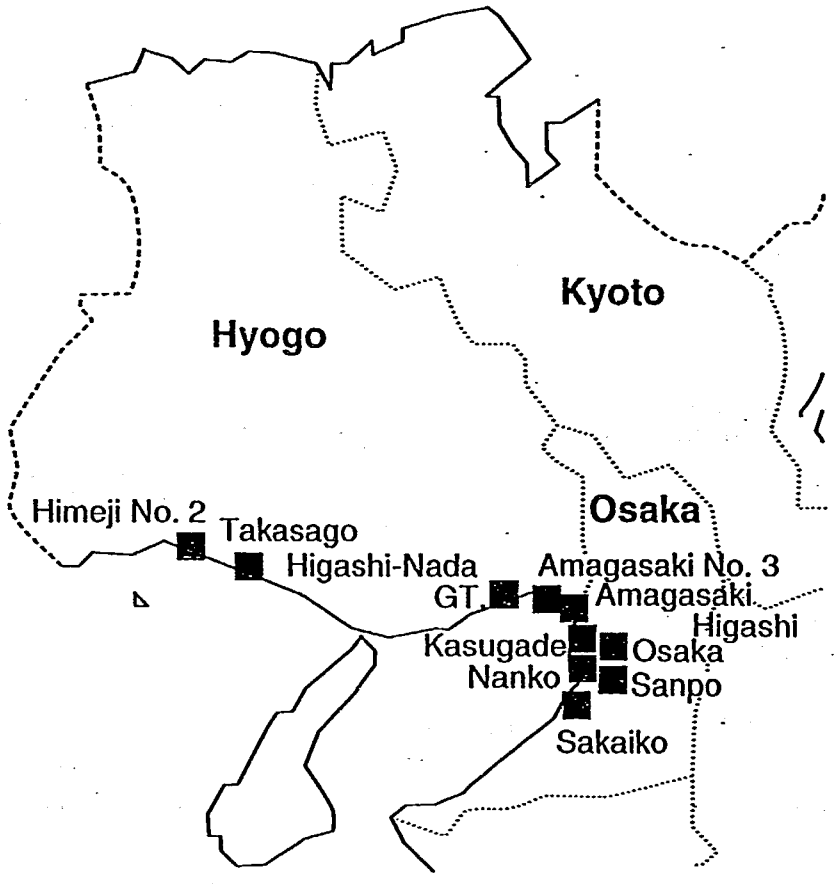



Figure-5 Power Stations Damaged by Earthquake

### 3-2 Transmission Lines and Substations

The earthquake did not cause any damage to the 500 kV facilities which form the backbone of power system. There was, however, substantial damage to the 275 kV and lower voltage facilities. Including minor incidents, damages occurred at 50 substations and along 112 transmission lines. (Figure-6)

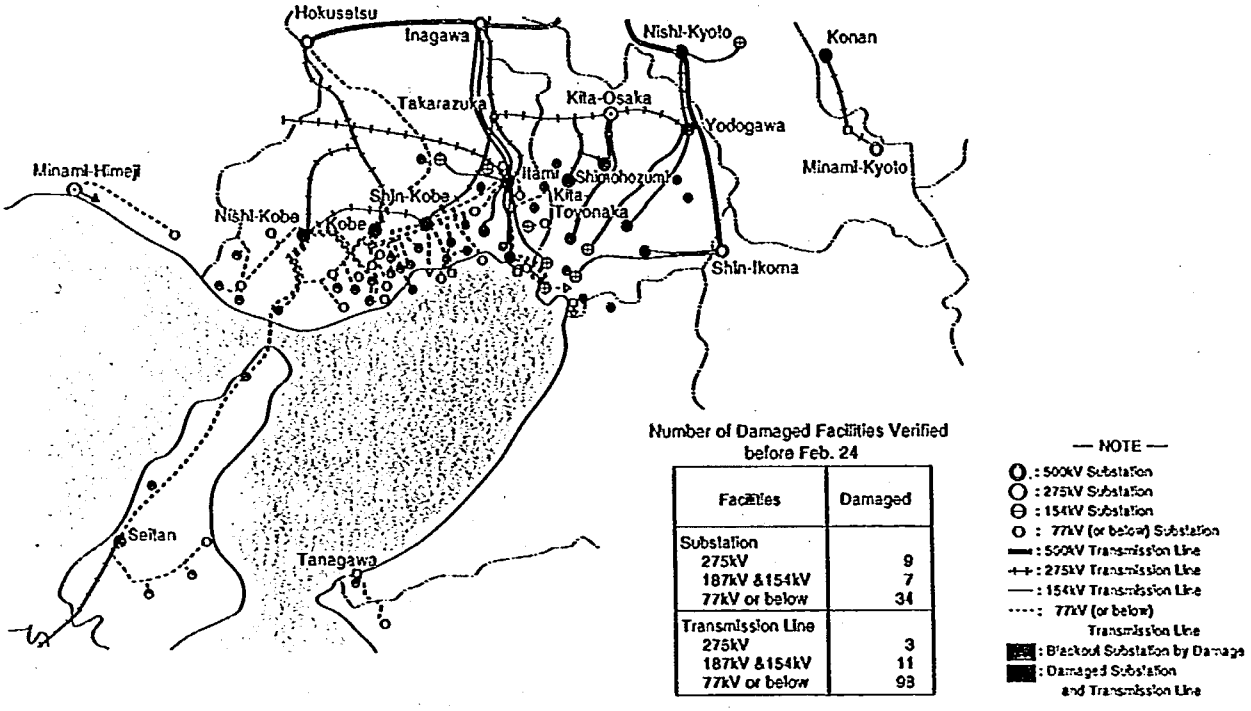



Figure-6 Substations and Transmission Lines Damages by the Earthquake

(Transmission Lines)

The overhead transmission lines suffered damages along 23 lines, mostly in the Kobe region. This included damage to structural members of the steel transmission-line towers and the damage to long-rod insulators used to fix jumpers. (Figure-7)

The damage to the steel towers was not directly caused by the earthquake motion. Rather, this damage was caused by fissures, slippage, and other dislocation in adjacent land areas, which displaced the tower foundations, and thus caused damaged to the structural members.

The damage to long-rod insulator was caused by the earthquake motion. Damage to underground transmission lines has been found along 102 lines, and the damage surveys in detail are still underway. The greatest damage was apparently located in those areas subject to the most intense earthquake movement, primarily in flat areas in the Kobe and Amagasaki regions along the waterfront of Osaka Bay.

A large number of the power cables suffered deformations and other abnormalities, but were still capable of power transmission. Only three of the cables were completely damaged and could no longer carry electricity.

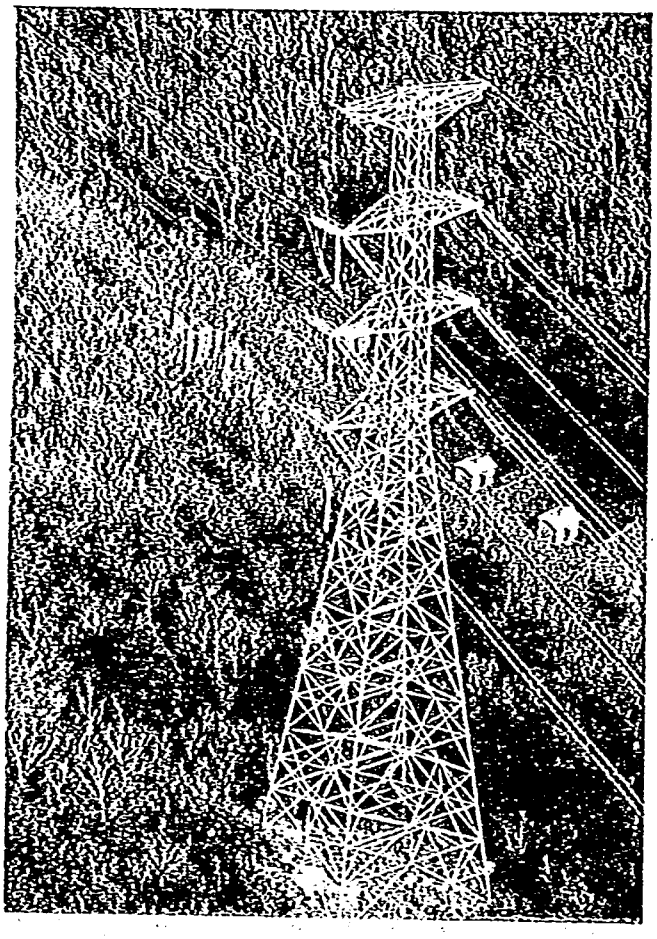
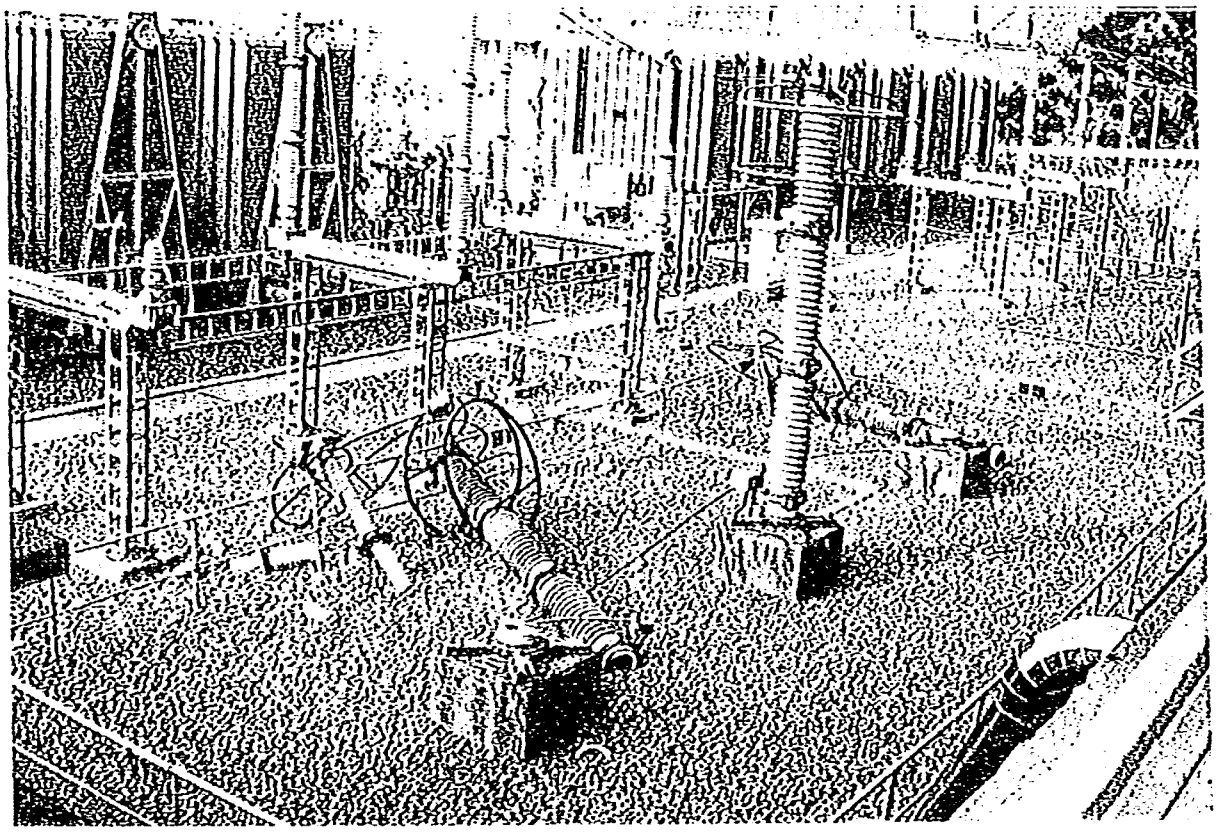


Figure-7 275 kV Hokushin-Line Tower No.37

(Substations)

The damage to the substations was also widespread, with a total of 181 incidents reported at 50 substations including the 275 kV Itami, Shin-Kobe, and Nishi-Kobe substations.

These incidents included damage to 17 transformers, which slipped out of place when the bolts which anchor these transformers to their foundations broke off; oil leakage from the bushings at 8 circuit breakers because the bushings slipped out of position; and breakage of the support insulators of 22 disconnect switches. (Figure-8)



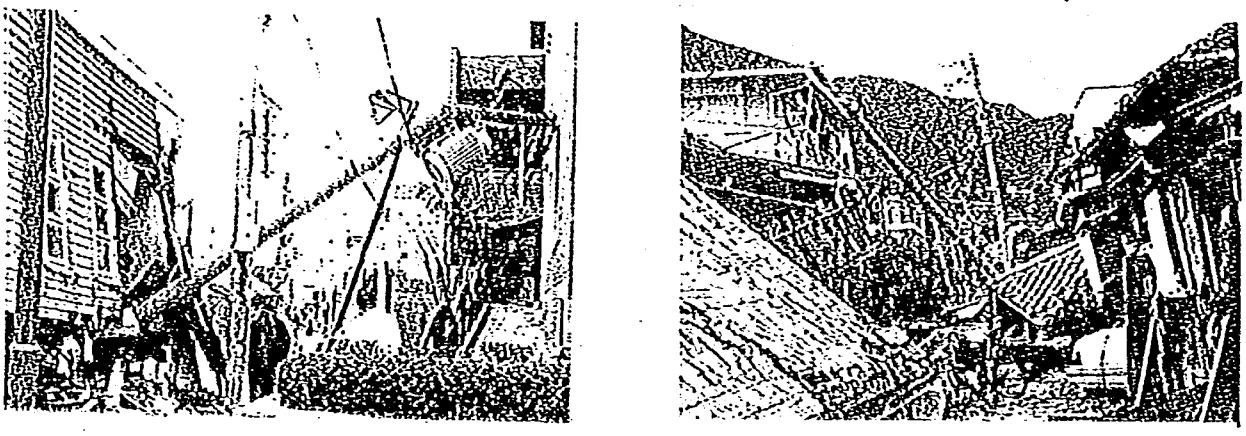
Figure–8 275 kV Arresters and Disconnect Switches

3–3 Distribution Lines

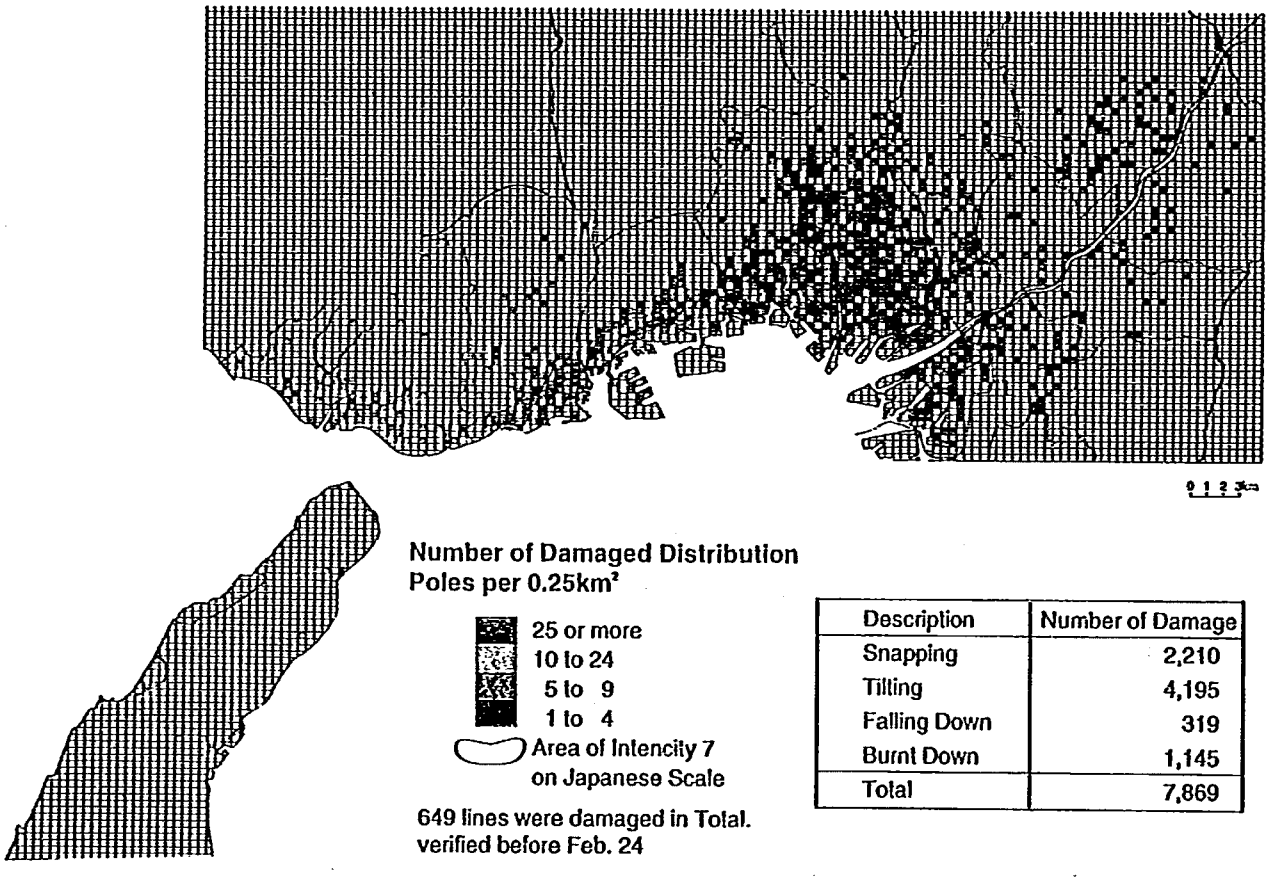
Troubles were reported at 649 circuits because of earthquake damage to the distribution lines.

Distribution poles fell over or were broken when buildings collapsed. (Figure -9) The distribution poles tilted over and the distribution lines were broken off because of problems in the underlying soil structure including liquefaction and subsidence.

Approximately 8,000 distribution poles were damaged by earthquake, and indeed the greatest damages occurred in those areas which were subject to intensity of "7" earthquake vibrations. (Figure-10)



Figure–9 Damage to the Overhead Distribution Lines




| Description | Number of Damage |
|---|---|
| Snapping | 2,210 |
| Tilting | 4,195 |
| Falling Down | 319 |
| Burnt Down | 1,145 |
| Total | 7,869 |

Figure–9 Distribution Chart of the Damage to the Distribution Poles

The underground distribution lines and their auxiliary equipment also suffered various types of damage. The transformers and other ground-mounted equipment for these lines were subject to tilting and deformations from shifts in the structure of the underlying soil.

Also, the underground ducts which the distribution cables run through suffered various damages, including the collapse of the ducts' side walls.

## 4. KEY POINTS FOR THE RAPID RESTORATION OF ELECTRICITY SUPPLY

As mentioned earlier, electric power was almost fully restored to the entire disaster area within seven days. Considering the extreme destruction caused by the earthquake in and around Kobe City, Kansai Electric was successful in restoring electricity supply rather quickly.

The following five points are considered as key which ensured the rapid restoration of electricity supply following the massive earthquake.

### 4-1 A Robust and Flexible Power System(Linked system with the 77 kV network)

The first critical point was a robust and flexible power system. In other words, to switch over from the damaged 275 kV system to the properly functioning 77 kV system reduced the area suffering from power outages within a relatively short period of time. (Figure-11)

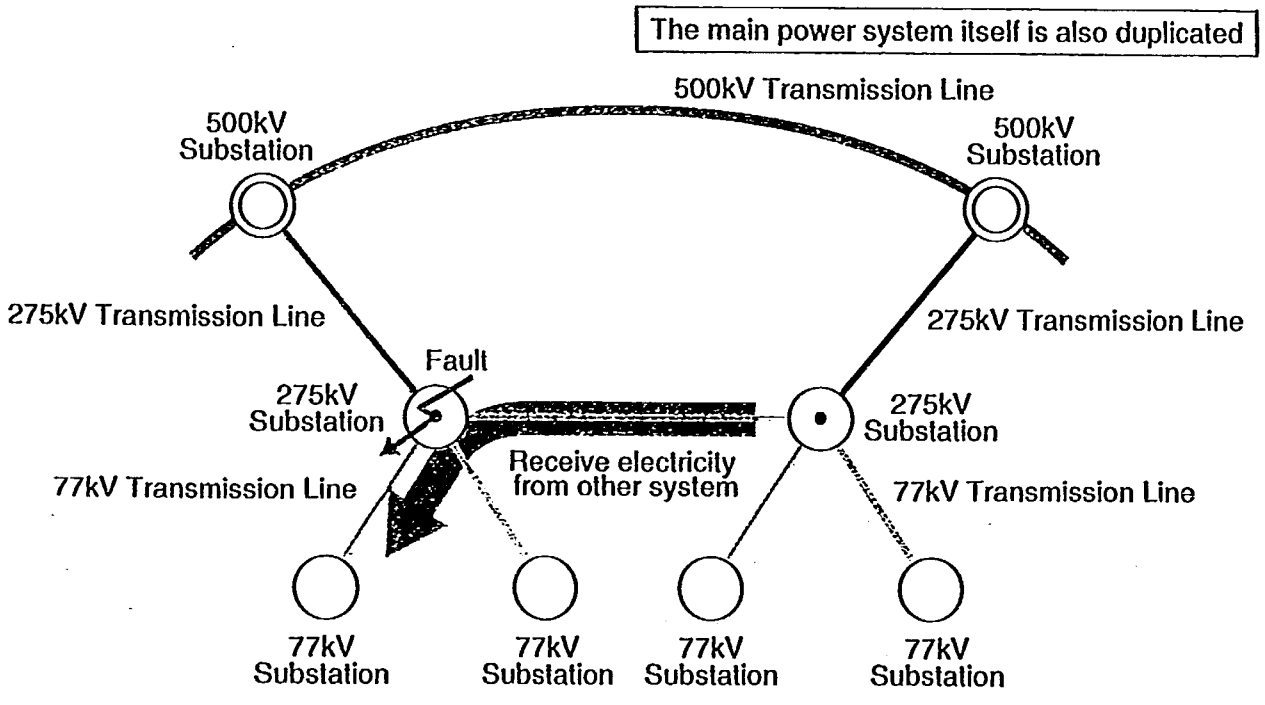



Figure-11 Switching Over to the 77 kV System when a 275 kV Substation Fails

### 4-2 Restoration by Overhead Distribution Lines

The second key point was the restoration of the damaged distribution network by using overhead distribution lines

The overhead distribution lines were used for temporary restoration in order to restore electricity supply quickly. Temporary restoration was conducted utilizing high-voltage power generation vehicles, and all the undamaged equipment and materials remaining at the damage sites to the greatest possible extent. That included reinforcement of broken power poles, straightening of tilted poles and so on. Damaged poles would be replaced along with reconstruction of roads.

In particular, because it takes a long time to identify the damaged sections of underground cables, overhead lines were used to by-pass the damaged cables for temporary restoration at several locations.

### 4-3 A Private Communications System with Strong Aseismic Design

The third factor contributing to the rapid restoration of power supply was the fact that the communications system was not damaged by the earthquake.

The Kansai Electric maintains a microwave communications system linking the central load dispatching center with all of the main power stations and substations. It has own independent telephone system using microwaves and fiber optic cables. Because these systems suffered no damages from the earthquake, it was very smooth to conduct all the communications necessary for the restoration works using private communications systems.

In the aftermath of the earthquake, the public telephone system were jammed so that the private telecommunications systems were a critical factor in the restoration works.

### 4-4 Nationwide System for Assistance from Other Electric Power Companies

The fourth factor contributing to the rapid restoration of electricity supply was the generous assistance provided by other electric power companies.

In addition to dispatching a total of 319 personnel, the electric power companies provided diverse types of material assistance including high-voltage power generation vehicles; working vehicles; vehicles equipped with satellite communications facilities; electrical materials. (Figure-12)

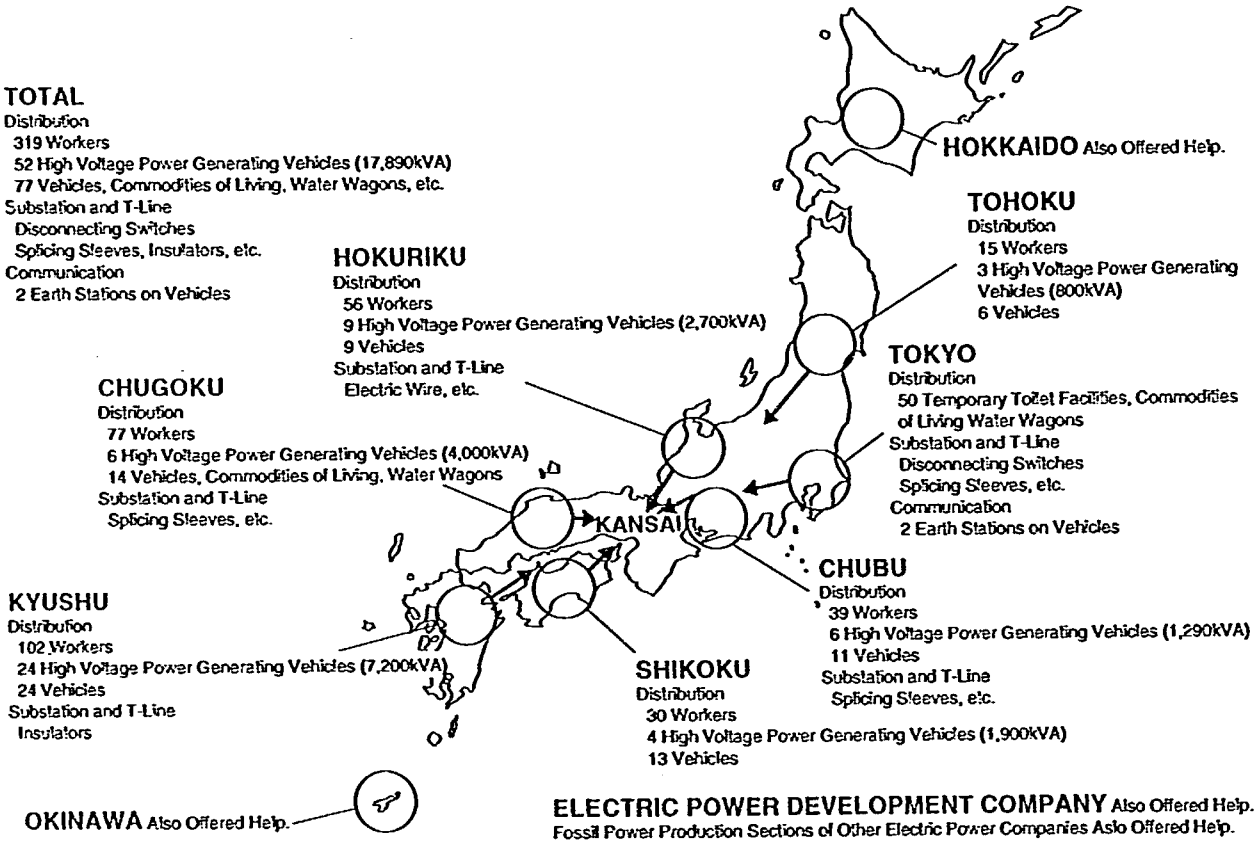



Figure-12 Assistance from Other Electric Power Companies throughout Japan

4-5 Aseismic Design

The fifth point was aseismic design that had been upgraded repeatedly based on past experience with earthquakes.

Kansai Electric has been systematically incorporating aseismic design for all main facilities ever since the 1978 Off-Miyagi earthquake. Although some facilities were damaged, application of aseismic design made it possible to avert any fatal damaged from this massive quake. In the areas which were subject to intensity of 7, 14 of 20 substations constructed before 1974 were damaged. But non of 9 substations constructed after 1975 were damaged. (Table-1)

Table-1 Evaluation of Aseismic Design at Substations in Seismic Intensity 7

| | before 1964 | 1965~1974 | 1975~1984 | after 1985 | Total |
|---|---|---|---|---|---|
| Damaged Substation | 7 | 7 | 0 | 0 | 14 |
| Substations Not Damaged | 0 | 6 | 6 | 3 | 15 |
| Total | 7 | 13 | 6 | 3 | 29 |
| % of Damaged Substations | 100% | 54% | 0% | 0% | 48% |

## 5. GEOLOGICAL ASPECT OF HEAVILY DAMAGED FACILITIES

### 5-1 Higashi-Nada Gas Turbine Power Station

This power station having two 60 MW generators, was constructed in 1974 on a corner of reclaimed land. It suffered a heavy damage from strong motion and geological disaster such as liquefaction and uneven settlement.

The ground is roughly composed of reclaimed soil of 15m thick, alluvial clay of 10 m thick and diluvial sand and gravel.

Each tank of water or fuel was supported by concrete slab and prestressed concrete piles driven into diluvial layer, N values of which were more than 35. But any countermeasures had not been carried out to liquefaction. Throughout the power station there were found reclaimed materials spouted by liquefaction and land subsidence. Tank itself did not suffer any damage or leakage of oil and water. (Figure-13)

The gravity-caisson type shore-protection walls had been put on rock mound, clay beneath which was replaced with sand. Displacement of these walls caused sinking and cracks of land.

Needless to say, these disasters in the ground caused damage, displacement and tilting of equipment and piping.

Reconstruction work of this power station including ground-improvement, is scheduled to complete before peak demand season next year.

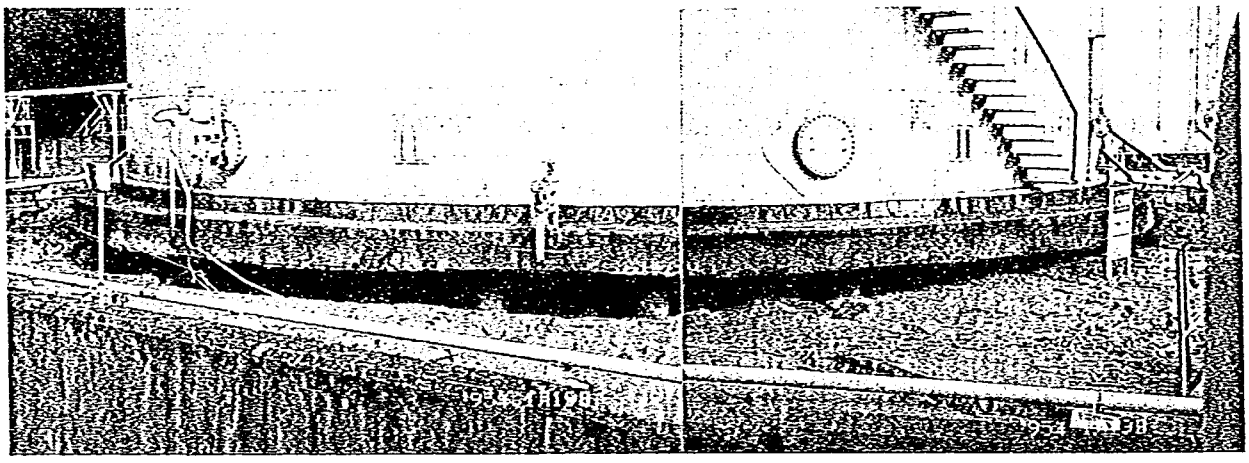


Figure-13 Liquefaction at Higashi-Nada Gas Turbine Power Station

5-2 Shin-Kobe Substation

This substation is located halfway up Rokko mountains and has four transformers constructed one-after other during 1962 through 1971. The land was developed cut and bank method. The maximum height of cutting was about 50 m and banking about 15 m. This substation is distant 24 km from the epicenter and observed acceleration was 584 Gal horizontally and 495 Gal vertically. (figure -14) The strong motion broke many equipments and the anchor-bolts of a transformer, slid the transformer, caused sinking and cracks in the ground and displaced the retaining walls.

Why so strong motion observed near rock foundation? Is it caused due to banking? It is most important to study about how the earthquake wave amplifies during transmission from underground to surface. Considering that rock foundation is not so deep and the observation of the earthquake is reliable, some geological surveys have been carried out at this substation.

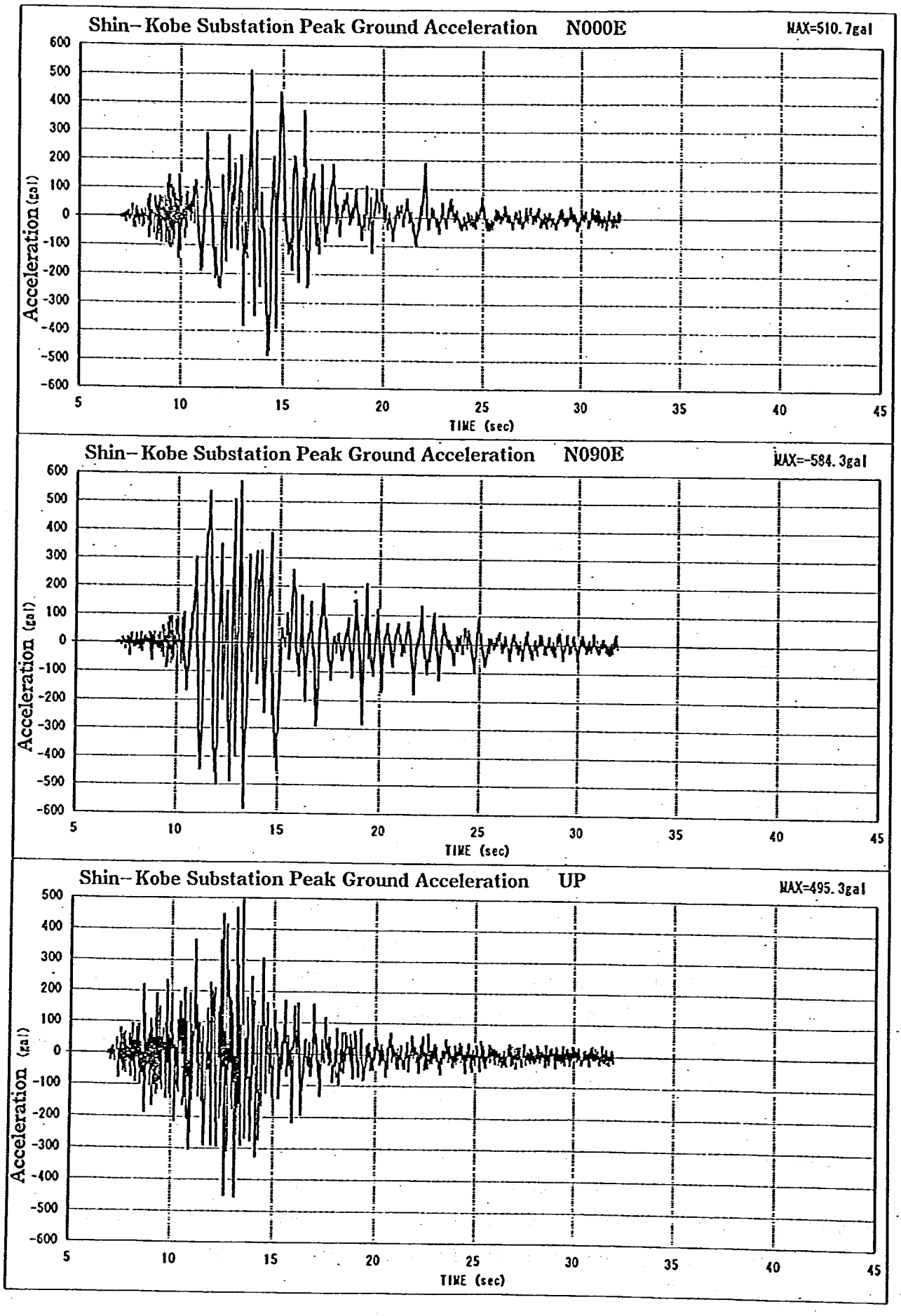



Figure-14 Acceleration Observed at Shin-Kobe Substation

## 6. CONCLUSION

6-1 The facilities operated by Kansai Electric suffered major damages, but the temporary restoration works were completed six days after the earthquake.

6-2 The followings points are considered as keys for rapid restoration of electricity supply.

(1) A robust and flexible power system
(2) Restoration by overhead distribution lines
(3) A private communications system with strong aseismic design
(4) A nationwide system to receive assistance from other electric power companies
(5) Application of aseismic design

6-3 It is verified that highly earthquake resistant facilities perform quite well.

6-4 Reliability of the facilities is greatly affected by geological condition as mentioned in the case of Higashi-Nada Gas Turbine Power Station. Some studies are being carried out to verify the relationship between ground motion and geological condition.

# Damage of Underground Telecommunication Facilities in the 1995 Great Hanshin Earthquake

by Kenichi Honda , Yuzo Yamaguchi and Shinji Mataki

NTT Access Network Systems Laboratories

## ABSTRACT

This paper shows that damage of underground telecommunication facilities in the 1995 Great Hanshin Earthquake. We had checked underground telecommunication facilities as soon as after this earthquake. And also we carried out the field survey of length between manholes and ground level of manhole sections in Port Island and Sumiyoshihama-cho area.
We have been investigating the trend of facilities damage in view of facilities type , ground condition and ground motion , by those results of facilities check and field survey.
In this paper, we mentioned about the trend of facilities damage and the relation between facilities damage and ground displacement by field survey.

## Introduction

The great earthquake that hit the southern part of Hyogo Prefecture on the morning of January 17, 1995, registered seven on the JMA scale, caused the worst disaster that had never happened before, and did serious damage to railways, highways, means of public transport and lifeline facilities. And telecommunication services suffered heavy damage from this earthquake on an unprecedented scale. Since the influence of the earthquake extended wide and far, the most severe damage by the earthquake was concentrated primarily in the whole areas of Kobe City, Ashiya City and Nishinomiya City.

## Damage to the communications service by the earthquake

On the morning of the earthquake, the telephone service with a total of 285,000 telephone lines was suspended because of the breakdown of a local exchange from power failure. It took about 2 weeks to restore this service. (Fig.1) In addition to the fact that the earthquake had a seismic intensity of seven on the JMA scale, the liquefaction of saturated sandy soils resulting from this

earthquake mostly in reclaimed land near Port Island and along the seashore caused the serious damage, which had to have a profound influence on the telephone service, to the underground facilities such as the conduit and manhole within which communications cables had been installed. Only part of the whole length of the underground cable of those earthquake-stricken areas suffered heavily damage.

The telecommunication network, cables laid in the area of a city falls into two classes: the overhead type one built with utility poles in the sky and the underground type. Generally speaking, the latter type suffered slight damage, while the former type suffered heavily either from fire or the collapse of houses. This fact conclusively has revealed that the latter is noted for reliability more than the former.

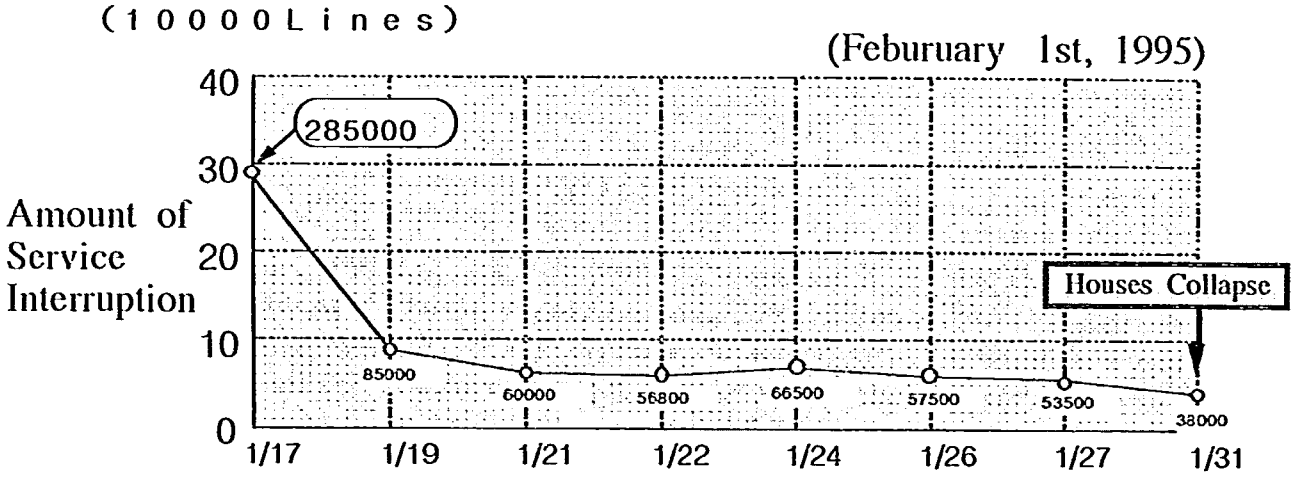



**Fig.1 Restoration of telephone service**

## Damage to the underground telecommunication facilities

### ◆ Outline of the damage

In the Table.1, the increase in the earthquake resistance of underground facilities was initiated in view of the dynamic characteristics of some of the strong earthquakes that had occurred in the past. Soon after the Miyagi-Ken Oki Earthquake occurred in 1978, a thorough investigation into the development of the duct sleeve and the seismic joint began. The former is set at the place where conduits and manholes are joined together and permits contraction or expansion of the joint, while the latter is inserted in a conduit run to provide for the expansion or contraction of the conduits and serves to prevent it from becoming separated. In 1982, the application of either of these devices to underground facilities began. The devices serve to improve either the ability of conduits to follow in response to the behavior of the ground during earthquakes or the resistance of underground facilities to earthquakes.(Fig.2)

| Events | Measures for underground facilities |
|---|---|
| 1964<br>Niigata Earthquake | ◇Improvement of steel conduit joints |
| 1968<br>Tokachi-oki Earthquake | ◇Laid direct burial cable into conduits |
| 1978<br>Miyagiken-oki Earthquake | ◇Improvement of conduit joints<br>(Duct Sleeve,Expansion Joint, Stopper Joint)<br>◇Apply stopper joint to approach bank of abutment |
| 1983<br>Nihonkai-chubu Earthquake | ◇Apply steel conduits,stopper joints and gavel drain method in liquefiable ground |

**Table.1 History of seismic measures for underground facilities**

The underground facilities to which one of the devices had been applied suffered little damage from this earthquake disaster. It has been shown that this type of conduits has much higher earthquake resistance. And it has been found that the damage done to an underground facilities varies in size according to the following three conditions: the first condition depends upon what structure the conduits is made up of; the second condition depends upon whether the ground, where it has been, is liquefied or not; and the third condition depends upon whether or not it is located in an earthquake-stricken area with a seismic intensity of 7 on the JMA scale. When it comes to damage, there is a significant difference in the amount of damage to underground

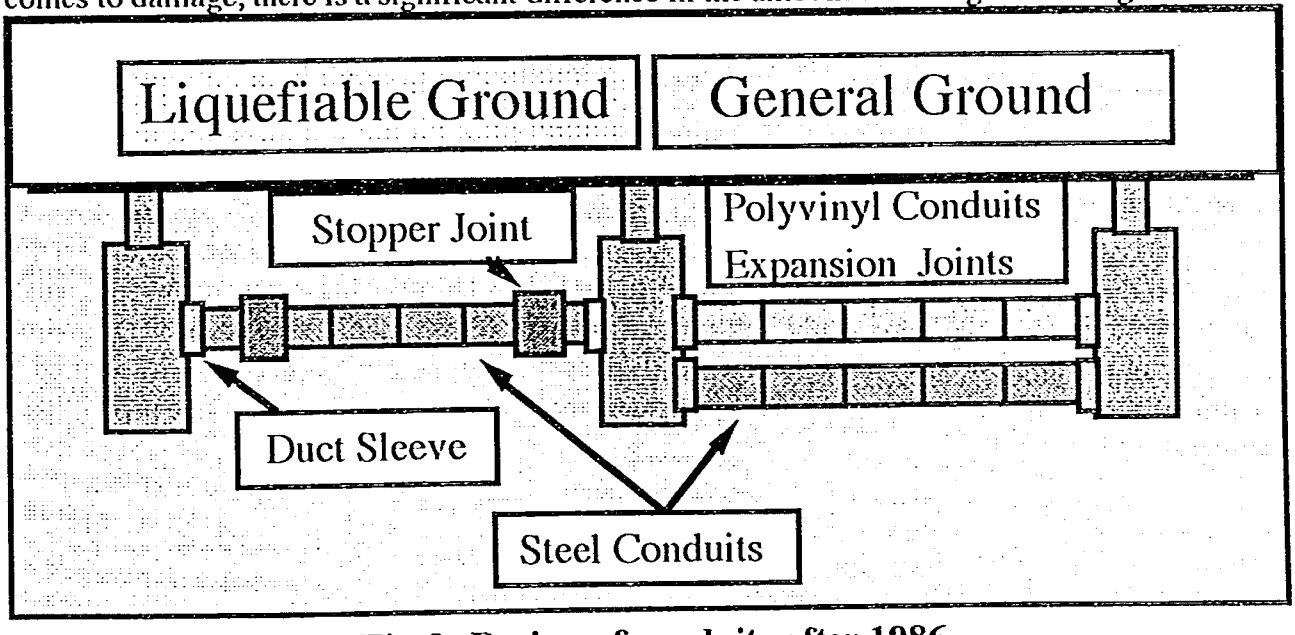



**Fig.2 Design of conduits after 1986**

facilities between the liquefied area with a seismic intensity of 7 and the unliquefied area with a seismic intensity of 6. Detailed surveys have revealed that the underground facilities made up of the same structure can be arranged, depending upon where they have been, in the order of decreasing damage: the liquefied area; the earthquake-stricken area with a seismic intensity of 7; and the earthquake-stricken area with a seismic intensity of 6. Support for the above argument can also be found from the observation. A thorough investigation of the damage done to those facilities in the liquefied and unliquefied areas is actively underway. It seems that the breaking off of conduits joints resulting from ground deformation in a liquefied area is more frequent than in an unliquefied area. A typical NTT underground conduits enclosing telephone cables that make connections between the subscriber's terminals and the telephone exchange center is given schematically in the Fig3. The main points of the damage to these systems may be summarized as follows.

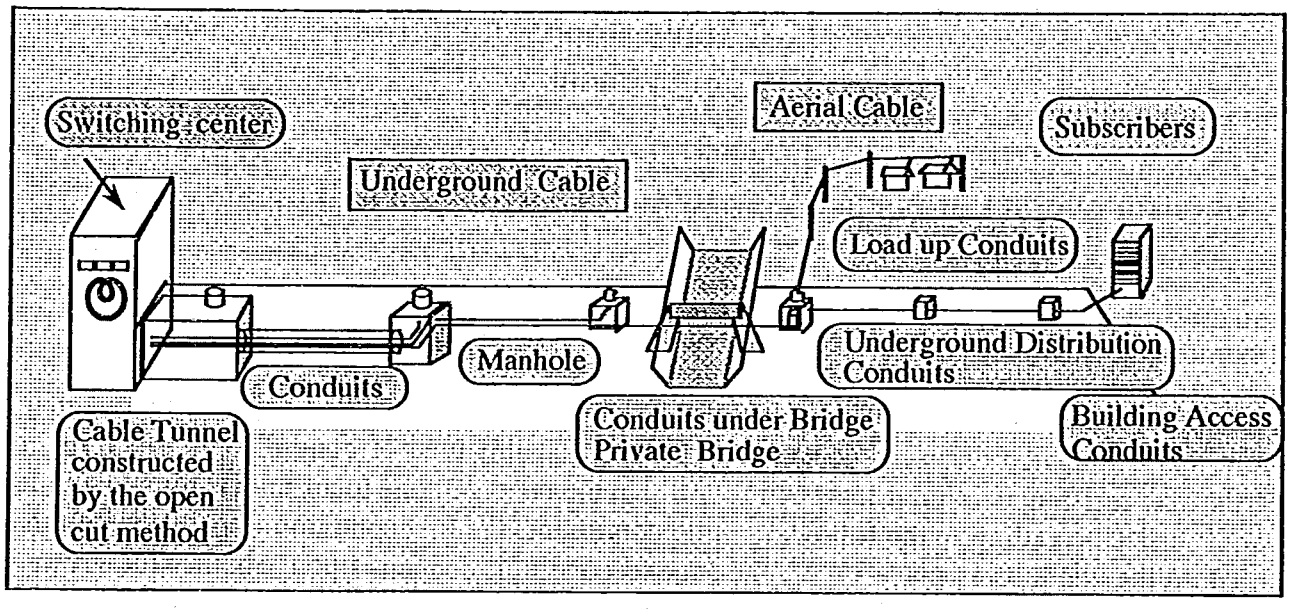



Fig.3 Underground telecommunication facilities from switching center to subscribers

## ◆ Open cut cable tunnels

There is an open cut telephone tunnel with a length of about 2 km in the City of Kobe. A quick check of the tunnel was made soon after the earthquake. As a result, a maximum of 18cm slide of expansion joint was found in the structurally-changing portion of the intermediate section between the telephone exchange center and the tunnel. On the other hand, muddy water gushed out of some parts of the tunnel, but all these problems exerted no bad influence on the whole structure of the tunnel. The exact place where liquefaction of the ground occurred was found to be one of the hardest hit sections of the open cut tunnel. However, this earthquake did no harm to shield cable tunnels.

### ◆ Conduits

A large system of conduits that had been connected with one another over a wide area suffered little damage that would have had a profound effect on the communications service. The coming off or breaking off of metallic conduits, the failure of polyvinyl conduits, and the peeling of cement mortar off the walls near the connections between the conduit and the manhole, which needed repairing, were found everywhere in some of the cities. Most of the conduits that had been laid throughout Kobe City were old and provided for no expansion or contraction. The damage by the earthquake was concentrated in those old type conduits. In the earthquake disaster survey that was carried out, a TV pipe camera was inserted into some 7,000 conduits, which had been laid in the underground of Kobe City, Ashiya City and Nishinomiya City, in order to make a quick check of the conduits. A detailed analysis of the check results is being made.

### ◆ Manholes

About 14,000 manholes had been installed chiefly in the hardest hit areas of Kobe City, Ashiya City, and Nishinomiya City, and then, about 15 % of these suffered some damage from the earthquake. The most common type of damage was cracks in the neck of some of the manholes. The dangerous crack that needed renewal was found in the body of some of the manholes. It has been found that uneven settlement of ground close to a manhole occurred in liquefied area.

### ◆ Building access conduits

It has been found in Port Island and the Kobe- Sannomiya Area that the settlement of about 30-50 cm in the ground near an approach to a building occurred. NTT uses an underground conduit enclosing communications cables to make connections to the subscriber's building. The uneven ground sinking due to liquefaction caused relative movement of different parts of the building , and led to the separation of some of the metallic conduits joints, the breakdown of polyvinyl conduits and the cutting off of some of the communications cables in the approach to the building.

### ◆ Conduits under bridges

The NTT communications cable conduits are usually used to the underside of a bridge girder, and receives the influence of the behavior of the bridge during earthquakes. The conduits under bridge were damaged in the past because of the inability of a conduit joint to follow in response to the behavior of the bridge. Recently efforts have been made to mount a newly-developed joint that allows sufficient expansion or contraction in execution of the work. The new joint suffered no damage from this earthquake. On the other hand, severe damage was done to every one of the joints that had been stipulated in the old specification, and that permitted less expansion or contraction. Some of the conduits were sometimes damaged by sinking of an embankment behind a bridge abutment during the earthquake.

◆ Underground cables

An underground cable did not suffer from this earthquake any of the damage that would have affected the telephone service, but relative movement of cable in a manhole occurred everywhere during the earthquake. The cable falls into 2 classes: the optical fiber cable and the metallic cable made up of copper wire. No significant difference in either of the classes that would have affected the telephone service was found.

## Relationship between damaged conduits and ground displacement

A field survey was conducted in the neighborhood of conduits which had been quickly checked, chiefly in Port Island and the Sumiyoshi-Hamachou Area. The comparison of the distance between manholes and of the ground level at the time of their completion with those after the earthquake makes it possible to estimate the amount of ground surface displacement and to carefully examine the relationship between damaged conduits and ground surface displacement. Since most of these were built in the period between 1975 and 1984, much attention was paid to the changes in the condition around the conduits. The distance between manholes and the ground level at the time of their completion were compared with those after the earthquake in view of the above circumstances.

### ● Nakahuto Area in Port Island

Sand boiling, which had covered almost the whole surface of sidewalks with soil and sand occurred because of liquefaction resulting from the earthquake was observed on a large scale in the Nakahuto Area on the east side of Port Island. Damage was also done to conduits buried in the neighborhood of this area.

It has been found that the ground level of a section of the conduit sunk by an average of about 20 cm on the general. (Fig.4) A survey has revealed that the difference in the ground level between before the earthquake and after the earthquake was found to be about 40 cm. And the separation of steel conduits joints were observed in this section.

In the Fig.5, this graph shows relative ground displacement that was obtainedby comparing measurement of relative ground level before and after earthquake.

We reduced the ground lebvel of after earthquake from those of before earthquake,and so we estimate the relative ground displacement.

The facilities damages occurred near at the point of which relative ground dispacement is large. And Maximum of relative ground displacement is less than 20cm.

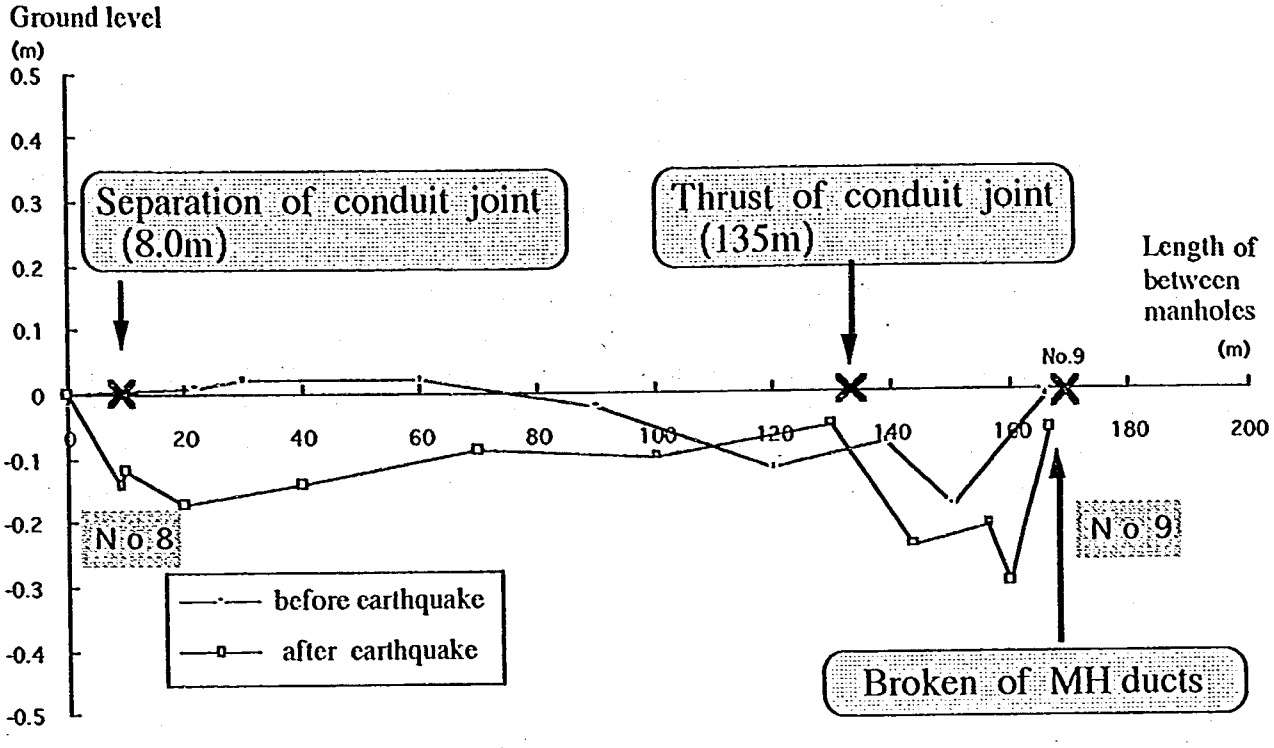



**Fig.4 Ground level of Port minami 8~9**

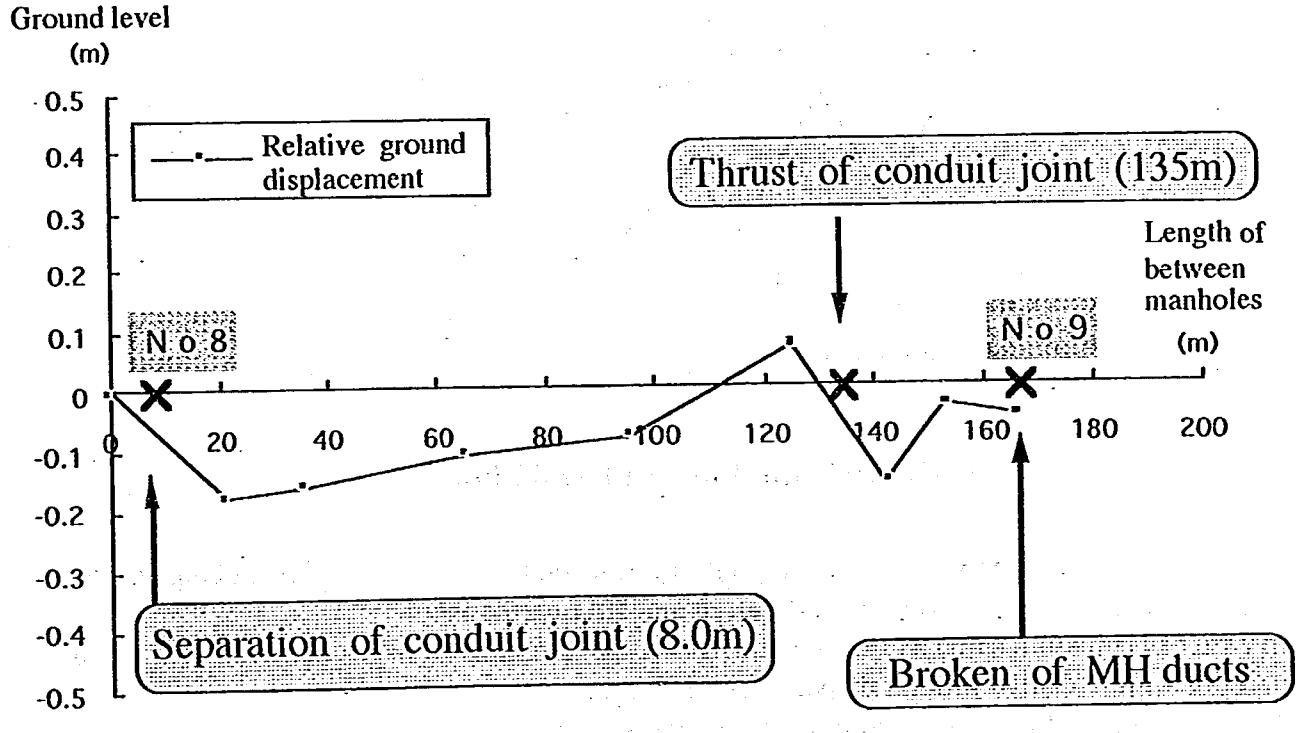



**Fig.5 Relative ground displacement of Port minami 8~9**

## ● Sumiyoshihama-cho Area

The elevated portion of the highway that makes connections between Rokko Island and the Sumiyoshihama-cho Area through the Rokko Bridge showed an undulating surface, or rose and fell in gentle slopes because of the liquefaction resulting from the earthquake. The figure shows the relative height of ground and manholes that has been determined on a base of one of the two measurements obtained before and after the earthquake. The ground level obtained after the earthquake generally sunk by an average of 20 cm or so and by a maximum of 50 cm or so in comparison with the one obtained before the earthquake. The ground surface that suffered heavy damage from the earthquake was found to be undulating. A survey has revealed that the difference in the ground level between before the earthquake and after the earthquake was found to be about 20 cm. A careful check of conduits joints by means of a TV pipe camera has revealed that polyvinyl conduits were damaged at a point 3 - 4 meters away from Manhole NO. 8.(Fig.6)

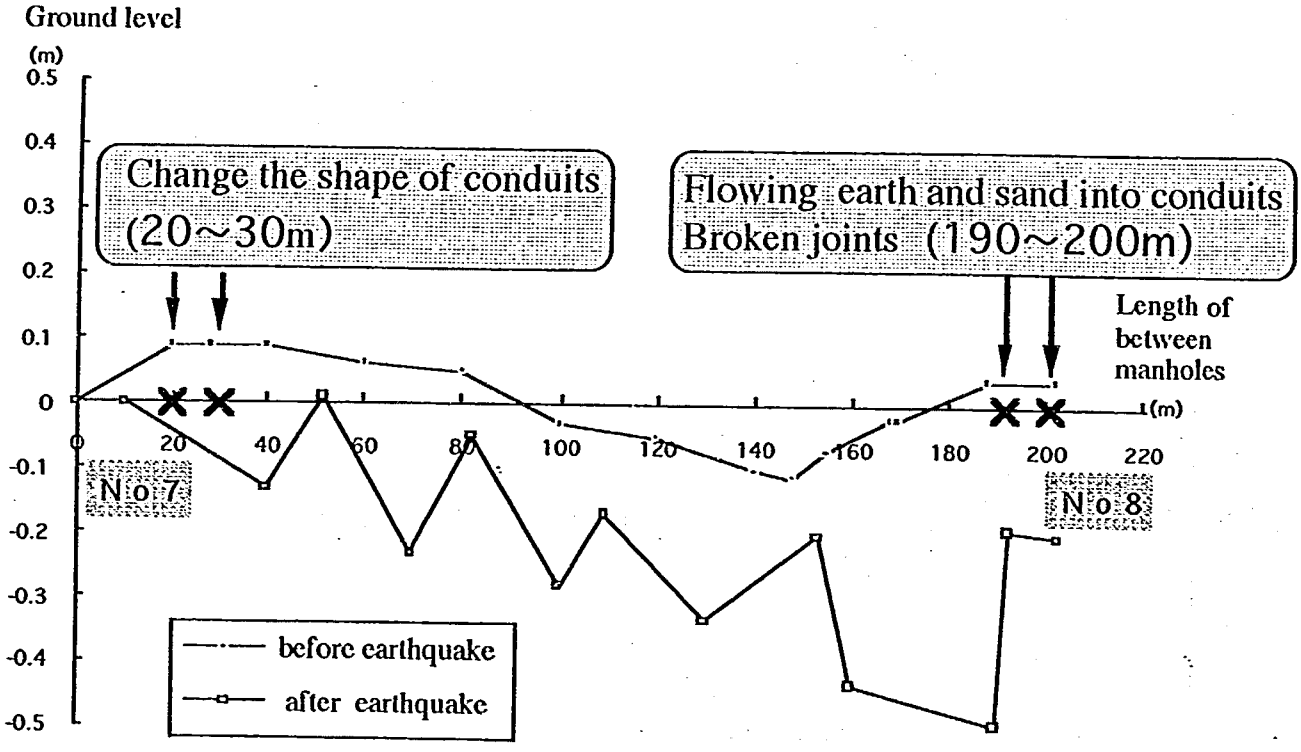



**Fig.6 Ground level of Dai2 koku 7~8**

In the Fig.7, this graph shows relative ground displacement that obtained from comparing measurement of relative ground level before and after earthquake.
In case of Dai2 koku same as Port minami 8~9, the facilities damages occurred near at the point of which relative ground dispacement is large.
And Maximum of relative ground displacement is about 50cm.

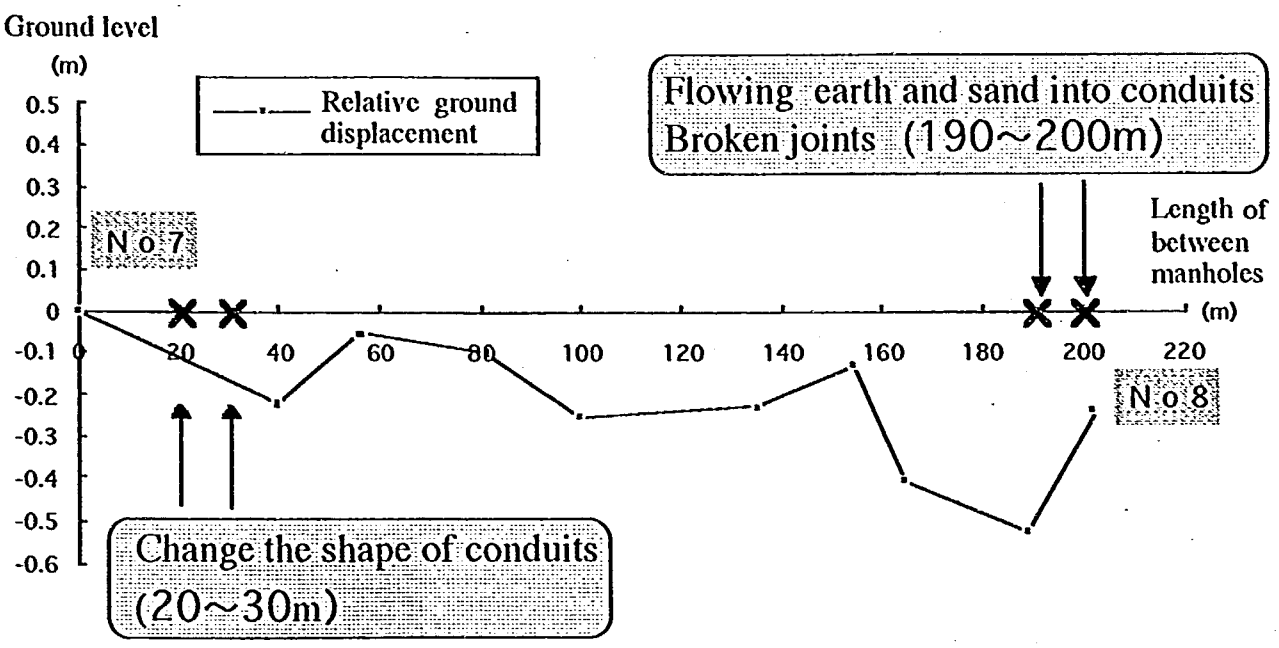



**Fig.7 Relative ground displacement of Dai2 koku 7~8**

## ● Relation between facilities damage and ground displacement

We carried out above mentioned measurements at about 16 locations in Port Island and Sumiyoshihama-cho.We calculated the average of relative ground displacement per 10m between manholes, and Fig.8 shows that total of manhole spans and damaged manhole spans to relative ground displacement.

And Fig.9 shows that total of manhole spans and damged manhole spans that compare the damage of conduits having expansion joints with the damage to conduits without expansion joints. Conduits having expansion joints have no damage , and most of conduits having no expansion joints suffered damage.

It made clear that facilities damage has a relationship with facilities type and amount of ground deformation.

We have already mentioned some of the damage done to conduits and the ground displacement caused by the earthquake. And we are now making a detailed analysis of these problems, and intend to carry out a thorough investigation into the close correlation between the damage done by the earthquake and the ground displacement furthermore.

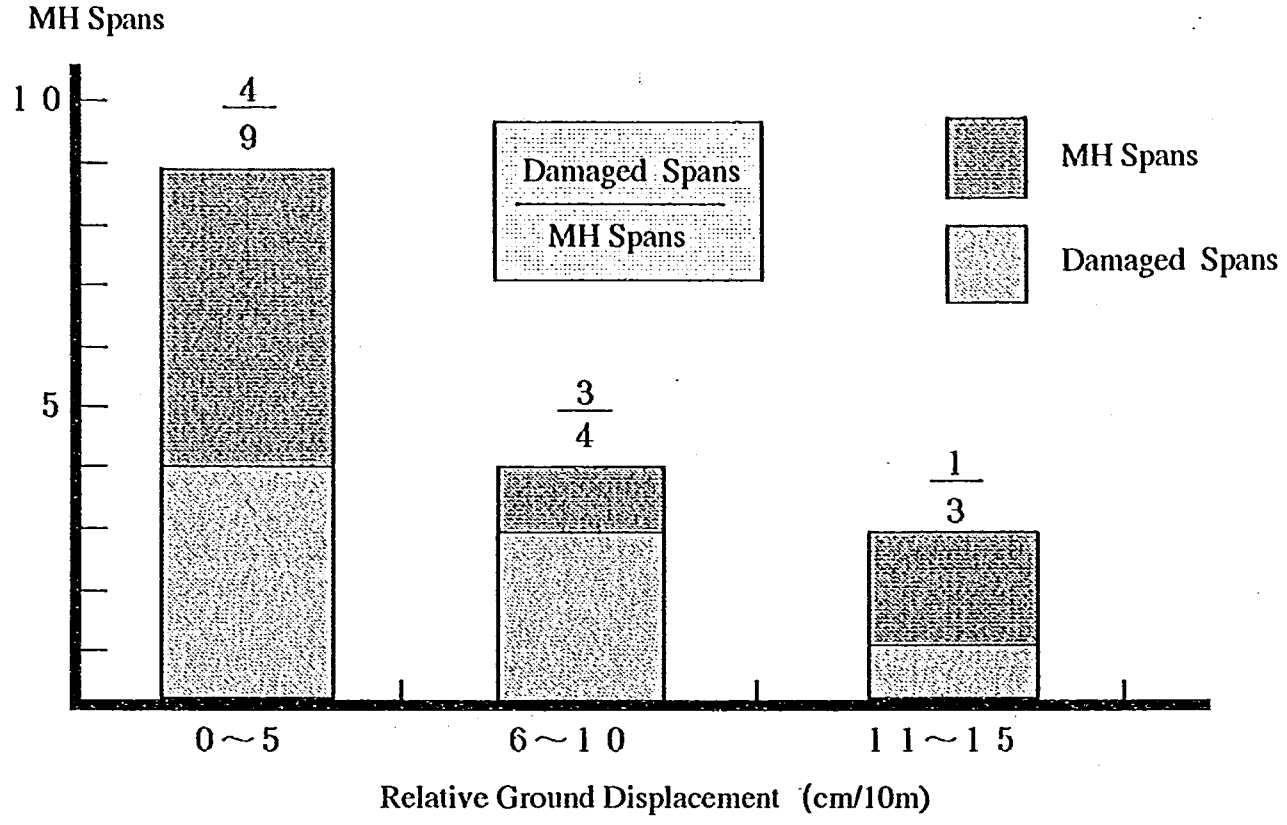



**Fig.8 Relationship between facilities damage and relative ground displacement**

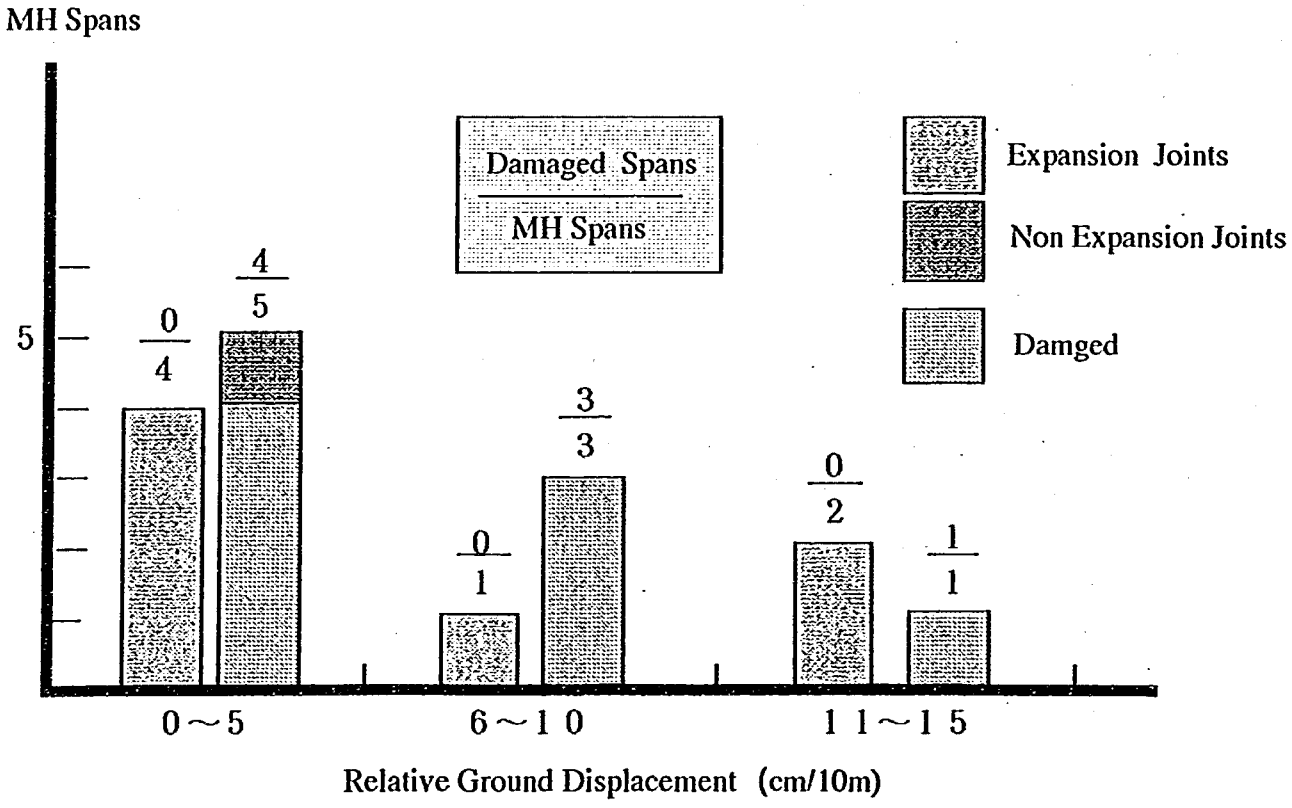



**Fig.9 Compare two types of conduits joints in liquefied ground**

## Summary

NTT learned some important lessons from strong earthquakes that had happened before. And the corporation has been concentrating on improving the resistance of underground facilities to strong earthquakes in view of these lessons since the days of the former Den Den Kosha. The underground facilities built according to the new specification which takes earthquake resistance into account suffered little damage from this earthquake. On the other hand, the occurrence of this earthquake disaster has made clear that there are some of the problems to be dealt with in the near future. Open cut cable tunnels and conduits suffered some type of damage from the ground settlement around the building caused by the earthquake. Further, it becomes necessary to make some improvement in the flexibility of connections between open cut cable tunnels and the building. In the case where the influence of an earthquake extends very wide and far, and the severe damage by that earthquake is concentrated primarily in an urbanized area, it takes a considerable amount of time to check the condition of the underground conduits that have been laid over the wide area. This may lead to an increase in the time necessary to restore these conduits, and therefore we are going to study the development of some kind of tool which enables us to make a quick check of them, and to predict the damage that would be done to them.

# POWER SYSTEMS: COMPARING THE KOBE AND NORTHRIDGE EARTHQUAKE EXPERIENCES

Anshel J. Schiff

Consulting Professor
Department of Civil Engineering
Stanford University

## ABSTRACT

The performance of power system equipment in the Kobe and Northridge earthquakes is compared. Seismic design and installation practices that could account for the differences in performance are reviewed. Changes and proposed changes in US practice following the Northridge earthquake are summarized. Research needed to improve power system equipment and system response are discussed.

# INTRODUCTION

## Basic Statistics Related to the Northridge and Hyogo-Ken Nanbu Earthquakes

The Northridge earthquake occurred at 4:31 A.M. local time on January 17, 1994. The 6.7 moment magnitude earthquake was located 30 km west-northwest of downtown Los Angeles in the San Fernando Valley. The hypocenter was 19 km deep but the fault rupture zone extended to within 7 km of the surface. There were 38 people killed (excluding those who died from heart attacks), and 10,177 injured were treated in emergency rooms of which 1525 were hospitalized (1). About 16,000 residential units were red tagged and about 43,000 were yellow tagged. Total direct losses are estimated at over $20 billion.

The Hyogo-Ken Nanbu (Kobe) earthquake occurred at 5:46 A.M. local time on January 17, 1995. The magnitude was 6.8 and the epicenter was located just off shore under Osaka Bay south of Kobe. There were 5,500 people killed, more than 26,000 injured, and over 300,000 made homeless. The total direct losses are estimated at over $200 billion.

## General Similarities

Both earthquakes were centered in large urban areas. The active fault zones of both earthquakes were shallow so that the ground motions were very severe. These events were the costliest earthquakes in their respective countries since the 1906 San Francisco and 1923 Tokyo earthquakes. In both events power systems experienced extensive damage, but service was restored to most areas within one day. Transportation and water systems were severely damaged. Communications systems suffered minor damage and disruption was primarily caused by system congestion.

## General Differences

Ground motions recorded at major power system sites in the Northridge earthquake tended to be more severe than in Kobe. There was liquefaction and significant ground deformation at several key power system sites and in many other areas in the Kobe area that had a large impact on power system damage and restoration time, particularly to the distribution system. Because of the extensive ground deformation there was extensive damage to the gas distribution system in Kobe. In the Northridge area there was one spectacular gas line failure and fire, but with the exception of an older gas transmission line in one canyon, there was relatively little gas system damage. The housing stock and many other structures in the strongly shaken areas in the Northridge earthquake were much newer than in Kobe. There were several fires following the Northridge earthquake, but due to little wind, the type of construction and lower density, fires did not spread. In Kobe several fires spread and destroyed large areas.

## Collection of Earthquake Damage Data

Most of the information on the Kobe earthquake described in this report was collected over a five day period one month after the earthquake. While Kansai Electric Power Company was very generous in sharing damage and system response information (2, 3), the short duration of the visit and the timing of the visit shortly after the earthquake when the recovery process was still underway limited the data that was available and that could be collected. The information on the Northridge earthquake was gathered through an intensive effort over several months after the earthquake and continued for over a year (4, 5). Because more detailed information was collected after the Northridge earthquake, this paper will primarily emphasize observations from Northridge. Comparisons of the equipment response between the two earthquakes will be made, but discussion about changes in design and installation practices will be limited to the Northridge earthquake.

It should be noted that throughout the paper reference is made to practices in the US and Japan. These references are limited to the damage areas in the respective earthquakes and not necessarily to practices outside of these limited areas.

## Organization of the Paper

The paper is divided into four technical section. The first section, Overview of Power Systems, contains a brief description of the power systems and design practices used prior to the earthquake. The second section, Comparison of Performance of power system equipment in Kobe and Los Angeles Area, describes power system equipment damage and compares differences in component performance of the transmission and distribution systems. The third section, Changes in Design Practices, describes changes in design, specifications and installation that have been made or are proposed by the LADWP. The next section describes research needed to improve power system equipment and system response based on observation made after the two earthquakes. The last technical section describes the major conclusions related to power systems that can be drawn from the two earthquakes.

# OVERVIEW OF POWER SYSTEMS

## Configuration of the Power Systems

Figure 1 shows a schematic diagram of the Kansai Electric Power Company (KEPCO) power system. The figure also shows peak accelerations recorded by KEPCO's network of strong motion instruments. In this figure the number of circuits and their voltages are not all shown. The heavy lines indicate 500 KV circuits, and the thinner lines indicate 275 KV or 154 KV circuits. The 500 KV system is located outside of the zone of severe or moderate ground shaking and it was not damaged. Several generating station located near Osaka Bay, some of which were damaged, are not shown.

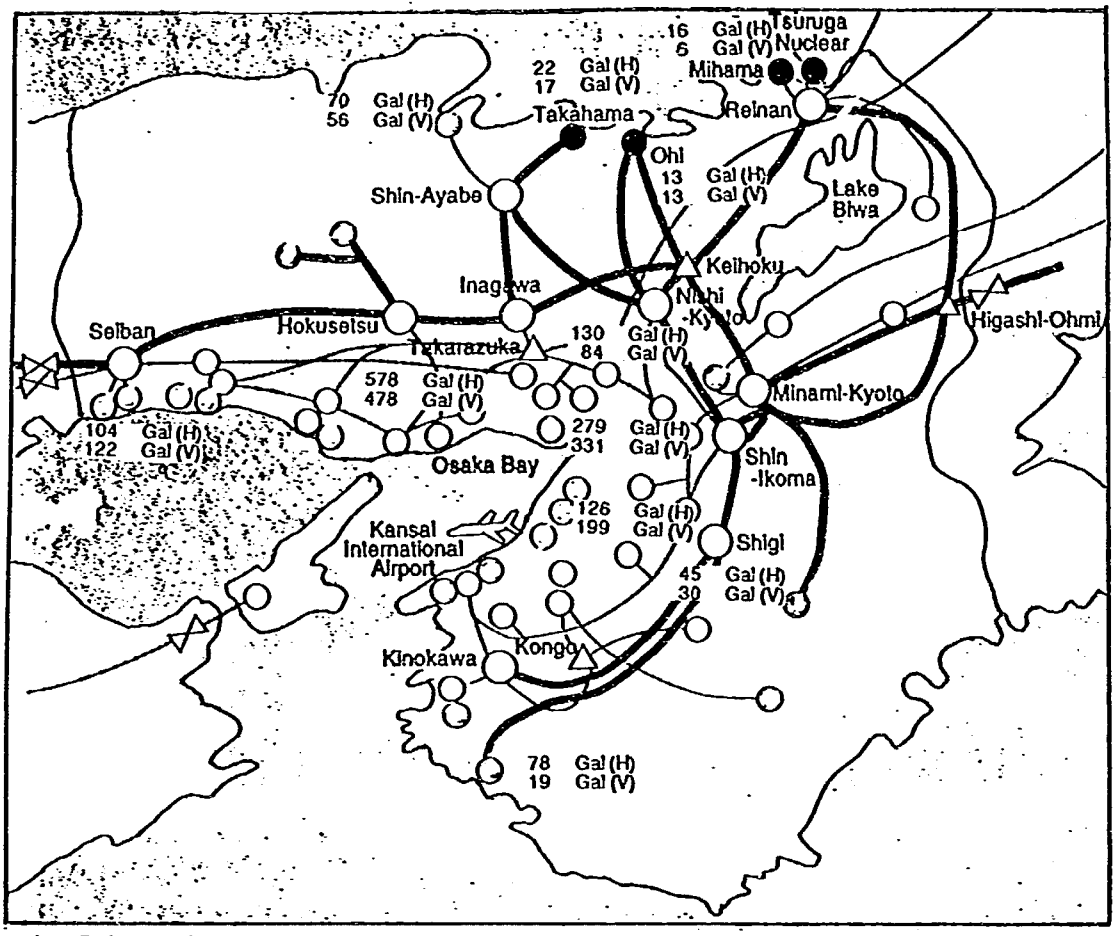



Fig. 1 Schematic Diagram of Kansai Electric Power Service Area and Peak Accelerations at Utility Instruments.

Most power in the area impacted by the Northridge earthquake is provided by the Los Angeles Department of Water and Power (LADWP) and the Southern California Edison Company (SCE). There are a few relative small municipal utilities, but their service area was outside of the severely shaken area. Figure 2 shows a schematic diagram of the LADWP system. The number of circuits and their voltages are not shown. In the northern part of the system there are a few 500 KV circuits and two Direct Current circuits, each operating at + and - 500 KV. Most of the other circuits operate at 230 KV. Only a few substations belonging to SCE bordering the north edge of the LADWP system experienced any damage. Two operated at 230 KV and one at 500 KV.

## Design Specifications and Practices

Reference 4 contains a summary of seismic design criteria published and adopted in Japan in 1980 (6). However, most of the equipment at KEPCO substation predated this guide and the older standards used for the design of the substation are not know by the author. Since the 1980 seismic criteria were not used for most equipment, they will not be described here. At the present time the

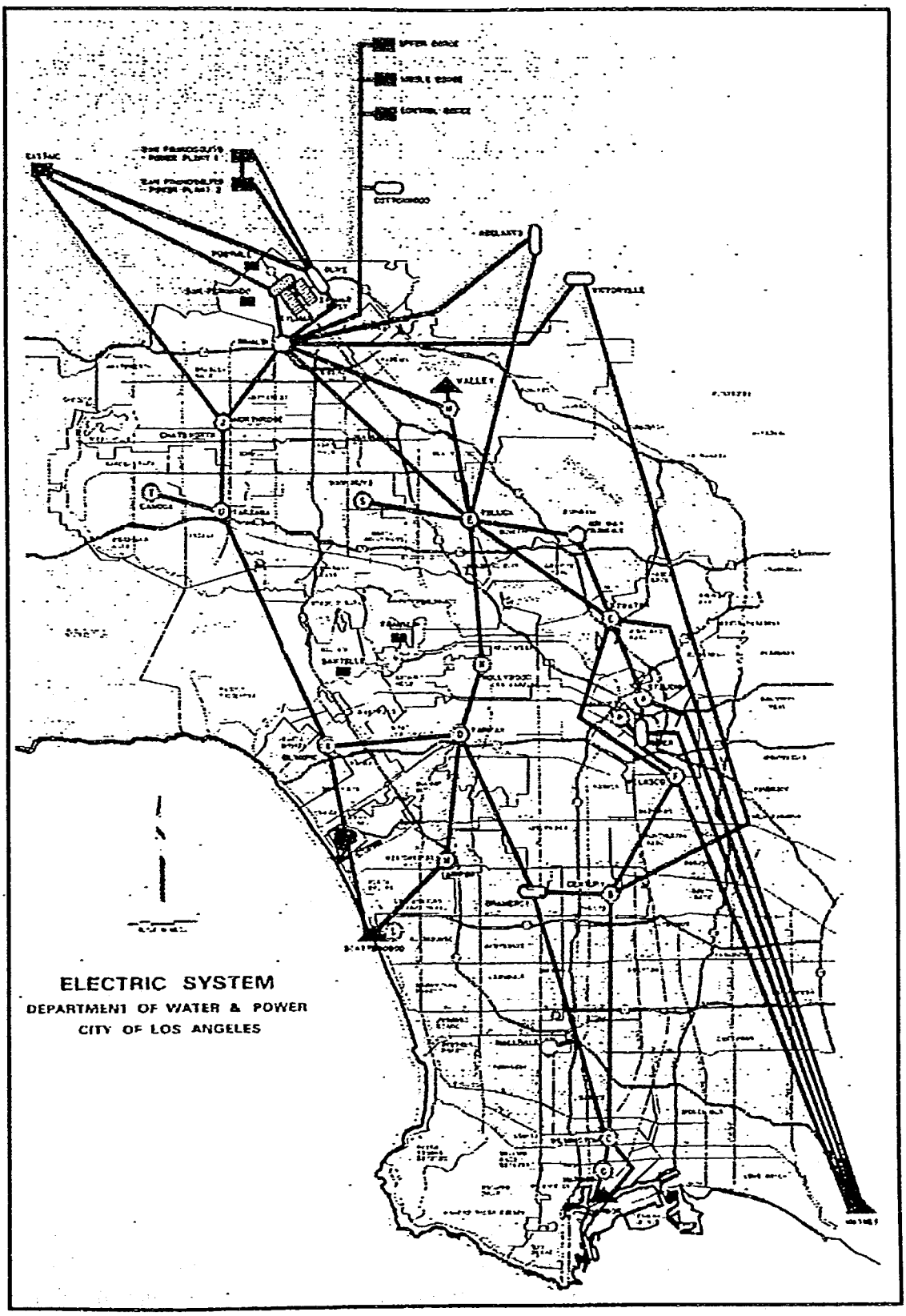



Fig. 2 Schematic Diagram of LADWP Power Transmission System.

1980 criteria, which were based on a peak ground motion of 300 gal, are being reviewed in light of the severe ground motions recorded in the Kobe earthquake.

The seismic design criteria for substation equipment used by LADWP and SCE are very similar. There was a significant change in design criteria following the 1971 San Fernando earthquake, which impacted much of the same areas as the Northridge earthquake, and caused extensive substation damage. A design spectrum was developed and for most service areas its level was adjusted for a peak acceleration of 0.5 g. The design criteria continued to evolve as experience was gained from subsequent damaging earthquakes. One significant difference between Kobe and the Los Angeles area is that there have been three major earthquakes in California (1971 San Fernando, 1987 Whittier Narrows, and 1989 Loma Prieta) and seven less significant earthquakes that caused power system damage. One of the key requirements is that certain classes of equipment must be seismically qualified by vibration testing rather than analysis. In general, rigid bus was not used. Finally, the LADWP eliminated all live-tank circuit breakers in their AC switchyard, following the San Fernando earthquake because of their poor performance.

## COMPARISON OF THE PERFORMANCE OF POWER SYSTEM EQUIPMENT IN KOBE AND LOS ANGELES AREA

### Transmission Lines

These earthquakes were unusual in that there was damage to high voltage transmission lines. In the US three towers located atop narrow ridges failed from ridge shattering or landslide damaged foundations. In one case two adjacent towers on each side of the failed tower also collapsed when all three conductors of the circuit parted. Foundations wee damaged in several other towers, but the towers did not collapse. Several towers at one site were damaged, one severely, due to liquefaction. The towers at this site, were fabricated from two-centimeter (.75-inch) plate, and had brittle failure of several welds. A failed tower on one critical line connecting a large pumped storage generating facility to the grid was temporarily replaced by a large crane rigged as a transmission tower. Prefabricated towers manufactured by a local company were also used to quickly restore service.

In Japan transmission lines dead end at the towers, and the lines passes under the cross arms. Post insulators are used to support lines under the tower cross arms and some of these failed. This damage did not put the line immediately out of service, but repairs were required. No towers collapsed.

### Transmission Substations

In the US most damage was to high voltage substations and the switchyards associated with DC converter stations. The damage in Japanese substations was relatively small, but the character of the damage to equipment serving the same function in the US and Japan was typically different.

The various classes of equipment will be discussed in the following sections. Table 1 summarized the performance of the equipment at damaged sites. Most transformer damage was associated with bushing damage. Note that items in the table refer to individual phases, with the exception of transformers which are a mix of single- and three-phase units.

Table 1 Summary of Performance of High Voltage Substation Equipment at Substations with Damage.

| Type of Equipment | Undamaged | Damaged |
|---|---|---|
| Transformers | 20 | 13 |
| Disconnect Switches | 536 | 209 |
| Potential Transformers | 32 | 8 |
| Current-Voltage Transformers | 154 | 39 |
| Wave Traps | 47 | 20 |
| Lightning Arresters | 59 | 35 |
| Circuit Breaker - SF-6 | 144 | |
| Circuit Breakers - Bulk Oil | 285 | |
| Circuit Breakers - Live-Tank | 5 | 10 |

Transformers

Transformers experienced a broad range of problems. In both the US and Japan there were anchorage problems. In the US, large bolts used to hold six single-phase transformers stretched and were deformed from shear loads. Two of four undersized welds failed on one transformer, allowing one end of the transformer to slide 25 cm (14 inches). Two transformers and their foundations pads rotated, and there were indications that other transformers may also have rocked. The rocking motion damaged low-voltage bus connections, which used rigid pipe bus and may have contributed to bushing failures. In Japan, bolts used to secure several large transformers and reactors that closely resembled distribution transformers failed in shear. The failure of these bolts allowed the transformers to slide as much as 46 cm (18 inches). As a result of the relative motion between a transformer and reactor a low voltage bushing failed due to the pull from the conductor. No high voltage bushings failed.

In the US approximately forty-two bushings required maintenance or had to be replaces. The porcelain on a few bushings cracked or was totally shattered. Most bushing problems were associated with the upper porcelain member sliding relative to its mounting flange, often allowing the bushing oil to leak. A factor contributing to these failures was the method used to support lightning arresters and connect them to the transformer. The impact of lightning arrester failure on bushings will be discussed below. Oil leaks required that the bushing be removed to be repaired, although temporary field repairs were sometimes made to keep the transformers in service. The loss of transformers due to bushing damage severely limited system capacity, but low winter loads allowed demand to be met. Bushings on two transformers exploded several weeks after the

earthquake, causing transformer fires that destroyed the transformers. An examination of the bushing indicated a failure in the insulation, but the cause of the problem is not well understood at this time. In Japan none of the transformer high voltage bushings failed.

Transformer radiators at a US substation site with relatively low ground motion were severely damaged. These radiators were supported from the transformer case and were unbraced. Their dynamic response caused pipe connecting the radiator to the transformer case to crack near the transformer body.

The only transformer radiator damage observed in Japan was in a distribution substation where the transformer anchorage failed. The transformer moved and the radiator hit a cable support, causing a leak.

## Circuit Breakers

After the 1971 San Fernando earthquake, the LADWP eliminated all of their live-tank circuit breakers, because their performance was very poor. In the Northridge earthquake severely shaken sites had bulk oil or single-phase gas insulated circuit breakers. There was no damage to any of these circuit breakers in this or any other US earthquake. SCE did have live-tank circuit breakers and 10 of 15 phases were damaged. The porcelain columns that supported the interrupter head on these units failed. In Japan, the upper part of bushings on several circuit breakers slipped. This damage was very similar to that observed on US transformer bushings. Bulk-oil circuit breakers and their bushings were much larger than their US counterparts.

## Disconnect Switches

About 28% of the disconnect switches (individual phases) at damaged substation were damaged in the US. Four types of failures were observed. Post insulators used to fabricate the disconnect switches failed at their lower sand ring; bolts used to hold the insulator post column failed; the aluminum plate that supports the insulator column deformed so that the disconnect switch would not close properly and the operating mechanism became misaligned so that the switch would not close properly. Damage was due to inertial loads or interaction with adjacent equipment due to the use of rigid bus or flexible bus with inadequate slack. In Japan, the few disconnect switched that were damaged had the insulator post split longitudinally.

## Bus Configurations and Substation Conductors

In the US most busses use the breaker-and-a-half configuration, although a few in the epicentral area used double-bus-double breaker configurations. In Japan the substations that were visited typically had double-bus-single-breaker configurations. In general, both countries use flexible bus. In the US there were two exceptions to this practice. One substation, because of the location of the transformer positions at the end of the bus, heavy rigid bus was needed because of the large

bus currents. This bus had a unique design, in that the rigid bus was supported on a short length of chain suspended from a porcelain support. This bus was severely damaged. One of the utilities also used a section of rigid bus between disconnect switches at line drop positions. There were indications that this caused interaction between the disconnects switches and subsequent damage. In many locations were flexible was used, adequate slack was not provided so that adjacent items of equipment could interact. In Japan flexible was consistently used, but as in the US, adequate slack was often not provided. The use of flexible bus and conductor when generous slack was beneficial when there was major deformations at sites, as observed in Japan.

In the US some sections of rigid bus were fabricated with cast aluminum fittings. These frequently failed and contributed to the failure of rigid bus.

Instrumentation Transformers

The performance of instrumentation transformers, potential transformers and current-voltage transformers, in the US was poor, with a failure rate of about 25% for non-suspended units. Most units failed at the lower sand ring of the porcelain. The units that failed were typically supported on a single tubular steel column. The typical design used a 17 cm (6-3/4 inch) diameter tube and the performance of these was poor compared to those that used a stiffer tube. In Japan, relatively stiff steel-frame structures were typically used to support instrumentation transformers. SCE suspends most of their current-voltage transformers. None of these units suffered any structural damage, but they frequently broke loose from their lower restraints, swung free, and damaged control cable connections and adjacent equipment. Even when units did not fail their lower restraints, they swung back and forth violently so that adjacent disconnect switches were damaged. In Japan instrumentation transformers were very large relative to those used in the US for equipment of similar voltage. The failures of these units in Japan was attributed to leaking "O" ring seal that joined the upper and lower halves. This failure was not observed in the US.

Wave Traps

In the US about 30% of wave traps failed. There were several failure modes that included internal structural failures between the coil and its center support; failure of end support members provided by the wave trap manufacturer, failure of post insulators supports; and failure of post insulators used to restrain suspended units. In Japan, two wave traps were observed in the damaged equipment "graveyard" at one of the substations, but the cause of their failure is not known.

Lightning Arresters

In the US lightning arresters are typically supported on booms mounted on the transformer case. The lightning arresters are typically supported on standoffs that are needed if strike counters are to be used. At 500 KV, the lightning arresters are typically supported on their own steel column near the transformer. About 38% of the lightning arresters failed. About half failed in the porcelain just

above the bottom mounting flange and the rest failed at the standoffs. Two types of standoffs are commonly used. One consists of a porcelain member with a steel stud protruding from each end. The second type of standoff, none of which failed, is a porcelain member that electrically isolates a bolt through center of the porcelain. The relatively flexible booms that supported the lightning arresters may have contributed to their failure. The lightning arresters were frequently connected directly to the bushing binding post. When a lighting arrester fails, it falls and an impact load can be applied to the bushing through its conductor connection. In Japan, lightning arresters were often supported on low concrete pads. Several arresters failed just above their lower mounting flange.

## Distribution System

Damage to the distribution system in the US was relatively minor as compared to the damage in Japan. This was primarily due to the large areas that experienced soil liquefaction and ground deformations in the latter case.

### Distribution System Substation

In the US there typically is very little damage to distribution substation equipment. In the Northridge earthquake this was generally true, but there were widespread brittle failures in cast aluminum hardware used to support rigid bus at 34.5 KV within the substations. Several transformers cracked anchor welds, but they did not move or cause disruption. In Japan transformers were typically surrounded by acoustical walls to reduce noise outside of the substation. At one substation the rocking of the walls, and possibly of the transformer, caused damage to the transformer bushings.

### Transformers

In the US, over 250 pad-mounted distribution transformers distributed in neighborhoods away from the distribution substations shifted on their pads up to about 30 cm (12 inches). These units were not anchored. Surprisingly, none of the power cables that enter the transformer though holes in the mounting pad were damaged, so that the movement of the transformer cause no disruption. The units did have to be repositioned on their pads. In the downtown area of Kobe the extensive damage to the buried distribution system could be seen by the shifting of the transformers and switchgear supported on pads adjacent to the street at the edge of sidewalks. Steel conduit was used and reportedly there was no damage to electrical cables, although extensive system repairs would be needed as sidewalks and streets were releveled.

Distribution Lines

In the US wooden poles are used to support distribution lines. There was essentially no damage to these poles. It is interesting to note that in the 1992 Petrolia earthquake (magnitude 6.9) in northern California no wooden poles were damaged even though 600 pole were in a deteriorated condition due to severe dry rot of the poles in which only an inch of sound material remained around the outside of the poles. In Kobe, many spun concrete poles were damaged. While many failed when they were hit by collapsed houses adjacent to them, many failed at their bases just above the ground or just below cross bars near the top of the pole.

## CHANGES IN DESIGN AND INSTALLATION PRACTICES

As a result of the Northridge earthquake several changes have been proposed or made in equipment specification and installation practices. New specifications have been developed for transformer bushings that mandate that they be tested. Because of the large size and weight of the transformers, the bushings can not be tested installed on the transformer. Now bushing will be tested separately and the transformer manufacturer will have to determine the amplification between the base of the transformer and the bushing mount. Also, composite rather than porcelain bushings are being sought.

To improve the seismic response of lightning arresters, standoffs, which were typically used on lightning arresters even when strike counters were not used, will be eliminated. When required, the standoff will be the bolted-through type. To reduce the impact of the failure of lightning arrester, the conductors that connect the lighting arrester to bushings will be reduced in size so that if the lightning arrester fails and falls, the connecting conductor will fail at a lower load so that the force applied to the bushing will be reduced. The use of lightning arresters made of composite material rather than porcelain is being explored.

The LADWP will be eliminating wave traps entirely. The plan is to have two methods of communications, probably both microwave based. Bonneville Power Administration has done this with the use of a microwave and optical fiber links.

Pad-mounted distribution transformers will be anchored in the future and existing units will be retrofitted.

Bracing has been added to large transformer radiators and purchase order specifications have been changed so that the radiators on new transformers must be braced.

## RESEARCH NEEDED TO IMPROVE EQUIPMENT AND SYSTEM RESPONSE

The performance of bushings on circuit breakers and transformers in Japan and the US was very different. In the US transformer bushings slipped and developed leaks and there were no problems with circuit breaker bushings. In Japan, the opposite was true. It would be mutually

beneficial if the differences that prevent or contribute to bushing damage in transformer and circuit breaker in Japan and the US could be identified. It has been suggest that in the US when bulk oil circuit breakers are closed, the internal end of the bushings are secured to each other and this may have contributed to their improved response.

There is a need to identify the main factors contributing to transformer bushing damage and to explore the possibility of low cost retrofits to improve their earthquake response. Factors that may contribute to bushing damage are flexibility of the turret that supports the bushing, flexibility of the top of the transformer in the area around the turret, and rocking of the transformer and its foundation pad. The long-term performance of restrainer rings to prevent bushings from slipping needs to be explored. There is also a need to develop a rapid restoration process to repair bushings that have slipped, rather than performing a total restoration.

A common practice in the US and Japan was to have a vertical line drop from a bus secured to the ground with a cable and insulator string. Just above the insulator string power connections were made to nearby equipment. Damage was observed to the adjacent equipment, apparently due to interaction with the line drop. Because of the low mass of the insulator string, the cause of these failures is not well understood and needs to be investigated.

The significant differences in the performance of instrumentation transformers in the US and Japan needs to be understood so that factors that contribute to the good performance in Japan can be incorporated into US practice

The installation of suspended equipment items, such as wave traps and instrumentation transformers, needs to be improved so that their dynamic response does not damage adjacent equipment.

There is a need to improve the procedures of documenting damage and restoration process so that a better accounting is obtained of the damage, the spare parts that are used and the labor needed for restoration. In the rush to restore service, much of this information is not gathered. It is needed to recover expenses when federal support is available or in making insurance claims.

In the Northridge earthquake most major substations recorded strong motion during the earthquake. There is a need for additional post-earthquake evaluation of dynamic response of substation equipment through low level vibration testing. The results of these tests should be used to relate site spectrum to the observed damage so that failures can be better understood and spectral based fragility data can be developed.

## CONCLUSIONS

Power utilities have again shown their resourcefulness in restoring severely damaged power systems. The loss of high voltage transformers presents a potential risk of long-term disruption, as the function of these units cannot be circumvented and repair times are lengthy. The high vulnerability of transformer bushings has been demonstrated. Older live-tank circuit breakers have

again been shown to be very vulnerable to earthquake damage. Newer units located in the DC switchyard performed well so that these designs may be more robust. Disconnect switches exhibited new failure modes: deformation of metal parts and of operating mechanisms. The detailed post-earthquake documentation of damage and response is important to understanding damage and improving equipment and system response. The impact of liquefaction at substations and in city centers where the distribution system is under ground has been shown to be very severe. This has implications to the eastern US were the potential of liquefaction is much higher than in California.

## ACKNOWLEDGMENTS

The authors acknowledges the cooperation and support of LADWP in collecting information on power system damage from the Northridge earthquake. He also gratefully acknowledges Kansai Electric Power Company for sharing data about the damage to their system from the Kobe earthquake.

## REFERENCES

1. "Northridge Earthquake Reconnaissance Report," EERI Earthquake Spectra, Supplement C to Volume 11, April 1995.

2. "Northridge Earthquake: Lifeline Damage and Post-Earthquake Response," Ed. A. J. Schiff Technical Council on Lifeline Earthquake Engineering, Monograph No. 8, August 1995, pp 9-97.

3. A report on the Northridge Earthquake by the Los Angeles Department of Water and power, in preparation.

4. "The Hyogo-Ken Nanbu Earthquake," Ed C. Farrar, Technical Council on Lifeline Earthquake Engineering, in preparation.

5. "Impact of the Earthquake of Southern Hyogo Prefecture on Electrical Facilities, Kansai Electric Power Co., Inc. March 7, 1995, unpublished report.

6. "Guide for Seismic Design of Substation Equipment," Japan Electric Association Guide: JEAG 5003-1980.

# Session-7

## Risk Assessment and Impact of Seismic Effects (1)

(U-4) Pipeline Performance Parameters for Earthquake Vulnerability
(Donald Ballantyne)

(U-5) Economic Impact of Lifeline Disruption: Current Models and Preliminary Observations from the Hanshin Earthquake
(Stephanie E. Chang and Wm. Jess Taylor)

(U-6) Application of GIS Technology to Seismic Risk Assessment of Lifeline Systems in Shelby County,Tennessee
(Howard H.M. Hwang)

# PIPELINE PERFORMANCE PARAMETERS FOR EARTHQUAKE VULNERABILITY

**Donald Ballantyne, P.E.**

**Associate**
**Dames & Moore**
**Seattle, Washington**

## ABSTRACT

This paper discusses the basis for the relative earthquake vulnerability of water pipeline systems as presented in the recent American Water Works Association publication, ***Minimizing Earthquake Damage, A Guide for Water Utilities*** by Donald Ballantyne, as summarized in Table 1. The paper provides a more in-depth background on pipeline failure modes than provided in the AWWA publication. The information is important and timely considering the Northridge and Kobe earthquakes.

Pipeline system materials include those for which AWWA has a current standard, and older pipeline system materials that have large installed inventories in the United States.

Earthquake pipeline damage mechanisms are described, and the ability of each pipeline system to resist those damage mechanisms is discussed. The pipeline vulnerability is related to pipe material and joint type as listed in Table 1.

## INTRODUCTION

Pipeline failure in earthquakes has lead to failure of systems to provide water for fire protection and drinking in the 1995 Kobe, Japan; 1994 Northridge and 1989 Loma Prieta, California earthquakes. Proper selection of pipe materials for new installations and replacement of vulnerable pipe segments critical to operation is important. In addition, there may be opportunities to improve existing pipe designs to make them more earthquake resistant.

The objective of this paper is to describe a method to rate the earthquake vulnerability of buried water pipe to earthquake induced deformation. The system can be used to:

1. Select appropriate pipe for new installations

2. Prioritize pipe within a water system to be replaced

3. Provide direction in developing an earthquake resistant pipe design.

The piping systems discussed in this paper are buried installations of pipe commonly used for transmission and distribution in the water supply industry. Service line piping system are not discussed.

## EARTHQUAKE HAZARDS

Earthquake hazards are the ground movement mechanisms associated with earthquakes. They include movement from earthquake wave propagation, as well as permanent ground deformation, PGD. In developing the method, it has been assumed that pipelines move with the ground.

### Wave Passage

Propagating earthquake waves move the soil as they pass. However, the soil moves back to its original position once the wave has passed. In terms of pipeline response, one can view wave propagation as inducing transverse or longitudinal ground deformations. For example, a shear wave, S-wave, traveling parallel to the pipeline axis induces transverse ground movement in the vertical or horizontal direction perpendicular to the pipe axis. In a continuous pipe, this transverse ground motion causes bending or flexure in the pipe. In a segmented pipe, we get some combination of bending in the segments between the joints, and relative angular rotation at the joints themselves.

On the other hand, Rayleigh waves, R-waves, traveling parallel to the pipeline axis induce longitudinal ground motion (ie., in a horizontal direction parallel to the pipe axis). In a continuous pipe, longitudinal ground motion causes alternating axial tension and compression in the pipe. In a segmented pipeline, we get some combination of axial stress, tension or compression, in the segments between joints, a relative axial extension or compression at the joints themselves.

Most pipe systems currently in use can accommodate some differential movement from wave passage by either accommodating it in the joint, or in pipe strain and ductility. Some damage from wave passage may occur, but it will be widely distributed throughout the system. If the length of pipe subjected to wave passage is much larger than that subjected to PGD, the total numbers of pipe failures from the two hazard may be comparable. Brittle pipe with rigid joints are subject to significant damage from wave passage.

### Permanent Ground Deformation

PGD can be caused by liquefaction, settlement, lurching, landslides, and fault rupture. It can put tension, compression, bending, and shear loads on pipelines.

PGD can occur as a result of liquefaction induced lateral spreading when the soil moves down a slope (a 2 percent slope is sometimes considered a threshold) or towards a free face. Liquefaction is caused by ground shaking that consolidates soils particles, forcing out water from between the particles. As the water tries to escape, it turns the soils into a quick condition. Liquefaction can also result in loss of bearing capacity or flotation of buried pipes. Significant flotation usually is limited to sewers that are not filled with liquid, making them more buoyant.

Settlement occurs when soil consolidation takes place, but there is no water present. Lurching occurs when soil masses are thrown by earthquake ground motion, and do not return to their original location.

Landslides move down slope in magnitudes ranging from millimeters when creep occurs, to tens and hundreds of meters when flow slides occur.

The surface expression of fault rupture moves soil on one side of the fault relative to the ground on the other side of the fault. The resulting effects of PGD on buried pipelines is similar to wave propagation effects. For example, a lateral spread in which the ground movement is parallel to the pipeline axis induced axial tension in a continuous pipeline near the head of the spread, and axial compression in the pipe near the toe. Hence the effects are similar to those due to longitudinal wave propagation. Similarly, a lateral spread in which the ground movement is perpendicular to the pipe induces bending in a continuous pipeline.

## PIPE MATERIAL AND JOINT TYPES

Materials commonly used for potable water transmission and distribution pipe include ductile iron, steel, concrete cylinder, and polyvinyl chloride, PVC. Polyethylene has only recently been approved as an AWWA standard, and is becoming a more accepted pipe material. Asbestos cement has been used extensively in the past, but sees minimal use for new installations. In the early 1970's, ductile iron replaced cast iron for new installations.

Pipelines can be classified into three groups, unrestrained segmented, restrained segmented, and continuous. The most commonly pipe used for potable water is a segmented pipe with bell and spigot joints with elastomeric gaskets. It may or may not be restrained (Figure 1). Another commonly used pipe is welded steel which is a continuous pipe (Figure 2) . Asbestos cement pipe is joined with couplings that work like a double bell, back-to-back. Steel and polyethylene, both continuous pipe systems, can employ butt joints that are welded (steel pipe) or fused (polyethylene pipe) together.

Older steel pipe barrels and joints were sometimes riveted. Until the 1950's, cast iron pipe joints were commonly sealed with lead or mortar, making them rigid.

When conducting an evaluation of an existing pipeline system, the pipe type and joint type can sometimes be identified by knowing the date of installation.

There are many variations on the pipe and joints described above.

## JOINT RESTRAINT

Joint restraint is an important parameter to evaluate earthquake vulnerability.

Bell and spigot pipe joints and coupled (asbestos cement) pipe are unrestrained unless special hardware is added.

Both bolted (Figure 3) and boltless (Figure 4) restrained joint designs have been developed to be an integral part of the joint design. Restrained joint systems available in the United States offer only minimal longitudinal deformation once the joint is installed. This means that any longitudinal movement from the ground deformation in the surrounding soil along the pipe must be dissipated in pipe strain. This may put very large longitudinal loads on pipe joints causing them to fail.

The Japanese have developed the "S" and "SII" restrained joint that allows some longitudinal movement, to a point, when the retainer ring stops pull out (Figure 5). With this design, when longitudinal deformation is initiated, it will be taken up in the first joint. If the first joint does not have the extension capacity, it is passed along to the second joint, and so on, similar to the way railroad train car connections take up slack when the train starts. Strain buildup is minimized which then controls longitudinal loading across pipe joints.

Welded steel and fused polyethylene joints are classified as continuous and are inherently restrained.

## PIPE PERFORMANCE PARAMETERS

Four pipeline performance parameters have been identified in an attempt to rate the earthquake vulnerability of pipelines. These parameters were selected based on pipe material and joint type, and their respective earthquake damage mechanisms. The pipeline performance parameters are:

1. Ruggedness
2. Resistance to Bending Failure

3. Joint Flexibility

4. Joint Restraint

Ruggedness is a function of pipe material strength and ductility. It is a factor in pipe failure in compression, shear, bursting, and to a lesser degree, tension and bending.

Resistance to bending failure of the pipe barrel (or body) is a function of the pipe barrel's strength in bending which is a function of the pipe's material properties, wall thickness, and it's length/diameter ratio. Non-ductile pipe such as cast iron and asbestos cement, 8-inch and smaller are particularly vulnerable in this category. Cast iron pipe may be slightly stronger, but the nominal laying lengths are half again as long as for asbestos cement pipe, allowing for a longer moment arm to cause bending failure. Large diameter, non-ductile pipe typically has adequate strength to resist failure in bending. Alternatively, if the pipe bends ductily without breaking, it is considered to be resistant to bending failure.

Joint flexibility is a function of a pipe's ability to extend, compress, or bend (or rotate) around the joint without breaking the joint's water-tight seal. For segmented pipe, joint flexibility is a function of joint geometry, and may be limited in large-diameter pipe joints such as concrete cylinder pipe (Figure 6). For continuous pipe, it is a function of the ductility of the pipe material.

Joint restraint is a function of the design of the pipe joint system holding pipe segments together in tension. For example, continuous welded steel pipe can have different designs that provide varying levels of restraint such as butt (stronger) versus lap (weaker) joints, and arc (stronger) versus gas (weaker) welds.

A fifth parameter, condition, should be considered for existing pipe. Pipe that has corroded, as identified by soil corrosivity, field inspection, or poor maintenance history, will likely perform worse than similar pipe in good condition.

## PIPE DAMAGE MECHANISMS

Pipe earthquake damage mechanisms are important to consider when rating earthquake vulnerability. Damage mechanisms can be segregated into two groups, pipe joint, and pipe barrel, and are listed below. The pipe performance parameter that is most significant in controlling the respective mechanism is listed following each, separated by a dash.

Pipe joints usually fail in the following ways:

- Extension (pulled joints) - joint restraint (Figure 7)
- Compression (split joints) - ruggedness (Figure 7)

- Bending/Rotation - joint flexibility and ruggedness (Figure 8)

In the Kobe Earthquake, approximately two-thirds of the pipe failures were from joint extension or compression. One reason that other types of failures were minimized in Kobe is that 89 percent of the pipe was either ductile iron or welded steel.

Pipe barrels usually fail in the following ways:

- Shear - ruggedness (Figure 9)
- Bending - resistance to bending failure and ruggedness (Figure 8)
- Hole (condition)
- Split/Burst - ruggedness and condition

Holes are usually a result of corrosion. Split of burst pipes can be the result of corrosion, often combined with water hammer. Pipes can collapse; usually this is limited to failure of non-pressure pipelines that have a weaker cross section.

Pipe failures are often associated with bends and fittings, hydrant connections, service connections, and valves where there is a discontinuity in the pipeline.

## WELDED STEEL PIPE JOINTS

Pipe joint welding should be further examined to differentiate vulnerability associated with a range of issues including gas versus arc welding, lap versus butt joints, and bell design.

In both the 1971 San Fernando and 1994 Northridge earthquakes, gas welded steel pipe performed much worse than arc welded steel pipe. Typically, the gas welded steel pipe was installed before 1940. Two considerations have been raised that may lead to its poor performance, 1) quality control, particularly of weld penetration, and 2) embrittlement of pipe material properties adjacent to the weld.

Welded lap joints allow some eccentric loading in the joint as compared to butt welded joints that minimize eccentric loads. To some degree, this can be controlled by providing equal welding on both the inside and outside of the joint. Interior welding is limited by pipe diameter.

It has been suggested that during the bell manufacturing process, material properties of the metal are changed when the bell is formed. This concern may be limited to larger diameter pipelines as a result of the limitation of the manufacturing equipment. The radius of the bend at the back of the bell may also influence pipe bell load transfer characteristics.

Therefore, gas welded pipe joints are rated much lower than arc welded joints in Table 1. Although not shown in Table 1, pipe with butt welded joints should be rated less vulnerable than pipe with lap welded joints.

## PIPE MATERIAL AND JOINT TYPE RATING

Based on observations of pipeline performance in recent earthquakes, pipe material and pipe joint types were rated for ruggedness, resistance to bending failure, joint flexibility, and joint restraint. The results are shown in Figures 10 through 13, respectively. The ratings for each parameter are summed to get a net vulnerability. Consideration was given to weighting one performance parameter higher than the others. Further evaluation comparing earthquake performance and vulnerability rating indicated even weighting seemed appropriate. The results are summarized in Table 1. It should be noted that there have been slight modifications to the pipe vulnerability ratings compared to those included in the original AWWA publication.

The results in Figure 10, Ruggedness, show that pipe manufactured from asbestos cement and cast iron have a moderate to high vulnerability. Concrete cylinder pipe, a composite of steel and concrete, PVC, and gas welded steel are considered to be moderately rugged.

The results in Figure 11, Resistance to Bending Failure, show that asbestos cement and cast iron pipe 8-inch and smaller is particularly vulnerable to bending. The rigid joint cast iron pipe includes all pipe diameters, so does not have as low a rating.

The results in Figure 12, Joint Flexibility, show that gas welded and rigid bell and spigot pipe are particularly vulnerable to joint movement.

The results in Figure 13, Joint Restraint, show that all unrestrained joint pipe is vulnerable to extension (pull apart) failures. Restrained joint concrete cylinder pipe and PVC are downgraded because the pipe barrel and restrainer attachments are not as strong as for steel and ductile iron pipe.

An additional level, very low vulnerability, is proposed. It would include butt welded steel, and ductile iron pipe with the Japanese "S", and "SII" joint. Butt welded steel joints are stronger than bell and spigot welded steel joints. S joint ductile iron pipe is designed to minimize strain buildup by providing some longitudinal extension before it restrains further movement.

## PIPELINE LININGS AND COATINGS

Pipelines have been evaluated on the merits of their basic material. In some cases, mortar and/or cement linings and coatings are added to pipelines to resist corrosion. These materials are less ductile than steel or concrete. In the case of mortar lined and coated ductile iron or steel pipe, the coating

may have a tendency to limit the ductile performance of the pipe. If the pipe loading forces the pipe to deform significantly, the mortar may spall, allowing corrosion to begin.

## PIPELINE FITTINGS AND APPURTENANCES

A pipeline system is only as strong as its weakest component. Therefore, fittings and appurtenances such as valves and hydrants should be constructed out of rugged materials. Air release valves should be designed to accommodate water hammer. Service connections should be designed to accommodate differential movement.

## CONCLUSIONS AND RECOMMENDATIONS

Pipelines are vulnerable to ground deformation. To mitigate earthquake damage there are several strategies listed below.

For new pipe:

- If possible, avoid high earthquake hazard areas.
- Use low vulnerability pipe in high hazard areas if they can not be avoided.
- Design appurtenances and connections to be as earthquake resistant as the pipeline itself..

For existing pipe:

- Upgrade vulnerable highly critical pipeline segments.
- Implement a long-term replacement program prioritized on pipe criticality and vulnerability.

For all pipeline systems:

- Install operational flexibility.
- Build in emergency response capability.

## ACKNOWLEDGMENTS

The author would like to thank Professor Michael O'Rourke of Rensselaer Polytechnic Institute for his insightful review comments. The U.S. Geological Survey is gratefully acknowledged for the funding to develop ***Minimizing Earthquake Damage, A Guide for Water Utilities.*** Funding from the National Center for Earthquake Engineering Research is appreciated for support of review of the document by the American Society of Civil Engineers Technical Council on Lifeline Earthquake Engineering.

## REFERENCES

1. American Water Works Association - Pipe Standards, See Table 1, Denver CO.

2 Ballantyne, Donald B., 1994, *Minimizing Earthquake Damage, a Guide for Water Utilities,* American Water Works Association, Denver CO.

3 Ballantyne, Donald B. , 1995, *Water System Damage in the Great Hanshin (Kobe) Earthquake,* presented at the American Water Works Association Conference, Anaheim, CA, June.

4 Eguchi, Ronald T., Mark Legg, Craig Taylor, Lloyd Philipson, and John Wiggins; 1983, *Earthquake Performance of Water and Natural Gas Supply Systems,* NSF Grant No. PFR-8005083, J.H Wiggins Company.

5. Miyajima, M. And K. Kitaura, 1989, *Effects of Liquefaction-Induced Ground Movement on Pipeline,* Proceedings from the Second U.S.-Japan Workshop on Liquefaction, Large Ground Deformation, and Their Effect on Lifelines, Grand Island, New York, September 26-29.

**Table 1**

**RELATIVE EARTHQUAKE VULNERABILITY OF WATER PIPE**

| Material Type/Diameter | AWWA Standard | Joint Type | Ruggedness | Bending | Joint Flexibility | Restraint | Total |
|---|---|---|---|---|---|---|---|
| *Low Vulnerability* | | | | | | | |
| Ductile Iron | C1xx Series | B&S, RG, R | 5 | 5 | 4 | 4 | 18 |
| Polyethylene | C906 | Fused | 4 | 5 | 5 | 5 | 19 |
| Steel | C2xx Series | Arc Welded | 5 | 5 | 4 | 5 | 19 |
| Steel | None | Riveted | 5 | 5 | 4 | 4 | 18 |
| Steel | C2xx Series | B&S, RG, R | 5 | 5 | 4 | 4 | 18 |
| *Low/Moderate Vulnerability* | | | | | | | |
| Concrete Cylinder | C300, C303 | B&S, R | 3 | 4 | 4 | 3 | 14 |
| Ductile Iron | C1XX Series | B&S, RG, UR | 5 | 5 | 4 | 1 | 15 |
| PVC | C900, C905 | B&S, R | 3 | 3 | 4 | 3 | 13 |
| Steel | C2xx | B&S, RG, UR | 5 | 5 | 4 | 1 | 15 |
| *Moderate Vulnerability* | | | | | | | |
| AC > 8" D | C4xx Series | Coupled | 2 | 4 | 5 | 1 | 12 |
| Cast Iron > 8" D | None | B&S, RG | 2 | 4 | 4 | 1 | 11 |
| PVC | C900, C905 | B&S, UR | 3 | 3 | 4 | 1 | 11 |
| Concrete Cylinder | C300, C303 | B&S, UR | 3 | 4 | 4 | 1 | 12 |
| *Moderate/High Vulnerability* | | | | | | | |
| AC <=8" D | C4xx Series | Coupled | 2 | 1 | 5 | 1 | 9 |
| Cast Iron <= 8" D | None | B&S, RG | 2 | 1 | 4 | 1 | 8 |
| Steel | None | Gas Welded | 3 | 3 | 1 | 2 | 9 |
| *High Vulnerability* | | | | | | | |
| Cast Iron | None | B&S, Rigid | 2 | 2 | 1 | 1 | 6 |

B&S - bell & spigot; RG - rubber gasket; R - restrained; UR - unrestrained

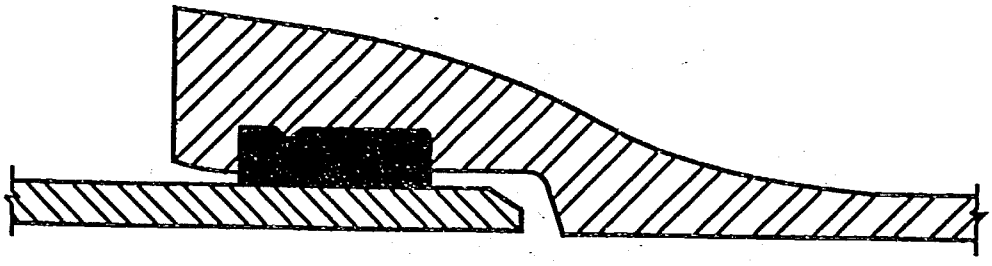


Figure 1
Tyton Type Bell and Spigot Joint

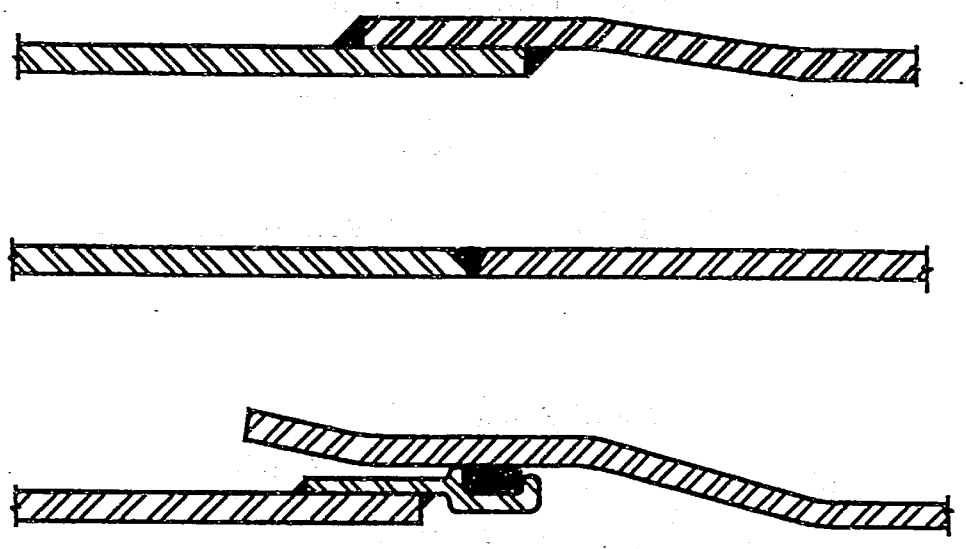


Figure 2
From Top to Bottom, Lap-Welded Slip, Single-Butt Weld,
and Carnegie-Shape Rubber Gaskets Joints

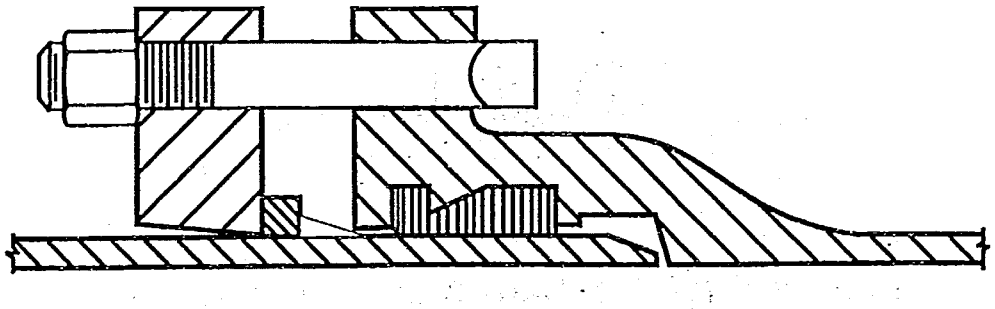


Figure 3
Bolted Restrained Push-on Joint

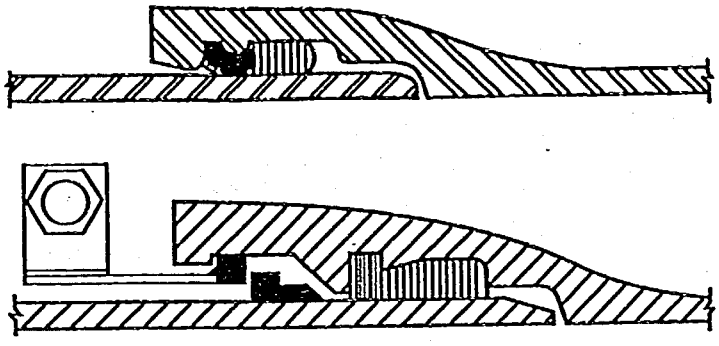
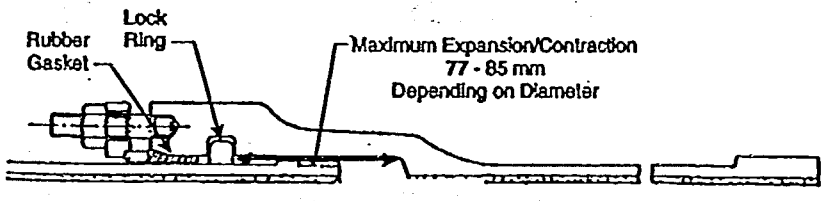
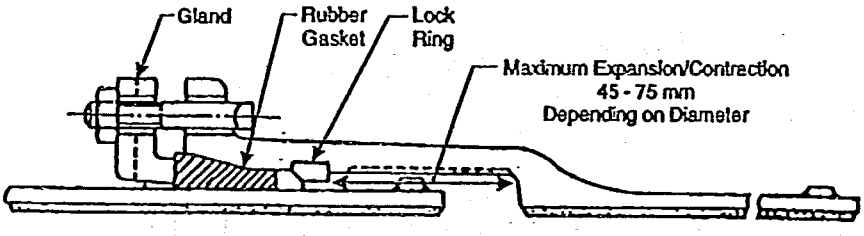


Figure 4
Boltless Restrained Joints




"S" Joint (500 - 2600 mm Diameter)




"SII" Joint (100 - 450 mm Diameter)

Figure 5
Seismic Joints (S ans SII)

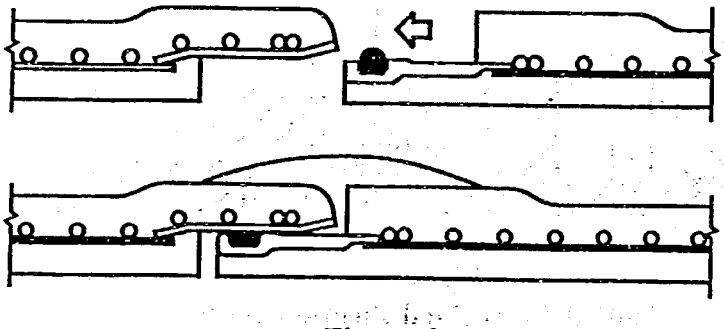


Figure 6
Concrete Cylinder Pipe Joint

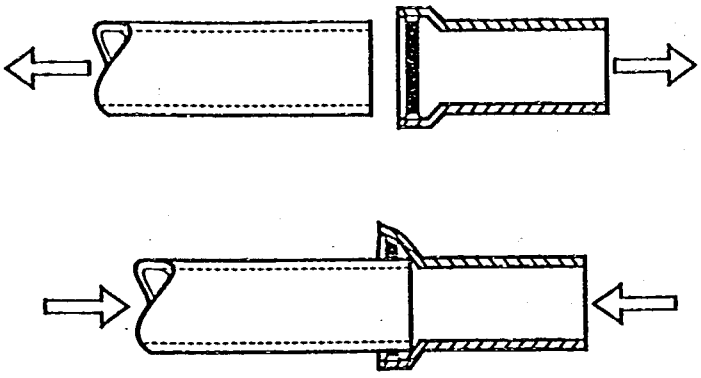


Figure 7
Extension (top) and Compression (bottom) Failures

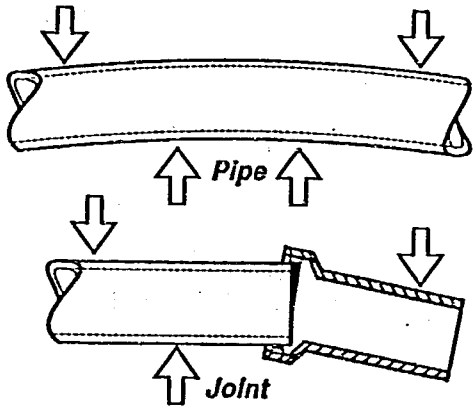



Figure 8
Bending

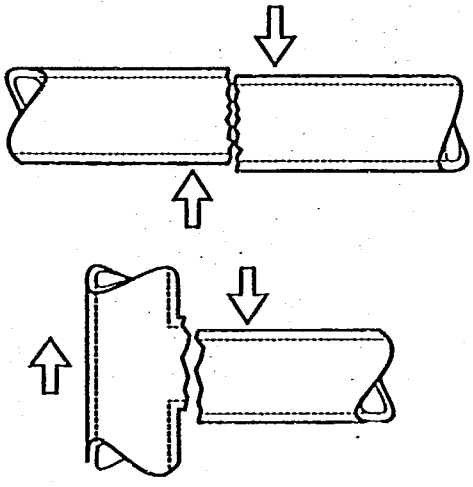


Figure 9
Shear

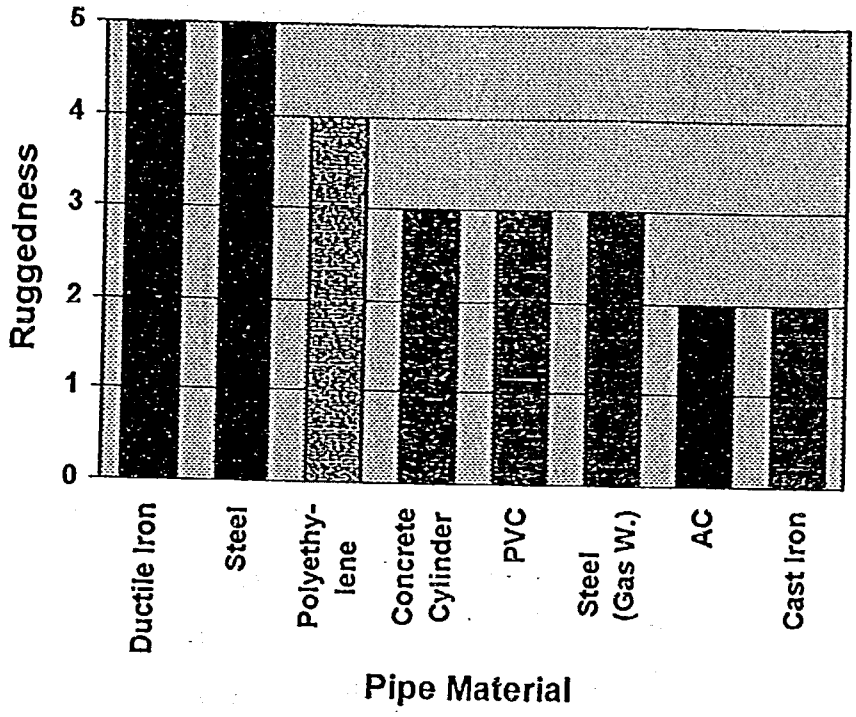



**Figure 10**
**Pipe Material Ruggedness**

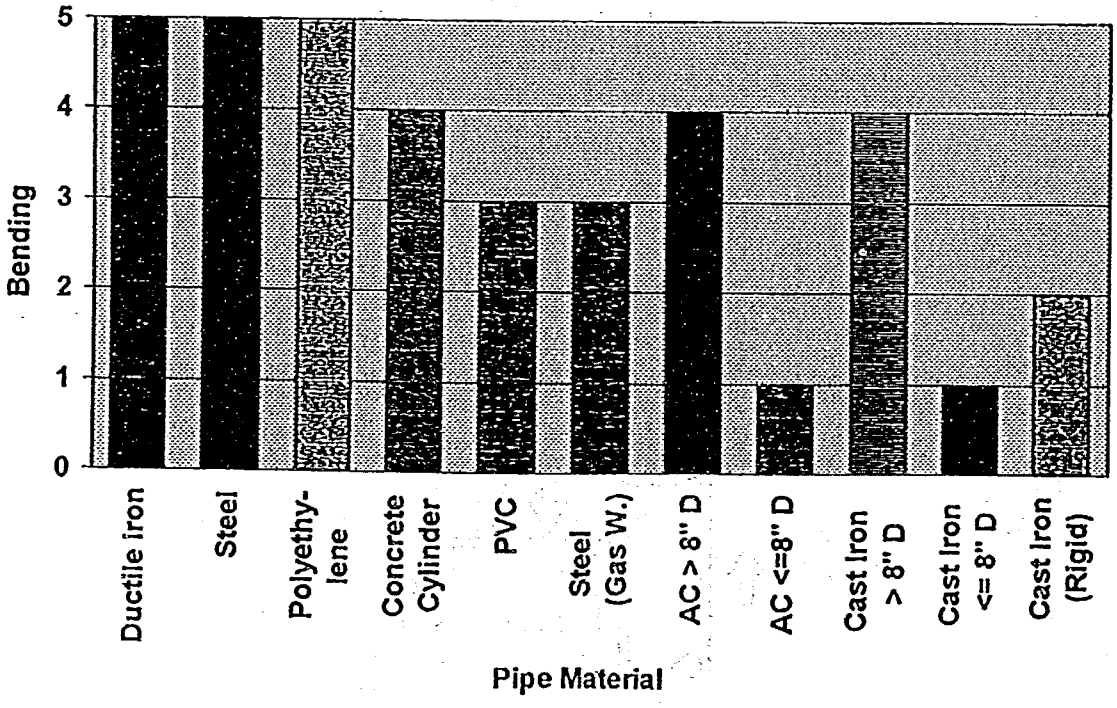



**Figure 11**
**Pipe Material Resistance to Bending**

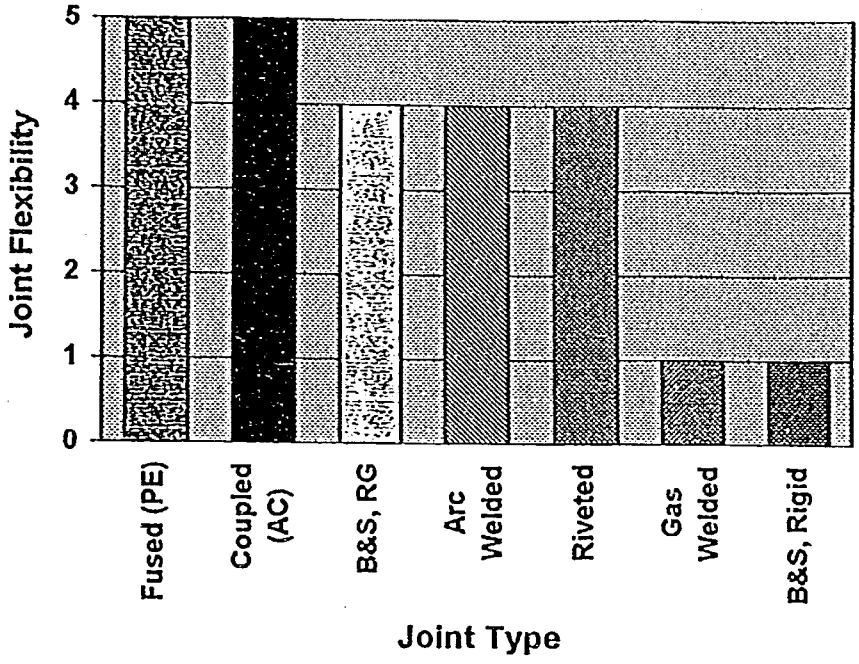



**Figure 12**
**Joint Flexibility**

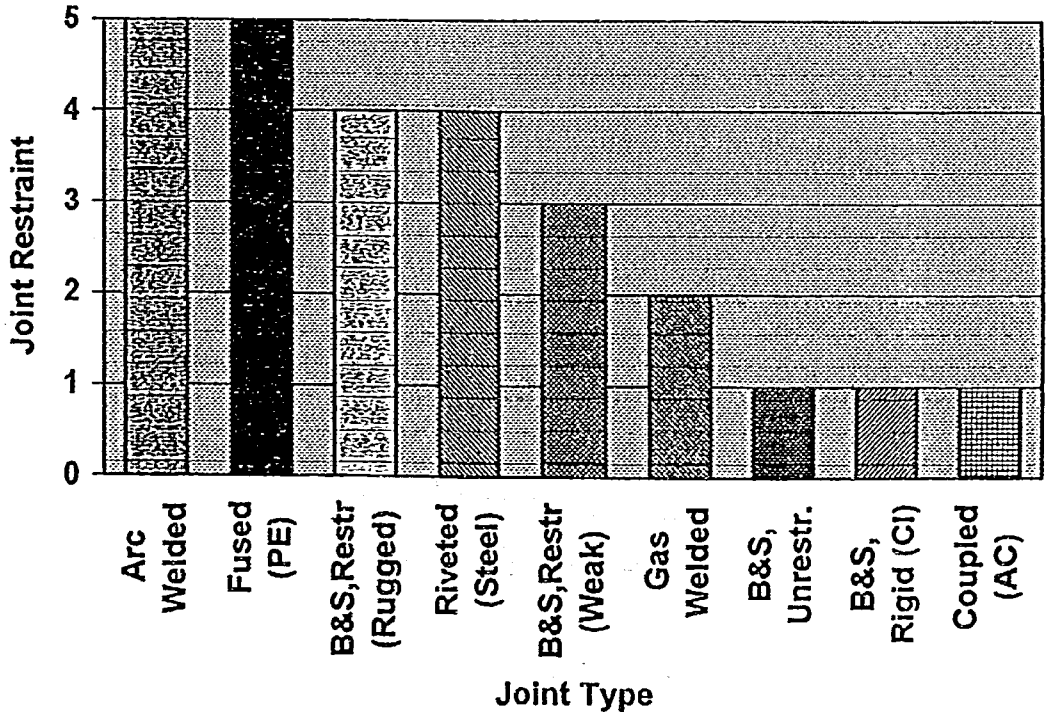



**Figure 13**
**Joint Restraint**

# ECONOMIC IMPACT OF LIFELINE DISRUPTION: CURRENT MODELS AND PRELIMINARY OBSERVATIONS FROM THE HANSHIN EARTHQUAKE

Stephanie E. Chang
Wm. Jess Taylor

EQE International, Inc.
Irvine, California

## ABSTRACT

Lifeline failures in the January 17, 1995 Hanshin earthquake disrupted the economy of the Kobe region with a severity previously unexperienced in any modern urban area. The potential for such catastrophic lifeline failures in a major seismic event also exists in the U.S.; however, disaster experiences in the U.S. do not provide a sufficient basis for estimating the likely economic impact of such events. This paper surveys current economic loss estimation methodologies associated with lifeline disruption, identifies their limitations, and presents a new regression-based methodology that addresses some of these issues. This methodology is then applied to evaluating the economic effects of lifeline disruption in the Hanshin earthquake, focusing on how disruption of different lifelines contributed to the total direct and indirect economic losses. The analysis is based on information for the first 10 weeks following the disaster and is sensitive to variations in damage and restoration between constituent subareas of the impacted region. Water, gas, and transportation lifeline disruption is evaluated in this context. While the results are preliminary, the model is shown to be robust and to have high explanatory power. Of the lifelines considered, transportation appears to have the greatest impact. Issues for further research are discussed.

## INTRODUCTION

Lifeline failures in the January 17, 1995 Hyogo-ken Nambu earthquake (also referred to as the Hanshin earthquake) disrupted the economy of the Kobe region with a severity previously unexperienced in any modern urban area. Widespread disruption of water and gas services and the massive, simultaneous failures of virtually all of Kobe's major transportation systems -- highways, local railways, the Shinkansen, and port facilities -- imposed an economic paralysis on the region that underscores the high degree to which modern urban functions depend upon effective lifeline services. With estimated restoration times of 3 to 6 months for the major rail lines connecting Kobe and Osaka and 6 months to 2 years for resumption of normal port services, the disruption of transportation in particular seems likely to entail economic consequences of a sort previously unexperienced in a modern urban economy.

Lifeline failures of this magnitude may also be experienced in the large urban earthquakes currently anticipated in California, as well as in moderate earthquakes striking less prepared areas in the eastern United States. However, our experiences of disasters in this country do not provide a sufficient basis for estimating the likely economic impact of such events, in which severe disruption is likely to be experienced simultaneously across several different types of lifeline systems. This paper focuses on the question of how disruption of different types of lifelines contributes to the total direct and indirect economic losses in a major urban disaster. An evaluative framework is proposed and applied to the experience of the Hanshin earthquake. First, however, current approaches to modeling the economic impact of lifeline disruption are reviewed.

## CURRENT MODELING APPROACHES

The economic impact of earthquakes and other natural disasters has been gaining attention in recent years, and many methodological improvements have been made with respect to estimating the direct and indirect regional economic losses beyond the costs of repairing physical damage. However, only a handful of studies have focused attention on lifelines.

Perhaps the most comprehensive study of the economic impact of lifeline disruption is ATC-25, "Seismic Vulnerability and Impact of Disruption of Lifelines in the Coterminous United States" (Applied Technology Council 1991). ATC-25 provides a methodology for estimating the direct business interruption losses associated with lifeline disruption at a business site. Specifically, for a particular lifeline $i$ and industry $j$, estimates of an "importance factor" $a_{ij}$ are provided, based on expert judgment. These importance factors indicate the percent of production that would be lost if lifeline service were completely disrupted. The relationship between lifeline disruption and production loss is assumed to be linear, so that partial lifeline service disruption is expected to induce a proportionate loss in output. The first 5 percent of lifeline outage is assumed to be absorbed without loss. The importance factors provide a simple means of comparison across different types of lifelines. In general, for example, electricity has a much higher importance factor than natural gas because few businesses are able to operate long without electricity.

A somewhat different, although complementary, approach is employed in a study by Eguchi et al. (1992) that was limited to evaluating energy systems. For a particular energy system and geographic area (e.g., state), a weighted average restoration time factor is multiplied with associated energy use factors and value added coefficients to obtain economic loss estimates. Unlike ATC-25, this approach does not rely upon importance factors determined by expert judgment. In addition, the spatial dimension of lifeline disruption and restoration is explicitly recognized insofar as meaningful geographic subareas comprising the impacted region are analyzed separately.

The preceding studies do not, however, evaluate indirect economic losses due to lifeline disruption. Indirect losses are defined here as downstream effects on other businesses that derive from reduced production by businesses suffering direct losses. Direct losses consist of those repair costs and business interruption losses caused by lifeline disruption at the business site. To estimate indirect losses, several studies have employed variations of input-output (I-O) analysis. I-O analysis is based upon a set of inter-industry production relations through which changes in one industry are propagated to other industries in the regional economy. I-O analysis has been applied to estimating lifeline-related losses both for a specific lifelines (Eguchi et al. 1990; Boisvert 1992; Rose and Benavides 1993) and within the context of a more comprehensive impact assessment (Kawashima and Kanoh 1990).

However, the application of I-O analysis to lifelines suffers from several important limitations. First, evaluation is based upon the pre-earthquake economic structure of the region. To account for earthquake-induced changes in economic structure, adjustments can be made to the inter-industry coefficients of the I-O model (e.g., Boisvert 1992; Rose and Benavides 1993); however, these adjustments must be arbitrarily imposed and may be infeasible to calibrate from actual experience. Second, because I-O analysis is based upon a rigid, fixed-coefficients vision of production technologies, it is inherently unable to capture the flexibilities, substitutions, and adaptations that households, businesses, industries, and economies appear to institute in the wake of a disaster. A third limitation consists of the difficulty of accommodating the spatial dimension of economic impact. Virtually all I-O analysis for earthquake hazards has been conducted without differentiating between areas within an impacted region. While a multi-subregion I-O model for a metropolitan area has been applied to estimating earthquake impact with a spatial dimension in Los Angeles (Gordon and Richardson 1992), in practice this is very difficult and expensive to implement. Finally, network effects -- the very quality that distinguishes lifeline impact from losses related to building damage -- cannot be captured within an I-O modeling framework. All of these factors limit the applicability of I-O analysis to evaluating the contribution of different lifelines to total regional economic loss.

With the advent of the Northridge earthquake, many studies are currently being conducted that will advance the state-of-the-art in modeling the economic impact of lifeline disruption, particularly in the case of transportation. The availability of empirical data from an actual, sizable urban earthquake disaster will certainly provide many new insights into the mechanisms and magnitudes of economic impact. One potentially important alternative framework to I-O analysis, econometric modeling, has so far only been applied to a hypothetical earthquake (Ellson et al.

1985). The severe lifeline disruption in the Hanshin earthquake provides a further, very valuable opportunity for developing new insights and improving models of economic loss associated with lifeline disruption.

## IMPACT IN THE HANSHIN EARTHQUAKE

### General Observations

Direct capital asset losses in the Hanshin earthquake have been estimated at approximately 9.9 trillion yen. (Hyogo Prefectural Government 1995) At an exchange rate of 85 yen to the dollar, this amounts to 116 billion dollars, or over 5 times the corresponding losses in the Northridge earthquake. Of this total, 5.8 trillion (59 percent) is buildings damage and 2.8 trillion (29 percent) consists of repair costs to lifelines. In other words, lifeline damage alone in the Hanshin earthquake exceeds total structural and infrastructure losses in the Northridge earthquake.

The total economic impact of the earthquake, however, includes direct and indirect business interruption losses as well as reconstruction costs. At the national level, the impact of the earthquake on Japanese gross domestic product (GDP) is expected to be measurable but small. Various economic research institutes in Japan have estimated the impact on GDP in fiscal year 1994 (ending in March 1995) to range from -0.5 percent to -0.03 percent. In fiscal year 1995, with the economic boost from reconstruction activity, the impact on GDP is expected to range from -0.3 percent to +2.0 percent. ("Disaster Impact Estimates..." 1995) For example, the Nomura Research Institute estimated that the earthquake would have a -0.6 percent impact on GDP in the first quarter of 1995, a -0.1 percent impact in the second quarter, and a +0.3 percent impact in the remaining two quarters of the year. (NRI Economic Research 1995)

While the national impact may be minimal, clearly the regional losses are very great. Soon after the earthquake, Nomura Research Institute estimated that the Kobe region would suffer a 15 percent loss in gross regional product (GRP) in the January-March 1995 period. Sanwa Bank Research Institute expected a 30 to 50 percent short-run production loss in the impacted region, before reconstruction effects are felt in the region. (Sanwa Bank Research Institute 1995) While actual figures have not yet been released as of this writing, available indicators support these estimates. Some preliminary figures collected by the Kobe City government are shown in table 1. Drops in department store sales peaked in February at a 91 percent loss; in March, the number of unemployed persons grew by 123 percent. (Kobe City Government 1995)

These studies do not, however, evaluate the contribution of lifeline disruption to total economic loss. In a qualitative sense, the speed of economic recovery is to a large extent dependent upon the speed of lifeline restoration. In the short run, this dependency arises because of the requirements for water, electricity, transportation access, and so on in production activities. In the long run, sustained lifeline disruption (such as closure of the port) may cause permanent shifts in economic behavior such as the relocation of plants to areas outside the earthquake-impacted region.

To evaluate the economic effect of lifeline disruption in the Hanshin earthquake, it will be important to take into account the very strong spatial effect deriving from the geography of lifeline damage and restoration. Generally speaking, the central and western wards of Kobe City suffered the greatest lifeline damage. The restoration of lifeline service also proceeded from areas of least damage inward to areas of greatest damage. This restoration pattern, which is clearest for the gas and transportation lifelines, can be expected to have a significant impact on economic loss and recovery in different parts of the impacted region.

## Methodological Approach

Because of the extent of lifeline disruption in the Hanshin earthquake, it is expected that the associated economic impacts should be both measurable and significant. This section presents a preliminary model of lifeline disruption impact based on data available within the first four months after the disaster. The objectives of this model are threefold: (1) to evaluate the contribution of lifeline disruption to the total direct and indirect regional economic loss; (2) to compare the impact across different types of lifelines; and (3) to develop a viable methodology for estimating lifeline disruption impact in future urban earthquake disasters in the U.S.

The methodological approach consists of developing a multivariate regression model to explain post-earthquake reductions in economic activity as a function of losses in various lifeline services. The model controls for factors other than lifeline disruption that also reduce economic activity. Two dimensions of the economic impact are particularly important to capture: the geographic variation in initial impact as well as subsequent lifeline restoration, and contrasts in the temporal restoration progress of different lifelines. Unlike other approaches such as input-output modeling, a regression model provides flexibility in evaluating economic impact without imposing an economic structure within which the effects propagate.

The general format of the model is as follows:

$$Q_{s,t} = \alpha + \sum_{l} \beta_{l,s,t} R_{l,s,t} + \sum_{j} \gamma_{j,s,t} P_{j,s,t} + \varepsilon \qquad (1)$$

where $Q$ is a measure of economic activity in subarea $s$ at time $t$ (normalized by expected economic activity without the earthquake), $R$ is a similarly normalized measure of post-earthquake lifeline $l$ service availability, $P$ is a measure of earthquake-related non-lifeline factors $j$ that influence economic loss, $\alpha$, $\beta$, and $\gamma$ are parameters to be estimated, and $\varepsilon$ is the error term.

It is important to select a time interval for analysis that is both meaningful from an analytical point of view and feasible from the standpoint of data availability. Because of the timeframe within which lifeline services are restored, intervals of less than a month are relevant; however, restoration data are generally not available on a daily basis. Datapoints were therefore evaluated on a weekly basis for this analysis. The duration of analysis was limited to 10 weeks because of data availability; however, this is probably sufficient in view of the fact that lifeline services were generally restored by the end of March. Exceptions include port facilities, segments of certain transportation routes and to a lesser extent natural gas service.

Similar considerations governed the choice of the basic spatial unit of analysis. The study area, shown in figure 1, includes Kobe and five other cities (Ashiya, Nishinomiya, Takarazuka, Itami, and Amagasaki). Kobe City itself is comprised of 9 city wards (Higashinada, Nada, Chuo, Hyogo, Nagata, Suma, Tarumi, Nishi and Kita) which are comparable in population to the other cities. However, not all of the information needed for the analysis is available at this level. In particular, electricity data was available for electric service areas, which are larger units. Their correspondence with the city and ward boundaries are also shown in figure 1. Since the city/ward delineation and the electric service area delineation both have advantages and disadvantages, analysis was conducted for each spatial system.

One of the principal difficulties with implementing equation (1) consists of obtaining economic data for $Q$ at the necessary level of spatial and temporal disaggregation. Fortunately, economic activity can be readily approximated by volume of electricity consumption, for which detailed data is generally available. Furthermore, electricity is frequently restored very quickly after an earthquake, in comparison with other lifelines such as natural gas or transportation. Following the Northridge earthquake, for example, the electrical service was essentially completely restored after four days (City of Los Angeles 1994); in Kobe, severely damaged buildings aside, electricity was completely restored within one week (The Kansai Electric Power Co., Inc. 1995). Once service is completely restored, electricity consumption can presumably serve as a reasonable indicator of economic activity.

Explanatory variables in the model were selected on the basis of their expected contribution to *loss* in economic production following the earthquake within the 10-week timeframe of analysis. These included availability of water and natural gas, transportation accessibility, and degree of buildings damaged in a particular ward, city, or electric service area. The latter variable is intended to serve as a control variable for the general extent of physical damage; the other variables are lifelines of interest. Given the 10-week timeframe of analysis, it is assumed that only short-term impacts will be measured. Therefore, no consideration was given to long-term changes in economic structure due, for example, to the closure of Kobe Port. It is important to note that the model is designed to investigate post-earthquake deviations from normal economic activity, rather than economic activity levels themselves. As a consequence, it does not include any typical economic variables such as interest rate, exchange rate, labor force characteristics, etc.

## Data

For this analysis, lifeline usage and restoration data pertaining to electricity, gas, water, rail and highway, and the Port of Kobe were used. Information on structural damage was also required. Data were collected in Japan from lifeline companies, government agencies, university researchers and published sources. The data were collected in May 1995 with the support of a "quick-response" grant from the National Science Foundation. Information was available in a variety of formats, including reports, press releases, unpublished charts, and maps; furthermore, information on different topics varied widely in terms of what was available four months after the disaster. Developing a consistent dataset proved to be an important challenge.

**Electricity.** Electric service was restored to virtually all customers within about a week after the earthquake. Because of this short restoration time, electricity can be used as a reasonable proxy for measuring post-earthquake economic output. Detailed electricity usage data was made available by the Kansai Electric Power Company and included usage by service area for each weekday between January 17, the day of the earthquake, and March 24, 10 weeks after the event. Comparable pre-earthquake usage data was available for only one date, Friday, January 13. Therefore, for this analysis, usage figures were used for each Friday in the 10 weeks following the earthquake for which data were available. Usage was normalized by the January 13 pre-earthquake level. This provides a measure of post-earthquake usage as a percentage of "normal" usage by electrical service area. Given the short time period of analysis, pre-earthquake electricity consumption may serve as a reasonable estimate of usage had there been no earthquake.

Because the electrical service areas span multiple wards and cities, a second dataset was constructed for wards and cities. The mapping of the electrical service areas to the ward/city level was performed (with one exception) by assigning unweighted values to the corresponding wards or cities. For the most part, wards and cities were contained within electric service areas. Specifically, the Nishi and Tarumi wards were assigned to the Akashi service area, the Suma, Nagata, Hyogo and Kita wards were assigned to Hyogo, and the Nada and Higashinada wards were assigned to Fukiai. The Chuo ward overlaps two service areas, Hyogo and Fukiai, and was assigned a weighted average of their electrical usage. The weights were based upon the area of overlap within each service area (4.4 $km^2$ in Hyogo and 17.6 $km^2$ in Fukiai). The cities of Ashiya and Nishinomiya were assigned to the Nishinomyia service area, Takarazuka and Itami cities to the Itami service area and Amagasaki city to the Tachibana service area.

**Gas.** Gas service was severely disrupted by the earthquake with full service restored in most areas by the end of March, over two months after the earthquake. Detailed daily gas restoration figures were obtained from Osaka Gas Company press releases at the ward/city level in terms of number of customers without gas and total customer base. Percentages of customers with gas service were calculated for each Friday between January 17 and March 24. For the last Friday, data was not available; inferences were therefore made by interpolating data from the last date for which information was available.

**Water.** The disruption of the region's water service was very similar to the gas service disruption, but restoration proceeded more quickly and was completed towards the end of March. Restoration data was provided by the Kobe City Waterworks Bureau and supplemented with information assembled by researchers from Hiroshima University of Technology for surrounding cities. The latter was accessed through the Hanshin earthquake clearinghouse located at Tokyo University. The data included weekly restoration figures (percent of normal availability) by ward/city from the date of the earthquake through the end of March.

**Structural Damage.** Within Kobe city alone, over 160,000 residential homes were severely damage or collapsed. Residential damage levels were available on a ward/city level from a report based on field surveys by the Architectural Institute of Japan (1995). Similar damage data for commercial buildings was unavailable. Based upon residential damage percentages, the Nagata

and Nada wards were the most heavily damaged. Specifically, estimates were made of *un*damaged buildings as a percent of pre-earthquake residential building stock. Over the time frame of this study, virtually no new construction was undertaken, although much debris was cleared. It was therefore assumed that these percentage estimates remained constant over the study period.

**Transportation.** Transportation availability was assessed in terms of the accessibility of a particular ward/city by railroad and highway. In order to derive a summary index of transportation availability, each of the 14 wards and cities can be conceptualized as a distinct cell intersected by rail and road lines. Each point at which a transport line crosses the cell border is identified as a "gate" or transportation access point. Because of the geography of the impacted area, in which the cities are roughly arrayed in a linear fashion along an approximately east-west axis, most of the gates are located on the eastern and western sides of the cities and wards. In the earthquake, various segments of the several transportation lines were damaged and closed. Restoration also proceeded segment by segment, allowing greater transportation access to some areas before others.

Within this conceptual framework, several indices of transportation accessibility can be developed. For the analysis presented in this paper, three sets of indices were implemented. The simplest index consists of the percent of a city/ward's "gates" that are open at a particular point in time. These include both railroad and highway gates, and are based on the assumption that the two modes are complete substitutes in terms of both passenger and freight traffic. In other words, the economic effects of a rail gate or a road gate being open (or closed) are the same. The second set of indices used here assume that, instead, railways and highways are not substitutes. Two indices are computed, one for the percent of gates open for each transportation mode.

However, these indices take no account of the direction in which gates are open. For example, consider the case where 50 percent of a ward's transportation gates are closed due to earthquake damage. The economic impact is likely to be more severe if all of these closed gates were located along the eastern side than if the gates were evenly distributed between the eastern and western sides. In the latter case, the ward is still connected with neighboring areas on both sides, permitting people and goods to flow between them. A third set of indices is therefore developed to take into account directionality:

$$T_{s,t}^{W} = 1 - \frac{1}{\sqrt{n}} \cdot \sqrt{\sum_{i} G_i^2} \qquad , \quad i = 1, \ldots, n \tag{2}$$

where $T^W$ is the direction-weighted transportation accessibility index for area $s$ and time $t$, $n$ is the number of sides to the area being considered (in most cases $n = 2$, i.e. east and west); $i$ is an index for the side; and $G_i$ is the percent of gates closed on side $i$. If $n = 2$, $G_1 = 0$ and $G_2 = 1$, then $T^W = 0.29$. If, $G_1 = G_2 = 0.5$, then $T^W = 0.50$. For the analysis presented below, $T^W$ is evaluated separately for roads and railways.

Data to estimate the transportation indices were obtained from a series of newspaper articles and maps. In the case of roads, only major highways were included in the analysis. These included the following 7 highways/expressways: Chugoku; Rt. 171; Meishin; Rt. 2; Rt. 43; Daini Shinmei; and Wangan. For railways, the following 10 were included: Hanshin; JR Tokaido; Hankyu Kobe line; Hankyu Itami line; Hankyu Imazu line; JR Fukuchiyama line; JR Sanyo line; Kobe Kaisoku/Sanyo Dentetsu; Kobe Dentetsu Arimasen; and the Kobe City subway. Indices were calculated for each Friday from January 20th through March 24th. For the few cases where sufficient data was not available, reasonable inferences were made as to when segments of the transportation routes reopened. In further analysis, more complete data can improve the accuracy of the transportation accessibility estimates.

**Port.** The Hanshin earthquake wrought severe damage on the Port of Kobe, effectively closing its operation for a period of months or years. It was not until the end of April, well beyond the timeframe of this study, that any substantial cargo operations were resumed. A few cargo berths in the Maya Pier, Port Island, and Rokko Island areas of the Port did reopen towards the end of March, mostly on or after March 20. By the last Friday of the study period (March 24), 8 of the 80 berths in these areas were accessible. In order to control for the effect of resumed access to parts of the port, dummy variables were included for the last two weeks of the study period.

**Electric Service Areas.** In the dataset where spatial units are taken to be electric service areas, estimates for the water, gas, structural damage and transportation variables were first evaluated for the 14 wards and cities. These data are then combined into the corresponding service areas by using population figures for weights. Specifically, numbers for labor force age population by place of residence were obtained from the Japanese Census.

## PRELIMINARY MODEL AND RESULTS

In light of the data available within the first few months after the disaster, the general model in equation (1) was implemented in the following format:

$$E_{s,t} = \alpha + \beta_1 G_{s,t} + \beta_2 W_{s,t} + \beta_3 S_s + \beta_4 P_t + \beta_5 T_{s,t} + \varepsilon \qquad (3)$$

where $E$, $G$, $W$, and $T$ are, respectively, measures of the percentage availability of electricity, gas, water, and transportation in area $s$ at time $t$. $S$ is a measure of structures (building) availability and is invariant over time for each area. This is a reasonable assumption given that very few new buildings were constructed within the first ten weeks after the earthquake. $P$ is a dummy variable indicating the restoration of port facilities at week $t$, as discussed above. In week 10 (March 24), $P$ is 1; in other weeks, it is zero. A dummy variable at week 9 (March 17) was also investigated, but this turned out to be uniformly insignificant and is disregarded in the remaining analysis. In some cases, the general transportation variable $T$ was substituted by two variables indicating railroad and highway accessibility, respectively (either unweighted by spatial direction, $R$ and $H$, or weighted, $R^w$ and $H^w$).

The base dataset consists of variables at the electric power service area (ESA) level and excludes the first week's observations. Recall that electricity was not fully restored to the study area until one week after the disaster. Reduced electricity consumption within the first week may therefore reflect supply constraints in addition to reduced demand from production losses. In other words, the accuracy of electricity consumption as a measure of economic activity may be questionable in the first week. An alternative dataset including the first week was also used. Because ESAs are larger than city wards, analysis at this level may miss some significant variations in impact and recovery; furthermore, the explanatory variables are more accurate at the ward/city level. Alternative datasets at this level (with and without the first week) were therefore also used.

Given the nature of damage and recovery in this earthquake, it is reasonable to expect that many of the explanatory variables will be highly correlated. With one principal exception, however, correlation coefficients between pairs of variables are less than 0.80. Water and gas availability are highly correlated, with a Pearson correlation coefficient ranging from 0.76 to 0.84 in the four datasets described above. In addition, in the ESA datasets, the weighted railroad variable $R^w$ is highly correlated with both water and gas, with coefficients in the 0.77 to 0.83 range. In terms of the transportation variables, it is interesting to note that the highway and railroad accessibility variables ($H$ and $R$; $H^w$ and $R^w$) are not particularly highly correlated, with coefficients ranging from 0.4 to 0.6. These results indicate that multicollinearity may present a problem with respect to the water and gas variables.

A number of different versions of equation (3) were estimated using ordinary least squares (OLS) regression. Results for some of these models, labeled examples 1 through 10, are presented in table 2. Example 1 constitutes the base case using the ESA database, the full set of variables ($T$ for transportation), and excluding the first week's observations. With 48 degrees of freedom, the explanatory power of this base model is quite high, as indicated by the adjusted $R^2$ value of 0.78. An F-test indicates the model is significant at the 1 percent level.

The structures, port dummy, and transportation variables are all significant at the 1 percent level, while neither gas nor water are significant at the 10 percent level. Since all variables are measured in the same units (percent availability relative to pre-earthquake levels), coefficient magnitudes can be directly compared as an indicator of impact on economic activity. The influence of the structures variable dominates, while transportation has slightly greater influence than the port dummy variable. Interpreted literally, a one percent increase in the transportation accessibility index is associated with a 0.22 percent increase in economic activity. One puzzling result, discussed below, is the negative sign appearing on the coefficient for the port dummy variable.

While the base case seems to provide a reasonable model, several other alternatives were also explored. Examples 2 and 3 respectively utilize unweighted and weighted mode-separated transportation variables instead of $T$. The results are robust with respect to the specification of transportation: the $R^2$ value is improved slightly, while the significance and coefficients of the other variables do not change much. Both railroads and highways are significant at the 1 percent level; however, based on the estimated coefficients, railroad access appears to have over twice as much impact on economic activity as does highway access. Example 4 eliminates the port dummy

variable from the regression. Several arguments can be made for this elimination: the negative sign in the base case is counter-intuitive; the actual extent of port restoration in week 10 is minor; and the dummy variable may be capturing any number of effects other than partial port restoration. However, eliminating the variable does not appear to improve the regression results.

Examples 5 and 6 explore the benefits of eliminating the water and gas variables, which were statistically insignificant in the base model. In example 5, eliminating the water variable improves estimation of the gas variable, so that it is significant at the 10 percent level. This indicates that the statistical insignificance on the variable in the base case may be a result of collinearity problems rather than a lack of actual influence on economic activity. The magnitude of the influence is relatively small, however, since the estimated coefficient is only 0.09 on the gas variable, as compared with 0.23 on the transportation variable and 1.17 on the structures variable. Excluding gas as well as water does not appear to improve the results.

Examples 7 and 8 include the first week's observations. Overall, the model is quite robust to this change. The explanatory power of the model and the coefficients on the other variables are stable. The principal effect of including the first week's observations is to improve estimation of the coefficient on the water variable. Gas is still statistically insignificant. The coefficient on the water variable is 0.17 and significant at the 5 percent level in example 8, the model that excludes the gas variable. This coefficient is still less than the 0.26 coefficient on the transportation variable, indicating less influence on economic activity. Since the impact of water disruption was most significant in the early part of the 10-week period, and particularly in the first week, it is reasonable that including the first week's observations improves the coefficient estimate.

Finally, examples 9 and 10 investigate the effect of using cities and wards rather than electricity as the spatial unit of analysis, respectively including and excluding the first week's observations. In general, using cities/wards reduces the explanatory power of the model to an $R^2$ value in the 0.55 to 0.60 range. However, it also provides two benefits: first, it lowers the Durbin-Watson statistic to a range where no serial autocorrelation is indicated; in addition, it improves estimation of the water variable. The coefficient in example 10, using the first week's observations, is 0.21 on the water variable and significant at the 1 percent level. Gas is still insignificant, and the coefficients on the structures, port and transportation variables are robust to this change.

To summarize, variations on the model indicate that equation (3) is a generally robust model with high explanatory power. Results are consistent with expectations. Structures/buildings availability appears to have the greatest impact on economic activity. Controlling for this effect, among the various lifelines, transportation accessibility has the most influence, with railroads appearing to be more important than highways in this regard. The influence of the port is indicated by the significance of a dummy variable indicating when partial service was restored. However, the negative coefficient on this variable is counter-intuitive and indicates that the dummy variable may be capturing some effect other than port restoration. Water and gas probably have some influence on economic recovery; however, because of collinearity problems, the coefficients are difficult to estimate reliably. Indicators suggest that water has more impact than gas, and that its influence is particularly important in the first weeks after the disaster.

## CONCLUSIONS

The economic impact of lifeline disruption represents an important yet poorly understood dimension of the total impact of earthquake disasters on regional economies. This paper has provided an overview of current methodologies for evaluating lifeline disruption impact and presented an alternative framework that addresses some of the principal limitations of these methods. In particular, the regression model presented here provides an assessment tool for evaluating the contribution of disruption of different lifelines to the total (direct plus indirect) losses. This model imposes a minimum of pre-earthquake information and assumptions about economic structure on the post-disaster economic situation. Also, it is able to flexibly capture the spatial dimension of disaster losses and recovery in the impacted region.

Preliminary applications of this model were made to analyzing the impact of lifeline disruption in the January 17, 1995 Hanshin earthquake. Data available for the first 10 weeks after the disaster by 6 electric power service areas (as well as 14 cities and city wards) were used. Because of data constraints, electricity consumption was used as an indicator of economic activity. Estimated models using availability of structures/buildings, water, gas, and transportation access were shown to have high explanatory power and to be robust to changes in the model specification and dataset characteristics. Of these variables, structures consistently had the greatest impact while transportation was also consistently significant. Railroad access appears to have greater influence on economic activity than highway access. Results regarding the impact of gas and water disruption were inconclusive, due in part to problems associated with multicollinearity between these variables. However, some findings did indicate that economic impact is smaller for gas than for water, which in turn is smaller than for transportation. These results, while preliminary, are surprisingly robust and consistent with expectations.

The approach developed in this paper provides a flexible, transparent evaluative tool that lends itself readily to at least two different applications. First, because it allows comparison of the economic losses associated with individual lifelines as well as structural damage, it can potentially provide evidence to support development of regional lifeline restoration priorities and recovery planning. Second, the approach can potentially be very useful for comparisons across different earthquakes. Such comparisons will allow development of patterns and generalizations about the economic impact of earthquakes that will enable researchers to step beyond case-by-case analysis. This capability will be particularly important in anticipating and mitigating the losses from future major urban earthquake disasters in the U.S.

Several important improvements can be made to the preliminary framework and analysis presented in this paper. Perhaps most importantly, with more complete data, losses should be recalibrated to reference expected economic activity had the earthquake not occured, rather than pre-earthquake economic activity. This recalibration includes adjusting for seasonal variations, to which electricity consumption is likely to be rather sensitive. In addition, direct measures of economic activity such as output levels or employment should be used as the dependent variable when data become available. Also, it may be useful to try to separate out debris removal and reconstruction-related activity from "normal" production, as they would exert a positive effect on

production that mitigates against the negative effect of lifeline disruption that the model is attempting to measure. Another area for further research consists of developing a more satisfactory method for assigning impacts in the presence of multiple lifelines disruption. The present framework assumes that lifeline impacts are separable and linearly additive. In further analysis, autocorrelation in the error terms should also be investigated further and accounted for, if necessary. Finally, while the spatial dimension of lifeline disruption impact is captured within this framework, network effects should be incorporated. In the present model, this is only indirectly accounted for through the direction-weighted transportation indices. At the very least, the preliminary analysis in this paper indicates that in terms of understanding the economic impact of lifeline disruption, the Hanshin earthquake provides a very important opportunity for advancing the state of the field.

## ACKNOWLEDGMENTS

The analysis presented in this paper was made possible by the generous assistance and cooperation of many individuals and institutions. The authors are grateful to Kansai Electric Power Company, Osaka Gas Company, Kobe Port and Harbor Bureau, Kobe Waterworks Bureau, Hyogo Prefectural Government and Kobe City Government (Economics Bureau) for providing published and unpublished data that were used in the analysis. In addition, secondary information directly used in this paper was provided by Nomura Research Institute, Mr. T. Hayashi of Cornell University, Mr. H. Kanda of JR Railways, Prof. T. Onishi of Tokyo University, and Profs. T. Okada and E. Taniguchi of Kyoto University. The authors especially appreciate the assistance of Profs. H. Kameda and H. Hayashi of Kyoto University and Prof. F. Yamazaki of Tokyo University in facilitating data collection in Japan. Finally, Dr. C. Scawthorn and Mr. R. Eguchi of EQE provided critical conceptual input and data collection contributions to the study. This material is based upon work supported by the National Science Foundation under Grant No. CMS-9521150. Any opinions, findings, and conclusions or recommendations expressed in this material are those of the authors and do not necessarily reflect the views of the National Science Foundation.

## REFERENCES

Applied Technology Council. 1991. *Seismic Vulnerability and Impact of Disruption of Lifelines in the Coterminous United States.* Redwood City, California: Applied Technology Council.

Architectural Institute of Japan. 1995. *Preliminary Reconnaissance Report of the 1995 Hyogoken-Nanbu Earthquake.* Tokyo: Architectural Institute of Japan.

Boisvert, R.N. 1992. "Indirect Losses from a Catastrophic Earthquake and the Local, Regional, and National Interest," in *Indirect Economic Consequences of a Catastrophic Earthquake.* Washington, D.C.: Federal Emergency Management Agency, pp. 141-206.

City of Los Angeles, Department of Water and Power. 1994. *January 17, 1994 Northridge Earthquake Major Emergency Report.*

"Disaster Impact Estimates by Survey Institutes." 1995. *Toyo Keizai Monthly Statistical Report.* April: 7-11. (in Japanese)

Eguchi, R.T. and S.D. Pelmulder. 1992. "Impact on the National Energy Distribution Network," in *Indirect Economic Consequences of a Catastrophic Earthquake.* Washington, D.C.: Federal Emergency Management Agency, pp. 141-206.

Eguchi, R.T., H.A. Seligson, and J.H. Wiggins. 1990. "Indirect Losses Caused by lifeline Damage or Disruption," in *Proceedings of the U.S.-Japan Workshop on Earthquake Disaster Prevention for Lifeline Systems.* Tsukuba Science City, Japan: Public Works Research Institute, pp.549-574.

Ellson, R.W., J.W. Milliman, and R.B. Roberts. 1984. Measuring the Regional Economic Effects of Earthquakes and Earthquake Predictions. *Journal of Regional Science,* 24(4): 559-579.

Gordon, P. and H. Richardson. 1992. *Business Interruption Effects of a Major Earthquake in the Newport/Inglewood Fault Zone (NIFZ).* A report submitted to the National Committee on Property Insurance, Boston, Massachusetts. Los Angeles: The Planning Institute, School of Urban and Regional Planning, University of Southern California.

Hyogo Prefectural Government. 1995. *Overview of Damage.* report, May 7th. (in Japanese)

The Kansai Electric Power Co., Inc. 1995. *Impact of the Earthquake of Southern Hyogo Prefecture on Electric Facilities.*

Kawashima, K. and T. Kanoh. 1990. "Evaluation of Indirect Economic Effects Caused by the 1983 Nihonkai-chubu, Japan, Earthquake." *Earthquake Spectra,* 6(4): 387-404.

Kobe City Government. 1995. Appendix to *Kobe Economy: Scale and Specialization.* (in Japanese)

NRI Economic Research, Tokyo Department. 1995. *Economic Effects of the Hanshin Earthquake.*

Rose, A.Z. and J. Benavides. 1993. "Interindustry Models for Analzing the Economic Impacts of Earthquakes and Recovery Policies. Presented at *40th North American Meetings of the Regional Science Association International,* Houston, Texas, November 11-14, 1993.

Sanwa Bank Research Institute. 1995. *Great Hanshin Earthquake.* (in Japanese)

## TABLES

**Table 1. Change in Economic Activity Following the Hanshin Earthquake, Kobe City**

| Month / Year | Department Store Sales | Unemployed Persons |
|---|---|---|
| January 1995 | - 44.7 % | - 12.0 % |
| February 1995 | - 90.5 % | + 47.7 % |
| March 1995 | - 81.0 % | + 122.9 % |
| April 1995 | - 52.7 % | not available |

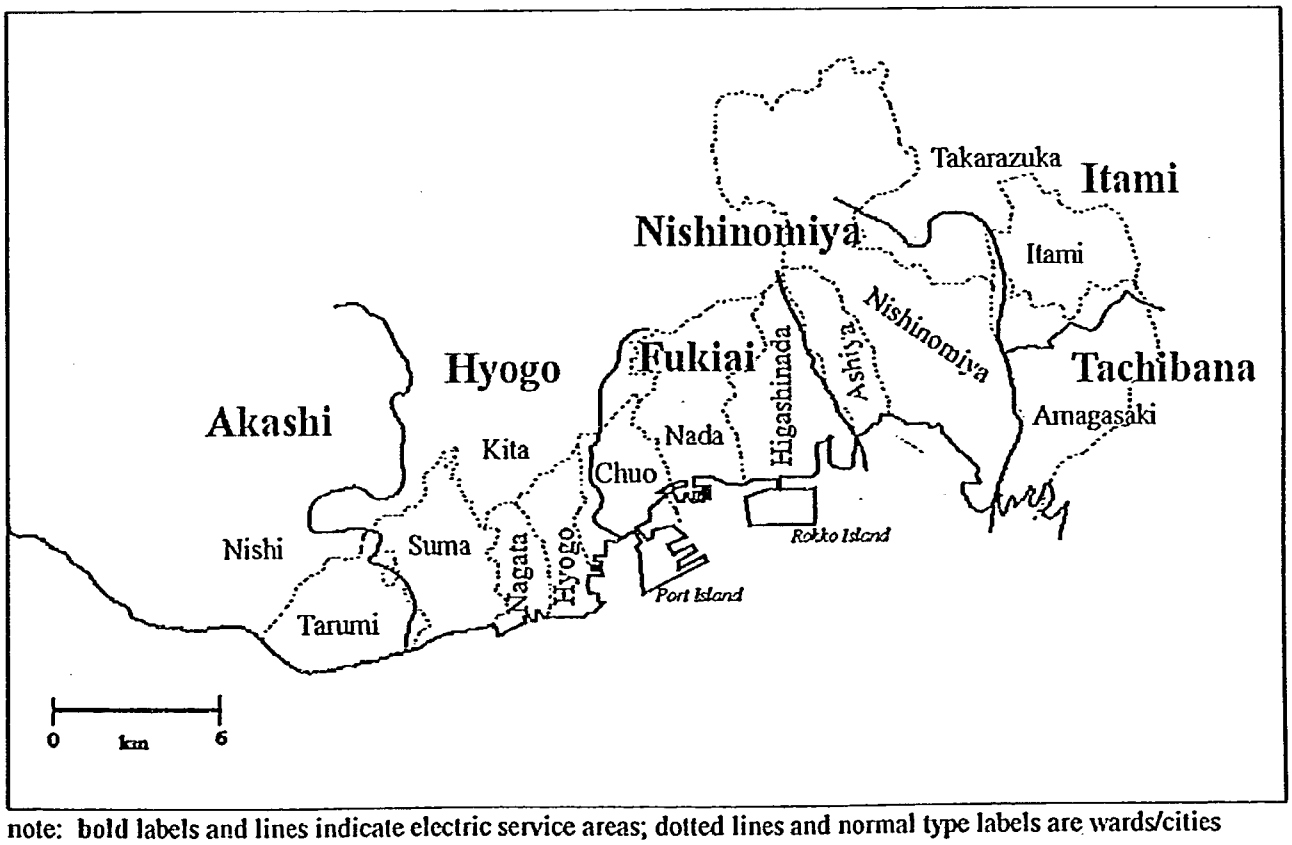
source: Kobe City Government

## Table 2. Regression Results

| Example | 1 | 2 | 3 | 4 | 5 | 6 | 7 | 8 | 9 | 10 |
|---|---|---|---|---|---|---|---|---|---|---|
| Spatial unit (a) | ESA | ESA | ESA | ESA | ESA | ESA | ESA | ESA | ward | ward |
| 1st week | exclude | exclude | exclude | exclude | exclude | exclude | include | include | exclude | include |
| Constant | -0.46** | -0.34* | -0.26 | -0.68*** | -0.43** | -0.51*** | -0.50** | -0.53*** | -0.004 | -0.04 |
| G | 0.08 | 0.002 | 0.04 | -0.19 | 0.09* | n/a | 0.006 | n/a | -0.006 | -0.04 |
| W | 0.03 | 0.004 | -0.06 | 0.06 | n/a | n/a | 0.16* | 0.17** | 0.12* | 0.21*** |
| S | 1.19*** | 1.00*** | 0.97*** | 1.48*** | 1.17*** | 1.29*** | 1.15*** | 1.16*** | 0.66*** | 0.61*** |
| P | -0.11*** | -0.10*** | -0.09*** | n/a | -0.11*** | -0.08*** | -0.10*** | -0.10*** | -0.09*** | -0.90*** |
| T1 | 0.22*** | n/a | n/a | 0.19** | 0.23*** | 0.28*** | 0.26*** | 0.26*** | 0.20*** | 0.24*** |
| R | n/a | 0.28*** | n/a | n/a | n/a | n/a | n/a | n/a | n/a | n/a |
| H | n/a | 0.12*** | n/a | n/a | n/a | n/a | n/a | n/a | n/a | n/a |
| RW | n/a | n/a | 0.27*** | n/a | n/a | n/a | n/a | n/a | n/a | n/a |
| HW | n/a | n/a | 0.11*** | n/a | n/a | n/a | n/a | n/a | n/a | n/a |
| adjusted $R^2$ | 0.78 | 0.82 | 0.80 | 0.72 | 0.78 | 0.77 | 0.78 | 0.79 | 0.55 | 0.58 |
| D-W | 2.36 | 2.70 | 2.60 | 1.75 | 2.38 | 2.15 | 2.10 | 2.10 | 1.81 | 1.68 |

notes: (a) ESA = electric service area; "ward"=ward/city; (b) significance levels: *=10%,**=5%,***=1%

## FIGURES




note: bold labels and lines indicate electric service areas; dotted lines and normal type labels are wards/cities

**Figure 1. Study Area**

# APPLICATION OF GIS TECHNOLOGY TO SEISMIC RISK ASSESSMENT OF LIFELINE SYSTEMS IN SHELBY COUNTY, TENNESSEE

Howard H. M. Hwang

Professor of Civil Engineering
Center for Earthquake Research and Information
The University of Memphis
Memphis, TN 38139, USA

## ABSTRACT

Geographic information system (GIS) technology is a powerful tool for collecting, managing, analyzing, and synthesizing spatial data; thus, it is increasingly being utilized in seismic hazard and seismic risk assessment. In this paper, we describe an on-going research on the application of GIS technology to seismic risk assessment of lifeline systems in Memphis and Shelby County, Tennessee. We have collected data relevant to geologic and geophysical features, local soil conditions, ground shaking, liquefaction potential, buildings, bridges, and lifelines in Memphis and Shelby County. These data have been implemented into a GIS database using ARC/INFO and MapInfo. Using these GIS data sets, a comprehensive seismic risk assessment of the lifeline systems in the Memphis area is being carried out. The results will be used by government agencies, professionals, and the general public to mitigate seismic risk in the Memphis area.

## INTRODUCTION

Memphis and Shelby County, Tennessee, are located geographically close to the southwestern segment of the New Madrid seismic zone (NMSZ), which is regarded by seismologists, engineers, and public officials as the most hazardous seismic zone in the eastern United States. Therefore, Memphis and Shelby County are exposed to significant seismic hazards. A large earthquake could cause widespread loss of life, damage to buildings and bridges, and interruption of essential services, such as water, gas, and electricity. To mitigate seismic risk, we need to collect geological and seismological data, predict seismic hazards, evaluate seismic vulnerability of buildings, bridges, and lifelines, estimate possible direct and indirect losses, and develop pre-earthquake preparedness and post-earthquake emergency response plans. In this way, the potential economic and societal impact caused by an earthquake can be minimized.

Geographic information system (GIS) technology is a powerful tool for collecting, managing, analyzing, and synthesizing spatial data (Aronoff 1989). The use of GIS facilitates the manipulation of spatial data, expands spatial analysis capabilities, and enhances visualization of analysis results. Thus, GIS technology is increasingly being used in seismic risk assessment studies. In this paper, we describe an on-going research on the application of GIS technology, such as ARC/INFO (ESRI 1991) and MapInfo (1994), to seismic risk assessment of lifeline systems in Memphis and Shelby County, Tennessee.

## DIGITAL BASE MAP AND GROUND FEATURES

The base map used in this project is the digital map implemented in the TIGER Files (1991). The scale of the map is 1:100,000, and it was prepared by the U.S. Geological Survey for the Bureau of the Census. The selection of a digital base map is one of the most critical tasks in carrying out a project using GIS, because this digital base map has a significant effect on the overall accuracy of the GIS work.

In this study, we implemented two kinds of municipal boundaries into the GIS database. The first one is the political boundaries that define Shelby County and the municipalities within the county, such as Memphis, Germantown, Collierville, Bartlett, Lakeland, Arlington, and Millington (Figure 1). These boundaries were digitized from the Official Map of Shelby County, Tennessee. The other is the boundaries of the 1990 census tracts, which were extracted from the TIGER Files. We use census tracts as the smallest units to represent the study area.

A GIS data set of the elevation in Shelby County was created from digitizing the USGS topographic quadrangle maps. The bedrock contours in the study area were determined using the geophysical log data of the five deep wells inside the county and 42 other wells in the vicinity of Shelby County. Furthermore, we collected, compiled, and analyzed about 8500 existing boring logs in the Memphis area to create representative boring logs in the cells resulting from applying a grid system to the entire study area (Ng et al. 1989). Then, we classified the soil profile in each cell into three soil-profile types, S2, S3, and S4, as specified in the Uniform Building Code (1991). On the basis of these data, we established a GIS coverage of soil-profile classification in Shelby County (Figure 2).

## SEISMIC HAZARDS

The seismic hazard data implemented in the GIS database are pertinent to ground shaking and soil liquefaction potential in Memphis and Shelby County. Both probabilistic and deterministic approaches have been used to estimate ground shaking. Hwang (1991) estimated the intensity of ground shaking in Memphis and Shelby County based on a moment magnitude 7.5 earthquake occurring at Marked Tree, Arkansas. For such a scenario earthquake, a seismologically based model was used to estimate the horizontal bedrock accelerations primarily caused by shear waves generated from the seismic source. The nonlinear site response analyses were then carried out to determine the dynamic site periods, acceleration time histories and corresponding response spectra at the ground surface for the study area. Furthermore, Hwang et al. (1995) performed a probabilistic seismic hazard analysis for Memphis and Shelby County based on the seismic source zones as shown in Figure 3. The resulting contours of peak ground acceleration in hard rock with 10% exceeding probability in 50 years and 250 years are shown in Figures 4 and 5, respectively.

The soil liquefaction potential in the Memphis area has been evaluated by Hwang and Lee (1992). The factor of safety against liquefaction $F_L$ was used to evaluate the liquefaction potential for a soil layer. The resistance of sandy and gravelly soils to liquefaction was determined using the empirical relation developed by Seed et al. (1983), while the liquefaction resistance for silty soils was determined using the empirical relation proposed by Shi (1987). The liquefaction potential of a site is affected by the severity, thickness, and depth of the liquefied layers. The site liquefaction potential index $P_L$ established by Iwasaki et al. (1982) was used to evaluate the severity of liquefaction potential at a site: little or no liquefaction ($P_L = 0$), minor liquefaction ($0 < P_L \leq 5$), moderate liquefaction ($5 < P_L \leq 15$), and major liquefaction ($P_L > 15$). The $P_L$ values of 575 representative boring logs were determined to establish a generalized map showing the areas of no, minor, moderate, and major liquefaction potential in the Memphis area (Figure 6).

## LIFELINE SYSTEMS

Memphis and Shelby County did not adopt any seismic design provisions until 1990. Consequently, most existing facilities in the Memphis area were not designed to resist earthquakes. These facilities may be vulnerable to ground shaking and ground failures in the event of an earthquake. The coverage of interstate highways and other critical routes in Shelby County (Figure 7) was established by extracting the data from the TIGER Files. Furthermore, data pertinent to 452 bridges in Shelby County, such as super- and sub-structures, year of construction, and average daily traffic volume, are being collected and implemented into the GIS database.

The utility systems delivering water, gas, and electricity to the people in the Memphis area are operated by the Memphis Light, Gas and Water Division (MLGW). The water in the Memphis water delivery system (Figure 8) is taken from underground aquifers by deep wells and delivered to the public after treatment. As of 1990, there are eight pumping stations in the low-pressure system and one pumping station in the high-pressure system. In addition to these pumping stations, six elevated tanks are used in the high-pressure system and nine booster pumps connect the low-pressure and high-pressure systems. Unlined cast iron pipes were used before 1960, while cement-lined cast iron pipes or ductile iron pipes were installed afterwards. Data pertinent to the entire Memphis water delivery system have been collected and implemented into the GIS database. Similarly, data pertinent to the MLGW gas transmission system (Figure 9) and standard-pressure distribution system have been collected and implemented into the GIS database.

The MLGW electric system receives 500 kV and 161 kV electric power from the Tennessee Valley Authority (TVA) at three locations: Cordova Substation, Thomas H. Allen Substation, and North Shelby Substation. The electric power is then transmitted to 44 substations throughout Memphis and Shelby County by means of 161 kV, 115 kV and 23 kV transmission circuits. Information relevant to the MLGW electric transmission system has been collected and implemented into the GIS database. Two GIS coverages were established: one for the substations, and the other for the transmission lines. Figure 10 shows the GIS-generated electric transmission system in Shelby County.

## SEISMIC RISK ASSESSMENT

The performance of water, gas, electricity utility systems in the event of a New Madrid earthquake is being evaluated by the NCEER lifeline research group. The resulting economic and societal impact is also being investigated. For example, the performance of MLGW water network subject to a large New Madrid earthquake has been evaluated by Shinozuka et al. (1992, 1993). From 25 simulations of damage

to the water network, average water head and average output flow were determined for each node. Then, the results were laid over the census tract coverage to estimate the effect of seismic damage to the network on the water supply in each census tract. Furthermore, Shinozula et al. (1994) also investigated the interaction of water and electric utility systems in the event of an earthquake.

## CONCLUDING REMARKS

In this paper, we describe an on-going research on seismic risk assessment of lifeline systems in Memphis and Shelby County, Tennessee. We have collected available data relevant to geologic and geophysical features, local soil conditions, ground shaking, soil liquefaction potential, buildings, bridges, and lifelines (water, gas and electric systems) in Memphis and Shelby County. These data have been implemented into a GIS database using ARC/INFO and MapInfo. By using these GIS data sets, a comprehensive seismic risk assessment of lifeline systems in Memphis and Shelby County is being carried out. The results will be used by government agencies, professionals, and the general public to mitigate seismic risk in the Memphis area.

We have learned that GIS technology is a powerful tool for collecting, managing, analyzing, and synthesizing spatial data. It provides an information management system which can be readily updated to reflect changes in analytical procedures and the availability of additional data. Furthermore, the use of GIS facilitates the visualization of analysis results, and thus GIS technology can provide a better communication between technical staff and decision makers, and between organizations with overlapping interests. Therefore, GIS technology is increasingly being used in seismic hazard, seismic risk, and seismic zonation studies.

## ACKNOWLEDGMENTS

This paper was prepared as a result of research sponsored by the National Center for Earthquake Engineering Research (NCEER) under contract numbers NCEER 933303 and 943301C (NSF grant number BCS-9025010). The support and guidance given by Professor Masanobu Shinozuka is greatly appreciated. In addition, the efforts made by Huijie Lin, Tien Chou, and Yu-Heng Yeh for implementing GIS data sets are also greatly appreciated.

## REFERENCES


Aronoff, S. (1989). *Geographic Information Systems: A Management Perspective.* WDL Publications, Ottawa.

Environmental Systems Research Institute (1991). *ARC/INFO Users Guide..* Redlands, CA.

Hwang, H. (1991). "Seismic Hazards for Memphis Water Delivery Systems." *Proceedings of the Third U. S. Conference on Lifeline Earthquake Engineering,* Los Angeles, CA, 510-519.

Hwang, H., and Lee, C.S. (1992). "Evaluation of Liquefaction Potential in Memphis Area, USA." *Proceedings of the Tenth World Conference on Earthquake Engineering,* Madrid, Spain, 1457-1460.

Hwang, H., Huo, J.R., and Lin, H. J. (1995). "Probabilistic Mapping of Peak Hard-Rock Acceleration in the Memphis Area, USA." to appear in the *Proceedings of 5th International Conference on Seismic Zonation,* Nice, France.

Iwasaki, T., Tokida, K., Tatsuoka, F., Watanabe, S., Yasuda, S. and Sato, H. (1982). "Microzonation for Soil Liquefaction Potential Using Simplified Methods." *Proceedings of the 3rd International Earthquake Microzonation Conference,* Seattle, WA, 3, 1319-1330.

Ng, K.W., Chang, T.-S. and Hwang, H. (1989). *Subsurface Conditions of Memphis and Shelby County.* Technical Report NCEER-89-0021, National Center for Earthquake Engineering Research, SUNY, Buffalo, New York.

Seed, H.B., Idriss, I.M. and Arango, I. (1983). "Evaluation of Liquefaction Potential Using Field Performance Data." *Journal of the Soil Mechanics and Foundations Division,* ASCE, 109(3), 458-482.

Shi, Z. (1987). "Study of Silt Liquefaction During Earthquakes." *Earthquake Research in China,* 1(3), 415-429.

Shinozuka, M., Hwang, H. and Murata, M. (1992). "Impact of Water Supply of a Seismically Damaged Water Delivery System." *Lifeline Earthquake Engineering in the Central and Eastern U.S.,* D.B. Ballantyne (ed.), Monograph No. 5, Technical Council on Lifeline Earthquake Engineering, ASCE, New York, 43-57.

Shinozuka, M., Hwang, H., and Tanaka, S. (1993). "GIS-Based Assessment of the seismic Performance of a Water Delivery System." *Proceedings of Fifth U.S.-Japan Workshop on Earthquake Disaster Prevention for Lifeline Systems,* K. Kawashima, H. Sugita, and T. Nakajima (eds.), PWRI 3198, Public Works Research Institute, Tsukuba, Japan, pp. 233-249.

Shinozuka, M., Shumuta, Y., Tanaka, S., and Koiwa, H. (1994). "Interaction of Lifeline Systems under Earthquake Condition." *Proceedings of Second China-Japan-U.S. Trilateral Systems on Lifeline Earthquake Engineering,* Xi'an, China, pp. 43-52.

*TIGER/Line Census Files, Technical Documentation* (1991). Bureau of the Census, Washington, DC.

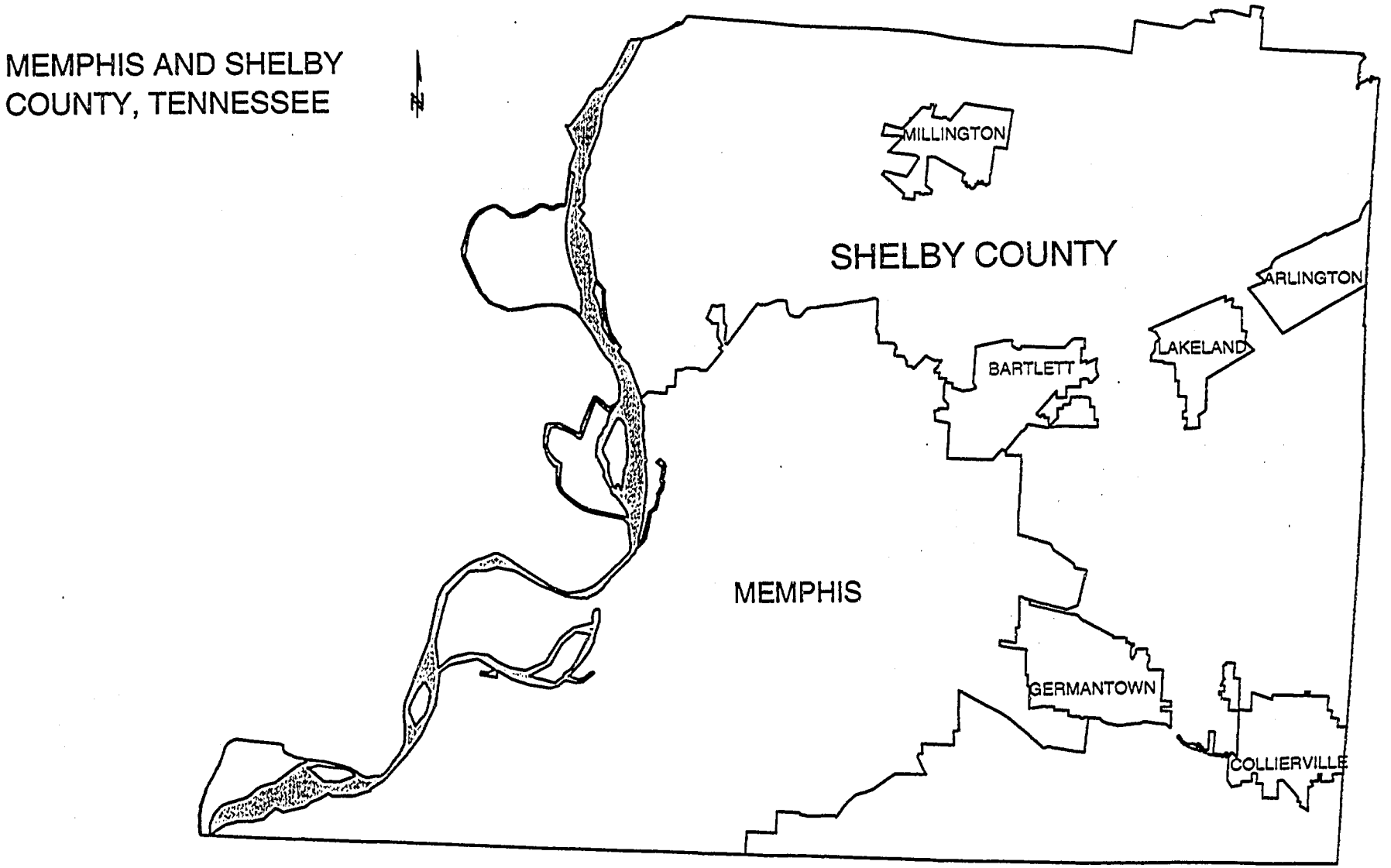



Figure 1 Memphis and Other Municipalities in Shelby County

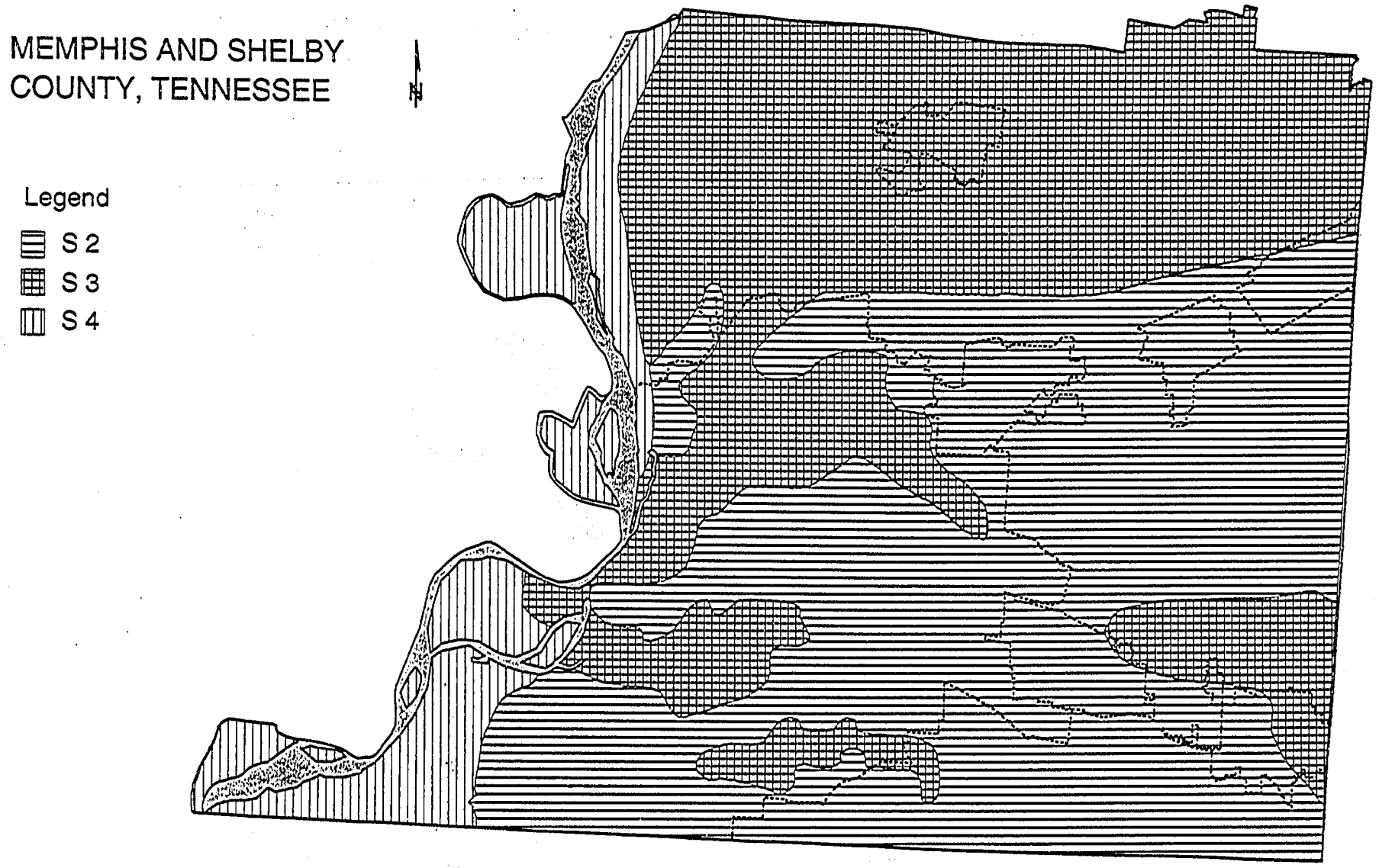



Figure 2 Soil-Profile Classification in Shelby County

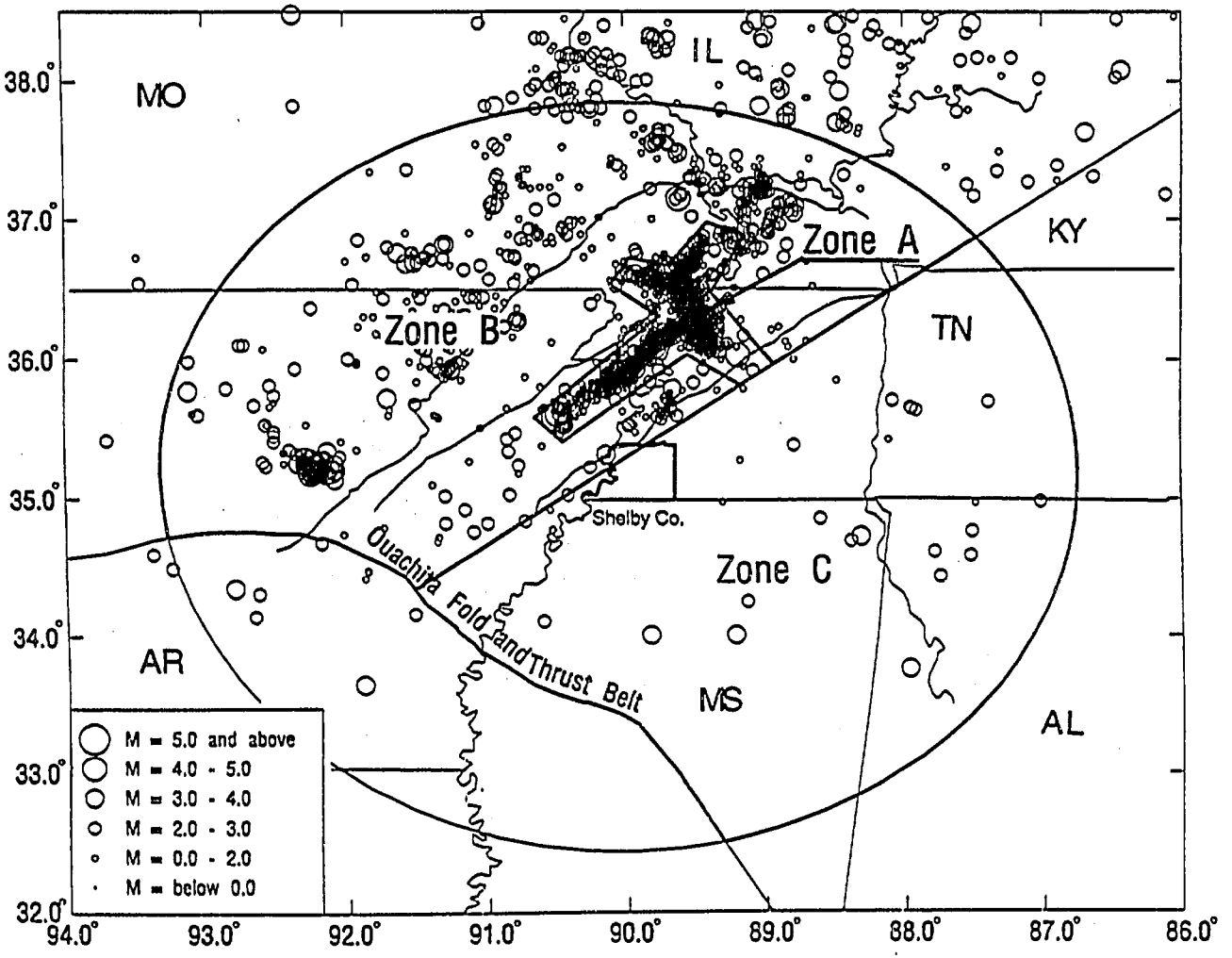



Figure 3 Seismic Source Zones in the Central United States

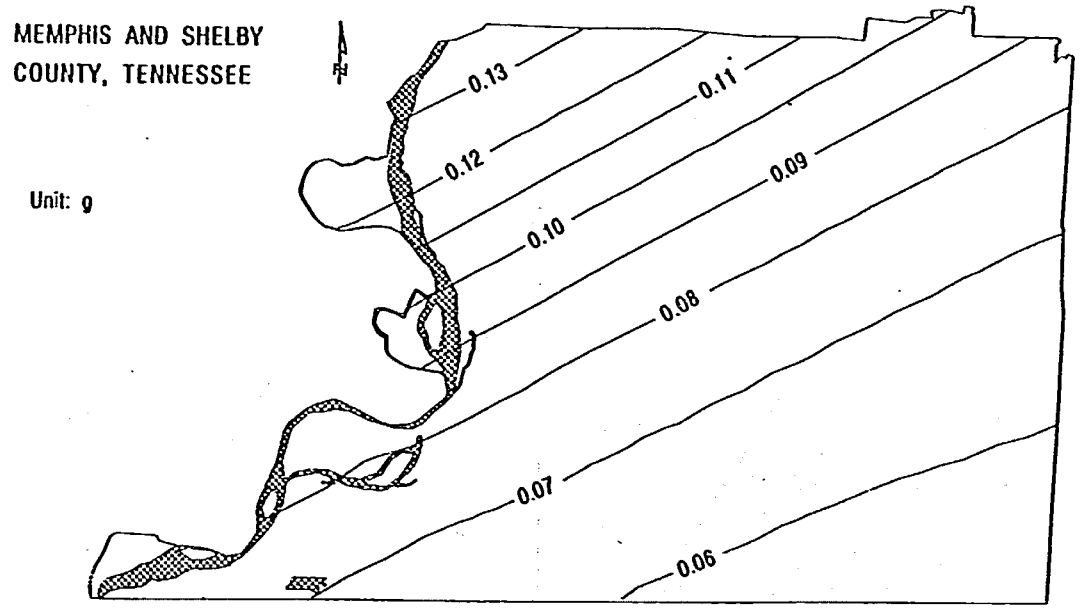



Figure 4 Contours of Peak Acceleration with 10% Exceeding Probability in 50 years

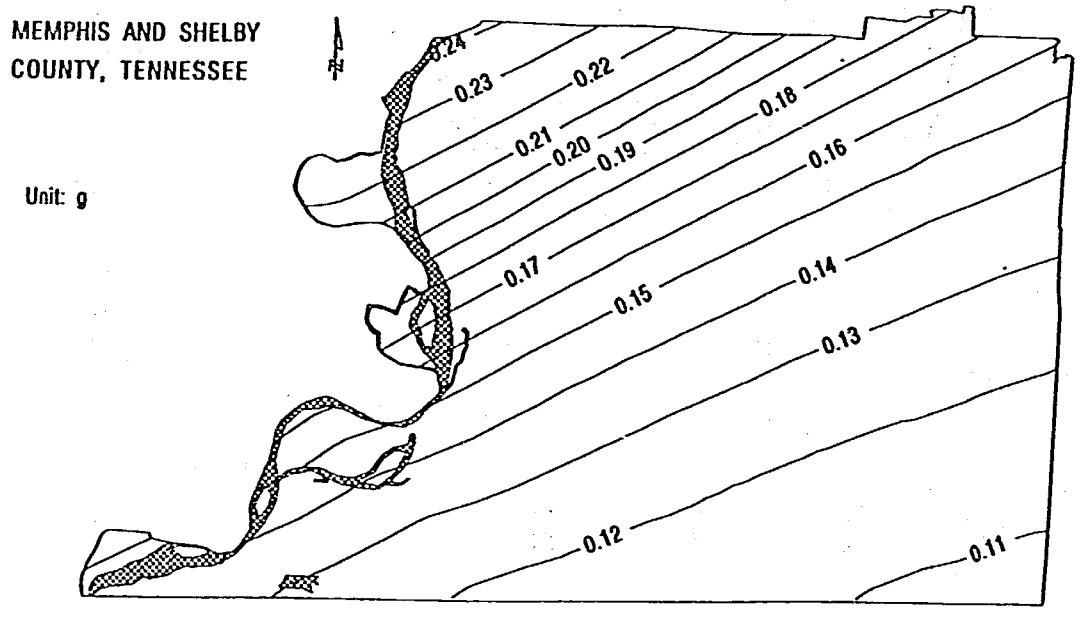



Figure 5 Contours of Peak Acceleration with 10% Exceeding Probability in 250 years

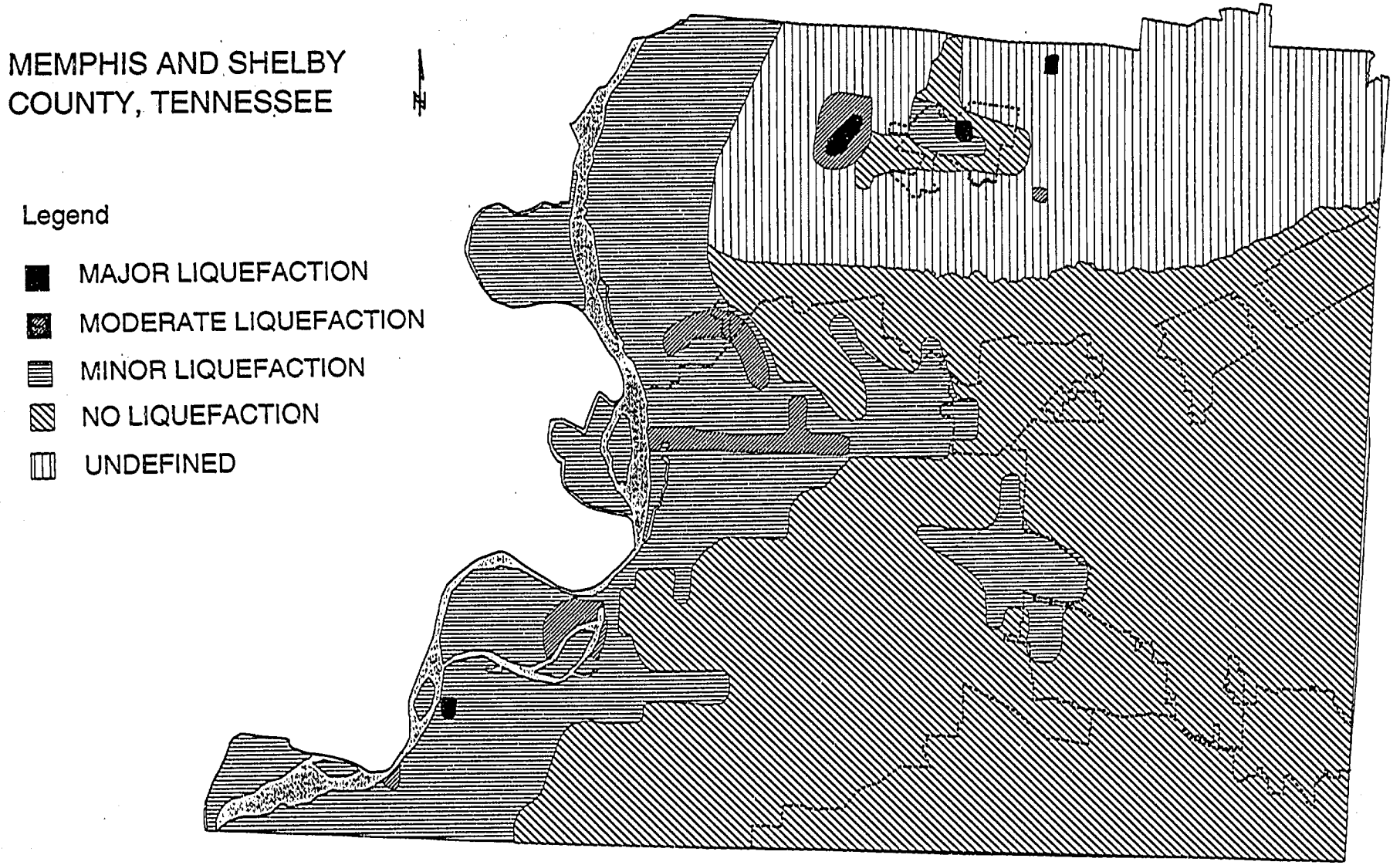



Figure 6 Soil Liquefaction Potential in Shelby County

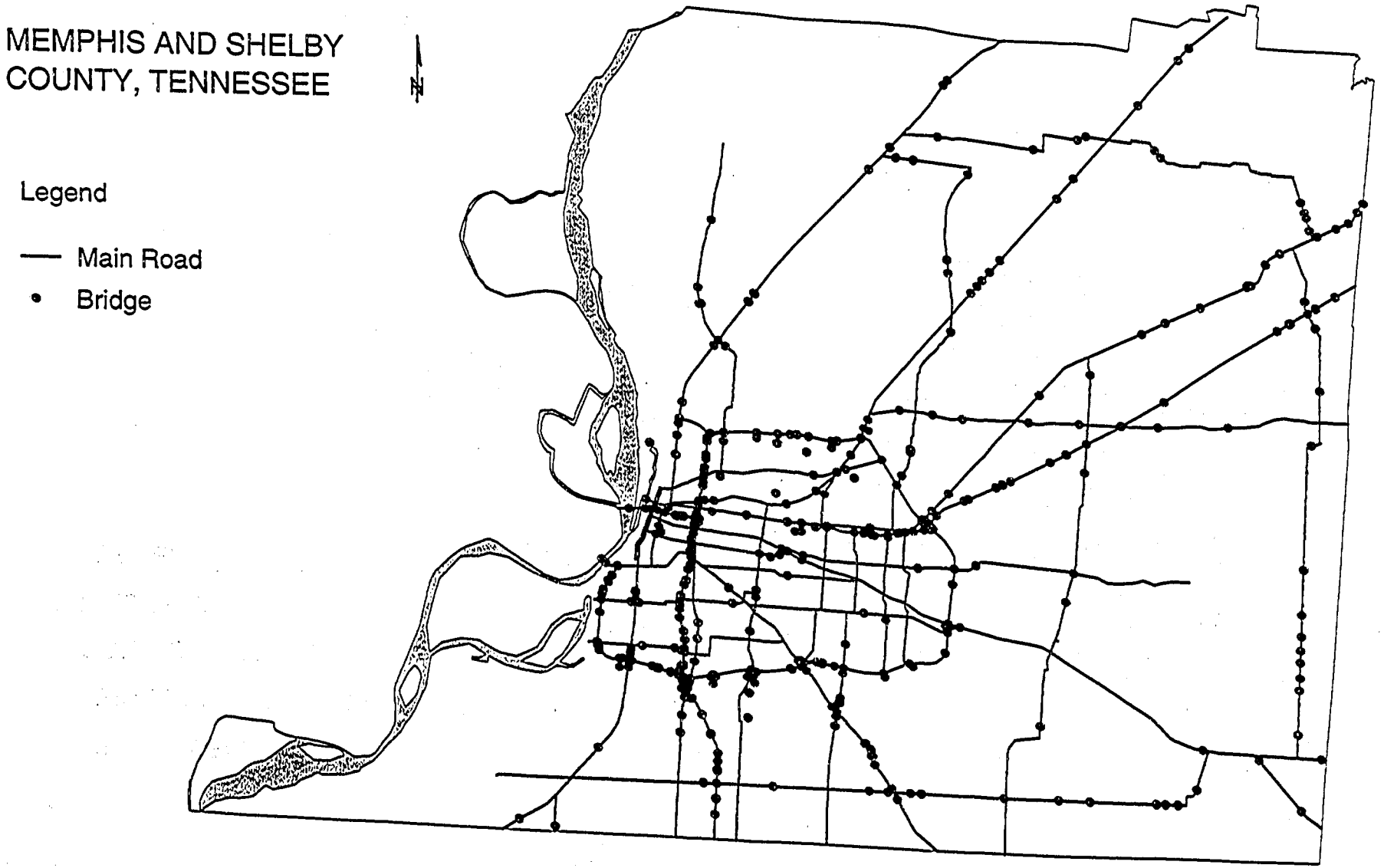



Figure 7 Main Roads and Bridges in Shelby County

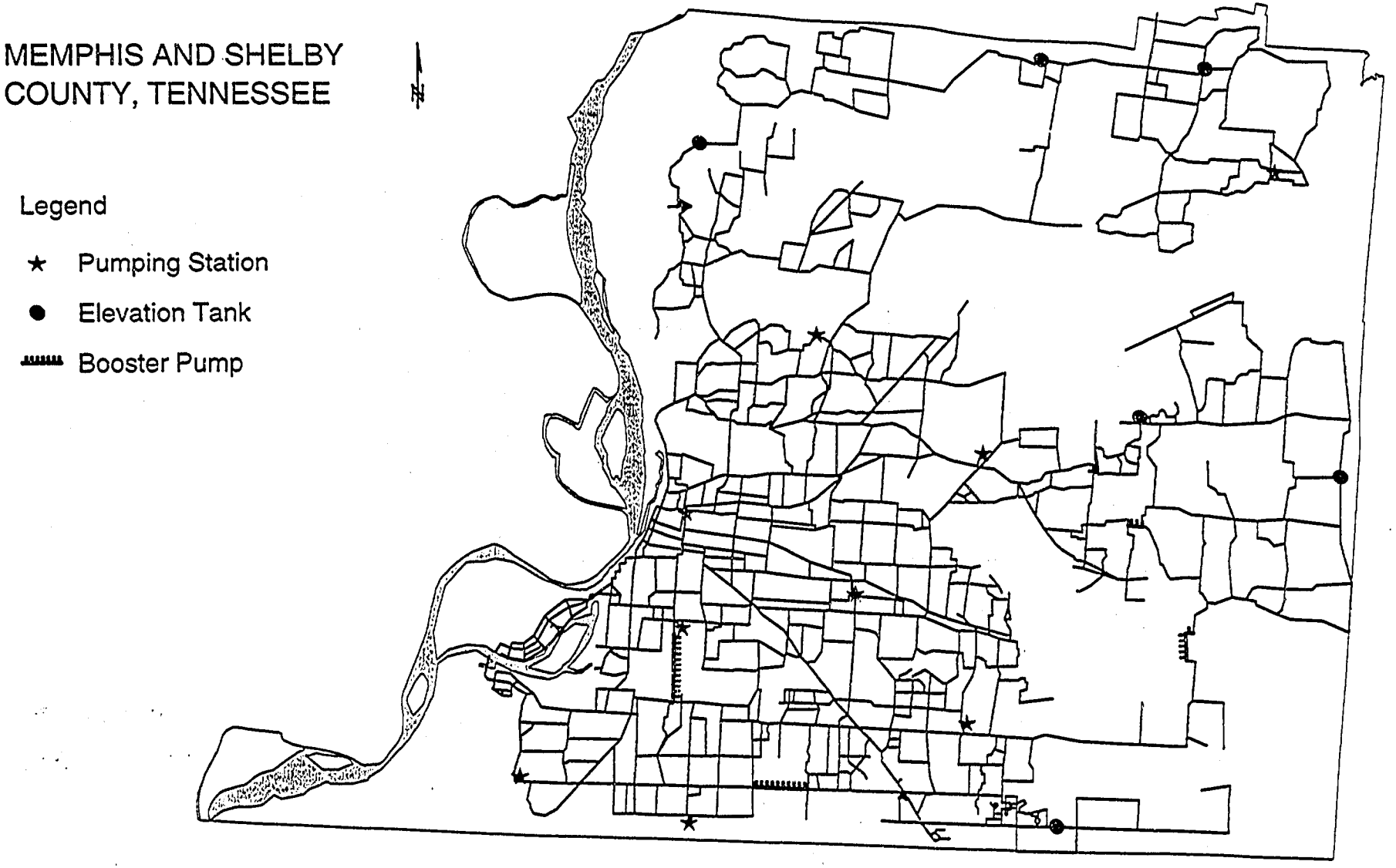



Figure 8 MLGW Water Delivery System

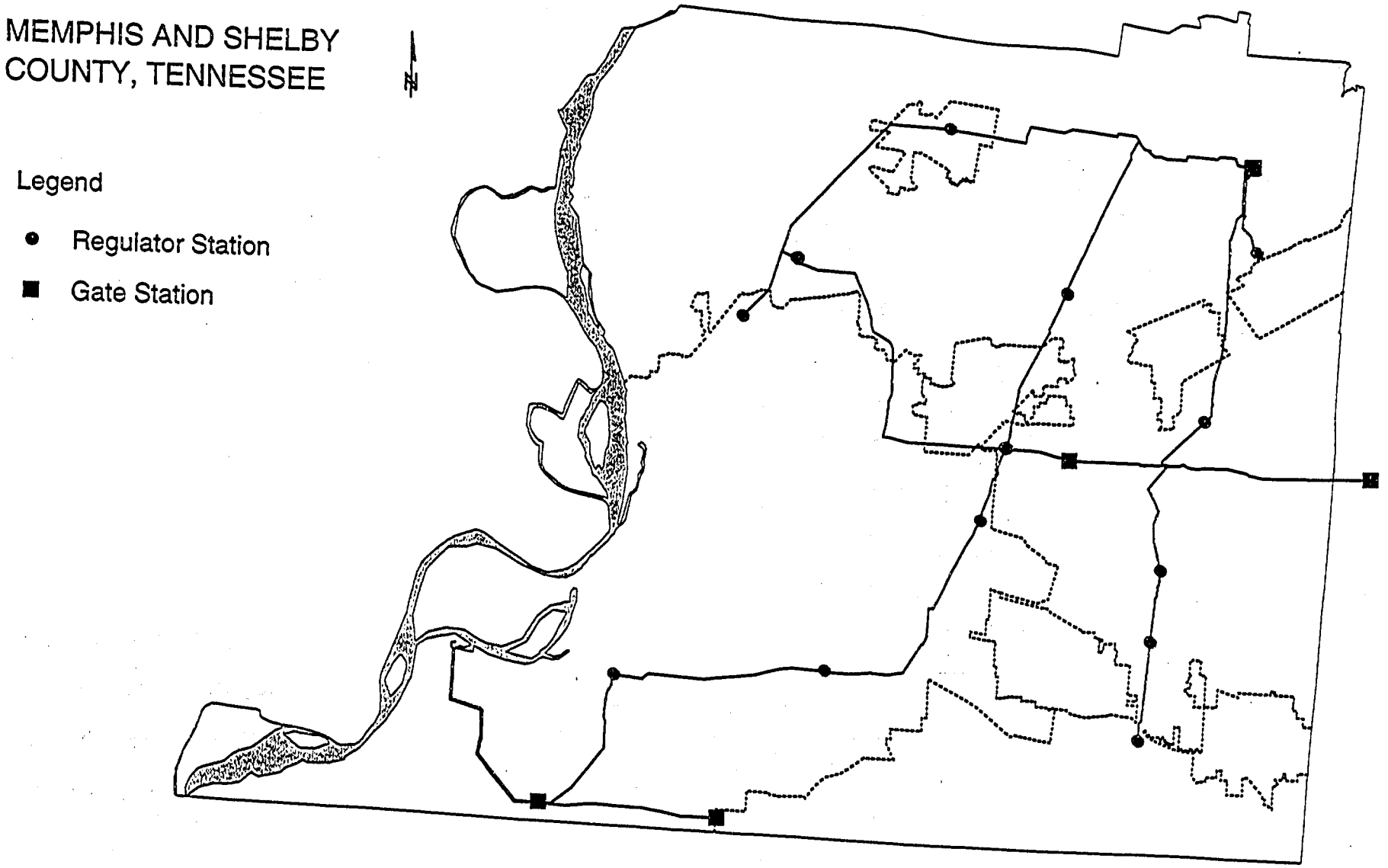



Figure 9 MLGW Gas Transmission System

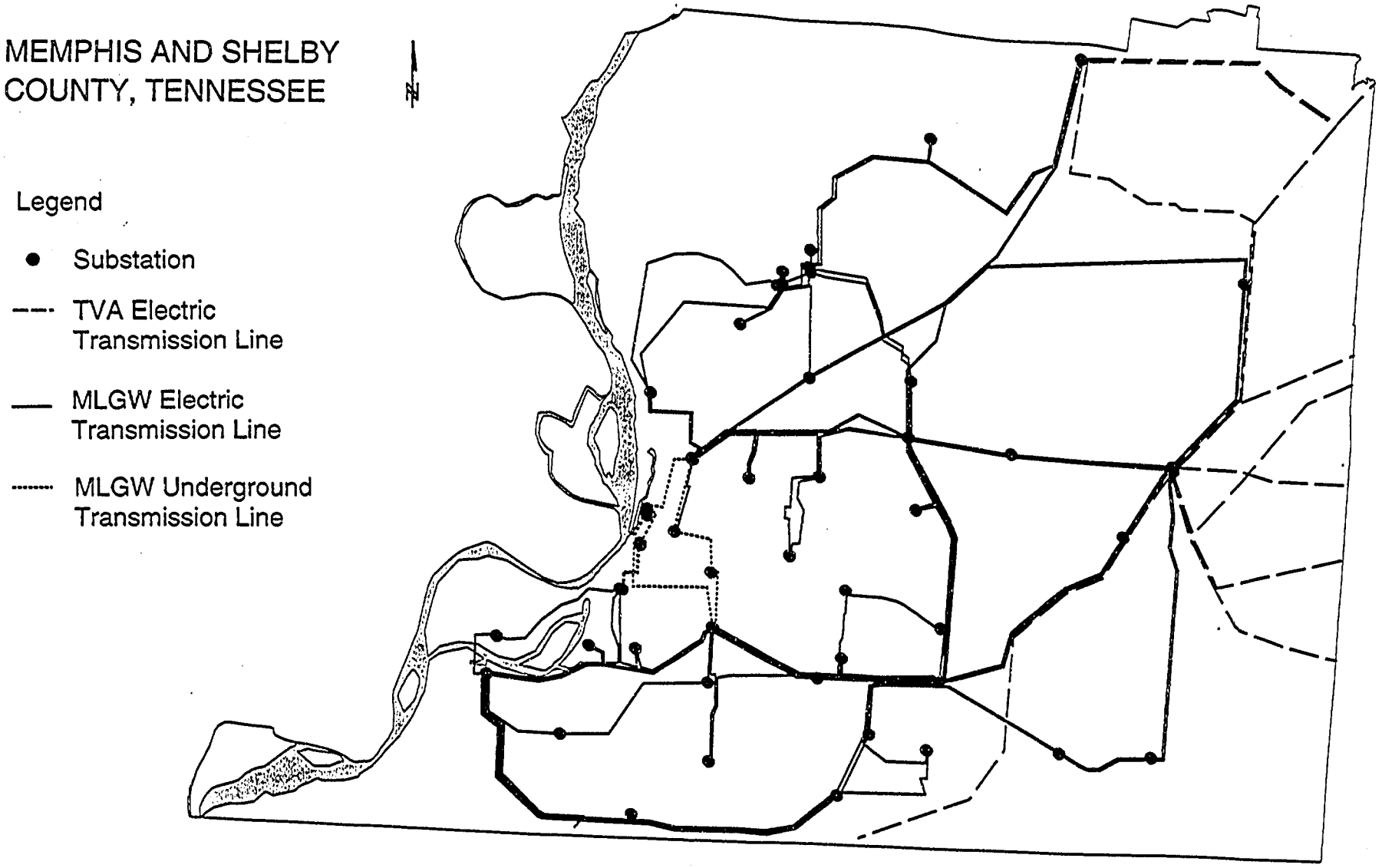



Figure 10 MLGW Electric Transmission System

# Session-8

## Risk Assessment and Impact of Seismic Effects (2)

(U-7) Functional Interactions of Lifeline Systems under Earthquake Conditions
(Masanobu Shinozuka and Satoshi Tanaka)

(N-1) Regional Approach to Assessment of Impact on Lifelines and Response to Earthquakes in New Zealand
(David C. Hopkins, John L. Lumsden and John A. Norton)

(U-8) New Trends in the Use of Earthquake Scenario Exercises: Opportunities for Mitigating Vulnerable Lifeline Systems
(Laurie A. Johnson)

(U-9) Rapid Post-Earthquake Damage Assessment for Lifeline Facilities
(Ronald T. Eguchi, Hope A. Seligson and James D. Goltz)

# Functional Interactions of Lifeline Systems under Earthquake Conditions

Masanobu Shinozuka
Champion Chair in Civil Engineering,
University of Southern California, Los Angeles, CA, USA

Satoshi Tanaka
Research Associate,
Disaster Prevention Research Institute, Kyoto University, Uji, Japan

## ABSTRACT

Lifeline system interactions have been suggested to occur and indeed have often been observed under earthquake conditions, particularly under severe ones. Indeed, the January 17, 1995 Hyogoken-Nambu earthquake showed that lifeline system malfunctions and interactions can severely impede the post-earthquake emergency response and delay the earthquake disaster mitigation process. This paper presents an analysis of such interactions that might occur between water delivery and electric power transmission systems subjected to a scenario earthquake. The basic data to describe physical characteristics of these lifeline systems are provided by MLGW (Memphis Light Gas and Water) Division, Memphis, Tennessee. However, some data necessary for the analysis are not available at this time and hence the models of the physical systems used in the analysis represent a simulated, but not precise, version of the water delivery and electric power transmission systems of MLGW. In view of this, the result of this analysis must be interpreted accordingly.

## INTRODUCTION

It is well known that the performance of a lifeline system during and following a severe earthquake depends on the seismic performance of other lifeline systems serving the same general urban or regional communities. Considering, for example, a water delivery system, its pumping stations, if not equipped with in-house emergency electric power generators (typically diesel engine-based), cannot function when the supply of electric power is interrupted as a result of the failure of the electric power transmission system due to a severe earthquake. Another example is the transportation lifeline system, typically a highway network whose functional failure significantly impedes post-earthquake emergency repair operations for all lifeline systems including itself. In this case, the functional failure results from the seismic damage sustained by its structural components such as embankments, bridges and road surface pavement, and/or from the debris on the road surface generated, for example, by damaged buildings along the roads and streets, which make the highways, roads and streets impassable. Such impassability also affects the mobility of fire-engines and thus seriously degrades the post-earthquake fire-fighting capability of the water delivery system. In fact, the January 17, 1995 Hyogoken-Nambu earthquake provided textbook examples of these and other lifeline system interactions.

The performance interaction of lifeline systems under earthquake conditions was studied earlier by many authors. Among others, Hoshiya and Ohno (1985)[1] developed a model that conceptually describes the seismic performance interaction between an electric power and a

water supply network system, Nojima and Kameda (1991)[2] demonstrated the use of cross impact analysis in estimating the performance interaction on the basis of observed performance data and Scawthorn (1992)[3] carried out similar analysis also utilizing the field data obtained from recent earthquakes.

The present paper further extends the scope of the earlier work by these and other authors which tended to be conceptual and qualitative, and performs a quantitative analysis through which the performance interaction between an electric power transmission and a water delivery system is evaluated. Such a quantitative analysis is extremely useful in identifying and prioritizing important performance parameters of the lifeline systems involved (such as the fragility curves of substations of the electric power system) for the retrofitting purposes.

In the following, numerical results are obtained using analytical models of electric transmission and water delivery systems developed on the basis of the corresponding Memphis systems. These are not exact models of the Memphis systems due to the unavailability of complete information, although the models developed are expected to represent approximately physical characteristics of the Memphis systems. In this regard, caution must be exercised if the numerical results obtained are to be used for the purpose of deriving specific technical and operational recommendations for the Memphis systems.

The criticism that such a quantitative analysis is not reliable in the face of many sources of uncertainty is misguided. Indeed, it is the purpose of this study to develop the basic models for system interaction analysis. These models can eventually be used under different modeling assumptions and with different parameter values for sensitivity analyses to determine the variability of the resulting lifeline performance under potential system interactions and to identity most critical modeling assumptions and parameters involved therein.

## ELECTRIC POWER SYSTEM

### Conditions for System Failure

MLGW's electric power transmission network is depicted in Fig. 1. It transmits electric power provided by TVA (Tennessee Valley Authority) through gate stations to 45 substations in the network consisting of 500kv, 161kv, 115kv and 23kv transmission lines and gate, 23kv and 12kv substations. The 500kv line and gate stations are operated by TVA, while other transmission lines and substations by MLGW. Each substation is associated with a service area, and usually one service area is served by only one substation except for two occasions.

In analyzing the functional reliability of each substation, the following modes of failure are usually taken into consideration; (1) loss of connectivity, (2) failure of substation's critical components, and (3) power imbalance. Each of these failure modes is addressed below from the viewpoint of the ensuing reliability analysis of the MLGW's electric power transmission system.

With respect to the loss of connectivity, it is noted that most of the transmission lines of the MLGW system are aerial supported by transmission towers. While by no means this implies that the transmission lines are completely free from seismic vulnerability, it is assumed in this study that they are, primarily for the purpose of analytical simplicity. Further study on this issue, particularly on the seismic vulnerability of transmission towers, needs to be carried out.

Substation Model

An electric substation consists of several electric nodes subjected to various values of voltage and connected each other through transformers in order to reduce the voltage and/or distribute the power to the service areas. Each electric node consists of many kinds of electric equipment such as buses, circuit breakers, and disconnect switches. The schematic diagram of an actual MLGW's substation is depicted in Fig. 2. Among the equipment, buses, circuit breakers and disconnect switches are seismically most vulnerable, as observed during the 1971 San Fernando, the 1989 Loma Prieta and the 1994 Northridge earthquake (Benuska 1990, Hall 1994, Goltz 1994)[4,5,6]. Figure 3 shows the damaged equipment of Moss Landing 500kv switchyard at the Loma Prieta earthquake (Benuska 1990)[4]. As shown in the figure, most of the live-tank circuit breakers and disconnected switches were damaged.

The physical damage thus sustained by the system produced corresponding system malfunction that required concentrated repair and restoration effort to make them operational again. However, in spite of the damage, the system performed reasonably well on the occasions of these earthquakes. Two factors played a significant role in this respect. First, the high voltage power transmission network is designed topologically with a sufficient degree of redundancy in transmission circuits. Second, substations are designed also with a sufficient degree of internal redundancy. Actual equipment configuration in a node is so complicated that it defies a rigorous modeling. Therefore, a simplified but essentially accurate configuration as shown in Fig. 4 is employed. In Fig. 4, if only one circuit breaker CB11 is damaged due to an earthquake, the node is still functional because all the lines remain connected each other. However, if CB11 and CB13 are damaged simultaneously, Line A and Line B are disconnected from the node, thus the function of the node is impaired. Table 1 shows partially the line status resulting from a combination (among possible 32) of the switch status at Position 1 in order to judge whether or not the corresponding mode of line connectivity still functions. In this study, it is assumed that buses and circuit breakers can be broken due to earthquake ground motion.

Utilizing the results of the previous studies by Shinozuka, et al. (1989)[7] and Ang, et al. (1992)[8], the fragility curve $F_c(a)$ for a circuit breaker is chosen to be a log-normal distribution function with the median and coefficient of variation equal to 0.45g and 0.38 respectively. This curve is assumed also applicable for the bus fragility for the purpose of analytical simplicity.

Monte Carlo Simulation

Utilizing the GIS (Geographical Information System)[9,10,11] capability existing at the University of Southern California, the map of the electric transmission network is overlaid with the map of PGA identifying the PGA value associated with each substation. The fragility curve developed for the equipment (buses and circuit breakers) can then be used to simulate the state of equipment damage involving the equipment in all the nodes at all the substations of the transmission system. For each damage state, the connectivity and flow analyses are performed with the aid of an computer code IPFLOW developed and distributed by Electric Power Research Institute (EPRI) (1992)[12].

The loss of connectivity occurs when the node of interest survives the corresponding PGA, but is isolated from all the generating nodes because of the malfunction of at least one of the nodes on each and every possible path between this node and any of the generating nodes. Hence, the loss of connectivity with respect to a particular node can be confirmed on each damage state by actually verifying the loss of connectivity with respect to all the paths that would otherwise establish the desired connectivity. The loss of connectivity is primarily due to the equipment failure not only at the node of interest but also all other nodes in the network.

As to the abnormal power flow, it is noted that the electric power transmission system is highly sensitive to the power balance and ordinarily some criteria are used to judge whether or not the node continues to function immediately after internal and external disturbances. Two kind of criteria are employed at each node for the abnormal power flow; (a) power imbalance and (b) abnormal voltage. When some nodes in the network are damaged due to an earthquake, the total generating power becomes greater or less than the total demanding power. For a normal condition, the power balance between generating and demanding power is in a certain tolerance range. Actually, the total generating power must be between 1.0 and 1.05 times the total demanding power for normal operation even accounting for the power transmission loss.

If this condition is not satisfied, the operator of the electric system must either reduce or increase the generating power to keep the balance of power. However, in some cases, supply cannot catch up with demand because the generating system is unable to respond so quickly. In this case, it is assumed that the generating power of each power plant cannot be quickly increased or reduced by more than 20% of the current generating power. When the power balance cannot be maintained even after increasing or reducing the generating power, the system will be down. This kind of outage is defined as a power imbalance. This situation, however, has never materialized in our analysis.

As for the abnormal voltage, voltage magnitude at each node can be obtained by power flow analysis. Then, if the ratio of the voltage of the damaged system to the intact system is out of a tolerable range (plus/minus 20% of the voltage for the intact system), it is assumed that a black out will occur.

The each node which makes up an substation has a different function. Some of them function as power receiving node that receives the high voltage power from the high voltage transmission line and transfer the power to the lower voltage nodes through transformers. On the other hand, some of them function as power distribution node that distribute the power to the service area. In this study, if the distribution node is failed or isolated from the network, or receives the abnormal power flow, the service area is assumed to be blacked out. Appropriate modification can be made to estimate the probability of malfunction of the service area served by more than one node.

For the Monte Carlo simulation, random numbers uniformly distributed between 0 and 1 are generated for every circuit breaker and bus in all nodes. These equipment are considered to be broken, when the random number is less than the value of failure probability of each equipment.

Each substation is examined with respect to its possible malfunction under these three modes of failure for each simulated damage state. In the present study, a sample of size 100 ($N=100$) is considered for the Monte Carlo analysis. The probability $P_{Em}$ of malfunction of a particular substation $m$ is then estimated as $N_m/N=N_m/100$ where $N_m$ is the number of simulated damage states in which the substation $m$ malfunctions in at least one of the three modes. On the basis of the flow analysis performed on the network in 100 simulated damage states, the ratio of the average electric power output (real-power in MW) of the damaged network to that associated with the intact network is computed and plotted in Fig. 5 under a scenario earthquake with M=7.5 epicentered at Marked Tree (see Fig. 6). The ratio is a convenient measure to show the degradation of the system performance due to the earthquake. The average is taken over the entire sample of 100.

## SYSTEM INTERACTION

The effect of the performance degradation of the electric power transmission system on the water delivery system serving the same regional community is analyzed here using the electric power transmission and water delivery system operated by MLGW as an example. Again, however, the analytical models to describe the seismic performance of these models are approximate due primarily to the lack of information on the technical and operational details of these systems.

Seismic reliability analysis has been performed for the water delivery system by the first author and his associates, Shinozuka et al. (1992)[13] and Tanaka et al (1993)[14], however, without taking the interaction effect into consideration. Figure 7 shows a map of the water delivery network and Fig. 8 the average water head (at each demand node) for the network damaged under the same scenario earthquake epicentered at Marked Tree. Figure 9 shows the ratio of these average values to the corresponding values of output flow rate of the intact network in Census tracts. The average is taken over the entire sample (sample size = 100) used in the Monte Carlo analysis from which these results are obtained.

Figure 10 shows a map of the electric power service areas together with the locations of the pumping stations and booster pumps of the water delivery system. For the numerical analysis, it is assumed that the pumping stations and booster pumps in a service area cease to operate for the lack of electric power if all the substations serving that service area malfunction. In the earlier study performed by Hwang et al. (1992)[15], the fragility curve of a pumping station in the MLGW's water delivery system is estimated. Hence, the probability $P_{Wj}$ of pumping station $j$ to malfunction under the scenario earthquake can also be estimated. If, therefore, this pumping station is located in the service area served by the substation $m$, then the probability $P_j$ of the pumping station $j$ to malfunction can be written as

$$\begin{aligned} P_j &= 1-(1-P_{Wj})(1-P_{Em}) \\ &\cong P_{Wj}+P_{Em} \end{aligned} \tag{1}$$

where the approximation is valid when both $P_{Wj}$ and $P_{Em}$ are small compared with unity and their occurrences are statistically independent. Appropriate modifications have been made to estimate the probability of malfunction of a pumping station located in the service area served by more than one substation. The probability of a booster pump to malfunction is simply equal to the probability $P_{Em}$ if the pump is located in the service area served by substation $m$ since, as in the earlier analysis performed by Shinozuka et al (1992)[13], the pumping stations are assumed to be not vulnerable seismically. This same analysis is repeated here with the added probability of malfunction for pumping stations and booster pumps due to the malfunction of electric power substations. Figures 10 and 11 show the ratios of the average water head at each demand node and output flow rate in Census tracts of the damaged water delivery network to the corresponding values of the undamaged network, respectively. Figures 11 and 12 clearly indicate the degrading effect of interaction when the impact of malfunction of electric power substations is incorporated into the analysis.

## CONCLUDING REMARKS

The analytical models are derived from the physical and operational data provided by Memphis Light, Gas and Water Division of Memphis, Tennessee, for its electric transmission and water delivery systems. The interaction effect of these two systems under a scenario earthquake is evaluated as quantitatively as possible on the basis of these analytical models. The numerical example utilizing Monte Carlo simulation techniques clearly indicates the degrading performance of the water delivery system due to the interaction effect between these two systems. In the numerical example, the interaction is assumed to materialize when the malfunction of substations interrupting the supply of electric power renders pumping stations and booster pumps of the water delivery system inoperational. Finally, it is noted that this paper represents a revised version of Shinozuka et al (1994)[16] accounting for substation redundancy and as such contains common materials.

## ACKNOWLEDGMENT

This work was carried out under NCEER Graut #94-3304B (under the auspices of the National Science Foundation). The authors wish to thank MLGW for the release of the information on its systems. They also wish to acknowledge the technical assistance provided by Professor H. Hwang of University of Memphis in completing this paper.

## REFERENCES

1. Hoshiya, M. and Ohono, H. (1985), "A System Dynamic Model in Seismic Performance Assessment of Electric Power and Water Supply Networks", Proc. of the Trilateral Seminar-Workshop on Lifeline Earthquake Engineering, Taipei, Taiwan, November, pp. 181-189.

2. Nojima, N. and Kameda, H. (1991), "Cross Impact Analysis for Lifeline Interactions", Proc. of the Third U.S. Conference on Lifeline Earthquake Engineering, Los Angeles, CA, August 22-23, pp. 629-638.

3. Scawthorn, C. (1992), "Lifeline Interaction and Post-Earthquake Functionality", Proc. of Fifth U.S.-Japan Workshop on Earthquake Disaster Prevention for Lifeline Systems, Tsukuba, Japan, October 26-27, pp. 441-450.

4. Benuska, L. (Ed.) (1990), "Loma Prieta Earthquake Reconnaissance Report", Earthquake Spectra, Earthquake Engineering Research Institute (EERI), Supplement to Vol. 6, May.

5. Hall, J. F. (Ed.) (1994), "Northridge Earthquake January 17, 1994", Preliminary Reconnaissance Report, Earthquake Engineering Research Institute (EERI), March.

6. Glotz, J. D. (Ed.) (1994), "The Northridge California Earthquake of January 17, 1994", General Reconnaissance Report, Technical Report, NCEER-94-0005, National Center for Earthquake Engineering Research (NCEER), State University of New York at Buffalo, Buffalo, NY, March.

7. Shinozuka, M., Mizutani, M., Takeda, M., and Kai, Y. (1989), "A Seismic PRA Procedure in Japan and Its Application to a Building Performance Safety Estimation, Part 3 Estimation of Build and Equipment Performance Safety", Proc. of ICOSSAR '89, pp. 637-644.

8. Ang, A.H-S., Pires, J., Schinzinger, R., Villaverde, R. and Yoshida, I. (1992), "Seismic Reliability of Electric Power Transmission Systems - Application to the 1989 Loma Prieta Earthquake", Technical Report to the NSF and NCEER, Dept. of Civil Engineering, Univ. of California, Irvine, January.

9. Environmental Systems Research Institute (ESRI) (1988), "ARC/INFO Users Manual", Environmental Systems Research Institute, Redlands, CA.

10. Burrough, P.A. (1986), "Principles of Geographic Information Systems for Land Resources Assessment", Oxford University Press, New York, NY.

11. Sato, R., M. Murata and M. Shinozuka (1991), "Seismic Risk Analysis of Water Delivery System based on GIS", Proc. of the Fourth International Conference on Seismic Zonation, Stanford, CA, August 25-29.

12. Electric Power Research Institute (EPRI) (1992), "Interactive Power Flow Version 1.0 Users Manual", Electric Power Research Institute.

13. Shinozuka, M., Hwang, H. and Murata, M. (1992), "Impact on Water Supply of a Seismically Damaged Water Delivery System", Lifeline Earthquake Engineering in the Central and Eastern US/TCLEE Council/ASCE Sessions Proc., ASCE National Convention, New York, NY, September 13-17, pp. 43-57.

14. Tanaka, S. et al. (1993), "User's Guide for Lifeline -W (II), a Program for Connectivity and Flow Analysis of a Water Delivery System under Intact and Seismically Damaged Conditions," Version 1, NCEER Technical Report, National Center for Earthquake Engineering Research (NCEER), State University of New York at Buffalo, Buffalo, NY, (in print).

15. Hwang, H., Ch'ng, A., and Hsu, H. (1992), "Seismic Fragility Analysis of Memphis Sheahan Pumping Building", Technical Report Center for Earthquake Research and Information, Memphis State University.

16. Shinozuka, M., Shumuta, Y., Tanaka, S., and Koiwa, H. (1994), "Interaction of Lifeline Systems under Earthquake Conditions", Proc. of the Second China-Japan-US Trilateral Symposium on Lifeline Earthquake Engineering, Xi'an, China, April 19-23, pp. 43-52.

Table 1 Status Table of Position 1

| Damaged Status of Switches | | | | | | | Line Status | |
|---|---|---|---|---|---|---|---|---|
| Bus 1 | CB 11 | Line A | CB 12 | Line B | CB 13 | Bus | Line A | Line B |
| 0 | 0 | | 0 | | 0 | 0 | 0 | 0 |
| 0 | 1 | | 1 | | 0 | 0 | 1 | 0 |
| 0 | 1 | | 0 | | 1 | 0 | 1 | 1 |
| 0 | 0 | | 1 | | 1 | 0 | 0 | 1 |
| 1 | 0 | | 0 | | 0 | 1 | 1 | 1 |
| 0 | 1 | | 1 | | 1 | 0 | 1 | 1 |
| 1 | 1 | | 0 | | 0 | 0 | 0 | 0 |
| 1 | 0 | | 1 | | 0 | 0 | 1 | 0 |
| 1 | 0 | | 0 | | 1 | 0 | 1 | 1 |
| 1 | 1 | | 1 | | 0 | 0 | 1 | 0 |

0: Operative 1: Inoperative

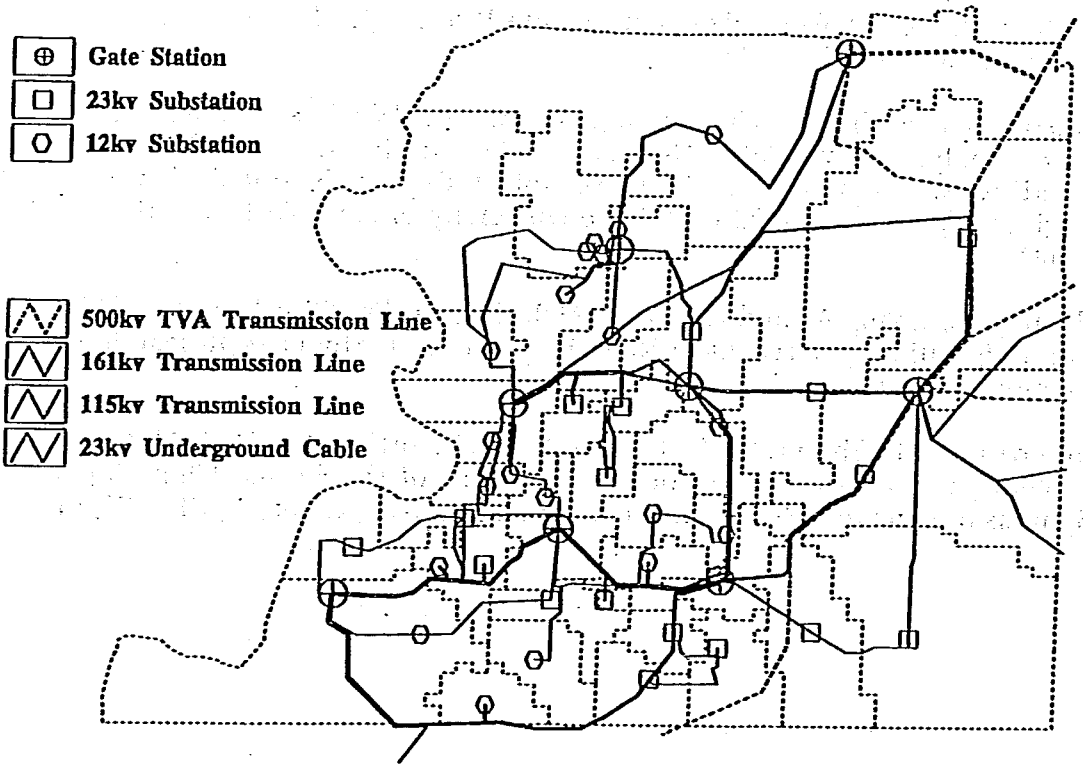



Fig. 1 MLGW's Electric Power Transmission Network

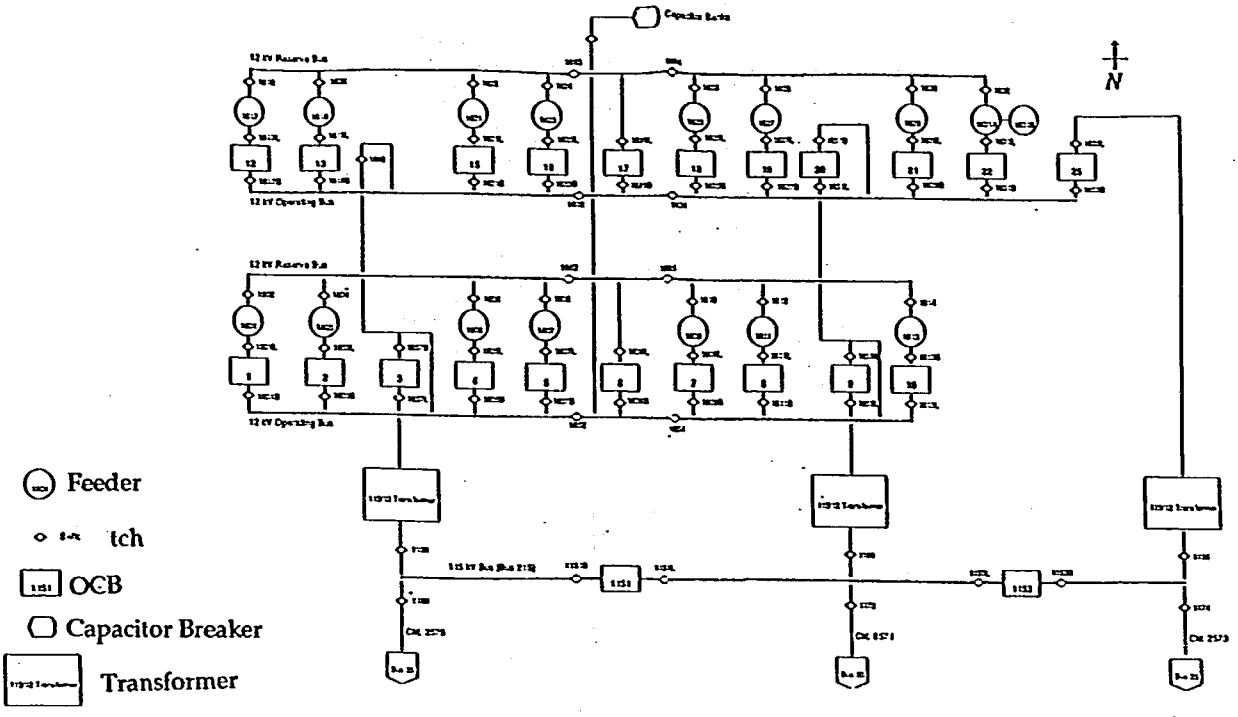
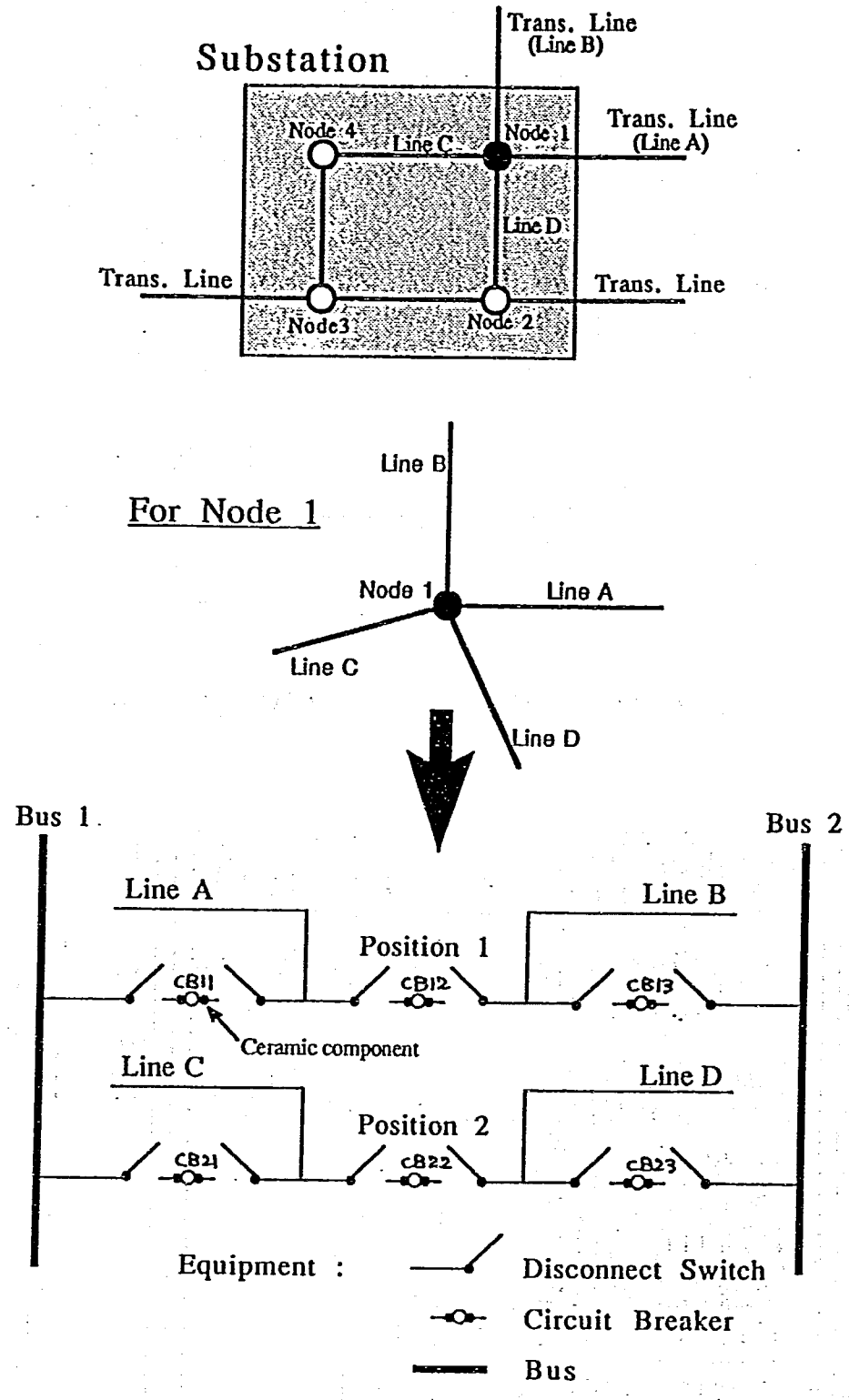



Fig. 2 Schematic Diagram of a MLGW's Substation



Fig. 3 Damaged Equipment of Moss Landing 500kV Switchyard at the 1989 Loma Prieta Earthquake




Note that disconnect switches are normally closed

Fig. 4 Typical Node Configuration Model

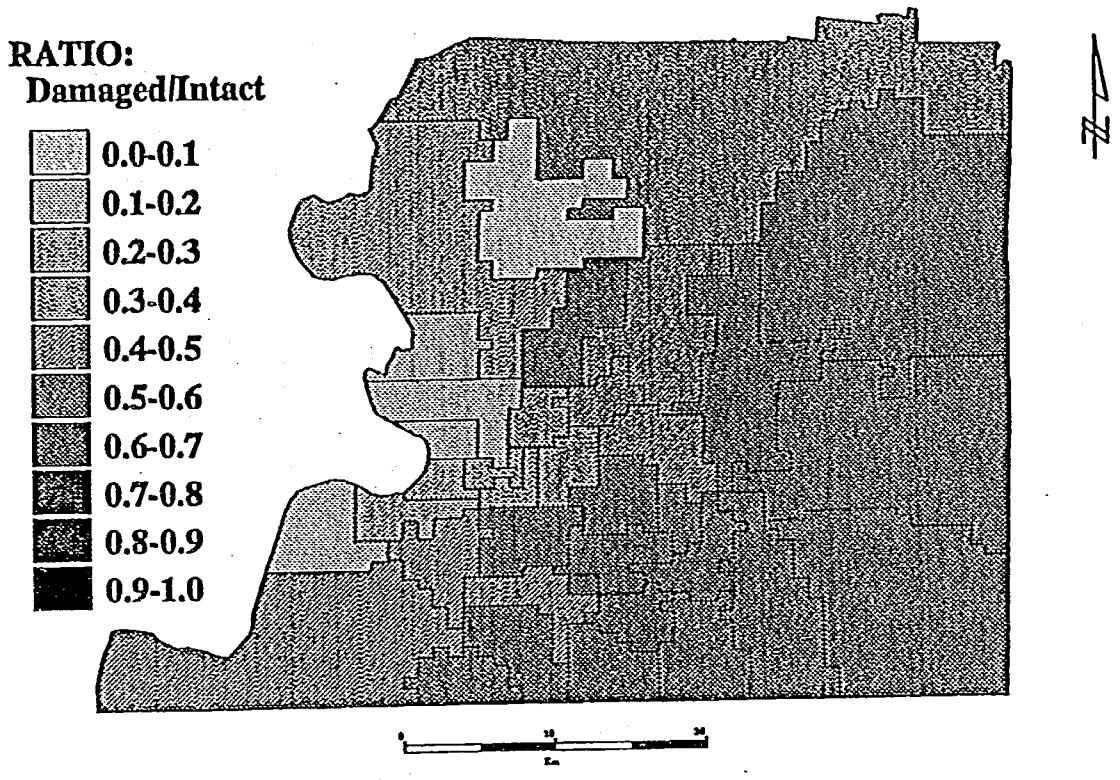



Fig. 5 Ratio of the Average Power Output under the Damaged Condition to the Intact Condition for Service Areas

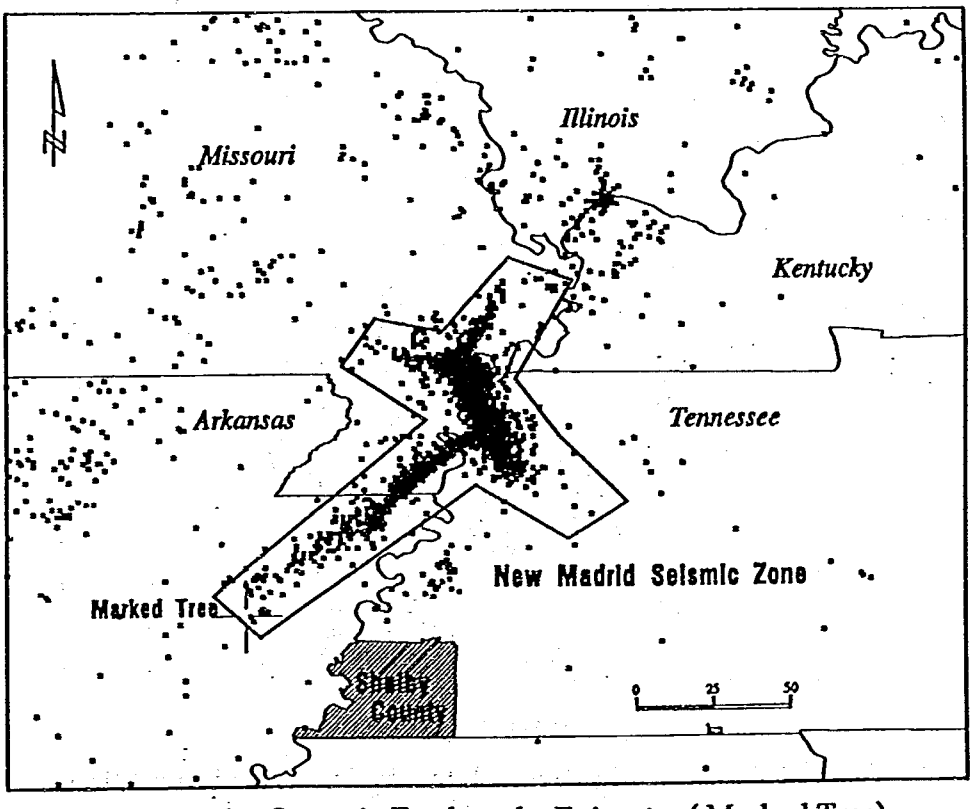



Fig. 6 Scenario Earthquake Epicenter ( Marked Tree)

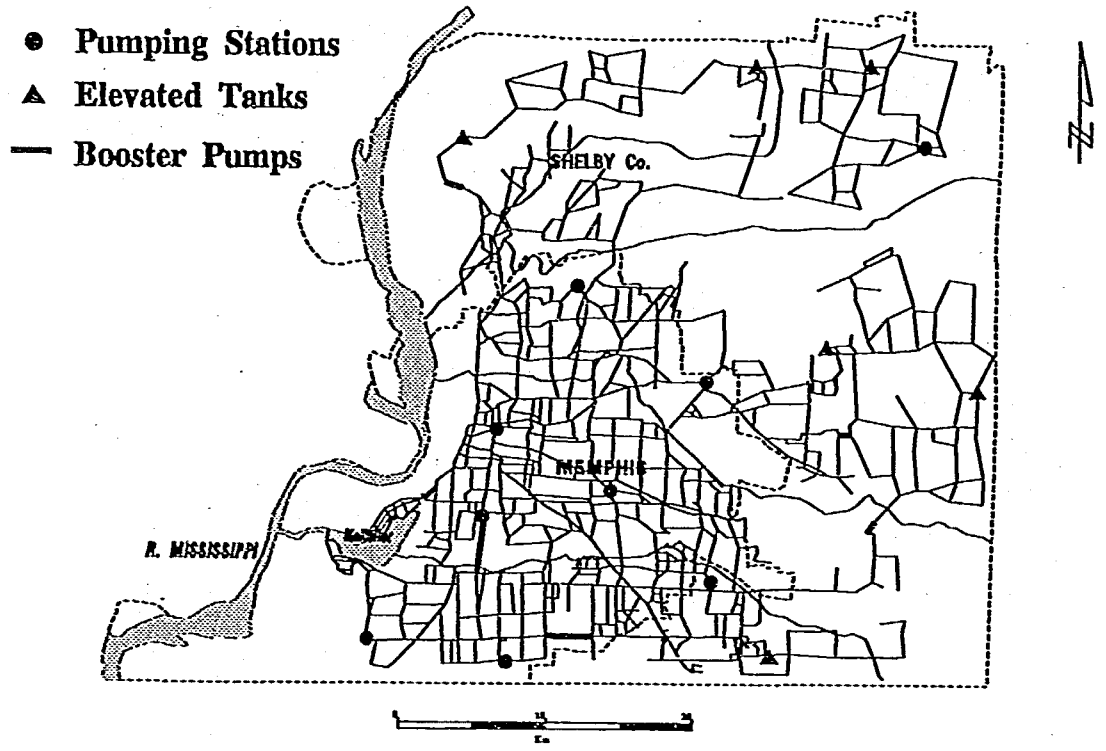



Fig. 7 MLGW's Water Delivery Network

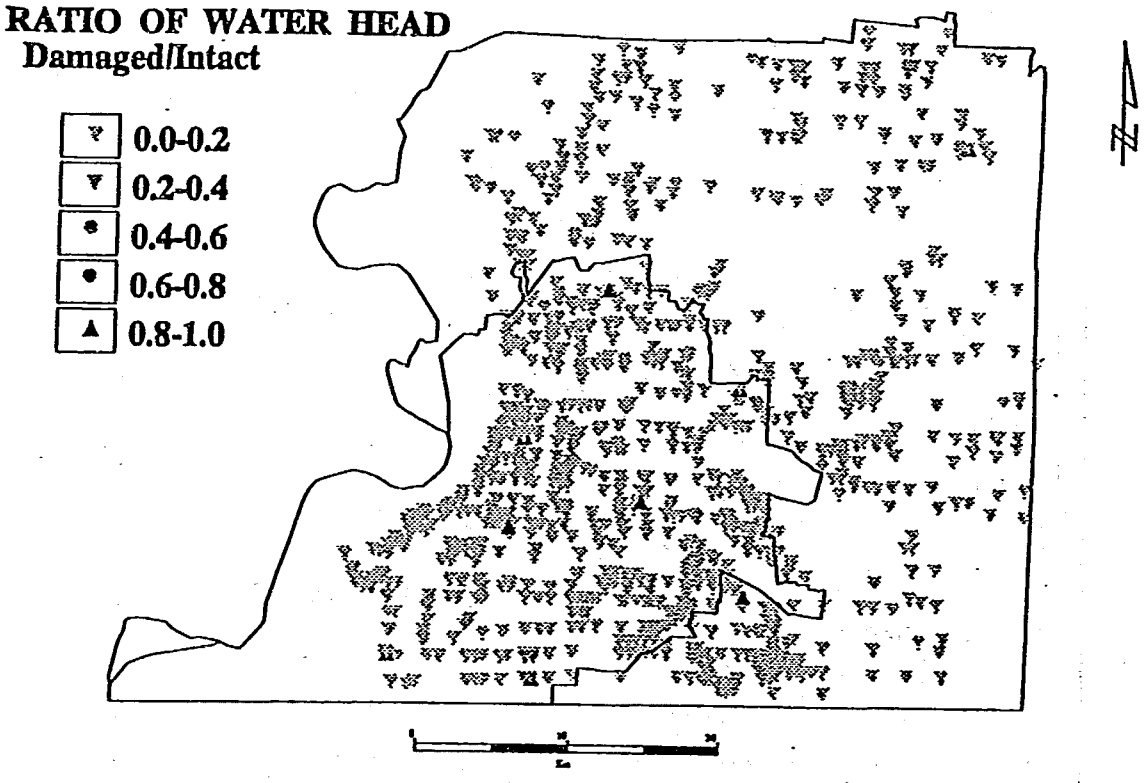



Fig. 8 Ratio of Water Head between Intact and Damaged Condition

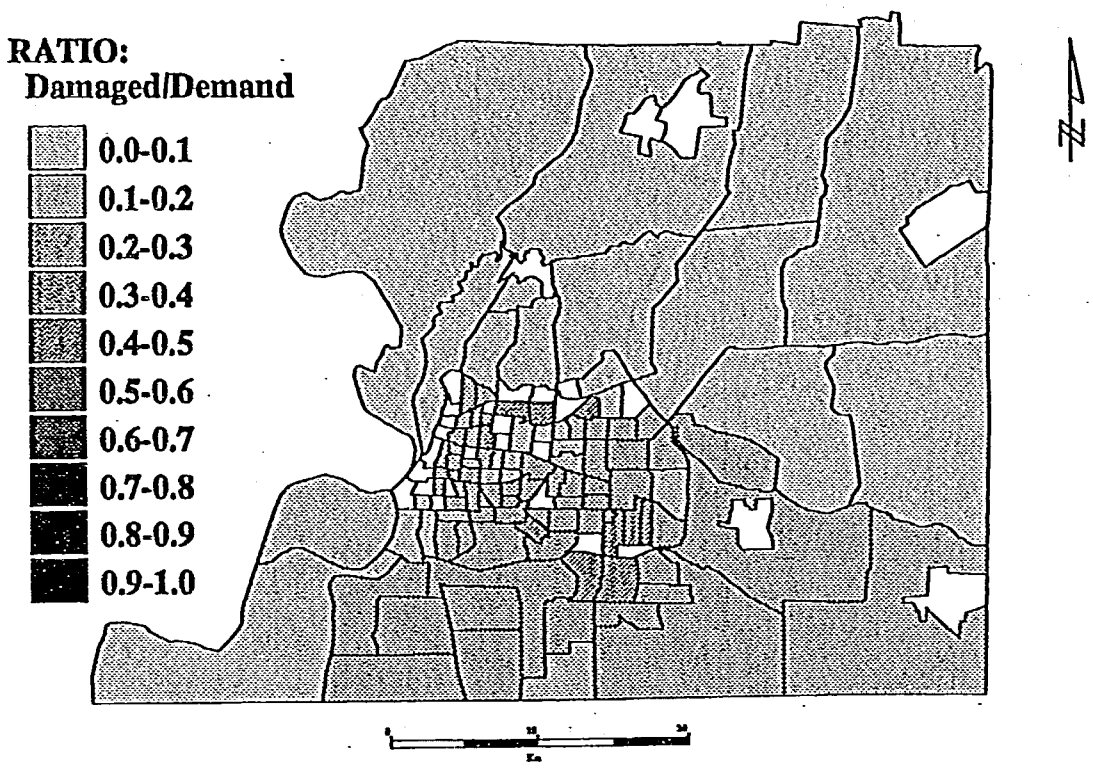



Fig. 9 Ratio of Output Flow between Intact and Damaged Condition in Census Tracts

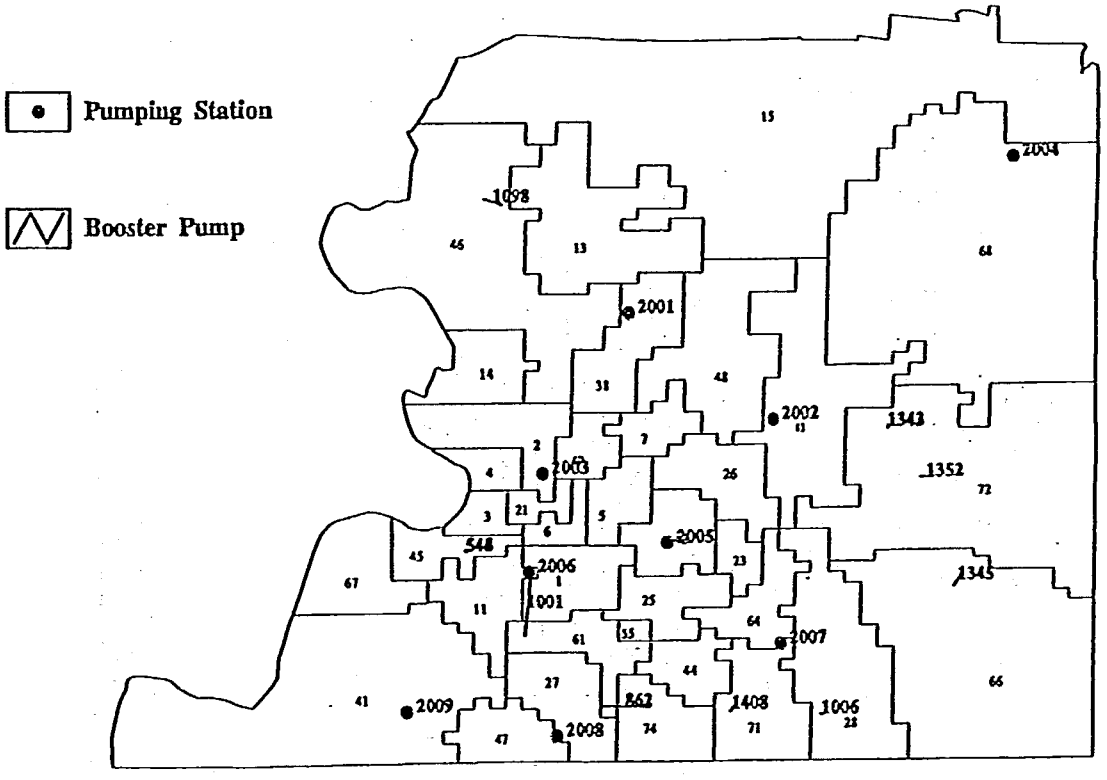



Fig. 10 MLGW's Pumping Stations and Booster Pumps on the Electric Service Area

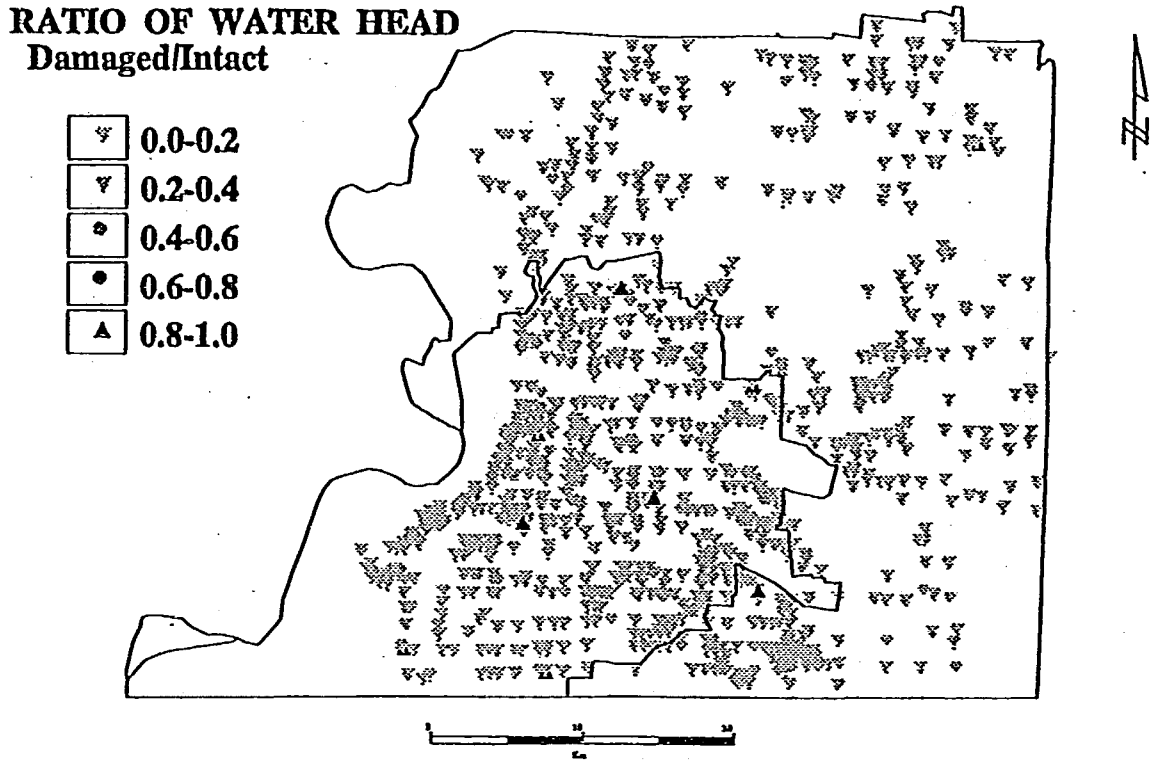



Fig. 11 Ratio of Water Head between Intact and Damaged Condition with System Interaction Effect

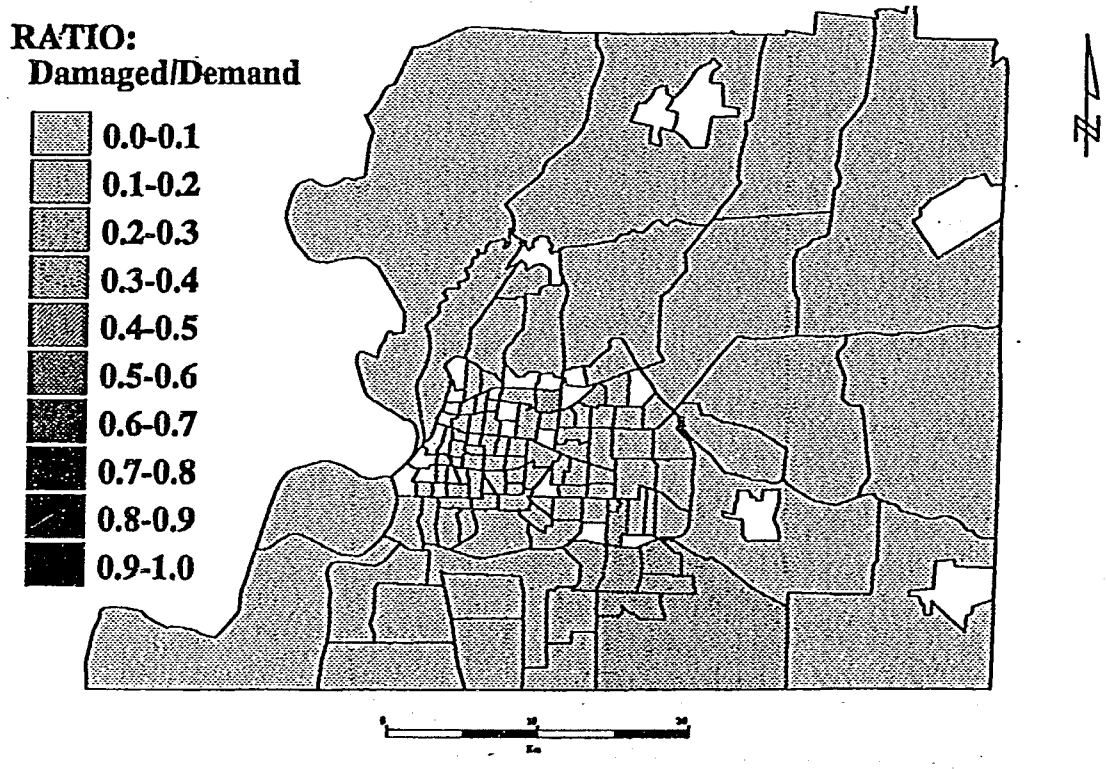



Fig. 12 Ratio of Output Flow between Intact and Damaged Condition in Census Tracts with System Interaction Effect

# A REGIONAL APPROACH TO ASSESSMENT OF IMPACT ON LIFELINES AND RESPONSE TO EARTHQUAKES IN NEW ZEALAND

David C Hopkins[1]
John L Lumsden[2]
John A Norton[3]

## ABSTRACT

New Zealand is no less vulnerable to earthquakes than are some of the other seismically active parts of the world, such as Japan and the west coast of the United States, where serious earthquakes have occurred during the past decade. Most New Zealanders have not had to cope with the impacts of a major earthquake during their lifetime and, therefore, there is much to be learnt from experiences overseas. The value of increasing international co-operation in this field is highlighted.

The role of effective lifeline earthquake engineering in saving lives and facilitating recovery after an earthquake has become recognised in New Zealand. This paper briefly describes the short history of lifeline engineering in New Zealand and presents a framework for response planning.

1 Director, Kingston Morrison Ltd., P O Box 10283, Welligton, New Zealand

2 Projects Director, Centre for Advanced Engineering, University of Canterbury, Private Bag 4800, Christchurch, New Zealand

3 Group Manager City Development, The Hutt City Council, Private Bag 31912, Lower Hutt, New Zealand

## INTRODUCTION

New Zealand is a country similar in size to California, located in the South Pacific Ocean within the rim of volcanic and seismic activity. By most standards, New Zealand lies in a zone of high seismic risk.

As a reminder of the seismicity of New Zealand, it is useful to compare some of the larger (Richter Magnitude > 6.5) events that have occurred in New Zealand and California since 1930. These are shown in Figure 1 and the similarities in terms of numbers and magnitude over the 65 year period will be apparent. What is, perhaps, disturbing from New Zealand's point of view is that since 1970 there has only been one event with a Richter Magnitude greater than 6.5 whereas there have been at least six such events in California. In the 40 years prior to 1970, the roles were reversed and New Zealand experienced five Magnitude 6.5 or greater earthquakes while California had just two (Lumsden, 1995).

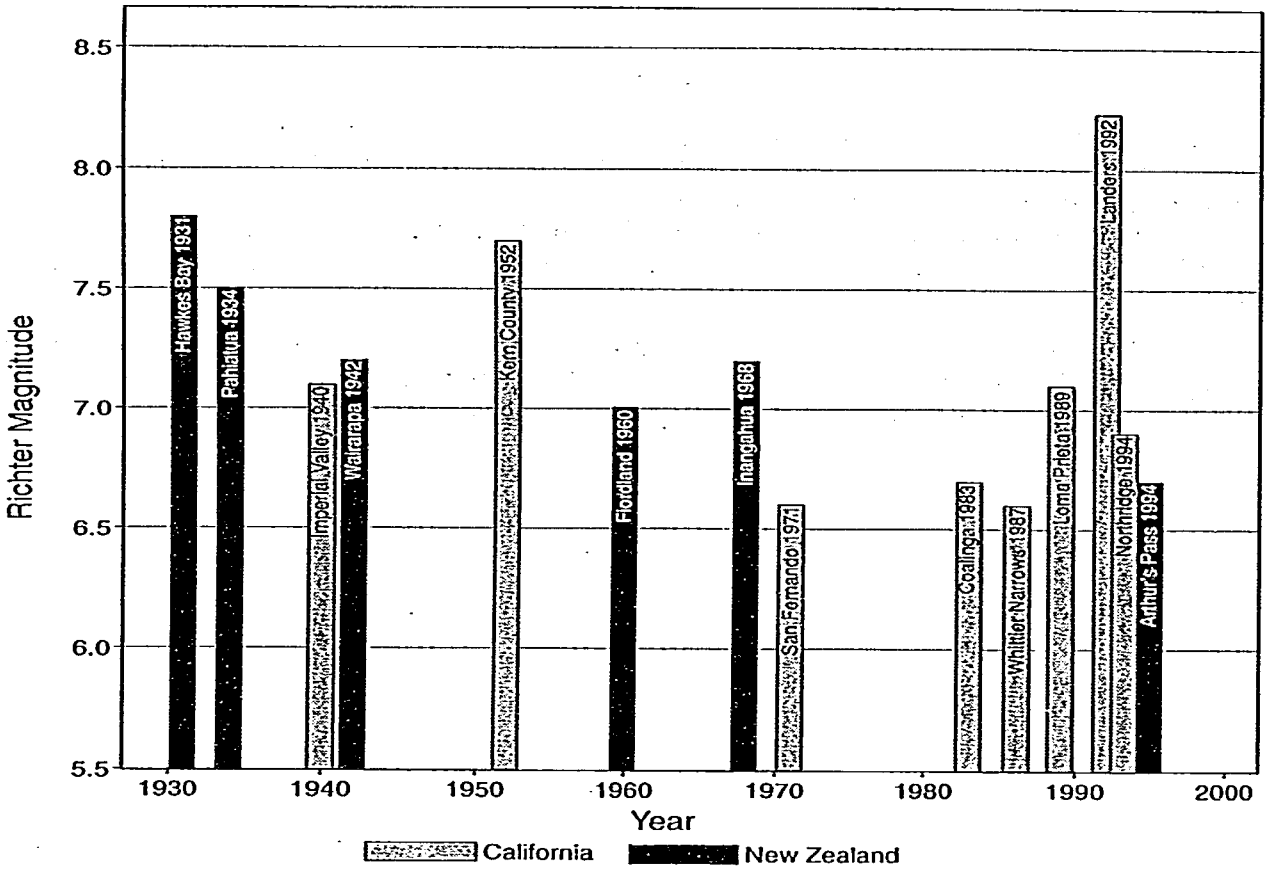



**Figure 1: Magnitude of Selected Earthquakes (M>6.5) in California and New Zealand 1930 to 1994**

It does not take too much imagination to suggest that a period of increased seismicity in New Zealand is long overdue.

In some ways New Zealanders have been fortunate in that the country is relatively sparsely populated and it is, in fact, over 60 years since an urban community of any size had to cope with the effects of a major earthquake. The downside of this is that New Zealand has few people with

any direct experience in earthquake recovery and therefore must learn from those overseas who have had such experience. New Zealand also has something to offer the lifeline community in other countries in that its relatively small population allows issues to be considered on a regional basis which, in turn, helps to bring a co-ordinated effort into problem-solving. It is considered that there is a need for more international co-operation in the field of lifeline engineering.

This paper briefly discusses the background to lifeline earthquake engineering in New Zealand and describes, in more detail, the important matter of response planning.

## LIFELINE EARTHQUAKE ENGINEERING IN NEW ZEALAND

While buildings in New Zealand can be expected to perform satisfactorily in an earthquake, the same cannot be said for other parts of the infrastructure, that is the lifelines and particularly those (pipelines, roadways, etc.) that link major elements together.

Major earthquakes in other countries in recent years have highlighted the fact that a significant part of the damage and loss of life can be attributed to failure of one or more lifeline systems. In other words, it is considered that significant reductions in the costs of future earthquakes can be made if steps are taken to reduce the risk of damage to the lifeline infrastructure.

It has become apparent from recent seismic events in California and Japan that, as society becomes technologically more sophisticated, the cost of recovery from an earthquake escalates. It is also apparent in New Zealand that the total costs of recovery from an event, on the scale, say, of the 1995 Hyogoken-Nanbu earthquake, in Wellington could represent a sum equal to as much as 70% of the country's gross national product, which would have a most serious impact on the economy.

The importance of lifeline engineering is, thus, becoming recognised as a matter of national importance in New Zealand. The catalyst for this recognition was the commencement of the Centre for Advanced Engineering[4] project in 1989 (CAE, 1991). This project examined the vulnerability of all the lifelines in the Wellington region to earthquake and, among other things, developed a methodology for prioritising the vulnerability of different elements in a lifeline network. The method involved preparing a hazard map of the region identifying the type and extent of the expected seismic hazards. Maps of each lifeline network were also prepared to the same scale and each was laid over the hazard map so that the vulnerable areas could be identified. The vulnerabilities of each network element were then given a numerical value based on a defined set of criteria that included importance and impact of failure.

During the course of the CAE project, it became clear that the vulnerability of any lifeline in an earthquake, or in other words, its ability to remain in service, could not be considered in isolation, and that its dependence on other lifelines was also an important factor. It was concluded that there has been a lack of appreciation of the importance of interdependence, particularly as it affects the recovery process. It was found that interdependence analysis is a fundamental part of response planning for lifeline utilities and assists in providing the earliest possible restoration of services.

Although, perhaps, it was not realised at the time, the CAE project is somewhat unique in its approach to lifeline engineering. This was mainly because of the way in which the project brought together academics, consultants, managers, etc., as well as representatives of all the lifeline service providers, to consider the vulnerability of the lifeline infrastructure throughout the whole region to selected seismic hazard scenarios.

---

4 The Centre for Advanced Engineering is a non-profit organisation, based at the University of Canterbury, Christchurch, New Zealand. It was established in 1987 to advance engineering knowledge in New Zealand in areas considered to be of national importance.

Since completion of the CAE project in 1991, interest in lifeline engineering has continued. A group in Wellington, formed in 1992, is continuing the work of the original project. This group consists of consultants, regional and city council staff and representatives of all the main utility service providers. Recently the work of this group has focused on integrated response planning and the findings are reported in the sections that follow (Wellington Earthquake Lifelines Group, 1994).

Another large group in Christchurch is undertaking a significant project examining the vulnerability of the lifelines in that city. This project is considering not only earthquake, but also the impact of other natural phenomena, including flooding, tsunami and various meteorological hazards on lifelines. The approach adds other dimensions to the problem, and the work completed suggests that, in some regions at least, lifeline engineering needs to look beyond seismic vulnerability.

## THE IMPORTANCE OF RESPONSE PLANNING

The importance of lifeline utilities in assisting and facilitating community response and recovery after a major earthquake cannot be over-emphasised. This has been illustrated in recent earthquakes in California and even more recently in Kobe, Japan.

Earthquake damage occurs instantly, and although a general pattern may be evident, precise details cannot be predicted before the event. Planning, therefore, cannot be carried out detail, but must be progressed to a level that increases the ability to cope with a wide range of circumstances.

It is fundamental that an effective response is planned. Utility managers must consider the sorts of effects they might have to deal with and how they would activate emergency management and allocate tasks. It is also crucial for them to consider how they would establish the status of their network and how they could effect a basic level of service as quickly as possible. Because utilities are complex hierarchies, it is essential that each does its own response planning. Nevertheless, having done its own planning, each utility should ensure that it has taken into account the possible effects of other failed or inoperative lifelines on its own ability to recover.

Analysis of the ability to respond has a direct bearing on the need or otherwise for physical mitigation measures. Appropriate response may obviate the need to spend large sums of money on mitigation. Alternatively, small amounts of money spent on mitigation may greatly facilitate response. Mitigation and response planning are therefore inextricably linked as is indicated in Figure 2 (Brunsdon *et al.*, 1995).

Figure 2 is derived from the normal circular diagram showing the phases of response, recovery, mitigation and preparedness. It indicates how the process of reducing a community's vulnerability to earthquake is a continuous one. Earthquake events provide lessons that need to be considered when decisions are made on risk assessment and on money to be spent on preparedness. It is not necessary to wait for actual events, as a third path of learning is available through research on hazards, risks, and physical mitigation.

Increasingly sophisticated data and techniques are now available that allow the benefits and the costs to be quantified and compared. Response planning is part of the cycle.

## FRAMEWORK FOR A RESPONSE PLAN

In order to promote a consistent approach amongst lifeline managers, a response planning framework has been developed This framework allows interdependence issues to be readily identified and provides for co-ordination with other emergency management organisations.

The, model framework addresses three phases of response. They are:

- the immediate response;
- the recovery of a basic or partial service; and
- the restoration of full service.

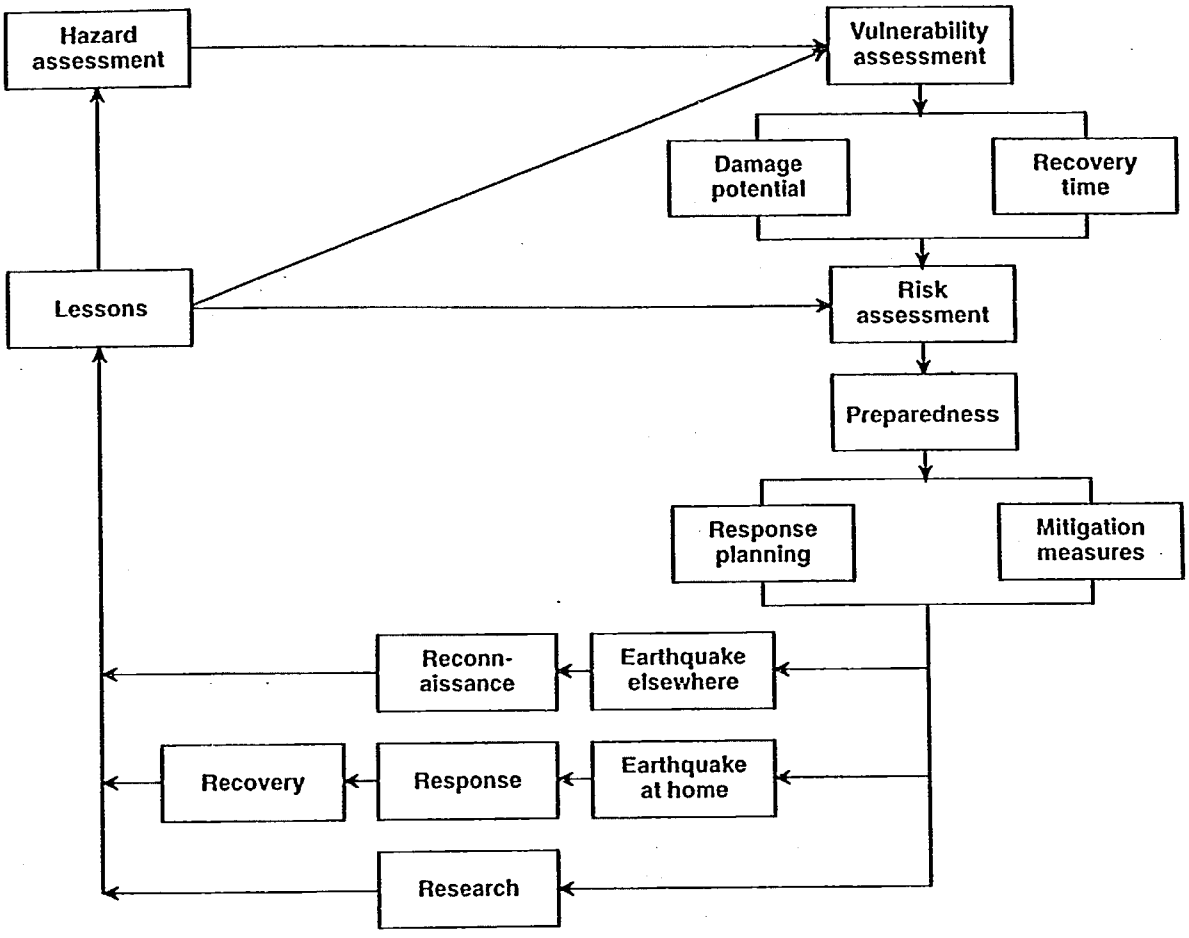



**Figure 2: Earthquake Risk Reduction Cycle**

The immediate response phase addresses; actions taken to make a site safe or secure, the activation procedures and formalities to set up an emergency response, and the initial response, which includes assessment of damage and status of the lifeline, review of available service and prioritising of response. This phase might cover up to the first 36 hours following an earthquake.

The recovery of a partial service phase addresses the establishment of resources and programmes to achieve a minimum service throughout the community. It also addresses the management of information and advice to the community. This phase might cover up to two weeks after the event.

The third phase covers the restoration of full service and addresses the organisation, policies and resources for continuing to provide a service while undertaking a restoration programme. This phase might take 6 months or more after the event.

The framework is based on a practical review of the lifeline hierarchy, its key elements and their relationship to local hazards. The procedure requires an identification of local hazards, an assessment of the network vulnerability to those hazards, a review of the key elements and customers of the network, and the definition of a minimum level of service by which a basic service to the community can be effected following an earthquake. The basis for an inspection procedure and prioritising of response requirements is included in the framework.

Any response plan developed from this framework for a particular utility identifies the processes by which the scope of damage to it can be assessed and the minimum level of service recovered as soon as possible after an event. It also identifies how the priorities and resources are to be managed to bring about the restoration of a full service.

A summary of the key points of the model, Utility Emergency Response Plan Framework, is given in Table 1. The detailed plan needs to provide specific direction and instruction to individuals, especially in the immediate response phase, in order that the response can be initiated as soon as staff are available. At the same time the plan needs to be simple to avoid confusion, and flexible enough to provide for a range of potential impacts.

It is vital to ensure that a viable organisational capability exists following an earthquake, and can be effectively mobilised at any time.

## CONCLUSIONS

New Zealand is situated in an area of high seismicity with well-developed building codes. A strong emphasis has been placed on lifeline work during the last five years in recognition of serious deficiencies in this area. A regional approach has been developed to address issues of:

- hazard identification;
- vulnerability assessment;
- mitigation measures; and
- response planning.

More recently, emphasis has been placed on developing a co-ordinated response planning framework focusing on planning within individual utility organisations but recognising, at the same time, the inevitable interdependence of lifelines. The framework is presented in this paper.

## REFERENCES


1. Lumsden, J.L; (1995), "Lifeline Engineering in New Zealand with Reference to Japan and California", In Proceedings 4th US Conference on Lifeline Earthquake Engineering, San Francisco, August 1995.
2. CAE, (1991), "Lifelines in Earthquakes Wellington Case Study", Project Report, Centre for Advanced Engineering, University of Canterbury, NZ., August, 1991, ISBN 0-9598002-1-2
3. Wellington Earthquake Lifelines Group, 1994 Report, Wellington Regional Council, November, ISBN 0-909016-22-4.
4. Brunsdon, D.R; Hopkins, D.C; Norton, J.A; (1995), "A Comprehensive Framework for Response Planning", In Proceedings 4th US Conference on Lifeline Earthquake Engineering, San Francisco, August 1995.

## Table 1: Utility Emergency Response Plan Framework

An Emergency Response Plan defines the procedures to be followed in the event of a significant earthquake. It defines the roles, responsibilities and authorities of personnel involved and actions to be undertaken or considered.

### PHASE 1 — IMMEDIATE RESPONSE

This phase is to secure hazardous components of a utility, to establish a control organisation and to provide an initial status report. First 36 hours.

a) Conditional Actions — to secure operational positions — address facility by facility
- What are they and what triggers them?
- Who does them?

b) Activation — initiating the Response procedures
- What constitutes activation and who does it?
- What management organisation is required?
- Where does it set up and where do staff report?
- Identify interfaces with other providers
- Communication arrangements
- Staff support needs
- Information handling/network maps/inspection forms

c) Initial Actions — how to address
- Inspections — to predetermined order — report on standard forms
- Identify status of critical customers
- Analyse and review available service
- Set priorities for response and control
- Identify equipment/staff needs
- Review ability to respond
- Media management/public information

### PHASE 2 — RECOVERY OF PARTIAL SERVICE

This phase is to effect a minimum service around the city given the status of available and recoverable supply points and networks. Up to 2 weeks.

Consider how to address:
- Organisation set up — make it secure
- Establish objectives and priorities
- Consider interdependencies
- What is a minimum level of service?
- Interface with other providers
- Check prime network lines for basic service
- Consider alternative supply options
- Identify access constraints
- Isolate major breakages
- Prioritise repair sequences given:
  - — spares/supplies
  - — equipment/resources
- Activate Mutual Aid Agreements
- Set procedures for managing external aid resources
- Record repairs, networks in place, temporary repairs
- Establish startup procedures
- Safety precautions/procedures
- Media management/public information

### PART 3 — RESTORATION OF FULL SERVICE

This phase is to provide an ordered programme to return to effective service as soon as possible. Two weeks to 6 months or more after the event.

Consider how to address:
- Personnel/Organisation/Authority
- Objectives/Priorities
- Standards policy
- Upgrading/retrofitting/replacement
- Taking on new technology
- Prioritise restoration sequence given:
  - — status of key customers
  - — spares/supplies
  - — equipment/resources
- Dependence on other utilities
- Procedures/safety precautions
- Media management/public information

# NEW TRENDS IN THE USE OF EARTHQUAKE SCENARIO EXERCISES: OPPORTUNITIES FOR MITIGATING VULNERABLE LIFELINE SYSTEMS

Laurie A. Johnson, AICP, Senior Planner
Spangle Associates, Urban Planning and Research
3240 Alpine Road, Portola Valley, CA 94028 USA

## ABSTRACT

If people and property are to be protected from the devastation earthquakes can cause, the hazards must be understood and the risk reduced. Earthquake scenario exercises are an effective tool to achieve both these ends, by bringing together four necessary elements for making decisions and policies. These key elements are a clear perception of the problem, viable solutions, involvement of key players providing leadership and advocacy, and an opportunity for action.

These conclusions are based on the experiences and findings of two projects undertaken by Spangle Associates. This first project was to design a one-day recovery exercise for local governments, and the second to create an earthquake scenario and mitigation workshop for Quito, Ecuador. This paper also draws on the observations of an earthquake scenario exercise conducted by the Earthquake Engineering Research Institute at its 1995 annual meeting. While the goals and targeted audiences for the three examples differ, the methods and lessons are directly transferable to the lifelines industry, particularly utility companies.

## INTRODUCTION

Earthquake damage scenarios are a useful and common way of presenting disaster-related information. Key ingredients of an earthquake scenario include a statement about the hypothesized earthquake, and a description, commonly including maps, of what is expected to happen. The process of developing a scenario can become quite technical, requiring the expertise of seismologists, geologists and structural engineers, in addition to those familiar with the community. The result is a detailed portrait of the impacts expected from the particular scenario earthquake.

Over the past 20 years, many earthquake damage scenarios have been prepared, especially for California and Japanese cities, and they are often presented in the form of loss estimation studies. In the United States, most of these studies have been sponsored by government agencies or the insurance industry. In general, the government-sponsored studies are for the purposes of emergency response planning, focusing on casualty estimates and assessing the functionality of emergency and critical facilities. The insurance industry sponsored studies have focused more on property losses to general building stock and other economic consequences.

Emergency responders and disaster planners have long understood the potential training and education opportunities provided by "exercising" earthquake scenarios. Typically, in these exercises, damage caused by a scenario earthquake is described in a compressed time period and participants are required to make emergency response decisions. These exercises, in effect, test the response system and indicate how improvements can be made. These efforts have proven to be very worthwhile.

More recently, there have been significant attempts in at least two countries to "exercise" earthquake scenarios with individuals not only concerned with emergency response, but also with how cities can be reconstructed after a major earthquake or how changes can be made before an earthquakes to make a city more resistant to earthquake damage. The major result of these activities is the development of hazard and risk reduction initiatives for reducing injuries and death, as well as property damage, and the active involvement of government and business leaders in the mitigation process.

Three examples of this type of scenario exercise are presented here. The first is an example of a model exercise based on a general scenario, leading players through a series of recovery related tasks. The second and third examples are based on specific earthquake studies--one in Quito, Ecuador, and the other in the San Francisco Bay Area. All three examples, represent instances in which policy makers and potential mitigation advocates were involved in the scenario creation, and each illustrates a different approach for focusing on hazard reduction as part of the scenario exercise. Following this, suggestions are made for the successful use of earthquake scenario exercises in mitigating vulnerable lifeline systems.

## EARTHQUAKE RECOVERY EXERCISE FOR LOCAL GOVERNMENTS

This one-day, table-top style exercise, created with support of the National Science Foundation (BCS-9025125), is designed to train local government officials in the typical recovery and rebuilding tasks and decisions following a damaging earthquake. (An exercise schedule is shown in Figure 1.) It is designed for 8 to 12 "players" who are mid-to high-level staff members of a single city or county, such as representatives from the chief administrative office and departments of planning, redevelopment, building, public works, housing, social services, as well as the traditional emergency responders, such as the police and fire departments.

The exercise consists of a sequence of twelve tasks, and it starts immediately after a damaging earthquake has struck. Each task in the exercise is introduced with a slide presentation giving the players background and examples of recovery from recent U.S. earthquakes to help them carry out the task instructions. In the first task, participants create a damage scenario depicting their best estimates of the impacts of a large earthquake on their community. The introduction to the first task illustrates the kinds of lands and buildings prone to earthquake failure, and with this general information, players are asked to use their expert knowledge of the community to identify on a base map:

"a) at least one area where you expect landslides, liquefaction failures, and/or fault ruptures;
b) at least two groups of blocks (one commercial and one residential) where you expect concentrated building damage;
c) major facilities such as hospitals, schools, government buildings, and high-rise buildings that you think are now at least temporarily unusable; and,
d) highway overpasses, roads, and other transportation facilities which might have collapsed or been left impassable by the earthquake."

Players have 45 minutes to complete the scenario, which serves as the basis for the rest of the exercise. Next, come emergency phase tasks concerning opening emergency shelters, cordoning off unsafe areas, rerouting traffic, and relocating essential activities. Then, more information is collected about both the damage and geologic stability of ground failure areas, and decisions are made about demolishing buildings. These tasks set the stage for early recovery--finding temporary space for displaced business and residents, adopting procedures to process permits for repairs, and finally preparing a reconstruction plan for a heavily damaged area.

**Figure 1.**
**Schedule for Earthquake Recovery Exercise for Local Governments**

| | | | Minutes |
|---|---|---|---|
| 8:00 - 8:25 | Introduction | | 25 |
| 8:25 - 9:30 | Task A. | Damage Scenario | 65 |
| 9:30 - 9:50 | Task B. | Emergency Shelter | 20 |
| 9:50 - 10:10 | Task C. | Closure and Relocation | 20 |
| *10:10 - 10:30* | *Break* | | *20* |
| 10:30 - 10:55 | Task D. | Damage Assessment | 25 |
| 10:55 - 11:15 | Task E. | Geologic Evaluation | 20 |
| 11:15 - 11:35 | Task F. | Demolition | 20 |
| 11:35 - 12:00 | Task G. | Temporary Business Sites | 25 |
| *12:00 - 1:00* | *Lunch* | | *60* |
| 1:00 - 1:25 | Task H. | Temporary Housing | 25 |
| 1:25 - 1:50 | Task I. | Permit Processing | 25 |
| 1:50 - 3:05 | Task J. | Reconstruction Planning | 75 |
| *3:05- 3:25* | *Break* | | *20* |
| 3:25 - 3:45 | Task K. | Timing and Recap | 20 |
| 3:45 - 5:00 | Task L. | Reducing Risks | 75 |

Throughout the day, as part of each exercise task, players are asked to identify actions that can be taken before an earthquake to reduce damages and to better prepare for each of the tasks. In the final exercise task, players are asked to review their list of recommended actions and compare it with a suggested list of actions, organized into the following categories: existing development, future development, emergency response, and public information and education. Players are then asked to select five high-priority actions, and for each outline the steps required to implement it, resources available and needed, responsible agencies and when the action would be taken. The high-priority risk reduction actions then form the core of a local earthquake risk reduction program.

To date, the exercise has been conducted in nine U.S. cities, most recently in Memphis, Tennessee and with the Los Angeles Community Redevelopment Agency. In each instance, the exercise provided participants with a first glimpse of what could be expected of them and their departments in the aftermath of an earthquake. The process of creating the damage scenario is also a powerful learning experience. Believing it portrays a realistic possibility, participants willingly turn to address the implications of the damage they have created. The sequence of do-it-yourself recovery tasks, also brings participants logically and necessarily to the question, "What can be done before the earthquake to make all this easier?"

An exercise manual, complete with all the materials needed to facilitate the exercise, has been published. The Federal Emergency Management Agency (FEMA) is currently publishing additional manuals and will distribute them to earthquake program managers in each state. Plans are also underway to train a cadre of facilitators to lead the exercise and to provide

exercise funding. FEMA is also funding the creation of similar exercises for flood and hurricane scenarios.

## QUITO EARTHQUAKE SCENARIO AND MITIGATION WORKSHOP

In July 1993, an interactive workshop was held in Quito, Ecuador, in which participants created an earthquake damage scenario and a risk reduction program based on the scenario. (A workshop schedule is shown in Figure 2.) The workshop was the final part of a two-year effort, known as Quito Earthquake Risk Management Project, funded and directed by Oyo Pacific (now Geohazards International), to develop an earthquake vulnerability analysis for Quito. In this project, Ecuadorian scientists and engineers conducted seismic studies with the advice and assistance of a committee of foreign experts and a committee including representatives from the Ecuadorian national government, Quito city government, and the insurance, banking, and petroleum industries.

The project was divided into three phases, and in the first phase, future earthquakes and their effects on Quito were analyzed. An international, interdisciplinary team of more than 40 seismologists, geologists, soils engineers, structural engineers, and city planners from Ecuador, Canada, France, Japan, and the United States estimated the magnitudes and locations of future earthquakes likely to affect Quito, the level of ground shaking that these earthquakes would create, and the damage to Quito's buildings and infrastructure. In the second phase, the impact on life in Quito during the month following one of these earthquakes was described in vivid, non-technical terms. This vulnerability study was performed by interviewing officials from 17 different city organizations, including sewer, water, power, and transportation departments; Civil Defense; and, fire and police departments.

During the third phase, all this information for a scenario earthquake was presented to over 60 public and private sector leaders at the opening sessions of the workshop. After this, the participants broke into four interest groups--banking and insurance, emergency services, lifelines, and buildings and planning--to detail the impacts of the scenario earthquake on each sector. The results of this session were then used by the four groups to develop specific recommendations within their fields of expertise for managing earthquake risk in Quito. Each group initially brainstormed to create a list of possible risk reduction actions. Then, the groups selected five high-priority actions and for each outlined the steps required to implement it, resources available and needed, responsible agencies and when the action would be taken. The high-priority risk reduction actions from all four groups comprise the core of an earthquake risk reduction program for Quito.

Most of the actions are broad in scope and include creating a Quito Earthquake Safety Advisory Board; adopting and enforcing an effective building code; supporting scientific research to improve earthquake scenarios; developing a workplace earthquake preparedness program; improving emergency response equipment and facilities; and, establishing a proper insurance tariff with underwriting guidelines. **The strength of a program assembled in this way is that it is created by those who have the main responsibilities for carrying it out. By working on the scenario, participants saw how their individual work lives would be affected in the aftermath of an earthquake, and thus, gained a personal stake in forging realistic solutions.**

Support for earthquake hazard reduction in Quito continues. The Quito School Earthquake Safety Project, which began in February 1995 and will be completed in October 1995, utilizes information on schools gathered during the earlier project. Retrofit designs and cost estimates, are being prepared for eight schools determined to be at highest risk, and for three popular

school designs used throughout the country. Funding for retrofitting three schools has already been secured, and an intent to fund four to five additional schools has been expressed by the Ecuadorian government, local philanthropic organizations, and local businesses.

**Figure 2.**
**Schedule for Quito Earthquake Scenario and Mitigation Workshop**

Day One

| | |
|---|---|
| 9:00 – 9:30 | Welcome and Introductions |
| 9:30 – 10:00 | Technical Summary<br>Part One: Quito's Earthquake Hazards--*frequency, magnitude, locations of faults, faulting, amplified ground shaking, landslides, liquefaction failure* |
| 10:00 – 10:30 | Part Two: Effects on Structures--*vulnerable buildings and infrastructure* |
| *10:30 – 11:00* | *Break* |
| 11:00 – 11:30 | Part Three: Effects on Government and Business--*results of interviews conducted with governmental and business leaders on potential impacts.* |
| 11:30 – 12:00 | Part Four: Examples of Types of Earthquake Damage |
| *12:00 – 1:00* | *Lunch* |
| 1:00 – 1:30 | Introduction to Group Sessions |
| 1:30 – 3:30 | Group Sessions: Assessing Impacts *(Groups meet to review and refine scenario information presented and to explore the implications of the damage on Quito's banking and insurance, emergency services, building and planning, and lifelines.)* |
| *3:30 – 4:00* | *Break (Group leaders and recorders prepare for general assembly presentations.)* |
| 4:00 – 6:00 | General Assembly: Assessing Impacts *(Group leaders describe the outcomes of their sessions and add information to the scenario map.)* |

Day Two

| | |
|---|---|
| 9:00 – 9:30 | Recap of Scenario |
| 9:30 – 10:00 | Organization and Program for Reducing Earthquake Risk – An Example from California. *The formation and structure of the California Seismic Safety Commission and its earthquake risk reduction program, "California at Risk".* |
| 10:00 – 10:30 | Example of a City Program to Reduce Earthquake Risk<br>*The earthquake risk reduction program of the City of Los Angeles.* |
| *10:30 – 11:00* | *Break* |
| 11:00 – 11:30 | Introduction to Group Sessions<br>*Mitigation examples and instructions for group sessions.* |
| 11:30 – 1:00 | Group Sessions: Reducing Impacts *(Groups meet to recommend actions for reducing the impacts identified in Day One sessions. The groups also assign priorities to the actions and indicate the schedule, resources needed, and agencies responsible for carrying them out.)* |
| *1:00 – 2:00* | *Lunch* |
| 2:00 – 3:30 | Group Sessions: Reducing Impacts *(continued)* |
| *3:30 – 4:00* | *Break (Group leaders and recorders prepare for general assembly presentations.)* |
| 4:00 – 6:00 | General Assembly: Reducing Impacts *(Group leaders present the list of actions developed in the group sessions.)* |
| 6:00 – 6:30 | Summary and Wrap-up |

## "A MAGNITUDE 7 ON THE HAYWARD FAULT"

The third scenario exercise example is the one-day symposium hosted by the Earthquake Engineering Research Institute (EERI), a multi-disciplinary and international organization for professionals in the earthquake field, at the organization's 1995 annual meeting in San Francisco. (A scenario schedule is shown in Figure 3.) The scenario considered the impacts of a magnitude 7 earthquake occurring on the northern segment of the Hayward fault. This fault runs along the hills flanking the eastern side of San Francisco Bay, and through one of the region's most heavily urbanized areas, including the cities of Oakland and Berkeley. While organized for months beforehand, the meeting took place coincidentally only three weeks after the Great Hanshin earthquake, drawing considerable media attention and also providing speakers with recent and eerily comparable illustrations of the scenario's likely effects.

**Figure 3. Schedule for "A Magnitude 7 on the Hayward Fault"**

| | |
|---|---|
| 9:05 – 9:15 | Introduction to Scenario |
| 9:15 – 9:35 | Hayward Fault Socio-Economic Setting |
| 9:35 – 9:55 | Geology and Seismology of the Hayward Fault |
| 9:55 – 10:15 | Ground Failure Phenomena: Surface Faulting, Landslides, Liquefaction, and Lateral Spreading |
| *10:15 – 10:45* | *Break* |
| 10:45 – 11:00 | Water and Sewer Delivery Systems Affected by Ground Failures |
| 11:00 – 11:15 | Transportation Systems and Buildings Affected by Ground Failures |
| 11:15 – 11:30 | Ground Motions: Site Response and Near-Fault Effects |
| 11:30 – 11:45 | Transportation Systems Affected by Ground Motions |
| 11:45 – 12:00 | Questions and Answers |
| *12:00 – 1:30* | *Lunch* |
| 1:30 – 1:45 | Power and Telecommunications Affected by Ground Motions and Fuel Delivery Systems Affected by Ground Failures |
| 1:45 – 2:10 | Critical Facilities Affected by Ground Motions |
| 2:10 – 2:35 | Commercial and Residential Buildings Affected by Ground Motions |
| 2:35 – 2:45 | Questions and Answers |
| *2:45 – 3:15* | *Break* |
| 3:15 – 3:35 | Emergency Response and Relief |
| 3:35 – 3:55 | Regional Response |
| 3:55 – 4:15 | Housing and Social Recovery |
| 4:15 – 4:30 | Regional Transportation Response |
| 4:30 – 4:50 | Economic Recovery |
| 4:50 – 5:00 | Questions and Answers |
| 5:00 – 5:15 | Wrap Up and Summary |

The scenario began with a description of the Bay Area's socio-economic setting, notably the region's world-wide, economic significance. Then, the geological and seismological aspects of the scenario event were described in detail. According to scientists, this highly probable scenario earthquake would probably last 20 seconds (twice as long as the Loma Prieta earthquake) and rupture a distance of 50 km--the same length as the Great Hanshin quake. Descriptions of the expected ground failure phenomenon and anticipated ground shaking were also presented. This information had been made available to other developers of the scenario well in advance of the meeting, and they used it to describe the effects on transportation systems, water, sewer, power, and fuel and delivery systems, telecommunications, critical facilities, commercial and residential buildings, emergency response and relief systems, as well as the impacts on social and economic recovery.

With respect to lifelines, speakers warned about the difficult transportation problems that would be experienced with this scenario. The audience heard that the Bay Area Rapid Transit (BART) would not be expected to be operational in the aftermath, and that freeways throughout the East Bay would be closed, including major north-south links and the Bay Bridge. The Oakland Airport would be expected to have heavy damage and extensive time closures. The scenario illustrated the need for a regional clearinghouse for transportation information in the wake of the next major earthquake, and the Metropolitan Transportation Commission and the state's Department of Transportation are now reportedly working to improve this communication link. Also, the Port of Oakland, which suffered severe damage in the 1989 earthquake and has since undertaken an extensive retrofit program, offered some good news, expecting to be functional after such an event. Furthermore, the East Bay Municipal Utility District announced the large pre-earthquake rehabilitation effort it is initiating for its water and sewer systems.

While this exercise did not specifically include in it the drafting of hazard reduction initiatives, it is a useful demonstration of how a complete earthquake scenario evaluation can be performed. The scenario presenters looked well beyond the initial impacts and damage and offered clear and appropriate statements about needed actions. Furthermore, the call to action was delivered to a large and diverse audience, and the responsibility for actions has been shared among many professions and governmental organizations. The day's final speaker offered the following statement about the picture that had been created: "In the end, it will be the will of the people expressed through personal acts to mitigate earthquake risks, as well as their support for earthquake programs, that will determine whether California attains an acceptable level of seismic safety by the end of this century." EERI plans to publish a summary of the scenario later in 1995.

## OPPORTUNITIES FOR USING SCENARIO EXERCISES TO MITIGATE VULNERABLE LIFELINE SYSTEMS

The three examples illustrate how earthquake scenario exercises can bring together the necessary elements for earthquake hazard reduction decisions and policies. The four key elements which must converge simultaneously are problems, solutions, participants, and opportunities. Suggestions for how earthquake scenario exercises can pull these elements together to mitigate vulnerable lifeline systems are as follows.

**Exercises increase awareness of the seismic hazard problem.**

Awareness is an essential precondition to risk reduction and an exercise, which creates a scenario and then addresses the damage, can effectively capture the attention of participants

and lead them to action. For example, in Los Angeles, information about the expected damages to lifeline systems presented in an earthquake damage scenario, motivated city officials to form new planning partnerships with utilities, the business community, and other governmental agencies.

Most lifelines operate as a system or network of many individual elements, often spread over a large geographical area. A highly detailed and technical scenario may be needed in order to fully understand the vulnerability of these complex systems, and to determine appropriate mitigation strategies. It is important to recognize, however, that this level of detail may not always be necessary to convince public officials and policy makers of the potential threat to life and property.

Furthermore, hazard and vulnerability information gathering can be a costly undertaking and attempts at hazard reduction sometimes fail to get beyond it. Funds may run out before any actual hazard reduction has occurred. A well designed scenario exercise, based on very general information, can increase awareness about the risk and provide direction for subsequent information gathering and analysis.

**Exercises can be used to develop comprehensive seismic hazard reduction plans.**

The first two exercises presented here relied upon the state of California's risk reduction program, "California at Risk", as a planning model and exercise participants developed comprehensive risk reduction programs, addressing four general categories of actions: existing development, new development, emergency response, and public information and education.

Because utilities are interconnected systems covering wide areas and facing a variety of earthquake effects, scenario exercises can be quite effective at illuminating the complex interplay of lifeline issues and convincing participants of the need to define realistic and comprehensive risk reduction strategies. It also can provide a framework for considering and prioritizing alternative mitigation measures, such as increased seismic (re)design, emergency response planning, redundancy, avoidance, and earthquake insurance.

**Exercises support and encourage advocates.**

Scenario exercises provide support for existing local advocates of earthquake safety and also encourage the emergence of new advocates. The scenario exercises presented here, not only involved earth science and engineering professionals, but also planners, policy makers, business managers, political officials, and others with significant decision making responsibilities. Many of these players have provided the much needed leadership and advocacy for continuing hazard reduction efforts. Furthermore, many are often very skilled at preparing strategic plans and programs, and they also understand the political process and how to win the necessary support to fund mitigation actions and continued research. Utility companies may also want to consider involving critical customers, regulators, and owners, in such efforts.

**Exercises create a "window of opportunity" for action.**

Policy decisions and actions most often occur when public concern is heightened. In California, most of the key seismic safety policies have been advocated and adopted during the window of opportunity opened following a damaging earthquake. Scenario exercises can also create such a "window", and a well-defined and politically acceptable plan, outlining post-exercise actions, can effectively seize this "opportunity".

## ACKNOWLEDGMENTS

This paper is partially based on work funded by the National Science Foundation under Grant Number BCS-9025125. Any opinions, findings, and conclusions, or recommendations expressed in this material are those of the author and do not necessarily reflect the views of the National Science Foundation.

## REFERENCES

Earthquake Engineering Research Institute, "Hayward Fault Scenario: What Would Happen If . . . ?", in *EERI Newsletter*, March 1995, Volume 29, Number 3.

Geohazards International, *The Quito, Ecuador, Earthquake Risk Management Project, An Overview*, May 1994.

Goode, Reka, "Kobe Redux: It Could Happen Here", in *Transactions*, April 1995, published by the Metropolitan Transportation Commission.

Mader, George G., "Creating the Scenario and Drafting Earthquake Hazard Reduction Initiatives", in *Issues in Urban Earthquake Risk*, edited by Brian E. Tucker et al., NATO ASI Series E: Applied Sciences - Vol. 271.

Mattingly, Shirley, "Socioeconomic and Political Considerations in Developing Earthquake Damage Scenarios in Urban Areas", in *Issues in Urban Earthquake Risk*, edited by Brian E. Tucker et al., NATO ASI Series E: Applied Sciences - Vol. 271.

Risk Management Software, Inc. (RMS) and California Universities for Research in Earthquake Engineering (CUREe), 1993, *Assessment of the State of the Art Earthquake Loss Estimation Methodologies, Task 1 Report*, October 1993.

Tyler, Martha Blair, and Johnson, Laurie A., "New Approaches to Encourage Earthquake Risk Reduction", in Proceedings of the 1994 National Conference on Earthquake Engineering, Chicago, Illinois.

Savage, William, personal communication, June, 1995.

Savage, William, et al., "Long-Term Risk-Management Strategy for Reducing Earthquake Vulnerability of Gas and Electric Systems," (PrePrint) *Proceedings of the 5th International Conference on Seismic Zonation*, Nice, France, October 17-19, 1995.

# RAPID POST-EARTHQUAKE DAMAGE ASSESSMENT FOR LIFELINE FACILITIES

Ronald T. Eguchi
Hope A. Seligson
James D. Goltz

EQE International, Inc.
Irvine, California

## ABSTRACT

Recent earthquakes in the U.S. have demonstrated the importance of rapid damage assessments for emergency response. At the time of the January 17, 1994 Northridge earthquake, several rapid damage assessment tools were in place to facilitate response and recovery decisions. Near real-time broadcasts of earthquake source information was available through the CUBE (Caltech-USGS-Broadcast-of-Earthquakes) system; early post-earthquake damage estimation was possible using a partially developed software tool entitled EPEDAT (Early Post-Earthquake Damage Assessment Tool). Both tools have undergone significant development since the Northridge earthquake, largely building on the lessons learned from the January 17, 1994 event. This paper provides a short summary of this development as well as pointing out future directions.

## INTRODUCTION

In the immediate aftermath of a damaging earthquake, local governments face the difficult task of rapidly allocating life safety services and identifying severely damaged structures, particularly damage to critical facilities. In the past, this task has often been characterized by a lengthy period of reconnaissance during which inaccurate reports, distortions and rumors must be separated from factual disaster intelligence painstakingly gathered from multiple sources. State government, responsible for assisting impacted cities and counties through the mutual aid system, also relies on this chaotic information gathering process.

Similar concerns affect utility and public works agencies. Isolation of severely damaged areas and rapid restoration of service must be based on reasonably accurate data on which parts of the system have suffered damage. Slow response may result in loss of critical water supplies, gas-initiated fires, and ineffective recovery actions.

During the Northridge earthquake, several rapid post-earthquake response systems were in place. An automated, real-time system which provides earthquake magnitude and location information to participating organizations through a commercial paging system within minutes of an earthquake was available through a joint Caltech-USGS effort. This system (CUBE Caltech-USG Broadcast of Earthquakes) experienced hardware and software problems during the earthquake; earthquake magnitude and location data were provided within one hour of the event, however. EPEDAT, which uses data from the CUBE system to initiate damage calculations, was only partially developed at the time of the earthquake. Nevertheless, estimates of damage, primarily damage to building stock, were provided to the State of California within days of the event.

In this paper, we examine these new technologies and the roles that they will play in future earthquake disasters. As Northridge and the recent Hanshin earthquake in Japan point out, rapid information on the severity of the earthquake can facilitate more systematic and effective response.

## NEW TECHNOLOGIES FOR REAL-TIME EARTHQUAKE HAZARD ASSESSMENT

This section discusses the CUBE and EPEDAT systems and the role each played during the recent Northridge earthquake. In addition, a detailed discussion of the individual models that make up the EPEDAT system is provided. This section is then followed by a discussion of the development goals that were used to constructing EPEDAT. As was discussed earlier, the emphasis in this development was on rapid response for emergency decisions.

## The Caltech-USGS Broadcast of Earthquakes (CUBE)

Although real-time seismic monitoring has been applied to promote public safety in Japan, similar applications have been slow to materialize in the United States. Following the Loma Prieta earthquake, a survey was conducted to assess the perceived utility of an earthquake early warning system which would provide a few seconds of warning in advance of damaging levels of shaking . Researchers found that most groups which were expected to enthusiastically endorse this new technology were luke-warm, at best, considering a few seconds warning too little time to take meaningful action in advance of a major earthquake. Nor was such a system regarded as a cost-effective strategy for hazard reduction and thus, unlikely to receive much support from users (Holden et al., 1989).

Despite this somewhat disappointing beginning for real-time monitoring, Caltech and the U.S. Geological Survey pushed ahead with plans to upgrade the Southern California Seismic Network (SCSN) to provide real-time broadcasts of earthquakes and seek the support of government agencies, large utilities and corporations for the potential post-event benefits these broadcasts might provide. Gradually, participants were recruited to participation in the Caltech-USGS Broadcast of Earthquakes (CUBE) and by the time of the Northridge earthquake, there were 18 Level III participants in the Earthquake Research Affiliates of Caltech (ERA), the organizational vehicle for provision of real-time earthquake broadcasts from SCSN. These participants made an annual contribution of $25,000 to the Caltech Development Fund (which helped support the purchase of new seismic monitoring equipment) and received reports of earthquakes via pagers which carried the magnitude, location, time and other earthquake data within 2-5 minutes of occurrence.

For approximately four years, CUBE reliably broadcasted earthquakes up to about M5.5 to participants. At 4:31 a.m. on January 17, however, the CUBE system experienced both hardware and software difficulties which resulted in delays of approximately one hour in providing information on the Northridge earthquake. A study currently under way is designed to determine how response of CUBE participants was affected by the performance of CUBE after the Northridge earthquake, and in general, how receipt of real-time earthquake information from SCSN has been integrated into the response plans of these organizations (Goltz, 1995).

Preliminary results from this study indicate that the CUBE system usually provides the first data upon which action may be taken. To assist in determining whether a response is justified, many CUBE participants have customized the Q-pager software (which displays spatial and other data on an earthquake) by adding overlays to the basic southern California map on which earthquake epicenters are plotted. These overlays include facilities such as transmission lines, dams, power stations or other critical structures. In a few instances, participants reported monitoring the patterns of small earthquakes in a particularly critical location under the assumption that these earthquakes may be precursors to a large damaging event.

Statewide real-time broadcasts are now available and have been adopted by those agencies (OES and Caltrans) and companies (utilities and railways) with statewide jurisdiction, facilities or distribution networks. These statewide broadcasts are available through a cooperative agreement between Caltech (CUBE) and the University of California at Berkeley (REDI or Rapid Earthquake Data Integration). In March, 1995, CUBE participants received software which permits the mapping of ground acceleration data broadcast in real-time from the SCSN. Most users consider this to be a very important development in that the potential impact on facilities can be more precisely estimated and mobilizations of personnel for inspections can be expedited.

The development of real-time monitoring and broadcast of seismic information appears to be in transition from concept and pilot project to a practical operational system. Under the strictest definition of real-time availability, the Northridge earthquake must be considered a missed event. It appears, however, that the January 17 event exposed a plethora of technical vulnerabilities in the CUBE system and triggered a concerted effort to remedy most, if not all of them. It does not appear that the failure of the CUBE system to provide rapid and accurate information on the earthquake had a dampening effect on the interest and enthusiasm of users.

**Loss Estimation and the EPEDAT system**

The Northridge earthquake was the first earthquake disaster to occur in the United States in which important emergency response and early recovery decisions were based on loss estimates as well as actual data gathered through standard reconnaissance procedures. The utilization of loss estimation techniques in the immediate post-earthquake context is a key development and marks a significant departure from conventional applications. For the last two decades, earthquake loss studies have addressed the pre-earthquake planning needs of utility operators and government agencies. Although the needs of these users vary, understanding risks and maintaining public safety have generally required similar scenario events, that is, those with the greatest impacts on the local population and economy.

Historically, loss estimation studies for planning purposes have identified scenario earthquakes as the focus for this development. These studies use existing knowledge of regional geology and seismology to generate maps with estimated intensities and, based on projected ground motion and other factors, estimate damage to buildings and structures, lifelines and impacts on population. Some studies also address potential secondary hazards such as fire, flood and hazardous materials releases. Presented in report or document form, often with fold-out and sometimes overlay maps, these earthquake scenarios have been employed by government and utilities to prepare and mitigate. Thus, the typical loss study has been single-event focused, applied in the long-term pre-event period and utilized primarily by those concerned with seismic safety planning and risk management.

Even before the Northridge earthquake, technological developments were rapidly rendering these scenarios and the formats in which they were presented obsolete. The advent of high speed computing, satellite telemetry and Geographic Information Systems (GIS) have made it possible to electronically generate loss estimates for multiple earthquake scenarios, provide a nearly unlimited mapping capability, and perhaps most important, develop estimates for an actual earthquake in near real-time given the source parameters of magnitude and location. For the last five years, real-time broadcasts of earthquake data including magnitude, location, depth and time of occurrence, have been available in southern California on an experimental basis from the Southern California Seismic Network operated jointly by the California Institute of Technology and the United States Geological Survey.

Currently under development by EQE International is a GIS-based system capable of modeling building and lifeline damage and estimating casualties in near real-time given the source parameters of an earthquake (Eguchi, et al, 1994). The Early Post-Earthquake Damage Assessment Tool (EPEDAT) will be completed in mid-1995, will utilize real-time seismic information from the Southern California Seismic Network and will operate on a personal computer. EPEDAT will utilize fault and seismicity data to locate the most likely source of an earthquake, as broadcast by CUBE. Applicable ground motion and soil amplification models will be employed to estimate the expected intensity patterns in the affected area. These intensities will then be overlaid onto the computerized data files containing an aggregate listing of buildings and lifelines in the region. Based on damage and casualty models already developed under contract with the State of California, and the intensity patterns computed, building and lifeline damage as well as casualties will be estimated for the impacted area. EPEDAT will also allow the user to update early estimates with actual reconnaissance data. Thus, as more accurate and specific data become available, they can be incorporated to refine or correct initial predictions.

Real-time loss estimation offers direct and tangible benefits over conventional loss studies. For the first time, loss estimation can be used in the emergency response and early recovery phases of a disaster as a decision support tool. Based on rapid receipt of magnitude and location, estimates of ground shaking and intensity can be calculated and mapped giving emergency responders a sense of the overall scope of an event minutes after it has occurred. Reconnaissance efforts can focus on those areas projected to be hardest hit based on estimates of intensity. Inspection teams can be dispatched, staging areas can be identified, medical emergency resources mobilized and sheltering needs considered, as responders are guided by estimates of damage, casualties and displaced persons. Recovery can be hastened by calculation of total dollar loss estimates and breakdowns of losses by facility or structural type, usage or other categorizations which expedite governmental disaster assistance.

Immediately following the January 17 earthquake, data and models which are the basis for EPEDAT in Southern California were utilized and, though the system was not fully operational at the time, produced timely and accurate information which was used by state and federal officials to support key policy and program decisions. Estimates of dollar losses and ground

shaking intensity were used by the California Office of Emergency Services to define the general regional scope of the disaster during the critical 24-48 hours after the event. The shaking intensity map was instrumental in approximating the locations of heaviest damage, used in briefing state agency executives, including the Governor, and in making decisions regarding shelter needs, locating Disaster Application Centers and "fast-tracking" the federal Disaster Housing Assistance Program. A total dollar loss estimate of $15 billion, generated within 24 hours of the earthquake, served as the basis for negotiation of a supplemental Congressional appropriation of $8.6 billion in federal disaster assistance.

**Basic Steps.** The methodology for estimating early post-earthquake damage consists of seven steps, some of which are interactive. Since the objective of this procedure is to provide the best estimate of damage based on all available data, including post-earthquake information, steps which compare or calibrate predictions with actual field data will be essential elements of the methodology. In general, these iterative loops involve refining estimates of earthquake source parameters or modifying damage algorithms for buildings and contents. The basic methodology for estimating early post-earthquake damage is presented in Figure 1. Seven essential steps are listed.

***Early Earthquake Magnitude Data.*** The first step consists of compiling early earthquake magnitude data. Usually this information consists of earthquake magnitude, the hypocenter or epicenter location, and perhaps, measurements of regional peak ground accelerations. For the EPEDAT prototype, the source for this information is the Caltech-USGS-Broadcast-of-Earthquake System (CUBE).

***Earthquake Source Parameters.*** The second step of this methodology is to identify the causative fault and to estimate the extent of fault rupture. It is important to estimate fault rupture lengths and their locations since ground motion patterns will depend on the distance to the fault rupture plane. Determination of this information will become more critical for large earthquakes that generate long rupture lengths. Smaller events may be modeled as point sources with little or no linear rupture length.

One of the more important tasks associated with this step is deciding on the causative fault. In southern California, where the fault system is complex, it may be difficult to initially determine the causative fault. This is further complicated by the recent introduction of faults that do not break the surface, i.e., "blind thrust" faults. In fact, during the Northridge earthquake, it took several days after the earthquake to finally identify the causative fault system and its mechanism of failure.

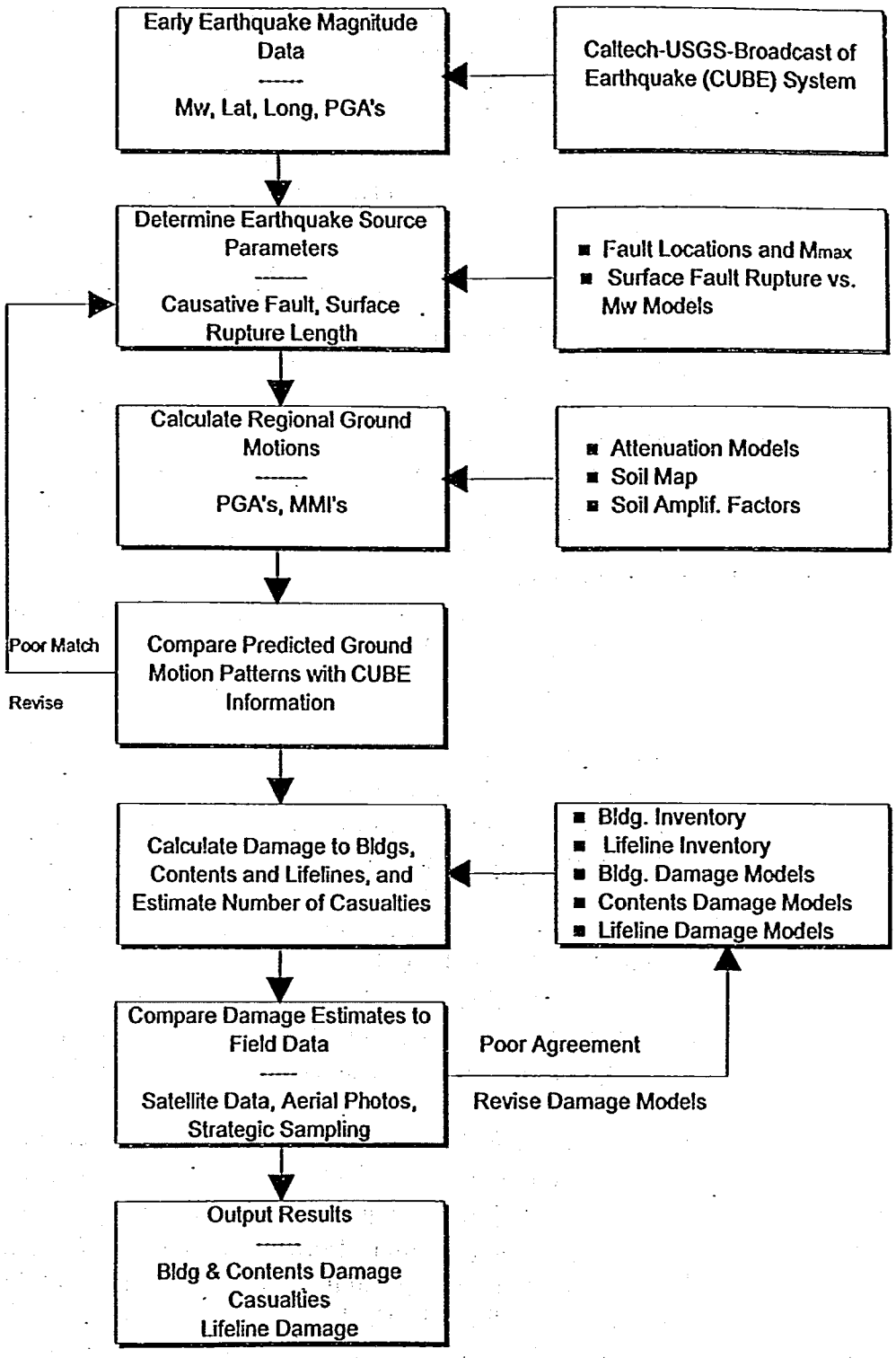



**Figure 1: Methodology for Estimating Early Post-Earthquake Damage**

To address this issue of fault assignment, we have developed the following procedure. A complete list of known active faults has been compiled and their locations have been digitally input into EPEDAT. For the most part, these are faults that have been identified as active or potentially-active by the California Division of Mines and Geology (CDMG, 1988, 1990). In addition, known blind thrust fault ramps have been added. In order to model these thrust ramps, it has been necessary to developed three-dimensional models of these source zones.

Next, we have developed a model which recognizes the maximum magnitude potential of each fault and its area of influence (i.e., zone of possible earthquake occurrence). The area of influence is based on knowing the type of fault, e.g:, strike-slip, reverse, thrust, etc.; the largest earthquake that can be generated by the fault; and the location of associated fault segments, i.e., secondary and branch faults. Based on this data, areas are drawn around each fault. When an earthquake is recorded, the location of the event is overlaid onto these areas. If the earthquake falls within one area of influence and the recorded magnitude is less than the maximum magnitude for that fault, the earthquake is assigned to that fault. If the earthquake falls within several areas of influence, a check is made regarding the maximum magnitudes for the possible causative faults. If the observed magnitude is below the maximum for each fault, then a final determination of the causative fault is made by comparing the prediction with actual data, as described below. Projected fault rupture lengths are computed from the magnitude data. Different models are used to determine fault rupture lengths depending upon fault type.

*Regional Ground Motion Intensities.* The next step involves the calculation of regional ground motion intensities. Based on the magnitude of the earthquake, the location of the projected fault rupture area or length, and the type of local soil conditions, ground motions are computed for a predetermined grid system. Currently, ground motion intensities are measured by two parameters: Modified Mercalli intensity and peak ground acceleration. In the future, other measures of instrumental intensity, e.g., peak ground velocity, or spectral ordinates for selected frequency ranges, may be calculated. As is characteristically done in most seismic hazard calculations, intensities are modified for each site based on local soil or geologic conditions. These factors are incorporated in the ground motion attenuation equation which considers the effects of source type, earthquake size and local soil amplification.

*Calibration of Projected Intensities with Post-Earthquake Data.* At this point in the analysis, a comparison is made between the ground motions calculated based on the attenuation model and those which are actually observed during the earthquake. As stated earlier, the CUBE system will produce early data on peak ground accelerations from the earthquake. When available, this data can be used to check, calibrate and perhaps even modify (in near-real time) the ground motion attenuation models contained within EPEDAT. For example, if the post-earthquake acceleration data appears to be biased towards higher ground motions (i.e., higher than normal), adjustments to the EPEDAT attenuation model can be made and regional motions recalculated. The more stations that are supplying accelerograph data to make these checks, the better the chance that unique ground motion patterns will be observed during the event. If no major

changes are necessary in modeling the intensity patterns from the earthquake, then the analysis proceeds to the next step.

*Damage Assessment.* At this point, it is possible to estimate regional damage to exposed facilities. In order to do this, several models must be inserted. The most important models are the exposure models. In general, there will be three sets of exposure models: buildings and contents, exposed populations, and lifelines. In addition to the exposure models, damage models for buildings and contents, and casualty models for exposed populations must be employed.

To date, we have incorporated exposure models that have been developed from county assessor's data for buildings, and census and employment data for exposed populations. EPEDAT currently has information for the following counties in southern California:

Los Angeles
Orange
Riverside
San Bernardino
Ventura
San Diego

The estimation of damage and casualties follows basic damage equations. In general, the following equation is used:

$$\text{Damage} = E[\text{Damage} \mid \text{Intensity}] \qquad (1)$$

where $E[\ ]$ represents the expected value of damage given a particular intensity level. That is, once the intensity is known for a particular site, the appropriate damage algorithm is selected and damage is estimated based on the intensity. Equation (1) is generally referred to as a damage function or algorithm. The development of these damage algorithms may follow two separate methods. The first set of models is constructed based on expert opinion. ATC-13 (ATC, 1985) is a good example of this type of development. The major benefit in using such an approach is that individual relationships can be developed for a wide range of facility types without much empirical data. Since their development is based on subjective opinions, basic trends can be developed or postulated for general facility types. Also, the judgment of experienced engineers can be used to help guide these relationships. The drawback of this approach is that these models may or may not replicate actual earthquake damage experience since little data used to construct these relationships.

A second set of models results from empirical analysis of past earthquake data. If large data sets are available to construct statistical models, this results in the most realistic representation of damage behavior. Unfortunately, these large data sets exist only for a few general construction categories.

EPEDAT uses the results from the building damage analysis to project impacts on exposed populations. Casualties are estimated by knowing the population levels within certain building types, and the extent of estimated building damage. Other impacts, such as displaced populations, are also calculated as a function of building damage.

*Comparison of Damage Projections with Post-Earthquake Data.* At this point in the analysis, a comparison can be made between estimated damage levels and observed post-earthquake damage data. Several techniques are being developed that will enhance our ability to calibrate regional damage after major events. Techniques being developed at the Jet Propulsion Laboratory (JPL) in Pasadena use satellite data and information to identify areas of massive ground movement (Crippen, 1992). By comparing pre- and post-earthquake satellite photos of the affected area, scientists at JPL have successfully identified areas of surface fault rupture. This technique was applied using data from the 1992 Landers earthquake in southern California. In a more refined application of these techniques, areas of liquefaction, ground movement or landslide could perhaps be identified. This information would be particularly useful in identifying areas of potential damage to underground utility systems.

The use of aerial photos can also help establish levels of regional damage. Hamada and O'Rourke (1992) have shown that aerial photos are extremely useful in identifying the magnitude and direction of significant land movements caused by liquefaction ground failure. This approach can also be used to calibrate specific predictions of site intensity by comparing the effects at sites with known seismic vulnerabilities to field observation data. Finally, a new technique being developed by EQE International is a rapid sampling scheme whereby predetermined sites or areas can be established within the southern California that will allow a limited but statistically significant sampling of post-earthquake damage. This approach is similar to the "Gallop Poll" or exit poll methodologies that are used to project "winning candidates" based on limited polling of voters. In the voter polls, demographic data plays an important element in the projections; in the damage assessment procedure, building inventory data plays a key role.

Using post-earthquake damage data collected from various sources, it is then possible to compare damage projections with actual field data. If the comparisons are not good, then modifications to the damage models must be made, in a manner similar to the changes needed to better project ground motion intensities. By incorporating this iterative step in the methodology, the procedure becomes dynamic, in the sense that new data are always being incorporated to improve the model predictions. As is evident from the recent Northridge earthquake, there are always surprises that occur, either in observed levels of ground motion or building damage. For an early post-earthquake damage assessment tool to be effective, it must incorporate the ability to merge actual data observed during the event into the analysis.

*Output of Results.* The final step involves the output of damage and casualty results. The most important factor here is to output the information in a form that can be input into a Geographical Information System (GIS). After a major disaster, many types of data must be

displayed to help make decisions. The Northridge earthquake showed the value of having a versatile GIS system. Important data, such as building damage, sheltered populations, and people needing aid were all displayed graphically using a GIS system. This information, when combined with a listing of resources, allowed a more effective match of need versus resource. In the future, GIS can be used in a more comprehensive way to decide on resource allocations. Figure 2. shows a sample screen from EPEDAT.

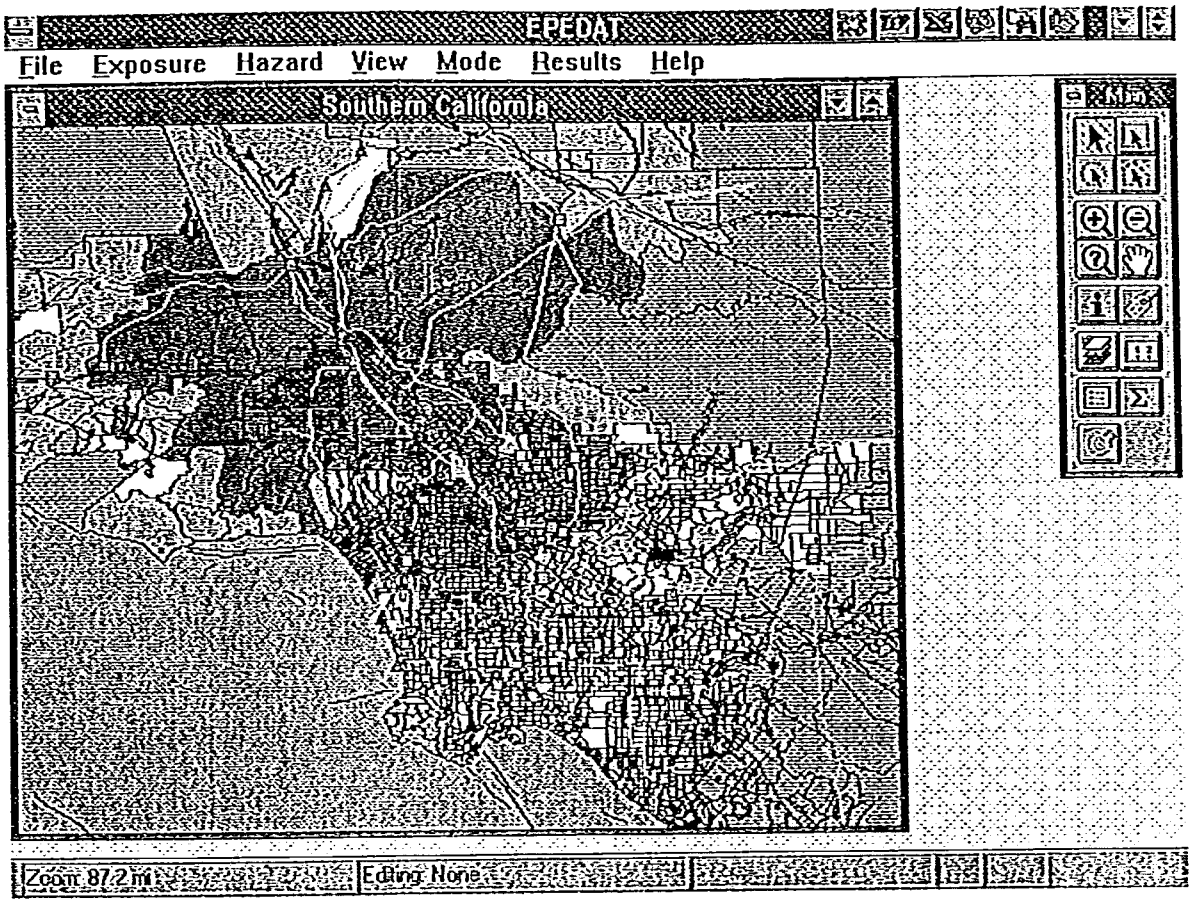



**Figure 2. Sample Screen from EPEDAT showing southern California Lifelines**

## DEVELOPMENT GOALS

While developing EPEDAT, the following goals were kept in mind:

1. Computerized data files on active fault systems, regional soil information, building inventories, and population distributions must be developed and made easily accessible.

2. Damage and casualty estimation models must allow for rapid calculations based on limited structural, building use and population exposure data.

3. Damage estimation routines must allow for updating of initial damage estimates in order to incorporate field reconnaissance information after the event.

4. The computer system must be user-friendly to allow easy access by emergency response personnel. This system should be PC-based to allow for independent usage as well as transferability.

5. The system should allow the user to construct various "what if" scenarios to investigate the range of impacts that may occur from various earthquake scenarios.

6. The system should incorporate effective graphic displays to allow the user to view projected damage scenarios. Separate screens should be developed to characterize the following risks on a regional scale:

   - Number of partially collapsed buildings
   - Number of totally collapsed buildings
   - Number of uninhabitable residential buildings
   - Number of essential buildings damaged (i.e., hospitals, fire and police stations)
   - Total damage to residential, commercial and industrial buildings, including damage to contents
   - Number of seriously injured
   - Number of deaths
   - Number of displaced individuals
   - Areas of potential utility outage
   - Potentially damaged highway structures
   - Areas potentially affected by hazardous materials release

7. The system should be modularized so that all computer models and databases can be easily updated.

## ACKNOWLEDGMENTS

The authors wish to thank the State of California, Office of Emergency Services, the U.S. Geological Survey and the California Institute of Technology for assistance in providing funding, documents or verbal information used in the preparation of this paper. The authors would also like to acknowledge the contributions of Dr. Thomas H. Heaton of Caltech, and Mr. Edward

Bortugno of the Governor's Office of Emergency Services. Finally, the authors would like to thank Mr. Paul Flores for his initial guidance and support of this effort. Without this guidance and support, this project never would have come to fruition.

## REFERENCES

ATC (1985). Earthquake Damage Evaluation Data for California, Applied Technology Council, ATC-13.

California Division of Mines and Geology (1988). Fault-Rupture Hazard Zones in California, CDMG Special Publication 42.

California Division of Mines and Geology (1990). Supplement No. 1 to Special Publication 42, CDMG.

Crippen, R.E. (1992). Measurement of Subresolution Terrain Displacements Using SPOT Panchromatic Imagery, *Episodes*, Vol. 15, No. 1.

Eguchi, R.T., J.D. Goltz, H.A. Seligson, and T.H. Heaton (1994). Real-Time Earthquake Hazard Assessment in California: The Early Post-Earthquake Hazard Assessment Tool and the Caltech-USGS Broadcast of Earthquakes, *Proceedings of the Fifth U.S. National Conference on Earthquake Engineering*, July 10-14, 1994.

Goltz, J.D. (1995). The Use of Real-Time Seismic Information by Government, Utilities and Corporations. Presentation at the California Institute of Technology, Seminar on Real-Time Seismology, April 20, 1995.

Hamada, M. and T.D. O'Rourke (1992), Case Studies of Liquefaction and Lifeline Lifeline Performance During Past Earthquakes, Technical Report NCEER-92-0001, Vols. 1 and 2.

Holden, R., R. Lee, and M. Reichle (1989). Technical and Economic Feasibility of an Earthquake Early Warning System in California, report to the California Legislature. California Division of Mines and Geology.

# Session-9

## Transportation and Fire

(N-2) Resources Required to Rebuild Wellington
(David C. Hopkins)

(J-19) A Fundamental Study on Innovative Menshin System for Underground Structures
(Hisanori Otsuka, Jun-ichi Hoshikuma and Kazuhiro Nagaya)

(U-10) A Bridge Prioritization Method Based on Transportation System Performance Using GIS
(Nesrin Basöz and Anne S. Kiremidjian)

(U-11) Fire Following the Hanshin and Northridge Earthquakes: A Comparative Analysis
(Charles Scawthorn and Andrew Cowell)

# Resources Required to Rebuild Wellington

## by David C Hopkins*

### *Synopsis*

*The process of restoring Wellington to normality after an earthquake will involve work on all elements of the built environment. This paper describes firstly the assessment of the costs of repairing damaged buildings and infrastructure, and then presents an analysis of the materials, plant and labour needed for reconstruction.*

*Buildings and infrastructure in the Wellington region are briefly described and their replacement values presented in various categories. Damage in dollar terms is assessed for each category, using existing knowledge of the likely effects of movement of the Wellington Fault, available damage ratio information, and engineering judgement.*

*The assessment of the type and amount of resources needed is made by broadly analysing the work content of each element of the repair work and allocating the required expenditure to various categories of materials plant and labour. These categories are chosen to match those normally used in resource assessment in the building industry.*

*The total resources likely to be needed for full reinstatement after a major earthquake in the Capital are thus presented in a form suitable as a starting point for assessing the implications for timing, availability and supply/demand.*

## 1. Introduction

Wellington's ability to recover from a major earthquake will depend on the nature and extent of damage, the overall costs involved, the resources required, and their availability, the economic impacts, the time taken to reconstruct and repair damaged facilities, and the logistics of applying resources to the task.

This paper presents an estimate of the resources required based on the analysis of the estimates of the cost of restoration, and the nature of the work involved. It makes no attempt to address issues of availability of resources, or other issues affecting recovery and restoration.

* Director, Buildings Division,
Kingston Morrison Limited, Architects Engineers Quantity Surveyors, Wellington

Recent damage assessments by public and private organisations have provided sufficient information to make a broad assessment of earthquake damage to the total built environment.

In this assessment existing data on damage has been used to cover the Wellington Fault Earthquake, and then analysed to determine required resources.

## 2. Wellington's Buildings and Infrastructure

The Wellington region today comprises four main cities, Wellington, Lower Hutt, Upper Hutt and Porirua, which account for the majority of the population in the whole region. The main areas of population are shown in Figure 1. The topography is generally steep with limited flat areas - most of the flat areas on the edge of the harbour are reclaimed land.

The early European settlers built in timber, matching familiar European styles and taking advantage of abundant natural timbers. After a damaging fire, emphasis turned to building in brick which in time proved to be vulnerable to earthquake. After the devastating Hawkes Bay Earthquake of 1931 codes were introduced requiring design for earthquake loads. In 1965, 1976, 1984, and 1992 changes were made to code requirements, each bringing more complex and generally more stringent requirements to deal with the greater sophistication of buildings and to take advantage of the ever increasing knowledge of their earthquake performance.

Houses in the Wellington are generally built in timber and masonry while most larger buildings are constructed in the indigenous material, concrete. Structural steel has not been used extensively except for industrial buildings, though more use is now being made of that material. Structural timber and concrete masonry are also commonly used for small to medium sized structures. The result is a wide range of building sizes and types, built to different codes.

Lifelines have not generally been subject to the same level of attention for seismic design , except bridges for road, rail and water supply, and electrical generation and transmission facilities. Thus, vulnerability of lifelines in the region is highly variable. A major study of Wellington's lifelines, completed under the auspices of the Centre for Advanced Engineering at the University of Canterbury in 1990, provides a comprehensive overview of all the systems and their vulnerability to earthquake. Since that time several studies of likely damage to selected lifelines have been carried out by the organisations responsible for them. In many cases this has been followed up with mitigation measures, with the result that most Wellington lifelines have received or are receiving attention. Recent earthquakes in California have added to the impetus of this gratifying trend, and interest has increased following the Hyogo-ken Nanbu earthquake which has particular relevance to Wellington lifelines.

## 3. Earthquake Damage Assessment

One of the most damaging earthquakes threatening the Wellington region is movement of the Wellington Fault. This event which has a 5 to 20% probability of occurrence in 50 years, has been used in making the damage assessments. Isoseismals used for this event are shown in Figure 2, and may be taken as applying to the data presented.

The overall damage assessment has been made on a broad basis, assigning a single damage ratio to each main class of asset.

The assessments are made on the basis that Wellington would be put back the way it was. No attempt has been made to allow for obsolescence, current under-utilisation of facilities, or any reduced demand for facilities in Wellington following the earthquake.

Table 1 shows the overall assessments of damage in dollar terms for the various asset categories. The value of contents has been derived from data in reports to the EQC, and has been taken as 21% of the building value in the case of commercial, industrial and rural buildings and 50% of the value for residential buildings and flats. The same damage ratio has been applied to the total of building value and to contents in each case.

Damage due to fire following earthquake was assessed to be 1% of replacement value for buildings and contents only, based on the report by Marsh and McLennan (1991). To highlight its inclusion in the figures, damage due to fire following earthquake has been shown separately.

Overall damage ratios (DR) are given for each group of assets. For buildings these have been taken from the overall results and the damage ratio curves used by Dowrick (1992) and from values derived from ATC 13 (1985). General values derived for other assets from a report by Holmes Consulting Group and DSIR to EQC (1991), and from Andrews et al (1993). Values for airport and rail infrastructure were taken from reports by Kingston Morrison. Where no studies had been done, assessments were made based on a New Zealand version of ATC13 prepared by Kingston Morrison and on specific damage assessments to assets in available reports. The values chosen represent reasonable estimates of likely damage, but even these should be interpreted in the light of the wide margin of uncertainty which exists in the derivation of damage ratios.

## 4. Assessment of Resources Required

The assessments of the resources required for reconstruction were obtained by a progressive splitting of the dollar amounts in each category of asset. Steps were:

*Step 1 - Split into Reconstruction Sub-Categories*

Building damage was split into sub-categories according to the nature of the likely reconstruction or repair. For each main building category, a distinction was made between complete replacement and repair since the split of resources was seen to be different in each case.

Table 2 shows the headings used and the resulting split of values.

*Step 2 - Sub-Division into Activities or Elements*

Each asset category or sub-category derived from Step 1 was further split into activities or elements according to the nature of the work to be done. The elemental split for buildings was chosen to match those in published handbooks on building costs.

*Step 3 - Split into Materials Plant and Labour*

Each activity or element was split between Materials, Plant and Labour in proportions according to the nature of the work involved. Each element or activity was assessed separately with the three splits adding up to 100% of the amount allocated to the element or activity.

*Step 4 - Split into sub-categories of Materials Plant and Labour*

Once the amount for Materials was determined for a particular activity from Step 3, it was further split into sub-categories according to the nature and range of work required. The same was done with the amounts allocated to that same element for Plant and for Labour. The sub-categories used here were selected to correspond to those used in the industry.

*Step 5 - Calculation of Resource Quantities*

Steps 1 through 4 resulted in a series of spreadsheets, one for each Reconstruction sub-category selected in Step 1. These contained dollar amounts allocated to the various sub-categories of Materials, Labour and Plant. Step 5 involved dividing these dollar amounts by a unit rates to determine the contribution to the overall resource requirement.

Table 3 is a sample of one spreadsheet showing the detailed split of dollar amounts and resource allocations for Commercial Buildings requiring complete replacement. This provides an insight into the method used to assess the resources, and to the range of sub-categories considered.

All other spreadsheets were compiled on similar lines.

*Step 6 - Summation of Resources Required*

This final step involved adding all the individual quantities and summarising them, a task made relatively simple by spreadsheet technology. Final totals are shown in Table 4.

## 5. Conclusions

- It is clear that a very considerable resource will be required and that the mobilisation and effectiveness of this resource will depend significantly on the degree of preparation and preparedness of key asset owners and managers.

- This assessment forms a valuable starting point for realistically assessing the time required for recovery and for assessing the likely availability of resources to carry out the reinstatement in a particular time frame. Because the quantities of most common building materials are assessed, it will provide separate sections of the building industry with their own perspectives on the likely impacts and opportunities.

- Other issues such as availability of resources, the time required for reconstruction, and the logistics of mobilising the required resources must be considered in conjunction with this resource assessment.

- The overall damage value as a percentage of the total assets at risk, while significant, is unlikely to be sufficient to undermine overall confidence in the city's future. This is borne out by experience from past earthquakes overseas which demonstrates that earthquake damage, while horrendous, has not led to significant relocation of people and assets.

- It would be possible to refine the analysis of the split of resources considerably and go into more detail on many of the aspects. It is hoped that this initial broad attempt will encourage others to examine the issues in a more comprehensive and detailed fashion.

## 6. Acknowledgements

This paper is based on a longer paper (Hopkins 1995) written at the request of EQC for the Wellington After the Quake Conference held in March 1995. They made available much background material on damage assessments and provided encouragement. The co-operation of organisations responsible for buildings and infrastructure in the Wellington region was extraordinary and without their readiness to provide information on the nature and value of their assets, the overall assessment could not have been made. It is a feature of Wellington that such co-operation is forthcoming and has enabled the region to progress its thinking and preparedness for earthquake. The support of each and every one of these organisations is gratefully acknowledged.

### References

Andrews, L A et al (1993) "Damage Ratios and Insurance Aspects for Services." Report of Project Group 2, Wellington Earthquake Lifelines Group 1993 Report, Wellington Regional Council, November.

Applied Technology Council (1985) "Earthquake Damage Evaluation Data for California - ATC13" Applied Technology Council, Redwood City, California, 1985.

Centre for Advanced Engineering (1991) "Lifelines in Earthquakes - Wellington Case Study." Project Summary and Project Report, Centre for Advanced Engineering at the University of Canterbury, Christchurch, NZ, August

Dowrick, D J (1990) " Study of Potential Losses to the EQC in Large Earthquakes in Central New Zealand." EQC Report, November.

Dowrick, D J (1991). "Study of Potential Losses to the EQC from Damage to Housing in Large Earthquakes in Central New Zealand." Report to EQC, August.

Dowrick, D J (1992) "Potential Loss Estimates for the EQC Derived Using Different Attenuation Models for Mercalli Intensity." Report to EQC, February.

DSIR/Holmes Consulting Group (1991) " Study of Potential Losses to Uninsured Property in a Large Earthquake in Central New Zealand" Report to EQC, October.

Hopkins, D C (1995) "Assessment of Resources Required for Reinstatement", Proceedings Wellington After the Quake Conference, Wellington, March.

Kingston Morrison Limited (1993 and 1994) Various Reports for Clients with Assets in the Wellington Region.

Marsh McLennan and Co (1991) " Review of the Earthquake and War Damage Commission" A Report presented to New Zealand Treasury, January.

## TABLE 1 - Wellington Infrastructure and Buildings

### Summary of Replacement and Reinstatement Values

All figures in NZ$M

| Item | Wellington | | | Hutt City | | | Upper Hutt | | | Porirua | | | Regional | | | Totals | |
|---|---|---|---|---|---|---|---|---|---|---|---|---|---|---|---|---|---|
| | Replace | D R | Reinst | Replace | D R | Reinst | Replace | D R | Reinst | Replace | D R | Reinst | Replace | D R | Reinst | Replace | Reinst |
| A Buildings | | | | | | | | | | | | | | | | | |
| 1 Commercial and Industrial | 15,058.8 | 0.18 | 2,710.6 | 3,668.0 | 0.15 | 550.2 | 739.2 | 0.15 | 110.9 | 770.0 | 0.15 | 115.5 | | | | 20,236.0 | 3,487.2 |
| 2 Residential | 6,371.0 | 0.15 | 955.7 | 3,095.0 | 0.12 | 371.4 | 1,148.4 | 0.12 | 137.8 | 1,589.5 | 0.12 | 191.9 | | | | 12,213.9 | 1,656.8 |
| 3 Flats | 1,809.9 | 0.13 | 235.3 | 917.1 | 0.10 | 91.7 | 277.2 | 0.10 | 27.7 | 177.8 | 0.10 | 17.8 | | | | 3,182.0 | 372.5 |
| 4 Other (Public) | 386.1 | 0.18 | 69.5 | 179.6 | 0.15 | 26.9 | 72.6 | 0.15 | 10.9 | 66.6 | 0.07 | 4.7 | | | | 704.9 | 112.0 |
| 5 Rural | 72.5 | 0.10 | 7.3 | 74.6 | 0.10 | 7.5 | 188.3 | 0.10 | 16.8 | 55.5 | 0.10 | 5.6 | | | | 370.9 | 37.1 |
| 6 Building Contents (21%) | 7,349.1 | | 1,359.1 | 2,829.7 | | 427.4 | 918.6 | | 147.6 | 1,075.9 | | 148.2 | | | | 12,173.3 | 2,082.3 |
| 7 Consequential Fire Losses(1%) | | | 39.8 | | | 10.5 | | | 3.0 | | | 3.4 | | | | | 56.7 |
| Total (no conts, no fire) | 23,698.3 | | 3,978.3 | 7,934.3 | | 1,047.7 | 2,405.7 | | 304.1 | 2,669.3 | | 335.4 | | | | 36,707.6 | 5,665.5 |
| B Roading | | | | | | | | | | | | | 670.0 | 0.08 | 53.6 | 670.0 | 53.6 |
| 1 Regional | | | | | | | | | | | | | | | | 731.6 | 58.5 |
| 2 District | 476.0 | 0.08 | 38.1 | 66.0 | 0.08 | 5.3 | 94.6 | 0.08 | 7.6 | 95.0 | 0.08 | 7.6 | | | | 220.9 | 33.1 |
| 3 Suburban | In B2 above | | | 220.9 | 0.15 | 33.1 | In B2 above | | | | | | | | | | |
| Total | 476.0 | | 38.1 | 286.9 | | 38.4 | 94.6 | | 7.6 | 95.0 | | 7.6 | 670.0 | | 53.6 | 1,622.5 | 145.3 |
| C Bridging | | | | | | | | | | | | | 360.0 | 0.30 | 108.0 | 360.0 | 108.0 |
| 1 Regional | | | | | | | | | | | | | | | | 66.7 | 20.0 |
| 2 District | 3.0 | 0.30 | 0.9 | 43.0 | 0.30 | 12.9 | 15.7 | 0.30 | 4.7 | 5.0 | 0.30 | 1.5 | | | | | |
| Total | 3.0 | | 0.9 | 43.0 | | 12.9 | 15.7 | | 4.7 | 5.0 | | 1.5 | 360.0 | | 108.0 | 426.7 | 128.0 |
| D Rail Network | | | | | | | | | | | | | 1,605.9 | 0.07 | 104.9 | 1,605.9 | 104.9 |
| 1 Formation ( incls track, tunnels bridges etc) | | | | | | | | | | | | | 213.8 | 0.18 | 38.4 | 213.8 | 38.4 |
| 2 Signals, communications, power | | | | | | | | | | | | | 55.1 | 0.20 | 11.0 | 55.1 | 11.0 |
| 3 Ways and Works Mech items | | | | | | | | | | | | | 795.5 | 0.03 | 23.9 | 795.5 | 23.9 |
| 4 Locos, rolling stock, misc | | | | | | | | | | | | | 2,670.3 | | 178.2 | 2,670.3 | 178.2 |
| Total | | | | | | | | | | | | | | | | | |
| E Airport Infrastructure | | | | | | | | | | | | | 42.1 | 0.08 | 3.5 | 42.1 | 3.5 |
| 1 Runways, taxiways etc | | | | | | | | | | | | | 60.4 | 0.06 | 3.7 | 60.4 | 3.7 |
| 2 Seawall and other civil works | | | | | | | | | | | | | 102.5 | | 7.3 | 102.5 | 7.3 |
| Total | | | | | | | | | | | | | | | | | |
| F Port Infrastructure . | | | | | | | | | | | | | | | | 306.0 | 61.2 |
| 1 Wharves ,Structures etc | 306.0 | 0.20 | 61.2 | | | | | | | | | | | | | 36.0 | 7.2 |
| 2 Cranes/equipment | 36.0 | 0.20 | 7.2 | | | | | | | | | | | | | 60.0 | 6.0 |
| 3 Containers/contents | 60.0 | 0.10 | 6.0 | | | | | | | | | | | | | | |
| Total | 402.0 | | 74.4 | | | | | | | | | | | | | 402.0 | 74.4 |

| | | | | | | | | | | | | | | | | | |
|---|---|---|---|---|---|---|---|---|---|---|---|---|---|---|---|---|---|
| G | Water Supply | | | | | | | | | | | | | | | | |
| | 1 Reticulation | 283.4 | 0.08 | 22.7 | 81.5 | 0.08 | 6.5 | 35.3 | 0.08 | 2.8 | 33.0 | 0.08 | 2.6 | 167.1 | 0.08 | 13.4 | 600.3 | 48.0 |
| | 2 Distribution Storage | 56.1 | 0.10 | 5.6 | 10.3 | 0.10 | 1.0 | 6.2 | 0.10 | 0.6 | 6.0 | 0.10 | 0.6 | 67.8 | 0.10 | 6.8 | 146.4 | 14.6 |
| | 3 Pumping stations | 2.8 | 0.10 | 0.3 | 0.8 | 0.10 | 0.1 | In G1 above | | | 0.7 | 0.10 | 0.1 | 20.6 | 0.10 | 2.1 | 24.8 | 2.5 |
| | 4 Plant and Misc Buildings | 2.0 | 0.10 | 0.2 | 0.8 | 0.10 | 0.1 | | 0.10 | 0.0 | 0.3 | 0.10 | 0.0 | 5.9 | 0.10 | 0.6 | 9.0 | 0.9 |
| | Total | 344.2 | | 28.8 | 93.4 | | 7.7 | 41.5 | | 3.4 | 39.9 | | 3.3 | 261.4 | | 22.8 | 780.4 | 66.0 |
| H | Sewerage | | | | | | | | | | | | | | | | | |
| | 1 Reticulation Main | 379.0 | 0.15 | 56.9 | 70.6 | 0.08 | 5.6 | In Hutt City | | | 38.0 | 0.08 | 3.0 | | | | 487.6 | 65.5 |
| | 2 Local Reticulation | In H2 above | | | 95.2 | 0.08 | 7.6 | 53.3 | 0.08 | 4.3 | | | | | | | 148.5 | 11.9 |
| | 3 Treatment Stations | 5.0 | 0.20 | 1.0 | In H2 above | | | 0.1 | 0.20 | 0.0 | 18.1 | 0.20 | 3.6 | | | | 23.2 | 4.6 |
| | Total | 384.0 | | 57.9 | 165.8 | | 13.3 | 53.4 | | 4.3 | 56.1 | | 6.7 | | | | 659.3 | 82.1 |
| I | Stormwater Reticulation | | | | | | | | | | | | | | | | | |
| | 1 Reticulation | 250.0 | 0.12 | 30.0 | 95.0 | 0.08 | 7.6 | 46.3 | 0.08 | 3.7 | 15.1 | 0.08 | 1.2 | | | | 406.4 | 42.5 |
| | Total | 250.0 | | 30.0 | 95.0 | | 7.6 | 46.3 | | 3.7 | 15.1 | | 1.2 | 0.0 | | 0.0 | 406.4 | 42.5 |
| J | Gas Network | | | | | | | | | | | | | | | | | |
| | 1 Regional(minimal) | 330.0 | 0.04 | 13.2 | | | | | | | | | | | | | 330.0 | 13.2 |
| | 2 Local | 55.5 | 0.08 | 4.4 | 47.2 | 0.08 | 3.8 | 16.1 | 0.08 | 1.3 | 18.4 | 0.08 | 1.5 | | | | 137.2 | 11.0 |
| | Total | 385.5 | | 17.6 | 47.2 | | 3.8 | 16.1 | | 1.3 | 18.4 | | 1.5 | 0.0 | | 0.0 | 467.2 | 24.2 |
| K | Electricity Network | | | | | | | | | | | | | | | | | |
| | 1 Regional Reticulation | | | | | | | | | | | | | 807 | 0.10 | 80.7 | 807.1 | 80.7 |
| | 2 Local Reticulation | 447.0 | 0.12 | 53.6 | 139.0 | 0.10 | 13.9 | 51.0 | 0.10 | 5.1 | 57.0 | 0.10 | 5.7 | | | | 694.0 | 78.3 |
| | 3 Nodes | | | | | | | | | | | | | | | | 0.0 | 0.0 |
| | Total | 447.0 | | 53.6 | 139.0 | | 13.9 | 51.0 | | 5.1 | 57.0 | | 5.7 | 807.1 | | 80.7 | 1,501.1 | 159.1 |
| L | Telecommunications | | | | | | | | | | | | | | | | | |
| | 1 Buildings and Plant | 269.0 | 0.20 | 53.8 | 49.0 | 0.15 | 7.4 | 20.0 | 0.15 | 3.0 | 52.0 | 0.15 | 7.8 | | | | 390.0 | 72.0 |
| | 2 Reticulation | 100.0 | 0.08 | 8.0 | 66.0 | 0.08 | 5.3 | 30.0 | 0.08 | 2.4 | 36.0 | 0.08 | 2.9 | | | | 232.0 | 18.6 |
| | Total | 369.0 | | 61.8 | 115.0 | | 12.6 | 50.0 | | 5.4 | 88.0 | | 10.7 | 0.0 | | 0.0 | 622.0 | 90.5 |
| M | Broadcasting | | | | | | | | | | | | | | | | | |
| | 1 State owned | | | | | | | | | | | | | 100.0 | 0.08 | 8.0 | 100.0 | 8.0 |
| | 2 Private | | | | | | | | | | | | | 30.0 | 0.08 | 2.4 | 30.0 | 2.4 |
| | Total | 0.0 | | 0.0 | 0.0 | | 0.0 | 0.0 | | 0.0 | 0.0 | | 0.0 | 130.0 | | 10.4 | 130.0 | 10.4 |
| | GRAND TOTALS | | | | | | | | | | | | | | | | | |
| | No contents, no fire | 26,759.0 | | 4,381.1 | 8,919.6 | | 1,168.4 | 2,774.3 | | 342.7 | 3,043.8 | | 376.9 | 5,001.3 | | 461.0 | 46,498.0 | 6,730.1 |
| | With contents and fire | 34,108.1 | | 5,740.2 | 11,749.3 | | 1,595.8 | 3,692.9 | | 490.3 | 4,119.7 | | 525.1 | 5,001.3 | | 461.0 | 58,671.3 | 8,812.4 |

# TABLE 2

## Summary of Materials, Plant and Labour by Asset Category

(includes construction costs plus planning, design etc and demolition)

| Category | Material | Plant | Labour | Total |
|---|---|---|---|---|
| Commercial Buildings - Complete Replacement | 220.5 | 114.4 | 247.7 | 582.5 |
| Commercial Buildings - Repairs>30% of Replacement | 296.9 | 155.3 | 444.0 | 896.2 |
| Commercial Buildings - Repairs<30% of Replacement | 430.4 | 178.0 | 823.1 | 1431.5 |
| Industrial Buildings - Replacement | 112.9 | 57.7 | 162.1 | 332.7 |
| Industrial Buildings - Repairs | 572.4 | 164.9 | 616.4 | 1353.7 |
| Residential Buildings - Replacement | 34.0 | 8.4 | 53.8 | 96.2 |
| Residential Buildings - Repairs | 343.3 | 212.7 | 1272.2 | 1828.2 |
| Other Buildings - Total Repairs and Replacements | 44.0 | 22.1 | 66.7 | 132.8 |
| Roading | 46.9 | 55.5 | 64.7 | 167.1 |
| Bridging | 45.9 | 31.4 | 82.7 | 160.0 |
| Rail Network | 52.9 | 68.9 | 79.6 | 201.4 |
| Airport | 2.1 | 2.6 | 3.7 | 8.4 |
| Port Infrastructure | 36.1 | 22.9 | 30.3 | 89.3 |
| Water Supply | 38.1 | 14.8 | 25.4 | 78.2 |
| Sewerage System | 37.1 | 19.7 | 33.5 | 90.3 |
| Stormwater System | 19.1 | 10.0 | 21.9 | 51.0 |
| Gas Network | 13.2 | 5.1 | 9.7 | 28.1 |
| Electricity Network | 64.9 | 45.8 | 56.6 | 167.3 |
| Telecommunications | 52.9 | 18.6 | 37.2 | 108.6 |
| Broadcasting Facilities | 6.4 | 1.8 | 3.7 | 12.0 |
| TOTALS | 2470.0 | 1210.7 | 4134.7 | 7815.3 |

Note! -Total for Construction Only from Table 1 6730.1

**Table 3**
**Sample Spreadsheet Calculation of Resources**

| Buildings | | | |
|---|---|---|---|
| Type | Commercial Complete Replacement | | |
| Damage = | 20.0% | of | $2,499.5 M |
| | | = | $497.9 |

| | Planning, Design, Procurement | | | Demolition | | | Preliminary | | | Substructure | | | Superstructure | | | Finishes and Fittings | | | Services (including external) | | | Totals | | |
|---|---|---|---|---|---|---|---|---|---|---|---|---|---|---|---|---|---|---|---|---|---|---|---|---|
| | Percent 12.0% | | | Percent 5.0% | | | Percent 8.0% | | | Percent 17.0% | | | Percent 30.0% | | | Percent 25.0% | | | Percent 20.0% | | | | | |
| | Value $59.75 | | | Value $24.89 | | | Value $39.83 | | | Value $84.64 | | | Value $149.37 | | | Value $124.47 | | | Value $99.58 | | | | | |
| Materials | Percent | Value | Quantity | Percent | Value | Quantity | Percent | Value | Quantity | Percent | Value | Quantity | Percent | Value | Quantity | Percent | Value | Quantity | Percent | Value | Quantity | Dollars | Quantities | Materials |
| concrete (m3) | | | | | | | 3.0% | 1.2 | 6,000 | 20.0% | 16.9 | 112,900 | 15.0% | 22.4 | 149,400 | | | | | | | 40.5 | 270,000 | concrete (m3) |
| timber (m3) | | | | | | | 2.0% | 0.8 | 800 | 10.0% | 8.5 | 8,500 | 10.0% | 14.9 | 14,900 | | | | | | | 24.2 | 24,000 | timber (m3) |
| reinforcing steel (tonnes) | | | | | | | 2.0% | 0.8 | 500 | 10.0% | 8.5 | 5,300 | 5.0% | 7.5 | 4,700 | | | | | | | 16.7 | 11,000 | reinforcing steel (tonnes) |
| structural steel (tonnes) | | | | | | | | | | 5.0% | 4.2 | 1,100 | 5.0% | 7.5 | 2,000 | | | | | | | 11.7 | 3,000 | structural steel (tonnes) |
| masonry, brickwork etc (m2) | | | | | | | | | | | | | 5.0% | 7.5 | 74,700 | | | | | | | 7.5 | 75,000 | masonry, brickwork etc (m2) |
| plaster board (m2) | | | | | | | | | | | | | | | | 15.0% | 18.7 | 933,600 | | | | 18.7 | 934,000 | plaster board (m2) |
| floor coverings (m2) | | | | | | | | | | | | | | | | 10.0% | 12.4 | 207,900 | | | | 12.4 | 208,000 | floor coverings (m2) |
| windows/glazing (m2) | | | | | | | | | | | | | | | | 20.0% | 24.9 | 124,800 | | | | 24.9 | 125,000 | windows/glazing (m2) |
| painting (m2) | | | | | | | | | | | | | | | | 10.0% | 12.4 | 1,244,700 | | | | 12.4 | 1,245,000 | painting (m2) |
| plumbing and drainage($1000 units) | | | | | | | 2.0% | 0.8 | 800 | | | | | | | | | | 10.0% | 10.0 | 10,000 | 10.8 | 11,000 | plumbing and drainage($1000 units) |
| electrical ($1000 units) | | | | | | | 2.0% | 0.8 | 800 | | | | | | | | | | 5.0% | 5.0 | 5,000 | 5.8 | 5,800 | electrical ($1000 units) |
| mechanical ($1000 units) | | | | | | | | | | | | | | | | | | | 20.0% | 19.9 | 19,900 | 19.9 | 19,900 | mechanical ($1000 units) |
| lifts and escalators per item | | | | | | | | | | | | | | | | | | | 15.0% | 14.9 | 120 | 14.9 | 120 | lifts and escalators per item |
| fill (m3) | | | | | | | | | | | | | | | | | | | | | | 0.0 | 0 | fill (m3) |
| basecourse/ballast (m3) | | | | | | | | | | | | | | | | | | | | | | 0.0 | 0 | basecourse/ballast (m3) |
| paving (m2) | | | | | | | | | | | | | | | | | | | | | | 0.0 | 0 | paving (m2) |
| Plant | Percent | Value | Hours | Percent | Value | Hours | Percent | Value | Hours | Percent | Value | Hours | Percent | Value | Hours | Percent | Value | Hours | Percent | Value | Hours | Hours | | Plant |
| bulldozers | | | | 5.0% | 1.2 | 6,600 | | | | 2.0% | 1.7 | 8,900 | | | | | | | | | | 2.9 | 10,000 | bulldozers |
| cranes | | | | | | | 19.0% | 7.6 | 108,100 | 3.0% | 2.5 | 36,300 | | | | | | | | | | 10.1 | 144,000 | cranes |
| trucks | | | | 25.0% | 6.2 | 124,500 | | | | 8.0% | 4.2 | 84,600 | 5.0% | 7.5 | 149,400 | 2.0% | 2.5 | 49,800 | 2.0% | 2.0 | 30,800 | 22.4 | 449,000 | trucks |
| graders | | | | | | | | | | | | | | | | | | | | | | 0.0 | 0 | graders |
| excavators | | | | 20.0% | 5.0 | 62,200 | | | | 5.0% | 4.2 | 52,900 | | | | | | | | | | 9.2 | 116,000 | excavators |
| rollers/pavers | | | | | | | | | | | | | | | | | | | | | | 0.0 | 0 | rollers/pavers |
| motor scrapers | | | | | | | | | | | | | | | | | | | | | | 0.0 | 0 | motor scrapers |
| loaders | | | | 5.0% | 1.2 | 11,300 | | | | | | | | | | | | | | | | 1.2 | 11,000 | loaders |
| misc small tools | | | | 5.0% | 1.2 | 124,500 | 15.0% | 6.0 | 597,500 | 10.0% | 8.5 | 846,400 | 20.0% | 29.9 | 2,987,400 | 8.0% | 10.0 | 995,600 | 13.0% | 12.9 | 1,294,500 | 66.5 | 6,646,000 | misc small tools |
| Labour | Percent | Value | Hours | Percent | Value | Hours | Percent | Value | Hours | Percent | Value | Hours | Percent | Value | Hours | Percent | Value | Hours | Percent | Value | Hours | Hours | | Labour |
| A Management | 10.0% | 6.0 | 49,800 | 0.5% | 0.1 | 1,000 | 1.0% | 0.4 | 3,300 | 0.2% | 0.2 | 1,400 | 0.2% | 0.3 | 2,500 | 0.2% | 0.2 | 2,100 | 0.2% | 0.2 | 1,700 | 7.4 | 62,000 | A Management |
| B Design & Contract Admin | 55.0% | 32.9 | 365,100 | 4.5% | 1.1 | 12,400 | 4.5% | 1.8 | 19,900 | 4.5% | 3.8 | 42,300 | 4.5% | 6.7 | 74,700 | 4.5% | 5.6 | 62,200 | 4.5% | 4.5 | 49,800 | 58.4 | 626,000 | B Design & Contract Admin |
| C Trades | 15.0% | 9.0 | 298,700 | 5.0% | 1.2 | 41,500 | 15.0% | 6.0 | 199,200 | 6.0% | 5.8 | 229,700 | 5.0% | 7.5 | 248,900 | 6.8% | 11.0 | 365,100 | 20.3% | 20.2 | 673,600 | 61.8 | 2,063,000 | C Trades |
| D Service Workers | 15.0% | 9.0 | 358,500 | 5.0% | 1.2 | 49,800 | 10.0% | 4.0 | 159,300 | 5.0% | 4.2 | 169,300 | 3.8% | 5.7 | 227,000 | 5.0% | 6.2 | 248,900 | 5.0% | 5.0 | 199,200 | 35.3 | 1,412,000 | D Service Workers |
| E Semi qualified & Plant Ops. | 5.0% | 3.0 | 119,500 | 20.0% | 5.0 | 199,200 | 14.5% | 5.8 | 231,000 | 7.3% | 6.2 | 247,200 | 16.5% | 24.6 | 985,800 | 16.5% | 20.5 | 821,500 | 5.0% | 5.0 | 199,200 | 70.1 | 2,803,000 | E Semi qualified & Plant Ops. |
| F Unqualified Labour | 0.0% | 0.0 | 0 | 5.0% | 1.2 | 58,600 | 10.0% | 4.0 | 181,100 | 5.0% | 4.2 | 192,400 | 5.0% | 7.5 | 339,500 | | | | | | | 19.3 | 770,000 | F Unqualified Labour |
| Total | 100.0% | 59.7 | | 100.0% | 24.9 | | 100.0% | 39.8 | | 100.0% | 84.6 | | 100.0% | 149.4 | | 100.0% | 124.5 | | 100.0% | 99.6 | | 562.5 | | |

Notes
1) Contingencies allowed for by adding appropriate percentage (1 to 1.5%) from Rawlinsons to Preliminary
2) All costs in millions of dollars
3) Preliminary includes establishment, disestablishment, contingencies etc

# Table 4
## Summary of Design, Demolition and Construction Costs and Quantities

(including Construction Costs plus Planning, Design etc and Demolition)

| | Dollars (NZ$M) | | | | Quantities | |
|---|---|---|---|---|---|---|
| **Materials** | Design | Demolition | Construction | Total | | Materials |
| concrete (m3) | | 1.1 | 289.7 | 290.8 | 1,939,000 | concrete (m3) |
| timber (m3) | | 1.1 | 349.2 | 350.2 | 350,000 | timber (m3) |
| reinforcing steel (tonnes) | | 0.4 | 148.7 | 149.0 | 103,000 | reinforcing steel (tonnes) |
| structural steel (tonnes) | | 1.1 | 134.6 | 135.7 | 42,000 | structural steel (tonnes) |
| masonry, brickwork etc (m2) | | 0.0 | 73.6 | 73.6 | 738,000 | masonry, brickwork etc (m2) |
| plaster board (m2) | | 0.0 | 194.7 | 194.7 | 9,734,000 | plaster board (m2) |
| floor coverings (m2) | | 0.0 | 165.6 | 165.6 | 2,761,000 | floor coverings (m2) |
| windows/glazing (m2) | | 0.0 | 199.6 | 199.6 | 998,000 | windows/glazing (m2) |
| painting (m2) | | 0.0 | 109.3 | 109.3 | 10,927,000 | painting (m2) |
| plumbing and drainage($1000 units) | | 0.0 | 254.9 | 254.9 | 263,000 | plumbing and drainage($1000 units) |
| electrical ($1000 units) | | 0.0 | 162.9 | 162.9 | 169,800 | electrical ($1000 units) |
| mechanical ($1000 units) | | 0.0 | 179.9 | 179.9 | 180,900 | mechanical ($1000 units) |
| lifts and escalators per item | | 0.0 | 132.2 | 132.2 | 1,110 | lifts and escalators per item |
| fill (m3) | | 0.0 | 15.4 | 15.4 | 617,000 | fill (m3) |
| basecourse/ballast (m3) | | 0.0 | 24.6 | 24.6 | 820,000 | basecourse/ballast (m3) |
| paving (m2) | | 0.0 | 31.5 | 31.5 | 158,000 | paving (m2) |
| **Plant** | | | | | Hours | Plant |
| bulldozers | | 7.9 | 4.5 | 12.4 | 67,000 | bulldozers |
| cranes | | 4.3 | 135.5 | 139.9 | 1,978,000 | cranes |
| trucks | | 86.2 | 274.5 | 360.7 | 7,215,000 | trucks |
| graders | | 0.6 | 11.3 | 11.9 | 149,000 | graders |
| excavators | | 37.5 | 74.5 | 112.0 | 1,485,000 | excavators |
| rollers/pavers | | 0.0 | 23.5 | 23.5 | 235,000 | rollers/pavers |
| motor scrapers | | 0.9 | 0.1 | 1.0 | 5,000 | motor scrapers |
| loaders | | 3.1 | 0.6 | 3.7 | 34,000 | loaders |
| misc small tools | | 53.2 | 492.5 | 545.7 | 54,569,000 | misc small tools |
| **Labour** | | | | | Hours | Labour |
| A Management | 54.5 | 2.2 | 35.3 | 92.0 | 770,000 | A Management |
| B Design & Contract Admin | 299.6 | 26.3 | 364.1 | 689.9 | 7,668,000 | B Design & Contract Admin |
| C Trades | 112.8 | 52.6 | 1025.0 | 1190.4 | 39,681,000 | C Trades |
| D Service Workers | 88.5 | 24.5 | 341.3 | 454.4 | 18,177,000 | D Service Workers |
| E Semi qualified & Plant Ops. | 31.7 | 88.6 | 1033.2 | 1153.5 | 46,142,000 | E Semi qualified & Plant Ops. |
| F Unqualified Labour | 4.0 | 100.0 | 450.5 | 554.4 | 25,203,000 | F Unqualified Labour |
| TOTALS | 591.2 | 491.4 | 6732.8 | 7815.3 | | |

# A FUNDAMENTAL STUDY ON INNOVATIVE MENSHIN SYSTEM FOR UNDERGROUND STRUCTURES

Hisanori Otsuka, Jun-ichi Hoshikuma and Kazuhiro Nagaya

1) Head, Earthquake Engineering Division, Public Works Research Institute, Ministry of Construction, Tsukuba Science City, Japan
2) Research Engineer, ditto
3) Assistant Research Engineer, ditto

## ABSTRACT

This paper presents a new construction technique for reducing the seismic effect in the design of underground structures. A concept of the technique, called herein "MENSHIN", is introduced and some appropriate menshin systems for underground structures are described. To examine the menshin system effect, a few case studies are carried out. Analytical results show that the menshin systems work well during an earthquake in shield tunnels and laterally wide underground structures.

## INTRODUCTION

The seismic design of underground structures has been recommended to be made by the Seismic Deformation Method (SDM) [1] . In the SDM, the displacement and deformation developed in the subsurface ground during an earthquake are taken as the major seismic effects to underground structures. The seismic response of underground structures is distinguished from the one of regular structures on ground by the small mass effect and large damping ratio. Therefore, it is assumed in the SDM that underground structures deform following the deformation of subsurface ground during the earthquake.

In the SDM, because the seismic deformation of underground structures follows that of the subsurface ground, structural seismic forces increase as the structure becomes stiffer. When the seismic effect to the underground structures is significant, the section area and/or the reinforcing bars shall be increased. In such case, it would be advantageous to reduce the seismic effect.

The concept of seismic effect reduction is called "BASE ISOLATION" or "MENSHIN" in the domain of bridge engineering. We propose a similar concept that will be also applicable to underground structures, thus it will be called herein as "MENSHIN" system.

There are two mechanisms for the menshin system of underground structures; to decrease the equivalent stiffness of the underground structures by using flexible joints; to isolate them from the seismic deformation of subsurface ground. The former technique has already been used in practice in the construction of submerged tunnels, common utility ducts and

shield tunnels, however, there are few studies on the latter one.
This research focuses on the menshin system by means of the menshin layer which can isolate the underground structures from the seismic deformation of the subsurface soil. In this paper, some appropriate sections for the menshin system of underground structures are introduced, and the effectiveness of the menshin system is examined based on a few case studies.

## APPROPRIATE SECTIONS FOR MENSHIN SYSTEM

The menshin system will be effective at the sections where the seismic effect is significant. Based on various previous studies and several damage observations due to past earthquakes, vulnerable sections have been summarized as shown in Fig. 1 [2].
Fig. 2 illustrates some effective sections for the menshin system application in underground structures, where the local seismic force develops; (a) underground pipelines passing through an irregular soil condition; (b) connection of the shield tunnel to the vertical shaft; (c) interaction system such as the underground pipeline passing closely to the bridge pile foundation; (d) laterally wide underground structures in a soft soil condition.
To show the effectiveness of the menshin system in the underground structures, (a)– and (d)–type structures are analyzed as discussed in the following sections.

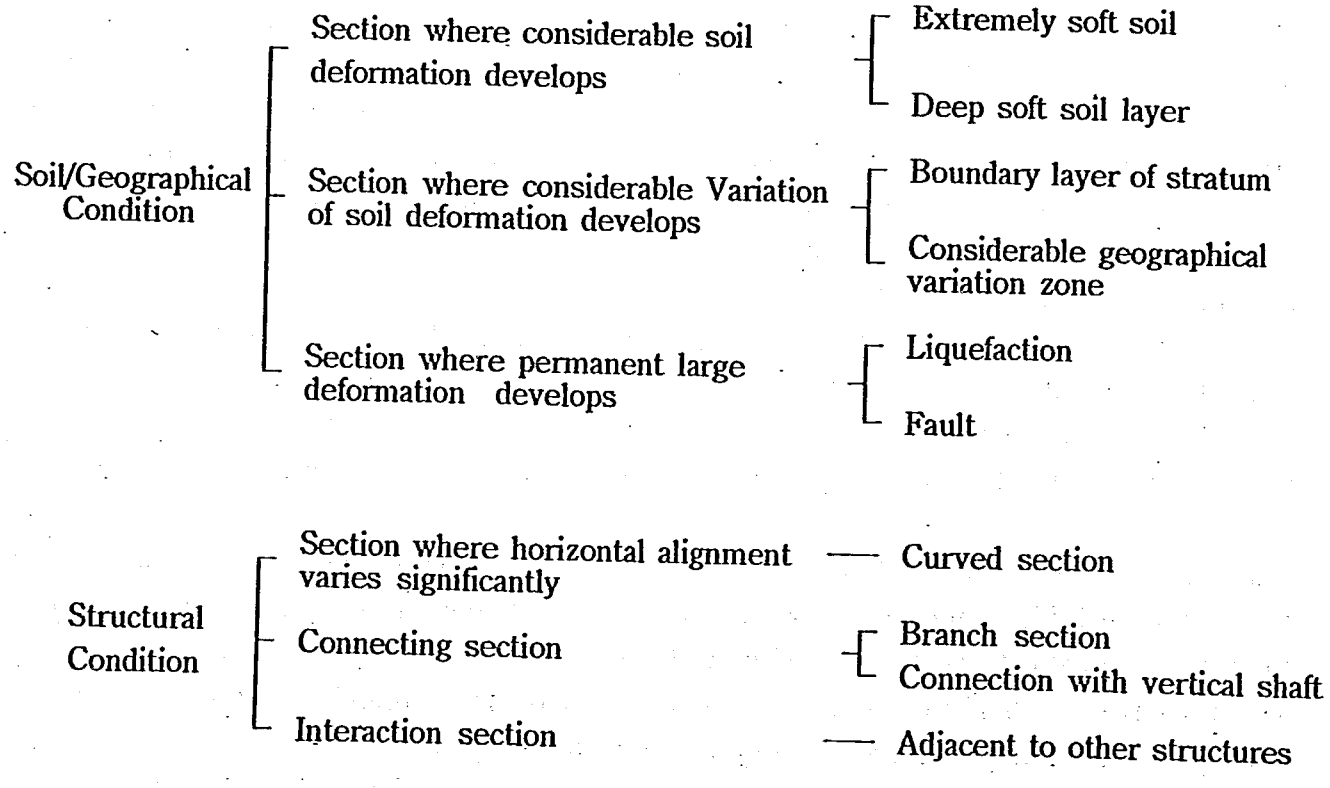
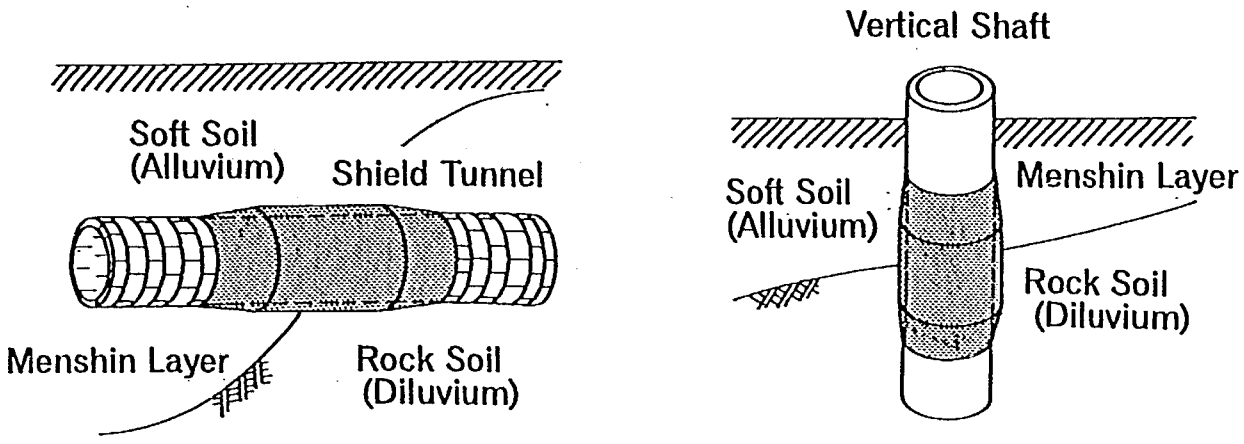
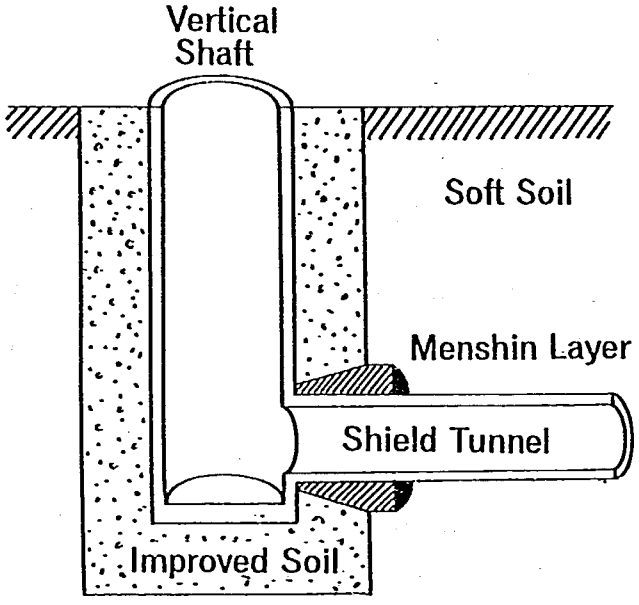


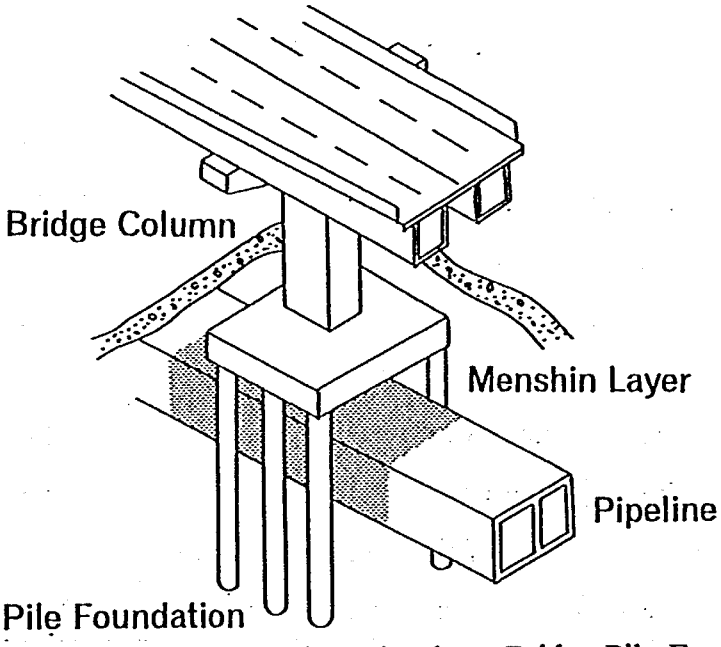

Fig. 1 Vulnerable Section in Underground Structures during an Earthquake




(a) Underground Pipeline Passing through an Irregular Soil Condition

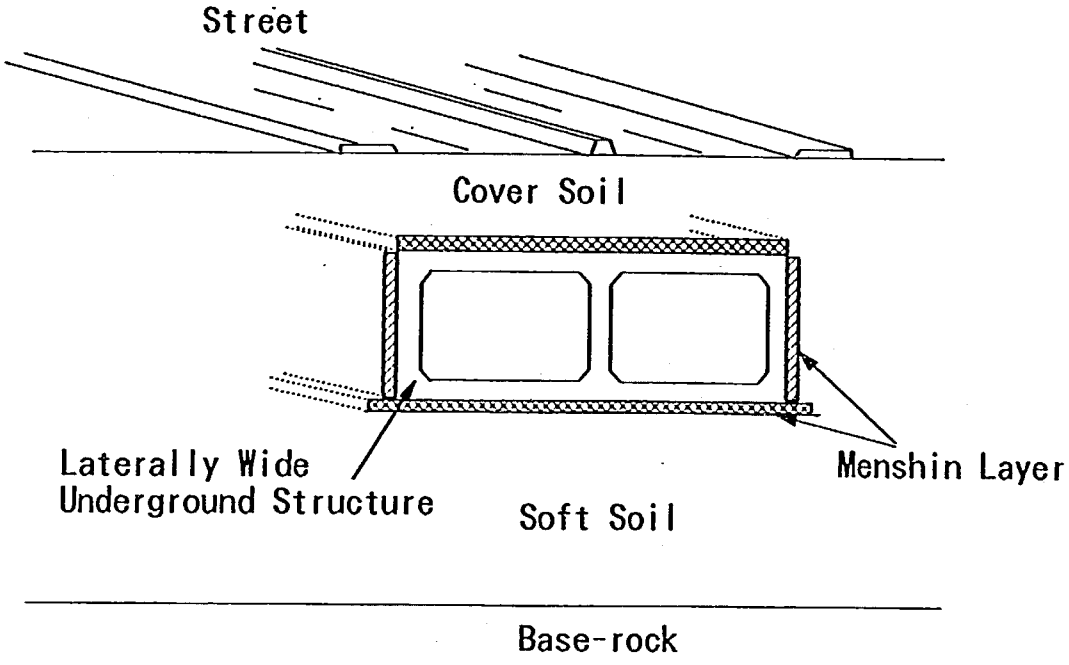



(b) Connection of Shield Tunnel to Vertical Shaft




(c) Underground Pipeline Passing Closely to Bridge Pile Foundation

Fig. 2–1 Effective Sections for Menshin System




(d) Laterally Wide Underground Structure Constructed by Cut–Cover Method

Fig. 2–2 Effective Sections for Menshin System

## MENSHIN EFFECT FOR SHIELD TUNNEL PASSING THROUGH IRREGULAR SOIL CONDITION

*Analyzed Menshin Shield Tunnel*

Structural details of the analyzed shield tunnel are shown in Table 1 and Fig. 3. External diameter of the shield tunnel is 5.1m, and the thickness of the inner lining is 20cm. The inner lining has minimum longitudinal reinforcing bars which is specified in the Guidelines for Seismic Design Methods of Large Underground Structures [1] .

Tabel 1 Structural Details of the Analyzed Shield Tunnel

| | |
|---|---|
| External Diameter (mm) | 5,100 |
| Thickness of Segment (mm) | 225 |
| Number of Segment Element | 6 |
| Width of Segment (mm) | 1,000 |
| Elastic Modulus of Segment (MPa) | $3.68 \times 10^4$ |
| Thickness of Inner Lining (mm) | 200 |
| Strength of Inner Lining Concrete (MPa) | 20.6 |
| Elastic Modulus of Inner Lining Concrete (MPa) | $2.30 \times 10^4$ |
| Material of Reinforcing Bar in Inner Lining | SD345, D22 |
| Reinforcing Bar in Inner Lining | 28 bars |

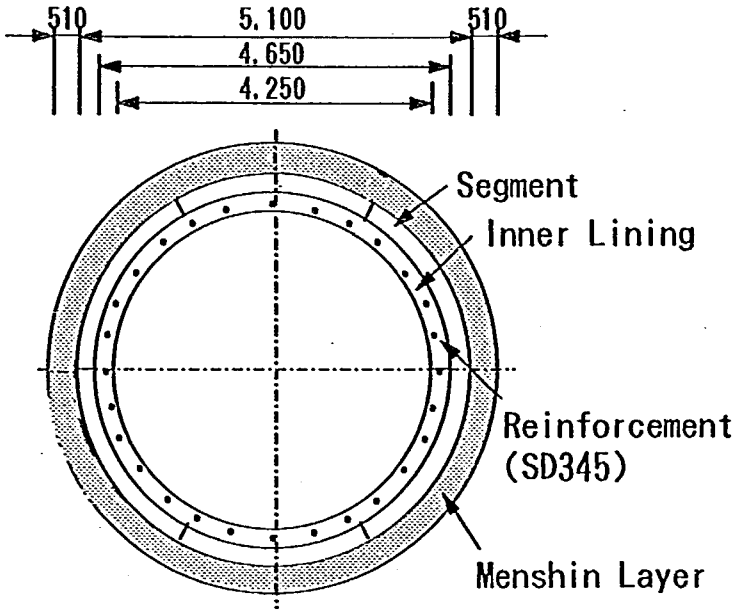



Fig. 3 Cross Section of the Analyzed Shield Tunnel

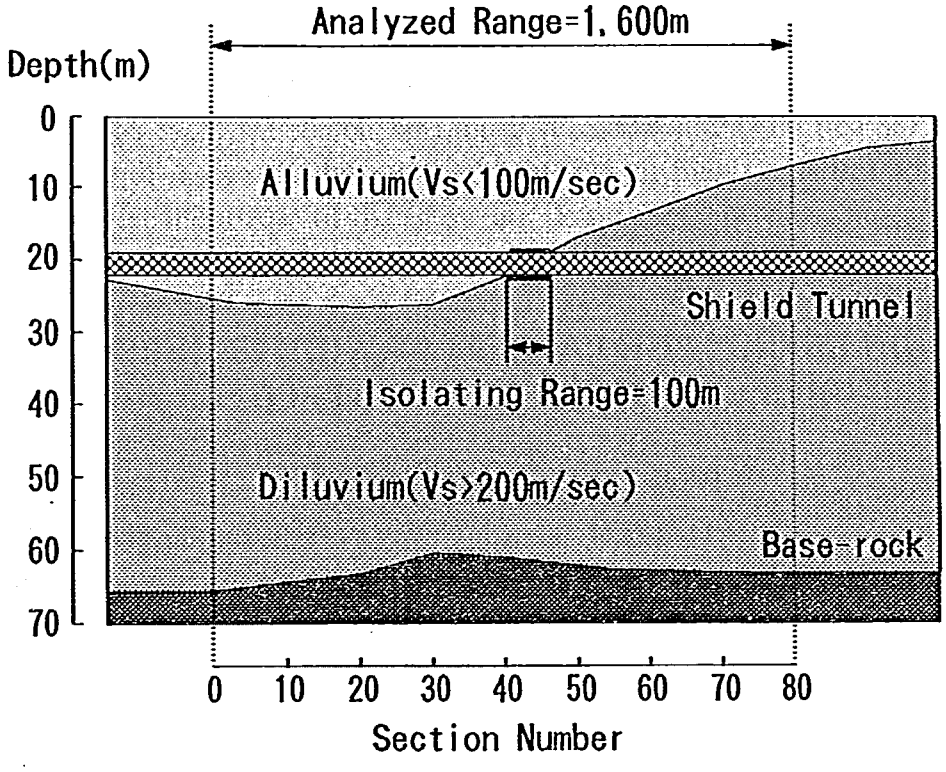



Fig. 4 Subsurface Ground Condition

The subsurface ground condition is shown in Fig. 4. The analyzed range has a length of 1600m in the longitudinal direction, and the depth from the ground surface to the tunnel axis is 21m. The shield tunnel passes through a boundary between alluvium to diluvium around the section No.40 (see Fig. 4), that is located at approximately the middle point in the analyzed range. The shear wave velocity of the alluvium and the diluvium are less than 100 m/sec and more than 200 m/sec, respectively. The base-rock appears at the depth of

approximately 60m from the ground surface. The ground condition is classified as group III, soft, according with the Specifications for Highway Bridges [3].
Thickness of the menshin layer is assumed here to be 51cm which corresponds to 10% of the external diameter. The tunnel is isolated from the subsurface ground by the menshin layer in the range of section No.40 to 45 (100m), that are in the edge of the diluvium. Although the appropriate elastic modulus of the menshin material is not yet clear, it is assumed here to be 5kgf/cm$^2$ (0.49MPa) which corresponds to approximately 0.3% of the one of the diluvium.

*Analysis of Menshin Effect by SDM*

The seismic analysis of the menshin shield tunnel was carried out by the SDM. The applied analytical procedure was based on reference [1]. To take into account the effect of the irregularity of soil condition into the SDM analysis, the seismic relative displacement developed between soils was modeled through a soil-tunnel spring. The soil-tunnel spring stiffness with the menshin layer was calculated by a static finite element analysis.
Fig. 5 shows the distributions of the seismic axial force and the seismic bending moment developed in the shield tunnels with/without the menshin layer. Both the peak axial force and the peak bending moment are observed around the section No.40 where the significant irregularity of the soil condition exists. It should be noted that these peak values decrease effectively in the menshin shield tunnel. In this case study, the axial force and the bending moment in the menshin shield tunnel are reduced to approximately 60% and 75%, respectively, of those in the non-menshin one.

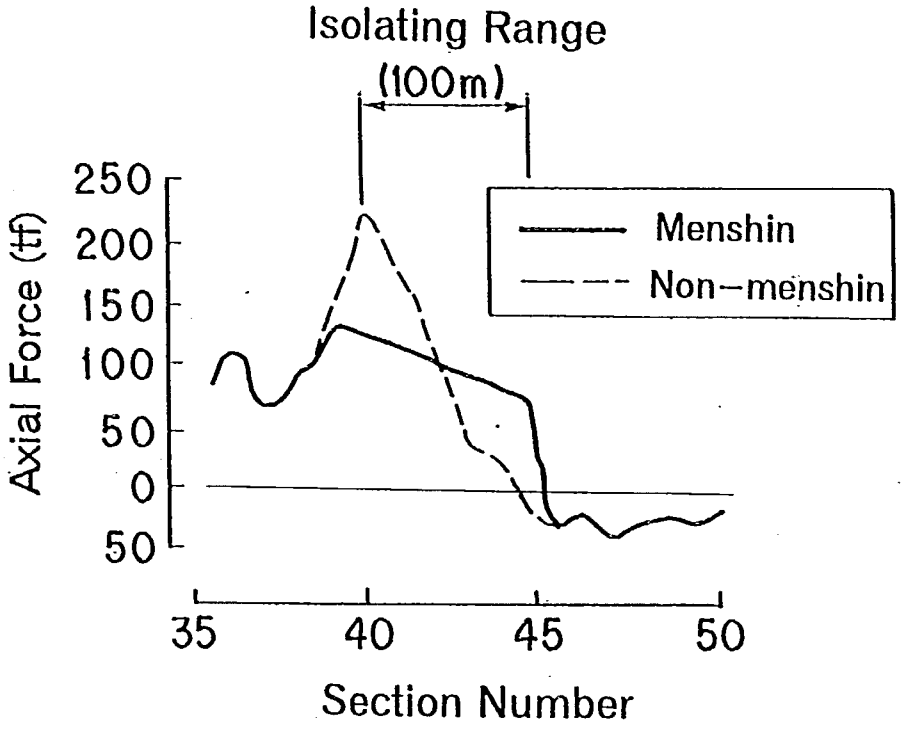
## MENSHIN EFFECT FOR LATERALLY WIDE UNDERGROUND STRUCTURES CONSTRUCTED BY CUT-COVER METHOD

*Analyzed Menshin Laterally Wide Underground Structures*

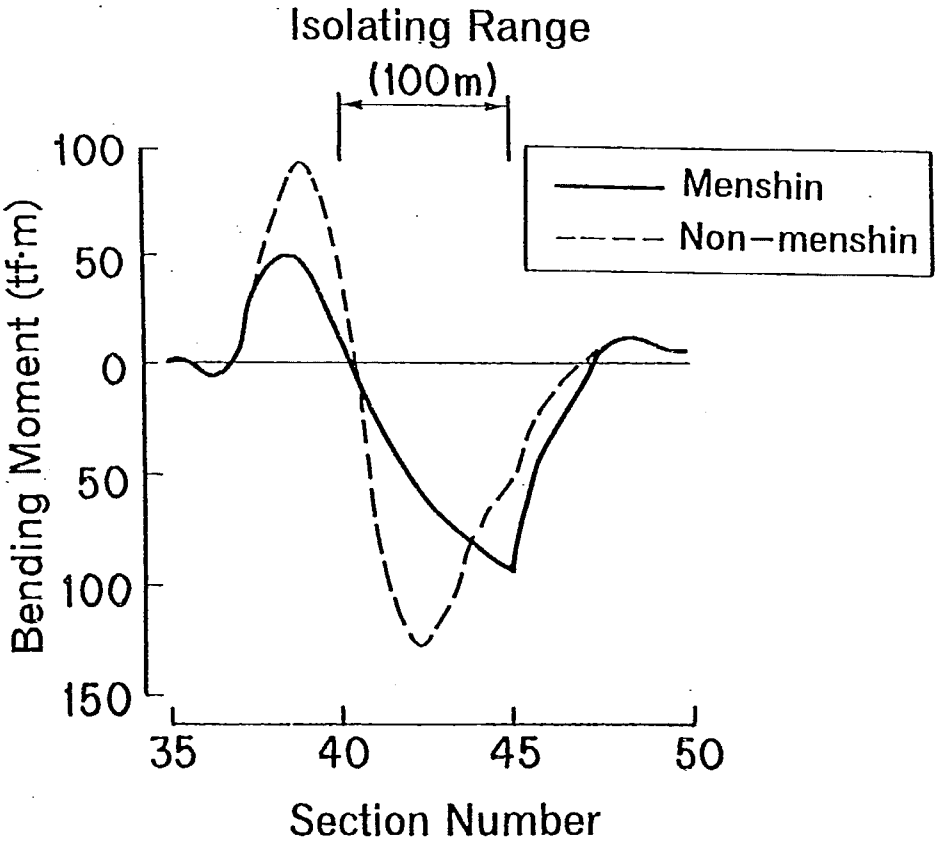
A box-type reinforced concrete tunnel for a highway passing on an alluvium was selected for the analysis. Structural details and the soil condition are shown in Fig. 6. The tunnel has a cross section with a width of 24.2m and a height of 9.1m. The depth of the covering soil is 5.0m. The alluvium with the depth of 28m is deposited on the diluvium, and the base-rock appears at the depth of 45m from the ground surface. The shear wave velocity of the alluvium is 100 to 120 m/sec.
The tunnel is covered by a menshin material with thickness of 50cm. The menshin material is assumed here to have the elastic modulus of 30kgf/cm$^2$ (2.94MPa) and the poisson ratio of 0.495.

*Dynamic Response Analysis by Two-Dimensional Finite Element Method*

A dynamic response analysis was made for the laterally wide underground structures with/without the menshin layer. A two-dimensional finite element model [1] was used in the analysis, since the dynamic characteristic of the underground structure and of the




(a) Distribution of Seismic Axial Force




(b) Distribution of Seismic Bending Moment

Fig. 5 Seismic Force Developed in Cross Section

subsurface ground, such as natural period, damping, stiffness, etc, can be adequately idealized. The stiffness of the subsurface ground is calculated in accordance with the Specifications for Highway Bridges [3], and the viscous damping is assumed here to be 10%. Although the input motion should be determined by the equivalent linearisation analysis of the subsurface ground, the standard acceleration waveform for the rock soil [3], with the peak of 102gal, was preliminarily inputed at the base-rock.

Fig. 7 shows the distributions of the peak seismic shear force and the peak seismic bending moment developed in the cross section. The effect of the shear stress around the surface is significant in laterally wide underground structures, so that the seismic forces develop especially at the corner sections. It is found that the menshin layer works well to reduce such forces. In this case analysis, the shear force and the bending moment in the menshin structure are reduced to approximately 63% and 75%, respectively, of those in the non-menshin one. From this results it is expected that the menshin system for laterally wide underground structures is an efficient way to reduce the seismic effects.

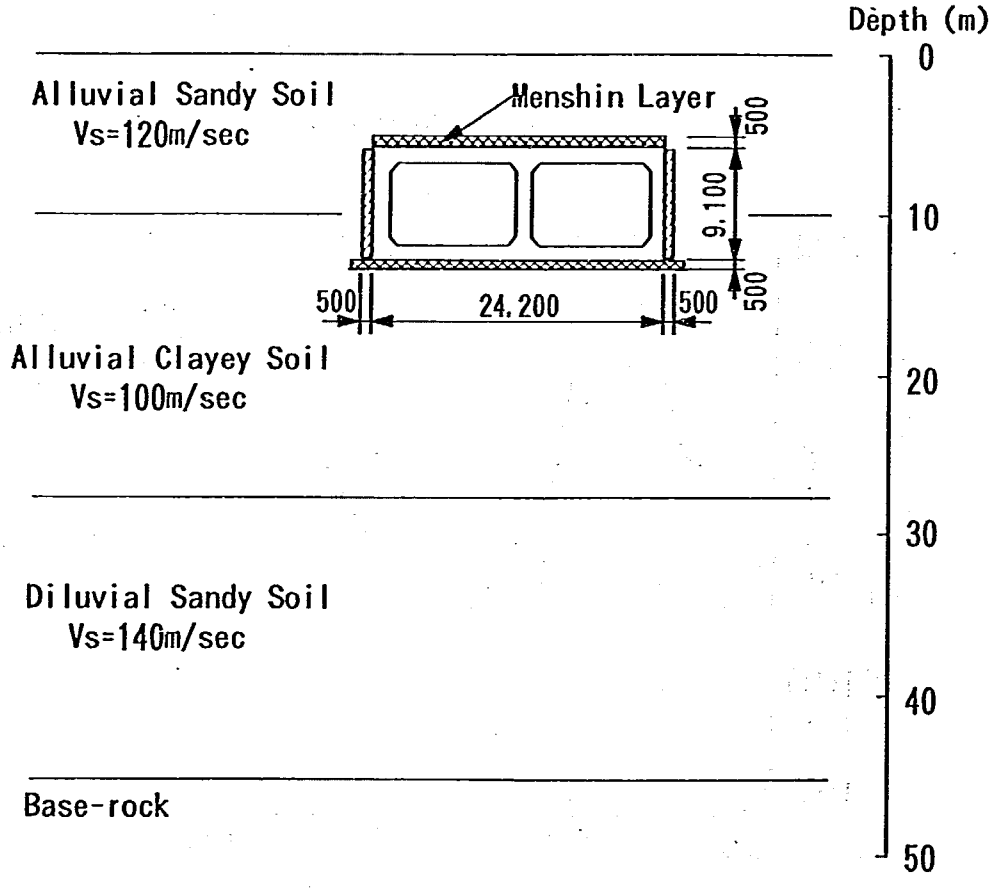
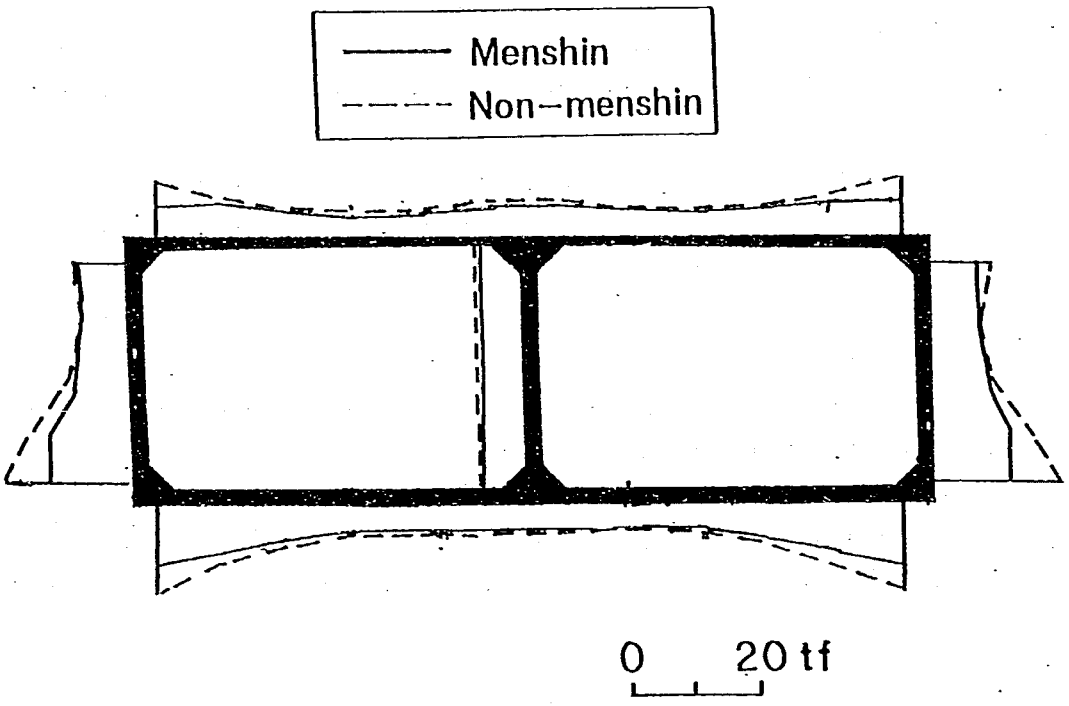
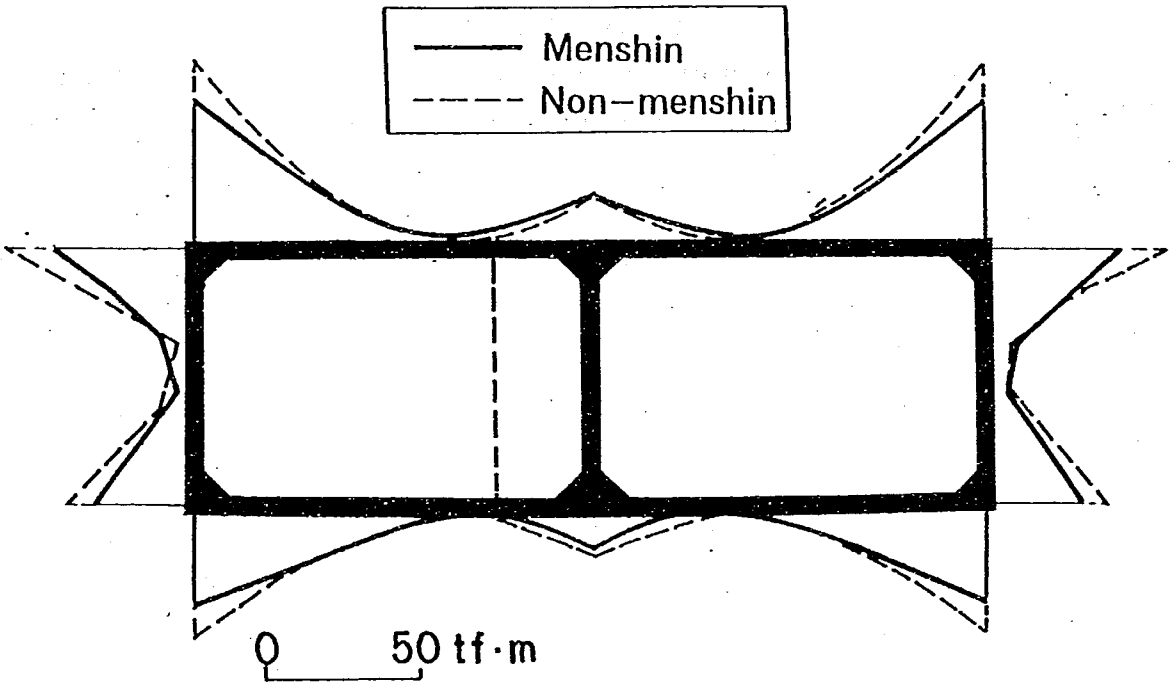



Fig. 6 Structural Details and Soil Condition




(a) Distribution of Peak Seismic Shear Force




(b) Distribution of Peak Seismic Bending Moment

Fig. 7 Seismic Shear Force and Bending Moment Developed in the Cross Section

## CONCLUDING REMARKS

A menshin system for underground structures by isolating them from the seismic deformation of the subsurface ground was introduced in this paper. Some appropriate sections for such menshin system were studied, and its effectiveness is examined based on a few case studies.

The menshin system is efficient in the sections where the seismic effect is significant. Appropriate sections were proposed as shown in Fig. 2. Based on some analytical case studies, it is apparent that the menshin system would be efficient at the underground structures. Although these studies have been just preliminary, over 20% to 30% reduction in the seismic force can be expected from the menshin system.

This research program has just initiated, so that a number of technical issues have to be studied in the future for the development of the menshin system. For that porpose, the Public Works Research Institute is going to initiate a three-year joint research program with several private companies. This joint research program will focus on the development of appropriate menshin materials and construction methods for the underground structures.

## REFERENCES


1) Asakura, H., Kawashima, K. and Sugita, H. : Guidelines for Seismic Design Methods of Large Underground Structures, 24th Joint Meeting of U.S.-Japan Panel on Wind and Seismic Effects, Gaithersburg, MD, U.S.A., May 1992.
2) Kawashima, K. : Seismic Design for Underground Structures, Kashima Publishing, 1994.
3) Japan Road Association : Specifications for Highway Bridges, Part 5, Feb. 1990. (in Japanese)

# A BRIDGE PRIORITIZATION METHOD BASED ON TRANSPORTATION SYSTEM PERFORMANCE USING GIS

Nesrin Basöz
Doctoral Candidate
The John A. Blume Earthquake Engineering Center
Department of Civil Engineering
Stanford University
Stanford, CA 94305-4020

and

Anne S. Kiremidjian
Professor and Director
The John A. Blume Earthquake Engineering Center
Department of Civil Engineering
Stanford University
Stanford, CA 94305-4020

## ABSTRACT

Bridges are critical components of transportation systems, thus mitigating their potential failure under seismic loads is essential for both the emergency response and for long term economic recovery of a region affected by an earthquake event. Seismic retrofitting decisions, used as a means of hazard mitigation, must be made under the constraint of limited resources. Proper allocation of available resources requires developing a prioritization method to identify and rank bridges that are in need of retrofitting. In this paper, a geographic information system (GIS)-based prioritization method is presented. The method requires assessing vulnerability and importance of all bridges in the seismic exposure region. The methodology is illustrated through an application to bridges in the Palo Alto, California area.

## INTRODUCTION

Bridges are important links to transportation systems. Damage to bridges can be particularly disruptive since the repair time can be lengthy and rerouting traffic can be difficult. Bridge damage as evidenced in earthquakes of the last few decades has emphasized the need for seismic hazard mitigation. As a first step towards the mitigation of bridge failures, it is necessary to assess the *vulnerability*, i.e., the damage potential of existing bridges subjected to future earthquakes, and the *importance*, i.e., the socio-economic impact of the failures to a community. Seismic retrofitting and upgrading to current design codes of all bridges that are in need of retrofitting is difficult and extremely costly. Retrofitting and upgrading decisions under limited resources require that the

ensemble of existing bridges be rank-ordered by their decreasing vulnerability and importance in order to identify the ones with the most need of retrofitting. For the purpose of achieving a rational ordering for bridges, prioritization methods need to be developed.

In order to insure the availability of a transportation system immediately after an earthquake and for long-term economic recovery, many states in the United States are currently in the process of prioritizing the bridges in their states. A detailed review of the following existing prioritization approaches is presented in Basöz and Kiremidjian (1995): the California Department of Transportation (Caltrans), the Applied Technology Council (ATC), the Illinois Department of Transportation (IDOT) and the Washington State Department of Transportation (WSDOT) approaches.

The developed prioritization method described in this paper is to be used for the formulation and implementation of a retrofitting program that optimally reduces the risk of seismic damage to bridges under limited resources. The resulting ranking is intended to be at the screening level leading to a possible more extensive analysis level for the bridges that are identified as candidates for seismic retrofitting. The general methodology presented herein can be applied to any state within the country and for different hazards.

In this paper, first the conceptual model for prioritization of bridges for seismic retrofitting is outlined. Then, the vulnerability and the importance criteria, their components and their synthesis under the GIS framework are summarized. An application of the developed method to the Palo Alto, California area is presented.

## CONCEPTUAL MODEL FOR PRIORITIZATION

A prioritization method has been developed for ranking a set of bridges based on their *vulnerability,* V, and *importance,* I. The rank order of bridges $\{R\}=\{R_1,R_2,...,R_N\}$ is defined such that:

$$R_1 > R_2 > ... > R_N \tag{1}$$

where the bridge assigned to $R_1$ is identified as the first candidate for seismic retrofitting. The ranking for bridge *i*, $R_i$, can be expressed as follows:

$$R_i = f(V_i, I_i) \tag{2}$$

where $R_i$ = Ranking of bridge *i* for seismic retrofitting,

$V_i$ = Vulnerability of bridge *i*, and

$I_i$ = Importance of bridge *i*.

The flowchart shown in Figure 1 illustrates the relationship between the main and sub-components of the conceptual prioritization method. For the final ranking, assessments for both vulnerability and importance are required.

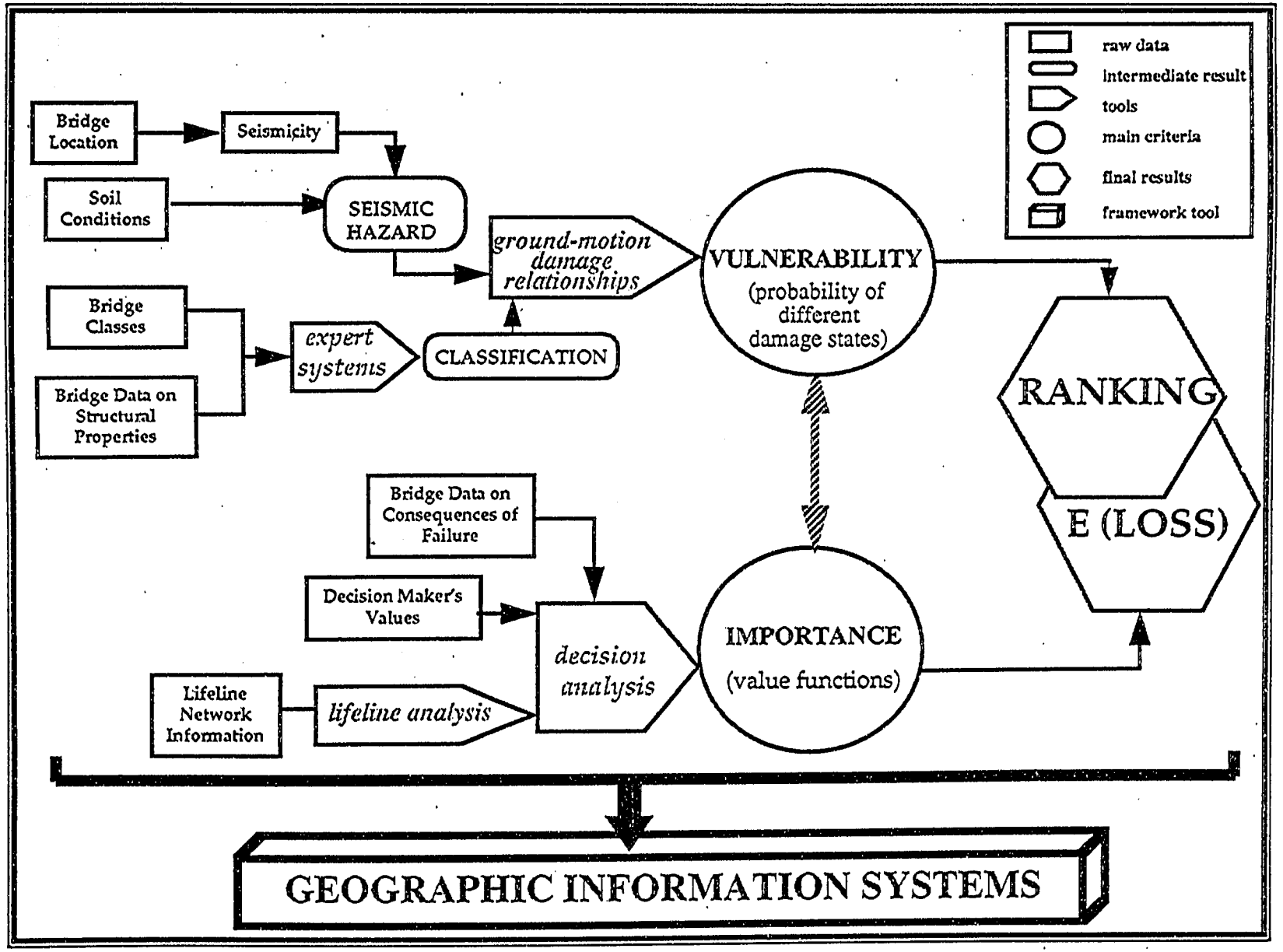



Figure 1. Components of Prioritization Method

## Vulnerability Assessment

Vulnerability is one of the main criteria in prioritization of bridges for seismic retrofitting. Seismic vulnerability, defined as the potential of a bridge to sustain a given level of damage, is expressed as a function of the site hazard and the structural properties of the bridge. The objective of the vulnerability assessment is to find $E[D|B_i]$ or $E[L|B_i]$ where

$$E[D|B_i] = E_i[D] = \text{Expected damage for bridge } i, \tag{3.a}$$

$$E[L|B_i] = E_i[L] = \text{Expected loss for bridge } i. \tag{3.b}$$

The expected damage for a bridge $i$, at a given site can be calculated as (Basöz and Kiremidjian, 1995):

$$v_{D_i} = E_i[D] = \iint_{AD} d f_{D|A}(d|a) f_A(a) da\, dd \tag{4}$$

where D = Damage state random variable,

$f_{D|A}(d|a)$ = Probability density function of damage D given the ground motion level A and

$$q_r(A) = \int_{d_i}^{d_j} d_r f_{D|A}(d|a) dd \tag{4.a}$$

where $q_r(A)$ = Expected value of being in a damage state $d_r$ given seismic hazard at site, A,

$f_A(a)$ = Probability density function of the ground motion level.

Therefore, vulnerability assessment requires the following:

- seismic hazard analysis at the bridge site,
- classification of bridges based on their structural characteristics and
- fragility analysis.

### *Seismic Hazard Analysis*

The presented prioritization considers vulnerability as a function of seismicity unlike other existing prioritization approaches (e.g., Caltrans and ATC). The seismic hazard is directly related to vulnerability and their relationship has to be examined.

The seismic load experienced by each bridge depends on the site of the bridge and its proximity to earthquake sources. A seismic hazard analysis which can be estimated by either a deterministic or a probabilistic approach, is necessary to identify the seismicity at a given bridge site. For the purpose of seismic hazard assessment at each bridge site, the level of ground motion should be calculated. Both ground shaking and collateral hazards such as liquefaction are considered in the seismic hazard assessment. Several ground shaking parameters can be used in seismic hazard analysis, such as Modified Mercalli Intensity (MMI), peak ground acceleration (pga) or spectral values (spectral acceleration ($S_a$), spectral velocity ($S_v$) or spectral displacement ($S_d$)). The selection of the ground shaking parameter depends on the ground motion parameter of the fragility curves that need to be developed.

### *Bridge Classification*

The seismic behavior of a bridge can be characterized based on its structural properties, location and construction. It is practical to group bridges with similar seismic behavior for prioritization purposes. Currently, only two bridge classifications exist: the Earthquake Engineering Facility Classification of ATC-13 (1985) and the bridge classification included in the National Institute of Building Sciences (NIBS) Technical Manual (Risk Management Solutions, 1995). However, neither of these classifications are detailed enough to distinguish different structural types and seismic behavior. In order to achieve a better understanding of the behavior of bridges under seismic loading, a more refined classification is developed (Basöz and Kiremidjian, 1995). For the purpose of this classification, the structural properties of a bridge are divided into primary and secondary attributes. The bridge classes are defined as a function of only the primary attributes which include substructure material type, superstructure material and structural type, number of spans, span continuity, abutment type and column bents. Ten bridge classes as listed in Table 1 are defined based on the substructure material type and superstructure type and material properties. Then, for each bridge class sub-categories are defined based on the other four primary attributes. Table 2 shows generic sub-categories for a bridge class. The secondary attributes include other structural properties such as skew, curvature and design year as an indication of the reinforcement practice. The effect of the secondary attributes is considered in the form of modifiers on the ground motion-damage relationships.

The bridge classes are defined to generalize the ground motion-damage relationships. For each bridge class, it is necessary to develop a ground motion-damage relationship in the form of fragility curves. The probability of a bridge being in a given damage level can be evaluated using the bridge classes and the respective fragility curves. However, bridge classes are rather general and serve for the purpose of capturing the ground motion-damage relationships for a limited number of attributes and over a specified range of values of these attributes. It is not always possible to have a bridge with the exact structural characteristics to match a bridge class sub-category. In order to classify existing bridges into one or more of the developed bridge classes, a classification method that uses a relational database management system (RDBMS) and a knowledge-based expert system (KBES) is developed. A detailed discussion of the bridge class definitions and the expert system **ESCOB** (Expert System for Classification of Bridges) that enables automated classification of a large set of bridges is included in Basöz and Kiremidjian (1995). The RDBMS is used to organize bridge attribute data in a systematic manner and **ESCOB** classifies the bridges in such a database. This system utilizes the classification developed by Basöz and Kiremidjian (1995) and is used to classify the bridges in the example application to Palo Alto, California.

| Bridge Class Identifier | Substructure Material | Superstructure Material/Type |
|---|---|---|
| 1 | concrete | concrete girder |
| 2 | concrete | steel girder |
| 3 | concrete | steel truss |
| 4 | steel | steel girder |
| 5 | steel | steel truss |
| 6 | concrete/steel | suspension/cable-stayed |
| 7 | concrete/steel/timber/masonry | arch |
| 8 | timber | any structure type except arch |
| 9 | masonry | any structure type except arch |
| 10 | concrete/steel/timber/masonry | others |

**Table 1. Bridge Classes**

**Bridge Class $C_n$**

single span bridges

$C_n^{sl}$ (least vulnerable single span sub-category)

| Attribute | Value |
|---|---|
| Abutment Type | monolithic |

$C_n^{sm}$ (most vulnerable single span sub-category)

| Attribute | Value |
|---|---|
| Abutment Type | non-monolithic |

multiple span bridges

$C_n^{ml}$ (least vulnerable multiple span sub-category)

| Attribute | Value |
|---|---|
| Abutment Type | monolithic |
| Span Continuity | continuous |
| Columns/bent | multiple |

$C_n^{mm}$ (most vulnerable multiple span sub-category)

| Attribute | Value |
|---|---|
| Abutment Type | non-monolithic |
| Span Continuity | discontinuous |
| Columns /bent | single |

**Table 2. Generic Sub-Category Definitions for Bridge Classes**

The prioritization methodology can be used with any of the well-defined bridge class definitions and ground-motion damage relationships. New bridge class definitions are developed as the existing ones are deemed to be inadequate.

### *Fragility Analysis*

The damage to a specific structural class can be expressed in terms of a ground motion-damage relationship. These are typically represented either in the form of fragility curves or damage probability matrices. Fragility curves express the probability of being or exceeding a specified damage level for a given ground motion damage. Damage probability matrices (DPM) relate the probability of being in a given damage state for a specified ground motion level. There is a unique functional relationship between these two representations, thus either one can be used without any limitations to the overall methodology.

The prioritization method presented in this paper requires that a ground motion-damage relationship exist for the bridge classes used in classifying existing bridges. DPMs and fragility curves are available for the ATC-13 and the NIBS bridge classes, respectively. In order to utilize the new bridge class definitions, fragility curves for each bridge class need to be developed. Several approaches can be used to develop fragility curves. These include the development of a system reliability formulations based on bridge component reliability where components are considered to be the physical components of a bridge, or identification of critical limit-states of a bridge system and use of analytical or simulation methods to calculate system reliability.

It is also important to clearly define the level at which the vulnerability should be evaluated as the definition of the damage level is an important aspect for the overall ranking. The overall ranking can be based on two damage levels: *collapse* and *serviceability*. For the vulnerability assessment, it is possible to define four or five physical damage states ranging from *no damage* to *collapse* as a function of the structural characteristics. Then, the relationship between physical damage states and functional characteristics of the damage have to be determined based on the respective importance factor that can be emergency response factor or long term economic impact factor explained in the following section. For example, for emergency response factor, the collapse damage might include only the *severe damage* and *total collapse* damage states. For the long term economic impact analysis, the physical damage states can be possibly grouped as *closed, limited use* and *open*. The fragility curves that need to be developed should contemplate these issues.

## IMPORTANCE ASSESSMENT

The prioritization of bridges for seismic retrofitting requires considering attributes that relate the consequences of failure of a bridge to the public safety and socio-economic well-being of a community. These factors are reflected in the importance criterion, I, for bridge prioritization. The bridge importance criterion for bridge *i* is defined as follows:

$$I = f(S, E, G, Q, L, H) \tag{5}$$

where S = Public safety factor,

E = Emergency response factor,

G = Long term economic impacts factor,

Q = Defense route factor,

L = Factor for interaction with other lifelines, and

H = Historical significance factor.

S reflects the risk of life loss on/under the structure due to failure of a bridge. E, is a measure of identifying the impacts of a failure immediately after the earthquake, especially for rescue operations and fire fighting purposes for which the availability of the transportation system is of primary concern. G considers the social impact usually for a period of time that starts a few days after the earthquake and extends anywhere from one to six months depending on the severity of the earthquake. The serviceability capacity of the transportation system to meet user's need constitutes the main concern. The factor, L is related to utilities carried on the bridge and represents the potential of physical damage to the bridge and possible disruption of services to the users. The Q and H factors are included to reflect different perspectives for the importance of the existing bridges on the transportation network system.

### *Value Tradeoff Model*

The effect of each factor on the importance criterion should be represented by a common measure. It is not possible to use monetary values or time loss because not all of the attributes can be represented by either of these terms. Thus, a value model is developed to properly evaluate the multi-attribute importance criterion. The decision maker's tradeoff values for each of the importance criterion factors need to be obtained through a separate analysis. The results of each analysis are combined by the use of the multi-attribute utility theory (Keeney and Raiffa, 1993). The general form of the value model that is used to properly assess the multi-attribute importance criterion for a given bridge *i* is expressed as follows:

$$U_{Ii} = \sum_{j \in I} k_j u_{ji} \tag{6}$$

where $U_{Ii}$ = Utility value (u-value) of the importance criterion for bridge *i* used in the final ranking,

$k_j$ = Scaling factor for each of the importance criterion factors listed in equation (5), and $\sum_{j \in I} k_j = 1$,

$u_{ji}$ = u-value of the importance criterion factor *j* for bridge *i*.

For this purpose, utility functions and scaling factors need to be defined for each of the factors listed above. The higher the $u_{ji}$, the more important is the bridge with respect to the given factor *j*.

### *Network Analysis*

Since the importance of a bridge is closely related to its function within the transportation network system, the u-value for the emergency response and long term economic impact factors requires conducting network analyses. For the emergency response factor, a connectivity network analysis is used to determine the critical bridge sets. Connectivity for a given group of origin-destination pair is defined as accessibility of the destination point from any of the origin points. A critical bridge set is defined as the set of bridges that would prevent the accessibility of the disaster area from the resource locations within an acceptable time frame for the emergency services. The analysis provides information about the available routes and the possible time delays for allocating resources for rescue and/or fire fighting to the disaster area. An algorithm based on the shortest path method (Ford and Fulkerson, 1964) is utilized for the connectivity analysis (Basöz and Kiremidjian, 1995). For the long term economic impact factor a serviceability analysis is required in order to estimate the economic loss due to damage to the bridges. The serviceability analysis can be conducted by solving the dynamic traffic assignment problem which includes the capacity and service level of the bridge in the analysis.

## GIS FRAMEWORK

Regional evaluation of transportation lifeline facilities that may be impacted by seismic hazard for emergency planning and retrofitting criteria can be accomplished by the use of Geographic Information Systems (GIS). The GIS-based approach provides a general, flexible methodology which enables the substitution or modification of any of the components such as damage model or hazard model. GIS can serve both as a tool for visualization and the analysis in the risk assessment process.
The spatial information about the highway network can be stored and manipulated in the relational database management system (RDBMS). Queries on the characteristics of the system can be displayed within GIS. Figure 2 shows bridge distribution in the Palo Alto area, California, based on number of spans. Furthermore, traffic flow constraints on a given link can be calculated in GIS to further obtain results such as time to travel on a given link. GIS also supports the analysis environment itself. Two fundamental analyses used for various applications, *path finding* and *allocation*, are supported by the network module in GIS. The path finding analysis is powerful in determining the best path to reach from an origin to a destination. Computational speed and comprehensible format of results are particularly valuable in various applications such as in

emergency response analyses. However, in order to consider the emergency response factor as part of the prioritization, the methodology requires an iterative and case - based solution. Hence, an external network analysis program is used for the identification of the critical bridge sets, possible time delays and the number of times that a given bridge is used for accessibility of the disaster area (Basöz and Kiremidjian, 1995). The external program is designed to utilize the already available network configuration information stored in the GIS. The results of the external program are displayed in the GIS. In the case of serviceability analysis which can be conducted for the long term economic impact purposes, the use of an external program is inevitable because GIS network analysis module is based on the assumption that a network maintains its original flow characteristics during an allocation of path finding session (Lupien et al., 1987).

In this paper, GIS is used to perform a risk analysis for bridges. Each of the steps for the vulnerability and importance assessment accomplished within GIS are summarized below by using the Palo Alto area, California as an example.

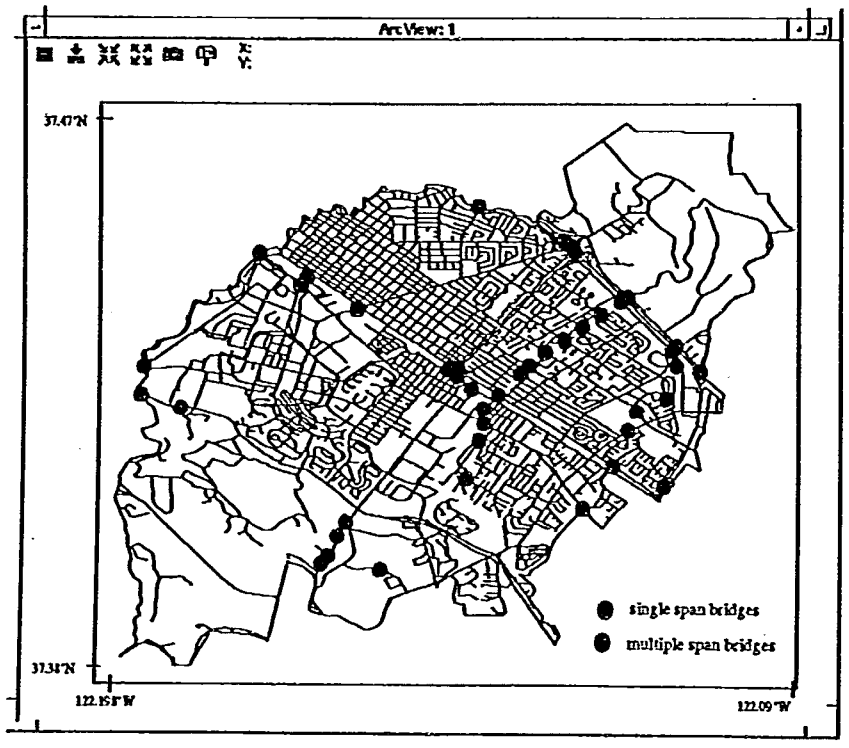



**Figure 2. Distribution of Multiple and Single Span Bridges**

## EXAMPLE STUDY: PALO ALTO AREA

In order to illustrate the bridge prioritization methodology, the bridges in the Palo Alto area are ranked for the emergency response condition. The area is the subject of a CUREe/Kajima joint project currently under progress at Stanford University for the regional damage and loss estimation. The available inventory used for prioritization purposes includes the fault locations near the area, seismic history of the area, local soil conditions, interstate to city level roads, local and state bridges. The inventory on the bridges includes the structural properties, traffic capacity and traffic flow direction.

Vulnerability Assessment: A probabilistic seismic hazard analysis is conducted for the area using the software program STASHA (Kiremidjian et al., 1994). The peak ground acceleration (pga) contour map for soft soil sites with 10 percent chance of being exceeded in 50 years is illustrated in Figure 3. Boore et al.'s (1993) attenuation relationship is used to include the effect of the soil conditions. Then, the bridge locations are overlaid with the seismicity map to obtain pga level at each bridge site. Each bridge is classified into bridge classes using its structural information.

The ground motion-damage relationships for the bridge classes and the pga level for a given bridge are used to obtain the probability of being in the collapse damage state, $q_c(A)$. Since the analysis is conducted for emergency response purposes, only the collapse damage state is considered.

Hypothetical values for $q_c(A)$ are used in the remaining parts of the example since fragility curves specific for the new bridge classes are not available at this time. Then, hypothetical modifiers are used to obtain the vulnerability which is expressed as the probability of being in a collapse damage state.

Importance Assessment: The importance assessment is performed primarily for the case of emergency response. A connectivity network analysis is conducted using the origin-destination (OD) pair (Stanford University Medical Center and Palo Alto Airport respectively) as identified in Figure 4. Only one origin-destination is selected for illustration purposes. In order to keep the computations manageable, several simplifying assumptions are made.

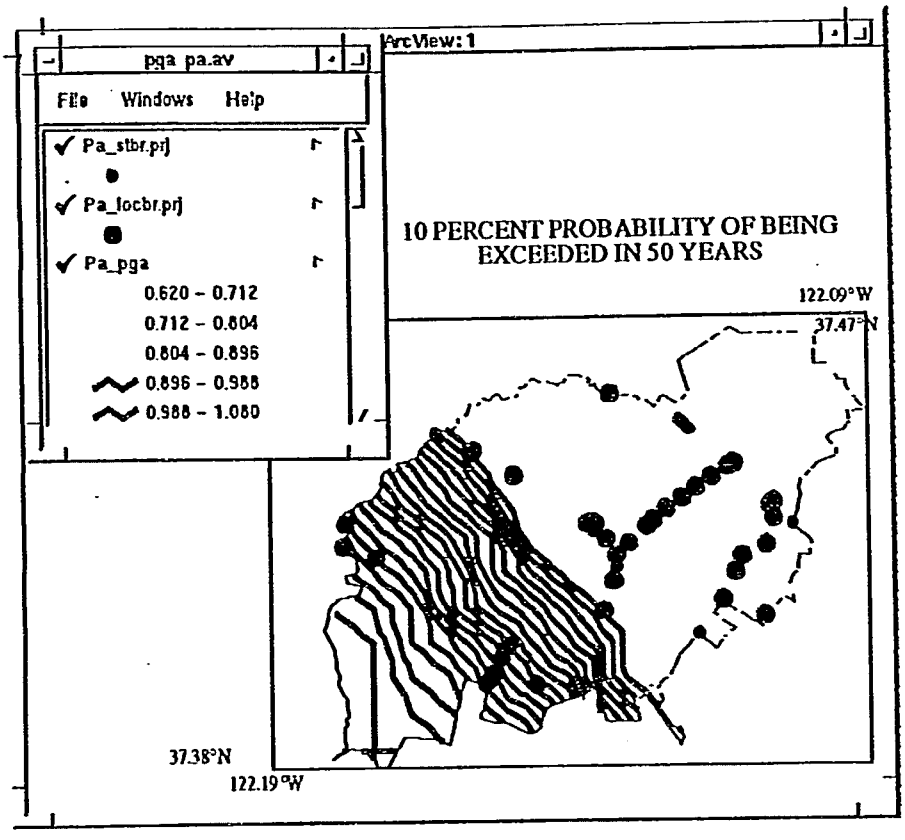



**Figure 3. Ground Motion Characteristics in the Palo Alto, California Area**

Hypothetical utility functions and scaling factors are used for the attributes of the emergency response factor. First the critical bridge sets are identified and then the bridges are ranked based on:

- the number of times that a bridge set is critical,
- time delay due to failure of a bridge, and
- the number of times that a bridge is used for accessibility of the disaster area.

If there are bridges that are not considered as part of any of the critical bridge sets due to their location with respect to the OD pair, then they are grouped and ranked in a separate set. Their ranking is obtained by sorting them in order of decreasing probability of being in the collapse damage level. This second set of bridges is ranked lower than the bridges included in the critical bridge sets. Figure 4 shows highest ranked ten bridges for seismic retrofitting when the objective is to reach the Palo Alto Airport from the Stanford University Medical Center for emergency response purposes.

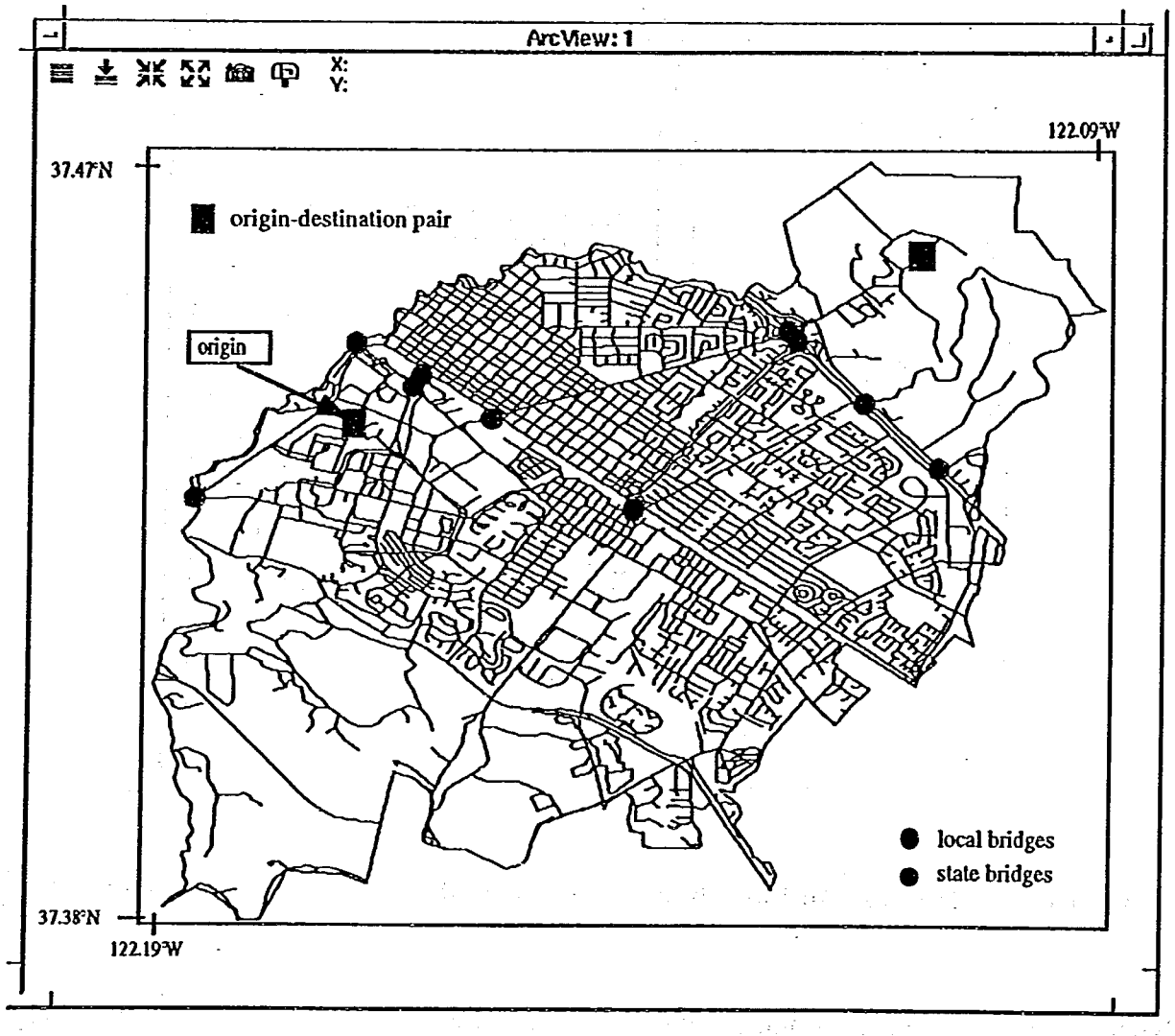



**Figure 4.** Origin and destinations for the Palo Alto, CA example

## CONCLUSIONS

A prioritization methodology developed to facilitate seismic retrofitting decisions for bridges is presented. The methodology considers the effect of the structural characteristics of the bridge on its vulnerability together with the importance of the network system performance, and the decision maker's values and preferences in retrofitting decisions. The integration of the vulnerability and the importance criteria is accomplished within the framework of GIS. An example is presented using the Palo Alto, California area to illustrate the general methodology. The final bridge ranking presented here is only for illustration purposes. A more detailed analysis requires that (1) fragility curves for the bridge classes defined in Basöz and Kiremidjian (1995) be developed and (2) modeling of the impact of unavailability of transportation routes to long-term economic be included in the final ranking.

## ACKNOWLEDGMENTS

The authors would like to express their deep appreciation to Dr. Ian Buckle, Jim Gates and Ann Sardo for their discussions regarding the seismic behavior of bridges. This research is funded by NCEER 91-3521A and the John A. Blume Earthquake Engineering Center.

## REFERENCES

ATC-13 (1985). "Earthquake Damage Evaluation Data for California", *Report ATC-13*, Applied Technology Council, Redwood City, California.

Basöz, N. and Kiremidjian, A. S., (1995). "Prioritization of Bridges for Seismic Retrofitting", *The John A. Blume Earthquake Engnrg Center Report No. 114.* Dept. of Civil Engnrg., Stanford Univ., Stanford, California.

Ford, L.R. and Fulkerson, D. R., (1962). *Flows in Networks*, Princeton Univ. Press, Princeton, NJ.

Boore D. M., Joyner W. B. and Fumal T. E. (1993). "Estimation of Response Spectra and Peak Accelerations from Western North American Earthquakes: An Interim Report", *US Geological Survey Open File Report 93-509*, Menlo Park, California.

Keeney, R. and Raiffa, H., (1993). *Decisions with Multiple Objectives: Preferences and Value Tradeoffs*, Cambridge Univ. Press, Cambridge, New York.

Kiremidjian, A. S., Mortgat, C. and Shah, H., (1994). *Stanford Seismic Hazard Analysis-STASHA,* The John A. Blume Earthquake Engrg. Center, Stanford Univ., Stanford, California.

Lupien, A. E., Moreland W. H. and Dangermond J. (1987). "Network Analysis in Geographic Information Systems", *Photogram. Engrg. and Remote Sensing*, Vol. 53, No. 10, 1417-1421.

Risk Management Solutions, Inc. (1995). *Development of a Standardized Earthquake Loss Estimation Methodology*, Vol. 1, Technical Manual (prepared for National Institute of Building Sciences), Menlo Park, California.

Shinozuka, M. and Sato, R., (1991). "GIS-based Interactive and Graphic Computer Systems to Evaluate Seismic Risks in Water Delivery Networks", *Proc. Third US National Conf. on Lifeline Earthquake Engrg.*, Los Angeles, California, 651-660.

# FIRE FOLLOWING THE HANSHIN AND NORTHRIDGE EARTHQUAKES: A COMPARATIVE ANALYSIS

by

Charles Scawthorn, S.E.
Senior Vice President

Andrew Cowell
Project Manager

EQE International,
San Francisco CA 94104 USA

## ABSTRACT

The 1994 $M_w$ 6.7 Northridge and 1995 $M_w$ 6.9 Hanshin earthquakes each resulted in MMI VIII or greater shaking intensity for about 2 million persons in the northern Los Angeles (US) and Kobe (Japan) areas, respectively. Ignition rates were comparable in the two events. The US earthquake resulted in about 110 fires in the earthquake affected area, 86% of which were structure fires. Of these, 60% were in single- or multi-family dwellings. All fires were out before noon, despite impaired communications, wide-scale failure of firefighting water supply in the large parts of the San Fernando Valley, and other problems. Alternative water supplies, such as backyard swimming pools, were employed in many cases. Mutual aid was requested by fire departments in the heavily affected area, but resources from outside the Los Angeles region were not required. The Japan event resulted in about 108 fires in the earthquake affected area, 97% of which were structure fires and about a dozen of which developed into conflagrations which burned for about 24 hours and destroyed about 5,000 buildings. Building density is greater in Kobe than in Los Angeles, but the major factors which impaired Kobe and other fire department response included a badly damaged water distribution system (resulting in near total loss of water supply), a badly damaged transportation system (exacerbated by heavy traffic), and a large number of collapsed buildings demanding their search and rescue attention.

## INTRODUCTION

Fires following large earthquakes are a potentially serious problem, due to the multiple simultaneous ignitions which fire departments are called to respond to while, at the same time, their response is impeded due to impaired communications, water supply and transportation. Additionally, fire departments are called to respond to other emergencies caused by the earthquake, such as structural collapses, hazardous materials releases, and emergency medical aid. Because of these factors, large earthquakes offer the potential for major conflagrations, which have occurred several times in this century. The worst of these post-earthquake conflagrations have occurred in Japan in 1923 (causing 140,000 fatalities) and in the United States in 1906 (destroying over 28,000 buildings). It is a matter of great concern that conflagrations of such large magnitude might recur in Japan or the US, in future earthquakes. The 1994 Northridge and 1995 Hanshin earthquakes offer strikingly parallel cases for data collection and assessment of the potential for future post-earthquake conflagrations. This paper reviews the two events in this context, and contrasts the fires that resulted.

## THE 1994 NORTHRIDGE, CALIFORNIA EARTHQUAKE

The Northridge earthquake was the largest earthquake to occur within a US city in more than 20 years. Because the earthquake primarily affected only a limited area, this paper focuses on the experiences of two heavily effected fire departments, the Los Angeles City Fire Department and the Santa Monica Fire Department.

**Affected Area and Fire Protection.** The 4:31 AM January 17, 1994 $M_w$ 6.7 earthquake was centered under the Northridge section of the San Fernando Valley area of the Los Angeles region. The event resulted in Modified Mercalli Intensity (MMI) shaking intensities greater than MMI VIII over approximately 700 square miles of the northern Los Angeles area, Figure 1. The population most heavily affected was in the San Fernando Valley, which is primarily protected by the Los Angeles City Fire Department. Table 1 lists fire departments significantly affected by the earthquake, and their summary statistics (see Scawthorn et al 1994 for additional detail).

**Response and Related Aspects in the Northridge Earthquake.** Approximately 110 fires were reported as earthquake-related on January 17, as shown in Table 2. For Los Angeles City, Santa Monica, Pasadena, Burbank, and Glendale, the number of fires is shown as reported by each fire department's incident reports. These reports reflect initial assessment of the probable cause, and may or may not

include all earthquake-related fires. Furthermore, what is counted as a single incident report may involve multiple structures. Lastly, in the case of mobile home parks, a single incident in some cases even involves multiple ignitions, since several mobile home parks had several fires, but were only listed as one incident, at one address. The major damage caused by the Northridge earthquake and the largest number of earthquake-related fires was concentrated in the San Fernando Valley. This area is served primarily by the Los Angeles City Fire Department (LAFD).

**Los Angeles City Fire Department.** The Northridge earthquake reportedly caused or was a contributing factor in 77 fires in the LAFD service area. These earthquake-related fires are located on the map in Figure 2. The 77 fires were among a total of 161 fires that occurred on the day of the earthquake. The time line in Figure 3 shows all calls for assistance with fires on the day of the earthquake. Earthquake-related fires predominate the calls for the first three hours. During the remainder of the day, the earthquake is a factor in almost one half of the fires. The presence of aftershocks, the shifting of damaged structures, and the turning off and on of utilities as a result of the initial shock had apparently caused new fires to occur. Structure fires predominate (86%) the earthquake-related fires. As noted above, each report of a mobile home fire may actually involve multiple structures, since a single report may have been written for an entire mobile home park consisting of multiple burn sites. Fires classified as "outside" include the incident on Balboa Boulevard in Granada Hills where ground movement broke gas and water mains beneath the street, igniting the escaping gas and causing fires in five surrounding homes. More than 70% (66) of the earthquake-related fires occurred in single- or multiple-family residences, as might be expected from the building stock that is typical in the San Fernando Valley. The major cause of ignition was electric arcing as the result of a short circuit, although gas flame from an appliance is also a recurring source of ignition.

The large number of dispatches at mid morning were mostly hazardous condition calls due to the reported leakage of natural gas. Hazardous condition dispatches and other public service assistance account for over 75% of the dispatches. The breakdown of the day's calls into dispatches categories is shown in Figure 4.

**Water Supply.** The Northridge earthquake effected the water supply for portions of the San Fernando Valley. The damage in that area is shown in Figure 5. Breaks occurred in at least six trunk lines and a large number of leaks occurred at other locations. The Department of Water and Power estimated that approximately 3,000 leaks were caused by the earthquake, including two lines of the Los Angeles Aqueduct. Pump stations and storage tanks also sustained damage. The damage to the system resulted in a water shortage that had to be made up by water tenders. LAFD reported lack of water pressure at hydrants in much of the west

and north portions of the San Fernando Valley. Due to this lack of water pressure, LAFD resorted to drafting from alternative sources, including the large number of backyard swimming pools in the area. SMFD reports the water supply system for Santa Monica suffered no significant impairment as a result of the earthquake.

## THE 1995 HANSHIN, JAPAN EARTHQUAKE

**Affected Area and Fire Protection.** The 5:46 AM January 17, 1995 $M_w$ 6.9 (JMA M7.2) Hanshin (official name: Hyogo-ken Nambu) earthquake was centered under the northern tip of Awaji island near Kobe, in the Kansai region of Japan. The event resulted in Modified Mercalli Intensity (MMI) shaking intensities greater than MMI VIII over approximately 400 square km of the Kobe-Ashiya-Nishinomiya area, Figure 6. Population of the affected area is given in Table 3.

The Kobe Fire Department (KFD) is a modern, well-trained fire response agency, organized into Prevention, Suppression, and General Affairs sections, and a Fire Academy. The city is divided into 11 wards for fire protection purposes. KFD maintains 11 fire stations and 15 branch stations, served by 1,298 uniformed personnel. Equipment includes two helicopters, two fireboats, and 196 vehicles. Other equipment includes 72 portable pumps. Fire engines carry predominantly 50- and 65-millimeter hose; larger hose is not available except for drafting purposes. KFD has a civil disaster prevention program as well as a cadre of volunteer fire corps with about 4,000 members. This corps provides the first on-scene engagement of the fire, performing functions such as giving directions to arriving emergency vehicles and helping to guide people to safety

**Response and Related Aspects in the Hanshin Earthquake.** KFD had minimal staffing on duty at the time of the earthquake, possibly because the previous day had been a holiday. Initial actions included recalling off-duty personnel and responding to fire calls. Approximately 100 fires broke out within minutes, primarily in densely built-up, low-rise areas of the central city, which comprise mixed residential-commercial occupancies, predominantly of wood construction. Within 1 to 2 hours, several large conflagrations had developed. There were a total of 108 fires reported in Kobe on January 17 (Kobe FD, 1995), the majority being in the wards of Higashi Nada, Nada, Hyogo, Nagata, and Suma, Figure 7 (after National Fire Research Institute, 1995). Modes of fire reporting were unclear as of this writing, and fire response was hampered by extreme traffic congestion, and collapsed houses, buildings, and rubble in the streets. Because of the numerous collapses, many areas were inaccessible to vehicles.

Fire spread was via radiant heat and flame impingement, building to building in the densely built-up areas. The wind was calm, and fire advance was relatively

slow. In a number of cases, fires were observed to have stopped at relatively narrow fire breaks (e.g., 10 meters) or, in at least one case, at a high-rise apartment building, probably as a result of active fire fighting. The final burned area in Kobe was estimated at 1 million square meters, with 50% of this in the Nagata Ward.

The Ashiya Fire Department reported 11 fires on January 17; nine of them were before 7:30 a.m. Distribution of the fires was along an east-west line about 1 kilometer wide centered on National Route 2. The total burned area for the 11 fires was about 4,400 square meters.

Water Supply. Fire water is primarily from the city water system, served by gravity from 30 reservoirs. Of these, 22 have dual tanks, with one tank having a seismic shutoff valve so that, in the event of an earthquake, one tank's contents is conserved for fire fighting. In this event, all 22 valves functioned properly, conserving 30,000 cubic meters of water, which, however, could not be delivered because of approximately 2,000 breaks in the underground piping. Kobe has approximately 23,500 fire hydrants, typically flush-mounted (i.e., under a steel plate in the sidewalk or street) with one 150-millimeter-diameter hose connection. The city has provided underground storage of water for disaster fire fighting in 968 cisterns, generally of 40,000-liter capacity, sufficient for about a 10-minute supply of a pumper. All engines carry hard suction, so that additional water can be drafted from Osaka Bay or the several streams running through Kobe.

Kobe sustained approximately 2,000 breaks in its underground distribution system. Water for fire-fighting purposes was available for 2 to 3 hours, including the use of underground cisterns. Subsequently, water was available only from tanker trucks. KFD attempted to supply water with a fireboat and relay system, but this was unsuccessful due to the relatively small hose used by KFD. The first author overflew the area at about 5:00 p.m. on January 17 and was able to observe all of the larger fires (about eight in all) from an altitude of less than 300 meters. No fire streams were observed, and all fires were burning freely—several with flames 6 meters or more in height. No fire apparatus were observed in the vicinity of the large fires, although fire apparatus could be seen at other locations (their activities were unclear from the air). Some residents formed bucket brigades (with sewer water) to try to control the flames.

## OBSERVATIONS

Several observations emerge from these two earthquakes:

Ignitions: There were a significant number of earthquake-related fires in both events. In fact, the total number of ignitions is comparable - 110 for the Northridge event, versus 108 for Kobe City. Considering that the great majority of

the 77 ignitions within the City of Los Angeles occurred within the MMI VII isoseismal, and that this area contains about one third of the total Los Angeles City population of 3.4 million, this equates to about 1 ignition per 14,719 population for the Northridge event. In the case of Kobe (population 1.5 million), the 108 ignitions equates to 1 ignition per 13,676 population. Thus, ignition rate is also comparable.

Response: In the case of Northridge, ignitions were all brought under control within several hours of the earthquake. Furthermore, the resources of the Los Angeles region were sufficient to deal with all fire ignitions, as well as other emergencies, such as search and rescue, hazardous materials releases, etc. This is an excellent response, and is due to the large well-equipped fire service in the Los Angeles region, which has dealt with a large number of fires and other emergencies in the last several years. The fire service in Los Angeles equates to approximately 1 firefighter per 1,338 population, while in Kobe this ratio is about 1/1,138, oi quite similar. However, Los Angeles region is significantly larger than Kobe, so that Los Angeles had more than four times the total resources of Kobe, a significant difference.

Weather Conditions: Wind, humidity and other conditions were favorable in both cases and not a major problem.

Water Supply: In Los Angeles, while firefighting water supply failed in the heavily affected portions of Northidge, firefighters were able to avail themselves of alternative sources (eg, backyard swimming pools). In Kobe, due to the more than 2,000 breaks in the underground water distribution system, the fire department was without water within several hours, and found it difficult to relay or otherwise obtain water for firefighting purposes. As a result, fire spread in Kobe was significantly greater than in Northridge, resulting in the destruction of perhaps 5,000 buildings in Kobe.

## Concluding Remarks

The 1994 Northridge and 1995 Hanshin earthquakes and associated fires reinforce the following points:

- earthquakes in urban areas continue to cause multiple simultaneous ignitions, and degrade emergency response due to impaired communications, transportation and water supply

- these events are replicable, as shown by comparison of the 1971 San Fernando and 1994 Northridge events (Scawthorn, et al, 1995), and by comparison of the ignition rates and other factors in the Northridge and

Hanshin events, providing some validation for simulation modeling and projections for larger events

- under adverse conditions, large conflagrations are possible in modern cities, as shown by events in California (i.e., the 1991 East Bay Hills Fire, and the 1993 Southern California wildfires), and by the Hanshin earthquake in Japan.

- projections for larger earthquakes in Los Angeles indicate perhaps 500 ignitions within several hours - the situation is worse in Tokyo.

This accumulation of experience leads to the conclusion that the potential exists for large conflagrations following a major earthquake in an urban area. Under adverse meteorological and other conditions, these conflagrations may burn for several days, replicating the events of 1906 in San Francisco, and 1923 in Tokyo. Extensive, well-drilled mutual aid systems are required, in order to mobilize large resources in response, but the deployment of these resources will be hampered by transportation difficulties and, perhaps most tellingly, failure of firefighting water supplies. Improvements in planning and infrastructure are absolutely essential to forestall this potential.

## ACKNOWLEDGMENTS

Portions of this work were performed under a grant from the National Science Foundation, which is gratefully acknowledged. We would like to thank the following individuals for the information and assistance that they provided in preparing this paper: Fire Marshall Michael Carter, Glendale FD; William Cass, Senior Arson Investigator, LAFD; Fire Marshall Darryl Forbes, Burbank FD; Battalion Chief Jim Hone, SMFD; John McIntyre and Vic Mesrobian, Information Management Division LACo FD; Leon Older, Information Services Department LAFD; Captain Roy Prince, LAFD; Dan Rosetti, Fire Investigation Unit, Pasadena FD. Lt. Nakachi, Kobe FD . and Dr. A. Sekizawa, National Fire Research Institute, Japan.

## REFERENCES

Anthony, D. F. , *Managing the Disaster*, Fire Engineering, Pennwell Publishing Company, August 1994.

Dewey, J.W., B.G. Reagor, and L. Dengler (1994) Isoseismal map of the Northridge California earthquake of January 17, 1994: Poster talk presented at the *89th Annual Meeting of the Seismological Society of American*, Pasadena CA.

Earthquake Engineering Research Institute (1995) *The Hyogo-Ken Nanbu Earthquake, January 17, 1995, Preliminary Reconnaissance Report,* Earthquake Engineering Research Institute, Oakland CA.

EQE International (1995) The January 17, 1995 Kobe Earthquake, An EQE Summary Report, EQE International, San Francisco CA.

Kobe Fire Department (1995) *Heisei 7 Hyogo Ken Nanbu Earthquake - Regarding Kobe City Damage and Fire Department Activities,* Kobe City.(in Japanese)

Los Angeles City Fire Department (1987), *Earthquake Emergency Operational Plan, 1987.*

Los Angeles City Fire Department (1994), *'94 Earthquake After Action Report,* March 9, 1994.

Los Angeles County Fire Department (1994) *Northridge Earthquake Fact Sheet.*

Manning, D. O., *Message from LAFD Chief Engineer and General Manager,* Fire Engineering, Pennwell Publishing company, August 1994.

National Fire Research Institute (1995) *Report on the Hyogo Ken Nanbu Earthquake and Urban Fires in Kobe City.*

Scawthorn, C. and Khater, M. (1994) *Fires Caused by Earthquakes: A Greater Threat Than Many Realize,* NFPA Journal, May/June, p. 82-86.

Scawthorn, C., Cowell, A. et al (1995) Fire-related Aspects of the January 17, 1994 Northridge Earthquake, Ch. 8, *Spectra,* Earthquake Engg. Research Inst., Oakland CA. (in press).

Table 1.
Fire Departments Affected by the January 17, 1994 Northridge Earthquake

| Fire Department | Estimated Population (thousands) | Area (Sq Miles) | Number of Stations | Fire Fighting Personnel | Number of Engines |
|---|---|---|---|---|---|
| Los Angeles City | 3,400 | 469 | 104 | 2,865 | 104 |
| Los Angeles County | 2,896 | 2,234 | 127 | 1,842 | 144 |
| Ventura County | 700 | 126 | 30 | 327 | 40 +/- |
| Santa Monica | 97 | 8 | 4 | 100 | 5 |
| Burbank | 94 | 17 | 6 | 120 | 6 |
| Pasadena | 132 | 23 | 8 | 150 | 8 |
| Glendale | 166 | 30 | 9 | 167 | 9 |
| South Pasadena | 25 | 3 | 1 | 27 | 2 |
| Beverly Hills | 34 | 6 | 3 | 81 | 7 |
| Culver City | 41 | 5 | 3 | 66 | 5 |
| Fillmore | 12 | 2 | 1 | 9 | 1 |

Table 2.
Fire Following the January 17, 1994 Northridge Earthquake

| Community | Number of Earthquake-Related Fires |
|---|---|
| Los Angeles City | 77 |
| Los Angeles County | ~15 |
| Ventura County | ~10 |
| Santa Monica | 4 |
| Burbank | 0 |
| Pasadena | 1 |
| Glendale | 0 |
| South Pasadena | 0 |
| Beverly Hills | 1 |
| Culver City | 0 |
| Fillmore | 2 |
| TOTAL | ~110 |

## Table 3.
## Hanshin Earthquake Population and Earthquake Casualty Data (EERI, 1995)

| Location (City/Ward) | Total Population[1] (x 1,000) | Earthquake Casualties[2] | | |
|---|---|---|---|---|
| | | Deaths | Injuries | Missing |
| Kobe-shi/Higashi-Nada-ku | 190 | 1,127 | 3,383 | 14 |
| Kobe-shi/Nada-ku | 130 | 782 | 1,112 | 33 |
| Kobe-shi/Chuo-ku | 116 | 207 | 3,327 | 3 |
| Kobe-shi/Hyogo-ku | 124 | 384 | 1,755 | 10 |
| Kobe-shi/Nagata-ku | 137 | 673 | 533 | 76 |
| Kobe-shi/Suma-ku | 188 | 314 | 637 | 24 |
| Kobe-shi/Tarumi-ku | 235 | 2 | 1,020 | 0 |
| Kobe-shi/Nishi-ku | 159 | 2 | 1,649 | 0 |
| Kobe-shi/Kita-ku | 198 | 1 | 817 | 0 |
| Kobe-shi (all wards) | 1,477 | 3,492 | 14,224 | 160 |
| Ashiya-shi | 85 | 393 | 2,759 | 3 |
| Nishinomiya-shi | 412 | 843 | 2,987 | 7 |
| Amagasaki-shi | 488 | 25 | 61 | 0 |
| Itami-shi | 184 | 10 | 923 | 0 |
| Kawanishi-shi | 142 | 1 | 73 | 0 |
| Takarazuka-shi | 203 | 84 | 1,100 | 0 |
| Sanda-shi | 79 | 0 | 15 | 0 |
| Akashi-shi | 278 | 5 | 965 | 0 |
| Kakogawa-shi | 247 | 2 | 15 | 0 |
| Awaji Island (northern section) | 56 | 56 | 712 | 0 |
| Other Hyogo-Ken cities | ~100 | 14 | 29 | 0 |
| Total for Hyogo-Ken cities | ~3,700 | 4,925 | 23,863 | 170 |
| Total for Osaka-Fu cities | ~200 | 11 | 1,941 | 0 |
| Total for other prefecture cities | ~100 | 0 | 98 | 0 |
| Total all cities (estimated) | ~4,000 | ~5,000 | ~25,000 | ~0 |

[1] *Monthly Statistics of Japan*, December 1994 (Kobe-shi ward populations), and *Japan Local Government Datebook 1993* (Hyogo-Ken city populations).
[2] *The Sankei Shimbun* (newspaper), January 21, 1995.

Table 4
Hanshin and Northridge Earthquakes: Comparative Analysis

| ASPECT | FACTOR | NORTHRIDGE | HANSHIN |
|---|---|---|---|
| Event | Magnitude ($M_W$) | 6.7 | 6.9 |
| | Date (winter) | Jan 17 | Jan 17 |
| | Time | 0431 | 0546 |
| Region | Population (MMI 8) | 1~1.5 million | 2 million |
| | Density (pop/sq km) | 1,000~1,500 | 4,000 |
| Ignitions | Number (total) | 110 | 108 |
| | Structural Fires | 86% | 97% |
| | Rate (MMI 7) Ign/pop: | 14,719 | 13,676 |
| Response | FD Communications | manual dispatch | |
| | Resources (ff/popul): | 1,338 | 1,138 |
| | Stations | 104 | 26 (Kobe) |
| | Traffic Congestion | Minor | Major |
| | Mutual Aid | Available - not needed | after 10 hrs |
| Water | Water System Damage | Some | Total? |
| | Cisterns | Swimming Pools | 946, mostly 40 tons (10 mins) |
| Wind | | Calm | Minor |
| Gas | Automatic Shut-offs | ? few % | 70% - ineffective due to structl collapse |
| Spread | | Minor | Major: 5,000 bldgs |

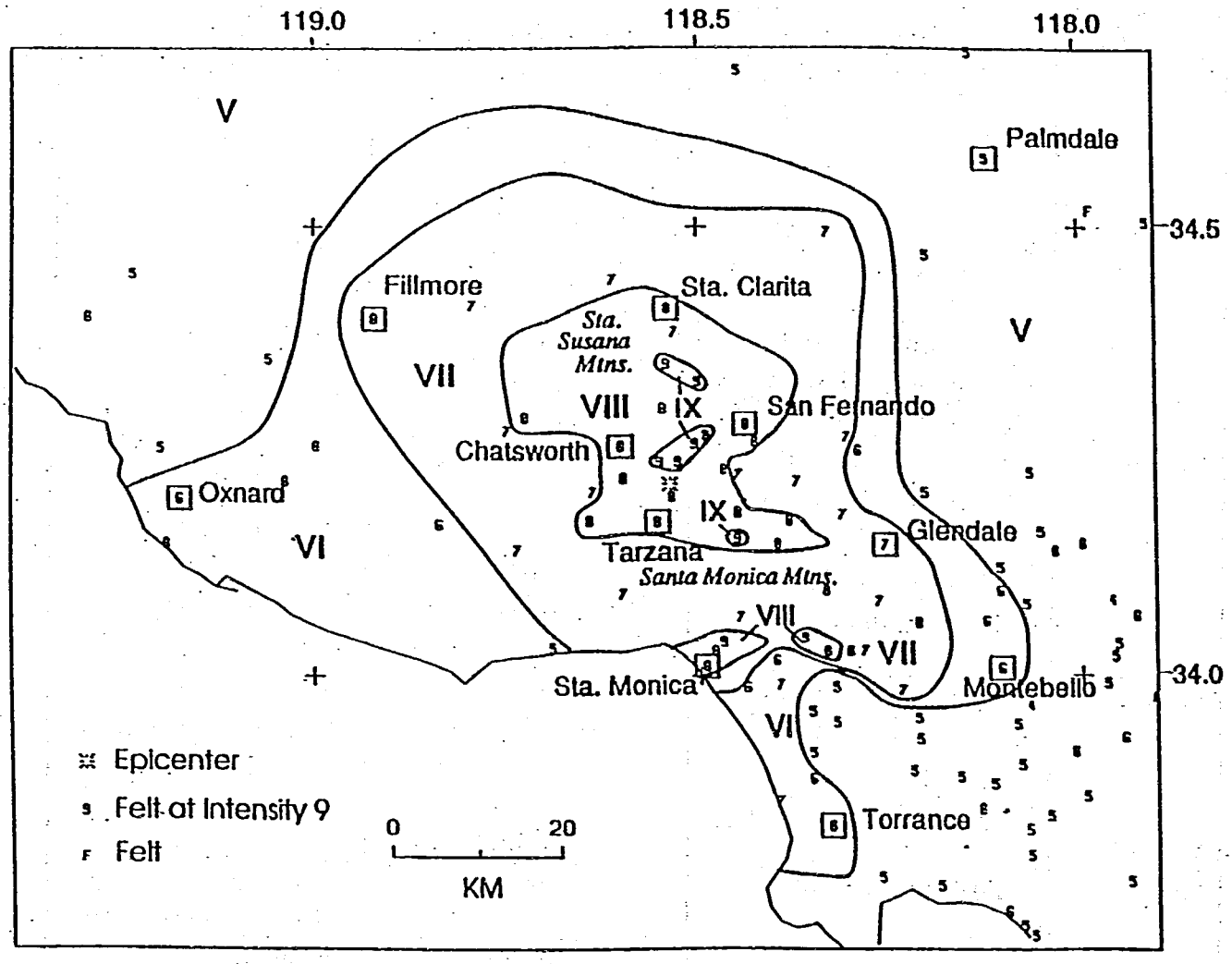



Figure 1. · MMI Map for the January 17, 1994 Northridge Earthquake (from J. Dewey, USGS)

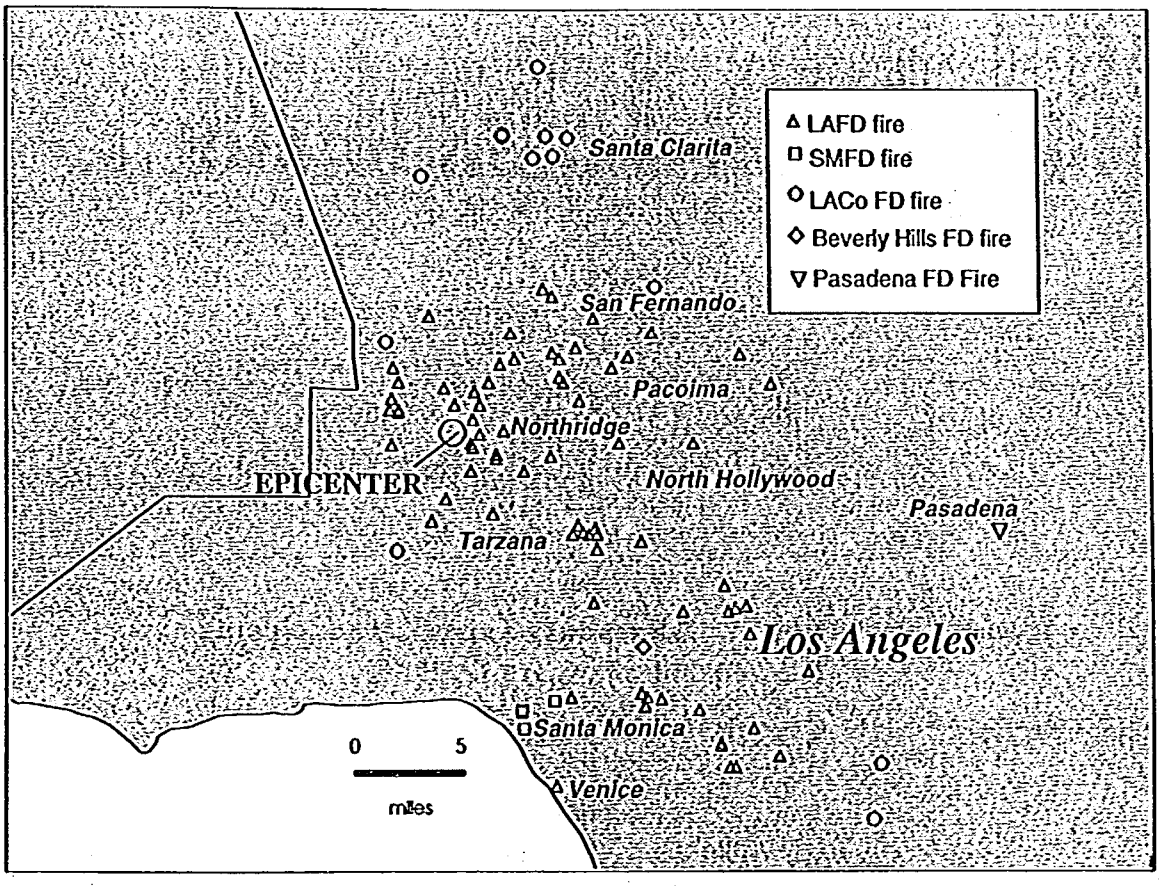



**Figure 2. Earthquake-Related Fires, January 17, 1994, LA County Fires Only.**

Figure 3. LAFD Fires, 4:31 to 24:00 hrs, January 17, 1994.

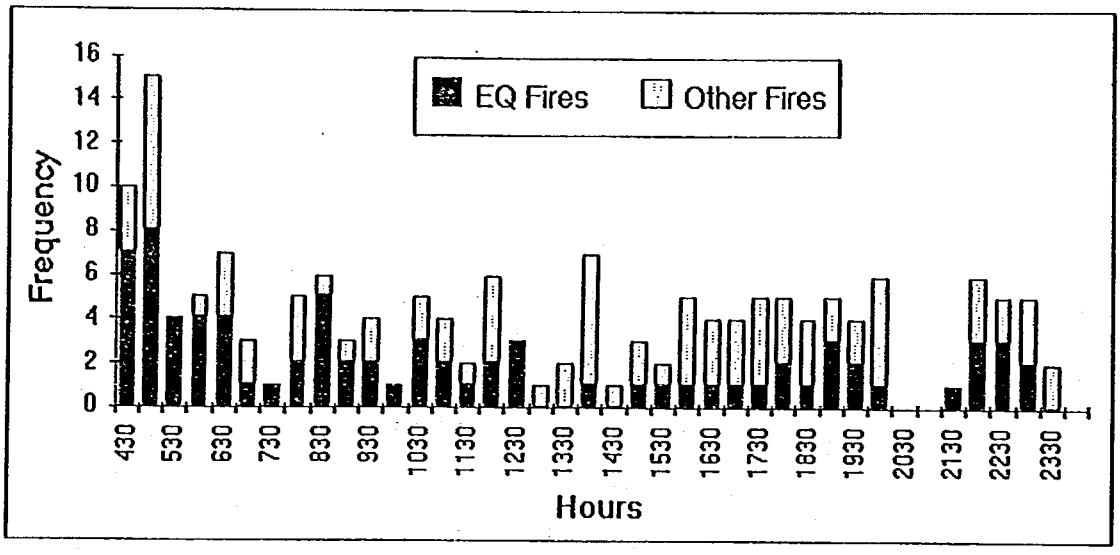
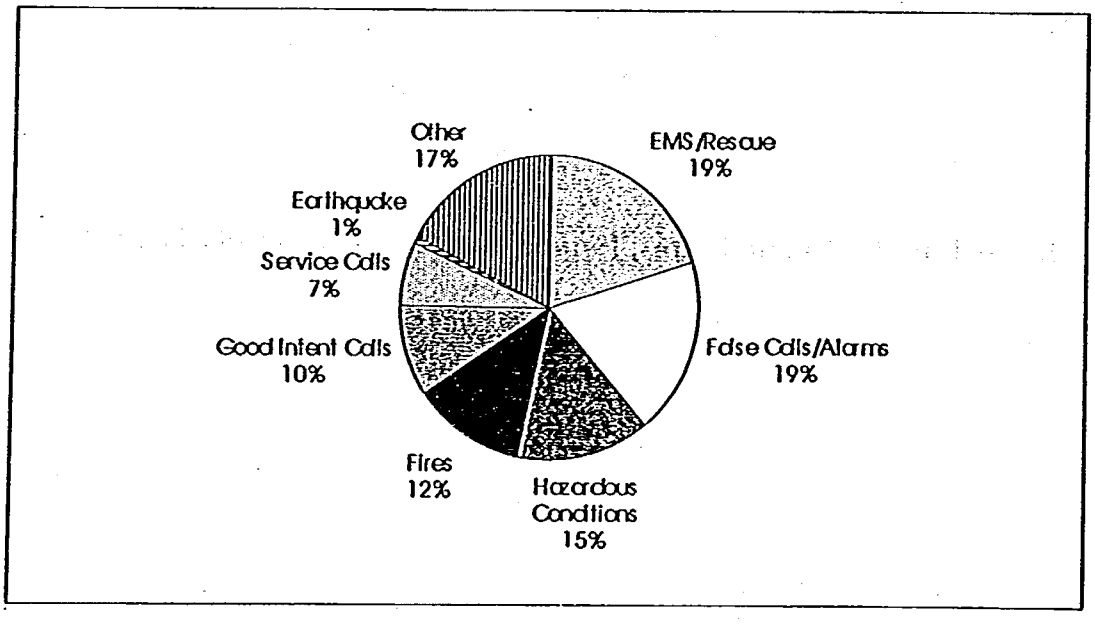



Figure 4. LAFD Incident Response Types, 1308 Incidents
4:31 to 24:00 hrs, January 17, 1994.



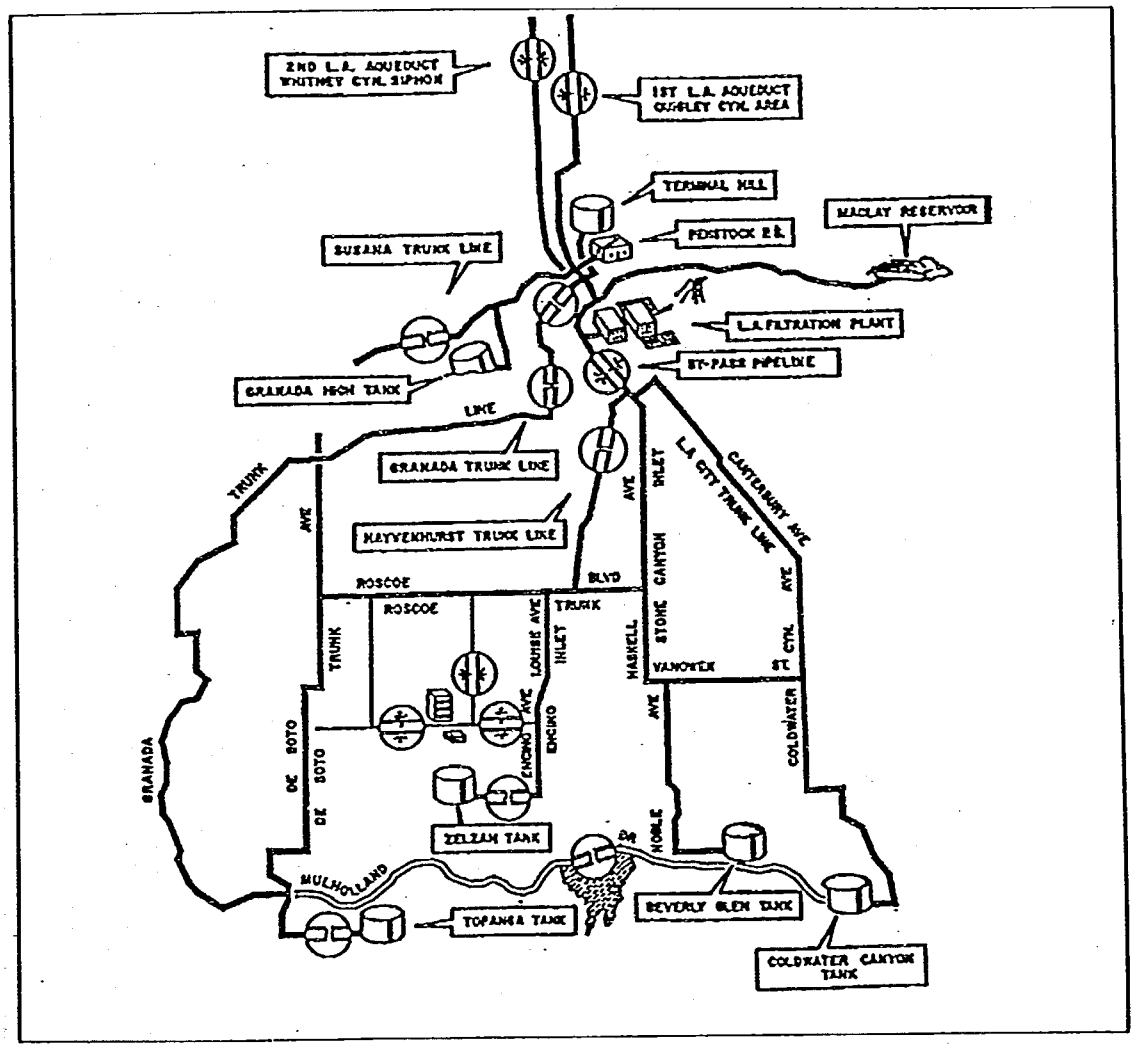



Figure 5. Water System Damage, Northridge Earthquake
(Drawing Courtesy of LAFD)

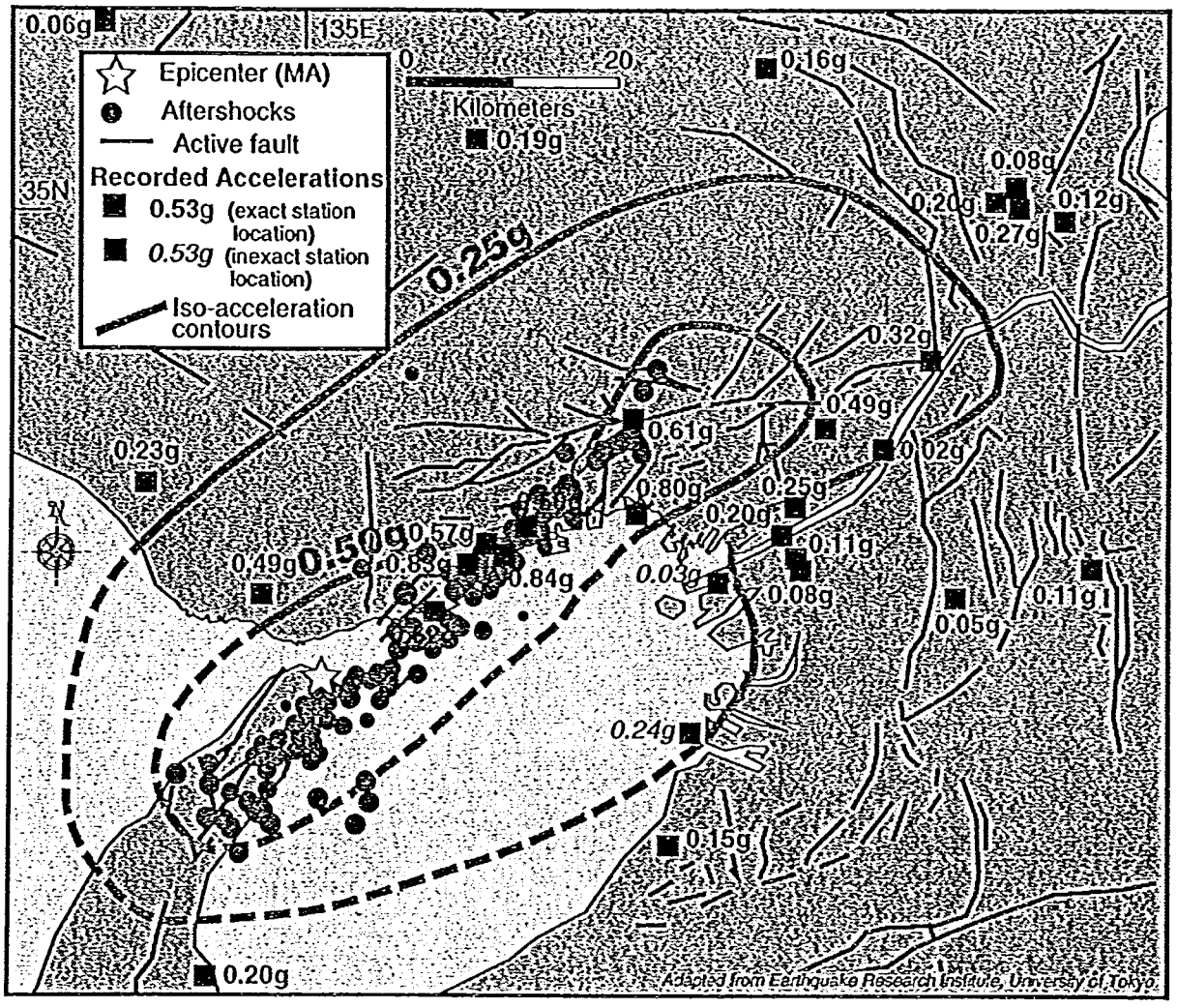



Figure 6. Shaking Intensity, Hanshin Earthquake (after EQE, 1995)

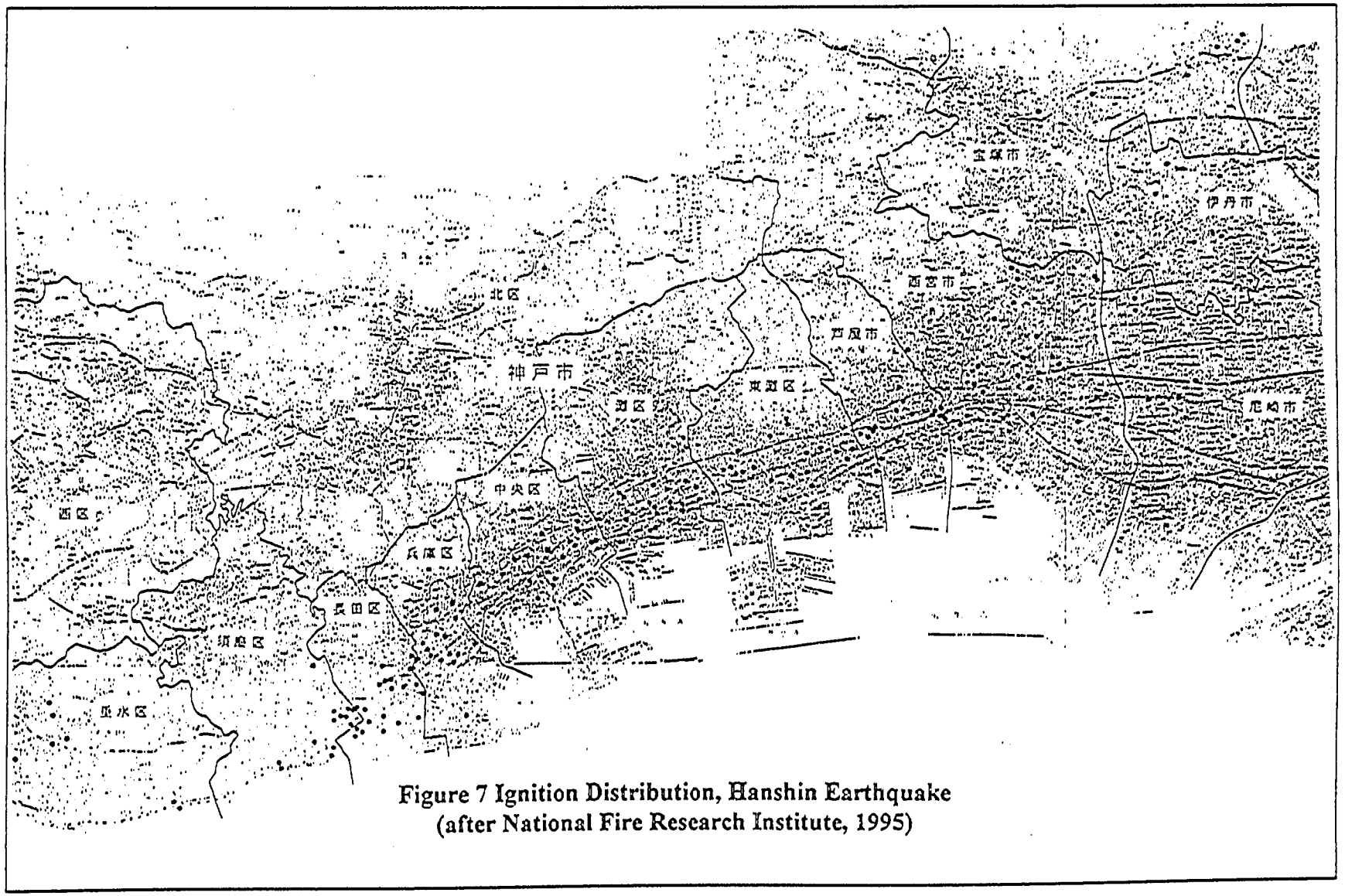



**Figure 7 Ignition Distribution, Hanshin Earthquake**
**(after National Fire Research Institute, 1995)**

# Resolutions

# RESOLUTIONS OF THE SIXTH U.S.-JAPAN WORKSHOP ON EARTHQUAKE DISASTER PREVENTION FOR LIFELINE SYSTEMS

*KKR HOTEL OSAKA, OSAKA*

*July 18-21, 1995*

The sixth U.S.-Japan Workshop on Earthquake Disaster Prevention for Lifeline Systems, co-sponsored by the Public Works Research Institute of Japan and the National Institute of Standards and Technology and the National Science Foundation of the United States under the auspices of Task Committee F, Disaster Prevention Methods for Lifeline System, UJNR Panel on Wind and Seismic Effects was held at KKR Hotel Osaka, Osaka, Japan, July 18-21, 1995. Sixty six experts, including three from New Zealand, representing government, academia, industry and private practice, participated in the workshop. Thirty two papers were presented, two of which by the New Zealand experts. In particular, results of the studies of the two most recent damaging earthquakes which occurred in the United States and Japan, i.e., the January 17, 1994 Northridge Earthquake and the January 17, 1995 Hyogo-ken Nanbu Earthquake, were presented and discussed.

The Workshop provided a most valuable forum to exchange information and ideas on technical as well as socioeconomic issues important to the lifeline earthquake engineering community of both countries. The following topics were addressed:

a. Lifeline systems such as water, sewerage, gas, electric power, telecommunication, and transportation damaged by recent earthquakes
b. Effects of liquefaction and its countermeasures.
c. Seismic monitoring
d. Risk assessment and socioeconomic impact
e. Postearthquake fires
f. Postearthquake lifeline function restoration
g. Seismic design and retrofit of lifeline facilities.

The Workshop participants has adopted the following resolutions:

1. The Workshop participants identified, without priority order, the following topics relevant to lifeline systems for future cooperative research programs:
   a. Exchange of information on the seismic design and performance of lifeline facilities;
   b. Field investigation of earthquake damages;
   c. Effect of liquefaction on the performance of lifeline systems,

d. Development of cost effective countermeasures against liquefaction for lifeline systems;
e. Repair and retrofit procedures and post-event service restoration strategies;
f. Improvement of post-earthquake fire suppression capabilities,
g. System analysis and network management strategies for improving lifeline performance during and after earthquakes;
h. Evaluation of the socioeconomic impacts resulting from a disruption of lifeline service after major earthquakes;
i. The adoption of emerging/mature methodologies, such GIS, GPS, real-time conditional simulation, from related field of expertise to lifeline earthquake engineering;
j. Enhancing communication between the private sector and government agencies in both countries.

2. The Workshop participants recognize the importance of continued exchange of personnel, technical information, research data and use of available research facilities in both countries, and the value of integrated multidisciplinary research. The workshop participants further recognize the benefit of identifying and executing specific activities comparing the results of different design, analysis and experimental methods, and disaster mitigation strategies in both countries.

3. In view of the most recent large earthquakes that caused significant damage to lifeline systems in the United States and Japan, the Workshop participants encourage the interaction of this Task Committee with other UJNR Task Committees to develop better methodologies for quantifying the vulnerability and implementing mitigation of lifeline systems to earthquakes.

4. The importance of continued support of "the International Decade for Natural Disaster Reduction (IDNDR)" has been acknowledged with respect to lifeline earthquake engineering and disaster mitigation research under the UJNR program. The Workshop participants consider the Sixth U.S.-Japan Workshop on Earthquake Disaster Prevention for Lifeline Systems a contribution to the achievement of the IDNDR goals.

5. Considering the importance of continued cooperative research programs on seismic effects and earthquake disaster prevention methods for lifeline systems, the Workshop participants recommend to hold the next workshop in 1997 in the United States. Location and time of the workshop will be determined through correspondence between the co-chairmen of Task Committee "F" of the UJNR Panel on Wind and Seismic Effects.

# Appendices

# KOBE AT SIX MONTHS

## A Phoenix on the Horizon

A Study Tour Report
by U.S. and New Zealand Delegates to the
Sixth U.S.-Japan Workshop on Earthquake Disaster Prevention for Lifeline Systems

Osaka, Japan
July 18-21, 1995

Workshop Co-chairs
Yasuyuki Koga
Riley Chung

Technical Editors
Laurie A. Johnson
Ronald T. Eguchi

*This report was supported by the National Science Foundation and the National Institute of Standards and Technology of the United States.*

## FOREWORD

July 17, 1995 marked the six-month anniversary of one of the greatest urban earthquake disasters this century. The statistics are still staggering: more than 5,500 lives lost, 27,000 injuries, 107,000 buildings damaged or destroyed, 300,000 people initially seeking shelter, and the most recent figure of over $140 billion (US) in economic losses. Officially titled the Hyogo-ken Nambu earthquake, the more popular names for the M7.2 JMA (6.9 moment magnitude) event are the Great Hanshin-Awaji earthquake, or simply the Kobe earthquake.

The six-month anniversary was also marked by Hyogo Prefecture's release of the much-anticipated reconstruction plan, commonly called the "Phoenix Plan". The plan is largely a series of policy statements about the region's vision for rebuilding and it incorporates the plans of city governments in the impacted area. Mitigation is a strong theme, and the document includes one-, three-, and ten-year targets for working toward a livable, economically healthy, and disaster resistant Kansai region. Posters and banners, containing the Phoenix symbol and accompanied by statements such as "We Love Kobe," are visible throughout the region, in store windows, draped over balconies, in train stations and rail cars, and mounted on construction screens. While more than 30,000 people are still homeless and rubble is still being cleared away, the spirit of recovery is strong.

Recovery and mitigation were on the minds of U.S. and New Zealand delegates participating in a two-day study tour to investigate the impacts to lifelines systems and the on-going recovery, six months after the earthquake. The study tour was part of the Sixth U.S.–Japan Workshop on Earthquake Disaster Prevention for Lifeline Systems, held in Osaka, Japan, on July 18-21, 1995. The workshop was co-sponsored by the Public Works Research Institute of Japan and the National Institute of Standards and Technology and the National Science Foundation of the United States, under the auspices of Task Committee F, Disaster Prevention Methods for Lifeline Systems, of the U.S.-Japan Natural Resources (UJNR) Panel on Wind and Seismic Effects.

Most of the delegates had visited the impacted area at least once before, offering each a unique set of perspectives on how the recovery and disaster prevention

activities were progressing. Snarled traffic problems in Kobe gave delegates plenty of time, as they traveled by bus between destinations, to observe and discuss key lessons learned. Many reports will undoubtedly document in greater detail the impacts to specific bridges or lifelines components and systems. This report is aimed at capturing the anecdotes--the raw but insightful collection of comments offered by this group as they observed Kobe's Phoenix emerging.

Laurie A. Johnson

## ACKNOWLEDGMENTS

The U.S. and New Zealand delegates wish to express our immense gratitude to our Japanese hosts from the Public Works Research Institute who arranged our study tour itinerary and managed the considerable logistics associated with the tour. This report would not be possible without their efforts. Our heartfelt thanks to each of them for identifying key people for us to talk to, serving as our interpreters, and so graciously and tirelessly accommodating our many diverse schedules and needs. We especially want to recognize Yasuyuki Koga, Director of the Earthquake Disaster Prevention Department, and Toru Terayama, Senior Research Engineer, as well as Yoshio Ninomiya, Tadashi Hamada, Shuichi Tamoto, Dong Gang, and Jorge Rodrigues.

We also want to extend our warm appreciation to the companies and organizations, and their respective staff members, who generously provided us tours of their facilities and willingly shared critical information, as well as first hand experiences. We wish to especially thank Tohru Yoshikawa, Deputy General Manager, Technical Research Center, Kansai Electric Power Company, Inc.; Toshikazu Inui, Deputy Manager, Central Load Dispatching Center, Kansai Electric Power Company, Inc.; Hiroshi Sumitomo, Manager, Earthquake Reconstruction Project, Corporate Planning Department, Osaka Gas Co., Ltd.; Makoto Matsushita, Assistant Manager, Planning Division, Kobe Municipal Waterworks Bureau; Yoshitaka Osanaga, Chief, Tobu Administrative Office, Kobe Municipal Sewage Bureau; and Atsushi Matsuura, Deputy General Manager, Tarumi Construction Office, Honshu-Shikoku Bridge Authority.

The U.S. delegates to the workshop and contributors to this report are: Donald Ballantyne, Dames and Moore; Stephanie Chang, EQE International; Riley Chung, National Institute of Standards and Technology; Ronald T. Eguchi, EQE International; LeVal Lund, consultant; Howard H.M. Hwang, University of Memphis; Laurie A. Johnson, Spangle Associates; Anne S. Kiremidjian, Stanford University; Thomas D. O'Rourke, Cornell University; Charles Scawthorn, EQE International; Anshel Schiff, consultant; and, M. Shinozuka, University of Southern California. The New Zealand delegates and report contributors are: John Lumsden, University

of Canterbury; John Norton, The Hutt City Council; and, David Hopkins, Kingston Morrison Ltd.

This report was supported by the National Institute of Standards and Technology (NIST) and the National Science Foundation (NSF) of the United States. Any opinions, findings, conclusions, or recommendations expressed herein are the authors' and do not necessarily reflect the views of NIST, NSF or the authors' organizations.

## TABLE OF CONTENTS


| | | Page |
|---|---|---|
| FOREWORD | | 476 |
| ACKNOWLEDGMENTS | | 478 |
| 1. | INTRODUCTION | 483 |
| 2. | REPORT ON LIFELINES | 484 |
| 2.1 | The Kansai Electric Power Company, Inc. | 484 |
| 2.2 | Osaka Gas Company, Ltd. | 487 |
| 2.3 | Kobe Municipal Waterworks Bureau | 489 |
| 2.4 | Kobe Sewage Works Bureau | 491 |
| 2.5 | Bridges and Roadways | 493 |
| 3. | REPORT ON OTHER ASPECTS OF RECOVERY | 496 |
| 3.1 | Debris Removal and Landfill Operations | 496 |
| 3.2 | Temporary Housing | 496 |
| 3.3 | Port Recovery | 497 |
| 3.4 | Business/Economic Recovery | 498 |
| 4. | KEY OBSERVATIONS AND LESSONS LEARNED | 499 |
| 4.1 | The Impact of This Earthquake was Extensive, Yet the Potential for Even More Destructive Earthquakes Still Exists | 499 |
| 4.2 | Good and Modern Design Does Pay Off | 500 |
| 4.3 | Traffic Congestion Has Had a Tremendous Effect on Both Response and Recovery | 500 |
| 4.4 | Effective Communication and Coordination Between Utility Companies and Government Agencies is Critical in All Aspects of the Disaster Cycle | 501 |
| 4.5 | Recovery is Not Only a Function of the Impacts, But Also Priorities and Resources | 502 |
| 4.6 | Notable Mitigation Efforts are Being Incorporated Into the Recovery. | 502 |

## TABLE OF CONTENTS (CONTINUED)


Page

4.7 Recovery As a Process Can be Enhanced by Good Leadership and Pre-event Planning. ..... 503

4.8 Response and Recovery Efforts Benefited From the Use of New Technologies. ..... 505

5. CONCLUSIONS ..... 506

6. REFERENCES ..... 508


## APPENDICES


A. Study Tour Schedule ..... 509

B. List of Materials Collected on the Study Tour ..... 511

# 1. INTRODUCTION

On July 20 and 21, 1995, U.S. and New Zealand delegates to the Sixth U.S.-Japan Workshop on Earthquake Disaster Prevention for Lifeline Systems participated in a two-day tour to study the impacts to lifelines systems and the on-going recovery, six months after the Great Hanshin-Awaji earthquake. The tour was designed and sponsored by the Public Works Research Institute of Japan. Delegates toured facilities of the Kansai Electric Power Company, Osaka Gas Company, Kobe Municipal Waterworks Bureau, and Kobe Municipal Wastewater Bureau, in addition to inspecting ground failure areas and a number of bridge repairs underway. A detailed itinerary for the study tour is provided in Appendix A.

This report is intended to document not only the activities related to the study tour, but the participants insights and observations. The remainder of this report is organized into three sections. The first section, "Report on Lifelines," is structured around the types of lifeline facilities toured. In addition to delegates' comments, each section contains a brief statement about the impact to a particular system, along with information about emergency services provided, the timing of recovery, an indication of the recovery priorities, and, when possible, an identification of countermeasures which are being addressed in the recovery. Telecommunications and rail systems were not included in the tour and therefore are not covered in this report.

The second section covers other aspects of recovery noted during the study tour. The third section addresses key observations and lessons learned for both the United States and New Zealand. These are followed by some concluding remarks and references. A list of materials collected on the study tour is provided in Appendix B.

## 2. REPORT ON LIFELINES

### 2.1 THE KANSAI ELECTRIC POWER COMPANY, INC.

With a generating capacity of 35,035 MW and supplying electricity to 11.7 million customers, the Kansai Electric Power Company is the largest power provider in the southern half of the Japanese archipelago (60 Hz area). Delegates visited the company's Central Load Dispatching Center and Training Simulator, which is located in the heart of downtown Osaka, more than 30 km from the epicenter of the quake. Mr. Tohru Yoshikawa, Deputy General Manager of the Technical Research Center, and Mr. Toshikazu Inui, Deputy Manager of the Central Load Dispatching Center, Kansai Electric Power Company, Inc. led their staff in an introductory presentation. They showed a video of the company's post-earthquake restoration efforts, and took delegates on a tour of the facilities. It was the first time for many of the delegates to visit a power dispatching center. Veterans noted the remarkable cleanliness of the facilities and superb quality of the equipment.

At the time of the earthquake, the center was controlling a light total electric power demand. The power supply was initially cut off to about 2.6 million customers, affecting a wide area stretching from Akashi city to the southwestern region of Kyoto Prefecture.

Some notes about the impacts and the power company's response and recovery efforts are as follows:

- More than 48 substations were damaged, eight of which were completely out of service. 446 distribution lines were damaged. The earthquake reduced the company's generating capacity by roughly 20%. No damage to hydropower generating stations or nuclear plants was observed. Thermoelectric power plants suffered damage to a total of 10 boilers due to ground settlement.

- In response to the earthquake, the Kansai Power Company organized its countermeasure unit in its head office in Osaka. The power dispatching center sustained no observable damage in this

event. Officials report that if damage had been more significant at this facility, the company would have operated its emergency response out of its backup center in Kyoto.

- The Kobe branch office of Kansai Electric Power served as the base for response and recovery activities in the Hanshin area. Although this office suffered structural and contents damage, it continued to serve as a customer service center to answer telephone calls from affected customers.

- A total of 4,700 workers were sent out to make repairs to the damaged system. According to the dispatching center, 60-70% of the employees that could be reached immediately after the earthquake did come to work by 12 noon that afternoon. In order to communicate with employees, a TV conference system, which had been partially damaged in the earthquake, was set up. During that first morning, after initial inspections and system adjustments, the number of customers without power was reduced to 1.0 million.

- Mobile transformers were also brought in to augment damaged substation equipment. Many supplies and equipment were brought in by sea, even though port facilities had suffered extensive damage.

- By January 19, all but 170,000 customers had power restored. By January 21, less than 30,000 customers were still without power. By January 23, almost all customers had power restored Only those buildings that were completely destroyed had no power. This general time frame marked the completion of the emergency restoration phase.

- Some of the community response activities that Kansai Electric Power directly supported included: 1) installing street lights in evacuation shelters, 2) installing electric water heaters in

evacuation shelters, 3) installing toilets and incinerators in hospitals, and 4) creating an employee support system.

- Full-scale restoration remains to be carried out. Kansai Electric representatives report that they are ready to respond and rebuild according to local government reconstruction plans.

Some comments and observations offered by delegates are:

- The power system was under light load at the time of the earthquake so there was enough available capacity and ample equipment to effectively transfer power needs to undamaged facilities.

- Because of good planning and fortuitous circumstances, the electric power system performed very well in this event. Some of the factors which contributed to this good performance include: having more dead vs. live tank circuit breakers, substations that were not located along the fault, and the time of day (i.e., low demand for power).

- Kansai Power operates as a linear network unlike the grid networks common in the U.S. Maintaining network stability was less of an issue in the Kobe earthquake. Network frequency was controlled by dropping the load to 500 KV substations. In the US, network frequency is controlled at the distribution station level (i.e., lower voltage levels). In Japan, controlling frequency by reducing loads to high voltage substations has the effect of disrupting power to larger service areas.

- The Japanese appear to rely less on network simulation exercises to develop contingency plans. This was evident in discussions with operators in the main control center. One possible reason for this lack of reliance on simulation studies may be differences in regulatory procedures and measures.

- Prior to the introduction of dynamic analysis requirements for high voltage substation equipment, Kansai Power used static analysis procedures (0.5g). It is not clear when the 0.5g criteria went into effect in Japan, however, this transition from static to dynamic analysis requirements parallels the development of seismic design criteria for high voltage equipment in the U.S.

- There were obvious psychological benefits shown by residents when the power was restored. This was evident in the videos shown by Kansai Power that highlighted their response and recovery efforts. Return to normalcy as soon as possible was an important goal for all affected utilities.

- In New Zealand, backup generators are rare commodities. The 67 backup generators used after the Kobe earthquake by Kansai Power offered significant advantages during the response and recovery periods.

## 2.2 OSAKA GAS COMPANY, LTD.

Delegates visited the supply center of Osaka Gas located on Port Island in Kobe. Ground settlement was evident around the base of the building and in the parking lot, but most equipment inside appeared intact and fully operational. Hiroshi Sumitomo, Manager, Earthquake Reconstruction Project, Corporate Planning Department, led the staff's presentation on the earthquake's impacts to the gas system. Staff also showed a video illustrating some of the problems they encountered in repairing the system.

Some notes on the impacts to the gas system and the company's response and recovery efforts are as follows:

- Ground shaking and permanent ground displacements severely damaged gas pipelines throughout the region. 838,000 customers were initially without gas.

- Reportedly, most pipeline damage occurred in low pressure gas pipes with screwed joints. Screwed joints have little flexibility for

movement. Earthquake damage to these kinds of pipes had been recognized by the Japanese from previous earthquakes in Japan. These pipes are being replaced with pipes having welded or mechanical joints.

- On January 24, Osaka Gas formally began its repair efforts. On January 28, 821,000 customers were still without service. February 6, the number had been reduced to 725,000 customers out of service. At the time of peak restoration activities, officials report that 9,700 people were involved in the repair work. By mid-March, officials report that the restoration was essentially complete. Restoration was a very time-consuming process which took 80 days instead of the initially estimated 45 days.

- According to company officials, Osaka Gas lost nearly $1 billion (US) in income in April 1995, as compared with income the same time the previous year.

- For about 10 years, Osaka Gas has had an ongoing program to mitigate seismic damage to their system. Following the earthquake, the company decided to increase its number of strong motion instruments which can provide early estimates of ground motion from 34 to 64. Within 3 minutes of the event, Osaka Gas expects to have information on peak accelerations and spectral intensities (SI) at all critical facilities. This system, when completed, will resemble the system in place at Tokyo Gas. The company also plans to further subdivided its distribution network into 100 blocks, rather than the present 55 blocks.

Some comments and observations offered by delegates are:

- In the U.S., it is generally acknowledged that liquefaction effects cause more dramatic damage to underground pipelines than wave passage effects. In the Kobe earthquake, Osaka Gas reported that areas of cut and fill were more significantly impacted. A

partial explanation for this discrepancy may be the fact that little distribution piping was located in these liquefied areas.

- One of the unexpected problems that occurred during the initial restoration period was the flooding of water into damaged gas pipelines. As a result of breakage of adjacent water lines, repairs to damaged gas pipes were slowed while flooded trenches were de-watered and gas pipes drained. To facilitate these repairs, Osaka Gas developed innovative methods and equipment to drain the system. In the U.S., this phenomena of water in gas pipes has not been observed.

- Robotic pigs were used to inspect and repair damage in underground pipelines, by examining joints with television cameras. Similar technology is available in the U.S., however, the Japanese also used these pigs to inspect and repair outer weld joints.

- To get around the transportation breakdown, collapsed buildings, etc., and to facilitate more effective response, the company set up a series of field offices right outside heavily damaged areas. Personnel and supplies were managed through these offices. This type of response required significant planning in order to implement. The company's actions can be a useful model for responding to future earthquakes in dense, urban areas.

## 2.3 KOBE MUNICIPAL WATERWORKS BUREAU

Delegates toured the Okuhirano Control Center of the Kobe Municipal Waterworks Bureau, located on the slopes of Mount Rokko above downtown Kobe. Assistant Plant Manager, Makoto Matsushita, guided delegates around the control center, which is also the site of the Okuhirano Purification Plant. It is one of two purification plants for the Kobe water distribution system. Water is primarily supplied into the area from the Yodo river via two east-west transmission tunnels, running roughly along the base of the mountains. Delegates viewed damaged pipe segments that had been retrieved from repair sites.

Mr. Matsushita reviewed the control center's emergency shut-off valve system which was engaged in the earthquake. Three seismometers are located on the first floor of the control center; the system control room is located on the fourth floor. The emergency shut-off valve system operates at three alarm levels. For Alarm Level 3 (80 gal or 0.08 g or less), the valves do not close. For Alarm Level 2 (80 to 250 gals, or 0.08 to 0.25 g), the valves shut-off automatically when two conditions are met in each service reservoir: 1) seismometer indicates over 80 gal; and 2) flow rate exceeds a threshold value. For Alarm Level 1 (250 gals or 0.25 g or greater), all valves shut-off automatically. During the earthquake, the center's seismographs recorded horizontal accelerations of 818 gal and 617 gal, and vertical accelerations of 332 gal. Alarm Level 1 was reached, and the system shut down.

Some notes about impacts as well as the bureau's response and recovery operations are as follow:

- In Kobe, 250,000 of 650,000 households were initially without water (39%). Extensive damage was observed throughout the roughly 4,000 km of water distribution pipe.

- The water bureau's headquarters, which was located on the 6th floor of the old Kobe City Hall, sustained a mid-floor collapse and has been uninhabitable since the earthquake. Significant damage also occurred at the Tobu branch office. The concrete tunnel of the Sengari aqueduct collapsed. Liquefaction and ground deformation was observed at the Uegahara Purification Plant and at the Egeyama Service Reservoir. Large distribution pipes attached to bridges failed because of collapsed or damaged bridge spans (e.g., Rokko Bridge which connects to Rokko Island; Kobe Bridge which connects to Port Island).

- In many cases, emergency water was supplied from fire-hydrants. Other emergency measures to supply water included the use of self-defense force ships drafting water from the bay to fill tank trucks.

- As of February 6, 29,000 households were still without water in Kobe. By February 20, almost all of the system was restored except for parts of the city's waterfront district. Officials report that the system was completely repaired by April 17. Approximately 900 repairs were reportedly made to the distribution system.

Some comments and observations offered by delegates are:

- In order to conserve water for drinking, approximately 20 reservoirs were intentionally shut down as a result of the earthquake. While this may appear to be a prudent action, it does cause some ancillary issues, such as inadequate water for fighting fires.

- Some innovative techniques were used for providing emergency water supplies. Some ideas that were presented included collapsible, spherical tanks (large yellow balloons), and long manifolds of house bibs. Many of these ideas could applied in the U.S.

- Suikin - manufactured flexible fittings for pipelines performed quite effectively. These fittings are designed to have super flexible-2 ball and socket joints with an expansive sleeve in between two balls and sockets. There were roughly 300 of these fittings in the Kobe area, with many of them on Port Island. No leakage was observed in any of these fittings following the earthquake. These fittings, however, are expensive.

## 2.4 KOBE MUNICIPAL SEWAGE WORKS BUREAU

The City of Kobe's wastewater system is designed to serve a regional population of over 1.5 million. There are seven treatment plants, one sludge center, and 3,315 km of wastewater pipes and 484 km of storm sewers. Delegates visited the Higashinada Wastewater Treatment Plant located in the port area, near downtown Kobe. Mr. Yoshitaka Osanaga, Chief of the Bureau's Tobu Administrative Office,

led delegates on a tour of the facilities. He reported that before the earthquake, the treatment plant had an estimated capacity of 225,000 cubic meters per day, although the actual operating level was around 160,000. After the earthquake, damage reduced the capacity to 187,000; the current operating level is about 180,000. He speculated that the 20,000 cubic meters per day increase is resulting from sewage infiltrating the system from nearby sewage pipes that have been damaged. Delegates also viewed a new building that houses the plant's emergency generator. The building's pile foundation sustained heavy damage. There was more than 1m of observable settlement around the building's base and nearly 2m of lateral displacement in a nearby quay wall due to liquefaction.

Some notes on the impacts to the wastewater system and the bureau's response and recovery efforts are as follows:

- Severe damage to the Higashinada, Chubu, and Nishibu treatment plants was observed. Capacities for these plants was initially reduced to 0%, 50%, and 20%, respectively.

- Typical sewer system failures involved abnormalities in manholes (uplift or settlement) and disruption of road surfaces. 1,414 repairs were reportedly made to the sewer system.

- The city estimates that it will take 3 years to reconstruct the damaged treatment plant facilities at a cost of 20 billion yen (approx. $200 million). The city is also undertaking a pipe restoration/repair program to check all buried pipes and fix those that are repairable.

Some comments and observations offered by delegates are:

- The City has done a significant amount of work since the earthquake (e.g. cleaning up, moving equipment, etc.) Delegates were particularly impressed with the efforts undertaken to get to where they are at this point in time.

- Most of the pipe damage in this earthquake occurred in non-liquefied regions.

- Sewer pipes connected to manholes were more severely damaged than other types of pipes. In the case of pipe breakage, pipes connected to manholes were damaged about ten times more than unconnected pipes.

## 2.5 BRIDGES AND ROADWAYS

A large number of bridges were damaged in this earthquake and one estimate puts the affected number at 60% of the total inventory. Permanent ground movements resulting from the earthquake were impressive. According to a land survey conducted by the Honshu-Shikoku Bridge Authority and the Geographical Survey Institute, displacements from 50 cm to 100 cm within the area from Northern Awaji Island to Tarumi Ward were observed. The ground under many bridge foundations also moved and consequently caused significant foundation damage.

On the first day of the tour, delegates visited the Rokko Island bridge repair. The north part of Rokko Island suffered severe liquefaction. The quay wall along the north end of the island moved about 3.5 m toward the sea. Subsidence of roughly 2.0m was also observed. At the same location, the simply-supported steel girder on the Port Liner Bridge dropped from the pier as a result of movement of the pier toward the sea. It was reported that the top of the concrete caisson displaced 80 cm toward the sea.

On the second day of the study tour, delegates changed into work clothes and took a boat ride to the north bridge tower of the Akashi-Kaikyo suspension bridge. At a total construction cost of 800 billion yen, the Akashi Kaikyo suspension bridge, scheduled to open in December 1998, was literally at ground zero during the January earthquake. Mr. Atsushi Matsuura, Deputy General Manager, Tarumi Construction Office, of the Honshu-Shikoku Bridge Authority led delegates on a tour of the bridge. Pier 3P has been permanently displaced by 80 cm in the horizontal direction and 20 cm in the vertical direction, relative to the rest of the bridge. Construction on the bridge resumed after a brief suspension in activities to assess the impacts of the earthquake. To study tour participants, this bridge was evidence that good modern seismic design and construction practices are paying off.

Also on the second day, delegates visited the Port Island bridge repair. In the north area of Port Island, the quay wall line moved toward the north with a maximum displacement of 4m. Significant subsidence was also observed in this area. A two-story steel bridge girder dropped due to a excessive movement of the pier. The end of the non-collapsed girder moved about 90 cm toward the sea.

For most of the world, probably the most memorable and devastating image of the earthquake was the failed Hanshin Expressway. Route 3 of the Hanshin Freeway is a privately-owned toll road. It is operated by the Hanshin Expressway Corporation, one of the largest corporations of its type in Japan. It is a predominantly elevated structure, supported on a majority of steel spans and columns. Eleven elevated spans of this system suffered major damage in the earthquake. One repair cost estimate puts damage at 500 billion yen (approx. $5 billion). Of the two routes most heavily impacted by the earthquake (i.e., Routes 5 and 3), Route 3 is the oldest by about 30 years, which accounts for the much higher damage rate experienced by this route as compared to the newer Route 5.

Despite this damage, Route 3 is expected to be open by the fall of 1995. Approximately 700 columns on Route 3 are being temporarily repaired and about 50 spans will be totally replaced before it is opened to traffic. Eventually 200 of these 700 columns will be replaced. The remainder of these columns will be strengthened to meet current seismic design criteria.

The Hanshin Expressway Corporation has an active earthquake maintenance program. The company currently spends about 30 billion yen (approx. $300 million) on approximately 200 km of freeway. It also has an ongoing seismic retrofit program and has for many years used earthquake couplers to restrain the free ends of simply-supported girders. The Hanshin Expressway Corporation has been investigating the use of steel jackets for enhancing the strength of concrete columns. In fact, several trial jackets on single column bents at the west end of Route 3 have already been installed. On the study tour, the delegates also noticed extensive epoxy repair to some damaged concrete columns. It was unclear whether these repairs were final or whether steel jackets would be added later on.

One delegate also commented that the repairs to damaged freeway overspans appeared to be slow compared to repairs made after the Northridge earthquake. A partial explanation for the rapid repairs after Northridge was the use of an incentive program instituted by CalTrans for early completion. For each day less than the pre-agreed opening or completion date, the contractor received $1 million. There was, therefore, significant incentive to complete reconstruction in the shortest period of time.

## 3. REPORT ON OTHER ASPECTS OF RECOVERY

Some additional aspects of recovery which delegates observed during the tour are included in this section.

### 3.1 DEBRIS REMOVAL/LANDFILL OPERATIONS:

A considerable amount of debris is still evident six months after the earthquake and Kobe city officials estimate that it will take one year to complete its demolition effort. Extensive landfill programs are underway on the bay sides of Port Island and Rokko Island and at other points along the margins of Osaka Bay. Interesting debris sorting procedures are also apparent for the recycling and reuse of various debris products. A steel melting and recycling area was observed.

Shortly after the earthquake, Kobe city officials established criteria for determining demolition priorities and these seem to be working well. According to one city representative, the priorities were: 1) buildings that blocked public access; 2) whole areas which contained many damaged buildings, especially those threatening neighboring buildings. All the areas were prioritized according to additional criteria and the city has been methodically working through clearing area by area. The city is allowing some building and property owners to perform their own demolitions with expenses reimbursed by the city.

### 3.2 TEMPORARY HOUSING

Large temporary housing projects are under construction. The number of temporary housing units is impressive and the effort to install working utilities and sanitary facilities for these units is also extraordinary. Some of the largest projects were under construction on the newly filled land at the bay sides of Rokko and Port Islands. Smaller projects are also visible throughout the heavily damaged areas of Kobe, especially in the few open areas, including parking lots.

Current reports are that 18,000 people are still living in tents and 40,000 are in temporary units. In addition, approximately 18,000 individuals have refused to move from their neighborhoods, even though housing in the area is unsafe and

uninhabitable. Delegates speculated that one of the key issues may be that many of these temporary housing areas are located far from familiar transportation systems, commercial centers, schools and work locations. Also, government officials are reportedly concerned that it will be hard to get people out of these temporary units, once more permanent housing has been constructed. Officials report that the temporary units will only be available for two years. Accommodating large homeless populations when the "big one" occurs, and facilitating smooth transitions from temporary to more permanent housing, are important questions for both U.S. and Japanese researchers to consider.

### 3.3 PORT RECOVERY

For more than a thousand years, the Kansai region flourished as Japan's gateway for foreign trade. However, once the capitol of Japan moved to Tokyo in the early 1800's, so also went the trading focus. Tokyo and Yokohama surpassed the region as the main trading hubs for the country. Ironically, it was the 1923 earthquake and fire which helped to obliterate both ports, and propel Kobe to the leading port status it held until this year. Now, another earthquake threatens to take this stature away.

Liquefaction and subsidence almost completely destroyed the world's sixth largest port. Following the earthquake, less than 10 berths were barely usable and almost all of the modern container cranes collapsed or suffered severe damage. The suspension of distribution functions due to this damage has affected economic activity locally, nationally, and even internationally.

At the time of our visit, officials reported that nearly three-quarters of the berths had been at least temporarily restored. Significant ground deformation and seawall failure was still evident. There was a perception on the part of several delegates that the repair activities in the port area were not as intense as in other areas of Kobe. There was less noise and less construction equipment visible. The delegates saw many tall cranes standing in what appeared to be good condition, but there was little cargo or other port related activities on-going. It is not clear to what extent the port of Kobe has retained or lost its pre-earthquake customers.

According to government officials, full restoration of port operations is not expected for approximately 2 years. Total repair costs are expected to exceed $9 billion (US).

### 3.4 BUSINESS/ECONOMIC RECOVERY

Commercial businesses appear to be recovering relatively quickly, at least based on our limited tour of the commercial areas of Kobe. Industrial business recovery seemed to be lagging, however, it is impossible to make a credible assessment based on the limited time spent on the study tour. There are many important lessons to be learned from this event about both commercial and industrial business recovery.

# 4. KEY OBSERVATIONS AND LESSONS LEARNED

The following notes represent key lessons learned from the Kobe experience. The comments compiled from study tour delegates (which are listed under each lesson) served as the basis for these observations. It is hoped that these lessons provide impetus to lifeline operators in the U.S. and New Zealand to enhance or accelerate the implementation of earthquake hazard reduction programs for their systems.

## 4.1 THE IMPACT OF THIS EARTHQUAKE WAS EXTENSIVE, YET THE POTENTIAL FOR EVEN MORE DESTRUCTIVE EARTHQUAKES STILL EXISTS

The range of lifelines and infrastructure affected by this event was immense, but the potential for even greater damage in a larger earthquake is apparent, especially given the scale and intensity of the region's infrastructure pattern.

The overall impact of liquefaction was staggering. Almost all facilities, regardless of size or configuration, moved with the shifted soil. Most transportation structures located on reclaimed land sustained damage and many buildings located in these areas showed signs of settlement at the base or movement of foundations. Several participants expected the effects from liquefaction to range from sand boils to structures sinking in place. They did not expect to see the massive movement of soil or land that actually occurred. As one New Zealand delegate put it, "the effects of liquefaction could be compared to putting thin porridge on a dinner plate and moving it from side to side."

Many delegates were concerned that the region's residents were reportedly so surprised by the earthquake, and, in particular, that they didn't realize that the potential for a large earthquake existed in this region. The region's future vulnerability to earthquakes depends in large part on the ability of the public and its decision makers to heed the lessons learned from this event and take action now to reduce future risks.

## 4.2 GOOD AND MODERN DESIGN DOES PAY OFF

While damage was extensive, Kobe also provides some sound examples of good structural design and construction practices. This was evidenced by the many well-designed buildings that survived, such as steel-frame buildings, and reinforced concrete structures built under Japan's most recent codes and standards. High-rise apartment and office buildings on both Port and Rokko Islands are another good example. These buildings were supported on pile foundations which performed well during the earthquake. The use of modern pipes with flexible fittings is yet another good example. These types of fittings, nearly 300 of them installed in the Kobe area, all demonstrated their capability to sustain the strong earthquake shaking without damage.

Many delegates cited the Akashi Kaikyo suspension bridge as an outstanding example of good modern design. Just as we have much to gain from observing damage, this earthquake can also provide the earthquake engineering community with some valuable "success" lessons.

## 4.3 TRAFFIC CONGESTION HAS HAD A TREMENDOUS EFFECT ON BOTH RESPONSE AND RECOVERY

Many delegates had visited the region in the early days of the disaster and recalled the giant traffic jams that impeded the operation of rescue workers, fire trucks, and relief providers. Most were amazed that six months after the earthquake, Kobe's traffic problems were still so significant. To a large degree, this situation arises due to the fact that the city of Kobe lies along a narrow strip of land, with mountains to the north and Osaka Bay to the south. All major road transportation systems are located in this east-west strip which is about 2½ miles (or 4.0 km) at its widest location. Many of these transportation systems were severely damaged during the earthquake. An often chaotic situation of traffic jams has been created as a result of significant efforts to repair, retrofit, and replace these systems, as well as a result of difficulties in re-routing traffic.

Traffic congestion is undoubtedly impacting the region's recovery, both physically and economically. It is interesting to note that in Kobe, the railway carries people

and the roads carry a large part of the freight. Clearly, the region's movement of goods continues to be impacted by this event.

U.S. delegates recalled how wide streets in the Northridge area easily accommodated emergency traffic. Many speculated whether congestion problems, of a magnitude similar to Kobe's, could occur in San Francisco, Oakland, or downtown L.A., after a large earthquake in California. A more moderate earthquake occurring in more densely developed cities of the Eastern U.S. could also have similar effects.

## 4.4 EFFECTIVE COMMUNICATION AND COORDINATION BETWEEN UTILITY COMPANIES AND GOVERNMENT AGENCIES IS CRITICAL IN ALL ASPECTS OF THE DISASTER CYCLE

There was an apparent lack of coordination between utilities both in the response and recovery related to this event, as well as in pre-event preparedness and response planning. The psychological boost to people when power was restored was noted which illustrates the importance of lifelines in the immediate aftermath. It also illustrates the value of response planning and a return to normalcy as soon as possible. There are reports, however, that early energizing of damaged electric power lines caused collateral damage in the form of fires resulting from leaking gas lines.

The decision to automatically shut down water supplies because of damage to water pipelines should be thoroughly reviewed. This decision may have resulted in the lack of sufficient water to fight ensuing fires. Better coordination between water and fire departments is essential in order to effectively address this issue.

Improving coordination between utilities was an issue addressed by a recent New Zealand study. Basic to this study was the organization of key players, including policy makers, utility operators, government officials, and researchers and engineers. Priorities were established by classifying impacts (whether damage related or due to disruption of service) on a qualitative scale. Part of the reason for the success of the program was that decisions were made based on how each action or mitigation reduced potential impacts. The methodology was systematic in the sense that it included a planning scenario, a vulnerability analysis, an impacts

analysis, and response planning to address the projected impacts. Perhaps, this type of approach could be extended to situations where close coordination between agencies is needed.

## 4.5 RECOVERY IS NOT ONLY A FUNCTION OF THE IMPACTS, BUT ALSO PRIORITIES AND RESOURCES

The scale of an earthquake disaster and its long-term impacts is often difficult to describe, more so to quantify. Earthquakes are often thought of as discrete individual happenings--reports of damage and response; recovery and the longer-term impacts are often seen as almost unrelated events. There is a great need to convey the scale of the disaster in terms of all the phases of the disaster, including response and recovery, and to illustrate the interconnectedness of these phases.

Many of the delegates were impressed with the resources being employed to reconstruct damaged urban facilities, particularly the transportation systems. For example, the amount of steel used and the ruggedness built into some of the repaired bridge elements amazed many. The speed at which damaged railways are being repaired was also impressive. While the full commitment of resources may not be known for some time to come, it appears that no amount of money is being spared in bringing damaged facilities back into operation, particularly the transportation systems.

Delegates noted that some longer-term impacts may be associated with those lifeline systems that cannot be repaired quickly or easily. For example, the long-term impacts associated with disruption of water, gas and electricity are expected to be low, since these systems were brought back into service in relatively short amounts of time. Other lifelines, such as the transportation systems (e.g., roads, highways, and port and harbor facilities) might have considerably longer-term impacts because of their longer repair times.

## 4.6 NOTABLE MITIGATION EFFORTS ARE BEING INCORPORATED INTO THE RECOVERY

As a result of this earthquake, Japan is now undertaking a comprehensive review of the nation's seismic design methods. The J.R. system in Japan has committed $1

billion a year for retrofit of seismically-vulnerable elements. Private companies and utilities are also looking closely at their exposure.

During our stay, the news reported that the National Reconstruction Committee in Tokyo had reviewed and accepted the recommendations of Hyogo Prefecture's "Phoenix Plan." The plan contains many references to mitigation, with one-, three-, and ten-year targets for working toward a livable, economically healthy, and disaster resistant Kansai region. Rebuilding guidelines are including statements about acceptable levels of risk for repairs and reconstruction.

A committee representing the region's major utilities, professional groups, and private companies, are also considering the possible construction of a large-scale "aseismic utility conduit" which would cross Kobe city from east to west, carrying trunk lines for major lifelines, including water, telecommunications, gas, and electricity. While some experts believe that the "lifeline box" as a completely aseismic design may not be possible, expectations are that quick restorations of enclosed pipelines would be possible without excavation.

The comparison might be premature but, to many delegates, Japan seems to leading California in the mitigation arena. Six years after the Loma Prieta earthquake, the Bay Bridge retrofit has still yet to begin.. California's AB 547 (a bill which mandates local jurisdictions to inventory seismically-vulnerable buildings) had some muscle in it, but it is for one class of building only, whereas Japan is now considering a major nationwide earthquake retrofit program for many classes of buildings.

## 4.7 RECOVERY AS A PROCESS CAN BE ENHANCED BY GOOD LEADERSHIP AND PRE-EVENT PLANNING

Management of the recovery will be a major issue everywhere. Delegates were interested in finding out what information was important to local and regional government officials in order for them to respond quickly and to conduct necessary assessments, allocate and manage available post-disaster resources and determine what additional resources are needed.

A considerable amount of attention has also focused on the problems and inadequacies by various government agencies during the response phase following this earthquake. Delegates noted that one reason why response to recent U.S. disasters may have appeared more immediate and focused is that we have had an amazing number of major natural disasters: hurricanes, floods, and earthquakes. Japan has been fortunate in that it has had very few. Perhaps this may have lulled many into a greater lack of awareness, or possibly even a bit of complacency. A certain amount of criticism in this Kobe event is appropriate because of the obvious gaps in preparedness and planning in the emergency phase. However, most delegates agreed that the leadership for the recovery is outstanding.

Many delegates were dismayed, but not surprised, to learn that certain recovery solutions, such as proposed street widenings, were receiving considerable resistance by residents. Some questioned whether the benefits of these measures were not fully recognized by the public or because there is a great incentive to return to normalcy as soon as possible. The decisions that take place after a major disaster are both difficult and traumatic. For example, the assessment of the safety of a building that houses many commercial establishments can be very difficult. There can be great political and economic pressure to get businesses back into operation as soon as possible. How certain decisions impact long-term needs is often difficult to assess in an emergency situation.

These issues illustrate the benefits of pre-earthquake recovery planning. Developing a post-earthquake recovery plan, such as what is being done in Kobe, is expected to be matched with strong resistance. Pre-earthquake planning efforts allow the public to participate in the selection and adoption of recovery strategies before pressures set in. Hopefully when the earthquake occurs, attention can be focused on the implementation of the plan rather than a debate on the policy aspects of the plan. One noteworthy example of this type of pre-planning in the U.S. is the PEPPER Study (Pre-Earthquake Planning for Post-Earthquake Rebuilding), which considers rebuilding options for a devastating earthquake in the Los Angeles area.

## 4.8 RESPONSE AND RECOVERY EFFORTS BENEFITED FROM THE USE OF NEW TECHNOLOGIES

The extensive use of robotic pigs to identify and repair damaged welds allowed faster restoration of the gas system. High-powered television cameras were mounted on these robotic pigs. This system is unique in that it allowed both the inspection and repair of exterior and interior welds. Television cameras were also reportedly used for inspecting for damage to sewer and conduits carrying telecommunication cables.

Digital accelerograph instruments were used to map peak ground motions in near-real time. Osaka Gas is planning to add 30 instruments to their existing 34-instrument network in order to provide more accurate and timely estimates of ground acceleration after major events. In conjunction with real-time estimates of ground motion there is also increasing interest in providing real-time estimates of damage. A map of peak ground motions can be constructed from limited network data, and when combined with damage assessment tools or methodologies, can be useful in determining the full scope of the disaster. This information can be particularly useful to local and regional governments responsible for making early and immediate decisions about response and relief.

It is evident that geographic information systems (GIS) played a major role in response and recovery following this earthquake, particularly for lifeline operators. Damaged facilities have been mapped relative to service populations and critical customers. This information has been used by companies in establishing restoration priorities, as well as identifying where emergency resources are needed. Many of the country's research organizations and university departments are also assembling extensive computer databases. A summary of the use of GIS tools and software in both the Kobe and Northridge earthquakes would be a valuable reference for many researchers, policy makers, lifeline operators, and government officials. It was suggested that an international conference on this topic be considered in the near future before precious data is lost.

## 5. CONCLUSIONS

Kobe is a very important event for more than just Japan. For U.S. delegates, Kobe probably best illustrates how lucky we have been. All the recent U.S. earthquakes have been moderate in magnitude or have generally missed densely populated areas. Recovery has been relatively rapid in these cases, largely because enough resources have been available both locally and regionally. In a catastrophic event in a densely populated area, all available resources will be heavily impacted, recovery will be significantly hampered both in time and scope because resources will have to come from distant locations.

There are many areas in the U.S. that are possible Kobe's. For example, seismic planning in the midwest is largely absent even though this region is a source of the largest earthquakes to have ever occurred in the contiguous U.S. What would happen if we had an earthquake such as Kobe in this area? In order to model this event, we need to learn how resources are stretched and how resilient response and recovery systems are when the demand for these resources exceed available capacity.

For the New Zealanders, the study tour illustrated the striking parallels between the nature and range of damage in the Kobe earthquake and the expected nature and range of damage in a Wellington fault scenario, such as the one portrayed in the Wellington Lifelines Project. To borrow from the workshop report prepared by David Hopkins, "the scale of infrastructure in the Kobe region is many times that of the Wellington region in particular, but the geology, soils and topography provide a similar range of environments. Lifelines generally are constructed in similar materials and the extensive range of conditions experienced by these facilities will provide a wealth of background for application to New Zealand situations. It is almost certain that the Kobe earthquake will provide the strongest parallels for New Zealand of any earthquake this century. Continuing study of the impacts of this earthquake will have significant potential benefits for New Zealand organizations involved in earthquake risk reduction, and in lifelines in particular."

As one delegate stated "visiting an disaster site transforms an earthquake from an engineering event to a societal event. You begin to develop a scenario for your

own city. You ask yourself questions like what will my city do with 300,000 homeless, and what are our resources?" Hopefully workshops such as this will continue to provide researchers and policy makers opportunities to exchange information, ideas, and real life experiences on the effects of these large and unexpected events. Participants agreed that future workshops, if appropriate, should include researchers from other earthquake-prone regions.

Finally, one of the most striking lessons we can learn from Kobe is that earthquakes are a percentage game. While no one will argue that the damage in Kobe was extraordinary and extensive, but looking around, one is also struck by how much survived, how many more buildings stand unscathed. The reality is that life carries on no matter what the scale, and six months later in Kobe, a great deal of life has resumed a good sense of normalcy.

## 6. REFERENCES

"Impact of the Earthquake of Southern Hyogo Prefecture on Electric Power Facilities," by Tohru Yoshikawa and Yoshiaki Mino, The Kansai Electric Power Company. Proceedings of the Sixth US/Japan Workshop on Earthquake Disaster Prevention for Lifelines Systems, Osaka, Japan, July 1995 (pre-print).

"Damages of Gas Facilities by Great Hanshin Earthquake and Restoration Process," by Shojiro Oka, Central Control Office, Distribution Department, Osaka Gas Co., Ltd. Proceedings of the Sixth US/Japan Workshop on Earthquake Disaster Prevention for Lifelines Systems, Osaka, Japan, July 1995 (pre-print).

"Damages of Kobe Water System by the Hanshin Awaji Great Earthquake and Restoration Plan," by Makoto Matsushita, Assistant Manager, Planning Division, Kobe Municipal Waterworks Bureau. Proceedings of the Sixth US/Japan Workshop on Earthquake Disaster Prevention for Lifelines Systems, Osaka, Japan, July 1995 (pre-print).

"Sixth US/Japan Workshop on Earthquake Disaster Prevention for Lifelines Systems, Osaka, Japan, July 1995." Report by David C. Hopkins, Kingston Morrison, dated August 2, 1995.

"Characteristics of the Southern Hyogo Earthquake, Damage to Urban Facilities", by Mitsuyuki Asano, in The Wheel Extended, No. 92, A Toyota Quarterly Review, published by Toyota, July 1995.

"Report from the Hanshin-Awaji Earthquake: Overview of Performance of Highway Bridges," by Ian G. Buckle, NCEER Bulletin, Volume 9, Number 2, April 1995.

## APPENDIX A

## STUDY TOUR ITINERARY

6th U.S.-Japan Workshop on Earthquake Disaster Prevention
for Lifelines Systems

July 20, 1995

| | |
|---|---|
| 9:00 am | KKR Hotel Osaka departure. Move to Kansai Electric Power Co. by bus |
| 9:30 am | Inspection of Kansai Electric Power Co., Osaka city |
| 10:30 am | Move to Osaka Gas Co., Kobe City, Port Island by bus |
| 12:30 pm | Inspection of Gas Supply Facility of Osaka Gas Co.; Lunch |
| 13:50 pm | Move to Kobe City, Water Supply Bureau by bus |
| 14:50 pm | Inspection of Kobe City, Water Supply Bureau, Okuhirano Purification Plan |
| 15:50 pm | Move to Kobe City Sewage Works Bureau by bus |
| 16:20 pm | Inspection of Sewage Works Bureau, Higashinada Wastewater Treatment Plant |
| 17:20 pm | Move to Rokko Island Bridge by bus |
| 17:50 pm | Inspection of deformation of bridge site ground, Kobe City Rokko Island |
| 18:05 pm | Move to hotel |
| 19:35 pm | KKR Hotel Osaka arrival |

July 21, 1995

| | |
|---|---|
| 8:00 am | KKR Hotel Osaka departure. Move to Akashi Suspension Bridge (under construction), Tarumi Work Office by bus |
| 10:30 am | Arrive at Tarumi Work Office. Change into work clothes |
| 11:20 am | Inspection of Akashi Suspension Bridge exhibition hall. Lunch |
| 13:30 pm | Leave 1A for tower 3P by ship |
| 13:50 pm | Climb tower 3P |
| 14:20 pm | Leave 3P for 4A by ship |
| 14:30 pm | Arrive at 4A. Inspection of Nojima Fault, Awaji Island |
| 15:20 pm | Leave 4A for Tarumi Work Office by ship |
| 15:40 pm | Arrive at Tarumi Work Office. Change clothes |
| 16:00 pm | Move to Kobe Bridge |
| 17:00 pm | Inspection of Kobe Bridge, deformation of bridge site ground |
| 17:20 pm | Move to Nishinomiya-port Bridge, Koshien-Hama, Nishinomiya City by bus |
| 18:10 pm | Inspection of damaged part of wharf and lateral displacement around the bridge |
| 18:30 pm | Leave Nishinomiya-port Bridge for hotel |
| 20:00 pm | KKR Hotel Osaka arrival |

## APPENDIX B

## LIST OF MATERIALS COLLECTED ON THE STUDY TOUR

"Controlling the Flow of Electricity", Central Load Dispatching Center, The Kansai Electric Power Co., Inc.

System Peak Record in 1994, The Kansai Electric Power Co., Inc.

Typical Daily Load Curves by Season, The Kansai Electric Power Co., Inc.

Hanshin-Awaji Earthquake Disaster, Photographs of Damages to Waterworks Facilities and Emergency Water Supply, July 1995, Kobe Municipal Waterworks Bureau.

Study Tour to Okuhirano Control Center, Kobe Municipal Waterworks Bureau.

"The Influence of the Southern Hyogo Earthquake upon the Akashi Kaikyo Bridge," Honshu-Shikoku Bridge Authority.

Excerpts from The Proceedings of Symposium on the Great Hanshin-Awaji Earthquake and Its Geo-Environments, June 20-21, 1995, Tokyo, Japan, The Committee of Environmental Geology, Geological Society of Japan, pages 14-31.

Paper written in Japanese on the Nojima Fault, including photographs of rupture effects on Awaji Island.



Photo 1



Photo 2

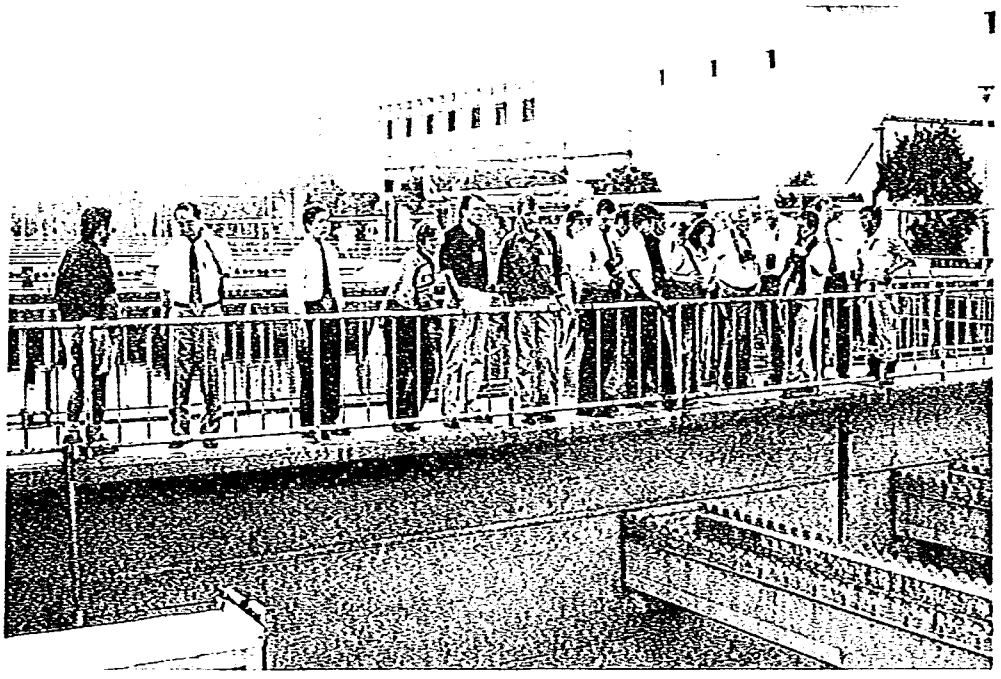


Photo 3

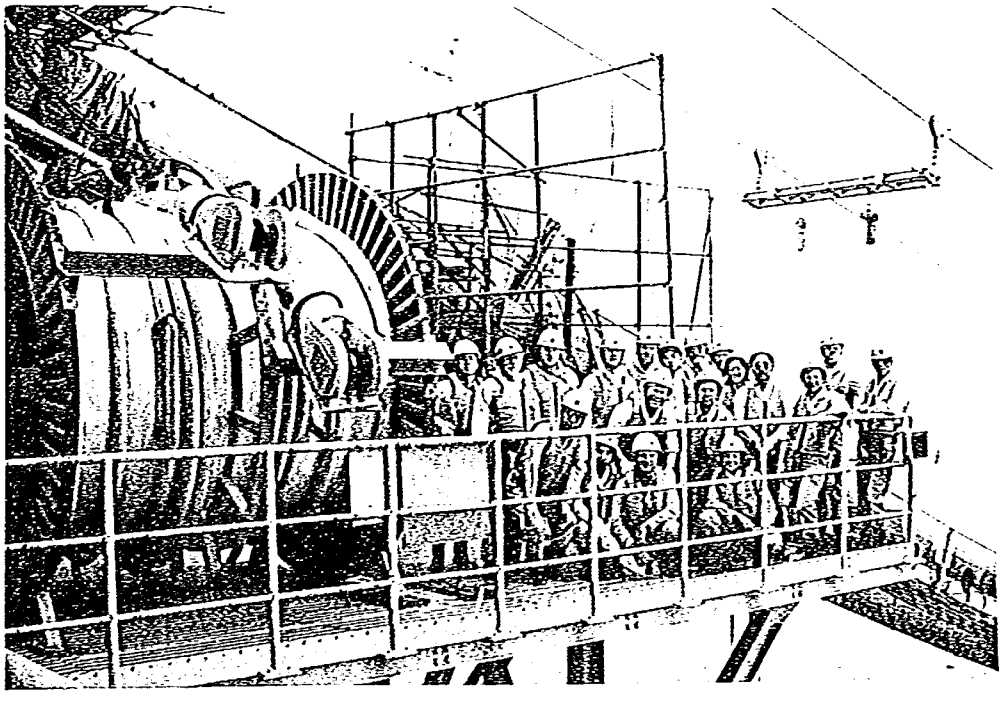


Photo 4

SIXTH U.S.–JAPAN WORKSHOP ON
EARTHQUAKE DISASTER PREVENTION FOR LIFELINE SYSTEMS
JULY 18 AND 19, 1995
KKR HOTEL OSAKA, OSAKA, JAPAN

WORKSHOP PROGRAM

July 18 (TUE)

8:50 Registration

9:00 Session–1 Opening Session

(Chairmen: H. Otsuka and Masanobu Shinozuka)

Welcome Remarks by Yasuyuki Koga
(Director, Earthquake Disaster Prevention Department)

Remarks by Riley Chung
(Leader, Earthquake Engineering Group Structures Division)

---

9:30 Session–2 Effects of Liquefaction (1)

(Chairmen: Y. Koga and L. Lund)

U–1) Case History of Pipeline Response to Ground Deformation at Balboa Blvd.,1994 Northridge Earthquake
(T.D. O'Rourke and S. Toprak)

J–1) Liquefaction–Induced Ground Displacement and Its Caused Damage to Lifeline Facilities
(Masanori Hamada, Ryoji Isoyama and Kazue Wakamatsu)

J–2) Microfine Cement Grouting as a Countermeasure against Liquefaction
(Osamu Matsuo, Junichi Koseki, Masaaki Sano and Masao Shimoda)

J–3) Analysis of Behavior and Effect of Geosynthetic Reinforced Embankments at the Occurrence Liquefaction
(Osamu Matsuo, Takao Shimazu, Junichi koseki Teruhisa Fujii and Naozo Fukuda)

10:30 Discussion

---

10:50 Break

---

11:00 Session–3 Effects of Liquefaction (2)

(Chairmen: M. Hamada and T. D. O'Rourke)

J–4) Study on Flow of Liquefied Ground by means of Model Pipe Tests
(Ikuo Towhata and William Vargas–Monge)

J–5) Countermeasures against the Floatation of Buried Pipes due to Liquefaction
(Susumu Yasuda, Hideo Nagase, Shigeru Itafuji and Keiichiro Mine)

J-6) Dependence of Longitudinal Subgrade Reaction to the Buried Pipe on Displacement Velocities and Cycles of the Ground.
(Mio Kobayashi, Hirokazu Ando and Noritake Oguchi)

11:45 Discussion

---

12:00 Lunch

---

13:00 Session-4 Water & Sewage

(Chairmen: S. Yasuda and D. Ballantyne)

J-7) Damages to Kobe Water System by the Hanshin Awaji Great Earthquake and Restoration Plan
(Makoto Matsushita)

J-8) Performance of Sewerage System During the 1994 Hokkaido Toho-oki Earthquake
(Masaru Kitaura and Masakatsu Miyajima)

J-9) Damage to Sewerage Facilities in Recent Earthquakes
(Shuji Tanaka)

U-2) Water and Sewer Lifelines: Lessons Learned from Recent Earthquakes
(Le Val Lund)

J-10) Performance of Lifeline Systems During the 1995 Great Hanshin Earthquake
(Shiro Takada and Junichi Ueno)

14:15 Discussion

---

14:40 Break

---

15:00 Session-5 Seismic Monitoring and Restoration

(Chairmen: S. Takada and A. S. Kiremidjian)

J-11) A Study on the Development of An Immediate Detection System for Seismic Damage to Lifelines Using GPS and GIS.
(Fusanori Miura and Junji Kiyono)

J-12) Development of SIGNAL : Seismic Information Gathering Network Alert System
(Yoshihisa Shimizu, Fumio Yamazaki, Shigeru Noda, Ryuji Isoyama and Youichi Yoshikawa)

J-13) Conditional Non-Gaussian Fields
(Masaru Hoshiya)

J-14) Real Time Conditional Simulation of Earthquake Ground Motion
(Tadanobu Sato and Hiroshi Imabayashi)

J-15) Optimization of Post-Earthquake Restoration of Lifeline Networks Using Genetic Algorithms
(Tadanobu Sato and Koji Ichii)

16:15 Discussion

16:40 Adjourn

17:30 Reception at the KKR HOTEL OSAKA – Akebono Room

July 19 (WED)

9:00 Session–6 Gas, Electricity and Telecommunication

(Chairmen: M. Miyajima and H. H.M. Hwang)

J–16) Damages of Gas Facilities by Great Hanshin Earthquake and Restoration Process
(Shojiro Oka)

J–17) Impact of the Earthquake of Southern Hyogo Prefecture on Electric Power Facilities
(Tohru Yoshikawa and Yoshiaki Mino)

J–18) Damage of Underground Telecommunication Facilities in the 1995 Great Hanshin Earthquake
(Kenichi Honda Yuzo Yamaguchi and Shinji Mataki)

U–3) Power Systems: Comparing the Kobe and Northridge Earthquake Experiences
(Anshel J. Schiff)

10:00 Discussion

10:20 Break

10:30 Session–7 Risk Assessment and Impact of Seismic Effects (1)

(Chairmen: H. Otsuka and L. A. Johnson)

U–4) Pipeline Performance Parameters for Earthquake Vulnerability
(Donald Ballantyne)

U–5) Economic Impact of Lifeline Disruption: Current Models and Preliminary Observations from the Hanshin Earthquake
(Stephanie E. Chang and Wm. Jess Taylor )

U–6) Application of GIS Technology to Seismic Risk Assessment of Lifeline Systems in Shelby County, Tennessee
(Howard H.M. Hwang)

11:15 Discussion

11:30 Lunch

13:00 Session−8 Risk Assessment and Impact of Seismic Effects (2)

(Chairmen: F. Yamazaki and S. E. Chang)

U−7) Functional Interactions of Lifeline Systems under Earthquake Conditions
(Masanobu Shinozuka and Satoshi Tanaka)

N−1) Regional Approach to Assessment of Impact on Lifelines and Response to Earthquakes in New Zealand
(David C. Hopkins, John L. Lumsden and John A. Norton)

U−8) New Trends in the Use of Earthquake Scenario Exercises : Opportunities for Mitigating Vulnerable Lifeline Systems
(Laurie A. Johnson)

U−9) Rapid Post−Earthquake Damage Assessment for Lifeline Facilities
(Ronald T. Eguchi, Hope A. Seligson and James D. Goltz)

14:00 Discussion

---

14:20 Break

---

14:40 Session−9 Transportation and Fire

(Chairmen: R. Hagiwara and A. Schiff)

N−2) Resources Required to Rebuild Wellington
(David C. Hopkins)

J−19) A Fundamental Study on Innovative Menshin System for Underground Structures
(Hisanori Otsuka, Jun−ichi Hoshikuma and Kazuhiro Nagaya)

U−10) A Bridge Prioritization Method Based on Transportation System Performance Using GIS
(Nesrin Basoz and Anne S. Kiremidjian)

U−11) Fire Following the Hanshin and Northridge Earthquakes : A Comparative Analysis
(C. Scawthorn and A. Cowell)

15:40 Discussion

---

16:00 Break

---

16:10 Session−10 Closing Session

(Chairmen: H. Otsuka and C. R. Scawthorn)

Settlement of Resolutions

Remarks by R. Chung
(Leader, Earthquake Engineering Group Structures Department)

Closing Remarks by Y. Koga (Director, Earthquake Disaster Prevention Department)

16:30 Closure

---

# LIST OF PARTICIPANTS
## -U.S. SIDE-


Mr. Donald Ballantyne
Dames & Moore
500 Market Place Twr.
2025 First Ave.
Seattle, WA 98121
(206) 728-0744 (T)
(206) 727-3350 (F)

Dr. Stephanie E. Chang
EQE International
Lakeshore Towers
18101 Von Karman Ave., Suite 400
Irvine, CA 92715
(714) 833-3303 (T)
(714) 833-3391 (F)

Dr. Riley Chung
National Institute of Standards / Technology
Bldg. 226, Rm B158
Gaithersbury,MD 20899
(301) 975-6062 (T)
(301) 869-6275 (F)

Mr. Ronald T. Eguchi
EQE International
Lakeshore Towers
18101 Von Karman Ave., Suite 400
Irvine, CA 92715
(714) 833-3303 (T)
(714) 833-3391 (F)

Prof. Howard H.M. Hwang
Center for Earthquake Research and Information
The University of Memphis
Memphis, TN 38152
(901) 678-4830 (T)
(901) 678-4734 (F)

Ms. Laurie A. Johnson
Spangle and Associates
3240 Alpine Rd.
Portola Valley, California 94028-7592
(415) 854-6001 (T)
(415) 854-6070 (F)

Prof. Anne S. Kiremidjian
Stanford University
Civil Engineering Dept.
Terman 238
Stanford, CA 94305
(415) 723-4164 (T)
(415) 725-9755 (F)

Mr.LeVal Lund
Civil Engineer
3245 Lowry Rd.
Los Angeles,California 90027
(213) 664-4432 (T/F)

Prof. Thomas D. O'Rourke
Civil-Envir. Engr.
265 Hollister Hall
Cornell University
Ithaca, NY 14853
(607) 255-6470 (T)
(607) 255-9004 (F)

Dr. Charles Scawthorn
EQE International
44 Montgomery Street
32nd, Floor
San Francisco, CA 94104
(415) 989-2000 (T)
(415) 397-5209 (F)

Prof. Anshel Schiff
Stanford University
27750 Edgerton Road
Los Altos Hills, California 94022
(415) 941-9233 (T/F)

Prof. M. Shinozuka
Fred Champion Chair in Civil Engineering
Dept. of Civil Engineering
University of Southern California
3620 S.Vermont Ave. KAP254
Los Angels, CA 90089-2531
(213) 740-9528 (T)
(213) 740-9529 (F)

# LIST OF INVITED PARTICIPANTS FROM NEW ZEALAND

Mr.John Lumsden
Center for Advanced Engineering
University of Canterbury
Christchurch 1, New Zealand
64-3-364-2478 (T)
64-3-364-2069 (F)

Mr.John Norton
The Hutt City Council
30 Laings Road, Lower Hutt
Private Bag 31912
Lower Hutt, New Zealand
64-4-570-6666 (T)
64-4-569-4290 (F).

Dr. David C. Hopkins
Kingston Morrison Ltd.
Mayfair House
54 The Terrace
PO Box 10283
Wellington, New Zealand
64-4-473-4265 (T)
64-4-473-3369 (F)

# LIST OF PARTICIPANTS

## -Japan SIDE-


Mr. Yukio Adachi
Hanshin Expressway Public Corporation
4-1-3 Kyutaro-machi Chuoku Osaka
541, Japan

Dr. Naozo Fukuda
Fukken Co.,Ltd
2-10-11 Hikari-cho Higashi-ku
Hiroshima 732, Japan

Dr. Dong Gang
Research Scholar
Earthquake Engineering Division
Public Works Research Institute
Tsukuba Sience City, 305, Japan

Mr. Ryoji Hagiwara
Head
Ground Vibration Division
Public Works Research Institute
Tsukuba Sience City, 305, Japan

Mr. Fumio Hakamada
Hanshin Expressway Public Corporation
4-1-3 Kyutaro-machi Chuoku Osaka
541, Japan

Prof. Masanori Hamada
Professor
School of Science and Engineering,
Waseda University
3-4-1 Okubo Shinjyukuku Tokyo, 169,
Japan

Mr. Tadashi Hamada
Research Engineer
Ground Vibration Division
Public Works Research Institute
Tsukuba Sience City, 305, Japan

Mr. Kenichi Honda
NTT Access Network Systems
Laboratories
1-7-1 Hanabatake, Tsukuba Science City
305, Japan

Mr. Masato Horie
Kansai Electric
3-3-22 Nakanoshima Kitaku, Osaka,
530-70, Japan

Mr. Junichi Hoshikuma
Research Engineer
Earthquake Engineering Division
Public Works Research Institute
Tsukuba Sience City, 305, Japan

Prof. Masaru Hoshiya
Professor
Department of Civil Engineering
Musashi Institute of Technology
1-28-1 Tamazutsumi Setagaya-ku, Tokyo,
158, Japan

Mr. Masato Hosokawa
Onoda Chemico Co.,Ltd
2-17-4 Yanagibashi, Daitoku, Tokyo,
111, Japan

Mr. Koji Ichii
Research Engineer
Port and Harbor Research Institute
3-1-1 Nagase Yokosuka, Kanagawa, 239,
Japan

Prof. Kenji Ishihara
Professor
Science University of Tokyo
2641 Yamazaki Nodashi, 278, Japan

Prof. Hiroyuki Kameda
Professor
Disaster Prevention Research Institute,
Kyoto University
Gokasho Ujishi, 611, Japan

Mr. Mio Kobayashi
Tokyo Gas Co., Ltd
1-16-25 Shibaura Minatoku Tokyo, 105,
Japan

Dr. Yasuyuki Koga
Director,
Earthquake Disaster Prevention
Department
Public Works Research Institute
Tsukuba Sience City, 305, Japan

Mr. Shinji Mataki
NTT Access Network Systems
Laboratories
1-7-1 Hanabatake, Tsukuba Science City
305, Japan

Mr. Makoto Matsushita
Kobe Municipal Waterworks Bureau
4-1-6 Isogamidori Chuoku Kobe, 651,
Japan

Mr. Yoshiaki Mino
Kansai Electric
3-3-22 Nakanoshima Kitaku, Osaka,
530-70, Japan

Prof. Fusanori Miura
Professor
Yamaguchi University
2557 Tokiwadai Ube, 755, Japan

Dr. Masakatsu Miyajima
Associate Professor
Kanazawa University
2-40-20 Kodatsuno Kanazawa, Ishikawa,
920, Japan

Mr. Toshihiko Naganuma
Hanshin Expressway Public Corporation
4-1-3 Kyutaro-machi Chuoku Osaka
541, Japan

Dr. Masahiro Nakano
Public Works Research Center
1-6-4 Taito Taitoku, Tokyo, 110, Japan

Mr. Yoshiro Ninomiya
Senior Research Engineer
Ground Vibration Division
Public Works Research Institute
Tsukuba Sience City, 305, Japan

Mr. Shojiro Oka
Osaka Gas Co.,Ltd
4-1-2 Hiranocho Chuoku Osaka, 541,
Japan

Dr. Hisanori Otsuka
Head,
Earthquake Engineering Division
Public Works Research Institute
Tsukuba Sience City, 305, Japan

Dr. Jorge Rodrigues
Research Scholar
Earthquake Engineering Division
Public Works Research Institute
Tsukuba Sience City, 305, Japan

Mr. Masaaki Sano
Onoda Chemico Co.,Ltd
2-4-2 Osaku Sakura, Chiba, 285, Japan

Prof. Tadanobu Sato
Professor
Disaster Prevention Research Institute,
Kyoto University
Gokasho Ujishi, 611, Japan

Mr. Yoshihisa Shimizu
Tokyo Gas.,Ltd
1-5-20 Kaigan Minatoku Tokyo, 105,
Japan

Dr. Hideyo Suzuki
Power R&D Center
Tokyo Electric Power
4-1, Egasaki-Cho, Tsurumi-ku,
Yokohama 230, Japan

Prof. Shiro Takada
Professor
Kobe University
Rokkoudaimachi Nadaku Kobe, 657,
Japan

Mr. Satoru Takahashi
Power R&D Center
Tokyo Electric Power
4-1, Egasaki-Cho, Tsurumi-ku,
Yokohama 230, Japan

Mr. Isao Takatori
Public Works Research Center
1-7-2 Taito Taitoku, Tokyo, 110, Japan

Mr. Shuichi Tamoto
Assistant Research Engineer
Soil Dynamics Division
Public Works Research Institute
Tsukuba Sience City, 305, Japan

Mr. Shuji Tanaka
Head,
Sewage Works Division
Public Works Research Institute
Tsukuba Sience City, 305, Japan

Dr. William Tanzo
Assistant Professor
Saitama University
255 Okubo Urawa, 338, Japan

Mr. Toru Terayama
Senior Research Engineer
Earthquake Engineering Division
Public Works Research Institute
Tsukuba Sience City, 305, Japan

Dr. Huanan Tong
University of Tokyo
7-22-1 Roppongi Minatoku, Tokyo, 106,
Japan

Prof. Ikuo Towhata
Professor
University of Tokyo
7-3-1 Hongo Bunkyoku, Tokyo, 113, Japan

Mr. Kiyoshi Tsuji
Toa Corporation
1-3 Anzencho Tsurumiku, Yokohama,
230, Japan

Mr. Jyunichi Ueno
Konoike Construction Co.,Ltd
3-6-1 Kitakyuhojimachi Chuo-ku, Osaka,
541, Japan

Mr. Kazuhiko Urano
Hazama Corporation
515-1 Azanishimukai Karima, Tsukuba
Science City, 305, Japan

Mr. Ryosuke Uzuoka
Hazama Corporation
2-5-8 Kitaaoyama Minatoku, Tokyo,
107, Japan

Mr. William Vargas-Monge
University of Tokyo
7-3-1 Hongo Bunkyoku, Tokyo, 113,
Japan

Mr. Yuzo Yamaguchi
NTT Access Network Systems
Laboratories
1-7-1 Hanabatake, Tsukuba
Science City, 305, Japan

Dr. Fumio Yamazaki
Associate Professor
University of Tokyo
7-22-1 Roppongi Minatoku, Tokyo
106, Japan

Prof. Susumu Yasuda
Professor
Tokyo Denki University
Ishizaka Hatoyamacho Hikigun,
Saitama-Ken, 350-03, Japan

Mr. Tohru Yoshikawa
Kansai Electric
3-3-22 Nakanoshima Kitaku, Osaka,
530-70, Japan

Mr. Hiroshi Yoshimura
Konoike Construction Co.,Ltd
4-3-55 Denpo Konohana-ku, Osaka,
554, Japan

# PROCEEDING OF FIFTH U.S.-JAPAN WORKSHOP ON EARTHQUAKE DISASTER PREVENTION FOR LIFELINE SYSTEMS

ISSN 0386-5878
Technical Memorandum of PWRI No.3415

Yasuyuki Koga
Hisanori Otsuka
Toru Terayama
Shuichi Tamoto

**Synopsis:**
These proceedings document the results of the U.S.-Japan Workshop on Earthquake disaster Prevention for Lifeline Systems which was held at KKR Hotel Osaka, Osaka, Japan, on July 18 and 19, 1995 under the auspices of the Panel on Wind and Seismic Effects, UJNR.The Workshop was organized by the Task Committee F "Disaster Prevention Methods for Lifeline Systems" (U.S. side chairman: R.M. Chung, NIST, Japan side chairman: Y.Koga, PWRI) of the Panel.

**Keyword: Earthquake Disaster Prevention, Lifeline Systems, Pipeline, Gas, Telephone, Electricity, Water Supply, UJNR**

○

郵 便 は が き

Postage stamp

3 0 5 - □ □

建設省土木研究所地震防災部耐震研究室
〒305 茨城県つくば市大字旭１番地

Earthquake Engineering Division,
Public Works Research Institute
Tsukuba Science City
Japan305

No.

No.

配布先住所 ○

配布先氏名

Receipt of

Technical Memorandum of PWRI No.3415

Name _____

Address _____

_____

_____